UNIVERSIDAD DE SALAMANCA

FACULTAD DE CIENCIAS QUÍMICAS

DEPARTAMENTO DE QUÍMICA ORGÁNICA

RECEPTORES MOLECULARES QUE SIMULAN AGUJEROS OXIANIÓNICOS: RECONOCIMIENTO MOLECULAR Y CATÁLISIS

TESIS DOCTORAL

José Javier Garrido González

Directores

Joaquín Rodríguez Morán

Laura Marcos Monleón

Ángel Luis Fuentes de Arriba

UNIVERSITY OF SALAMANCA

FACULTY OF CHEMICAL SCIENCES

ORGANIC CHEMISTRY DEPARTMENT

MOLECULAR RECEPTORS WHICH MIMIC OXYANION HOLES: MOLECULAR RECOGNITION AND CATALYSIS

PhD Thesis

José Javier Garrido González

Supervisors

Joaquín Rodríguez Morán

Laura Marcos Monleón

Ángel Luis Fuentes de Arriba

UNIVERSIDAD DE SALAMANCA

FACULTAD DE CIENCIAS QUÍMICAS

DEPARTAMENTO DE QUÍMICA ORGÁNICA

VNiVERSiDAD D SALAMANCA

CAMPUS DE EXCELENCIA INTERNACIONAL

RECEPTORES MOLECULARES QUE SIMULAN AGUJEROS OXIANIÓNICOS: RECONOCIMIENTO MOLECULAR Y CATÁLISIS

TESIS DOCTORAL

Memoria que presenta **D. José Javier Garrido González** para optar al título de Doctor por la Universidad de Salamanca, con la mención de "Doctor Internacional"

VNiVERSiDAD D SALAMANCA
CAMPUS DE EXCELENCIA INTERNACIONAL

DEPARTAMENTO DE QUÍMICA ORGÁNICA
FACULTAD DE CIENCIAS QUÍMICAS
UNIVERSIDAD DE SALAMANCA

D. Joaquín Rodríguez Morán, Director del Departamento de Química Orgánica de la Universidad de Salamanca

CERTIFICA:

Que la presente memoria titulada "Receptores moleculares que simulan agujeros oxianiónicos: Reconocimiento Molecular y Catálisis" ha sido realizada por D. José Javier Garrido González en el Departamento de Química Orgánica de la Universidad de Salamanca para optar al título de Doctor por la Universidad de Salamanca, con la mención de "Doctor Internacional", y ha sido desarrollada bajo la dirección del Dr. D. Joaquín Rodríguez Morán, Catedrático del Departamento de Química Orgánica de la Universidad de Salamanca, la Dra. Dña. Laura Marcos Monleón, Profesora Contratada Doctora del Departamento de Química Orgánica de la Universidad de Salamanca y el Dr. Ángel L. Fuentes de Arriba, Investigador Beatriz Galindo del Departamento de Química Orgánica de la Universidad de Salamanca.

Y para que así conste a efectos oportunos, firma el presente documento

Fdo. Joaquín Rodríguez Morán

D. Joaquín Rodríguez Morán, Catedrático del Departamento de Química Orgánica de la Universidad de Salamanca, Dña. Laura Marcos Monleón, Profesora Contratada Doctora del Departamento de Química Orgánica de la Universidad de Salamanca y el Dr. Ángel L. Fuentes de Arriba, Investigador Beatriz Galindo del Departamento de Química Orgánica de la Universidad de Salamanca

CERTIFICAN:

Que la presente memoria titulada "Receptores moleculares que simulan agujeros oxianiónicos: Reconocimiento Molecular y Catálisis" ha sido realizada por D. José Javier Garrido González para optar al título de Doctor por la Universidad de Salamanca, con la mención de "Doctor Internacional", y ha sido desarrollada bajo su dirección conjunta en el Departamento de Química Orgánica de la Universidad de Salamanca y autorizan su presentación para ser calificada como Tesis Doctoral.

Y para que así conste a efectos oportunos, firman el presente documento

BECAS Y PROYECTOS DE INVESTIGACIÓN

El doctorando José Javier Garrido González ha disfrutado durante la realización de la Tesis Doctoral de un contrato predoctoral al amparo del Programa III de la Universidad de Salamanca (Programas Propios, año 2018), por el que se convocan "ayudas para financiar contratos predoctorales de la Universidad de Salamanca, cofinanciados por el Banco Santander".

Para optar a la mención de "Doctor Internacional" el doctorando José Javier Garrido González ha realizado una estancia de investigación de 3 meses en la Universidad de Bristol bajo la supervisión del profesor Anthony P. Davis. Esta estancia ha estado cofinanciada por el programa IV de la Universidad de Salamanca (Programas Propios, año 2021), por el que se convocan ayudas para la "movilidad del Personal Investigador".

El trabajo de investigación contenido en la presente memoria ha sido financiado parcialmente por los siguientes proyectos de investigación:

- Ministerio de Ciencia e Innovación: PID2019-108994RB-I00 y PID2020-118732RA-I00.
- Junta de Castilla y León: Fondos FEDER – SA069P17.
- Universidad de Salamanca: Programas Propios – KCEP/463AC01 y 18K155/463AC01.
- Fundación Memoria de D. Samuel Solórzano Barruso: FS/8-2019.

También destacar la labor de los servicios de apoyo a la investigación (Resonancia Magnética Nuclear, Espectrometría de Masas y Difracción de Rayos X) de la plataforma NUCLEUS de la Universidad de Salamanca, cuya labor permite el correcto desarrollo de parte del desarrollo experimental de esta Tesis.

CONTRIBUCIONES CIENTÍFICAS DERIVADAS DE LA TESIS DOCTORAL

Se detallan a continuación los artículos científicos publicados en revistas científicas y contribuciones presentadas en congresos y simposios, que recogen parte de los resultados obtenidos en la presente memoria de Tesis Doctoral:

Publicaciones en revistas científicas.

1. Turiel, M. G.; Garrido-González, J. J.; Simón, L.; Sanz, F.; Lithgow, A. M.; Morán, J. R.; Fuentes de Arriba, Á. L.; Alcázar, V. "Highly Enantioselective Extraction of Phenylglycine by a Chiral Macrocyclic Receptor based on Supramolecular Interactions", *Org. Lett.* **2020**, *22*, 867 – 872. https://pubs.acs.org/doi/10.1021/acs.orglett.9b04379

   Factor de impacto: 6.005 (JCR, 2020).
   Ranking: Q1 (6 de 57).

2. Garrido-González, J. J.; Iglesias Aparicio, Mª M.; Martínez García, M.; Simón, L.; Sanz, F.; Morán, J. R.; Fuentes de Arriba, Á. L. "An Enzyme Model Which Mimics Chymotrypsin and N-Terminal Hydrolases", *ACS Catal.* **2020**, *10*, 11162 – 11170. https://pubs.acs.org/doi/10.1021/acscatal.0c02121

   Factor de impacto: 13.084 (JCR, 2020).
   Ranking: Q1 (15 de 162). Primer decil.

3. Garrido-González, J. J.; Boya del Teso, I.; Fuentes de Arriba, Á. L.; Sanz, F.; Martín del Valle, E. M.; Morán, J. R.; Alcázar, V. "An Adjustable Cleft Based on an 8-Sulfonamide-2-Naphthoic Acid with Oxyanion Hole Geometry", *Chem. Eur. J.* **2021**, *27*, 14605 – 14609. https://doi.org/10.1002/chem.202102137

   Factor de impacto: 5.236 (JCR, 2020).
   Ranking: Q2 (52 de 178).

Contribuciones presentadas en congresos y simposios.

1. - Título: "Charge Transfer Complexes of an Artificial Oxyanion-Hole Enzyme Mimic with an Adaptable Cleft"
   - Tipo de contribución: Póster.
   - Autores: José J. Garrido-González,* Asmaa Habib, Estela Sánchez Santos, Irene Boya del Teso, Ángel L. Fuentes de Arriba, Joaquín R. Morán, Victoria Alcázar.
   - Nombre de la conferencia: RSEQ Symposium. 27/10/2021 – 30/09/2021.
   - Entidad Organizadora: Real Sociedad Española de Química.
   - Lugar de celebración: Formato on-line, España.

2. - Título: "A Supramolecular Enzyme Model which Mimics Chymotrypsin and N-Terminal Hydrolases"
   - Tipo de contribución: Póster.
   - Autores: José J. Garrido-González.*
   - Nombre de la conferencia: III Jornadas de Jóvenes Investigadores en Ciencia y Tecnología Químicas. 15/07/2021 – 16/07/2021.
   - Entidad Organizadora: Facultad de Ciencias Químicas, USAL.
   - Lugar de celebración: Salamanca, Castilla y León, España.

3. - Título: "Synthetic Enzyme as Transacylation Organocatalyst"
   - Tipo de contribución: Comunicación Oral.
   - Autores: Ángel L. Fuentes de Arriba, Luis Simón, Joaquín R. Morán, José J. Garrido-González.*
   - Nombre de la conferencia: I Jornada de Jóvenes Investigadores del GEQOR (GEQOR – Jóvenes). 16/06/2021.
   - Entidad Organizadora: Grupo Especializado de Química Orgánica, Real Sociedad Española de Química.
   - Lugar de celebración: Formato on-line, España.

4. - Título: "Estructura, síntesis y reconocimiento molecular de compuestos orgánicos"
   - Tipo de contribución: Comunicación Oral.
   - Autores José J. Garrido-González.*
   - Nombre de la conferencia: II Jornadas de Jóvenes Investigadores en Ciencia y Tecnología Químicas. 28/11/2019 – 29/11/2019.
   - Entidad Organizadora: Facultad de Ciencias Químicas, USAL.
   - Lugar de celebración: Salamanca, Castilla y León, España.

5. - Título: "New achievements in the development of organocatalyst for transacylations"
   - Tipo de contribución: Póster.
   - Autores: José J. Garrido-González,* Mª Mercedes Iglesias Aparicio, Miguel Martínez García, Vega Rodríguez Gil, Joaquín Rodríguez Morán.
   - Nombre de la conferencia: XXXVII Reunión Bienal de la RSEQ. 26/05/2019 – 30/05/2019.
   - Entidad Organizadora: Real Sociedad Española de Química.
   - Lugar de celebración: Donostia-San Sebastián, País Vasco, España.

6. - Título: "Estrategias de Química Supramolecular en Organocatálisis"
   - Tipo de contribución: Comunicación Oral.
   - Autores: José J. Garrido-González.*
   - Nombre de la conferencia: I Jornadas de Jóvenes Investigadores en Ciencia y Tecnología Químicas. 04/10/2018 – 05/10/2018.
   - Entidad Organizadora: Facultad de Ciencias Químicas, USAL.
   - Lugar de celebración: Salamanca, Castilla y León, España.

7. - Título: "Supramolecular Chemistry: from enzyme to biodiesel"
   - Tipo de contribución: Póster.
   - Autores: José J. Garrido-González,* Jorge Martín García; Antonio Santos Antón, Joaquín Rodríguez Morán.
   - Nombre de la conferencia: XXVII Reunión Bienal de Química Orgánica. 20/06/2018–22/06/2018.
   - Entidad Organizadora: Grupo Especializado de Química Orgánica, Real Sociedad Española de Química.
   - Lugar de celebración: Santiago de Compostela, Galicia, España.

8. - Título: "Imitando la vida: desde el enzima hacia el biodiésel"
   - Tipo de contribución: Comunicación Oral.
   - Autores: José J. Garrido-González,* Jorge Martín García; Joaquín Rodríguez Morán.
   - Nombre de la conferencia: III Jornada de Promoción de la Investigación Básica para Estudiantes de Ciencias e Ingenierías. 12/04/2018 – 13/04/2018.
   - Entidad Organizadora: Universidad Rey Juan Carlos.
   - Lugar de celebración: Móstoles, Comunidad de Madrid, España.

"Si quieres llegar rápido, viaja solo. Si quieres llegar lejos, viaja acompañado"

Proverbio africano.

"Lo que conocemos es una gota, lo que no conocemos es un océano"

Isaac Newton.

"La ciencia, muchacho, está hecha de errores, pero de errores útiles de cometer, pues poco a poco, conducen a la verdad"

Profesor Otto Lidenbrock en "Viaje al centro de la Tierra" – Julio Verne.

A mi madre, hermana y abuela

Y especialmente a Sara, mi compañera de vida.

AGRADECIMIENTOS

Quisiera comenzar estos agradecimientos a mis directores: Quino, Laura y Ángel. Gracias por toda la ayuda recibida durante este tiempo, por vuestros consejos, desvelos y disposición a ayudarme en cualquier cosa que he necesitado a lo largo de estos años.

También quisiera expresar mi agradecimiento a la Universidad de Salamanca, por el contrato de investigación predoctoral que he disfrutado (Programas Propios de la USAL – Programa III cofinanciado por el Banco Santander, **2018**) durante el desarrollo de la Tesis Doctoral. También a la Junta de Castilla y León por el proyecto de Investigación (Fondos FEDER – SA069P17) que me permitió acceder a dicha ayuda.

Esta aventura comenzó realizando la asignatura de Prácticas en Empresa del Grado en Química y Quino nos recibió entusiasmado, como siempre, y con la misión de hacer un enzima artificial e imitar a la Naturaleza. Y tan bonita es la idea que en cuento acabé el Máster volví a tu laboratorio y trabajamos codo con codo hasta hoy (¡y lo que nos queda!). Siempre has tenido esa ilusión por tu trabajo y ganas de ayudar al prójimo que te caracteriza. Gracias por transmitirme esa ilusión y ganas de aprender, de buscar la explicación de lo que estaba sucediendo en el balón para aprender cada día un poquito más, espero llegar a ser tan gran científico como tú algún día. Sobre todo, porque después de todo este tiempo no has sido solo un director, sino que eres un buen amigo. Especial mención a Carmen, que después de haber oído tanto de ti eres como una más entre nosotros en el laboratorio, ayudándonos a ser "*persistentes en esta vida"*. Por fortuna te pude conocer en persona, antes de la pandemia en la San Silvestre salmantina, y descubrí lo encantadora y buena persona que eres.

En mis primeros pasos en el laboratorio conocí mucha gente encantadora. A Laura y a Omayra, un gran equipo que conocí trabajando mano a mano en el laboratorio, y que me han ayudado siempre en todo lo que he necesitado. Gracias Laura por todos tus consejos, ayuda y por tener las puertas de tu despacho siempre abiertas para cualquier cosa que he necesitado. Gracias por todo el trabajo de ordenador que haces, que nos proporcionó el proyecto de la Junta que me permitió disfrutar del contrato de investigación. Gracias por esas jornadas en el Bruker enseñándonos a manejar el equipo, e intentando pasar espectros (¡cuando quería!).

Este trabajo no sería el mismo sin ti, Ángel. Recuerdo que cuando estaba realizando el TFG en el Departamento te acercaste de visita una vez, ¡y había una expectación enorme! Venías de visita desde Santiago completando tu fantástico currículum, donde nos encontramos por segunda vez en la Bienal de Química Orgánica. Fue una gran alegría para todos que pudieses volver de nuevo al Departamento, esta vez a trabajar codo con codo con nosotros, y poder descubrir que, efectivamente, la fama era muy cierta. Desde entonces he podido disfrutar de tu inestimable ayuda, siempre disponible para ayudar y a hacer todo lo que estaba en tu mano para resolver cualquier mínimo problema que me surgía. Gracias por nuestras jornadas maratonianas, media jornada de trabajo, nuestras particulares reuniones de grupo con Quino en el Bruker para resolver lo que nos muestra la pantalla, con un trozo de papel y un lápiz.

Gracias por todos los fines de semana que nos hemos quedado a trabajar, ayudándome desinteresadamente, y por todo tu esfuerzo, ganas y entrega. Gracias por todo este tiempo de trabajo, y sobre todo de amistad, y el que nos queda por delante de disfrutar juntos.

Durante todo este tiempo trabajando en el laboratorio he podido conocer a muchísima gente del grupo con un gran corazón y ganas de trabajar, que me han ayudado infinitamente en todo lo que estaba en su mano.

A Victoria, me alegro mucho de haberte conocido. Eres una persona espectacular, siempre dispuesta a ayudar en todo lo que puedes. Siempre que pasamos por tu taquilla cando estamos en el laboratorio nos acordamos de ti, y de lo desordenada que la tenemos para cuando vuelves. Pero en el fondo nos quieres como somos, aunque intentas mejorarnos siempre. Gracias por sacar siempre algo de tiempo para poder hablar o acercarte a Salamanca y hacernos una visita que a los tres nos llena de alegría.

A Simón, nuestro teórico en el grupo. Muchas gracias por hacernos cuantas modelizaciones te hemos mandado, y que más de una y más de dos han sido duras de pelar. Gracias siempre por escuchar nuestros problemas en el laboratorio, y al rato ya tenía en el correo recetas nuevas para probar, o aplicaciones para algún producto que parecía que no valía la pena.

A Muñiz, por estar disponible siempre que es necesario desde el otro lado del charco. Gracias por los mensajes en el móvil que tanto me hacen reír, y que te hacen sacar una sonrisa cada día. Siempre que acaba el año y empezamos el nuevo cuatrimestre, cabe la posibilidad de que Victoria y tú nos hagáis una visita al laboratorio, y podamos trabajar codo con codo con vosotros.

A todos los profesores del Departamento de Química Orgánica, especialmente a Josefa, Gracias por dirigir mi TFG y enseñarme a trabajar en un laboratorio, además de preocuparte siempre por mí. Gracias por todos los momentos que hemos disfrutado, en especial el día de tu jubilación, en la que pudimos disfrutar enormemente de tu compañía y de tu entorno. Gracias Paco por las charlas mañaneras comentando la actualidad, y por todas las prácticas que nos han tocado dar juntos y que he aprendido de ti. También a vosotras, Rosa y Cruz.

Su labor en el Departamento y en la Facultad es esencial. Gracias Mari José y Javier, por estar disponibles en cada documento nuevo que aparecía y teníamos que rellenar, por equipar el laboratorio con todo lo necesario para las prácticas, por los pedidos interminables (así como los papeles que los acompañan), por tramitar las facturas. Fundamentalmente, por mantener el orden del Departamento. Mención especial también al equipo de limpieza, que nos permite poder trabajar cómodamente y nos mantienen todo en perfectas condiciones. Especialmente a Toñi, por todo el cariño y charlas a primera hora de la mañana (que para vosotras es media mañana ya).

También quiero destacar la labor de la Agencia de Gestión de la Investigación, en particular de Carmen. Muchas gracias por estar siempre disponible para resolver cualquier duda

relacionada con cualquier papel pendiente de contratos o proyectos. Por estar siempre disponible tanto telemáticamente como presencialmente.

A Esther del Olmo y a Mario de Juan, del departamento de Ciencias Farmacéuticas, siempre dispuestos a ofrecer su ayuda. Gracias sobre todo por cuidar a mi Sara, que es lo más importante de mi vida. Aunque ya no estás en Farmacia, gracias, Mónica. Mucha suerte en tu nueva etapa y extender el agradecimiento por acompañar a Sara en Farmacia.

Sin ellos, el trabajo de investigación iría a paso de caballo, pero cojo de tres patas. Nos permiten resolver nuestros problemas con su gran trabajo y múltiples técnicas. Para todos los que trabajáis en los servicios de apoyo a la investigación. Gracias a José y Paqui, del Servicio de Difracción de Rayos X, gracias por resolver tantos cristales como os hemos llevado, aunque las estructuras morfológicas de algunos dejaban algo que desear. Gracias José por todos tus conocimientos, ayuda con los archivos de los compuestos, y por nuestro café diario en el bar a media mañana, para coger fuerzas para el resto del día. Gracias a César, Juan y Clara, del Servicio de Espectrometría de Masas, gracias por los miles y miles de compuestos que hemos llevado a analizar, y que en muchas ocasiones os ha llevado a pelearos con la estructura para poder sacar el resultado. Gracias Juan por tu alegría mañanera en el café, siempre con una sonrisa y alegría contagiosa. Gracias a Anna, del Servicio de Resonancia Magnética Nuclear, gracias por ampliar mis conocimientos en resonancia, siempre disponible para ayudar cuando tenía dudas a la hora de manejar el Varian y el Bruker, o queríamos hacer algún experimento especial con nuestra chicha.

A todas las nuevas generaciones del Departamento, tanto lo que estamos actualmente como los que han pasado por nuestras manos en algún momento. Gracias a mis compañeros de Villabajo, especialmente a mi compañero Alberto, siempre alegre y con ganas de trabajar y ayudar. Este tiempo hemos compartido buenos momentos, como la Bienal de Donosti o la estancia en Bristol, gracias por tu compañía y ayuda. Porque la investigación es trabajo en equipo, ellos me han ayudado con el trabajo experimental y espero haber podido contribuir brevemente a su formación, enseñándoles algo de lo poco que sé. A todos los TFGs, TFMs y alumnos de prácticas del Grado en Química y del Grado Superior de Técnico de laboratorio: Antonio, Nacho, Darío, Daniel, Irene, Borja, Merce, Miguel, Vega, Jorge, Ariadna, Elena, Estela, Alicia, Lucía, Noemy, Guillermo, Álvaro, Andrea, Pablo, Álex, Inés, Daniel, Andrea, Celia, Bayron, Vego, Héctor, Ana, Ruth, Aurora, Mónica... A todos los Villarribianos (nuestros gemelos, Rachid, …) que, aunque no hayamos coincidido en el tiempo en la A3, muchos nos reunimos bajo el paraguas común de haber estado trabajando con Quino y compartimos nuestras experiencias cuando nos encontramos.

La facultad, que viene siendo nuestra segunda casa, tiene su gran espacio polivalente. ¡Qué sería de nosotros sin nuestro BAR! Gracias Vicen, Estrella y Sonia por no solo alimentarnos a lo largo del día, sino por hacer de nuestra estancia allí un momento de desconexión y disfrute. Gracias por todos los cafés y comida *off the record* que nos dais para subirnos al despacho y recuperar la energía. Por todos los desayunos con un gran café, hecho con un cariño especial,

por todos los platos de comida riquísimos, siempre disponibles a la hora que haga falta, y un largo etcétera. Antes de la pandemia disfrutábamos del pincho del Grupo del Quino al mediodía (variando un poco los horarios para evitar la estampida de toda la chavalería buscando su pincho para recuperar fuerzas) y de las comidas semanales donde nos preparáis un buen menú para aguantar la tirada. Por suerte el primero lo hemos podido recuperar, y espero pronto recuperar el segundo.

En este templo que es el bar nos reunimos varios monjes, el Grupo de los Fieles Madrugadores: Quino, Eva, Chema, Juan, Ángel, Álvaro, Diego, Patri y servidor. Gracias por compartir ese momento en la mañana para ponernos al día en cualquier tema, ya sea el precio del cereal, la Universidad o cómo llevamos la investigación. Gracias Eva por tus consejos y poder trabajar contigo.

En este viaje se conoce a gente encantadora de otros ámbitos de la Química, y juntos aprendemos un poquito más. Gracias a Diego, Ghibom e Iria. Es un placer haberos conocido y poder disfrutar de vuestra compañía, ayuda y experiencia, de la que aprendo cada día más. Por más excursiones como la de la Fregeneda, una gran aventura justo antes de que tuviéramos que estar encerrados en casa por la pandemia. ¡Ahora podremos volver a retomarlas!

A Alberto, nuestro informático del grupo, especializado en ponernos a punto el ordenador y hacernos los conectores de los modelos CPK. Gracias por tus visitas al departamento y animarnos y ofrecernos tu ayuda siempre, por informarte desinteresadamente de cualquier cosa que necesitábamos y solucionar los problemas informáticos y no informáticos que nos surgen cada día.

A Enol, que lleva poco tiempo con nosotros, pero se ha convertido en uno más del grupo, así como Noelia y Javier, que le dan vidilla al laboratorio y a las comidas.

A las nuevas generaciones del grupo: Asmaa y Estela. Espero que disfrutéis de esta etapa tanto como lo he disfrutado yo. Espero haberos podido ayudar en todo lo que ha estado en mi mano, aunque este último año ha sido más complicado poder estar pendiente de todos. Lo bueno que tiene el grupo es que somos como una pequeña familia, y cuidamos los unos de los otros.

Durante mi estancia en Madrid en el Máster tuve la suerte de conocer a más gente encantadora. Comenzando por mi homónimo José, quien fue mi director del TFM. Espero que esta tesis te resulte *"seria y formal a la par que juvenil y dinámica"*. Gracias por el entusiasmo que le pusiste junto a Andrés a la hora de explicar vuestro proyecto, y que hizo que os conociera mucho más de cerca, y que esa amistad haya llegado hasta hoy en día. A nuestro torbellino MJ, que revolucionaba el laboratorio QB404 y que no te faltaban nunca las ganas de trabajar. A todos los que hemos coincidido en el QB404, en un laboratorio de "retales" queha hecho que nos juntásemos gente de muchas áreas: Antonio, Marta, Laura y el grupo Analítico. Especialmente a Sandra, que ponía siempre una chispa de alegría en todo momento.Gracias a todos por acogernos a Sara y a mí como si lleváramos toda la vida allí, hemos

disfrutado mucho de todas nuestras escapadas a la Universidad Rey Juan Carlos, a la defensa de la Tesis de nuestro querido Antonio y posterior celebración entre otros.

Hay un madrileño-castellano que merece una dedicatoria especial, y ese es mi buen amigo enantiomérico Antonio. Desde el primer momento que pisé el laboratorio me di cuenta de lo buena persona que eres, y ya me lo habían advertido previamente, pero la realidad superaba claramente la ficción. Aunque no era tu labor, eras prácticamente el encargado del laboratorio. Y yo, recién aterrizado, que te preguntaba cualquier cosa que necesitaba, recibía toda tu ayuda que con gran amabilidad me brindabas. Gracias por estar ahí siempre que lo he necesitado, por las comidas viendo Los Simpson en el laboratorio, con nuestra Coca Cola Zero, y nuestra lista en la pizarra de los capítulos que habíamos visto de la serie House of Cards. Gracias por hacerme partícipe de Jornadas y Cursos, de nuestro primer artículo con el espectroscopio o del botafumeiro en el laboratorio, con ambientador para evitar ciertos olores que nos hicieron famosos en la Facultad. Gracias por extender esa amistad en todos los aspectos posibles, y que cada vez que vuelvo a Madrid me sienta como en casa, así como ese mismo cariño y amistad que profesas a Sara, mi alma gemela. Gracias por ser como eres y por dejarnos formar parte de tu vida.

Thank you so much Tony for giving me the opportunity to be part of your group, I had a good time there. Thank you to all the researches from Davis Group: Sergio, Nick, Richard, Federica, Suresh, Danny, Al, Claire, Tom, Soumen and Daniel. Thank you for all the knowledge that I had acquired in these three months. Thank you Maddie for taking care of me at home. Gracias al grupo de españoles: Sergio, Inma, Javi, Alberto, Laia, Noelia y Jana, que aun viniendo de esquinas diferentes de España somos todos vecinos. Buenos ratos de juegos de mesa hemos disfrutado tras el curro.

A Isa y Paco de La Dama I, gracias por cuidarnos y tratarnos como su fuéramos vuestros hijos. Por la alegría con la que nos recibís en vuestra casa y os preocupáis por que no nos falte de nada. Es un placer poder contar con vosotros.

A Juan y Noe. Aunque ya sabéis que el trabajo me lo permite poco, y a vosotros menos todavía, siempre sacamos un ratito para poder encontrarnos y comentar cómo nos va la vida. Gracias por todo el tiempo compartido en el Domino's Pizza, y por el que nos queda por compartir.

A mis Parroquianos de Béjar: Sergio, Jesús, Arturo, Jorge y Guille. Que, aunque el trabajo me absorba, siempre estáis disponibles para poder tomar un descanso con una buena cerveza o un buen vino. Por supuesto, gracias al resto de amigos que en Béjar nos reunimos.

En esta aventura he estado acompañado por mi amigo Álvaro, con el que embarqué en las jornadas de gimnasio que nos servían para liberar la tensión acumulada de las reacciones que no salen. Además de aprender Inglés. La verdad es que no parábamos, ¡a ver si ahora que ha pasado la pandemia vuelvo a la carga! Gracias por tu amistad y por ayudarme en todo. Con muchas ganas de seguir disfrutando de tu compañía en esta nueva etapa, y siempre. Extiendo

este agradecimiento a Miriam. Muchas gracias por estar a su lado y permitirnos disfrutar de tu compañía.

Gracias Paco, Flori y Javi, porque desde el primer momento me habéis abierto las puertas de vuestra casa y me habéis tratado como uno más, con gran cariño. Me habéis ayudado en todo lo que estaba en vuestra mano y más. Este agradecimiento se extiende, por supuesto, a toda la familia de Sara (abuelos, tíos y primos), que se han convertido en mi familia también.

A mi madre María Ángeles y a mi hermana Patricia. Gracias mamá por todo el sacrificio que has hecho para que mi hermana y yo estemos hoy donde estamos. Gracias a tu esfuerzo hemos conseguido llegar alto, porque unos buenos cimientos son imprescindibles para construir un rascacielos. Gracias a mi hermana, por acompañarme durante todo este proceso, por disfrutar del poco tiempo libre que tengo para estar con vosotras. Y siento si a veces no he podido estar tan pendiente de vosotras como debería. Todo este agradecimiento lo extiendo a mi familia: a mis tíos (Tenty y Edu, José y Mari Carmen, Juancar y Lola), que me han tratado siempre como a un hijo, que es lo bonito de las familias unidas, disfrutar y cuidar los unos de los otros. A todos mis primos y pequeños sobrinos, que no hay cosa más feliz que veros crecer. También gracias a por todos los que ya no están entre nosotros, que nos han enseñado tanto de la vida, y que siguen ocupando un grandísimo lugar en nuestros corazones.

El Lugar de Honor de estos agradecimientos lo ocupa la persona más importante de mi vida: Sara, mi alma gemela, mi mejor amiga y compañera de viaje. No se qué sería de esta vida sin ti, llenas mis días de alegría y diversión y haces que cada momento a tu lado sea inmejorable. Gracias por acompañarme de la mano en cada momento de mi vida haciendo que cuando algo va mal en el trabajo, todo sea llegar a casa para que se vea distinto. Gracias por ayudarme siempre en todo lo que necesito. Gracias por completar mis frases, hacerme reír, quererme y aguantarme cuando a veces me pongo un poco pesado y me repito como las persianas o me pongo a hacer un monólogo. Enhorabuena por todos tus logros, comienza una nueva etapa en nuestra vida que vamos a exprimir al máximo. Gracias por las noches de sofá y Masterchef cogidos de la mano (o Poirot, o Sherlock o cualquier película o serie) que nos duran toda la semana, por los paseos a la Alamedilla a ver los patitos, por los desayunos en La Dama, por los viajes que compartimos a cualquier lado del mundo, y por toda nuestra vida.

Porque cualquier lado del mundo a tu lado es nuestro Hogar.

Table of contents

Abbreviations and acronyms 1

General Objectives and Introduction 3

CHAPTER 1 7

1. Objectives 7

2. Introduction 11

2.1. Supramolecular chemistry 11

2.1.1. Classification. 11

2.1.2. Types of interactions found in Supramolecular Chemistry 12

2.2. Association of amino acids 15

2.3. Antecedents of the research group 23

3. Methods and Results 33

3.1. Macrocyclic receptor **2** 33

3.2. Receptor **20** 42

3.3. Receptor **28** 52

3.4. Receptor **29** 54

3.5. Receptor **46** 63

4. Conclusions 71

5. Experimental Section 75

5.1. Materials and instrumentation 75

5.2. Synthetic details and characterization 78

5.3. General procedures for NMR titrations 101

5.4. General procedure for amino acid extraction 101

5.5. Resolution of macrocyclic receptor 2 enantiomers using TLC impregnated with L-amino acids 102

5.6. Chiral HPLC chromatograms 102

5.7. ORTEP diagrams and X-ray crystal structure data 102

5.8. Modelization studies 103

CHAPTER 2 107
1. Objectives 107
2. Introduction 111
2.1. Catalysis 111
2.1.1. Definition and classification 111
2.1.2. Organocatalysis 115
2.1.3. Nobel Prize in Asymmetric Organocatalysis 119
2.2. Enzymes as models for the development of new organocatalysts 121
2.2.1. Hydrolytic enzymes as models for the design of new organocatalysts 122
2.2.2. Chymotrypsin and *N*-terminal hydrolases: Active center studies 123
2.2.3. Catalytic mechanism of hydrolytic enzymes 126
2.2.4. State-of-the-art. Hydrolytic enzyme mimics in the literature 128
2.3. Hydrolases mimics in our research group. Previous work 130
3. Methods and Results 139
3.1. Configuration between amino and hydroxyl group. Organocatalysts **5**, **11** and **16**. First generation organocatalysts 139
3.1.1. Catalyst **5** 141
3.1.2. Catalyst **11** 145
3.1.3. Synthesis of catalyst **16** 151
3.1.4. Summary and conclusions for organocatalysts **5**, **11** and **16** 156
3.2. Improved version of catalyst **16**: Catalysts **21**, **22**, **25** and **29** 157
3.2.1. Catalyst **21** 157
3.2.2. Catalyst **22** 160
3.2.3. Catalyst **25** 161
3.2.4. Catalyst **29** 162
3.2.5. Summary and conclusions for catalysts **21**, **22**, **25** and **29** 174
3.3. Oxyanion-hole improvement: Second generation organocatalysts 176
3.3.1. Narrow and adjustable oxyanion hole 176
3.3.2. Catalyst **33** 178
3.3.3. NH acidity studies. Catalysts **35**, **37** and **39** 181
3.4. Hydrogen bond network. Third generation organocatalysts 187

3.4.1. NH acidity studies. Catalysts **52**, **56**, **60** and **61** 195
3.5. Kinetic studies for catalyst **5**, **39** and **60** 203
3.6. Summary and conclusions for 2nd and 3rd generation catalysts (2nd & 3rd Gen.) .. 204
3.7. Improve association constant. Oxyanion-hole models **64**, **67** and **69** 205
3.7.1. Receptor **64** 206
3.7.2. Receptor **67** 208
3.7.3. Receptor **69** 211
3.7.4. Summary and conclusions for oxyanion-hole mimics **64**, **67** and **69** 214
4. Conclusions 217
5. Experimental Section 221
5.1. Materials and instrumentation 221
5.2. General Procedures 224
5.3. Synthetic details and characterization 227
5.4. Kinetic studies 290
5.4.1. Methanolysis studies 290
5.4.2. Transesterification Studies 299
5.5. Titration studies 300
5.6. Computational studies 302
Annex I – Final compound list 305
Annex II – Publications 311
Annex III – NMR Spectra 335
Annex IV – Kinetic Studies 375

ABBREVIATIONS AND ACRONYMS

Throughout this manuscript, abbreviations and acronyms recommended by the American Chemical Society in the Organic Chemistry Area (updated in the Journal of Organic Chemistry on April 2018; https://pubs.acs.org/paragonplus/submission/joceah/joceah_authguide.pdf) have been employed.

Å	Ångström
Ac	Acetyl group
Ac_2O	Acetic anhydride
AcOH	Acetic acid
Ala	Alanine
Arg	Arginine
Asn	Asparagine
Asp	Aspartic acid
Boc	*tert*-butyloxycarbonyl
Bu	Butyl group
^{13}C NMR	^{13}C Nuclear Magnetic Resonance
CD_3OD	Deuterated methanol
$CDCl_3$	Deuterated chloroform
COSY	COrrelation SpectroscopY
Cys	Cysteine
δ	Chemical shift
d	Doublet
DCM	Dichloromethane
dd	Doublet of doublets
DMSO	Dimethylsulfoxide
dt	Doublet of triplets
E	Enzyme
E_a	Activation energy
ee	Enantiomeric excess
EI	Electron-impact Ionization
E-P	Enzyme-Product associate
Eq	Equivalent
E-S	Enzyme-Substrate associate
ESI	Electrospray Ionization
Et	Ethyl group
EtOAc	Ethyl acetate
Gly	Glycine
h	Hours
^{1}H NMR	^{1}H Nuclear Magnetic Resonance
His	Histidine
HMBC	Heteronuclear Multiple Bond Correlation
HOMO	Highest Occupied Molecular Orbital
HPLC	High Performance Liquid Chromatography
HRMS	High Resolution Mass Spectrometry
HSQC	Heteronuclear Single Quantum Correlation
Hz	Hertz
IR	Infrarred spectroscopy
J	Coupling constant
k	Rate constant
K_{ass}	Association constant
λ	Wavelength
Leu	Leucine
LUMO	Lowest Unoccupied Molecular Orbital
Lys	Lysine
m	Multiplet
m.p.	Melting point
Me	Methyl group
min	Minutes
MS	Mass spectrometry
o	*Ortho*
p	*Para*
Pd/C	Palladium over carbon
Phe	Phenylalanine
ppm	Parts per million
Pr	Propyl group
Pro	Proline
Pyr	Pyridine

q	Quartet
quant.	Quantitative
r.t.	Room temperature
ROESY	Rotating frame Overhauser Effect SpectroscopY
s	Singlet
Ser	Serine
t	Triplet
$t_{1/2}$	Half-life
^{t}Bu	Tert-butyl group
TEA	Triethylamine
THF	Tetrahydrofurane
Thr	Threonine
TLC	Thin Layer Cromatography
Tyr	Tyrosine
UV	Ultraviolet

Bibliographic citations have been placed as footnotes in the pages where they were first cited in the section; they were added independently at every section or chapter, so they are duplicated in different chapters when necessary.

General Objectives and Introduction

General Objectives and Introduction

The general objective of this Thesis is the design and synthesis of small organic molecules which mimic the oxyanion-hole scaffold found in hydrolytic enzymes. They employ this structural motif to associate anions and electronegative groups such as carbonyls from esters and amides and reduce the activation energy of many reactions in which a negatively-charged transition state is generated.

These artificial oxyanion-hole mimic will be used to associate the carboxylic acid group of amino acids in order to carry out the chiral resolution of racemic mixtures of amino acids. In addition, they will be employed to catalyse the transesterification of non-activated esters by mimicking the mechanism of natural hydrolases.

Chapter 1

Catalytic properties of enzymes are basically sustained by their ability in the association of a substrate and keeping it close to the active centre. A preorganized tertiary structure allows them to play as catalysts, setting up the space where the substrate interacts with the enzyme and the reaction takes place.

For example, the active centre of proteases, such as chymotrypsin, is formed by a catalytic triad, an hydrophobic pocket, and an **oxyanion hole**. The last two moieties bind the aromatic unit and the amide carbonyl, respectively. The oxyanion hole contains **hydrogen bond donor groups** which stabilise the carbonyl group and the negatively charged oxygen atom of the tetrahedral intermediate in the hydrolysis reaction. Backbone amides usually act as hydrogen bond donor groups. As the oxyanion hole can bind anions, the development of**supramolecular receptors** with an **oxyanion-hole geometry** is a good starting point for anionbinding.

Amino acids are the building blocks in protein synthesis and are essential in human nutrition. There are several industrial syntheses of amino acids which include an enzymatic step and generate enantiomerically pure L amino acids, the enantiomer required for human diet. Organic syntheses of amino acids are usually cheaper and do not require the specific conditions of enzymatic synthesis, however they generally afford the amino acids racemic mixture.

Racemic synthesis combined with chiral supramolecular receptors could improve and reduce costs in the industrial obtention of amino acids.

Chapter 2

Enzymes are the most efficient catalysts in Nature. The configuration of their active centre, established by the three-dimensional structure of the protein, allows them to increase the rate of reactions that otherwise would be very slow or even could not take place.

Supramolecular interactions, such as hydrogen bonding, π- π stacking or hydrophobic interactions, among others, are essential to set up and maintain the three-dimensional structure of enzymes, and they also play an important role for the enzyme-substrate association. All these concepts explain the catalytic activity of the enzymes and are essential to understand how to improve artificial enzymes designs.

Hydrolases enzymes catalyses the cleavage of many different bonds, such as amide or ester bonds. These compounds are widely employed in food and pharmacy industries, even though their use is conditioned by the strict enzyme stability requirements (pH, ionic strength or temperature affect the enzyme structure); they usually are more expensive than synthetic catalysts.

Most hydrolases have an active center formed by a hydrophobic pocket, a **catalytic triad** and an **oxyanion hole**. The catalytic triad is in charge of the nucleophilic attack on the substrates while the oxyanion hole stabilises both the substrate and the negatively-charged intermediate. These two features are the main responsible for the reaction rate acceleration. Thus, mimicking the catalytic triad and the oxyanion hole with a small organic molecule with a similar geometry should provide comparable reaction rates. The design and synthesis of organocatalysts that are as efficient as enzymes would be ideal to improve many synthetic and industrial processes and is still a challenge in Organic Chemistry.

Chapter 1 - Objectives

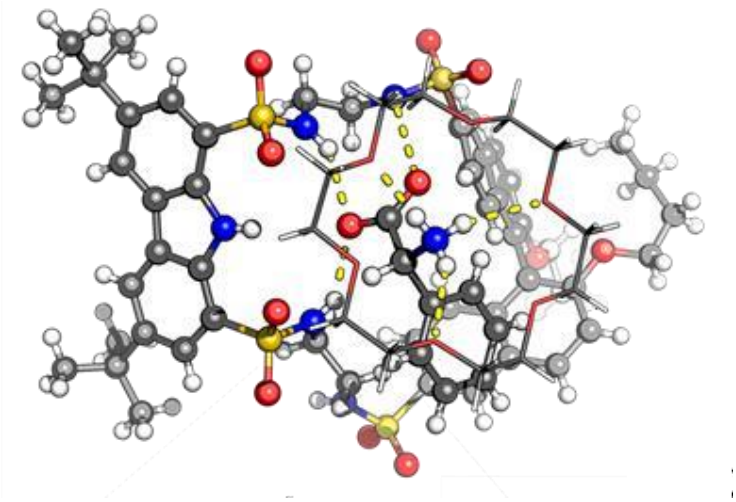

In **Chapter 1**, supramolecular receptors with an oxyanion-hole geometry will be discussed. They will be modified with a crown ether to bind amino acids. Several linkers will be considered, and structural studies combined with computational analysis of the receptors will guide us to find the better design.

The **main objective** of this chapter is the synthesis of a series of supramolecular receptors with and oxyanion-hole geometry. These receptors will be employed to perform the chiral resolution of amino acids racemic mixtures. To achieve this goal, the specific objectives shown below are proposed:

- **Objective 1**: Oxyanion-hole mimics design based on 1,8-disulfonamidecarbazole, 8-nitro-2-naphthoic acid and 1,8-diaminoxanthene skeletons.

- **Objective 2**: Synthesis and characterization of the supramolecular receptors.

- **Objective 3**: Chiral resolution of amino acid racemic mixtures by the supramolecular receptors synthesised in Objective 2, using liquid-liquid extraction.

Chapter 1 - Introduction

2. Introduction

2.1. Supramolecular chemistry

In 1987, the Royal Swedish Academy of Sciences awarded the Nobel Prize in Chemistry for the development and use of molecules with specific structural interactions with high selectivity to Jean-Marie Lehn (Louis Pasteur University, Strasbourg), Donald J. Cram (University of California) and Charles J. Pedersen (DuPont Company, Wilmington).[1] It was then that what is now known as Supramolecular Chemistry began to develop.

Supramolecular Chemistry can be defined as a branch of chemistry that studies intermolecular interactions, as well as the thermodynamic and kinetic factors involved in the formation of supramolecular complexes. It can be described as chemistry beyond molecules. Jean-Marie Lehn, one of the Nobel laureates mentioned above, defined it as "the chemistry of intermolecular bonds, covering the structures and functions of entities formed by the association of two or more chemical species".[2] He also introduced the term supramolecule as "an organised entity created by the association of two or more chemical species joined by intermolecular forces whose properties as a whole are better than the sum of the properties of each individual species".[3]

Later, thanks to the studies of the scientist Fritz Vögtle, the importance of supramolecular chemistry in chemical and biological processes, in which molecular interactions play an important role, was understood. Vögtle defined supramolecular chemistry as "chemistry beyond the molecular level, a chemistry of designed intermolecular interactions". In recent years, the field of Supramolecular Chemistry has experienced a big development with a myriad of new applications in sensing, molecular imaging, metal extraction, and drug formulation and delivery.[4]

Nowadays, Supramolecular Chemistry can be considered as an independent scientific area. This was recognized in 2016 when Jean-Pierre Sauvage (University of Strasbourg), Sir James Fraser Stoddart (Northwestern University, Evanston) and Bernard Lucas Feringa (University of Groningen) were awarded the Nobel Prize in Chemistry for the design and synthesis of molecular machines.[2]

2.1.1. Classification.

Supramolecular Chemistry can be classified in two categories related to the size of the molecular system: molecular recognition (host-guest association), and self-assembly.[3]

---

[1] https://www.nobelprize.org/prize/chemistry/1987/press-release/ (accessed on June, 2020).
[2] Mondragón Vásquez, K.; Domínguez Chávez, J.G.; Pacheco, F.A. *Ciencia*, **2018**, *69*, 8.
[3] Ariga, K.; Kunitake, T. Supramolecular Chemistry-Fundamentals and Applications. Advanced Textbook, Ed. Springer, **2006**, 1.
[4] Kolesnichenko, I. V.; Anslyn, E. V. *Chem. Soc. Rev.* **2017**, *46*, 2385 – 2390.

Molecular recognition (host-guest processes) studies how a larger molecule, called host, associates or wraps a smaller molecule, called guest, through non-covalent interactions. These associations are strongly conditioned by the size and shape of the participating molecules.[5]

Self-assembly consists of the directed association of several molecules to form a larger, highly ordered structure under reversible and spontaneous conditions controlled by non-covalent interactions. Accordingly, it is possible to define a supramolecular polymer as a macromolecule containing low-mass entities (monomers) linked together by non-covalent interactions.[6]

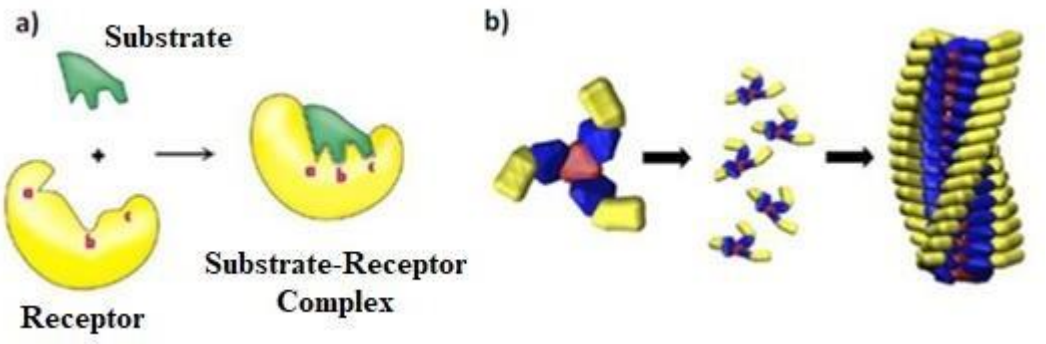

Figure 1. *a) Host-guest or receptor-substrate interaction model. b) Self-assembly model.*

2.1.2. Types of interactions found in Supramolecular Chemistry

Supramolecular Chemistry studies the formation of molecular or ionic aggregates by different non-covalent interactions such as electrostatic interactions, dipolar interactions, hydrogen bonds and van der Waals forces,[7] which are much weaker than covalent bonds. The energies corresponding to these types of bonds and a comparison with intramolecular bonds are shown in Figure 2.

[5] Steed, J. W.; Turner, D. R; Wallace, K. J. Core Concepts in Supramolecular Chemistry and Nanochemistry, John Wiley & Sons, Inc., **2007**.
[6] Aparicio, F.; García, F.; Sánchez, L. Supramolecular Polymers; In Encyclopedia of Polymer Science and Technology, Ed. Peterca, M.; John Wiley & Sons, Inc., **2012**.
[7] (a) Steed, J.W.; Turner, D.R.; Wallace, K.J. *Core Concepts in Supramolecular Chemistry and Nanochemistry*, Wiley, **2007**, 1 – 27. (b) Steudel, R. *Chemistry of the Non-Metals*, Walter de Gruyer & Co, **1976**, 112 – 115 and 163 – 172.

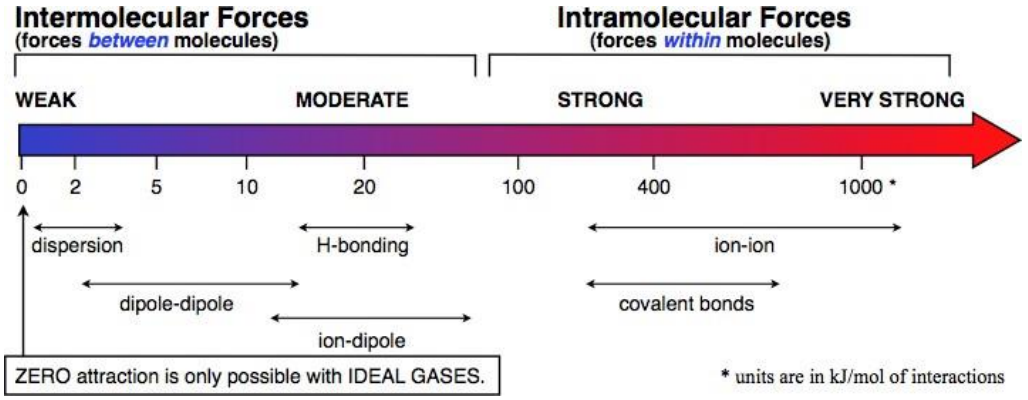

Figure 2. *Energies of non-covalent interactions.*

Ionic interactions: Interactions between charged species.

- Ion-ion: This interaction occurs between a cation and an anion. An example of this type of interaction can be found in biological systems such as the amino acid side chains of a protein. In this case, the interactions occur between the carboxylate and ammonium groups present in these chains.

- Ion-dipole: This interaction takes place between a charged species and an uncharged or neutral species with dipolar moment. An example would be the association of cations (Na^+ or K^+) by crown ethers.

Dipole-dipole interactions: Interactions between uncharged species, but whose structure has a local charge distribution that generates areas of positive charge density and areas of negative charge density. An example of this type of interaction takes place between molecules with polar functional groups such as -COOR, -NO_2 or -CN, among others.

Van der Waals interactions: Interactions due to the electronic distribution of the molecules. Depending on the degree of polarity, several types of these interactions can be distinguished. The higher the degree of polarity, the stronger the interaction.

- Keesom interaction: It takes place between permanent dipoles.

- Debye interaction: It is formed between an induced dipole and a permanent dipole.

- London interaction: It is stablished between induced dipoles.

In addition, there is also π-π interactions that occur when p-orbitals overlap in aromatic systems.

Hydrogen bonds: These are interactions of the dipole-dipole type; however, they are considered a separate group due to their own characteristics. These interactions occur between a hydrogen bond donor and a hydrogen bond acceptor. The so-called hydrogen bond donor is

a hydrogen atom bonded to an electronegative atom (O, N, F), while the hydrogen bond acceptor is an electronegative atom with free electron pairs available for sharing. An example of this type of interaction can be found in the tertiary structure of proteins, as well as in the bonding of the base pairs of DNA (Figure 3).

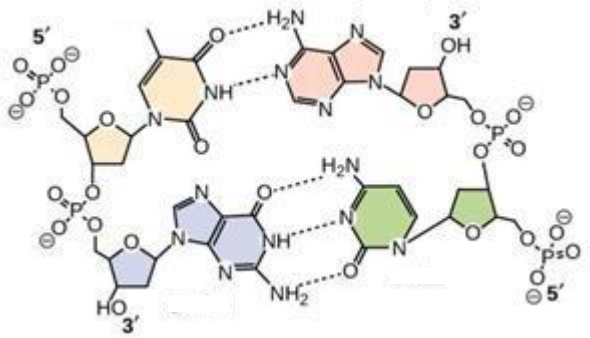

Figure 3. *Bonding of DNA base pairs by hydrogen bonds.*[8]

It is important to note the **low-barrier hydrogen bond** is especially strong hydrogen bond where the acceptor and donor atoms are very close to each other and generates a free movement of the proton between them. These bonds show great stability.[9]

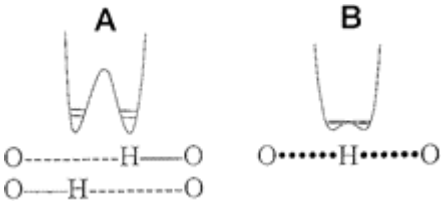

Figure 4. *Energy diagrams of usual hydrogen bonding (left) and low-barrier hydrogen bonding (right).*

The non-covalent interactions described above can be used in the design of new molecular receptors for species (charged or neutral) such as those shown in Figure 5.

[8] https://courses.lumenlearning.com/microbiology/chapter/structure-and-function-of-dna/ (accessed on June, 2020).
[9] (a) Cleland, W. W; Frey, P. A.; Gerlt, J. A. *J. Biol. Chem.* **1998**, *273*, 25529 – 25532. (b) Cleland, W. W.; Kreevoy, M. M. *Science* **1994**, *264*, 1887 – 1890.

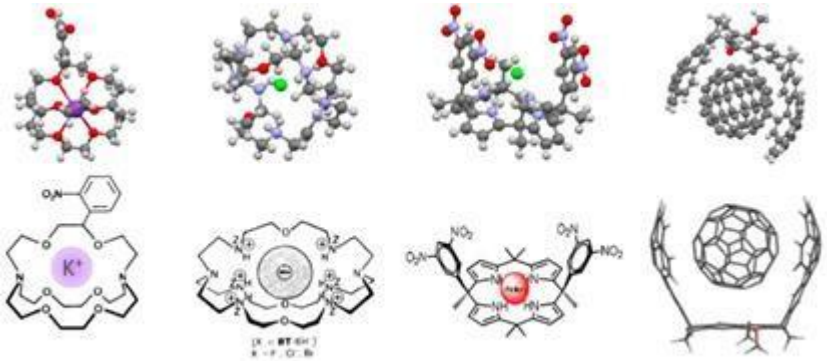

Figure 5. *Receptors based on non-covalent interactions.*[10]

2.2. Association of amino acids

Host-guest chemistry offers the possibility to design almost any molecule whose shape is complementary to a given guest. Molecular receptors are usually organic compounds designed to work in organic solvents, because many of the intermolecular interactions used by molecular receptors are usually weakened in aqueous solutions and, therefore, the complexation of hydrophilic molecules such as sugars or amino acids are still a challenge.

Although elegant receptors have already been designed for carbohydrates, like the receptors for glucose synthesized by Davis,[11] the association of amino acids is complicated.

[10] (a) Kim, A.; Ali, R.; Park, S. H.; Kim, Y.; Park, J. S. *Chem. Commun*. **2016**, *52*, 11139 – 11142. (b) Abeyratne Kuragama, P.L.; Fronczek, F.R.; Sygula, A. *Org. Lett.* **2015**, *17*, 5292 – 5295. (c) Warmutha, R.; Grell, E.; Lehn, J. M.; Bats, J. W.; Quinkert, G. *Helv. Chim. Acta* **1991**, *74*, 671 – 681. (d) Dietrich, B.; Guilhem, J.; Lehn, J. M.; Pascard, C.; Sonveauz, E. *Helv. Chim. Acta* **1984**, *67*, 91 – 104.
[11] Tromans, R. A.; Carter, T. S.; Chabanne, L.; Crump, M. P.; Li, H.; Matlock, J. V.; Orchard, M. G.; Davis, A. P. *Nat. Chem.* **2019**, *11*, 52 – 56.

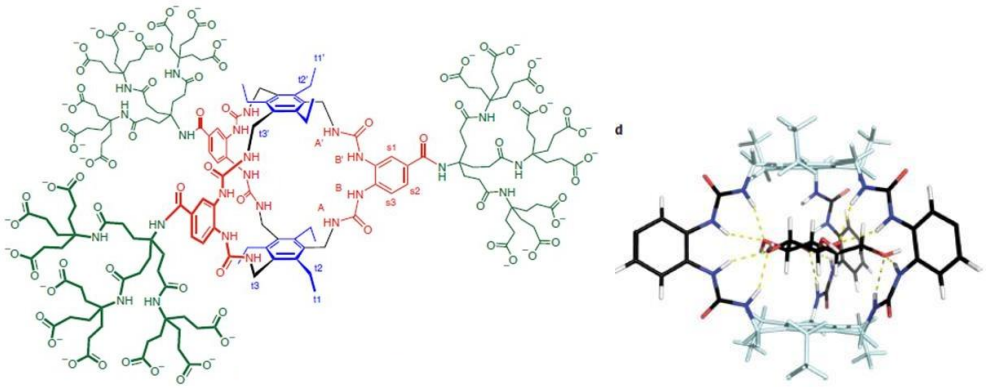

Figure 6. *Molecular receptor synthesised by Davis able to associate glucose in water.*

The presence of a positive charge and a negative charge in the amino acid should favour the formation of a complex by electrostatic interactions with the receptor. The same electrostatic interactions make amino acids more soluble in aqueous media, which means that the strong ion-dipole interactions between the ion and the water molecules need to be broken for the association with the receptor to succeed.

The industrial obtention of enantiopure amino acids is very important. The global amino acid market was assessed in 21.18 billion dollars in 2019 and it is expected to keep growing by an annual rate of 7.8% from 2020 to 2027.[12] Amino acids are widely used in pharma, agrochemical, food, and fragrance industries. While L amino acids are the components of proteins, D enantiomers have found interesting applications in antibiotics, chemotherapeutics, immunosuppressives, deodorants, fluorescent markers of DNA, sweeteners, pesticides, etc.[13] In fact 5% of the top 200 brand name drugs by retail sales in 2018 possessed a D amino acid in their structure.[14]

The main procedures used to obtain amino acids are extraction from natural sources, fermentation processes, chemical synthesis, and enzymatic catalysis.

The amino acid **extraction procedure from natural sources** consists of the hydrolysis of proteins and the subsequent separation of the desired compounds. However, the result is a very complex mixture of amino acids where the separation and purification of the products are generally complicated and expensive.[15] In addition, the protein source limits the amounts of

[12] https://www.grandviewresearch.com/industry-analysis/amino-acids-market (accessed on November, 2021).
[13] Martínez-Rodríguez, S.; Martínez-Gómez, A. I.; Rodríguez-Vico, F.; Clemente-Jiménez, J. M.; Las Heras-Vázquez, F. J. *Chem. Biodivers.* **2010**, *7*, 1531 – 1548.
[14] (a) https://njardarson.lab.arizona.edu/content/top-pharmaceuticals-poster (accessed on August, 2019). (b) McGrath, N.; Brichacek, M.; Njardarson, J. T. *J. Chem. Ed.* **2010**, *87*, 1348 – 1349.
[15] Moore, S.; Stein, W. H. *J. Biol. Chem.*, **1951**, *192*, 663 – 681

amino acids produced, therefore, it is not the most suitable method to obtain amino acids in bulk. Also, the process is limited to the obtention of L-amino acids, which is the main enantiomer in natural sources.

The **fermentation process** consists of the decomposition of the protein by microorganisms in a series of reactions that can involve up to 30 types of enzymes.[16] The volume of amino acid production will depend on the quality of the enzymes used; therefore, the improvement and development of new strains is pursued to achieve the maximum production. It is a widely used method to produce amino acids in bulk. However, it must be taken into account that it is only possible to obtain the L enantiomer. Also, it usually requires large volumes of water, big fermenters capacity, strict sterility and costly methods for product recovery that boosts the capital investment.[17]

Numerous **synthetic routes** have been developed to produce amino acids; however, these routes are often long and expensive. Likewise, they present a great limitation since, in general, each of the enantiomers is not obtained separately, but rather the racemic mixture is obtained, creating the need to add a separation step. Despite the fact that a multitude of **enantioselective amino acid syntheses** have also been designed,[18] obtaining L-amino acids from fermentations is still preferred since the cost is lower. In situations in which obtaining the D or L enantiomer does not make a difference, as is the case of glycine, which does not have a chiral centre, or of methionine, intended for poultry feed,[19] chemical synthesis can be cheaper than fermentation by microorganisms.

Finally, in the **enzyme catalysed processes**, one or two types of enzymes are used to convert an amino acid precursor to the desired amino acid.[16] It is a method that does not need to use microorganisms so if the precursor substance has low cost it can be profitable.

The method of choice will depend on the available technology, the cost of the raw materials, the market characteristics and the environmental impact of the method itself.

An interesting way to synthesise amino acids rely on **racemic synthesis followed by a chiral resolution step**. One of the advantages of this method is that it can be used for the synthesis of D-amino acids.

---

[16] https://www.ajinomoto.com/aboutus/amino-acids/how-amino-acids-are-made (accessed on July, 2021).

[17] Sugimoto, M. Amino Acids, Production Processes. In: *Encyclopedia of Industrial Biotechnology: Bioprocess, Bioseparation, and Cell Technology*; Flickinger, M. C., Ed.; John Wiley & Sons, **2010**.

[18] (a) O'Donnell, M. J. *Acc. Chem. Res.* **2004**, *37*, 506 – 517. (b) O'Donnell, M. J.; Drew, M. D.; Cooper, J. T.; Delgado, F.; Zhou, C. *J. Am. Chem. Soc.* **2002**, *124*, 9348 – 9349.

[19] https://en.engormix.com/poultry-industry/articles/role-methionine-poultry-its-t38926.htm (accessed on July, 2021).

Traditional syntheses of amino acids are the Strecker,[20] Erlenmeyer[21] and Bucherer-Bergs[22] reactions (Figure 7).

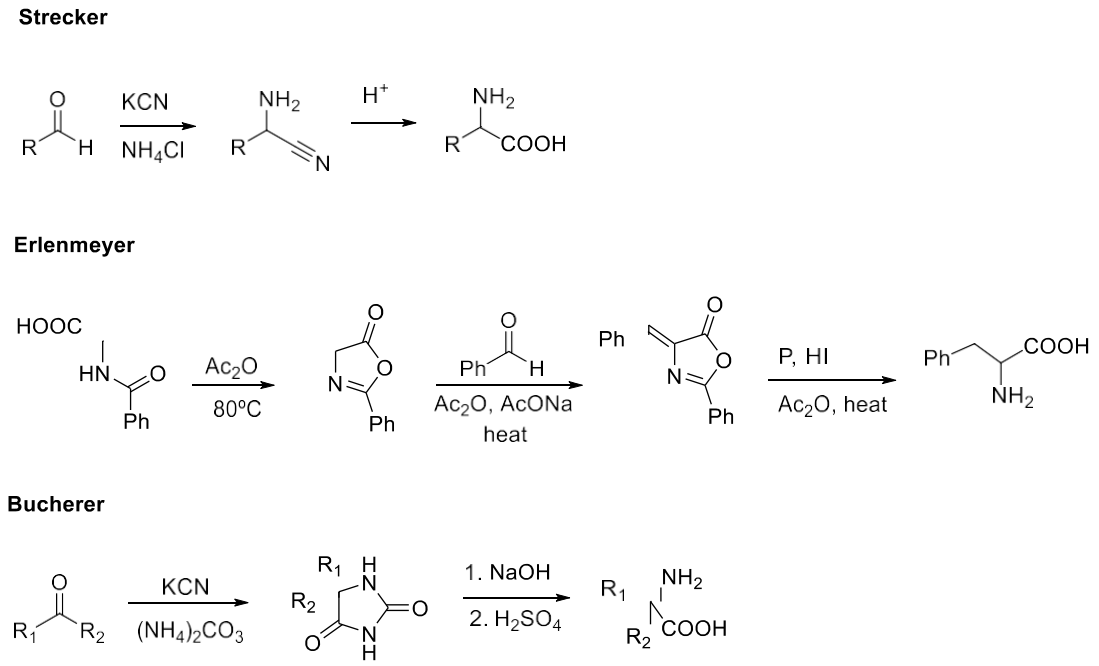

Figure 7. *Racemic syntheses of amino acids.*

Racemic synthesis is easier and cheaper than asymmetric synthesis as it does not require the employment of chiral auxiliaries or chiral catalysts. Also, different options are available for the chiral resolution step, such as crystallization, chromatography, electrophoresis, or liquid-liquid extraction. In the last years, **enantioselective liquid-liquid extraction** has appeared as an appealing option because of the low energy consumption that the technique requires, the recyclability of the method, also it is easy to handle and easy to scale up.[23]

In order to be able to separate enantiomers by liquid-liquid extraction, this technique requires a chiral receptor able to transport one of the amino acid enantiomers from an aqueous phase to an organic phase (Figure 8).

[20] Strecker, A *Ann. Chem. Pharm.* **1850**, *75*, 27 – 45.
[21] Erlenmeyer, F. *Liebigs Ann. Chem.* **1893**, *275*, 1 – 8.
[22] Bergs, H. Verfahren zur Darstellung von Hydantoinen. German Patent DE566094, 1932.
[23] Schuur, B.; Verkuijl, B. J. V.; Minnaard, A. J.; de Vries, J. G.; Heeres, H. J.; Feringa, B. L. *Org. Biomol. Chem.* **2011**, *9*, 36 – 51.

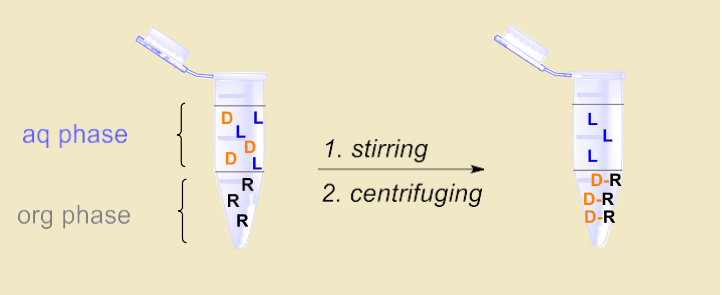

Figure 8. *Concept of enantioselective liquid-liquid extraction.*

However, this is a challenging task, due to the ionic nature of zwitterionic amino acids, *i.e.* when they are at neutral pH, they are highly hydrophilic and extremely soluble in aqueous solutions, thus increasing the energetic cost associated with their desolvation. This makes them difficult to extract to organic phases due to the charge of the ammonium and carboxylate groups, preventing them from being stabilised by hydrogen bonds, which is the case in aqueous media.

Also, the receptor needs to be able to simultaneously associate the positively charged ammonium group and the negatively charged carboxylate group of the amino acids which are arranged in a specific tridimensional disposition. All these features increase the complexity of the receptor structure.

Amino acid derivatization has been proposed as an option to facilitate the extraction; however, a further deprotection step that increases the cost of the process is required. In order to make it profitable, it would be more attractive to find a receptor able to directly extract zwitterionic amino acids from aqueous solutions with high selectivity.

Different strategies have been used in literature to form stable complexes with amino acids and make them soluble in organic solvents. These receptors can associate either the carboxylate group and/or the ammonium group of the amino acids although most systems possess moderate operational selectivities.

- Recognition by electrostatic interactions. The strength of the hydrogen bonds used in molecular recognition decreases as the polarity of the solvent increases. For effective recognition of amino acids in aqueous media, ionic interactions have been used to increase the binding affinity of hydrogen bonds.[24] Classical examples are the receptors developed by

[24] Gale, P.; Steed, J. *Synthetic Receptors for Biomolecules. Design principles and Applications*, Royal Society of Chemistry, **2015**, 331.

Rebek[25] and Mendoza.[26] More recently, as selected examples, researchers such as Schmuck or Suzuki have developed positively charged receptors based on molecules with guanidinium groups,[27] You and Lan used imidazolium groups[28] and Ramaiah employed viologen groups.[29]

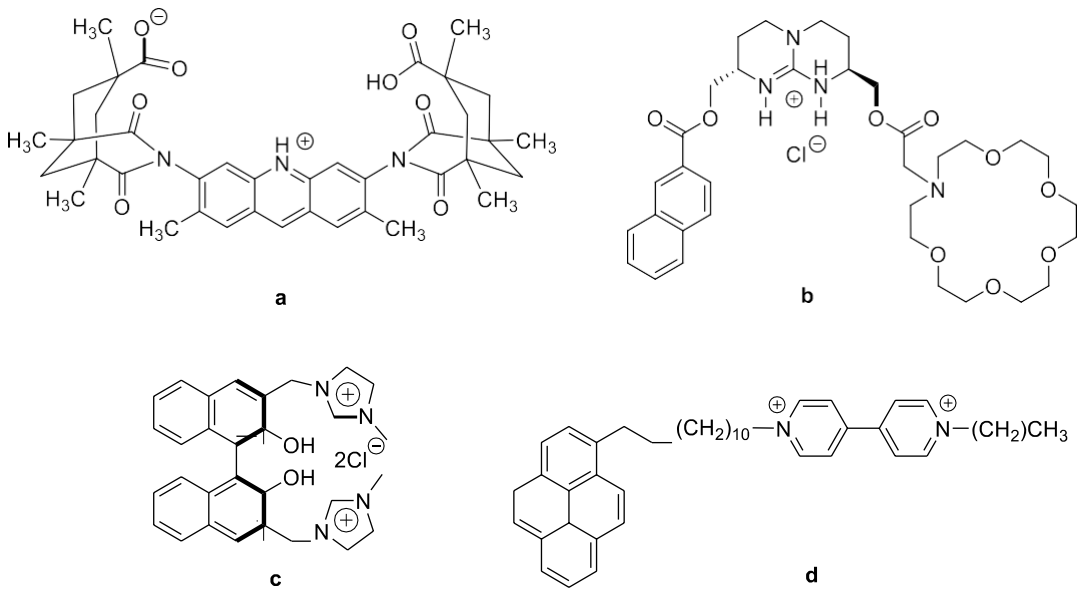

Figure 9. *Acridinium (a), guanidinium (b), imidazolium (c) and viologen (d) based receptors.*

- **Recognition by hydrogen bonding**. Classic Cram receptors based on crown ethers lies in this category.[30] More recently, Chan investigated the binding functions of a neutral

[25] (a) Rebek, Jr. J.; Nemeth, D. *J. Am. Chem. Soc.* **1985**, *107*, 6738 – 6739. (b) Rebek, J.; Marshall, L.; Wollak, R.; Parris, K.; Killoran, M.; Askew, B.; Nemeth, D.; Islam, N. *J. Am. Chem. Soc*. **1985**, *107*, 7476 – 7481. (c) Rebek, J.; Askew, B.; Nemeth, D.; Parris, K. *J. Am. Chem. Soc*. **1987**, *109*, 2432 – 2434.

[26] (a) Galan, A.; Andreu, D.; Echavarren, A.; Prados, P.; De Mendoza, J. *J. Am. Chem. Soc.* **1992**, *114*, 1511 – 1512. (b) Blondeau, P.; Segura, M.; Pérez-Fernández, R.; de Mendoza, J. *Chem. Soc. Rev.* **2007**, *36*, 198 – 210.

[27] Schmuck, C. *Chem. Commun.* **1999**, 843 – 844.

[28] Yang, L.; Qin, S.; Su, S.; Yang, F.; You, J.; Hu, C.; Xie R.; Lan, J. *Org. Biomol. Chem.* **2010**, *8*, 339 – 348.

[29] Hariharan, M.; Karunakaran, S. C.; Ramaiah, D. *Org. Lett.*, **2007**, *9*, 417 – 420.

[30] Selected examples: (a) Kozbial, M.; Pietraszkiewicz, M.; Pietraszkiewicz, O. *J. Incl. Phenom. Mol. Recognit. Chem.* **1998**, *30*, 69 – 77. (b) Lingenfelter, D. S.; Helgeson, R. C.; Cram, D. J. *J. Org. Chem.* **1981**, *46*, 393 – 406. (c) Hernández, J. V.; Oliva, A. I.; Simón, L.; Muñiz, F. M.; Grande, M.; Morán, J. R. *Tetrahedron Lett.* **2004**, *45*, 4831 – 4833.

fluorescent receptor based on cholic acid.[31] Pre-organisation of this receptor allows binding of the receptor to amino acids at three sites, thus increasing complexation.

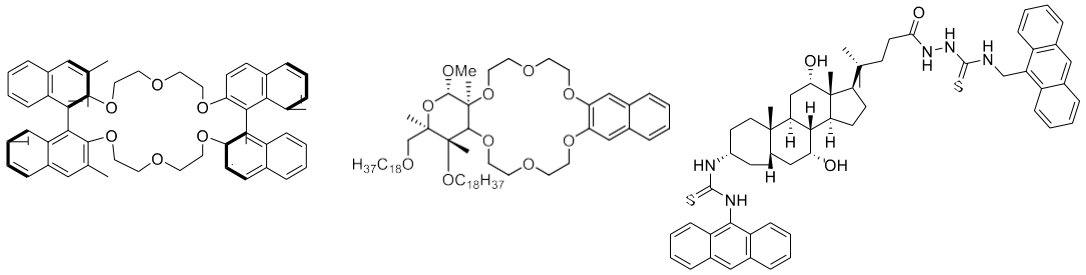

Figure 10. *Receptors based on hydrogen bonds.*

- Metal coordination recognition. One of the most straightforward ways for reversible association of amino acids in water is to employ a receptor that possesses a metal centre able to chelate with the nitrogen of the amino group and the oxygen of the carboxyl group.[24] Taglietti and Yu have developed a series of complexes where the metal used was copper,[32] Buryak and Severin[33] used rhodium and Yang employed gold.[34] De Vries and Feringa have used palladium complexes[35] whereas lanthanides have been exploited by Yonemitsu.[36]

[31] Liu, S.; Fang, L.; He, Y.; Chan, W.; Yeung, K.; Cheng, Y.; Yang, R. *Org. Lett.*, **2005**, *7*, 5825 – 5828.
[32] (a) Hortalá, M. A.; Fabbrizzi, L.; Marcotte, N.; Stomeo, F.; Taglietti, A. *J. Am. Chem. Soc.* **2003**, *125*, 20 – 21. (b) Liu, X.; Ma, Y.; Cao, T.; Tan, D.; Wei, X.; Yang, J.; Yu, L. *Sep. Purif. Technol.* **2019**, *211*, 189 – 197.
[33] Buryak, A.; Severin, K. *J. Am. Chem. Soc.* **2005**, *127*, 3700 – 3701.
[34] Yang, Y.; Shim, S.; Tae, J. *Chem. Commun.* **2010**, *46*, 7766 – 7768.
[35] (a) Verkuijl, B. J. V.; Minnaard, A. J.; de Vries, J. G.; Feringa, B. L. *J. Org. Chem.* **2009**, *74*, 6526 – 6533. (b) Verkuijl, B. J. V.; Schoonen, A. K.; Minnaard, A. J.; de Vries, J. G.; Feringa, B. L. *Eur. J. Org. Chem.* **2010**, 5197 – 5202.
[36] Selected examples: Tsukube, H.; Uenishi,J.-i.; Kanatani, T.; Itoh, H.; Yonemitsu, *Chem. Commun.* **1996**, 477 – 478.

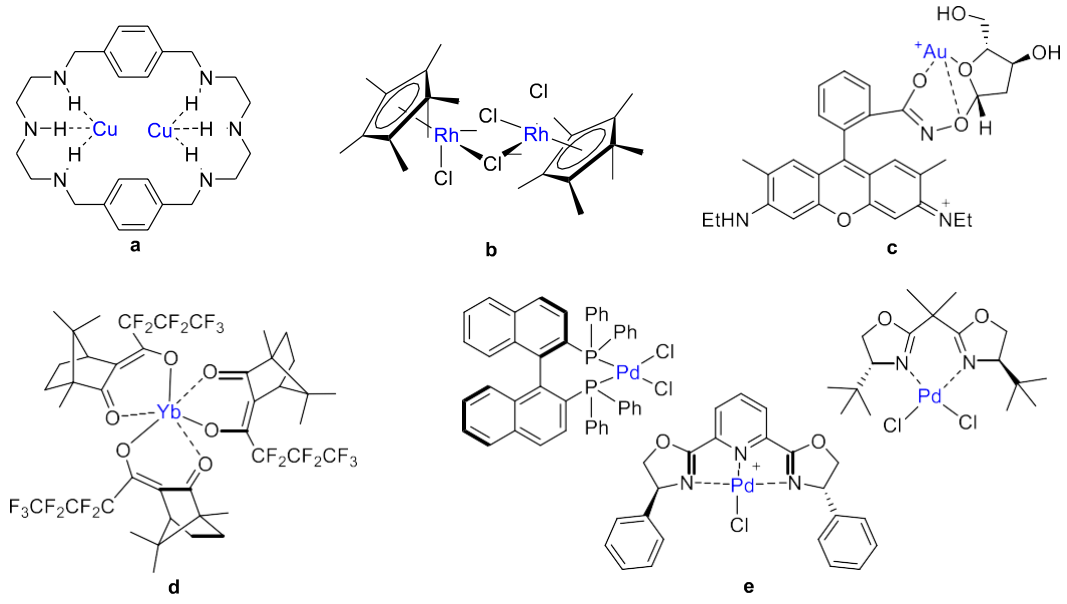

Figure 11. *Receptors based on metals such as copper (a), rhodium (b), gold (c), ytterbium (d) and palladium (e).*

- **Nanoparticle-based recognition**. This kind of recognition relies on electrostatic interactions that occur on the surface of the nanoparticle. For example, Patel and Menon investigated the recognition of some amino acids such as lysine, arginine or histidine by gold nanoparticles functionalised with *p*-sulfonatocalix[4]arene thiol in aqueous solution.[37]

[37] Patel, G.; Menon, S. *Chem. Commun.* **2009**, 3563 – 3565.

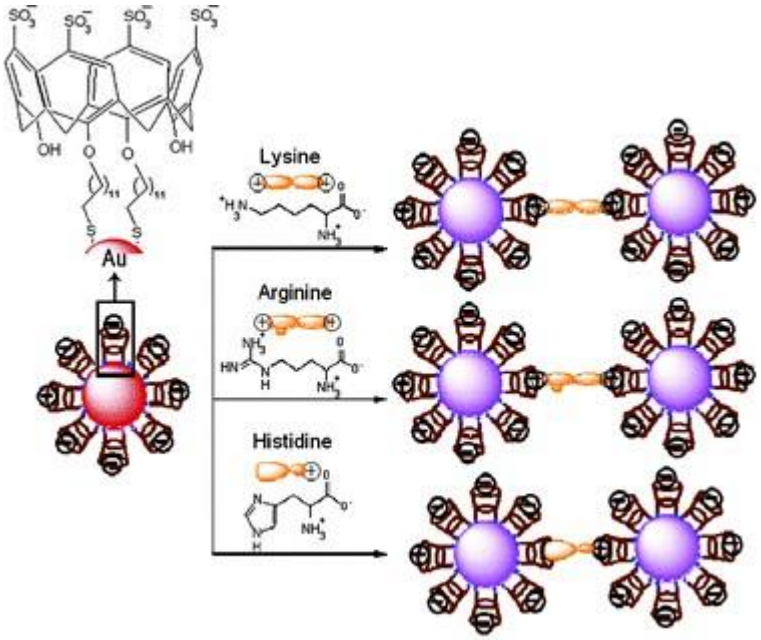

Figure 12. *Receptor based on nanoparticles.*

2.3. Antecedents of the research group

Our research group has a large experience in the association of zwitterionic amino acids in non-polar solvents. This topic is a real challenge, because amino acids are ionic, polar compounds, soluble in water, but very insoluble in organic solvents. The high melting points of amino acids show that they form a very stable crystalline network and breaking it with a molecular receptor implies the formation of even more stable bonds than those between amino acid molecules. As an additional challenge, once a sufficiently efficient receptor is obtained to break this crystalline structure, it must be adapted to only one of the two enantiomers of the amino acid, since the final challenge would be to obtain a molecular receptor that allows the resolution of amino acid racemic mixtures.

To extract zwitterionic amino acids from an aqueous phase to an organic phase it is necessary to establish a strong association complex between the receptor and the host amino acid. Traditionally, crown ethers have shown good properties to complex the ammonium group. However, many other solutions exist to complex the carboxylate moiety.

In our group, we have used the oxyanion-hole structure of hydrolytic enzymes (Figure 13) as inspiration for the design of carboxylate receptors. Hydrolytic enzymes use the oxyanion

hole to bind the substrate carbonyl group with two or three hydrogen bonds and stabilize the generated transition state (Figure 13).[38]

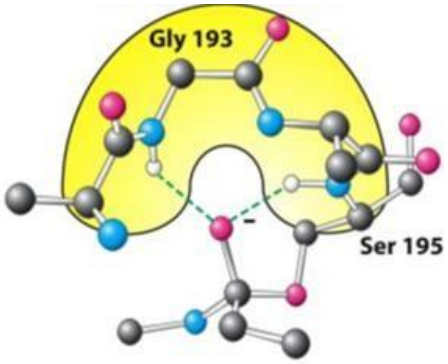

Figure 13. *Oxyanion hole of chymotrypsin.*[39]

Figure 14 shows some of the receptors developed in our research group[40] to mimic the oxyanion-hole structure with xanthone, thioxanthone and dihydroanthracene skeletons. All of them possess a pair of NHs to associate the carbonyl group through hydrogen bonds. The presence of an oxygen atom in the xanthone skeleton creates a narrower oxyanion hole than the one in dihydroanthracene or thioxanthone.

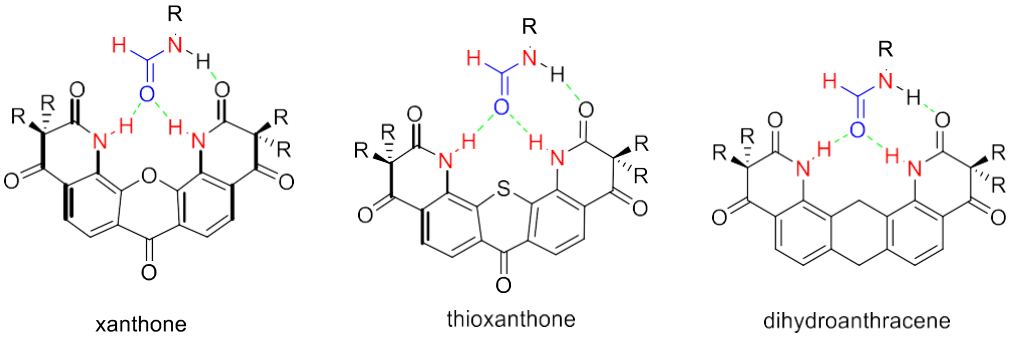

Figure 14. *Receptors developed in the research group.*[41]

[38] Copeland, R. A. *ENZYMES: A Practical Introduction to Structure, Mechanism, and Data Analysis.* 2nd ed. Wiley-VCH, **2000**.
[39] Tymoczko, J. L.; Berg, J. M.; Stryer, L. Biochemistry: A Short Course, 3rd ed, W. H. Freeeman, **2015**.
[40] (a) Martín, M.; Raposo, C.; Almaraz, M.; Crego, M.; Caballero, C.; Grande, M.; Morán, J. R. *Angew. Chem. Int. Ed. Engl.* **1996**, *35*, 2386 – 2388. (b) Almaraz, M.; Raposo, C.; Martín, M.; Caballero, M. C.; Morán, J. R. *J. Am. Chem. Soc.***1998**, *120*, 3516 – 3517. (c) Muñiz, F. M.; Simón, L.; Alcázar, V.; Raposo, C.; Fuentes de Arriba, Á. L.; Morán, J. R. *Eur.J. Org. Chem.* **2009**, 5350 – 5354. (d) Simón, L.; Muñiz, F. M.; Fuentes de Arriba, Á. L.; Alcázar, V.; Raposo, C.; Morán, J. R. *Org. Biomol. Chem.* **2010**, *8*, 1763 – 1768.
[41] Hernández Rubio, O. Tesis Doctoral, **2019**, *Universidad de Salamanca.*

However, none of the receptors shown in Figure 14[42] were able to extract zwitterionic amino acids from water to chloroform, as the amino acid has a bigger tendency to remain solvated in the aqueous phase due to the lack of ammonium association.

This problem was solved by the incorporation of other groups able to accept the hydrogen bonds of the ammonium moiety. For example, the catalyst in Figure 15 allowed the selective proline extraction.[43]

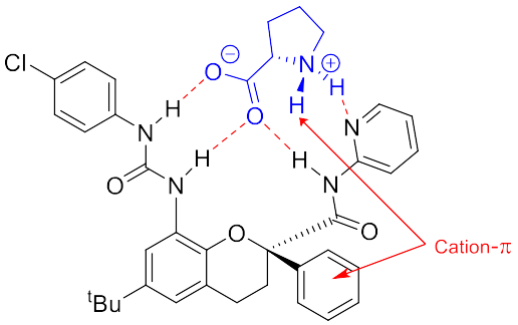

Figure 15. *Molecular receptor that extracts proline selectively from an aqueous mixture of amino acids to chloroform at 20°C.*

This molecular receptor combines the hydrogen bonds donors of the oxyanion hole with the hydrogen bond acceptors provided by the pyridine moiety. Also, cation-π interactions help to stabilise the complex. They allow the highly selective proline association. However, the enantioselectivity obtained was poor.

Another receptor that allowed the selective extraction of phenylalanine[44] is shown in Figure 16. The combination of hydrogen bonds with π- π stacking effects makes possible to extract phenylalanine from an aqueous solution to chloroform particularly well. However, both phenylalanine enantiomers adapted well to the molecular receptor, so enantioselective recognition was poor.

---

[42] (a) Pérez, E. M.; Oliva, A. I.; Hernández, J. V.; Simón, L.; Morán, J. R.; Sanz, F. *Tetrahedron Lett.* **2001**, *42*, 5853 – 5856. (b) Oliva, A. I.; Simón, L.; Muñiz, F. M.; Sanz, F.; Morán, J. R. *Chem. Commun.* **2004**, 426 – 427. (c) Oliva, A. I.; Simón, L.; Muñiz, F. M.; Sanz, F.; Ruiz–Valero, C.; Morán, J. R. *J. Org. Chem.* **2004**, *69*, 6883 – 6885.

[43] Temprano, Á. G.; Monleón, L. M.; Rubio, O. H.; Rubio, L. S.; Pérez, A. B.; Sanz, F.; Morán, J. R. *Org. Biomol. Chem.* **2016**, *14*, 1325 – 1331.

[44] Herrero, F. G.; Rubio, O. H.; Monleón, L. M.; Fuentes de Arriba, Á. L.; Rubio, L. S.; Morán, J. R. *Org. Biomol. Chem.* **2016**, *14*, 3906 – 3912.

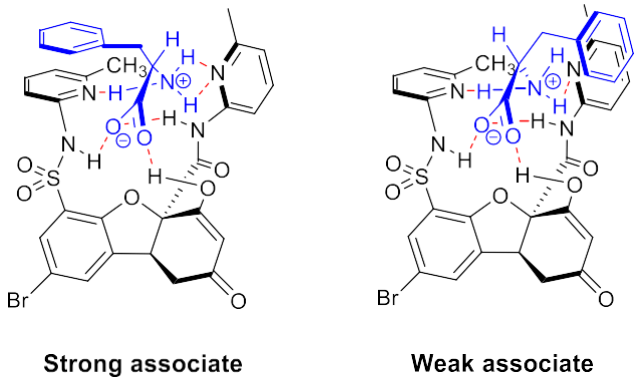

Figure 16. *Molecular receptor selective for phenylalanine.*

Although none of the receptors shown in Figure 15 and Figure 16 had been designed with a specific cavity to accommodate the ammonium group of the amino acid, their ability to extract zwitterionic amino acids from the aqueous phase into the chloroform phase was remarkable. However, it was difficult to improve their design to get enantioselective recognition in a rational way.

In order to carry out a rational design of an enantioselective receptor for amino acids, it is necessary to combine a binding group for the carboxylate and another specific group able to interact with the ammonium group.

In principle, the binding moieties for carboxylate and ammonium groups does not necessarily need to be attached to the same platform. In fact, the macrocycle of Figure 17 in combination with 18-crown-6 ether was able to extract phenylglycine easily from an aqueous solution and also showed moderate enantioselectivity (a ratio up to 9 for phenylglycine was obtained between the two association constants of both diastereomeric complexes).[30(c)]

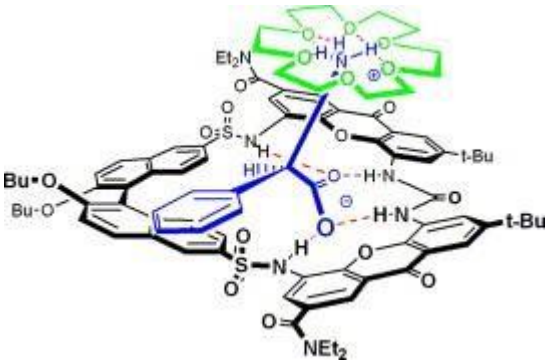

Figure 17. *(Left) Structure of the ternary complex formed between a macrocycle designed in our group with phenylglycine and 18-crown-6 ether.*

To improve the previous results, we thought the combination of the carboxylate binding unit with the crown ether in the same platform would provide higher enantioselectivities. A more rigid receptor would have more chances to distinguish between the two amino acid enantiomers.

To prove our hypothesis, Figure 18 receptor was synthesised. First, an achiral receptor was considered in order to facilitate its synthesis and study the amino acid extraction from the water phase.[45]

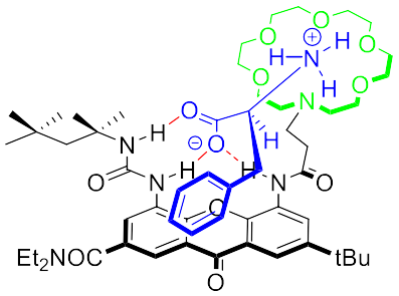

Figure 18. *Non-enantioselective receptor for amino acids.*

This compound extracted particularly well lipophilic amino acids such as phenylalanine, phenylglycine, leucine, isoleucine and alanine from water to chloroform, but since it lacked any chiral centre, it did not allow any enantioselective discrimination between amino acids.

The introduction of a chiral centre into the above structure seemed straightforward at first sight, as it would only require either methacrylamide or the corresponding crotonamide instead of acrylamide for the synthesis of the spacer.

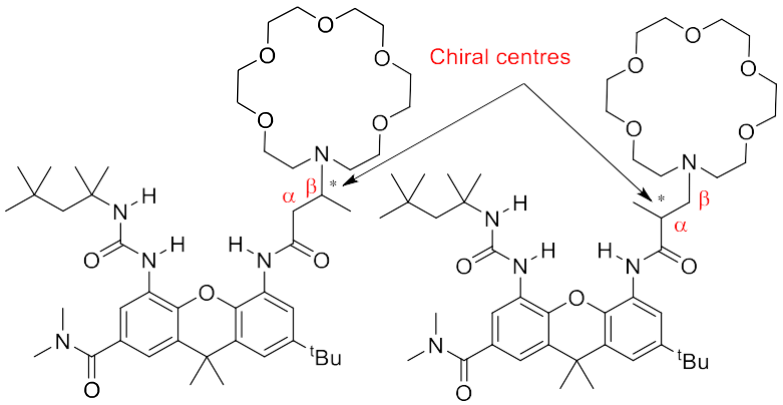

Figure 19. *Asymmetric proposals for the receptor of Figure 18.*

[45] Hernández, J. V.; Muñiz, F. M.; Oliva, A. I.; Simón, L.; Pérez, E.; Morán, J. R. *Tetrahedron Lett.* **2003**, *44*, 6983 – 6985.

Surprisingly, neither of the two receptors of Figure 19 proved useful in the extraction of amino acids. Apparently, the additional steric hindrance created by the methyl groups in either the α or β position of the propionamide fragment is responsible for the lack of stability of the associates.

Figure 20 shows a different design in which the chiral centre was located in the chromane backbone instead of the spacer between the carboxylate binding unit and the crown ether.[46]

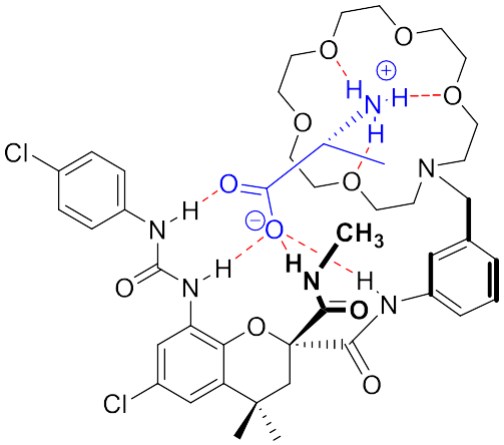

Figure 20. *Receptor with a chromane skeleton and an aza-crown ether attached to it.*

This receptor proved to be highly selective for alanine, probably because only the methyl group from the lateral chain of alanine fits inside the cavity. However, enantioselective recognition was poor. Most likely, the main problem lies in the planar geometry of the oxyanion hole, which allows the fitting of both enantiomers of alanine inside the cavity (Figure 21). X-ray analysis corroborates this fact.

[46] Rubio, O. H.; Taouil, R.; Muñiz, F. M.; Monleón, L. M.; Simón, L.; Sanz, F.; Morán, J. R. *Org. Biomol. Chem.* **2017**, *15*, 477 – 485.

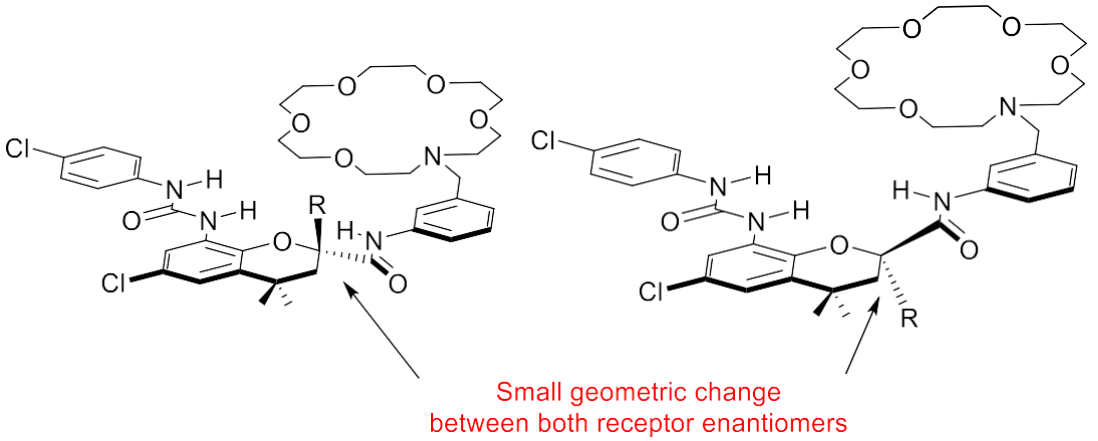

Figure 21. *Explanation of the small enantioselective recognition showed by the receptor of Figure 20.*

Molecular modelling studies showed that a receptor in which the chiral centre closer to the amino acid α could show much higher enantioselective recognition, as the chiral centre of the receptor should be closer to the chiral centre of the amino acid.

A rational understanding of the complex formed between receptor and amino acid is still required to be able to carry out the chiral extraction of amino acids from aqueous media with high enantioselectivity.

Chapter 1 – Methods and Results

3. Methods and Results

3.1. Macrocyclic receptor 2

We have previously reported[47] a carbazole-based receptor **1** (Figure 22A) functionalized with two sulfonamide groups as hydrogen bond sites for anion complexation.

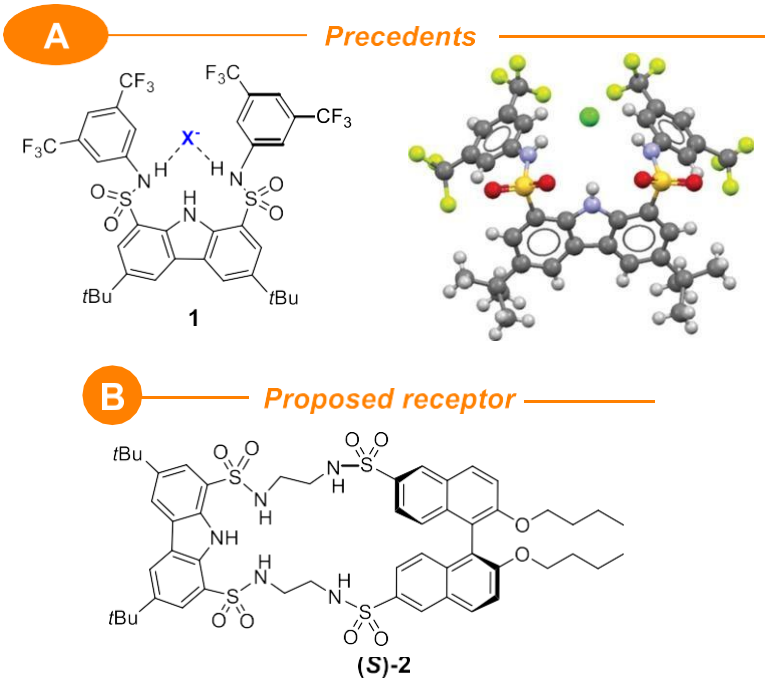

Figure 22. *(A) Precedents in the group for anion recognition with a carbazole scaffold. (B) Proposed novel chiral macrocyclic receptor based on a carbazole-BINOL scaffold.*

While excellent affinities were obtained for halide anions (K_a= 7.9 ×10^6 M^{-1} for Cl^- in $CHCl_3$), a strong decrease in binding was observed for oxyanions. This behavior, according to the X-ray structural analysis and modeling studies,[47] was attributed to the importance of the CH···X (halogen) interactions in the binding process and the steric hindrance and receptor conformational changes observed for oxyanion association.

Trying to develop a more efficient synthetic host for oxyanions and eventually for zwitterionic amino acids, the macrocyclic structure **2** (Figure 22B) was designed with several improved features: (i) two more H-bond donor groups; (ii) the macrocyclic structure ensures

[47] Fuentes de Arriba, Á. L.; Turiel, M. G.; Simón, L.; Sanz, F.; Boyero, J. F.; Muñiz, F. M.; Morán, J. R.; Alcázar, V. *Org. Biomol. Chem.* **2011**, *9*, 8321 – 8327.

a higher degree of preorganization reducing the entropic cost of association;[48] (iii) a chiral binaphthyl unit enables the enantioselective recognition of chiral anions and (iv) the steric hindrance around the sulfonamide NHs has been reduced replacing the bis(trifluoromethyl)anilines by ethylenediamines. Thus, anion binding can be expected in the hydrogen bonding donor pocket of the preorganized receptor **2**, while a chiral BINOL building block should be able to preferentially select one of the enantiomers. Not only but also, (i) sulfonamide based carbazole receptors provide more acidic NHs than carboxamides and hence, potentially stronger associates; (ii) do not require transition metals and (iii) their synthesis can be easily carried out on a multigram scale from inexpensive starting materials.

Receptor **2** *synthesis*

The synthetic strategy for the preparation of compound **2** was a convergent synthesis where ring closure could be achieved by the simultaneous formation of two sulfonamide bonds. While two different approaches were considered (disconnections *a* and *b*), as shown in Figure 23, route *a* afforded macrocycle **2** in higher yield (36 % *vs* 25 % in route *b*).

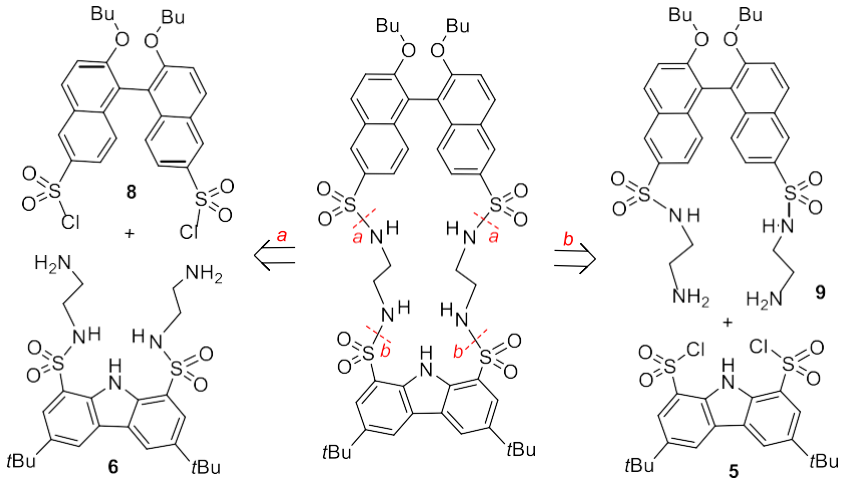

Figure 23. *Synthetic strategies a and b leading to macrocycle* **2**.

As illustrated in Figure 24, starting from the readily available 3,6-di-*tert*-butyl-9*H*-carbazole **3**[49] and 2,2'-dihydroxy-1,1´-binaphthyl **4**,[50] the synthesis of **2** was straightforward, involving as key intermediates the disulfonyl dichlorides **5**[47] and **8**,[51] previously synthesized

[48] (a) Martí-Centelles, V.; Pandey, M. D.; Burguete, M. I.; Luis, S. V. *Chem. Rev.* **2015**, *115*, 8736 – 8834. (b) *Macrocyclic Chemistry. Current Trends and Future Perspectives*; Gloe, K., Ed.; Springer, Dordrecht, **2005**.

[49] Yang, X.; Lu, R.; Gai, F.; Xue, P.; Zhan, Y. *Chem. Commun.* **2010**, *46*, 1088 – 1090.

[50] Kyba, E. P.; Siegel, M. G.; Sousa, L. R.; Sogah, G. D.; Cram, D. J. *J. Am. Chem. Soc.* **1973**, *95*, 2691 – 2692.

[51] Hernández, J. V.; Oliva, A. I.; Simón, L.; Muñiz, F. M.; Grande, M.; Morán, J. R. *Tetrahedron Lett.* **2004**, *45*, 4831 – 4833.

by our group. NMR experiments were carried out to unambiguously assign the chemical shifts for protons, both in $CDCl_3$ and in DMSO-d_6 solvents.

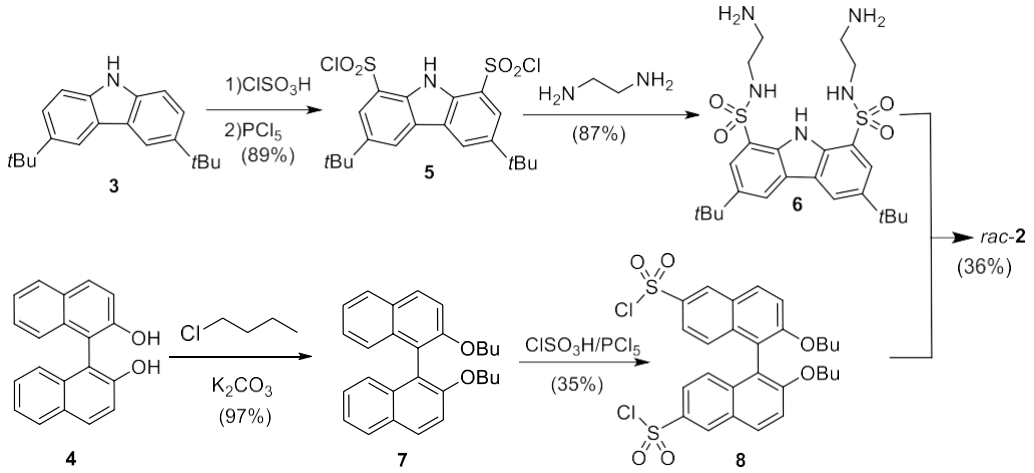

Figure 24. *Synthesis of the racemic macrocycle* **2** *via route a.*

The racemic macrocycle **2** anion binding affinity was explored and compared to acyclic receptor **1** by ^{1}H NMR titrations in $CDCl_3$ as solvent. Halide and acetate anions were selected to compare with previous results obtained with receptor **1**.[47]

Table 1. *Association constants K_a (M^{-1}) for the complexes formed by macrocycle* **2** *and receptor* **1** *and selected anions (added as tetrabutyl or tetraethyl ammonium salts) at 298 K in $CDCl_3$. Errors estimated to be ≤ 10%.*

Entry	Anion	Receptor **1**	Receptor **2**
1	Cl^-	7.9×10^6 [a]	8.0×10^5 [b]
2	I^-	4.2×10^5 [a]	5.0×10^5 [b]
3	AcO^-	[c]	2.8×10^5

[a]Measured by fluorescence. [b]Measured by ^{1}H NMR competitive titration with receptor **1**. [c]Data could not be fitted to a binding model due to the possible receptor **1** deprotonation with the acetate.

While receptors **1** and **2** were found to display similar high affinities for halides (Table 1, entries 1 and 2), macrocycle **2** was able to bind acetate with an association constant higher than 10^5 M^{-1} (Table 1, entry 3). Thus, the replacement of the bis(trifluoromethyl)aniline with ethylenediamine in the sulfonamide linkages proved to be effective to avoid deprotonation (previously observed for receptor **1**), resulting in hydrogen bonds acetate binding.

Extraction studies

Encouraged by these results, we next explored the association of amino acids in their zwitterionic form. Macrocycle **2** combines an oxyanion hole moiety[52] for binding of carboxylates and a binaphthyl unit to impart chirality. Ammonium binding was achieved using 18-crown-6 ether.[53] This binding site combination allows this receptor to extract zwitterionic amino acids from an aqueous solution into a chloroform phase.[51]

In a typical liquid-liquid extraction experiment, a saturated aqueous solution of the amino acid was added to a solution of macrocycle **2** and 18-crown-6 ether in $CDCl_3$, followed by vigorous stirring. ^{1}H NMR analysis of the organic phase was used to estimate the extraction efficiency (Table 2).

Table 2. *Extraction of zwitterionic amino acids from aqueous solution into $CDCl_3$ by combination of macrocycle* **2** *and 18-crown-6 ether.*

Entry	Amino acid[a]	Extraction[b] (%)
1	D,L-alanine	-
2	D,L-leucine	-
3	D,L-phenylalanine	Quant. (*56.4%* ee)[c]
4	D,L-phenylglycine	Quant. (*91.8*% ee)[c]
5	D,L-serine	-
6	D,L-tryptophan	-
7	D,L-tyrosine	-
8	D,L- valine	-

[a]0.5 mL of an aqueous saturated solution of the amino acid was added to 0.5 mL of a $CDCl_3$ solution of **2** (1.15×10^{-2}M) and 18-crown-6 ether (2.65×10^{-2}M), followed by vigorous stirring and centrifugation. [b]Single extraction experiment; extraction percentages based upon the macrocycle concentration in the organic phase and determined by integration of the ^{1}H NMR signals. [c]Determined by HPLC when receptor (*S*)-**2** is used.

[52] (a) Simón, L.; Goodman, J. M. *Org. Biomol. Chem.* **2012**, *10*, 1905 – 1913. (b) Simón, L.; Goodman, J. M. *J. Org. Chem.* **2010**, *75*, 1831 – 1840. (c) Simón, L.; Muñiz, F. M.; Fuentes de Arriba, Á.; Alcázar, V.; Raposo, C.; Morán, J. R. *Org. Biomol. Chem.* **2010**, *8*, 1763 – 1768. (d) Pihko, P.; Rapakko, S.; Wierenga, R. K. in *Hydrogen Bonding in Organic Synthesis*, Wiley-VCH Verlag GmbH & Co. KGaA, 2009, 43 – 71. (e) Muñiz, F. M.; Montero, V. A.; Fuentes de Arriba, A. L.; Simón, L.; Raposo, C.; Morán, J. R. *Tetrahedron Lett.* **2008**, *49*, 5050 – 5052. (f) Simón, L.; Muñiz, F. M.; Sáez, S.; Raposo, C.; Morán, J. R. *ARKIVOC* **2007**, iv, 47 – 64. (g) Simón, L.; Muñiz, F. M.; Sáez, S.; Raposo, C.; Morán, J. R. *Eur. J. Org. Chem.* **2007**, 4821 – 4830.

[53] (a) Späth, A.; König, B. *Beilstein J. Org. Chem.* **2010**, *6*, DOI:10.3762/bjoc.6.32. (b) Gokel, G. W.; Leevy, W. M.; Weber, M. E. *Chem. Rev.* **2004**, *104*, 2723 – 2750.

Macrocycle **2** proved to be highly selective for aromatic amino acids phenylglycine and phenylalanine which were quantitatively extracted into $CDCl_3$ with 1:1 macrocycle to amino acid binding stoichiometry; the rest of the tested amino acids were not extracted to any measurable extent. Figure 25 displays the aromatic region of the ^1H NMR spectra of macrocycle **2** before (a) and after the extraction with a saturated solution of D-phenylglycine (b) and D-phenylalanine (c), where the appearance of the aromatic ring signals of both amino acids can be observed.

Amino acid recovery from the chloroform phase was easily achieved by removing the aqueous phase and washing the organic phase with one equivalent of potassium decanoate in water. 18-crown-6 ether traces were eliminated by washing twice the aqueous phase with chloroform.

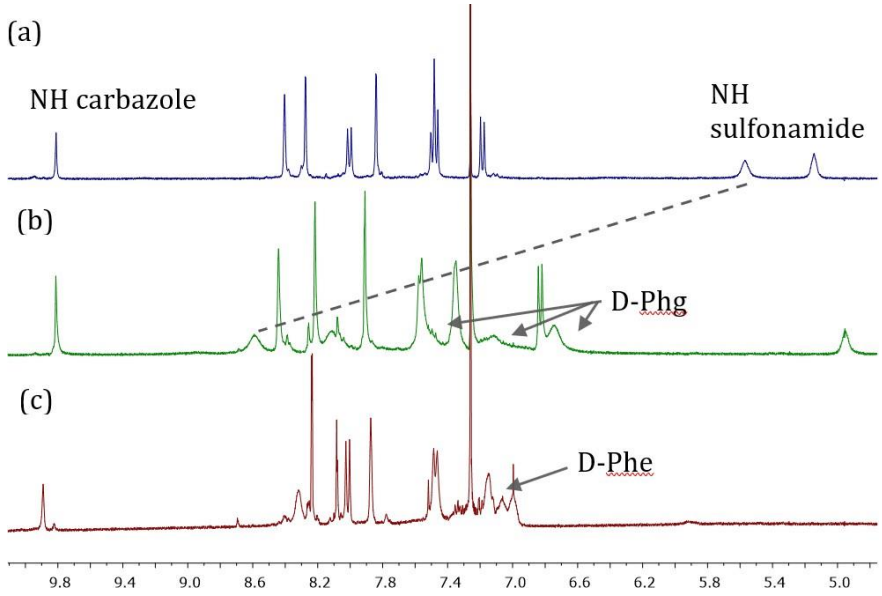

Figure 25. *Partial ^1H NMR spectra (5.0-10.0 ppm) of macrocycle (S)-**2** before (a) and after liquid-liquid extraction with a saturated solution of D-phenylglycine (b) and D-phenylalanine (c).*

The fact that, among the natural amino acids tested, only phenylalanine was extracted, could be used in the preparation of food supplements for the treatment of Phenylketonuria.[54]

The observed selectivity in the extraction of the underivatized amino acids prompted us to prepare the enantiopure receptor *(S)*-**2** starting from *(S)*-2,2´-dihydroxy-1,1´-binaphthyl **4**.[55] While chiral macrocycle **2** was being synthetized, further evidence for enantioselective

[54] Al Hafid, N.; Christodoulou, J. *Transl. Pediatr.* **2015**, *4*, 304 – 317.
[55] Tanaka, K.; Okada, T.; Toda, F. *Angew. Chem. Int. Ed.* **1993**, *32*, 1147 – 1148.

binding was obtained using a methodology our group has successfully applied for the resolution of racemic receptors.[51,56] Conventional TLC plates were impregnated with a 1.5% aqueous solution of L-phenylglycine and the stoichiometric amount of 18-crown-6 ether and dried (Figure 26). Elution of the racemic macrocycle afforded two separated spots, corresponding to the diastereomeric complexes of L-phenylglycine with each enantiomer of racemic **2**. At the same time, elution of *(S)*-**2** in TLC plates impregnated with L-phenylglycine and D-phenylglycine clearly showed that the strong complex is formed with D-phenylglycine, affording a spot with larger R_f than the spot generated after elution in the L-phenylglycine impregnated TLC (Figure 27).

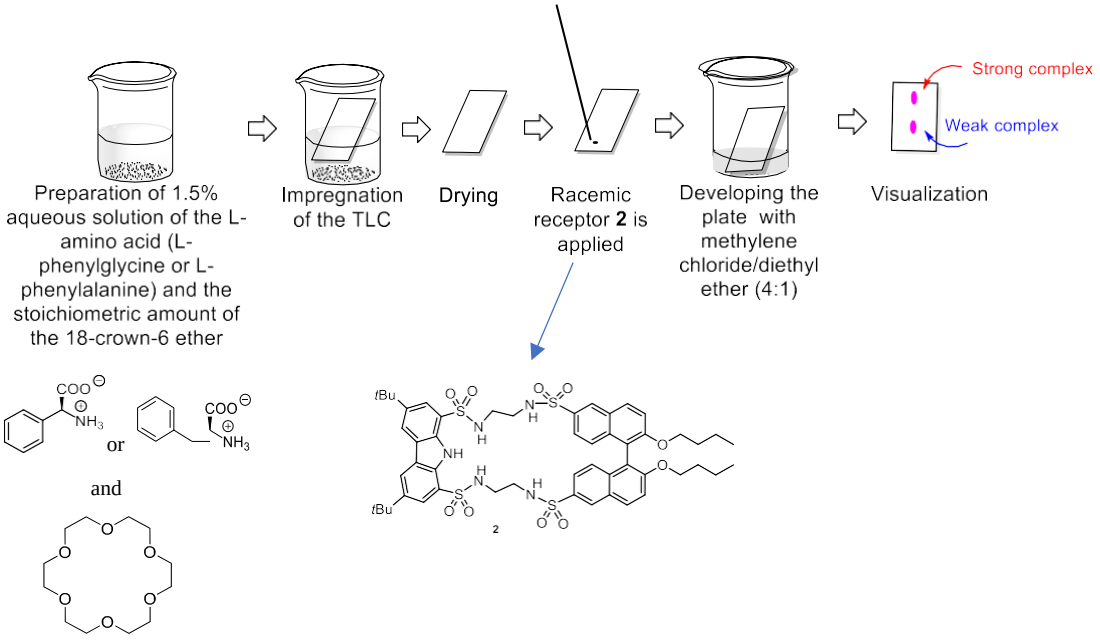

Figure 26. *Scheme of the TLC resolution of racemic macrocycle* **2**.

[56] (a) Temprano, Á. G.; Monleón, L. M.; Rubio, O. H.; Simón, L.; Pérez, A. B.; Sanz, F.; Morán, J. R. *Org. Biomol. Chem.* **2016**, *14*, 1325 – 1331. (b) Herrero, F. G.; Rubio, O. H.; Monleón, L. M.; Fuentes de Arriba, Á. L.; Simón, L.; Morán, J. R. *Org. Biomol. Chem.* **2016**, *14*, 3906 – 3912. (c) de Juan Fernández, L.; Fuentes de Arriba, Á. L.; Monleón, L. M.; Rubio, O. H.; Alcázar, V.; Simón, L.; Morán, J. R. *Eur. J. Org. Chem.* **2016**, 1541 – 1547. (d) Fuentes de Arriba, Á. L.; Herrero, A. G.; Rubio, O. H.; Monleón, L. M.; Simón, L.; Alcázar, V.; Sanz, F.; Morán, J. R. *Org. Biomol. Chem.* **2015**, *13*, 493 – 501.

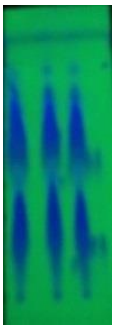

Rac-**2** eluted in a TLC impregnated with L-phenylglycine showed two spots corresponding to the diastereomeric complexes.

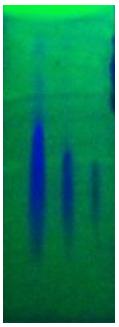

Rac-**2** eluted in a TLC impregnated with L-phenylalanine showed that the two spots are not well separated.

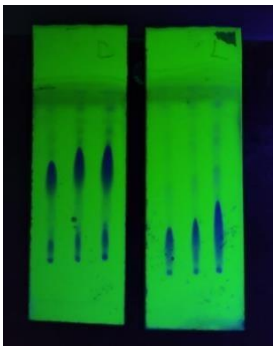

(S)-**2** eluted in a TLC impregnated with D-phenylglycine (left) showed a less polar spot than *(S)*-**2** eluted in a TLC impregnated with L-phenylglycine (right)

Figure 27. *TLC impregnated with L- and D-phenylglycine and L-phenylalanine.*

These preliminary results were later confirmed by the liquid-liquid extraction experiments with the enantiopure macrocycle *(S)*-**2** and the racemic amino acids. To our delight, analysis by chiral HPLC showed a preference of macrocycle *(S)*-**2** for D-enantiomers, reaching a 91.8% *ee* for phenylglycine (Table 2, entry 4) and 56.4% *ee* for phenylalanine (Table 2, entry 3). The selectivity obtained for zwitterionic phenylglycine (α = 11.2) is, to our knowledge, the best result for this amino acid obtained so far.

To understand the origin of this enantiodiscrimination, NMR studies were carried out on the diastereomeric receptor *(S)*-**2** complexes with L- and D- phenylglycine in the presence of 18-crown-6 ether. The chemical shifts showed that the carbazole NH is not involved in the binding with the amino acid while the carbazole sulfonamide NHs are shifted from 5.57 ppm to 8.59 and 8.43 ppm in the complexes, as expected when hydrogen bonds are formed (Figure 25). It is remarkable the very different chemical shifts of the *meta* protons of both phenylglycine enantiomers in the complexes, which seems to indicate associates with very different geometries.

Crystallographic and modelling studies

X-ray crystallographic analysis turned to be a powerful tool to clarify the geometry of the complexes. When an equimolecular mixture of racemic macrocycle **2**, racemic phenylglycine and 18-crown-6 ether were dissolved in a chloroform/methanol solution, crystals of the ternary complexes 1:1:1 were obtained, with the configurations *(S)*-**2**•D-phenylglycine and *(R)*-**2**•L-phenylglycine (Figure 28).

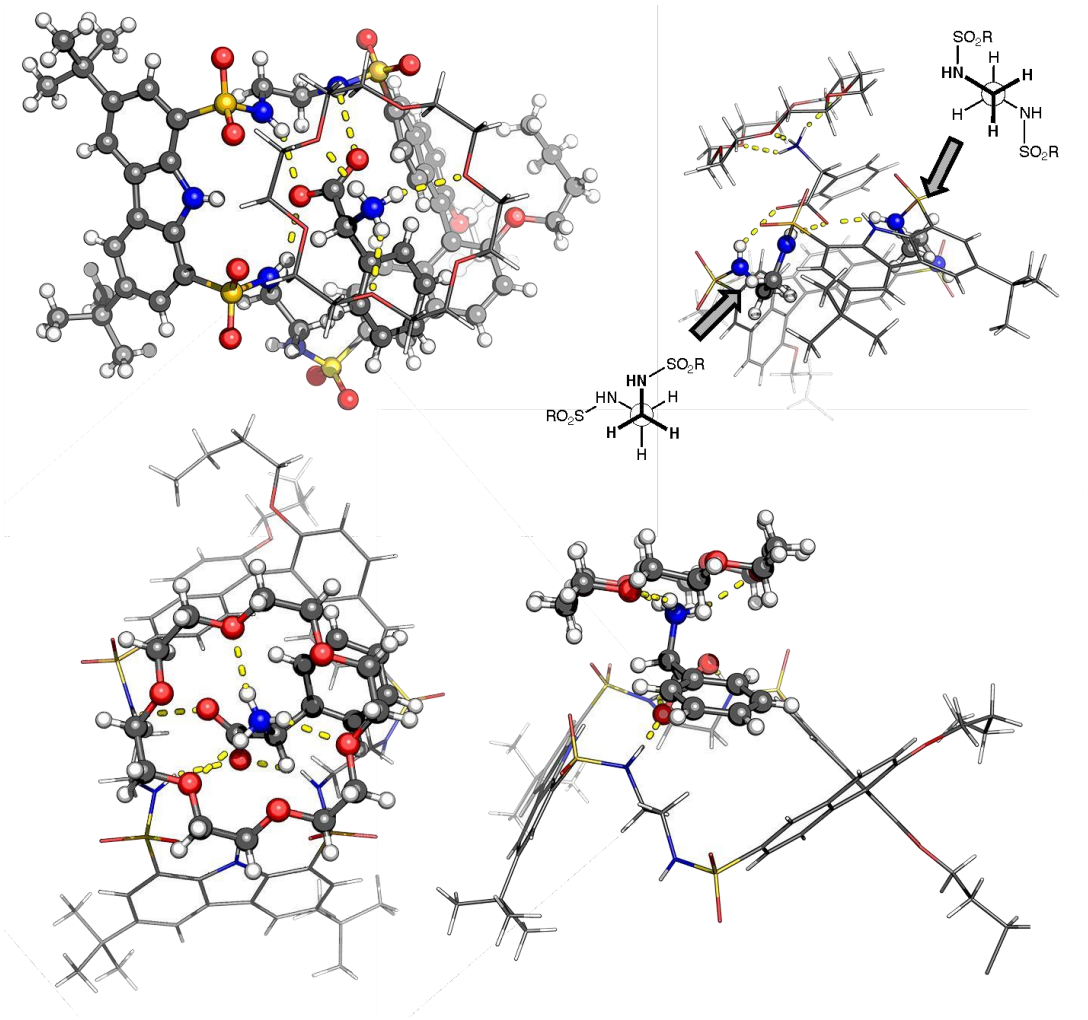

Figure 28. *X-ray structure of the ternary complex (S)-***2***•D-phenylglycine•18-crown-6 ether with hydrogen bonds as yellow dotted lines. For clarity the ternary complex is shown in two views: amino acid and macrocycle (above) and amino acid with crown ether (below). The dihedral angles of the ethylenediamine groups are shown in the top-right view.*

The X-ray structure shows that the carboxylate is bound to the macrocycle through three hydrogen bonds: two formed with both carbazole sulfonamide and the third one with one of the binaphthyl sulfonamides. The fourth sulfonamide NH is not involved in the binding, pointing outside the cavity. As expected, the ammonium group is encapsulated by the crown ether, forming several hydrogen bonds. The crown ether is tilted toward the hydrogen atom in the amino acid, to prevent steric interactions with the larger α-carbon substituents (Figure 28, bottom). In addition, two intramolecular hydrogen bonds are formed in the macrocycle, between the carbazole NH and one of the oxygen atoms of the sulfonamide linked to the carbazole ring (2.450 Å and 2.466 Å).

The phenyl substituent is in the gap left by the binaphthyl group; the conformation adopted by the nearest ethylene diamine (Figure 28, top-right), which directs the fourth NH out of the cavity, contributes to enlarge this gap. In addition, the upfield shift of the phenylglycine *meta* ^{1}H signals (6.74 ppm) in the *(S)*-**2**•D-phenylglycine complex can be attributed to the proximity of these protons to the binaphthyl aromatic sheet.

Since no crystals were obtained for the weak complex, DFT calculations were performed to explain the enantioselectivity. The structure of the most stable *(S)*-**2**•D-phenylglycine complex (Figure 29) is like the X-ray structure. For the *(S)*-**2**•L-phenylglycine complex, two structures were found. The first one shows the carboxylate and the phenyl group occupying the same positions as in the strong complex, leading the H substituent (and the bulky crown ether that is tilted toward it) in the direction of the other binaphthyl sheet. Alternatively, the gap occupied by the phenyl group in the stronger complex can be used to accommodate the amino substituent bound to the crown ether. The latter structure is 2.3 kcal/mol more stable, but still is highly destabilized respect to the *(S)*-**2**•D-phenylglycine complex (7.9 kcal/mol). A similar study on the complexes with phenylalanine shows a smaller energy difference (4.5 kcal/mol).

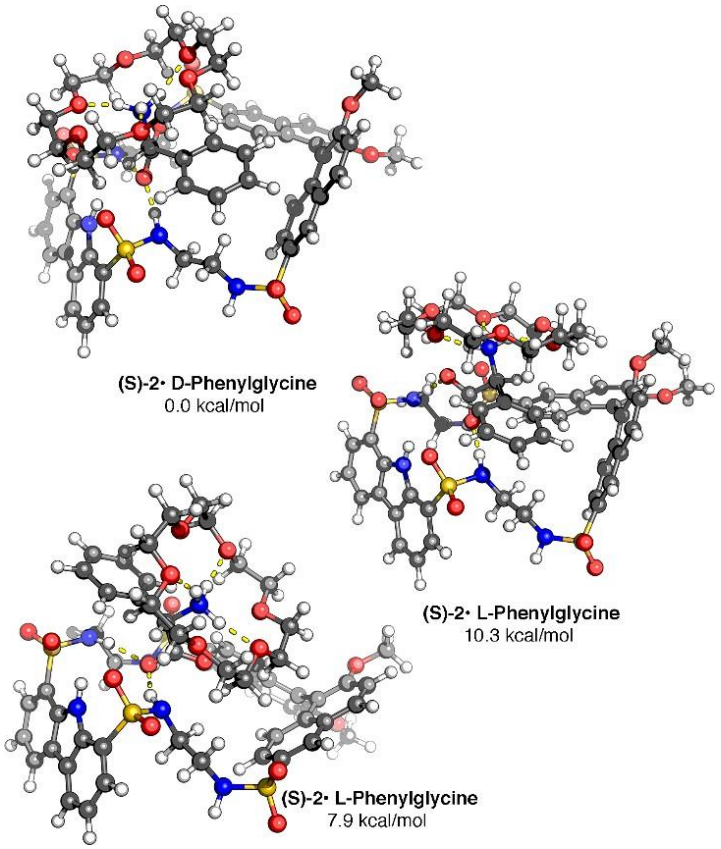

Figure 29. *DFT optimized structures (HF) for the complexes of (S)-***2** *and phenylglycine.*

In conclusion, we have shown that using supramolecular interactions, a new chiral macrocyclic receptor is able to selectively extract zwitterionic phenylglycine from aqueous solutions with high enantioselectivity. X-ray diffraction and DFT studies analysis explained the high enantiodiscrimination observed and will be helpful to further improve the receptor design in a near future.

3.2. Receptor 20

Receptor *(S)*-**2** was able to extract L-phenylglycine from a saturated aqueous solution with 18-crown-6 ether as ammonium binding moiety but, in our opinion, the results could be improved by placing both the carboxylate and the ammonium binding groups in the same molecule. This should reduce the entropic cost for the association.

As receptor *(S)*-**2** does not have any evident anchoring point to attach the crown ether, a different design was considered (Figure 30). This new receptor involves a 2-naphthoic acid platform where both the oxyanion-hole mimic and the crown ether are attached. This scaffold had already provided good results for anion association in our research group.[57] In this case, a phenylenediamine unit, which is a common motif in the synthesis of molecular receptors,[58] was also incorporated to act as hydrogen bond donor. The crown ether unit associates the ammonium group of the amino acid, while NH groups provide the necessary hydrogen bonds to bind the carboxylate group. The ethylsulfone and cyclohexyl groups increases the solubility of the receptor in organic media, and avoid possible π-π stacking between the aromatic rings which could cause dimerisation troubles. Also, the ethylsulfone increases the NH acidity at position 8.

[57] Pacho, D. Trabajo de Fin de Grado, **2019**, *Universidad de Salamanca.*
[58] (a) Ultowski, F.; Jurczak, J. *Tetrahedron: Asymmetry* **2014**, *25*, 962 – 968. (b) Ghosh, K.; Saha, I. *Tetrahedron Lett.* **2008**, *49*, 4591 – 4595. (c) Brooks, S. J.; Gale, P. A.; Light, M. E. *Supramol. Chem.* **2007**, *19(1 – 2)*, 9 – 15. (d) Gale, P.A *Acc. Chem. Res.* **2006**, *39*, 465 – 475.

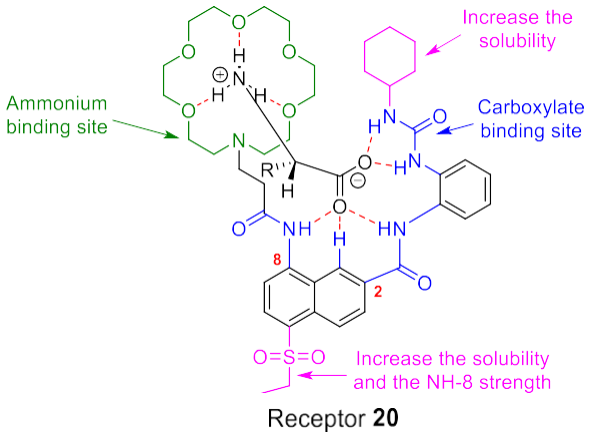

Figure 30. *Associate model between receptor* **20** *an a generic α-amino acid.*

Receptor 20 *synthesis*

2-Naphthoic acid can be easily modified at C–8 by electrophilic aromatic substitution, such as nitration. Nevertheless, this reaction cannot be carried out directly because C–5 is more reactive than C–8. Therefore, naphthoic acid C–5 must be blocked first, for example by bromination. The synthesis began with the bromination of 2-naphthoic acid to obtain 5-bromo-2-naphthoic acid **10**. This procedure has been optimized in our research group,[59] since the original procedure[60] using molecular bromine and AcOH led to mixtures of brominated compounds at C–5 and C–8 (Figure 31) difficult to purify by crystallization or chromatography. To increase the reactivity at C–5, 98% H_2SO_4 was employed as solvent for the reaction but, unfortunately, a mixture of compound **10** and dibrominated compounds in C–5 and C–8 (Figure 31) was obtained, even adding substoichiometric amounts of Br_2. This result can be explained if the bromide is reoxidised to bromine by H_2SO_4.

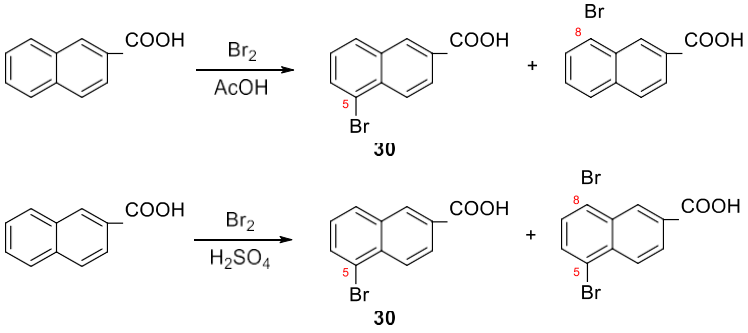

Figure 31. *Bromination of 2-naphthoic acid in AcOH (above) and in 98% H_2SO_4 (below).*

[59] Rodríguez Gil, V. *Trabajo de Fin de Grado*, **2019**, Universidad de Salamanca.
[60] Prager, B.; Jacobson, P. *Beilsteins*, 4th ed. **1926**, *9*¸ 652.

To optimize the reaction, NaBr was used as a source of bromine since as it is a stable solid, it is easier to handle and measure an exact amount (Figure 32). Pleasingly, the portion-wise addition of NaBr to a solution 2-naphthoic acid in 98% H_2SO_4 afforded a crude reaction mixture in which the major compound was the brominated compound in C–5. With the amount of solvent used in these conditions, compound **10** crystallizes out of the reaction, reducing the amount of the dibrominated compound. The reaction was worked up over ice and the subsequent recrystallization of the solid in a mixture of 20% MeOH in DCM yielded 5-bromo-2-naphthoic **10** as a white solid.

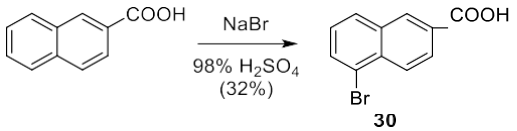

Figure 32. *Bromination of 2-naphthoic acid with NaBr in 98% H_2SO_4.*

The nitration of 5-bromo-2-naphthoic acid **10** was carried out with a solution of 60% HNO_3 in H_2SO_4 (4:40 mL) keeping the reaction below 25°C to avoid the naphthtlene polynitration. The reaction was worked up with ice and the solid obtained was recrystallized in AcOH to eliminate polybrominated and polynitrated side products.

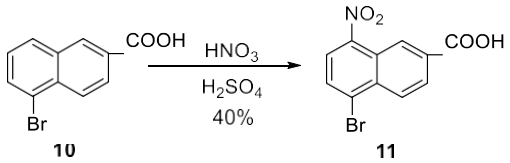

Figure 33. *Nitration of compound* **10**.

Then, the nitro group of compound **11** was reduced to amine. Previous experiments in our research group[61] had shown that the bromine atom at C-5 was sensitive to both Zn / AcOH and H_2 / Pd reduction conditions, and complex mixtures were obtained. To avoid this problem, bromine atom was replaced by an ethylsulfone. Also, the ethyl group increases the solubility of the receptor and the presence of the bulky sulfone reduces π-π stacking interactions between the aromatic rings of the receptor while increasing the NH acidity in C-8.

The nucleophilic aromatic substitution of compound **11** was performed with sodium ethanethiolate under reflux. The deprotonation of the thiol was carried out with NaOH, which also deprotonates compound **11** carboxylic acid, so the reaction can take place in water.

To avoid the propagation of bad odors the oxidation of the thiol to the sulfone was carried out *in situ*, without the isolation of compound **12** (figure 9). Oxidation was peformed in an aqueous basic medium with Oxone® as oxidizing agent and K_2CO_3 as auxiliar base. Under

[61] Gacho Temprano, A. Trabajo de Grado, **2016**, *Universidad de Salamanca.*

these reaction conditions, the excess of ethanethiol was also oxidized and removed from the reaction media after acidification with 35% aqueous HCl and sulfone **13** filtration.

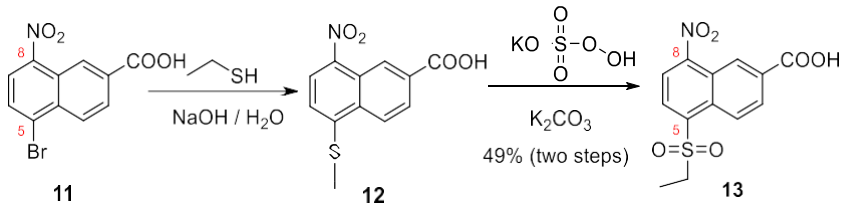

Figure 34. *Nucleophilic aromatic substitution at C-5 favoured by the nitro group at C-8 and thioether oxidation to obtain compound* **13**.

Commercially available *o*-phenylenediamine was used as starting material. However, the reaction between *o*-phenylenediamine and cyclohexyl isocyanate did not generate the expected product but a mixture of unreacted phenylenediamine and a phenylendiamine with two ureas attached to each amino group. We believe that, once the first amino group reacts with one molecule of cyclohexyl isocyanate, the urea catalyses the reaction between the free amino group and a second molecule of cyclohexyl isocyanate, as it is shown in Figure 35.

To solve this problem, the reaction was run in the presence of tetraethylammonium chloride, which should block the first urea by hydrogen bonding (Figure 10). However, double functionalization was obtained again.

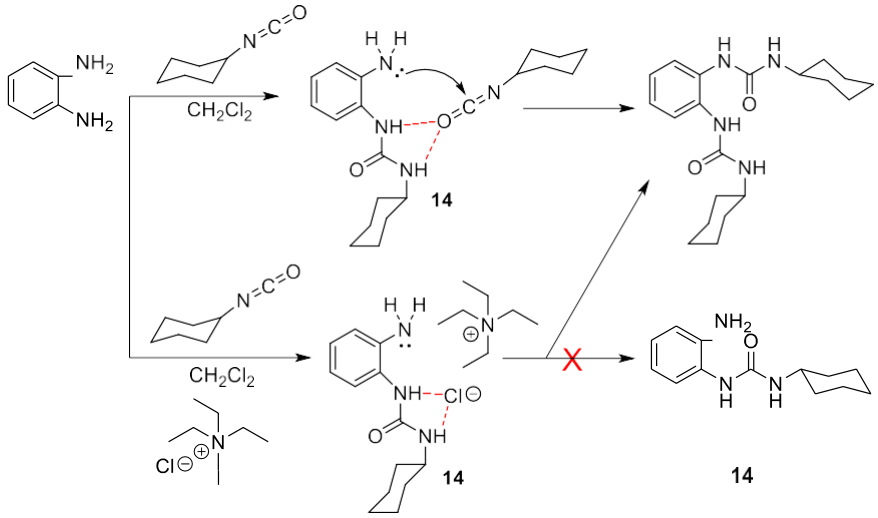

Figure 35. *Reaction between o-phenylenediamine and cyclohexyl isocyanate and proposed associate to yield the double urea product.*

To avoid these problems, 2-nitroaniline was mixed with cyclohexyl isocyanate in EtOAc at room temperature, however no reaction was observed. The nitro group makes the aromatic ring so electron-deficient, that the amino becomes a poor nucleophile. It was necessary to remove the solvent and heat the reaction to 160°C for 16 hours to obtain the desired product. Pleasingly, urea **15** crystallised under the reaction conditions, and it was purified by filtration.

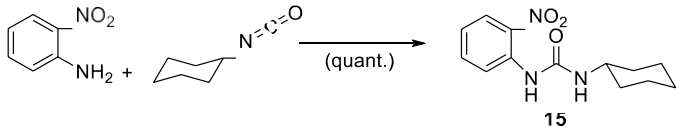

Figure 36. *Synthesis of compound* **15**.

Curiously, compound **15** characterization was tricky since two sets of signals in both ^{1}H and ^{13}C NMR spectra were observed. Since the mass spectrum confirmed the structure, in our opinion the duplicated signals corresponded to two different spatial arrangements (Figure 37). In both conformers, the same number and type of spectroscopic signals are obtained, but with different chemical shifts since the protons environment is different.

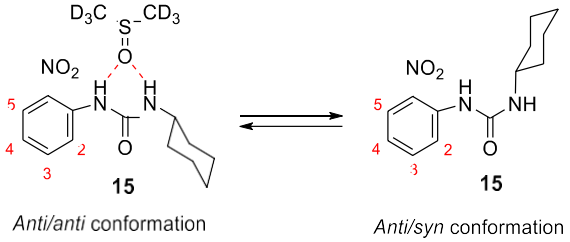

Figure 37. *Anti/anti and anti/syn urea conformations in compound* **15**.

The ^{1}H spectrum was recorded in DMSO-d_6. The largest change was observed for the cyclohexyl NH doublet, which in the *anti*/*syn* conformation resonates at 5.55 ppm and in the *anti*/*anti* conformation resonates at 7.48 ppm. This impressive shift can be explained because in this conformation the NH is hydrogen bonded to the oxygen of DMSO-d_6, as shown in Figure 37. The aromatic NH singlet resonates in the *anti*/*syn* conformation at 9.29 ppm, while in the *anti/anti* conformation appears at 10.50 ppm. In addition, 4 triplets corresponding to H-3 and H-4 were observed. They resonate between 7.05 and 7.73 ppm. The same trend is observed for H-2 and H-5, where 4 doublets appears between 7.94 and 8.37 ppm.

Once structure **15** was confirmed, the nitro group was reduced to the amino group. The first attempt was carried out with Zn / AcOH at 60°C following the standard conditions previously developed in the research group[61] but, unfortunately, this option did not lead to the desired

product with good yield. A literature search showed that Medvedeva[62] had reported that this type of compounds could be easily reduced with $(NH_4)_2S$ in an alcoholic solvent. In our case, the addition of Na_2S in 25% EtOH/THF and heating under reflux reduced compound **15** to compound **16** quantitatively.

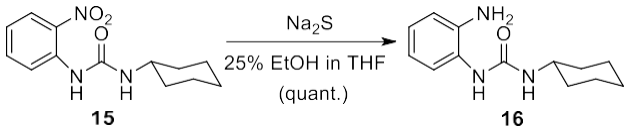

Figure 38. *Compound* **15** *reduction using* Na_2S.

In order to attach compound **16** to the naphthalene skeleton, compound **13** was treated with PCl_5 in DCM at room temperature for 30 minutes. After solvent distillation under low pressure the acid chloride was obtained. The coupling between compound **13** acid chloride and amine **16** was carried out using Schotten-Baumann conditions in a standard procedure.[63] The amine **16** was dissolved in EtOAc with a saturated Na_2CO_3 aqueous solution, maintaining vigorous stirring. The acid chloride, dissolved in EtOAc, was added over this mixture. Compound **17** was obtained after decantation and solvent distillation.

Compound **17** characterization by ^1H NMR showed an interesting fact. As shown in Figure 39, the urea carbonyl bond changes its conformation and behaves as a hydrogen bond acceptor of carboxamide NH at C-2. This pattern is consistent with the strong deshielding of H-1 at 8.96 ppm and the absence of a deshielded doublet for H-5 which should have a similar shift as H-2 in $CDCl_3$. H-2 resonates at 7.85 ppm due to the presence of the carboxamide carbonyl group.

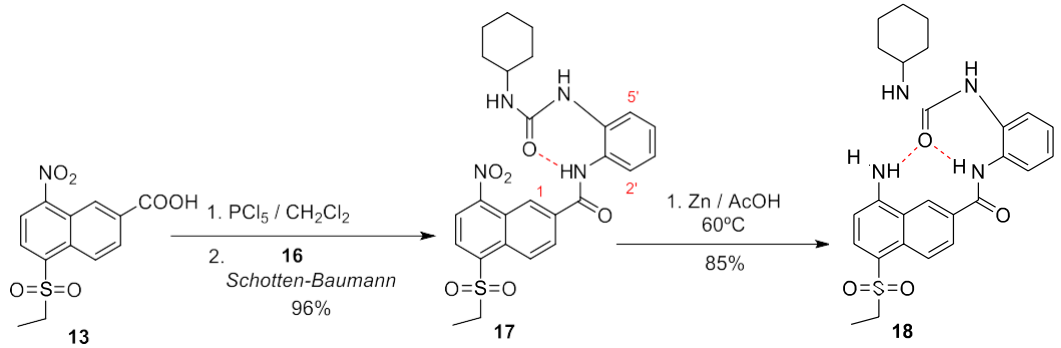

Figure 39. *Compound* **17** *synthesis using Schotten-Baumann conditions and subsequent nitro reduction with Zn.*

[62] Medvedeva, M.M.; Pozharskii, A.F.; Kuz'menko, V.V.; Bessonov, V.V.; Tertov, B.A. *Chem. Heter. Comp.* **1979**, *15*, 166 – 172.
[63] Wade, L.G. *Química Orgánica.* 5th ed. Pearson-Prentice Hall, Madrid, España, 2004, p. 859.

The reduction of the nitro group was achieved using the standard conditions developed in the research group.[61] A mixture of Zn and AcOH was maintained at 60°C with vigorous stirring and compound **17** was added. The temperature increased since the reaction is exothermic and the reaction color turned from yellow (typical of the nitro group) to a greenish color as the reaction proceeded. After 5 minutes, the reaction was diluted with EtOAc and metallic Zn was filtered off. The ^{1}H NMR spectrum of compound **18** also showed two intramolecular hydrogen bonds between the urea carbonyl group and the NHs of the carboxamide and the amine groups.

Then, acryloyl chloride was coupled with amine **18**. This step required the synthesis of acryloyl chloride by treating freshly distilled (24 mmHg) acrylic acid with thionyl chloride (b.p. 76°C) and subsequent purification by low pressure distillation (24 mmHg). Compound **18** was reacted with acryloyl chloride in TFH at reflux to afford compound **19**. No auxiliar base was necessary in the reaction because the sulfone makes the aromatic ring electron-deficient and therefore the aromatic amine is poorly basic. Compound **19** crystallized in the reaction media after Et_2O addition.

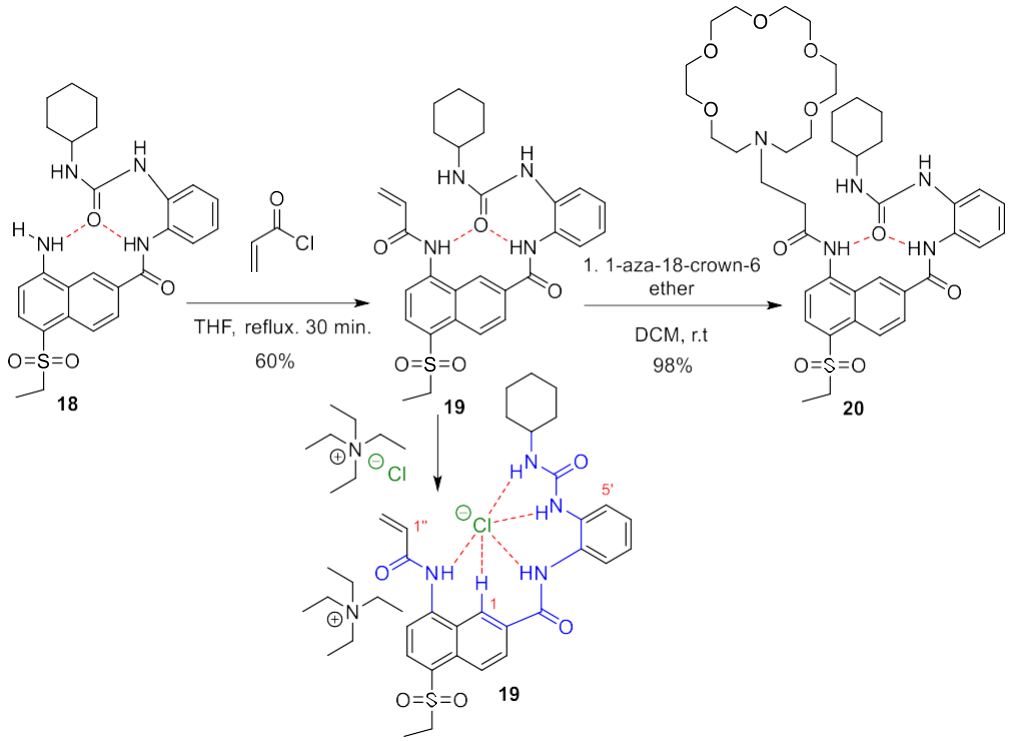

Figure 40. *Amide* **19** *synthesis and reaction with 1-aza-18-crown-6 ether to yield receptor* **14**. *Tetraethylammonium chloride association in compound* **19**.

To prove the receptor ability to complex anions, tetraethylammonium chloride was added to a compound **19** solution (*ca.* 5 mg in 400 μL $CDCl_3$). The first interesting observation was that the H-5 doublet deshielded from 7.20 to 7.85 ppm. This shift evidences the chloride

association in the receptor cavity and the change in the urea conformation. The NH protons involved in the association are also strongly deshielded: H-1 shifted from 8.94 to 9.64 ppm and the vinyl proton H-1" from 6.77 to 7.36 ppm.

Once the association ability of compound **19** was confirmed, 1-aza-18-crown-6 ether was coupled to the alkene following a standard procedure developed in our research group.[64] The Michael addition was carried with more than 2 equivalents of 1-aza-18-crown-6 ether under high concentration conditions in DCM as solvent for 16 hours.

Once the reaction was finished, more DCM was added, and the organic phase was washed with distilled water to get rid of the crown ether excess. Again, the ^{1}H NMR spectrum showed the association of the urea carbonyl group inside the receptor cavity.

Extraction studies

In order to study the ability of receptor **20** to extract amino acids from an aqueous solution, the following methodology was developed:

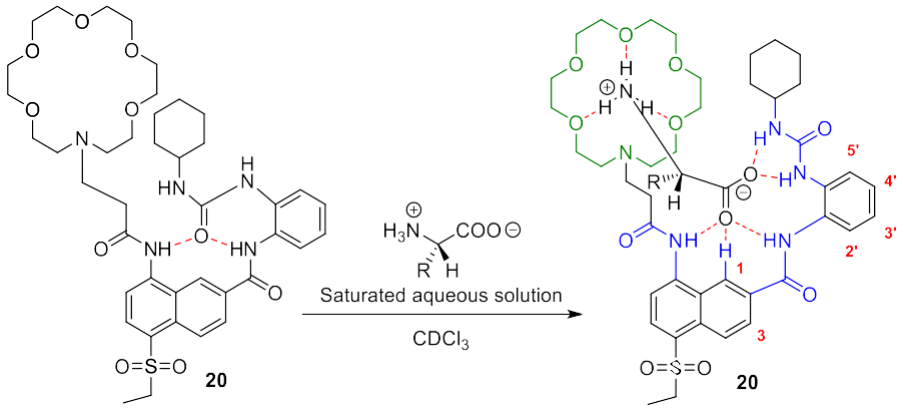

Figure 41. *General scheme for the extraction studies with receptor* **20**.

- Preparation of a receptor **20** solution (*ca.* 10 mg/1 mL in $CDCl_3$).
- Preparation of a saturated amino acid solution (*ca.* 500 µL of distilled water).
- Addition of 500 µL of the amino acid solution to a vial with 500 µL of the previously prepared receptor **14** solution, and vigorous shaking, mixing the two phases.
- The mixture is transferred to an NMR tube, centrifuged and the ^{1}H spectrum is recorded.

[64] Muñoz Muñiz, F. Tesis Doctoral, **2007**, *Universidad de Salamanca.*

The amino acids studied using this methodology were L-leucine, L-phenylalanine and glycine, covering a range of different lipophilicity from higher to lower lipophilic character. The results obtained are shown in Figure 42.

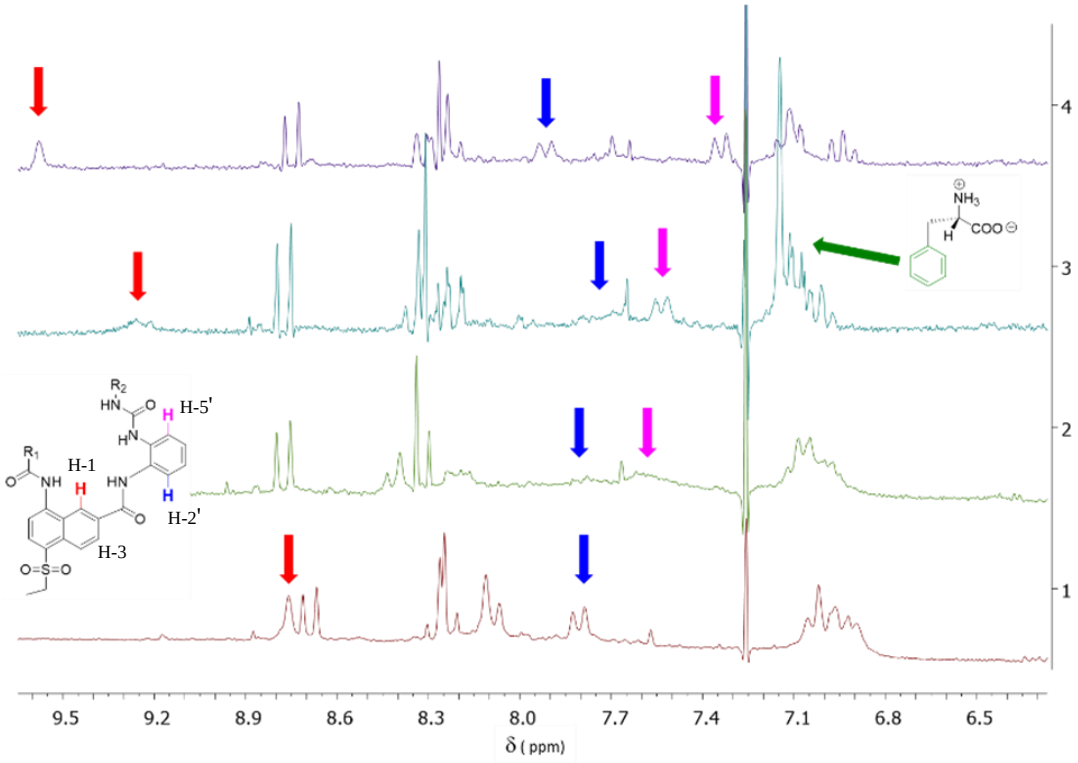

Figure 42. *Extraction studies: ^{1}H NMR spectra of receptor* **20** *(1), in the presence of L- leucine (2), L-phenylalanine (3) and glycine (4). Selected protons are indicated with coloured arrows.*

The biggest changes observed in the ^{1}H NMR spectrum of receptor **20** after amino acid addition takes place in the aromatic region. The amino acid association forces a change in the conformation of receptor **20**, as it was observed with compound **19**. It is remarkable the deshielding experienced by H-1 from 8.76 ppm in the free receptor to 9.28 ppm (associate with L-phenylalanine) and 9.58. ppm (associate with glycine).

Also, H-5 deshields from 7.15 ppm to 7.60 ppm after amino acid association, while H-2' barely shifts (around 7.8 ppm). In the case of glycine, all phenylenediamine protons are very well resolved, with H-5' more shielded (7.35 ppm) than the corresponding protons in the other associates.

In the cases where the signals were broad and their assignment was complicated, a series of irradiation experiments were carried out in the areas where these signals were expected, and the changes associated with vicinal signals were interpreted. For H-1 (coupled in *meta* with H-3), the irradiation confirmed its position by the transformation of the broad doublet at 8.10ppm to a narrow doublet. In the case of H-2' and H-5', irradiation experiments confirmed their position by transforming the triplets corresponding to H-3' and H-4' in doublets, respectively, which resonate 6.92 and 7.01 ppm.

Quantification of the extent of amino acid extraction constituted a challenge. Although a single set of signals was observed in the ^{1}H NMR spectra, this fact does not indicate the complete formation of the associate, since if the associate is weak the observed signal is an average between the associated and the free receptor. Unfortunately, the signal from the amino acid α proton was masked under the crown ether signals, so it was necessary to find another way to analyze the amino acid extraction extent.

Pleasingly, in the case of L-phenylalanine, the aromatic signals between 6.96 and 7.19 ppm allowed to integrate the amount of amino acid extracted to the organic phase. Indeed, this value matched with the amino acid total extraction, highlighting the potential of receptor **20** to extract phenylalanine.

So far, no associates of receptor **20** have been crystallized with any amino acid or organic or inorganic anion to determine the associate geometry by X-ray diffraction analysis. Anyway, the good result obtained with phenylalanine encouraged us to modify the receptor structure with a chiral auxiliary in order to carry out the chiral extraction of amino acids.

Chiral version of receptor **20**

In order to have a chiral receptor based on the structure of compound **20**, the acrylic acid moiety was replaced by metacrylic acid. Compound **21** (Figure 18) was obtained following the methodology described to obtain compound **19**. However, subsequent 1,4-addition of 1- aza-18-crown ether to the α,β-unsaturated carbonyl group did not take place even after the addition of general and Lewis acid catalysts.

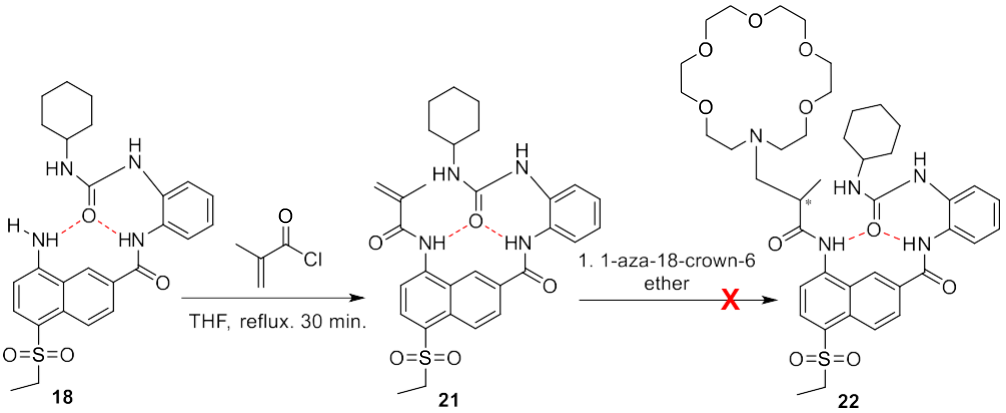

Figure 43. *Synthesis of compound **21** and expected reactivity with 1-aza-18-crown-6 ether.*

3.3. Receptor 28

Since compound **22** could not be obtained, other designs were considered. Phenylenediamine was removed from the initial design to avoid the intramolecular hydrogen bonds between the urea carbonyl group and the two NHs of the oxyanion hole. To facilitate the introduction of the 1-aza-18-crown-6 ether and generate the chiral center, a 2-bromophenylacetic moiety was proposed. The position of the bromine leaving group in alpha position to a carbonyl group and in a benzylic position should favour the S_N2 reaction.

As these two moieties could not be attached to the 2-naphthoic acid scaffold, a 4,5-diaminoxantene skeleton was contemplated (Figure 19). Although receptor **28** provides only three NH bonds (receptor **20** contributed with four NH bonds), this skeleton has been successfully used previously in the research group as oxyanion-hole mimic to associate anions and oxyanions (such as acetates or amino acids).[64]

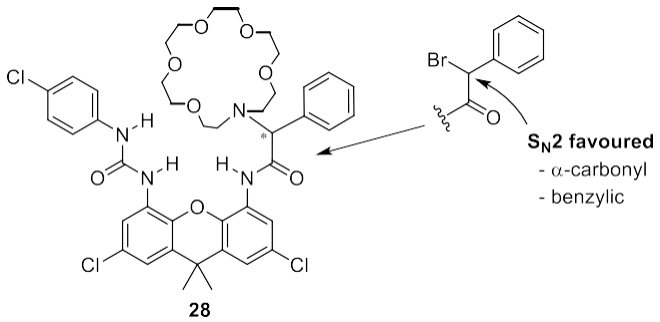

Figure 44. *Receptor **28** based on a 4,5-diaminoxantene scaffold.*

The synthesis of receptor **28** employed amine **23** as starting material (its synthesis was previously optimized in the group).[64] The reaction of amine **23** with *p*-chlorophenyl isocyanate

yielded compound **24**, which crystallized from the crude reaction mixture after Et_2O addition. Then, Boc group was deprotected in neat trifluoroacetic acid to generate compound **25** as the trifluoroacetate salt, which was treated with compound **26** under Schotten-Baumann conditions to afford compound **27**. Finally, the addition of 1-aza-18-crown-6 ether under the reaction conditions already optimised in the synthesis of receptor **20** afforded receptor **28**.

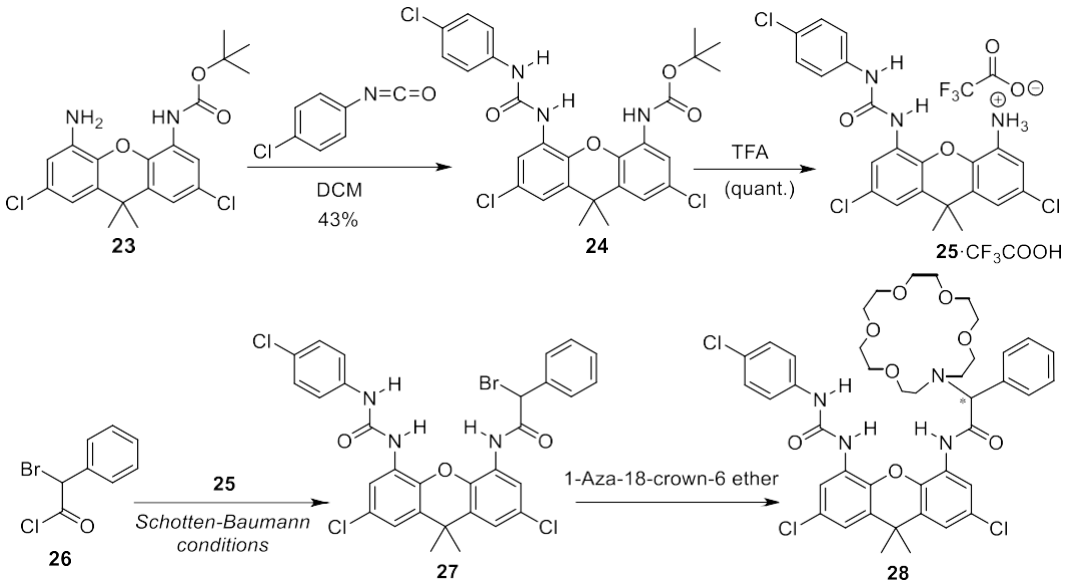

Figure 45. *Synthesis of receptor* **28**.

Interestingly, the ^{1}H NMR of compound **28** showed a complicated set of signals for the alpha protons of the aza-crown ether nitrogen. Usually, all the protons of the aza-crown ether appear as a broad singlet. However, in this case, a strong intramolecular hydrogen bond between the aza-crown ether nitrogen and the carboxamide NH was proposed to explain the signal splitting caused by the diastereotopic protons adjacent to the nitrogen atom of the aza-crown ether.

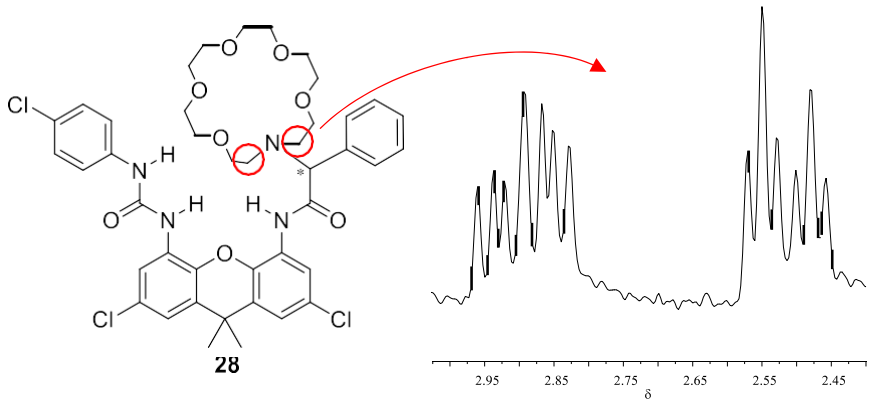

Figure 46. *^{1}H NMR spectrum (2.95 - 2.45 ppm) of compound* **28**.

Extraction studies

Following the methodology described in the previous section, extraction studies with different amino acids were carried out. Surprisingly, no changes were observed in the ^{1}H NMR spectra after amino acid addition. We believe that the strong intramolecular hydrogen bond between the aza-crown ether nitrogen and the carboxamide NH prevents the receptor to associate amino acids. Only potassium acetate, where the potassium cation fits perfectly in the 18-crown-6 ether, showed a weak association with the acetate molecule.

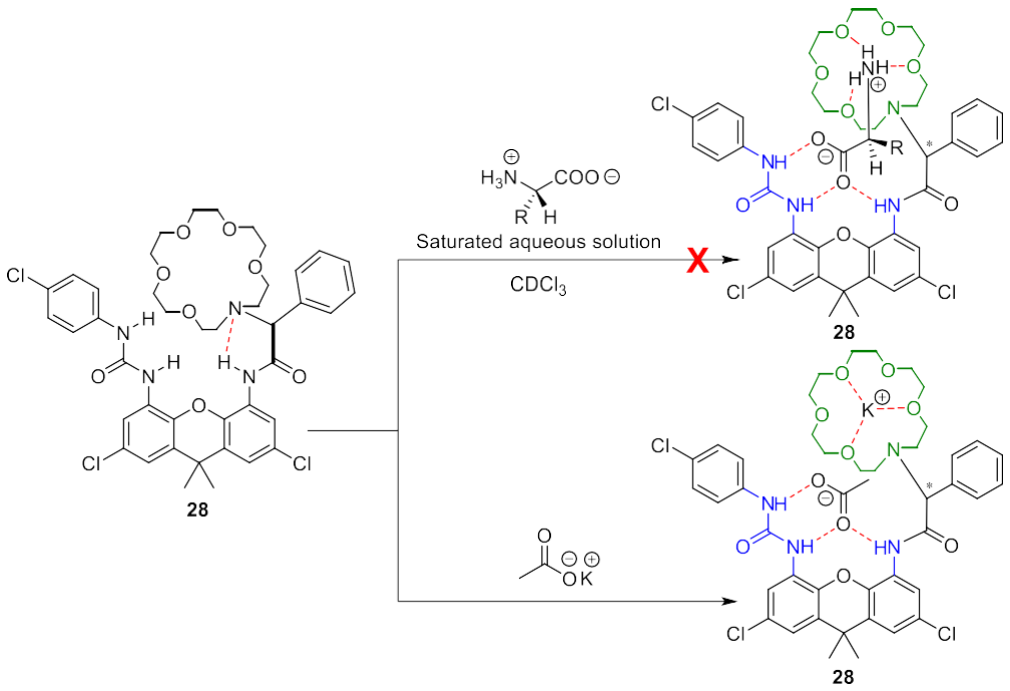

Figure 47. *General scheme for extraction studies with receptor* **28**.

3.4. Receptor 29

In order to avoid the intramolecular hydrogen bond which prevents amino acid extraction in receptor **28**, a larger spacer between the xanthene skeleton and the aza-crown ether was required. To this end, tyrosine was chosen. In addition, tyrosine has a methylene group which confers more flexibility to the spacer, allowing the aza-crown ether to adapt better to the ammonium group of the amino acid. Also, the presence of a hydroxyl group on the tyrosine aromatic ring facilitates the incorporation of an anchoring point by chloromethylation of the electron-rich aromatic ring (Figure 48). The utilisation of chiral L-tyrosine allows the direct

introduction of the chiral auxiliary in the receptor and avoids tedious racemic mixture resolution procedures.

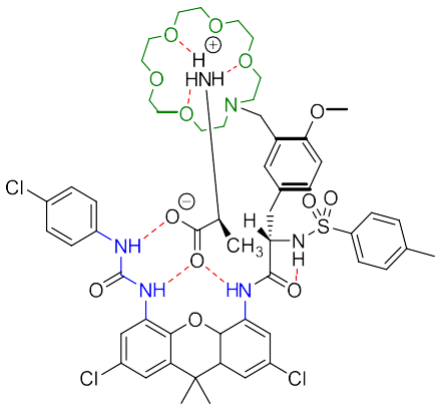

Figure 48. *Associate model between receptor* **29** *and L-alanine.*

An additional intramolecular hydrogen bond between the sulfonamide group and the carboxamide carbonyl group should make receptor **29** more rigid and therefore its ability to carry out the enantioselective extraction of racemic mixture of amino acids should be favored.

To prove this hypothesis, modelling studies of the complex between receptor **29** and L-alanine were performed (Figure 49). The DFT model shows that the distance between the nitrogens of the aza-crown ether and the ammonium group is only 3.23 Å, which is short enough to ensure the formation of the complex. The distance between the α–carbon of the amino acid and the carboxamide receptor is 4.30 Å, which indicates that the amino acid fits freely in the cavity. The distance between the hydrogens in the α position of the aforementioned carbons corresponds to 2.60 Å, 0.60 Å longer than the distance between them if they were in contact, which again confirms that there should be no steric hindrance and the formation of the complex should be facilitated. Enantioselective recognition lies in the steric hindrance between the lateral chain of the amino acid and the tyrosine spacer, as the substitution of the α–hydrogen of L-alanine by the methyl group of D-alanine generates steric hindrance.

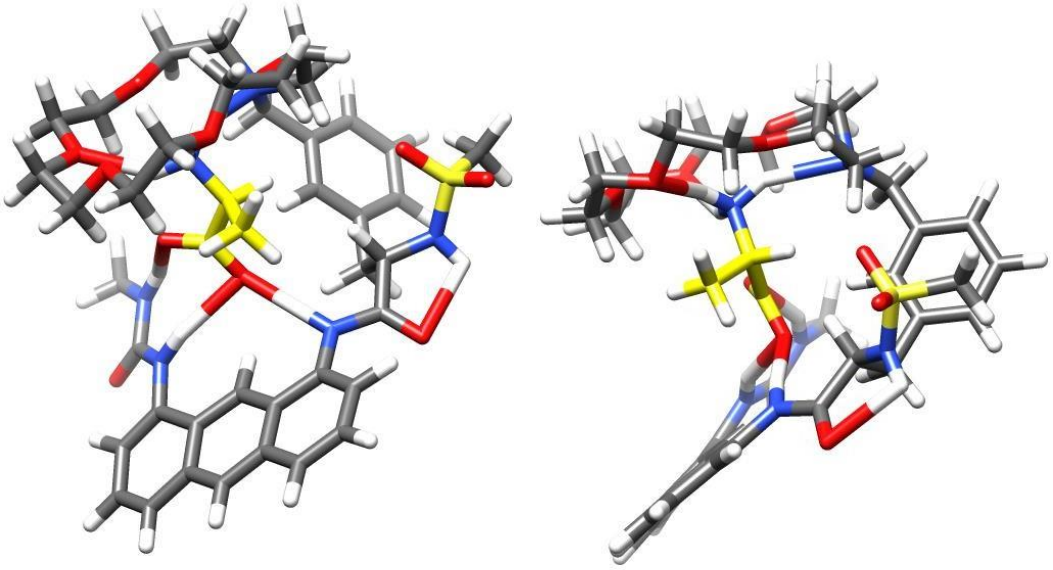

Figure 49. *DFT optimized (HF) structure for receptor* **29**. *Chlorourea and xanthene scaffolds were simplified to shorten the calculation time.*

Receptor* 38 *synthesis

The first attempt to tosylate the amino group of L-tyrosine in basic aqueous conditions, using NaOH and TsCl at reflux, afforded a solid precipitate where the tosyl ^{1}H NMR signals were duplicated. ^{1}H NMR interpretation revealed that the ditosylated compound **30** was obtained instead, with a tosyl group on the amino and another on the phenolic OH, as it is shown in Figure 50.

Although we were planning to protect the OH group of the tyrosine aromatic ring, maintaining the tosyl group in the phenolic OH could increase the steric hindrance too much. At this point, two possible strategies were proposed to avoid the ditosylation: (i) hydrolysis of the tosylated phenol or (ii) finding other reaction conditions where the phenol does not react with TsCl.

Considering that compound **30** was very insoluble in basic aqueous medium (which is a surprising result, since the sodium salt of compound **30** would be expected to be soluble in water), the first strategy would require a co-solvent as DMSO and maintain a reflux system. Alternatively, the second strategy would require a less polar solvent than water, for example methanol. In this scenario, the generation of the phenolate necessary to react with TsCl is discouraged.

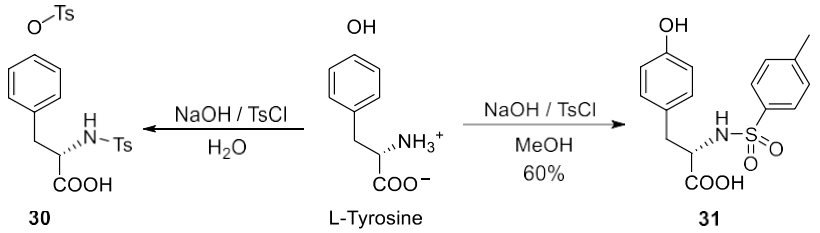

Figure 50. *Synthesis of monotosylated* **31** *and ditosylated* **30** *from L-tyrosine.*

The more atom-economical second strategy was addressed first. L-tyrosine was dissolved in MeOH while keeping the mixture at reflux and then TsCl was added. After 10 minutes, the reaction mixture was filtered under vacuum to remove undesired ditosylated compound **30**. Acidification of the mother liquors allowed the isolation of monotosylated compound **31**.

Then, compound **31** phenolic OH was methylated with CH_3I and NaOH in THF to afford compound **32** upon acidification. Compound **32** was chloromethylated with paraformaldehyde and 35% aqueous HCl at 35°C using AcOH as solvent. However, the ^1H NMR spectrum of the product revealed that the desired compound was not obtained, but a mixture of starting material and a compound containing a six-membered ring formed between the aromatic ring and the tosyl amino group with formaldehyde in a Pictet-Spengler reaction (Figure 51)[65].

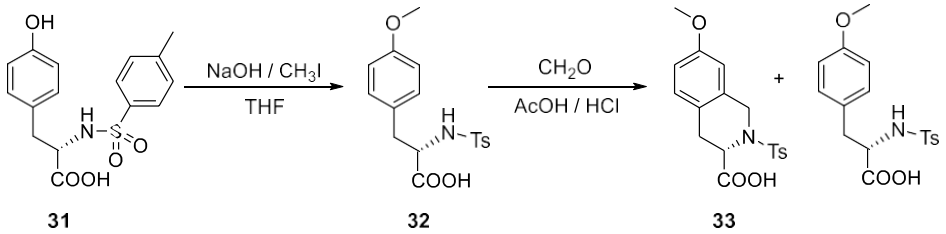

Figure 51. *Phenolic OH methylation and chloromethylation of compound* **32**, *where a Pictet-Spengler-type reaction was observed.*

To avoid the formation of compound **33**, the NH of compound **32** was methylated with CH_3I and NaOH. Compound **34** was obtained after acidification (Figure 52).

[65] Pictet, A.; Spengler, T. *Berichte der Deutschen Chemischen Gesellschaft*, **1911**, *44*, 2030 – 2036.

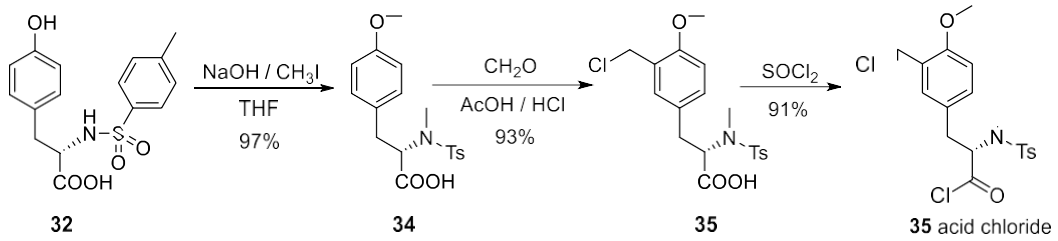

Figure 52. *Methylation of compound* **32** *and chloromethylation to afford compound* **35** *and acid chloride formation with* $SOCl_2$.

Compound **34** chloromethylation was carried out following the same reaction conditions described above to afford compound **35**, which was activated using $SOCl_2$ to generate compound **35** acid chloride.

The first attempt to couple amine **25** with **35** acid chloride was carried out in EtOAc as solvent using pyridine as auxiliar base. Curiously, the ^{1}H NMR spectrum of the reaction crude showed the consumption of the starting materials but the appearance of a novel compound with more signals than expected. After purification by silica gel column chromatography, ^{1}H NMR characterization and irradiation experiments confirmed the structure **36** proposed in Figure 54. We believe that the presence of the pyridinium cation stabilizes the chloride by electrostatic interactions with the help of the oxyanion-hole NHs, as it is shown in Figure 54.

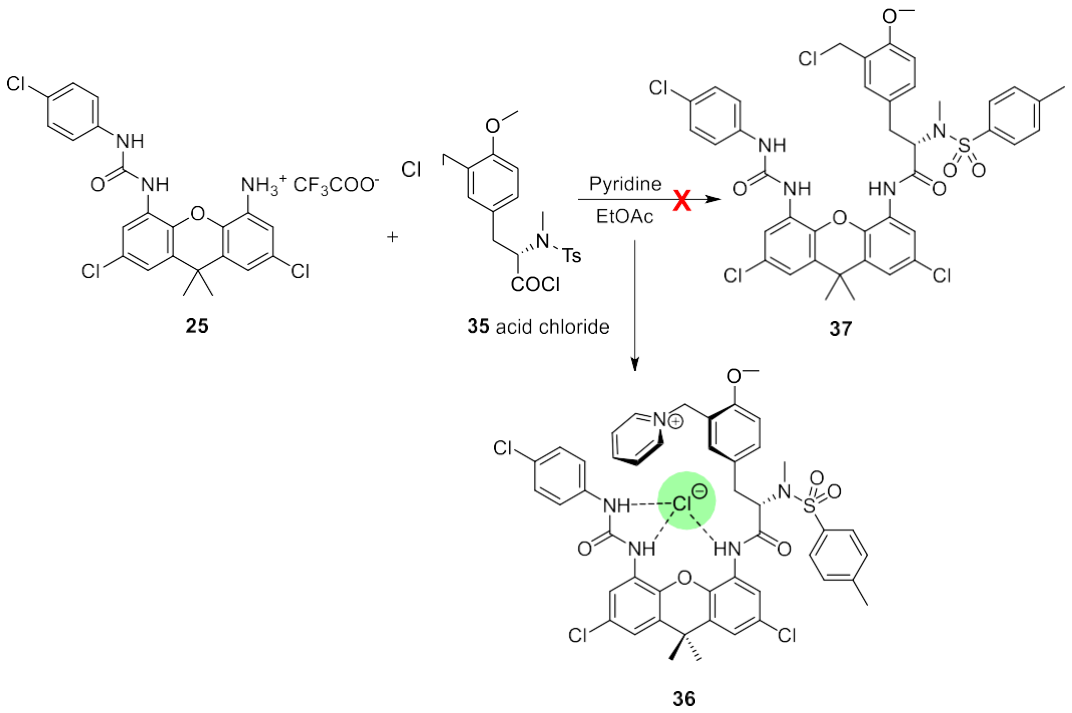

Figure 53. *Unexpected product* **36** *obtained after coupling compound* **25** *with* **35** *acid chloride.*

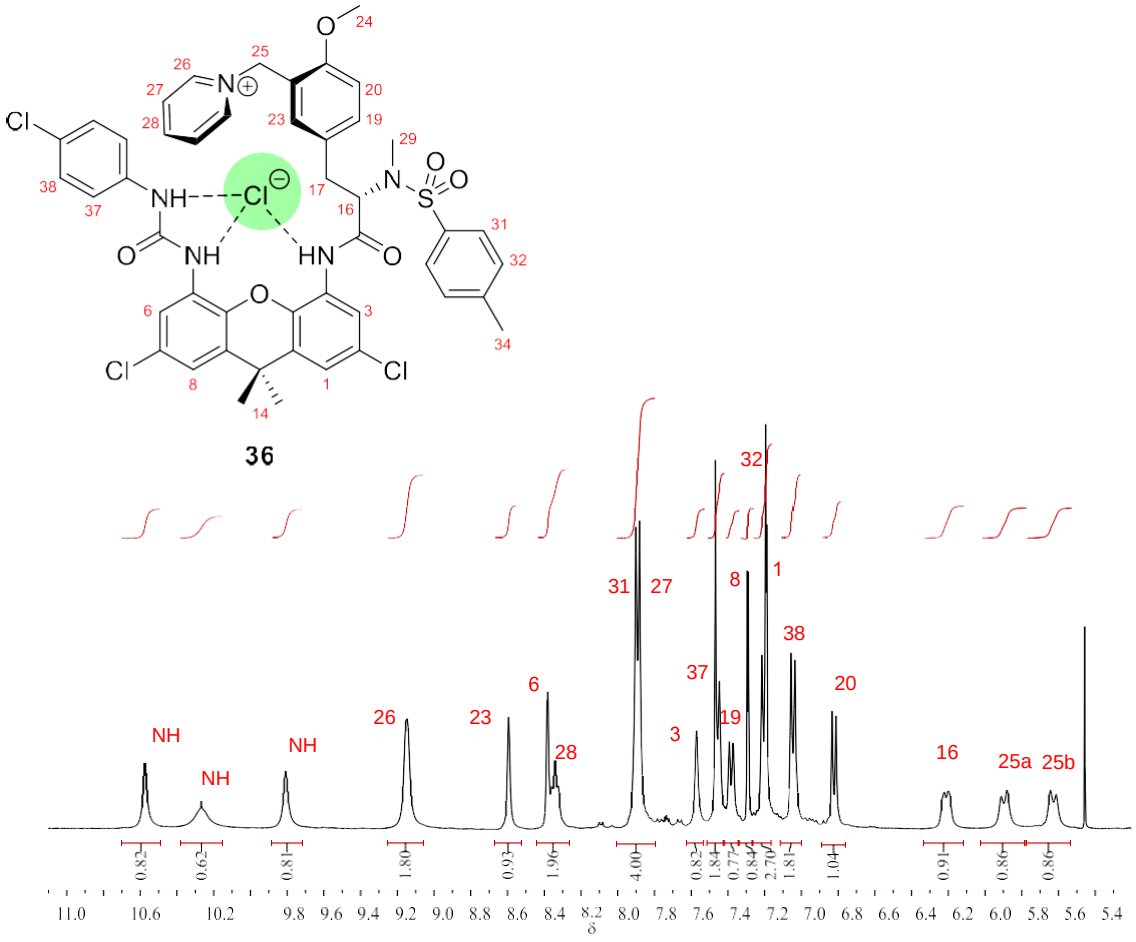

Figure 54. *^{1}H NMR spectrum (11.0 – 5.4 ppm) of pyridinium chloride* **36** *and protons assignment.*

To solve this synthetic problem, pyridine was replaced by non-nucleophilic collidine. The reaction was carried out in neat collidine, but in this case complex mixtures were obtained. Alternatively, compounds **25** and **35** were dissolved in EtOAc and then 3 equivalents of collidine were added to the reaction mixture, but compound **37** was obtained in low yield recovering both unreacted starting acid and the amine in a 1:1 ratio.

We believe that the presence of water in the reaction mixture could explain the low yields obtained. As in the reaction conditions the amine is protonated, the water molecules react first with the acid chloride. Probably, after deprotection of carbamate **24**, the **25** trifluoroacetate salt crystallized with one water molecule responsible which was responsible for the hydrolysis of **35** acid chloride.

In this scenario, we decided to carry out the coupling under Schotten-Baumann conditions. Amine salt **25** was dissolved in EtOAc in the presence of a saturated solution of Na_2CO_3 keeping the reaction at 0°C with ice to minimize the acid chloride and benzyl chloride

hydrolysis. **35** acid chloride was added slowly while maintaining vigorous stirring. It was necessary to purify the compound by column chromatography over silica gel before introducing the aza-crown ether into compound **37** to prevent the latter from associating any cation from silica gel during column chromatography.

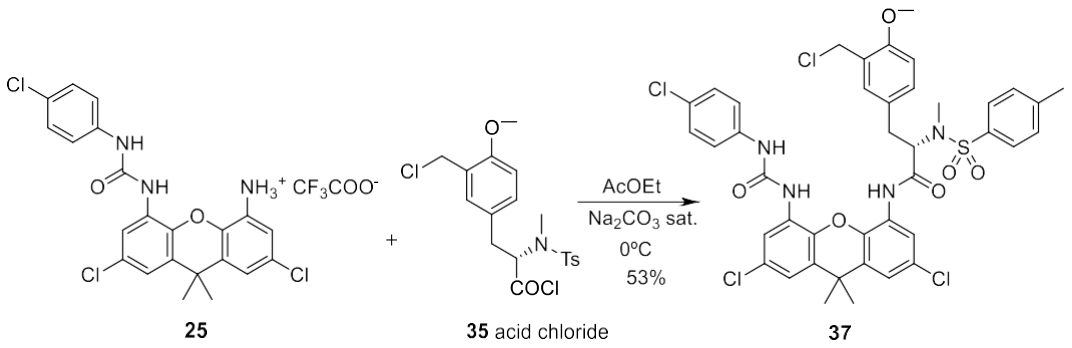

Figure 55. *Compound* **37** *synthesis using Schotten-Baumann conditions.*

The last step consisted in the benzylic chloride S_N2 substitution with 1-aza-18-crown-6 ether. Compound **37** and aza-crown ether were dissolved in the minimum amount of DCM. An excess of crown ether was added to minimize the risk of nitrogen dialkylation which would have generated a quaternary ammonium salt. The use of deionized water in the work-up is important since otherwise the salts from tap water could be associated by the receptor, which has suitable cavities for both cation and anion binding.

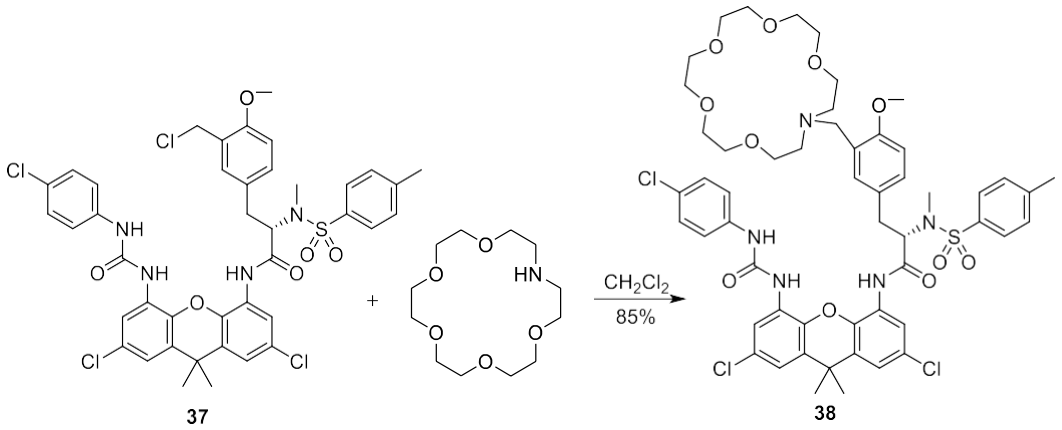

Figure 56. *Receptor* **38** *synthesis.*

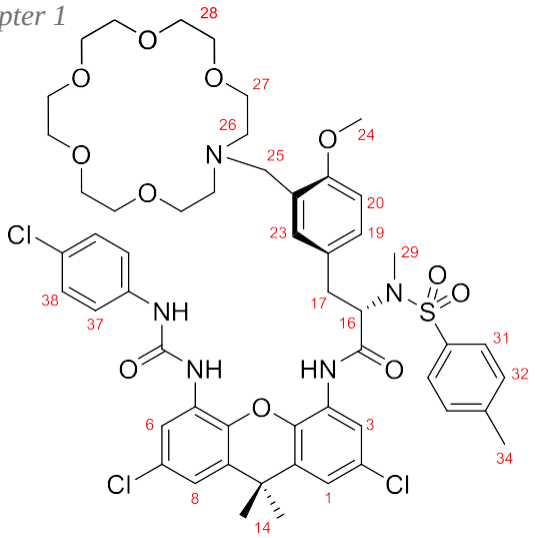

38

Figure 57. *^{1}H NMR spectrum (9.0 – 0.0 ppm) of receptor* **38** *and protons assignment.*

Extraction studies

Extraction studies were carried out following the methodology explained before. As receptor **38** is enantiomerically pure, a racemic amino acid (D and L) mixture was used in the experiments because, if association of the amino acids is successful, the splitting of the proton signals corresponding to both diastereomeric associates would facilitate the interpretation of the extraction experiments and the potential of the receptor to carry out the chiral resolution of racemic mixtures of amino acids. In this case, the amino acid studied were D,L- phenylalanine, D,L-leucine and glycine.

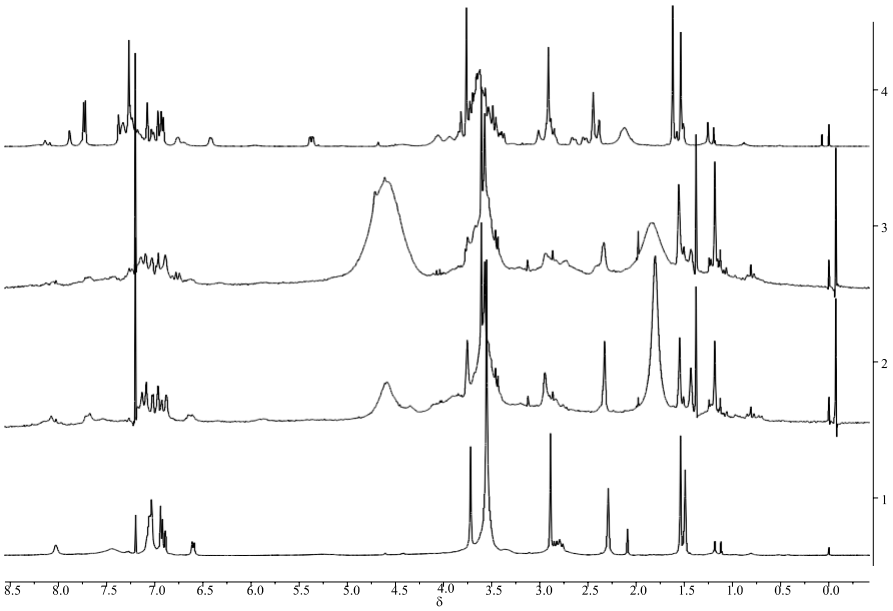

Figure 58. *^{1}H NMR spectra (8.5 – 0.0 ppm) from extraction studies: receptor* **38** *(1), receptor* **38** *with D,L-phenylalanine (2), D,L-leucine (3) and glycine (4) in $CDCl_3$.*

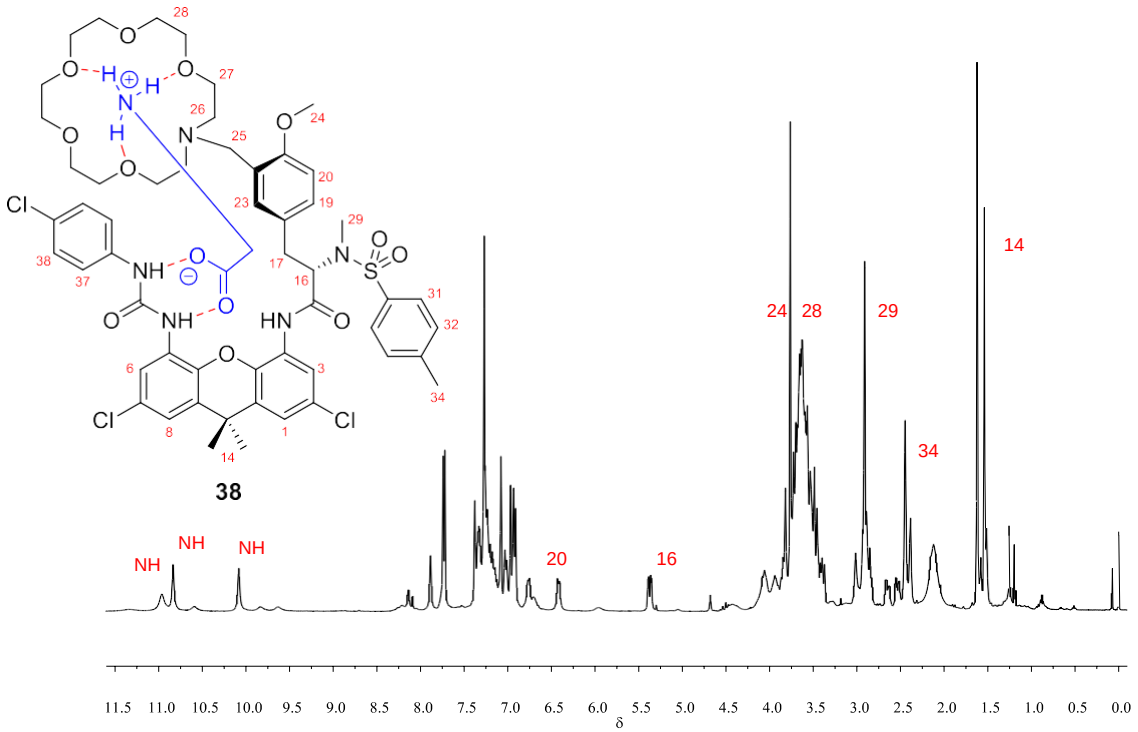

Figure 59. *^{1}H NMR spectrum (11.5 – 0.0 ppm) of the complex formed between receptor* **38** *and glycine in $CDCl_3$ and protons assignments.*

The ^{1}H NMR spectra of Figure 58 showed that receptor **38** was only able to extract glycine, which was the only guest able to induce changes in the ^{1}H NMR spectrum. This result is surprising because glycine is one of the most polar amino acids and consequently one of the most difficult to extract from water. Since glycine is the smallest amino acid, it seems logical to conclude that the reason why the less hydrophilic amino acids are not extracted is steric hindrance. We believe that the cavity of receptor **38** is very small, and can only host glycine.

To confirm that the receptor cavity can only accommodate glycine, a DFT study was performed for the associate between glycine and receptor **38**, as it is shown in Figure 60. This study shows how small the cavity is and the difficulty to place any group bigger than a hydrogen atom in the amino acid α carbon. Apparently, this narrow cavity is a consequence of the methylated sulfonamide nitrogen, which is placed near the cavity reducing its size, so only the smallest amino acid can fit inside.

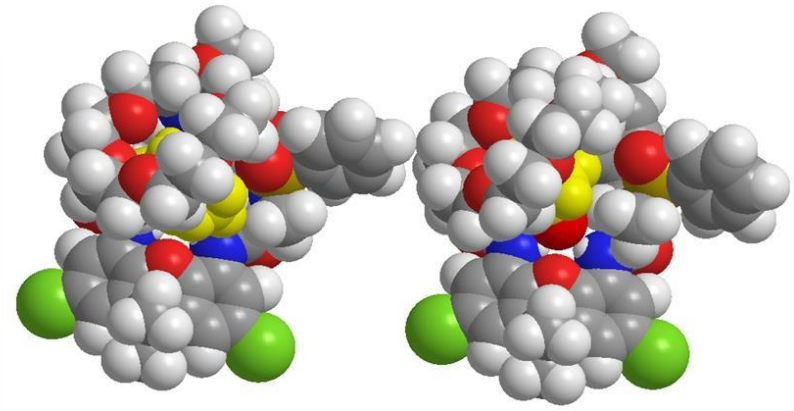

Figure 60. *DFT optimized (HF) structure for receptor* **38** *and glycine associate.*

3.5. Receptor 46

To avoid the negative effect of the *N*-methylsulfonamide on the receptor structure, a new design which exhibit less steric hindrance between the cavity and the associated amino acid was considered. Logically, two hydrogens at the α-carbon of the carboxamide would have caused minimal steric hindrance, but the chiral center would have been lost, so it was proposed to replace one of them with a methyl group.

Following this requirement, racemic receptor **46** was designed (Figure 61, left). DFT optimized structure for the complex between receptor *(S)*–**46** and L-alanine showed that this complex should be feasible as no steric hindrance was observed (Figure 61, right).

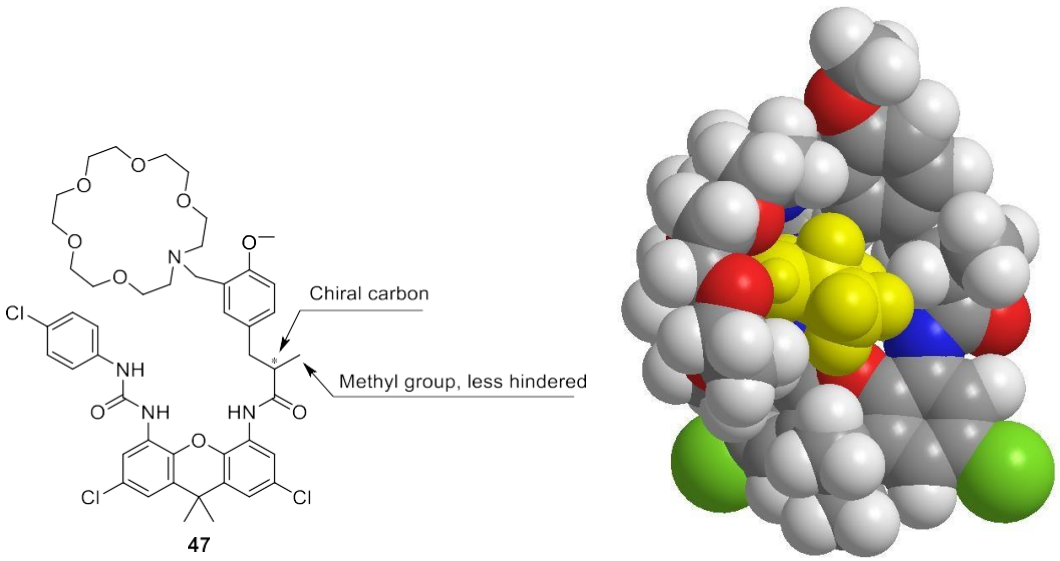

Figure 61. *Proposed receptor* **46** *(left) and DFT optimized (HF) structure for receptor* **46** *complex with L-alanine.*

Receptor 46 *synthesis*

Once all the synthetic problems in the preparation of receptor **38** were known, the preparation of receptor **46** should be straightforward. Also, the absence of heteroatoms that can generate cyclizations prevents the Pictet-Spengler reaction. In this case, *p*-anisaldehyde was chosen to construct the spacer. The aldehyde was easily reduced to the alcohol **39** with $NaBH_4$ in MeOH. Then, the alcohol was treated with $SOCl_2$ to synthesise the chlorinated derivative **40**.

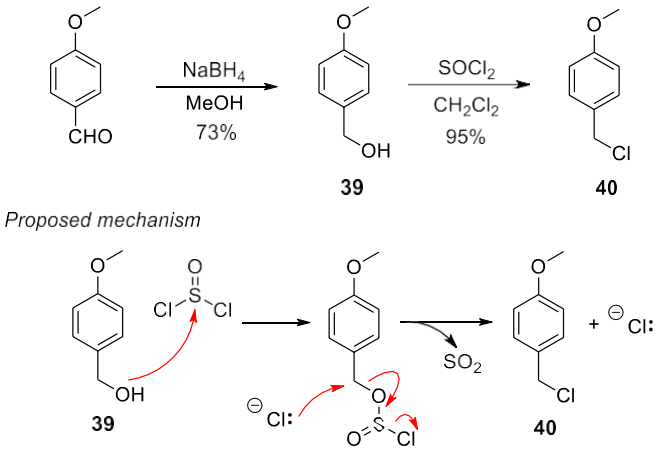

Figure 62. *Anisaldehyde reduction and proposed mechanism for benzyl alcohol substitution by chlorine.*

The next step consisted of a malonic synthesis to replace the chloride with an acid derivative. To introduce a chiral centre in the spacer, diethyl 2-methylmalonate was employed. First, sodium ethoxide was formed dissolving metallic sodium in absolute EtOH, keeping the reaction at reflux until the sodium dissolved. Once the mixture was homogeneous, diethyl 2-methylmalonate was added to obtain the carbanion and then *p*-methoxybenzyl chloride **40** was incorporated into the reaction mixture to obtain compound **41**. The hydrolysis of the ester groups was carried out with KOH in EtOH. The last step consisted of the decarboxylation of compound **42** heating it at 180°C.

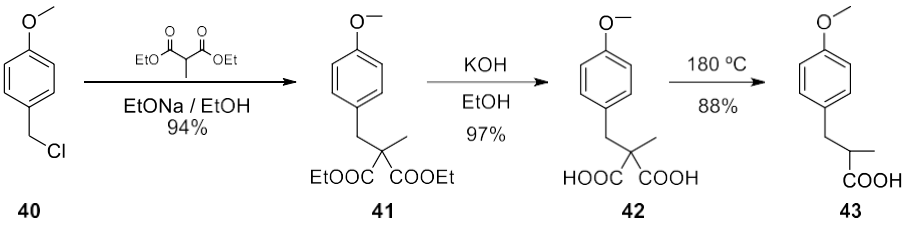

Figure 63. *Synthesis of compounds* **41**, **42** *and* **43**.

Chloromethylation of compound **43** was performed following the same procedure used in compound **34** with paraformaldehyde, 35% aqueous HCl solution and AcOH at 35°C. Then, **44** acid chloride was obtained with $SOCl_2$. Coupling reaction between **44** acid chloride and **25**·CF_3COOH was carried out under Schotten-Baumann conditions, following the same procedure to obtain compound **37**.

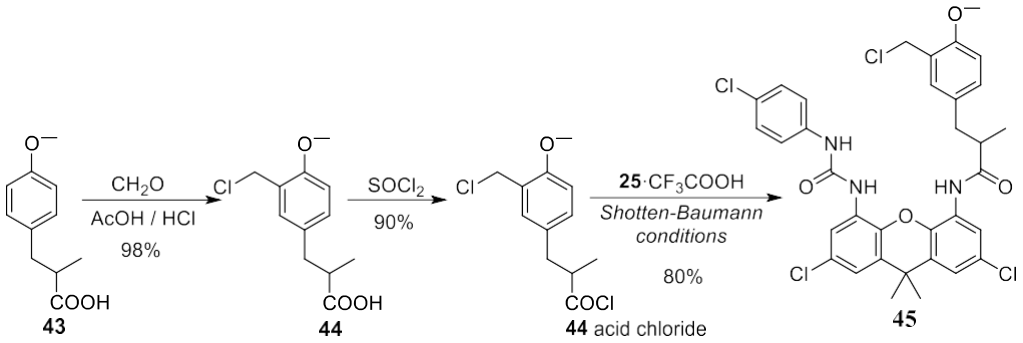

Figure 64. *Synthesis of compound* **45**.

Finally, compound **45** and 1-aza-18-crown-6 ether were dissolved in the minimum amount of DCM and, after 16 hours, EtOAc was added, the organic solvent was washed with distilled water to get rid of the aza-crown ether excess, and receptor **46** was obtained.

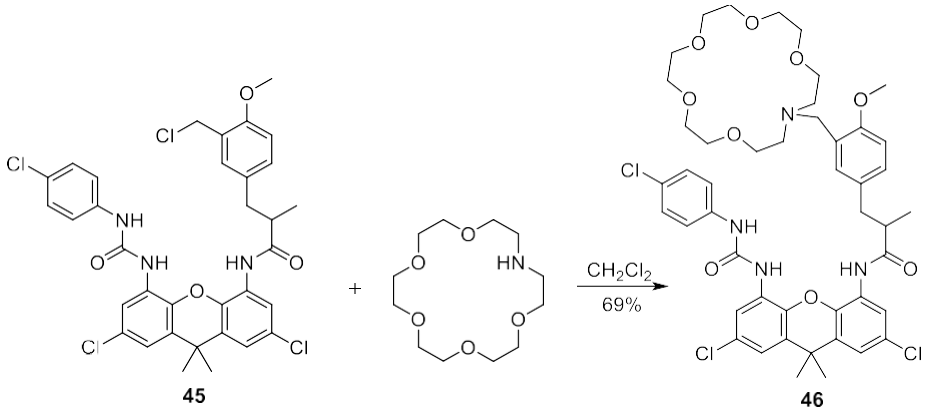

Figure 65. *Receptor* **46** *synthesis.*

Extraction studies

Following the same methodology described with the other receptors, extraction studies were performed. As in this case receptor **46** was obtained as a racemic mixture, enantiomerically pure amino acids (L enantiomer) were used in order to observe the splitting of the signals corresponding to both diastereomeric associates.

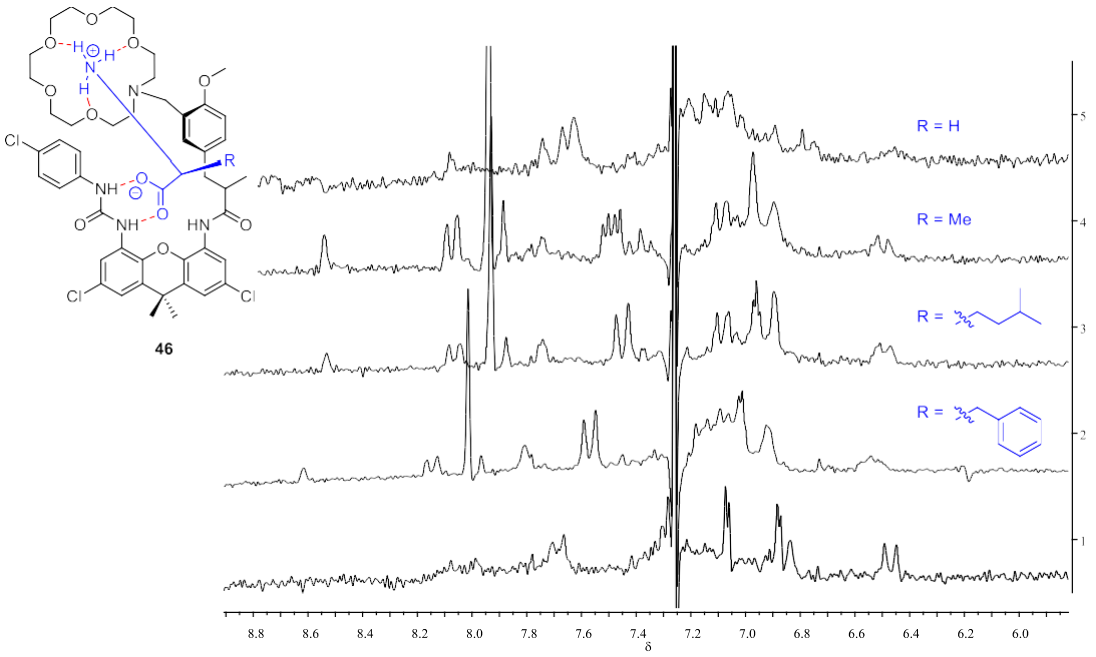

Figure 66. *^{1}H NMR spectra (8.8 – 6.0 ppm) of receptor* **46** *(1) with L-phenylalanine (2), L-leucine (3) and glycine (4).*

The ^{1}H NMR spectra of Figure 66 showed that receptor **46** was able to extract quantitatively all amino acid tested from water to the chloroform phase, which demonstrates the strength of the associates formed and the suitability of the spacer attached between the xanthene and the aza-crown ether. However, it is surprising that no enantioselective recognition was found in the extractions, since both receptor enantiomers associated L-amino acids equally well.

As discussed above, a strong complex was expected to form between the L-amino acids and the (*S*)–receptor, in which the hydrogen at the α position of the amino acid and the hydrogen at the chiral center of the receptor face each other to minimize steric hindrance. If the amino acid configuration was reversed, the hydrogen at α position would change its position with the side chain, and now the side chain would experience steric hindrance with the hydrogen at the chiral center of the receptor. On the other hand, if the configuration of the receptor had been reversed, it would have been the methyl group of the receptor which would have experienced steric hindrance with the hydrogen at position α of the amino acid. In either situation, a steric hindrance would have appeared and consequently the complex should have shown a smaller association constant.

To try to understand the reasons why repulsions between the large groups described above do not show up experimentally in the complex, a new modeling study was carried out. This new study demonstrated that it was possible to keep a close contact between the hydrogen at the α position of the amino acid and the hydrogen at the chiral center of the receptor by changing the position of the aromatic group of the spacer. Figure 67 compares the diastereomeric complexes formed between both enantiomers of receptor **46** and L-alanine. Both structures have a very similar geometry, with similar energies. In both DFT optimized structures, the L-alanine α hydrogen occupies a similar position, which is close to the position of the proton in the chiral center of the receptor.

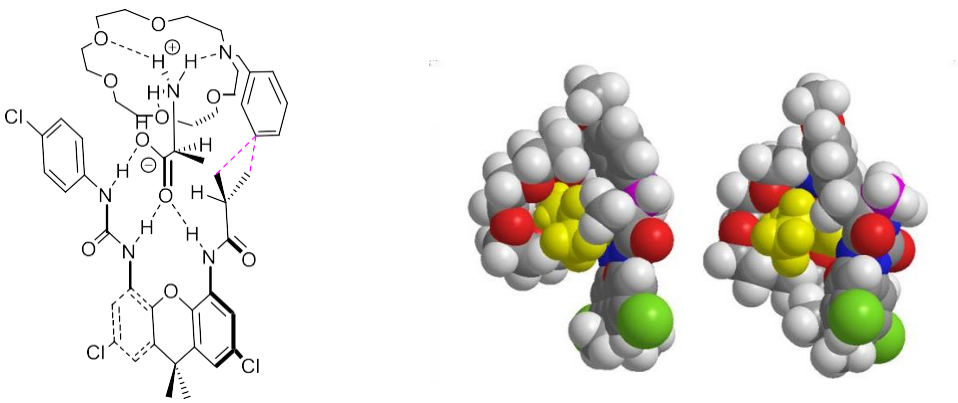

Figure 67. *DFT optimized (HF) structure of the complexes formed between receptor (S)-**46** (left) and (R)-**46** (right) with L-alanine (depicted in yellow).*

In the *(S)*-receptor the spacer group is attached to the carbon located at the right side of the plane of the xanthene (Figure 67), while in the *(R)*-receptor, the spacer is attached to the carbon located to the left side of the xanthene plane. We believe that the aromatic ring of the spacer group can flip between these two positions, which does not affect the whole geometry of the complex, so the two possible diastereomeric associates obtained between L-alanine and the racemic receptor **46** are thermodynamically similar. Therefore, they are extracted in the same proportion from the aqueous solution.

Although the receptors with the aza-crown ether directly attached to the carboxylate binding moiety did not provide amino acid enantiodiscrimination, they were able to quantitatively extract phenylalanine, glycine and leucine from aqueous media, and many of them in a selective way.

Chapter 1 - Conclusions

4. Conclusions

The following conclusions are extracted from this chapter:

- Receptors *(S)*-**2**, **20**, **28**, **38** and **46** were synthesised and fully characterised.

- The combination of a carbazole-BINOL macrocycle *(S)*-**2** with 18-crown-6 ether allowed to extract D-phenylglycine with 91.8% *ee* and D-phenylalanine with 56.4% *ee*.

- Achiral receptor **20**, which combines an aza-crown ether and an oxyanion-hole mimic in the same platform was able to extract racemic phenylalanine from aqueous solution quantitatively.

- Chiral receptor **22** analogue to receptor **20** was not synthesised because of the low reactivity of the aza-crown ether in the addition reaction.

- Receptor **28** based on 1,8-diaminoxanthene scaffold was not able to extract amino acids due to the presence of an intramolecular hydrogen bond between the crown-ether nitrogen and the carboxamide NH. However, potassium acetate was successfully extracted.

- Receptor **38** with a L-tyrosine spacer was synthesised, and the extraction experiments showed a small cavity only available for glycine.

- Chiral receptor **46** analogue to receptor **38** showed quantitative extractions for both enantiomers of hydrophobic amino acids.

Chapter 1 – Experimental Section

5. Experimental Section

5.1. Materials and instrumentation

Reagents

Reagents were purchased and used without further purification unless otherwise noted. The solvents used were purified and dried following the standard methods.[66]

Purification of reaction crudes

Reactions were monitored by analytical thin layer chromatography (TLC) using pre-coated aluminium-backed plates (0.2 mm silica gel 60 F_{254}, Merck®) and visualized by UV light (254 or 365 nm) or different stains such as $KMnO_4$, iodine of phosphomolybdic acid. Compounds purification was performed using silica gel column chromatography (Chromagel 60A SdS. C.C. 70-200 μm) with solvent mixtures with increasing polarity as eluents and crystallization in different solvent mixtures.

Melting Points (m.p.)

Melting points were measured in a Leica Galen III microscope and were reported in ºC.

IR spectroscopy

IR spectra were recorded using a Nicolet IR100 with NaCl crystals as films or with Nujol slurry for solids.

NMR spectroscopy

^{1}H and ^{13}C NMR spectra were recorded at room temperature using Bruker models WP-200-SY, Varian Mercury 200 MHz (200 MHz to ^{1}H and 50 MHz to ^{13}C) and Bruker Advance NEO 400 MHz with a Prodigy CPPBBO BB-H&F z-gradient cryo-probe (400 MHz to ^{1}H and 100 MHz to ^{13}C) spectrometers. Chemical shifts were reported in parts per million (ppm) to the nearest 0.01 ppm for ^{1}H and to the nearest 0.1 ppm for ^{13}C, with TMS or the solvent signal as an internal standard using reported shifts (^{1}H/^{13}C): deuterated chloroform $CDCl_3$ 7.26/77.2 ppm, dimethylsulfoxide DMSO-d_6 2.49/39.5 ppm or methanol CD_3OD-d_4 3.3/49.0 ppm and tetramethylsilane TMS 0.00 ppm.[67] Coupling constants (*J*) were reported in Hertz. The following abbreviations were used to explain the multiplicities: s, singlet; d, doublet; t, triplet; q, quartet; quin, quintet; sext, sextet; m, multiplet; br, broad.

Mass spectrometry

Mass spectra were recorded on a cuadrupole-TOF Applied Biosystems QSTAR XL and Waters ZQ 4000 spectrometers using electrospray ionization (ESI) or electronic impact (EI).

---

[66] Armarego, W. L. F.; Perrin, D. D. Purification of Laboratory Chemicals; 3rd ed.; Pergamon Press: Oxford, 1988.
[67] Gottlieb, H. E.; Kotlyar, V.; Nudelman, A. *J. Org. Chem.* **1997**, *62*, 7512–7515.

Mass spectra were recorded with an Applied Biosystems QSTAR XL using ESI and a quadrupole TOF mass analyzer. Enantiomeric excess (*ee*) was determined with an Agilent 1100 series HPLC, using a Daicel CHIRALPAK ZWIX(+) (analytical Column, 3 µm, ID 3.0 mm x L 150 mm) and a mixture of two solvent systems as eluent: solvent A 98:2 (4:1 mixture of acetonitrile and methanol/ water containing 20 mM formic acid and 20 mM ammonium formate) and solvent B 98:2 (methanol/ water containing 40 mM formic acid and 20 mM ammonium formate).

X ray diffraction studies

X-ray diffraction structures were measured in a Bruker Kappa Apex II with a CCD detector diffractometer. Data were collected at 298(2) K using Cu K_α radiation (λ = 1.54178 Å) and ω scan technique and were corrected for Lorentz and polarization effects.

A series of narrow frames data were collected with a scan width of 0.5º in ω and an exposure time of 10 s per frame. The data were integrated with SAINT[68] to a resolution of 0.78Å using a narrow-frame algorithm. Data were corrected for absorption effects using the multi-scan method using SADABS.[69]

[68] SAINT-NT Version 6.0, Madison, Wisconsin, USA: Bruker –AXS, **2001**.
[69] SADABS 2008/1, L. Krause, R. Herbst-Irmer, G. M. Sheldrick, D. Stalke. *J. Appl. Crystallogr*. **2015**, *48*, 3-10.

Modelling studies

Theorical studies were carried out using GAMESS interface for Chem3D 19.1 software[70] using the semiempirical method AM1 and theorical Hartree-Fock. Calculations were made using Gaussian16 software[71] The M06-2X DFT functional[72] combined with 6-31G(d,p) basis set[73] was employed, along with the GD3 empirical dispersion correction.[74] Gibbs free energy was calculated on the optimized structures using the Quasy rigid rotor harmonic oscillator approximation implemented in Goodvibes.[75] Molecular graphics were prepared using *Pymol*.[76]

[70] G. M. J. Barca, C. Bertoni, L.Carrington, D. Datta, N. De Silva, J. E. Deustua, D. G. Fedorov, J. R. Gour, A. O. Gunina, E. Guidez, T. Harville, S. Irle, J. Ivanic, K. Kowalski, S. S. Leang, H. Li, W. Li, J. J. Lutz, I. Magoulas, J. Mato, V. Mironov, H. Nakata, B. Q. Pham, P. Piecuch, D. Poole, S. R. Pruitt, A. P. Rendell, L. B. Roskop, K. Ruedenberg, T. Sattasathuchana, M. W. Schmidt, J. Shen, L. Slipchenko, M. Sosonkina, V. Sundriyal, A. Tiwari, J. L. Galvez Vallejo, B. Westheimer, M. Włoch, P. Xu, F. Zahariev, M. S. Gordon, *J. Chem. Phys.* **2020**, *152*, 154102.

[71] Frisch, M. J.; Trucks, G. W.; Schlegel, H. B.; Scuseria, G. E.; Robb, M. A.; Cheeseman, J. R.; Scalmani, G.; Barone, V.; Petersson, G. A.; Nakatsuji, H.; Li, X.; Caricato, M.; Marenich, A. V.; Bloino, J.; Janesko, B. G.; Gomperts, R.; Mennucci, B.; Hratchian, H. P.; Ortiz, J. V.; Izmaylov, A. F.; Sonnenberg, J. L.; Williams; Ding, F.; Lipparini, F.; Egidi, F.; Goings, J.; Peng, B.; Petrone, A.; Henderson, T.; Ranasinghe, D.; Zakrzewski, V. G.; Gao, J.; Rega, N.; Zheng, G.; Liang, W.; Hada, M.; Ehara, M.; Toyota, K.; Fukuda, R.; Hasegawa, J.; Ishida, M.; Nakajima, T.; Honda, Y.; Kitao, O.; Nakai, H.; Vreven, T.; Throssell, K.; Montgomery Jr, J. A.; Peralta, J. E.; Ogliaro, F.; Bearpark, M. J.; Heyd, J. J.; Brothers, E. N.; Kudin, K. N.; Staroverov, V. N.; Keith, T. A.; Kobayashi, R.; Normand, J.; Raghavachari, K.; Rendell, A. P.; Burant, J. C.; Iyengar, S. S.; Tomasi, J.; Cossi, M.; Millam, J. M.; Klene, M.; Adamo, C.; Cammi, R.; Ochterski, J. W.; Martin, R. L.; Morokuma, K.; Farkas, O.; Foresman, J. B.; Fox, D. J. *Gaussian 16 Rev. B.01*, Wallingford, CT, **2016**.

[72] (a) Zhao, Y.; Truhlar, D. G., *Acc. Chem. Res.* **2008**, *41*, 157–167. (b) Zhao, Y.; Truhlar, D. *Theor. Chem. Account.* **2008**, *120*, 215–241. (c) Zhao, H.; Truhlar, D. G., *Theor. Chem. Acta* **2007**, *120*, 215–241.

[73] (a) Hariharan, P. C.; Pople, J. A. *Theor. Chem. Acc.* **1973**, *28*, 213–22. (b) Francl, M. M.; Pietro, W. J.; Hehre, W. J.; Binkley, J. S.; DeFrees, D. J.; Pople, J. A.; Gordon, M. S. *J. Chem. Phys.* **1982**, *77*, 3654–3665.

[74] Grimme, S.; Antony, J.; Ehrlich, S.; Krieg, H. *J. Chem. Phys*. **2010**, *132*, 154104.

[75] (a) Grimme, S. *Chem. Eur. J.* **2012**, *18*, 9955–9964. (b) Funes-Ardoiz, I.; Paton, R. S. (2016) GoodVibes v3.0.1. http://doi.org/10.5281/zenodo.595246.

[76] The PyMOL Molecular Graphics System, Version 1.8 Schrödinger, LLC.

5.2. Synthetic details and characterization

Synthesis of racemic macrocycle* 2 *through disconnections a and b

Route a

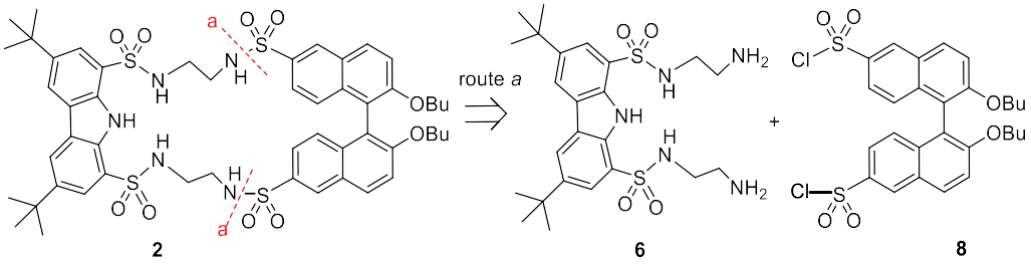

N^1,N^8-bis(2-aminoethyl)-3,6-di-*tert*-butyl-9*H*-carbazole-1,8-disulfonamide (6)

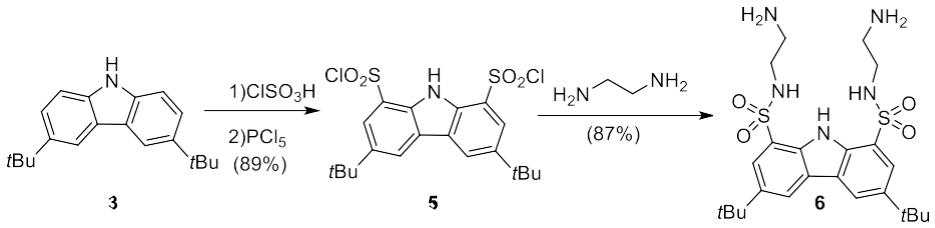

Compounds **3** and **5** were prepared according to published procedures.[77] To a solution of ethylendiamine (2.05 mL, 30 mmol) in methylene chloride (100 mL) was added dropwise a solution of the disulfonyl dichloride **5** (1.60 g, 3.38 mmol) in CH_2Cl_2 (60 mL) with continuous stirring. Once the addition of the disulfonyl dichloride **5** was finished, stirring was kept until the reaction was complete. The progress of the reaction could be monitored by TLC (methylene chloride as eluent). Then, the solvent was removed under reduced pressure and the crude residue was triturated with water. The precipitate thus obtained was filtered, washed and dried under vacuum, to afford 1.52 g (87%) of the desired diamine **6**.

m.p.: 147ºC.

IR (thin film, υ in cm^{-1}): 3423, 3098, 2955, 2864, 1612, 1573, 1495, 1437, 1327, 1288, 1197, 1145, 1041, 963, 898, 736.

^{1}H NMR (200 MHz, 5% CD_3OD in $CDCl_3$) δ 8.23 (s, 2H), 7.83 (s, 2H), 2.95 – 2.80 (m, 4H), 2.80 – 2.65 (m, 4H), 1.37 (s, 18H).

[77] (a) Yang, X.; Lu, R.; Gai, F.; Xue, P.; Zhan, Y. *Chem. Commun*. **2010**, *46*, 1088 – 1090. (b) Fuentes de Arriba, Á. L.; Turiel, M. G.; Simón, L.; Sanz, F.; Boyero, J. F.; Muñiz, F. M.; Morán, J. R.; Alcázar, V. *Org. Biomol. Chem*. **2011**, *9*, 8321 – 8327.

^{13}C NMR (50 MHz, 5% CD_3OD in $CDCl_3$) δ 143.5, 134.1, 124.8, 123.9, 121.9, 121.2, 44.6, 40.8, 35.1, 31.9.

HRMS (ESI+): Calculated for $C_{24}H_{38}N_5O_4S_2$ $[M+H]^+$ 524.2359, found 524.2354.

2,2'-dibutoxy-1,1'-binaphthyl-6,6'-disulfonyl dichloride (8)

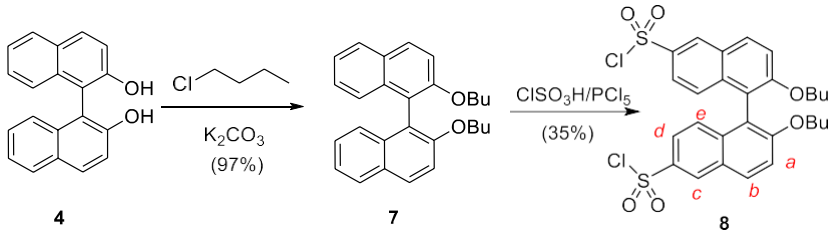

4 7 8

Compound **4** was prepared according to the literature.[78] Compound **8** has been previously prepared in our group,[79] but here we include the detailed procedures for compounds **7** and **8**. 1,1'-binaphthyl-2,2'-diol (BINOL) **4** (20.0 g, 69.9 mmol) was dissolved in DMF (300 mL) in a 1 L round-bottom flask equipped with magnetic stirrer, condenser and under argon. Finely powdered K_2CO_3 (138.0 g, 1 mol) was added followed by addition of butyl chloride in excess (40 mL, 380 mmol) and the reaction mixture was heated at 110ºC for 5 hours. Once the reaction was finished, the mixture was poured onto water and extracted several times with ethyl acetate. The combined organic layers were dried over sodium sulfate and the organic solvent was removed under reduced pressure. The crude residue was purified by crystallization(CH_2Cl_2/ hexane) to afford 27.04 g (97%) of the desired compound **7**.

m.p.: 90ºC.

IR (thin film, υ in cm^{-1}): 3377, 3046, 2955, 2936, 2871, 1619, 1593, 1508, 1469, 1333, 1275, 1255, 1080, 821, 756.

^{1}H NMR (200 MHz, $CDCl_3$) δ 8.02 – 7.90 (m, 4H), 7.58 – 7.21 (m, 8H), 4.15 – 3.91 (m, 4H), 1.58 – 1.38 (m, 4H), 1.18 – 0.98 (m, 4H), 0.80 – 0.62 (m, 6H).

^{13}C NMR (50 MHz, $CDCl_3$) δ 154.9, 134.6, 129.6, 129.4, 128.1, 126.3, 125.8, 123.7, 121.0, 116.1, 69.7, 31.7, 19.1, 13.9.

HRMS (ESI+): Calculated for $C_{28}H_{31}O_2$ $[M+H]^+$ 399.2319, found 399.2323.

---

[78] Kyba, E. P.; Siegel, M. G.; Sousa, L. R.; Sogah, G. D.; Cram, D. J. *J. Am. Chem. Soc.* **1973**, *95*, 2691 – 2692.
[79] Hernández, J. V.; Oliva, A. I.; Simón, L.; Muñiz, F. M.; Grande, M.; Morán, J. R. *Tetrahedron Lett.* **2004**, *45*, 4831 – 4833.

Compound **7** (10.0 g, 25.0 mmol) was dissolved in methylene chloride (300 mL) in a three necked round bottom flask, equipped with magnetic stirrer, a pressure-equalising dropping funnel and under argon atmosphere. The reaction mixture was cooled down to -20ºC. Then, a solution of chlorosulfonic acid (4.5 mL, 65 mmol) in methylene chloride (5 mL) was added dropwise and the reaction mixture was stirred for one hour. The progress of the reaction could be monitored by ^{1}H NMR analysis of aliquots. Once starting material was no longer present, a bubbler was mounted to the flask and PCl_5 in excess (21.4 g, 101.33 mmol) was added. The mixture was stirred until evolution of gas ceased. ^{1}H NMR spectra of aliquots allowed us to follow the progress of the reaction and, if necessary, small amounts of PCl_5 could be added until the reaction finished. Then, the reaction mixture was poured onto ice and water. The organic layer was separated and the aqueous phase was extracted several times with ethyl acetate. The combined organic layers were dried with Na_2SO_4 and the solvents were evaporated. Silica gel column chromatography with CH_2Cl_2 afforded the disulfonyl dichloride **8** (5.6 g, 35%).

^{1}H NMR (200 MHz, $CDCl_3$) δ 8.64 (s, 2H), 8.20 (d, *J* = 8.9 Hz, 2H), 7.75 (d, *J* = 8.3 Hz, 2H), 7.62 (d, *J* = 8.9 Hz, 2H), 7.27 (d, *J* = 8.3 Hz, 2H), 4.09 (t, *J* = 6.8 Hz), 1.52 – 1.40 (m, 4H), 1.10 – 0.90 (m, 4H), 0.65 (t, *J* =6.8 Hz, 6H).

Compound **8** is relatively unstable and no further characterization was done.

Synthesis of the racemic macrocycle 2. *Route a*

Acetonitrile (400 mL) and triethyl amine (6.0 mL, 43.28 mmol) were added to a 1 Liter 2-neck round bottom flask equipped with magnetic stirrer, two pressure-equalising dropping funnels and under nitrogen atmosphere. A solution of the diamine **6** (1.52 g, 2.90 mmol) in CH_3CN (100 mL) was added to one of the funnels while the disulfonyl dichloride **8** (1.73 g, 2.90 mmol) in CH_3CN (100 mL) was put in the other. Next and simultaneously, both solutions were dropwise added and at the same speed. Once the additions were finished, stirring was kept until aliquot analysis by TLC and ^{1}H NMR showed that the reaction had finished. The solvent was evaporated and the crude residue was purified by silica gel column chromatography (CH_2Cl_2/ EtOAc 4:1 as eluent) to afford 1.11 g (36%) of the macrocycle **2**.

m.p.: 199 ºC.

IR (thin film, υ in cm^{-1}): 3429, 3273, 1619, 1463, 1333, 1281, 1145, 957, 898.

^{1}H NMR (400 MHz, $CDCl_3$) δ 9.81 (s, NH), 8.40 (d, *J* = 1.6 Hz, 2H), 8.27 (d, *J* = 1.6 Hz, 2H), 8.00 (d, *J* = 9.0 Hz, 2H), 7.84 (d, *J* = 1.6 Hz, 2H), 7.49 (dd, *J* = 8.0 and 1.6 Hz, 2H), 7.47 (d, *J* = 9.0, 2H), 7.19 (d, *J* = 8.0 Hz, 2H), 5.58 (s, 2 NH), 5.14 (s, 2 NH), 4.02 – 3.93 (m, 4H), 3.21

– 2.99 (m, 4H), 2.98 – 2.86 (m, 4H), 1.46 – 1.36 (m, 4H), 1.42 (s, 18H), 1.07 – 0.96 (m, 4H), 0.66 (t, *J* = 7.2 Hz, 6H).

^{13}C NMR (101 MHz, $CDCl_3$) δ 156.83, 143.68, 135.68, 134.03, 132.97, 131.01, 128.93, 127.22, 126.80, 124.69, 123.83, 122.67, 122.18, 120.32, 119.20, 115.96, 68.81, 42.67, 42.02, 34.93, 31.70, 31.07, 18.69, 13.47.

HRMS (ESI+): Calculated for $C_{52}H_{63}N_5O_{10}S_4Na$ $[M+Na]^+$ 1068.3350, found 1068.3352.

Route b

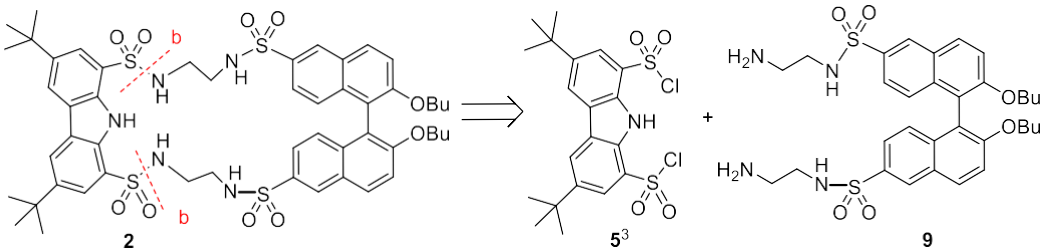

The compound **5**, 3,6-di-tert-butyl-9*H*-carbazole-1,8-disulfonyl dichloride, was synthesized according to a published procedure.[77]

***N*^{1},*N*^{8}-bis(2-aminoethyl)-2,2'-dibutoxy-1,1'-binaphthyl-6,6´-disulfonamide (9)**

To a solution of ethylenediamine (2.0 mL, 30 mmol) in diethylether (120 mL) was added dropwise a solution of the disulfonyl dichloride **8** (1.0 g, 1.68 mmol) in diethylether (20 mL) with continuous stirring. Once the addition of the disulfonyl dichloride **8** was finished, stirring was kept until the reaction was complete. The progress of the reaction could be monitored by ^{1}H NMR analysis of aliquots. Once the reaction was finished, water (100 mL) was added and the phases were separated. The organic layer was dried with Na_2SO_4 and the solvent was evaporated. Column chromatography with methanol/ ethyl acetate 1:1 afforded the desired diamine **9** (0.96 g, 88%).

m.p.: 105ºC.

IR (thin film, υ in cm^{-1}): 3280; 2955; 2923; 2865; 2365; 2326; 1619; 1502; 1469; 1327; 1275; 1151; 1100; 1035.

^{1}H NMR (200 MHz, CD_3OD) δ 8.47 (d, *J* = 1.6 Hz, 2H), 8.17 (d, *J* = 9.0 Hz, 2H), 7.64 (d, *J* = 9.0 Hz, 2H), 7.55 (dd, *J* = 9.0, 1.6 Hz, 2H), 7.16 (d, *J* = 9.0 Hz, 2H), 4.05 – 3.90 (m, 4H), 2.99 – 2.93 (m, 4H), 2.81 – 2.75 (m, 4H), 1.42 – 1.32 (m, 4H), 1.02 – 0.92 (m, 4H), 0.62 (t, *J* = 7.0 Hz, 6H).

^{13}C NMR (50 MHz, CD_3OD) δ 157.1, 135.6, 134.4, 131.2, 128.6, 127.7, 126.3, 122.6, 119.1, 116.2, 68.6, 43.9, 40.6, 31.1, 18.7, 12.8.

HRMS (ESI+): Calculated for $C_{32}H_{43}N_4O_6S_2$ $[M+H]^+$ 643.2618, found 643.2625.

Synthesis of the racemic macrocycle 2. *Route b*

Acetonitrile (200 mL) and triethyl amine (3.0 mL, 21.64 mmol) were added to a 1 Liter 2-neck round bottom flask equipped with magnetic stirrer, two pressure-equalising dropping funnels and under nitrogen atmosphere. A solution of the diamine **9** (0.96 g, 1.45 mmol) in CH_3CN (50 mL) was added to one of the funnels while the disulfonyl dichloride **5** (0.72 g, 1.45 mmol) in CH_3CN (50 mL) was put in the other. Next and simultaneously, both solutions were dropwise added and at the same speed. Once the additions were finished, stirring was kept until aliquot analysis by TLC and ^{1}H NMR showed that the reaction had finished. The solvent was evaporated and the crude residue was purified by silica gel column chromatography (CH_2Cl_2/ EtOAc 4:1 as eluent) to afford 770 mg (25%) of the macrocycle **2**.

Synthesis of the enantiopure receptor (*S*)- 2

Starting from the 1,1'-binaphthyl-2,2'-diol (BINOL) **4** enantiomerically pure,[80] and following the synthetic strategy via route *a*, the receptor (*S*)-**2** was prepared. $[\alpha]_D^{20}$=105.9 $degcm^3g^{-1}dm^{-1}$(c=1.0 gcm^{-3} in chloroform).

[80] Tanaka, K.; Okada, T.; Toda, F. *Angew. Chem. Int. Ed.* **1993**, *32*, 1147 – 1148; *Angew. Chem.* **1993**, *105*, 1266 – 1267.

Acryloyl chloride

Freshly distilled acrylic acid (4.0 g, 55.5 mmol) was dissolved in thionyl chloride (3,8 mL, 52.4 mmol) and left without stirring for two hours. Then, the reaction mixture was distilled under vacuum (75°C, 25 mmHg) yielding 2.2 g (44%).

^{1}H NMR (200 MHz, $CDCl_3$) δ 6.64 (d, *J* = 17.0 Hz, 1H), 6.35 (dd, *J* = 17.0 and 11.0 Hz, 1H,), 6.17 (d, *J* = 11.0 Hz, 1H).

5-Bromo-2-naphthoic acid (10)

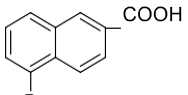

10

Finely powdered 2-naphtoic acid (10.0 g, 58.1 mmol) was dissolved in 250 mL of 98% H_2SO_4 and 50 mL of AcOH, keeping the solution below 20ºC. Then, NaBr (6.0 g, 58.3 mmol) was added portionwise under stirring for 15 minutes. Then, the reaction mixture was left without stirring for one hour and a precipitate appeared. 100 g of ice were added portionwise keeping the reaction mixture below 30ºC and the solid was filtered under vacuum, yielding 14.5 (quant.) of compound **10**, which was used without further purification in the next reaction.

^{1}H NMR (200 MHz, $CDCl_3$) δ 8.49 (d, *J* = 1.5 Hz, 1H), 8.16 (d, *J* = 8.5 Hz, 1H,), 8,03 (dd, *J* = 8.5 and 1.5 Hz, 1H,), 7,82 (d, *J* = 8.0 Hz, 1H,), 7,77 (d, *J* = 8.0 Hz, 1H), 7.28 (t, *J* = 8.0 Hz, 1H).

5-Bromo-8-nitro-2-naphthoic acid (11)

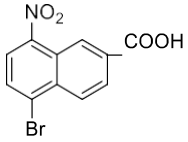

11

A solution of 4 mL of HNO_3 60% in 40 mL of H_2SO_4 95% was added dropwise over a solution of compound **10** (14.5 g, 57.8 mmol) in 200 mL of H_2SO_4 95%, keeping the temperature below 25ºC. Then, the reaction mixture was left without stirring for one hour, 100 g of ice were added and the solid which appeared was filtrated under vacuum and recrystallised in AcOH, yielding 7.6 g (40%) of compound **11**.

m.p.: 215 – 216°C.

IR (thin film, υ in cm^{-1}): 3377, 2916, 1690, 1534, 1456, 1340, 1281, 917, 756.

^{1}H NMR (400 MHz, DMSO-d_6) δ 8.98 (d, *J* = 1.5 Hz, 1H), 8.37 (d, *J* = 9.0 Hz, 1H), 8.28 (dd, *J* = 9.0 and 1.5 Hz, 1H), 8.26 (d, *J* = 8.0 Hz, 1H), 8.18 (d, *J* = 8.0 Hz, 1H).

^{13}C NMR (101 MHz, DMSO-d_6) δ 166.3 (C), 146.3 (C), 133.2 (C), 131.8 (C), 131.2 (CH), 128.7 (C), 128.3 (CH), 128.1 (CH), 125.3 (CH), 125.2 (CH), 124.5 (C).

HRMS (ESI+): Calculated for $C_{11}H_6{}^{79}BrNNaO_4^+$ $[M+Na]^+$ 317.9372, found 317,9396

5-(Ethylsulfonyl)-8-nitro-2-naphthoic acid (13)

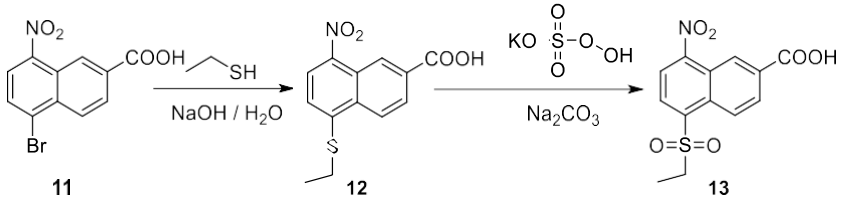

NaOH (3.3 g, 82.5 mmol) and ethanethiol (5 mL, 4.3 g, 69.4 mmol) were dissolved in 90 mL of H_2O and the solution was heated at 40ºC. To this solution, compound **11** (6.0 g, 20.3 mmol) was added, and the reaction mixture was stirred for 10 minutes at 40ºC. Then, the reaction was cooled down to room temperature and a solution of Na_2CO_3 (9.0 g, 84.9 mmol) in 90 mL of H_2O was added slowly. Next, Oxone (9.0 g, 79.6 mmol) was added portionwise for 10 minutes with vigorous stirring. When the addition was finished, the solution was acidulated with 2M aqueous HCl until acidic pH. The solid which appeared was filtered under vacuum and recrystallised in CH_2Cl_2, yielding 3.1 g (49%) of compound **13**.

m.p.: 182 – 185°C.

IR (thin film, υ in cm^{-1}): 2923, 1690, 1528, 1456, 1294, 1132, 814, 723.

^{1}H NMR (200 MHz, DMSO-d_6) δ 8.91 (d, *J* = 9.0 Hz, 1H), 8.89 (d, *J* = 1.7 Hz, 1H), 8.50 (d, *J* = 8.2 Hz, 1H), 8.47 (d, *J* = 8.2 Hz, 1H), 8.36 (dd, *J* = 9.0 and 1.7 Hz, 1H), 3.57 (c. *J* = 7.5 Hz, 2H), 1.14 (t, *J* = 7.5 Hz, 3H).

^{13}C NMR (50 MHz, DMSO-d_6) δ 166.2 (C), 151.0 (C), 138.3 (C), 131.8 (CH), 131.6 (C), 131.1 (C), 129.0 (CH), 125.5 (CH), 125.2 (CH), 124.3 (C), 122.7 (CH), 49.7 (CH_2), 7.0 (CH_3).

HRMS (ESI+): Calculated for $C_{13}H_{11}NNaO_6S^+$ $[M+Na]^+$ 332.0199, found 332.0188.

1-cyclohexyl-3-(2-nitrophenyl)urea (15)

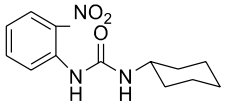

15

2-Nitroaniline (10.0 g, 72.4 mmol) and cyclohexyl isocyanate (10.0 g, 79.9 mmol) were heated in a pressure reactor at 160°C for 16 hours. Then, the solid was filtered under vacuum and washed with Et_2O, yielding 19.0 g (quant.) of compound **15**.

m.p.: 156 – 158°C.

IR (thin film, υ in cm^{-1}): 3299, 2949, 1658, 1560, 1515, 1450, 1385, 1281, 1223, 860, 743.

^{1}H NMR (200 MHz, DMSO-d_6) δ 10.05 and 9.29 (broad s, NH), 8.35 and 8.03 (d, *J* = 8.2 Hz, 1H), 8.03 and 7.96 (d, *J* = 8.2 Hz, 1H), 7.69 and 7.62 (t, *J* = 8.2 Hz, 1H), 7.28 and 7.08 (t, *J* = 8.2 Hz, 1H), 7.48 and 5.55 (broad d, NH), 3.58 – 3.39 (m, 1H), 1.90 – 1.45 (m, 5H), 1.45 – 0.96 (m, 5H).

^{13}C NMR (50 MHz, DMSO-d_6) δ 155.8 (C), 152.4 (C), 140.4 (C), 136.9 (C), 136.6 (C), 135.4 (CH). 134.9 (CH), 133.5 (C), 125.7 (CH), 125.6 (CH), 124.3 (CH), 124.0 (CH), 122.2 (CH), 121.5 (CH), 48.6 (CH), 33.8 and 33.2 (2 CH_2), 25.7 (CH_2), 24.9 and 24.8 (2 CH_2).

1-(2-Aminophenyl)-3-cyclohexylurea (14)

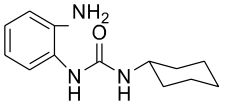

14

Sodium sulfide (30.0 g, 0.38 mol) was added over a solution of compound **15** (4,0 g; 15,2 mmol) in 30 mL of THF and 10 mL of EtOH and refluxed for 30 minutes. Then, the solvent was evaporated under reduced pressure and the crude was dissolved in 50 mL of EtOAc. The organic phase was washed twice with 10 ml of H_2O, dried over anhydrous Na_2SO_4, filtered and concentrated under reduced pressure, yielding 3.5 g (quant.) of compound **14**.

m.p.: 194 – 196°C.

IR (thin film, υ in cm^{-1}): 3312, 2929, 2858, 1619, 1573, 1463, 1379, 1320, 1223.

^{1}H NMR (200 MHz, DMSO-d_6) δ 7.41 (br s, NH). 7.29 (dd, *J* = 8.0 an 1.5 Hz, 1H), 6.76 (dt, *J* = 8.0 and 1.5 Hz, 1H), 6.69 (dd, *J* = 8.0 and 1.5 Hz, 1H), 6.52 (dt, *J* = 8.0 and 1.5 Hz, 1H), 6.10 (br d, NH), 3.52 – 3.38 (m, 1H), 1.89 – 1.44 (m, 5H), 1.39 – 0.96 (m, 5H).

^{13}C NMR (50 MHz, DMSO-d_6) δ 155.0 (C), 140.1 (C), 125.8 (C), 122.8 (CH), 116.8 (CH), 115.8 (CH), 47.7 (CH), 33.0 (2 CH_2), 25.3 (CH_2), 24.4 (2 CH_2).

HRMS (ESI+): Calculated for $C_{13}H_{20}N_3O^+$ $[M+H]^+$ 234.1601, found 234.1608.

_N_-(2-(3-Cyclohexylureido)phenyl)-5-(ethylsulfonyl)-8-nitro-2-naphthamide (17)

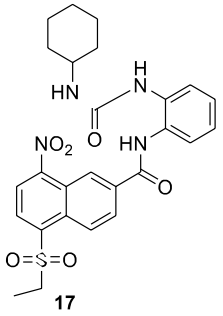

17

Compound **13** (1.0 g, 3.2 mmol) was added over a solution of PCl_5 (1.0 g, 4.8 mmol) in 20 mL of CH_2Cl_2 and left under stirring for 15 minutes. Then, the solvent was concentrated under reduced pressure, and the crude acid chloride was dissolved in 50 mL of EtOAc and added over a biphasic mixture of compound **14** (760 mg, 3.3 mmol) in 50 mL of EtOAc and 5 mL of a saturated aqueous solution of Na_2CO_3 with vigorous stirring. After 5 minutes, the two phases were separated, the organic phase was washed with 2M aqueous HCl (2x10 mL), 4% aqueous Na_2CO_3 (2x10 mL), dried over anhydrous Na_2SO_4, filtered, and concentrated under reduced pressure, yielding 1.63 g (96%) of compound **17**.

m.p.: 127 – 130°C.

IR (thin film, υ in cm^{-1}): 3306, 3163, 2916, 2838, 1658, 1541, 1469, 1336, 1307, 1119, 1048, 749, 730.

^{1}H NMR (200 MHz, DMSO-d_6) δ 10.62 (br s, NH). 8.96 (d, *J* = 9.0 Hz, 1H), 8.92 (s, 1H), 8.53 – 8.44 (m, 3H), 7.88 (br s, NH), 7.85 (d, *J* = 7.8 Hz, 1H), 7.44 (d, *J* = 7.8 Hz, 1H), 7.21 (t, *J* = 7.8 Hz, 1H), 7.05 (t, *J* = 7.8 Hz, 1H), 6.64 (br d, NH), 3.60 (c, *J* = 7.5 Hz, 1H), 3.55 – 3.39 (m, 1H), 1.85 – 1.75 (m, 1H), 1.75 – 1.57 (m, 2H), 1.57 – 1.44 (m, 1H), 1.16 (c, *J* = 7.5 Hz, 3H), 1.37 – 0.97 (m, 6H).

^{13}C NMR (50 MHz, DMSO-d_6) δ 164.0 (C), 156.6 (C), 154.9 (C), 151.3 (C), 137.9 (C), 135.0 (C), 134.9 (C), 131.4 (CH), 130.5 (C), 128.3 (CH), 127.0 (CH), 126.5 (CH), 125.2 (CH), 124.2 (C), 122.9 (CH), 122.2 (CH), 122.0 (CH), 121.1 (CH), 49.7(CH_2), 48.0 (CH). 47.5 (CH), 33.3 (CH_2), 33.0 (CH_2), 25.3 (CH_2), 25.3 (CH_2), 24.4 (CH_2), 7.0 (CH_3).

HRMS (ESI+): Calculated for $C_{26}H_{28}N_4NaO_6S^+$ $[M+Na]^+$ 547.1622, found 547.1622.

8-Amino-*N*-(2-(3-cyclohexylureido)phenyl)-5-(ethylsulfonyl)-2-naphthamide (18)

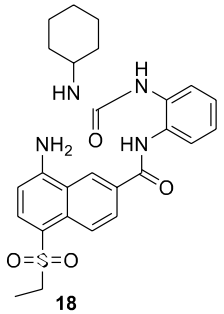

18

Compound **17** (1.5 g, 2.9 mmol) was added over a dispersion of 16.0 g of Zn in 15 mL of AcOH heated at 60ºC with vigorous stirring. After 10 minutes, 50 mL of EtOAc were added and the reaction mixture was filtered to remove Zn. Then, the organic phase was washed with water (2x10 mL), dried over anhydrous Na_2SO_4, filtrated and concentrated under reduced pressure, yielding 1.2 g (85%) of compound **18**.

m.p.: 195 – 196°C.

IR (thin film, υ in cm^{-1}): 3442, 3371, 3319, 3247, 2923, 2852, 1658, 1632, 1580, 1547, 1450, 1379, 1119, 762, 723.

^{1}H NMR (200 MHz, DMSO-d_6) δ 10.1 (br s, NH). 8.96 (s, 1H), 8.57 (d, *J* = 9.0 Hz, 1H), 8.17 (d, *J* = 9.0 Hz, 1H), 7.95 (d, *J* = 9.0 Hz, 1H), 7.88 (d, *J* = 9.0 Hz, 1H), 7.43 (dd, *J* = 8.0 and 2.0 Hz, 1H), 7.19 (dt, *J* = 8.0 and 2.0 Hz, 1H), 7.12 (br s, NH), 7.04 (dt, *J* = 8.0 and 2.0 Hz, 1H), 6.80 (d, NH), 6.70 (d, *J* = 8.0 Hz, 1H), 3.26 (c. *J* = 8.0 Hz, 2H), 1.84 – 1.74 (m, 2H), 1.67 – 1.57 (m, 2H), 1.57 – 1.46 (m, 1H), 1.34 – 1.20 (m, 2H), 1.05 (t, *J* = 8.0 Hz, 3H), 1.06 – 0.96 (m, 4H).

^{13}C NMR (50 MHz, DMSO-d_6) δ 165.2 (C), 154.8 (C), 152.3 (C), 135.0 (C), 134.5 (CH), 132.0 (C), 129.8 (C), 127.4 (C), 127.0 (CH), 126.5 (CH), 126.2 (CH), 123.9 (2 CH), 121.9 (CH), 121.1 (CH), 121.0 (C), 117.3 (C), 105.7 (CH), 49.7 (CH_2), 48.1 (CH), 33.0 (2 CH_2), 25.2 (CH_2), 24.5 (2 CH_2), 7.5 (CH_3).

HRMS (ESI+): Calculated for $C_{26}H_{30}N_4NaO_4S^+$ $[M+Na]^+$ 517.1880, found 517.1876.

8-Acrylamido-*N*-(2-(3-cyclohexylureido)phenyl)-5-(ethylsulfonyl)-2-naphthamide (19)

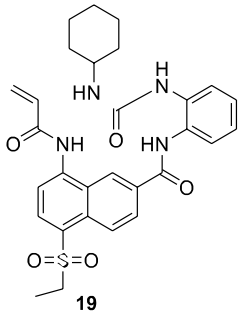

19

Acryloyl chloride (50 μL, 55 mg, 0.6 mmol) was added over a solution of compound **18** (300 mg, 0.6 mmol) in 10 mL of THF and refluxed for 30 minutes. Then, the solvent was eliminated under reduced pressure and the crude was crystallised in Et_2O, yielding 200 mg (60%) of compound **19**.

m.p.: 158 – 160°C.

IR (thin film, υ in cm^{-1}): 3280, 2962, 2929, 2845, 1664, 1547, 1469, 1372, 1301, 1139, 769, 723.

^1H NMR (200 MHz, DMSO-d_6) δ 10.75 (br s, NH). 10.40 (br s, NH), 9.13 (s, 1H), 8.79 (d, *J* = 9.0 Hz, 1H), 8.37 – 8.26 (m, 3H), 7.94 (br s, NH), 7.89 (d, *J* = 8.0 Hz, 1H), 7.46 (d, *J* = 8.0 Hz, 1H), 7.20 (dt, *J* = 8.0 and 2.0 Hz, 1H), 7.05 (dt, *J* = 8.0 and 2.0 Hz, 1H), 6.88 (dd, *J* = 17.0 and 10.0 Hz, 1H), 6.72 (br d, NH), 6.42 (dd, *J* = 17.0 and 2.0 Hz, 1H), 5.90 (dd, *J* = 10.0 and 2.0 Hz, 1H), 3.46 (c, *J* = 7.5 Hz, 2H.), 1.85 – 1.74 (m, 2H), 1.69 – 1.56 (m, 2H), 1.56 – 1.46 (m, 1H), 1.34 – 1.19 (m, 2H), 1.12 (t, *J* = 7.5 Hz, 3H), 1.19 – 1.02 (m, 4H).

^{13}C NMR (50 MHz, DMSO-d_6) δ 165.0 (C), 164.2 (C), 154.8 (C), 140.6 (C), 134.9 (C), 132.6 (CH), 132.1 (C), 131.5 (CH), 130.6 (C), 129.1 (C), 128.3 (CH_2), 127.2 (C), 126.9 (CH), 126.9 (CH), 126.3 (CH), 124.5 (CH), 124.2 (CH), 121.9 (CH), 121.2 (CH), 118.8 (CH), 49.7 (CH_2), 48.1 (CH), 33.0 ($2CH_2$), 25.2 (CH_2), 24.5 ($2CH_2$), 7.3 (CH_3).

HRMS (ESI+): Calculated for $C_{29}H_{32}N_4NaO_5S^+$ $[M+Na]^+$ 571.1986, found 571.1990.

8-(3-(1-Aza-18-crown-6-1-yl)propanamido)-*N*-(2-(3-cyclohexylureido)phenyl)-5-(ethylsulfonyl)-2-naphthamide (20)

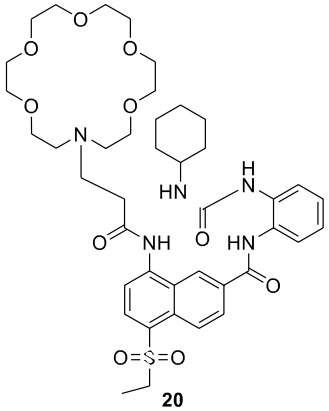

20

Compound **19** (100 mg, 0.2 mmol) and 1-aza-18-corona-6 ether (72 mg, 0.3 mmol) were mixed in 100 μL of CH_2Cl_2 and left without stirring for 16 hours. Then, 15 mL of CH_2Cl_2 were added and the organic phase was washed with water (2x10 mL), dried over anhydrous Na_2SO_4, filtered under vacuum and concentrated under reduced pressure, yielding 145 mg (98%) of compound **20**.

m.p.: oily compound.

IR (thin film, υ in cm^{-1}): 3267, 2962, 2936, 2852, 1651, 1541, 1469, 1385, 1314, 1100.

^{1}H NMR (200 MHz, $CDCl_3$) δ 10.61 (br s, NH), 8.76 (s, 1H), 8.69 (d, *J* = 9.0 Hz, 1H), 8.28 (d, *J* = 8.5 Hz, 1H), 8.23 (d, *J* = 8.5 Hz, 1H), 8.09 (d, *J* = 9.0 Hz, 1H), 7.81 (d, *J* = 8.0 Hz, 1H), 7.22 – 6.80 (m, 3H), 6.04 (br d, NH), 3.26 (c, *J* = 7.5 Hz, 2H), 3.78 – 2.56 (m, 29H), 1.90 – 1.71 (m, 2H), 1.66 – 1.42 (m, 3H), 1.23 (t, *J* = 7.5 Hz, 3H), 1.35 – 1.14 (m, 2H), 1.10 – 0.90 (m, 3H).

^{13}C NMR (50 MHz, $CDCl_3$) δ 132.7 (C), 131.2 (C), 125.6 – 123.5 (CH), 70.6 – 69.5 (CH_2), 52.7 (CH_2), 50.4 (CH_2), 49.0 (CH), 48.8 (CH_2), 33.4 ($2CH_2$), 25.5 (CH_2), 24.8 ($2CH_2$), 7.4 (CH_3).

HRMS (ESI+): Calculated for $C_{41}H_{58}N_5O_{10}S^+$ $[M+H]^+$ 812.3899, found 812.3900.

Tert-butyl (2,7-dichloro-5-(3-(4-chlorophenyl)ureido)-9,9-dimethyl-9*H*-xanthen-4-yl)carbamate (24)

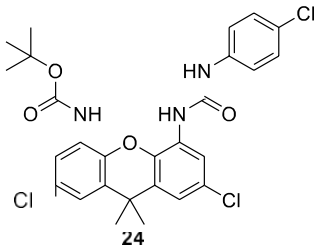

24

p-Chlorophenyl isocyanate (202 mg, 1.3 mmol) dissolved in 2.5 mL of CH_2Cl_2 was added over a solution of compound **23** (510 mg, 1.3 mmol) in 2.5 mL of CH_2Cl_2. Then, the solvent was evaporated under reduced pressure and after diethyl ether addition, a white solid precipitated in the reaction media. The white solid was collected by filtration under vacuum, yielding 298 mg (43%) of compound **24** as a white solid.

m.p.: 145ºC.

IR (thin film, υ in cm^{-1}): 3520, 3381, 3128, 2924, 2855, 1739, 1712, 1691, 1651, 1624, 1602, 1549, 1492, 1413, 1313, 1278, 1237, 1211, 1151, 1091, 1062, 984, 873, 851, 831, 769, 735.

^{1}H NMR (200 MHz, $CDCl_3$) δ 9.53 (s, 1H), 9.07 (d, *J* = 17.9 Hz, 1H), 8.81 (s, 1H), 7.99 – 7.86 (m, 2H), 7.50 (d, *J* = 8.7 Hz, 2H), 7.38 (d, *J* = 8.7 Hz, 2H), 7.31 – 7.25 (m, 2H), 1.50 (s, 6H), 1.45 (s, 9H).

^{13}C NMR (50 MHz, $CDCl_3$) δ 152.6 (C), 152.1 (C), 138.2 (C), 137.9 (C), 131.8 (C), 131.4 (C), 128.9 (2CH), 128.3 (2CH), 127.9 (2C), 127.5 (2C), 125.8 (2C), 119.5 (4CH), 80.1 (C), 31.0 ($2CH_3$), 27.9 ($3CH_3$), 15.2 (C).

HRMS (ESI+): Calculated for $C_{22}H_{19}^{35}Cl_3N_3O_2^+$ $[M\text{-Boc}]^+$ 462.0537, found 462.0531.

Tosyl-L-tyrosine (31)

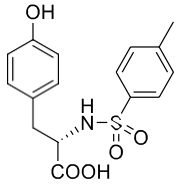

31

L-tyrosine (10.20 g, 56.3 mmol) and NaOH were dissolved in 100 mL of methanol and refluxed until the mixture become homogenous. Then, tosyl chloride (5.27 g, 27.6 mmol) was added. After 5 minutes, the reaction mixture was filtered, and the filtrate was concentrated under reduced pressure. 5 mL of 35% aqueous HCl were added and the aqueous phase was

extracted with EtOAc (2x50 mL). The organic phase was dried over anhydrous Na_2SO_4, filtered, and evaporated under reduced pressure, yielding 5.59 g (60%) of compound **31**.

^{1}H NMR (200 MHz, 5% CD_3OD in $CDCl_3$) δ 7.59 (d, *J* = 8.2 Hz, 2H), 7.23 (d, *J* = 8.2 Hz, 2H), 6.95 (d, *J* = 8.4 Hz, 2H), 6.67 (d, *J* = 8.4 Hz, 2H), 4.03 (t, *J* = 5.9 Hz, 1H), 2.94 (qd, *J* = 13.9 y 6.0 Hz, 2H), 2.40 (s, 3H).

All the spectroscopic properties matched the characterisation described in literature.[81]

(*S*)-2-((*N*,4-Dimethylphenyl)sulfonamido)-3-(4-methoxyphenyl)propanoic acid (34)

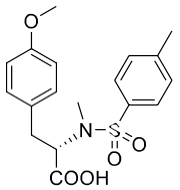

34

NaOH (2.29 g, 57.4 mmol) and CH_3I (10 mL, 0.16 mol) were added over a solution of compound **31** (4.45 g, 13.3 mmol) in 100 mL of THF. The reaction mixture was stirred for 16 hours. Then, 2.5 mL of 35% aqueous HCl were added and the aqueous phase was extracted with EtOAc (2x50 mL), dried over anhydrous Na_2SO_4, filtrated and evaporated under reduced pressure, yielding 4.66 g (97%) of compound **34**.

^{1}H NMR (200 MHz, 5% CD_3OD in $CDCl_3$) δ 7.38 (d, *J* = 8.1 Hz, 2H), 7.15 (d, *J* = 8.1 Hz, 2H), 7.09 (d, *J* = 8.5 Hz, 2H), 6.79 (d, *J* = 8.5 Hz, 2H), 4.88 (dd, *J* = 9.8 and 5.8 Hz, 1H), 3.81 (s, 3H), 3.24 (dd, *J* = 14.4 y 5.8 Hz, 1H), 2.85 (s, 3H), 2.30 (dd, *J* = 14.4 and 9.8 Hz, 1H), 2.39 (s, 3H).

The spectroscopic properties matched the characterisation described in literature.[82]

[81] Sahoo, S. P.; Subudhi, B. B. *Med. Chem. Res.* **2014**, *23*, 3039 – 3048.
[82] Peterson, R. L.; Hubele, K. W.; Niemann, C. *Biochemistry* **1963**, *2*, 942 – 946.

(*S*)-3-(3-(Chloromethyl)-4-methoxyphenyl)-2-((*N*,4-dimethylphenyl)sulfonamido) propanoic acid (35)

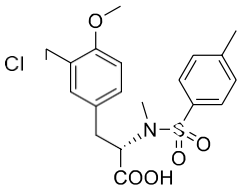

35

2 mL of 35% aqueous HCl were added over a solution of compound **34** (1.02 g, 2.7 mmol) and paraformaldehyde (1.04 g, 34.6 mmol) in 20 mL of AcOH. The reaction mixture was kept at 35ºC for 3 hours and then it was added over 50 mL of H_2O and extracted with EtOAc (3x25 mL). The organic phase was separated, dried over anhydrous Na_2SO_4, dried and evaporated under reduced pressure to yield 1.08 g (93%) of compound **35** as a yellow solid.

m.p.: 130ºC.

IR (thin film, υ in cm^{-1}): 2924, 2854, 1707, 1612, 1502, 1350, 1325, 1256, 1209, 1157, 1117, 1088, 1061, 1028, 985, 924, 889, 817, 743, 714, 653.

^{1}H NMR (400 MHz, $CDCl_3$) δ 7.41 (d, *J* = 8.1 Hz, 2H), 7.14 (d, *J* = 8.1 Hz, 2H), 7.10 (s, 1H), 7.09 (dd, J = 8.1 and 2.1 Hz, 1H), 6.76 (d, *J* = 8.1 Hz, 1H), 4.91 (dd, *J* = 9.6 and 6.0 Hz, 1H), 4.59 (d, *J* = 11.3 Hz, 1H), 4.55 (d, *J* = 11.3 Hz, 1H), 3.86 (s, 3H), 3.21 (dd, *J* = 14.4 and 6.0 Hz, 1H), 2.86 (s, 3H), 2.80 (dd, *J* = 14.4 and 9.6 Hz, 1H), 2.38 (s, 3H).

^{13}C NMR (101 MHz, $CDCl_3$) δ 175.1 (C), 156.5 (C), 143.3 (C), 136.1 (C), 131.2 (CH), 130.5 (CH), 129.5 (2CH), 128.4 (C), 127.3 (2CH), 126.0 (C), 111.1 (CH), 60.6 (CH), 55.8 (CH_3), 41.5 (CH_2), 34.5 (CH_2), 30.2 (CH_3), 21.6 (CH_3).

HRMS (ESI+): Calculated for $C_{19}H_{22}NO_5S^+$ $[M\text{-}Cl]^+$ 376.1213, found 376.1204.

(*S*)-3-(3-(Chloromethyl)-4-methoxyphenyl)-*N*-(2,7-dichloro-5-(3-(4-chlorophenyl)ureido)-9,9-dimethyl-9*H*-xanthen-4-yl)-2-((*N*,4-dimethylphenyl)sulfonamido)propanamide (37)

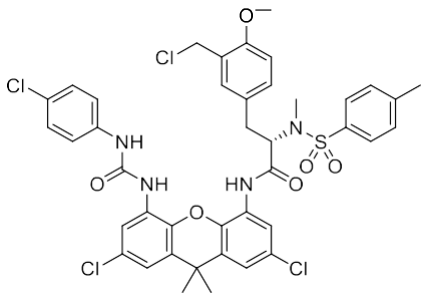

37

Compound **24** (202 mg, 0.4 mmol) was dissolved in 2 mL of CF_3COOH and refluxed for 15 minutes. Then, the solvent was evaporated under reduced pressure, yielding 205 mg (quant.) of compound **25** as a white solid, which was used without further purification in the next reaction.

Compound **35** (206 mg, 0.5 mmol) was dissolved in 2 mL of $SOCl_2$ and refluxed was 30 minutes. Then, the solvent was evaporated under reduced pressure, yielding 196 mg (91%) of compound **35** acid chloride as a dark oil, which was used without further purification in the next reaction.

Using Schotten-Baumann conditions, compound **35** acid chloride (166 mg, 0.4 mmol) was dissolved in 15 mL of EtOAc and added dropwise over a solution of compound **25** (126 mg, 0.2 mmol) in 20 mL of EtOAc and 10 mL of a saturated aqueous solution of Na_2CO_3 under vigorous stirring at 0ºC. Then, the organic phase was separated, washed with 15 ml of H_2O, dried over anhydrous Na_2SO_4, filtrated and evaporated under reduced pressure. The crude obtained was purified by silica gel column chromatography using CH_2Cl_2 as eluent, yielding 100 mg (53%) of compound **37**.

m.p.: Oily compound.

IR (thin film, υ in cm^{-1}): 3753, 3395, 2968, 2372, 1701, 1599, 1539, 1496, 1412, 1310, 1260, 1214, 1156, 1089, 910, 815, 731.

^{1}H NMR (400 MHz, $CDCl_3$) δ 8.72 (s, 1H), 8.31 (d, *J* = 1.7 Hz, 2H), 7.83 (s, 1H), 7.43 – 7.31 (m, 2H), 7.21 – 7.07 (m, 5H), 6.91 – 6.78 (m, 3H), 6.70 (d, *J* = 8.1 Hz, 1H), 5.06 – 4.91 (m, 1H), 4.58 (d, *J* = 11.1 Hz, 1H), 4.51 (d, *J* = 11.1 Hz, 1H), 3.83 (s, 3H), 3.38 – 3.24 (m, 1H), 2.93 (s, 3H), 2.80 (s, 1H), 2.41 (s, 3H), 1.63 (s, 3H), 1.51 (s, 3H).

^{13}C NMR (101 MHz, $CDCl_3$) δ 167.2 (C), 156.6 (C), 152.3 (C), 145.0 (C), 138.1 (C), 137.5 (C), 137.0 (C), 134.7 (C), 131.5 (CH), 131.3 (C), 130.9 (CH), 130.7 (C), 130.3 (CH), 129.1 (C), 128.9 (C), 128.5 (CH), 128.4 (C), 128.2 (C), 127.7 (C), 127.2 (CH), 126.5 (C), 126.3 (C),

121.4 (CH), 120.4 (2 CH), 119.4 (2CH), 119.3 (2 CH), 119.1 (CH), 119.0 (CH), 111.1 (CH), 62.3 (CH), 55.8 (CH_3), 41.3 (CH_2), 34.8 (C), 33.6 (CH_3), 33.0 (CH_2), 30.4 (CH_3), 29.8 (CH_3), 21.2 (CH_3).

HRMS (ESI-): Calculated for $C_{41}H_{38}{}^{35}Cl_5N_4O_6S^-$ $[M-Cl]^-$ 889.0960, found 891.0931.

(*S*)-3-(3-((1-Aza-18-crown-6-1-yl)methyl)-4-methoxyphenyl)-*N*-(2,7-dichloro-5-(3-(4-chlorophenyl)ureido)-9,9-dimethyl-9*H*-xanthen-4-yl)-2-((*N*,4-dimethylphenyl)sulfonamido)propanamide (38)

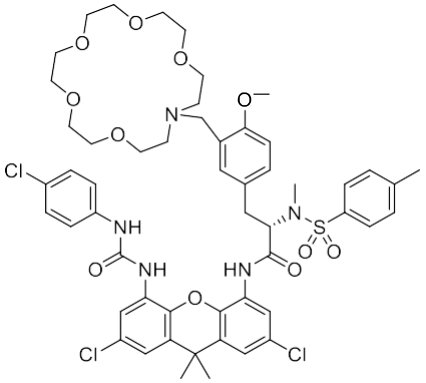

38

Compound **37** (37 mg, 0.04 mmol) and 18-crown-6 ether (25 mg, 0.09 mmol) were dissolved in 500 μL of CH_2Cl_2 and left without stirring for 16 hours. Then, the solvent was evaporated under reduced pressure, 10 mL of EtOAc were added and the organic phase was washed with deionized water (2x5 mL). Then, the organic phase was separated, dried over anhydrous Na_2SO_4, filtrated and evaporated under reduced pressure, yielding 40 mg (85%) of compound **38**.

m.p.: Oily compound.

IR (thin film, υ in cm^{-1}): 3837, 3744, 3672, 3648, 3187, 2922, 2359, 2247, 1699, 1617, 1546, 1496, 1419, 1338, 1311, 1252, 1219, 1158, 1112, 952, 915, 817, 732, 662.

^{1}H NMR (400 MHz, $CDCl_3$) δ 8.02 (s, 1H), 7.64 – 7.30 (m, 4H), 7.13 – 6.98 (m, 6H), 6.96 – 6.86 (m, 3H), 6.60 (d, *J* = 8.2 Hz, 1H), 3.72 (s, 3H), 3.55 (s, 20H), 2.89 (s, 3H), 2.81 (dd, *J* = 23.8 y 12.6 Hz, 9H), 2.29 (s, 3H), 1.54 (s, 3H), 1.49 (s, 3H).

^{13}C NMR (101 MHz, $CDCl_3$) δ 179.0 (C), 156.7 (C), 153.0 (C), 143.9 (2 C), 138.0 (2 C), 137.7 (2 C), 135.7 (2 C), 131.2 (CH), 130.1 (CH), 129.9 (2 CH), 128.8 (2 C), 128.6 (CH), 128.3 (2 CH), 127.2 (2 CH), 121.6 (CH), 121.1 (2 CH), 121.1 (4 C), 118.6 (2 CH), 110.6 (CH), 70.7 (5 CH_2), 70.2 (5 CH_2), 55.5 (CH), 54.2 (3 CH_2), 41.4 (CH_2), 34.8 (C), 33.4 (2 CH_3), 27.6 (CH_3), 25.6 (CH_3), 21.6 (CH_3).

HRMS (ESI+): Calculated for $C_{53}H_{63}{}^{35}Cl_3N_5O_{11}S^+$ $[M+H]^+$ 1082.3305, found 1082.3291.

(4-Methoxyphenyl)methanol (39)

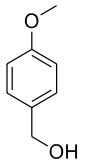

39

$NaBH_4$ (400 mg, 10.6 mmol) was added portionwise over a solution of *p*-anisaldehyde (2.00 mL, 16.5 mmol) in 20 mL of MeOH. The reaction was kept at room temperature for 10minutes and then the solvent was evaporated under reduced pressure and 20 mL of water wereadded. The aqueous phase was extracted with EtOAc (2x25 mL), the organic phases were combined, dried over anhydrous Na_2SO_4, filtrated and evaporated under reduced pressure, yielding 1.66 g (73%) of compound **39** as a colourless oil, which was used without further purification in the next reaction.

^{1}H NMR (200 MHz, $CDCl_3$) δ 7.79 (d, *J* = 8.6 Hz, 2H), 7.39 (d, *J* = 8.6 Hz, 2H), 5.10 (s, 2H), 4.31 (s, 3H).

All the spectroscopic properties matched the characterisation made in the literature.[83]

1-(Chloromethyl)-4-methoxybenzene (40)

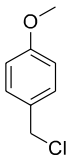

40

A solution of $SOCl_2$ (2 mL, 27.6 mmol) in 5 mL of CH_2Cl_2 was added over compound **39** (1.66 g, 12.0 mmol). The reaction was kept at room temperature for 15 minutes, then the solvent was evaporated under reduced pressure, yielding 1.78 g (95%) of compound **40** as a dark oil.

^{1}H NMR (200 MHz, $CDCl_3$) δ 7.31 (d, *J* = 8.6 Hz, 2H), 6.88 (d, *J* = 8.6 Hz, 2H), 4.56 (s, 2H), 3.80 (s, 3H).

All the spectroscopic properties matched the characterisation made in the literature.[84]

---

[83] Coufourier, S.; Ndiaye, D.; Gaillard, Q. G.; Bettoni, L.; Joly, N.; Mbaye, M. D.; Poater, A.; Gaillard, S.; Renaud, J. L. *Tetrahedron*, **2021**, *90*, 132187

[84] Sait, N.; Aliouane, N.; Toukal, L.; Hammache, H.; Al–Noaimi, M.; Helesbeux, J. J.; Duval, O. *Journal of Molecular Liquids*, **2021**, *326*, 115316.

Diethyl 2-(4-methoxybenzyl)-2-methylmalonate (41)

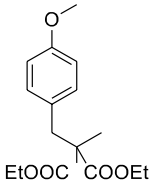

41

Small portions of Na (230 mg, 10.0 mmol) were dissolve in 10 mL of anhydrous EtOH in a reaction flask equipped with a reflux condenser. When all Na had dissolved, diethyl 2-methylmalonate (900 μL, 5.2 mmol) was added followed by a solution of compound **40** (790 mg, 5.0 mmol) in 2 mL of anhydrous EtOH. Then, the solvent was evaporated under reduced pressure and the crude was dissolved in 50 mL of EtOAc and washed with H_2O (2x15 mL), dried over anhydrous Na_2SO_4, filtered and concentrated under reduced pressure, yielding 1.40 g (94%) of compound **41** as dark oil, which was used without further purification in the next reaction.

^{1}H NMR (200 MHz, $CDCl_3$) δ 7.03 (d, *J* = 8.6 Hz, 2H), 6.79 (d, *J* = 8.6 Hz, 2H), 4.19 (c, *J* = 7.1 Hz, 4H), 3.77 (s, 3H), 3.16 (s, 2H), 1.32 (s, 3H), 1.25 (t, *J* = 7.1 Hz, 6H).

All the spectroscopic properties matched the characterisation made in the literature.[85]

2-(4-Methoxybenzyl)-2-methylmalonic acid (42)

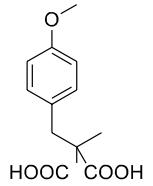

42

KOH (860 mg, 15.3 mmol) was added over a solution of compound **41** (1.40 g, 4.7 mmol) in 20 mL of EtOH and the reaction was refluxed for one hour. Then, the reaction mixture was added over 20 mL of 2M aqueous HCl and extracted with EtOAc (2x30 mL). The combined organic phases were separated, dried over anhydrous Na_2SO_4, filtrated and evaporated under reduced pressure, yielding 1.10 g (97%) of compound **42** as dark brown oil, which was used without further purification in the next reaction.

[85] Tsuji, H.; Hashimoto, K.; Kawatsura, M. *Org. Lett.* **2019**, *21*, 8837 – 8841.

^{1}H NMR (200 MHz, $CDCl_3$) δ 7.12 (d, *J* = 8.5 Hz, 2H), 6.82 (d, *J* = 8.5 Hz, 2H), 3.79 (s, 3H), 3.23 (s, 2H), 1.45 (s, 3H).

All the spectroscopic properties matched the characterisation made in the literature.[86]

3-(4-Methoxyphenyl)-2-methylpropanoic acid (43)

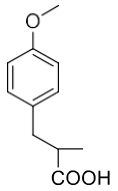

43

Compound **42** (1.10 g, 4.6 mmol) was heated at 180ºC for one hour. Then, it was dissolved in 50 mL of EtOAc and extracted with 4% aqueous solution of Na_2CO_3 (2x25 mL). The aqueous phase was acidulated with 35% aqueous HCl and extracted with EtOAc (2x25 mL). The combined organic phases were dried over anhydrous Na_2SO_4, filtered and evaporated under reduced pressure, yielding 790 mg (88%) of compound **43** as an oil, which was used without further purification in the next reaction.

^{1}H NMR (200 MHz, 10% CD_3OD in $CDCl_3$) δ 7.10 (d, *J* = 8.5 Hz, 2H), 6.83 (d, *J* = 8.5 Hz, 2H), 3.79 (s, 3H), 3.01 (dd, *J* = 12.4 y 6.6 Hz, 1H), 2.82 – 2.55 (m, 2H), 1.17 (d, *J* = 6.6 Hz, 3H).

All the spectroscopic properties matched the characterisation made in the literature.[87]

3-(3-(Chloromethyl)-4-methoxyphenyl)-2-methylpropanoic acid (44)

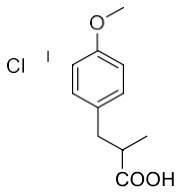

44

Compound **43** (790 mg, 4.1 mmol), paraformaldehyde (791 mg, 26.3 mmol) and 3 mL of 35% aqueous HCl were dissolved in 15 mL of AcOH and heated at 35ºC for 16 hours. Then, the reaction mixture was added over 50 mL of H_2O and extracted with EtOAc (3x25 mL). The combined organic phases were separated, dried over anhydrous Na_2SO_4, filtered and

[86] Johansson, A. M.; Mellin, C.; Hacksell, U. *J. Org. Chem.* **1986**, *51*, 5252–5258.
[87] Zhu, Y.; Chen, X.; Yuan, C.; Li, G.; Zhang, J.; Zhao, Y. *Nat. Commun*. **2017**, *8*, 14904.

evaporated under reduced pressure, yielding 952 mg (98%) of compound **44** as a dark brown oil, which was used without further purification in the next reaction.

m.p.: Oily compound.

IR (thin film, υ in cm^{-1}): 2972, 2839, 1707, 1614, 1504, 1462, 1379, 1259, 1184, 1160, 1122, 1031, 941, 902, 814, 753, 681.

^{1}H NMR (400 MHz, $CDCl_3$) δ 7.18 (d, *J* = 1.6 Hz, 1H), 7.12 (dd, *J* = 8.5 y 1.6 Hz, 1H), 6.82 (d, *J* = 8.4 Hz, 1H), 4.63 (s, 2H), 3.86 (s, 3H), 3.01 (dd, *J* = 13.5 y 6.9 Hz, 1H), 2.73 (hex, *J* = 6.9 Hz, 1H), 2.63 (dd, *J* = 13.5 y 6.9 Hz, 1H), 1.18 (d, *J* = 6.9 Hz, 3H).

^{13}C NMR (101 MHz, $CDCl_3$) δ 182.5 (C), 156.1 (C), 131.2 (CH), 131.2 (C), 130.6 (CH), 125.8 (C), 110.9 (CH), 55.7 (CH_3), 41.7 (CH_2), 41.5 (CH), 38.4 (CH_2), 16.6 (CH_3).

HRMS (ESI-): Calculated for $C_{12}H_{15}O_3^-$ $[M-Cl]^-$ 207.1016, found 207.1009.

3-(3-(chloromethyl)-4-methoxyphenyl)-*N*-(2,7-dichloro-5-(3-(4-chlorophenyl)ureido)-9,9-dimethyl-9*H*-xanthen-4-yl)-2-methylpropanamide (45)

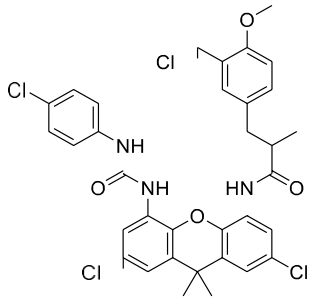

45

Compound **44** (165 mg, 0.7 mmol) was dissolved in 2 mL of $SOCl_2$ and refluxed for 30 minutes. Then, the solvent was evaporated under reduced pressure to yield 160 mg (90%) of compound **44** acid chloride, which was used without further purification in the next reaction.

Following Schotten-Baumann conditions (as described in section 4.2.5.), compound **44** acid chloride (64 mg, 0.25 mmol) dissolved in 15 mL de EtOAc was added over a solution of compound **25**·CF_3COOH (88 mg, 0.15 mmol) in 20 mL of EtOAC and 10 mL of a saturated aqueous solution of Na_2CO_3 under vigorous stirring at 0ºC. Then, the organic phase was separated, washed with 15 mL of H_2O, dried over anhydrous Na_2SO_4, filtered and evaporated under reduced pressure. The crude was purified by silica gel column chromatography with mixtures CH_2Cl_2/EtOAc 9:1 as eluent and mixtures with higher polarity. 84 mg (80%) of compound **45** were obtained as an orange oil.

m.p.: Oily compound.

IR (thin film, υ in cm^{-1}): 3319, 2969, 1669, 1598, 1541, 1499, 1417, 1307, 1254, 1220, 1031, 910, 860, 820, 732.

^{1}H NMR (400 MHz, $CDCl_3$) δ 7.69 – 7.63 (m, 4H), 7.45 – 7.39 (m, 2H), 7.22 – 7.01 (m, 3H), 6.83 – 6.77 (m, 2H), 5.30 (s, 2H), 3.72 (s, 3H), 2.95 – 2.84 (m, 1H), 2.77 – 2.62 (m, 2H), 1.82 (s, 6H), 1.55 (s, 3H).

^{13}C NMR (101 MHz, $CDCl_3$) δ 182.5 (C), 156.1 (C), 131.2 (CH), 131.2 (C), 130.6 (CH), 125.8 (C), 110.9 (CH), 55.7 (CH_3), 41.7 (CH_2), 41.5 (CH), 38.4 (CH_2), 16.6 (CH_3).

HRMS (ESI-): Calculated for $C_{34}H_{31}{}^{35}Cl_5N_3O_4^-$ $[M+Cl]^-$ 720.0763, found 722.0745.

3-(3-((1-Aza-18-crown-6-1-yl)methyl)-4-methoxyphenyl)-*N*-(2,7-dichloro-5-(3-(4-chlorophenyl)ureido)-9,9-dimethyl-9*H*-xanthen-4-yl)-2-methylpropanamide (46)

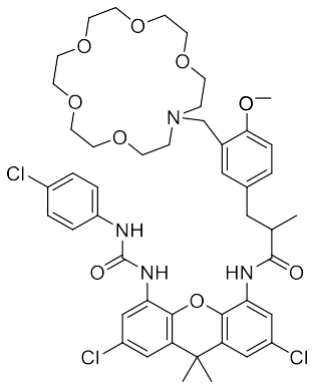

46

Compound **45** (52 mg, 0.08 mmol) and 18-crown-6 ether (93 mg, 0.35 mmol) were dissolved in 500 μL of CH_2Cl_2 and left without stirring for 16 hours. Then, the solvent was evaporated under reduced pressure and 10 mL of EtOAc were added. The organic phase was washed with deionized water (2x5 mL), dried over anhydrous Na_2SO_4, filtrated and evaporated under reduced pressure, yielding 48 mg (69%) of compound **46**.

m.p.: Oily compound.

IR (thin film, υ in cm^{-1}): 3462, 3268, 3115, 2916, 1705, 1601, 1543, 1494, 1434, 1354, 1310, 1254, 1218, 1111, 1208, 954, 913, 830, 732.

^{1}H NMR (400 MHz, $CDCl_3$) δ 7.98 (s, 1H), 7.83 (s, 1H), 7.64 (d, *J* = 6.1 Hz, 2H), 7.22 (d, *J* = 8.0 Hz, 2H), 7.16 – 6.94 (m, 4H), 6.87 (s, 2H), 6.79 (s, 1H), 6.45 (d, *J* = 8.3 Hz, 1H), 4.18 (d, *J* = 14.2 Hz, 1H), 3.65 (s, 3H), 3.80 – 3.29 (m, 26H), 2.96 – 2.79 (m, 1H), 2.57 (d, *J* = 11.2 Hz, 1H), 1.67 (s, 3H), 1.38 (s, 3H), 1.33 (d, *J* = 5.6 Hz, 3H).

^{13}C NMR (101 MHz, $CDCl_3$) δ 178.8 (C), 176.5 (C), 156.6 (C), 153.2 (2C), 140.3 (C), 138.9 (2C), 138.3 (C), 133.8 (CH), 133.1 (2CH), 132.0 (C), 130.7 (2C), 128.8 (CH), 128.1 (2C), 126.8 (C), 122.7 (2CH), 120.3 (CH), 119.6 (CH), 117.1 (2CH), 111.5 (CH), 70.7 ($4CH_2$), 70.0 ($4CH_2$), 69.9 ($2CH_2$), 55.3 (CH), 46.5 ($2CH_2$), 39.2 (CH_2), 35.2 (C), 33.7 (CH_3), 29.8 (CH_2), 27.6 (CH_3), 24.9 (CH_3), 19.5 (CH_3).

HRMS (ESI-): Calculated for $C_{46}H_{56}{}^{35}Cl_3N_4O_9^+$ $[M+H]^+$ 913.3107, found 913.3093.

5.3. General procedures for NMR titrations

Measurement of binding constants by absolute ^{1}H NMR titrations

A typical procedure for NMR titrations is described. A solution of receptor **2** (2 mM, 2 mL) in $CDCl_3$ was prepared and a volume of 500 μL was added to a standard NMR tube. The ^{1}H NMR spectrum of this sample was then collected at 298 K. A solution of the tetrabutylammonium salt (0.01 M) was prepared by dissolving the exact amount of the salt in the remaining solution (1.5 mL) of receptor **2**. Aliquots of this solution were then added to the NMR tube, mixing well after each addition and recording the corresponding ^{1}H NMR spectra. The concentration of receptor **2** was kept constant during the titration as the anion solution also contained receptor **2** at its initial concentration. The chemical shifts of selected protons were analyzed and plotted against the ratio of concentrations [Guest]/[Host]. K_a values were calculated using a Monte Carlo nonlinear curve-fitting method.

Measurement of binding constants by competitive ^{1}H NMR titrations

For competitive titrations, a solution of both receptors in $CDCl_3$ (2 mL) was prepared with similar concentrations of the receptors [**1**]= [**2**] =10^{-2}M. A volume of 500 μL of this solution was added to a standard NMR tube and the ^{1}H NMR spectrum of the sample was collected at 298 K. A solution of the tetrabutylammonium salt (0.025 M) was prepared by dissolving the exact amount of the salt in the remaining solution (1.5 mL) of the receptors. Aliquots of the solution containing the salt were then added to the NMR tube, mixing well after each addition and recording the corresponding ^{1}H NMR spectra. The chemical shifts of selected protons from both receptors were analyzed and plotted against each other. The relative association constant was calculated using a Monte Carlo nonlinear curve-fitting method.

5.4. General procedure for amino acid extraction

In a typical liquid-liquid extraction experiment, the organic layer was prepared by dissolving together 24 mg (22.9 mmol) of the macrocycle **2** and 14 mg (53.0 mmol) of the 18-crown-6-ether in 2 mL of $CDCl_3$ ([**2**] =1.15×10^{-2}M; [crown ether]= 2.65×10^{-2}M). A portion of this solution (0.5 mL) was added to 0.5 mL of an aqueous saturated solution of the corresponding amino acid. The mixture was stirred for 15 minutes, centrifugated and the ^{1}H NMR spectrum of the organic layer was obtained. The extraction efficiency (in terms of extracted equivalents of amino acids) was determined by integration of the ^{1}H NMR signals .

5.5. Resolution of macrocyclic receptor 2 enantiomers using TLC impregnated with L-amino acids

Conventional TLC plates were impregnated with a 1.5% aqueous solution of the L-amino acid (phenylglycine or phenylalanine) and the stoichiometric amount of the crown ether (18-crown-6-ether) and dried. The chiral stationary phase thus obtained was useful for the separation of the macrocycle enantiomers: elution with the solvent system methylene chloride/diethyl ether (4:1) afforded two separated spots, corresponding to the diastereomeric complexes of L-phenylglycine with each enantiomer of the racemic macrocycle **2**.

On the other hand, for L-phenylalanine, both spots were not well separated.

5.6. Chiral HPLC chromatograms

Enantiomeric excess (ee) was determined with an Agilent 1100 series HPLC, using a Daicel CHIRALPAK ZWIX(+) (analytical Column, 3 µm, ID 3.0 mm x L 150 mm) and a mixture of two solvent systems as eluent: solvent A 98:2 (4:1 mixture of acetonitrile and methanol/ water containing 20 mM formic acid and 20 mM ammonium formate) and solvent B 98:2 (methanol/ water containing 40 mM formic acid and 20 mM ammonium formate).

5.7. ORTEP diagrams and X-ray crystal structure data

A suitable single crystal of the ternary complex (macrocycle **2**/ phenyl glycine/ 18-crown-ether-6) was mounted on glass fiber for data collection on a Bruker Kappa Apex II CCD diffractometer. Data were collected at 298 K using Cu K_α radiation (λ = 1.54178 Å) and ω scan technique, and were corrected for Lorentz and polarization effects. The crystal structure was solved by direct methods combined with difference Fourier synthesis and refined by full-matrix least-squares fitting on F^2 by the SHELXTL-97 program.[88] All the non-hydrogen atoms, except some disordered atoms and some isolated water solvent molecules, were refined anisotropically. The carbon atom sites (labeled C46, C47, C48 and C52) of the butyl groups are split on two positions each with an occupancy factor of 50%. The hydrogen atoms were positioned geometrically. Due to diffuse electron density associated with solvent molecules of crystallization, the hydrogen atoms on solvent molecules cannot be generated but they are included in the molecular formula directly. The high R_1 and wR_2 factor both of the complex might be due to the disorder of the solvent and the weak crystal diffraction. CCDC-1441451

[88] (a) G. M. Sheldrick, SHELXS 97, Program for crystal Structure Solution, **1997**, University of Göttingen. (b) G. M. Sheldrick, SHELXL 97, Program for crystal Structure Refinement, **1997**, University of Göttingen.

contains the supplementary crystallographic data for this paper. These data are provided free of charge by The Cambridge Crystallographic Data Centre.

5.8. Modelization studies

All calculations were done using Gaussian16 software. Geometry optimizations were performed in the gas phase using the M06-2X functional, along with 6-31G(d,p) basis set. Grimme´s dispersion term was included by means of the "empiricaldispersion=GD3" keyword. Gibbs free energy correction was calculated at the same level of theory employed during the optimization. A quasi-harmonic rotor approximation was used, as suggested by Grimme, as it is implemented in "Goodvibes" Software developed by Robert Paton and Funes-Ardoiz. The default settings (100 cm^{-1} cutoff) were used. This correction to the Gibbs free energy was added to the single point energy calculated at the M06-2X-D3/6-311+G(d,p) level of theory in which solvent effects (chloroform) were included by means if an implicit SMD solvation model.

In addition to the geometry obtained from the X-ray diffraction experiments, an alternative geometry was considered for the receptor in which the four NH sulfonamides were directed toward the cavity. This was accomplished by establishing a gauche conformation in the ethylenediamine moiety instead of the alternated conformation shown in the X-ray diffraction structure (see Figure 3). The energies of the complexes are larger with this alternative geometry in all structures, except for the structure of the (*S*)-**2•** L-phenylglycine complex in which the gap toward the binaphthyl sheet is occupied by the phenyl ring. However, the energy of this structure is large compared with the other (*S*)-**2•** L-phenylglycine complex in which the gap is occupied by the crown ether. A third set of structures was also sought, in which the gauche/alternate configurations of the ethylenediamine moieties are reversed with respect to the most stable structures. The energies are, however, considerably larger in all cases, and therefore these structures were not sought for the complexes with phenylalanine.

Binding constant titrations, HPLC traces, ORTEP diagrams and X-ray crystal structure data and modelling studies coordinates are freely available at:
https://pubs.acs.org/doi/suppl/10.1021/acs.orglett.9b04379/suppl_file/ol9b04379_si_001.pdf

Chapter 2 – Objectives

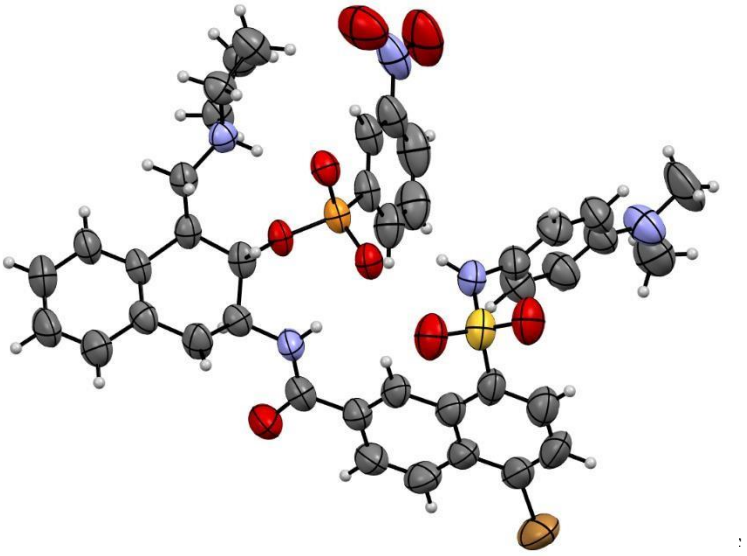

In **Chapter 2**, organoc hydrolytic enzymes will be discussed. Spectroscopic and structural analysis, as well as the study of the catalytic properties of these compounds will show the structural requirements that are necessary to mimic the reaction rates provided by enzymes.

The **main objective** of this chapter is the synthesis of a series of artificial hydrolases which mimic the active centre of chymotrypsin and *N*-terminal hydrolases. They will be tested as catalysts for transesterification reactions. To achieve this goal, the specific objectives shown below are proposed:

- **Objective 1**: Structural studies of the active centre X-ray structure of chymotrypsin and *N*-terminal hydrolases. Inhibited enzymes with tetrahedral intermediate analogues will be explored. This knowledge will show the relative geometry between the functional groups which will be mimicked to synthesise the organocatalysts.

- **Objective 2**: Design and modelling studies of small-molecule hydrolase mimics.

- **Objective 3**: Synthesis and characterization of the organocatalysts.

- **Objective 4**: Kinetic, association and structural studies. The knowledge generated will be used to modify the catalysts structure accordingly.

Chapter 2 – Introduction

2. Introduction

2.1. Catalysis

2.1.1. Definition and classification

Both in research and industrial processes, **catalysis** is fundamental to facilitate the obtention of new compounds such as drugs, agrochemicals, cosmetics, food industry compounds, etc. The concept of **catalysis** was established by J. J. Berzelius[89] in 1835 and corresponds to the process of increasing the rate of a chemical reaction by the addition of a substance, called **catalyst**, which is not consumed. These catalysts usually interact with one or more reagents to form intermediates or associates, which are transformed into the products without modifying the structure of the catalyst. In general, catalysts provide an alternative mechanism in which the activation energy is lower than the reaction without the catalyst, as it is shown in Figure 68.

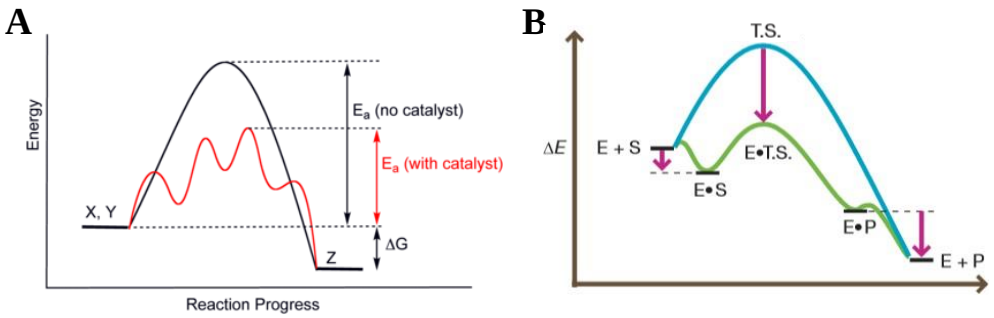

Figure 68. *(A) Potential energy diagram for a reaction with (red line) and without (black line) the presence of a catalyst. (B) Potential energy diagram for an enzymatic reaction with (green line) and without (blue line) catalysis.*[90]

Many industrial processes have one step in which a catalyst is necessary in the reaction mixture to obtain the desired compound. For example, Contact Process uses vanadium (V) oxide as catalyst to oxidize sulfur dioxide to sulfur trioxide which is employed to produce around 200 million tons of sulfuric acid per year.[91] Another example are epoxy-adhesives, or polyepoxides, whose monomers contain an epoxide which is responsible of the polymerization. It is usually carried out with a wide range of co-reactants such as acids, alcohols, phenols, amines, or thiols (curatives in the cross-linking reaction)[92] or using either acids or bases in a catalytic homopolimerization process (Figure 69).

---

[89] Trofast, J. *The Concept of Catalysis. In Perspectives in Catalysis- In Commemoration of Jöns Jacob Berzelius*; Larsson, R., Ed.; Gleerup:Lund, **1981**; p 9-17.
[90] Vranken, D. V.; Weiss, G. A. *Introduction to Bioorganic Chemistry and Chemical Biology*, **2012**, *I*, 237.
[91] https://www.essentialchemicalindustry.org/chemicals/sulfuric-acid.html (accessed on October, 2021).
[92] May, C. *Epoxy Resins: Chemistry and Technology*. 2nd ed.; CRC Press, New York, **1988**.

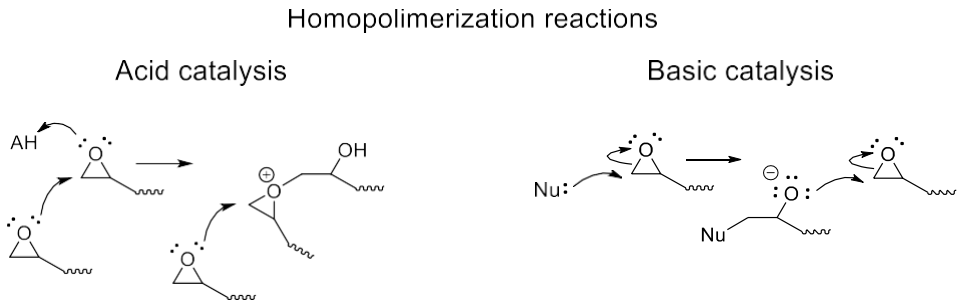

Figure 69. *Homopolymerization of epoxy-adhesives under acid (left) and basic (right) conditions.*

According to the medium where the catalyst performs its function, catalysis can be classified as: **heterogeneous** and **homogeneous catalysis**.

In **heterogeneous catalysis**[93] reagents and catalyst are in different phases. Most of the heterogeneous catalysts are solids which interact with the reagents in liquid or gaseous mixtures, and they can be removed easily by filtration. Zeolites, alumina, metals, or metal oxides, among others, are well known catalysts for several chemical transformations. The reaction takes place in the active sites of the catalyst, which are planar surfaces, surface imperfections or cavities. Also, unusual metal valences responsible of the catalysis are present in the solid.

Haber Process[94] is one example of an industrial transformation where a heterogeneous catalyst is employed. In this reaction ammonia is obtained from bimolecular nitrogen and hydrogen gas using finely divided iron as catalyst. The reagents are adsorbed onto the catalyst and the triple bond from the dinitrogen is broken. This process is used in industry to obtain around 230 million tons of ammonia per year,[95] which is essential in fertilizers production. It has been estimated that 50% of the human nitrogen atoms have a synthetic origin.[96]

In heterogeneous catalysis, it is usual to support the catalysts on a non-active material, such as alumina, silica or activated carbon, to improve their effectiveness and minimize costs. For example, in organic synthesis, the traditional method to reduce an alkene to the corresponding hydrocarbon with H_2 takes place in the presence of nanoparticles of palladium supported on active carbon.

---

[93] Schlögl, R. *Angew. Chem. Int. Ed.* **2015**, *54*, 3465 – 3520.
[94] Appl, M. Ammonia, 2. Production Processes in *Ullmann's Encyclopedia of Industrial Chemistry*, WILEY-VCH, **2011**.
[95] Production capacity of ammonia worldwide from 2018 to 2030. https://www.statista.com/statistics/1065865/ammonia-production-capacity-globally/ (accessed on October, 2021)
[96] https://ourworldindata.org/how-many-people-does-synthetic-fertilizer-feed (accessed on October, 2021).

On the other hand, in **homogeneous catalysis**[97] all the components are dissolved in the same phase. Homogeneous catalysts are usually organic compounds or single-atom metals with organic ligands, which interacts with the reagents in a liquid or gaseous phase. There are four main categories in homogeneous catalysis: **acid-base catalysis**, **transition metal catalysis**, **biocatalysis** and **organocatalysis**.[97]

Transition metal catalysis

In this group the catalyst contains one metal atom, such as iron, palladium, titanium, aluminium, or iridium, among others, which is stabilized with different organic ligands. They can catalyse many different reactions such as the polymerization of terminal alkenes using Ziegler-Natta catalyst[98] (Figure 70A) or the late-stage C-H functionalization of pharmaceutical compounds (Figure 70B).[99]. Photocatalysis, where the catalyst receive light to generate an excited state responsible for catalysis, has become an important field with novel applications, such as singlet oxygen generation ($^1O_2$) produced by a metal-transition catalyst (Figure 70C).[100]

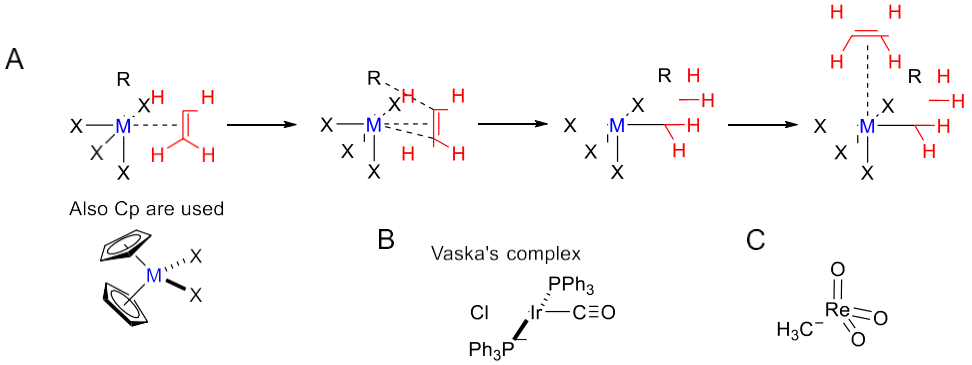

Figure 70. *(A) Ziegler-Natta catalyst mechanism for terminal alkenes polymerization.*[98] *(B) Vaska's complex employed in Strecker C-H late-stage amide and lactam cyanation.*[100] *(C) Photocatalysts employed on singlet oxygen ($^1O_2$) generation.*[99]

Biocatalysis

In biology, enzymes are the main catalysts in catabolism and anabolism processes. Enzymes are proteins formed by sequentially linked amino acids (secondary structure), where intermolecular interactions (such as disulfide bonds and hydrogen bonds, stacking, ionic bridges, among others,) set up the ternary and quaternary structure with a specific three-dimensional shape. The active centre, where the reaction takes place, usually consists of a

---

[97] van Leeuwen, P. W. N. M. *Homogeneous Catalysis. Understanding the Art*, Kluwer Academic Publishers, Dordrecht – Boston – London, **2004**.
[98] Cossee, P. *Journal of Catalysis* **1964**, *3*, 80 – 88.
[99] Fuentes de Arriba, A. L.; Lenci, E.; Sonawane, M.; Formery, O.; Dixon, D. J. *Angew. Chem. Int. Ed.* **2017**, *56*, 3655 – 3659.
[100] Sánchez Arroyo, A. J. Tesis Doctoral, **2019**, Universidad Complutense de Madrid.

specific cavity with functional groups which participate in the reaction. Temperature, ionic strength or pH have a big influence in the geometry of the ternary and quaternary structures and, subsequently, are able to modify the active centre's configuration and its catalytic properties. Unlike transition metal catalysis, many enzymes do not need any metals in its structure to catalyse the reaction.

Thanks to its selectivity, enzymes are used in several industrial syntheses, where the target is very specific. For example, the highly selective 11-hydroxylation of 11-deoxycortisol to yield cortisol by 11-β-hydroxylase is a good example.[101]

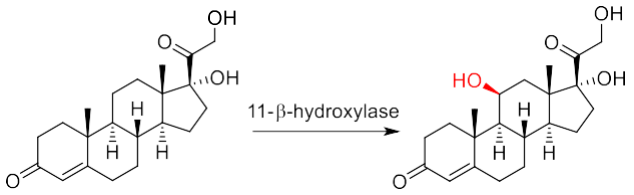

Figure 71. *Industrial synthesis of cortisol using 11-β-hydroxylase.*

One of the main problems of using enzymes is that its obtention is very expensive and they are sensitive to changes in the pH, temperature, ionic strength, etc. Most of them only work in aqueous media under mild reaction conditions.

Organocatalysis

The use of small organic molecules to increase the rate of a reaction is called organocatalysis. Whereas transition metal catalysis uses metal atoms to produce catalysis, organocatalysts do not have any metal atom in its structure.

Several advantages for the use of organocatalysts are listed below:[102]

- Most of them do not require mild reaction conditions (they tolerate humidity, oxygen, wet solvents, etc).
- Small organic molecules have higher stability than enzymes, so they can be used in more extreme conditions. For example, enzymes usually could not be used over 60ºC.
- They are usually cheaper than enzymes and transition-metal catalysts.
- They can be used in a wide range of applications.
- They contribute to Green Chemistry avoiding toxic metals in its structure. They can be used safely in food and pharmaceutical industries.

---

[101] (a) Buchholz, K.; Kasche, V.; Bornscheuer, U. T. *Biocatalysts and Enzyme Technology*. 2nd ed. WILEY-VCH, Weinheim, **2012**. (b) Slater, L. B. Industry and Academy: The Synthesis of Steroids. *Hist. Stud. Phys. Biol. Sci.* **2000**, *30*, 443–480.

[102] (a) Juaristi, E. *Educ. quim.* **2010**, *22*, 12 – 14.
(b) http://www.scielo.org.mx/scielo.php?script=sci_arttext&pid=S0187-893X2011000100003 (accessed on October, 2021).

2.1.2. Organocatalysis

Background and classification

During the last decades organocatalysis has been developed exponentially, even though it is not a modern concept. The first record for an organocatalytic reaction is the hydrolysis of cyanogen to oxamide in the presence of aqueous acetaldehyde by Liebig in 1860.[103] Some important events in organocatalysis field are shown below:

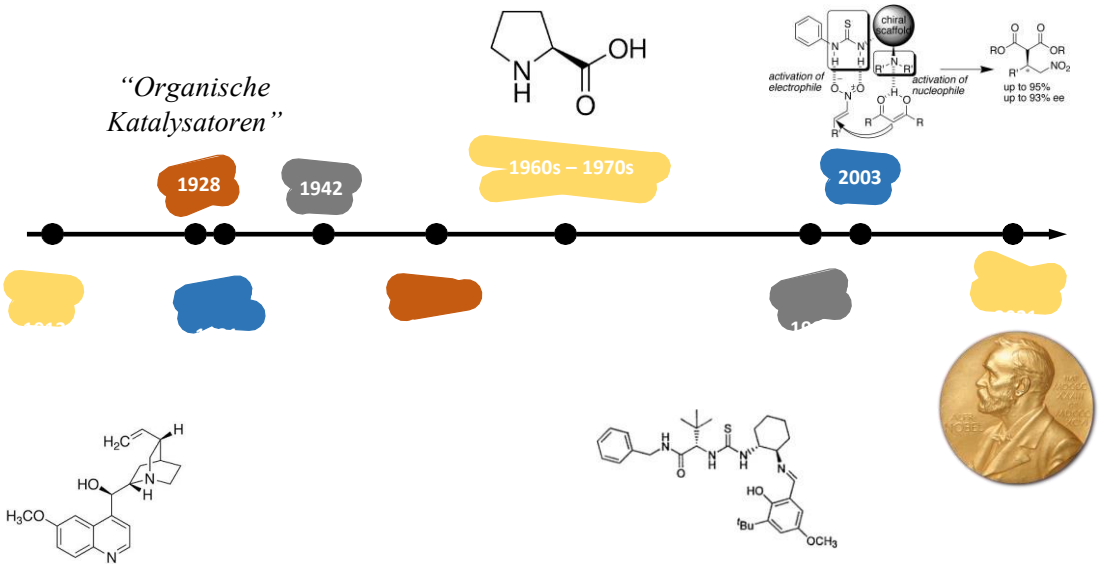

- ✓ **1912**. Bredig and Fiske[104] reported the addition of HCN to benzaldehyde using quinine and quinidine.
- ✓ **1928**. Langenbeck[105] coined the term *organocatalysis*: catalytic activity of small organic molecules and enzymes.
- ✓ **1931**. Fischer and Marschall[106] used amino acids to catalyse aldol reactions. In **1942**, Langenbeck and Borth[107] used chiral amino acids in this reaction.
- ✓ **1950s**. Pracejus[108] reported a quinine derivative to catalyse the asymmetric addition of MeOH to methylphenylketene. Wynberg[109] used quinine in a Michael addition of β-keto esters or nitroalkanes to unsaturated ketones.
- ✓ **1960s-1970s**. General mechanism for class I aldolases[110] through an enamine intermediate was revealed.

---

[103] von Liebig, J. *Justus Liebigs Ann. Chem. (Ann. Chem. Pharm.)* **1860,** *113*, 246 – 247.
[104] Bredig, G.; Fiske, W. S., *Biochem. Z.* **1912**, *46*, 7 – 23.
[105] Langenbeck, W. *Angew. Chem.* **1928**, *41*, 740 – 745.
[106] Fischer, F. G.; Marschall, A. *Ber.* **1931**, *64*, 2825 – 2827.
[107] Langenbeck, W.; Borth, G. *Ber.* **1942**, *75B*, 951 – 953.
[108] (a) Pracejus, H.; Mätje, H. *J. Prakt. Chem.* **1964,** *24*, 195 – 205. (b) Pracejus, H. *Justus Liebigs Ann. Chem.* **1960**, *634*, 9 – 22.
[109] Wynberg, H.; Helder, R. *Tetrahedron Lett.* **1975**, *16*, 4057 – 4060.
[110] (a) Lai, C. Y.; Nakai, N.; Chang, D. *Science* **1974**, *183*, 1204. (b) Rutter, W. J. *Fed. Proc. Am. Soc.*

Exp. Biol. **1964**, *23*, 1248 – 1257.

✓ **1998**. Jacobsen[111(a)] reported a Strecker reaction catalysed by hydrogen bonding between N-allylbenzaldimine and HCN. The catalyst has a thiourea which acts as bifunctional catalyst, activating both electrophile and nucleophile simultaneously. In **2003**, Takemoto[112] reported a simple bifunctional thiourea derivative for Michael and Aza-Henry reactions.

These examples involve different types of organocatalysts and mechanisms which can be classified in different ways. According to the catalyst's nature or mechanistic role there are **acid-base Brönsted** and **acid-base Lewis catalysts**; if the difference lies in the interaction between reagents and catalyst there are **non-covalent** and **covalent organocatalysis**, and the last one focus on the stereochemistry, and distinguish between **non-chiral** and **chiral** organocatalysis.

Acid-base Brönsted and acid-base Lewis catalysis

Most organocatalysts can be classified in line with their mechanistic role or the reactions that they promote. According to their mechanistic role, they can be classified as **Lewis acid or base** and **Brönsted acid or base**.[113] Figure 72 shows the different mechanisms involved within this classification.

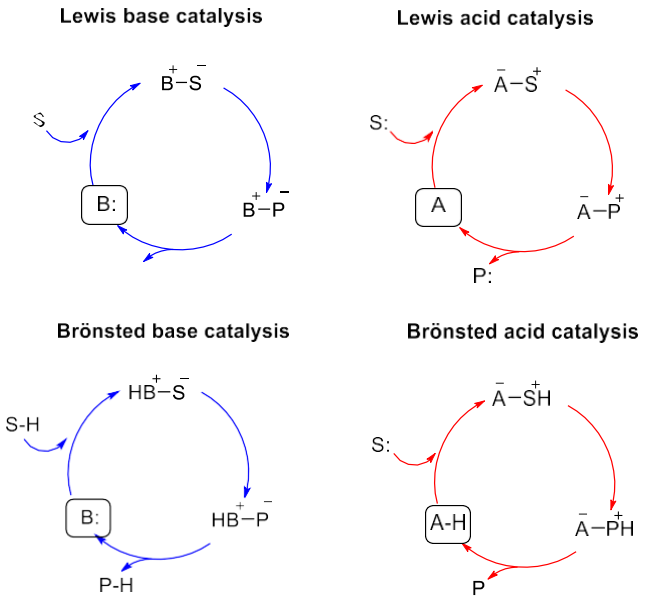

Figure 72. *Catalytic cycles with Lewis acid (A) or base (B:) (above) and Brönsted acid (A-H) or base (B:) (bottom).*[113] *S stands for substrate and P for product.*

[111] (a) Sigman, M. S.; Jacobsen, E. N. *J. Am. Chem. Soc.* **1998**, *120*, 4901 – 4902. (b) Zuend, S. J.; Coughlin, M. P.; Lalonde, M. P.; Jacobsen, E. N. *Nature* **2009**, *461*, 968 – 970.
[112] Okino, T.; Hoashi, Y.; Takemoto, Y. *J. Am. Chem. Soc.* **2003**, *125*, 12672 – 12673.
[113] Seayad, J.; List, B. *Org. Biomol. Chem.* **2005**, *3*, 719 – 724.

In Lewis acid or base (A / B:) mechanisms, the organocatalyst starts the cycle ~~by~~ binding ~~to~~ the substrate (S), with a subsequent reaction to generate the product and, in the end the catalyst is released again. On the other hand, Brönsted acid or base (AH / B:) mechanisms starts with the protonation or deprotonation of the substrate, respectively. Usually the catalyst remains attached to the substrate as a ionic pair. Simón and Goodman[114] reported the mechanism of a Strecker reaction using chiral phosphoric acids as organocatalysts, which have a Lewis base and a Brönsted acid in its structure to activate both nucleophile and electrophile.

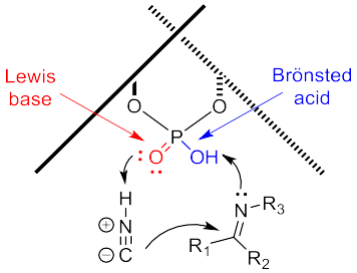

Figure 73. *Mechanism of a Strecker reaction reported by Simón and Goodman using chiral phosphoric acids as catalysts. The Lewis base actives the nucleophile whereas the Brönsted acid protonates the electrophile to enhance its reactivity.*[114]

Non-covalent and covalent organocatalysis

Organocatalysis can also be classified according to the substrate's interaction with the organocatalyst: in **covalent organocatalysis** the catalyst forms a covalent bond with the substrate, which will break down at the end of the reaction in order to regenerate the catalyst; in **non-covalent organocatalysis**, the catalyst stablishes non-covalent interactions with the substrate, such as hydrogen bons.

Several examples have been reported where L-proline acts through covalent catalysis, reacting with the substrate to form a reactive enamine intermediate which can be used, for example, to functionalize the carbonyl α-carbon in aldol reactions between ketones and aromatic aldehydes. Jacobsen and co-workers[111] reported that thioureas and ureas catalyse the Strecker reaction between HCN and *N*-allylbenzaldimine through hydrogen bonding.

[114] Simon, L.; Goodman, J. L. *J. Am. Chem. Soc.* **2009**, *131*, 4070 – 4077.

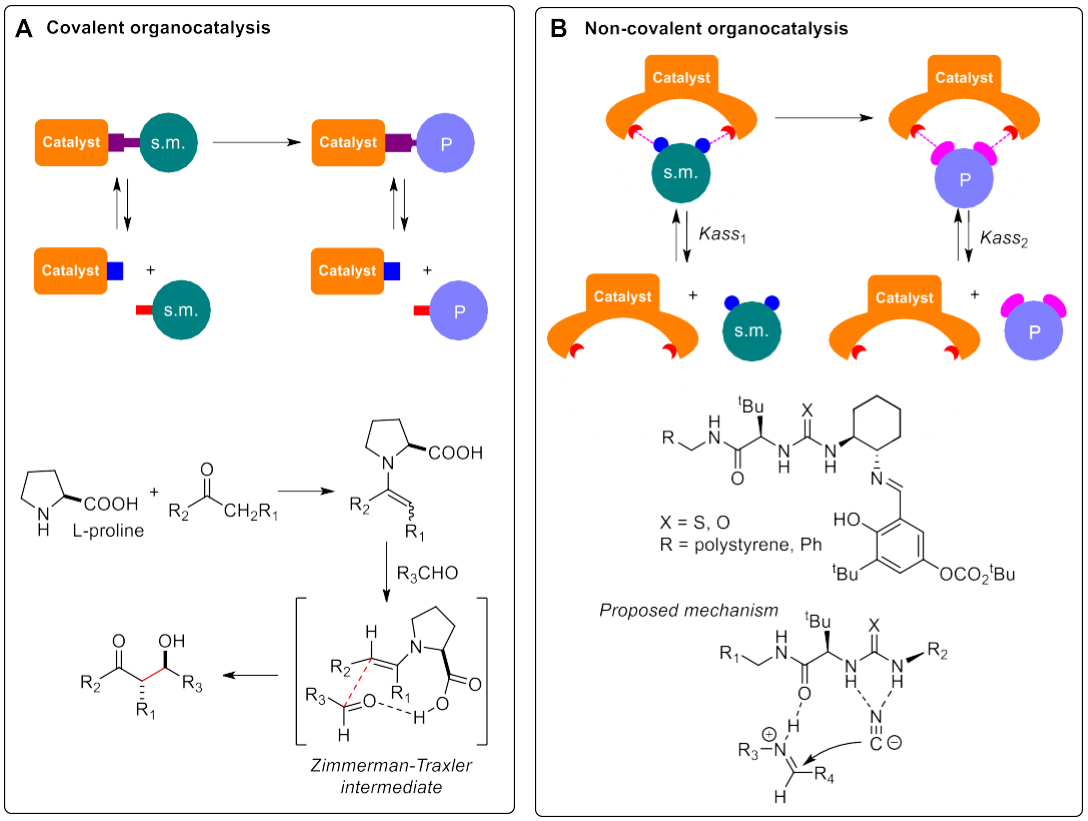

Figure 74. *(A, up) Schematic cartoon to explain covalent organocatalysis and (A, down) example using L-proline in an intermolecular aldol reaction. (B, up) Schematic cartoon to explain non-covalent organocatalysis and (B, down) catalysts based on ureas and thioureas reported by Jacobsen in Strecker reactions. s.m. stands for starting material and P for products.*

Non-chiral and chiral organocatalysis

The last classification can be stablished according to the chirality of the reaction. In **non-chiral organocatalysis** the reaction leads to non-chiral compounds whereas in **chiral organocatalysis** the reaction leads to chiral compounds. The last one is very interesting in drug development, as almost all of these compounds are enantiomerically pure since the opposite enantiomer can be inactive or even toxic.

Even though organocatalysis can be classified in these three groups, usually organocatalytic processes and organocatalysts can be part of several groups at the same time, because they have features of different groups.

2.1.3. Nobel Prize in Asymmetric Organocatalysis

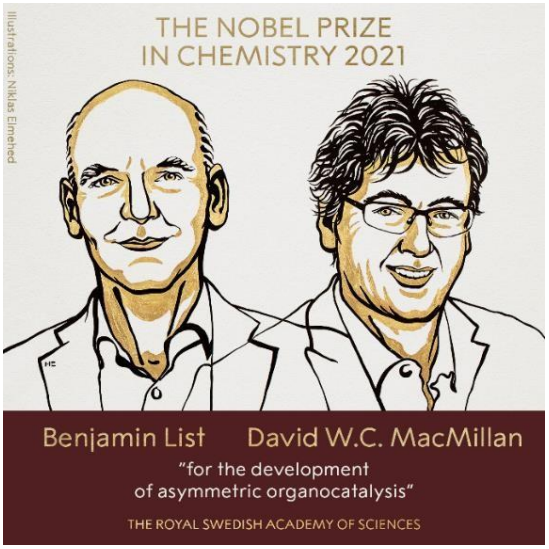

*"The Royal Swedish Academy of Sciences has decided to award **Benjamin List** and **David W. C. MacMillan** the Nobel Prize in Chemistry 2021, for the development of asymmetric organocatalysis."*[115]

In October 2021, Benjamin List and David W. C. Macmillan were awarded with the Nobel Prize in Chemistry due to their work from 2000 in which they introduced the **enamine and iminium ion mechanisms** in organocatalysis. "*Their work conceptualized the area of organocatalysis, focusing on asymmetric catalysis, and indicated principles for designing new organocatalytic reactions based on modern concepts such as LUMO lowering and HOMO raising.*" [115]

Benjamin List – Enamine catalysis / Lewis base catalysis

In 2000, List, Lerner and Barbas described an intermolecular aldol reaction catalysed by L-proline, where a new carbon-carbon bond is formed between acetone and several aromatic aldehydes.[116]

They proposed a mechanism where the L-proline forms an enamine with the acetone, raising up the Highest Occupied Molecular Orbital (HOMO) and therefore its nucleophilicity. The carboxylic group from L-proline helps to stabilize the metal-free Zimmerman-Traxler transition state by

---

[115] (a) Advanced information. NobelPrize.org. Nobel Prize Outreach AB 2021. Sun. 10 Oct 2021. https://www.nobelprize.org/prizes/chemistry/2021/advanced-information/.
(b) https://www.nobelprize.org/prizes/chemistry/.
(c) https://www.nobelprize.org/uploads/2021/10/advanced-chemistryprize2021-2.pdf (accessed on October, 2021).

[116] List, B.; Lerner, R. A.; Barbas, C. F. *J. Am. Chem. Soc.* **2000,** *122* (10), 2395 – 2396.

hydrogen bonding. The asymmetric feature is transferred from the catalyst through covalent bonding with the substrate.[115(c)] L-proline had been widely employed previously in organocatalysis, for example by Hajos and Parrish[117] and Eder, Sauer and Wiechert[118] to synthesise the Hajos-Wiechert and Wieland-Miescher ketones, which are valuable starting materials in several steroids synthesis.

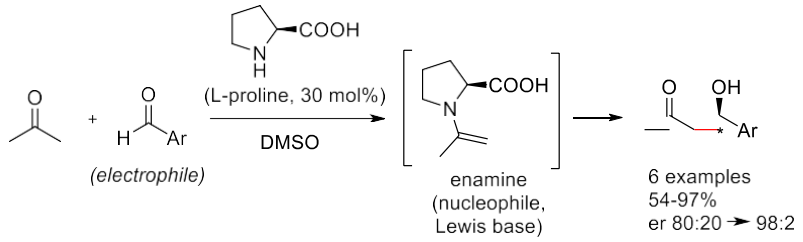

Figure 75. *Asymmetric aldol reaction using L-proline as catalyst.*[115(c), 116]

David W. C. MacMillan – Iminium ion catalysis / Lewis acid catalysis

In 2000, Ahrendt, Borths and MacMillan described the Diels-Alder reaction between α,β-unsaturated aldehydes and dienes using chiral imidazolidinones as catalysts.[119]

They proposed a mechanism where an iminium ion is formed between the aldehyde and the catalyst, in which the energy of the Lowest Unoccupied Molecular Orbital (LOMO) is lower than the energy of the aldehyde.[115(c)] Similar reactivity could be observed using traditional metal-based Lewis acids catalysts.

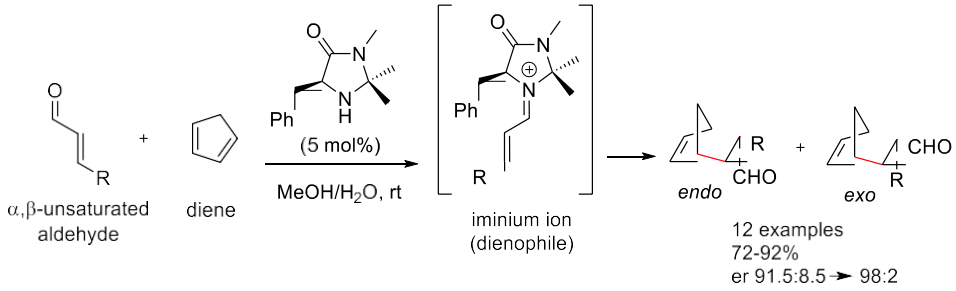

Figure 76. *Asymmetric Diels-Alder reaction using imidazolidinones as catalysts.*[115(c), 119]

[117] (a) Hajos, Z. G.; Parrish, D. R. German Patent DE2102623, July 29, 1971. (b) Hajos, Z. G.; Parrish, D. R. *J. Org. Chem.* **1974**, *39*, 1615 – 1621.
[118] Eder, U.; Sauer, G.; Weichert, R. *Angew. Chem. Int. Ed.* **1971**, *10*, 496 – 497.
[119] Ahrendt, K. A.; Borths, C. J.; MacMillan, D. W. C. *J. Am. Chem. Soc.* **2000**, *122* (17), 4243 – 4244.

This is not the first Nobel prize in this field, catalysis has been awarded seven times: W. Ostwald (1909, catalysis), P. Sabatier (1912, hydrogenation using metal catalysts), K. Ziegler and G. Natta (1963, developing catalysts for polymer synthesis), J.W. Cornforth (1975, stereochemistry of enzyme-catalysed reactions), W.S. Knowles, R. Noyori and K. B. Sharpless (2001, asymmetric catalysis), Y. Chauvin, R. H. Grubbs and R. R. Schrock (2005, olefin metathesis), and R. F. Heck, E.-i. Negishi and A. Suzuki (2010, palladium-catalysed cross couplings).[120]

2.2. Enzymes as models for the development of new organocatalysts

Enzymes, which are Nature's catalysts, are able to catalyse a huge number of different chemical transformations. According to the reaction in which they are involved, enzymes are classified in seven groups: oxidoreductases, transferases, hydrolases, lyases, isomerases, ligases and translocases.[121] As examples, esters, carbohydrates and amides are hydrolysed by esterases, glycosidases and proteases, respectively, which belong to hydrolases group.

In 1972, Breslow coined the term **Biomimetic Chemistry** as Chemistry inspired by Nature.[122] One branch on this field, called **Enzyme Mimicry**, studies the imitation of the catalytic processes developed by enzymes, with the objective of reaching reaction rates and selectivities comparable to that of enzymes. To achieve this goal is not necessary to imitate the whole enzyme but the essential features in enzyme-based transformations: (i) well-defined active site structure, (ii) complementarity and association between the enzyme and thesubstrate in the active site and (iii) intermediate-reaction stabilization.[121]

Merging principles from biocatalysis and organocatalysis is a good starting point to design, synthesise and evaluate new small organic molecules as actives as enzymes, able to improve industrial processes, synthetic chemistry, and the knowledge about how enzymes work. Also transition-metal catalysis could be included in the study, as many enzymes has a transition-metal atom in its active center.

Enzyme mimicking is still a challenge, as it requires not only to decorate an organic molecule with the appropriate functional groups but including them in the correct three-dimensional configuration in which they are active. Furthermore, right geometry and rigidity are very important to achieve this goal.

---

[120] Further information at: https://www.nobelprize.org/prizes/list/all-nobel-prizes-in-chemistry/ and in reference 115(c).
[121] Nelson, D. L.; Cox, M. M.; Hoskins, A. A. *Lehninger. Principles of Biochemistry.* 8th ed. Macmillan learning. **2021**. pp 734 – 735.
[122] Breslow, R. *Artificial Enzymes*. WILEY-VCH. Weinheim. **2005**.

A wide number of enzyme mimics have been reported.[122,123] They can imitate very different enzymes such as cytochrome P-450, enolases, hydrolases, aldolases and many metalloenzymes, and catalyse a myriad of reactions such as aromatic substitution reactions, photochemical reactions, redox reactions, hydrolytic reactions, etc.

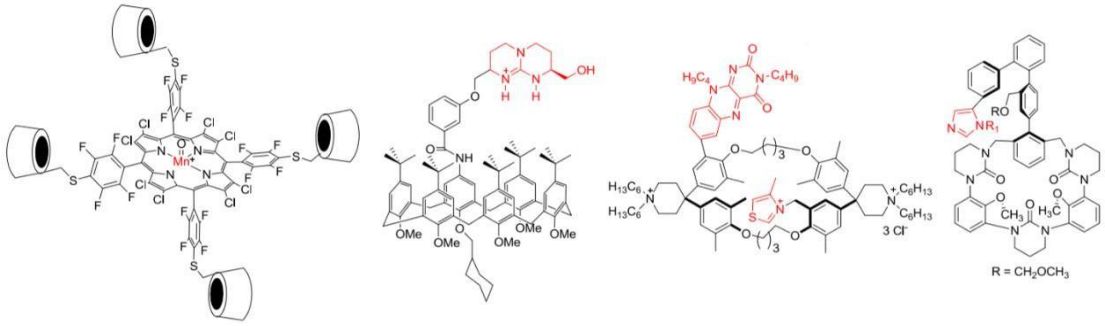

Breslow, **2002** de Mendoza, **2000** Diederich, **1997** Cram, **1986**

Figure 77. *Artificial enzymes mimicking: cytochrome P-450, acetylcholinesterase, oxidase and transacylase.*

2.2.1. Hydrolytic enzymes as models for the design of new organocatalysts

Hydrolytic enzymes are a family of more than 200 enzymes which catalyse the hydrolysis of different kind of bonds, such as ester, amide or glycosidic bonds, but also C–C, C–O, C, N, C–halide, P–N, S–N, C–P, S–S and C–S bonds.

In particular, esterases and peptidases are widely used in industry to hydrolyse ester and peptidic bonds; however, as it has been reported before, their use is restricted to a narrow window of aqueous solvents, pH, temperature and salt conditions.

The development of synthetic hydrolase mimics would allow to solve the problems described above. These organocatalysts could find application in biodiesel production because they should be able to catalyse the transesterification of triglycerides with methanol. They can be attractive molecules to catalyse the biodegradation of polymers such as polyethylene terephthalate (PET) plastics, CO_2 capture or be used as drugs.

---

[123] (a) Yang, J.; Gabriele, B.; Belvedere, S.; Huang, Y.; Breslow, R. *J. Org. Chem.* **2002**, *67*, 5057 – 5067; (b) Cuevas, F.; Di Stefano, S.; Magrans, J. O.; Prados, P.; Mandolini, L.; de Mendoza, J. *Chem. Eur. J.* **2000**, *6*, 3228 – 3234; (c) de Mendoza, J.; Alcázar, V.; Botana, E.; Galán, A.; Lu, G.; Magrans, J. O.; Martín-Portugués, M.; Prados, P.; Salmerón, A.; Sánchez-Quesada, J.; Seel, C.; Segura, M. *Pure Appl. Chem.* **1997**, *69*, 577 – 582; (d) Magrans, J. O.; Ortiz, A. R.; Molins, A.; Lebouille, P. H. P.; Sánchez-Quesada, J.; Prados, P.; Pons, M.; Gago, F.; de Mendoza, J. *Angew. Chem. Int. Ed. Engl.* **1996**, *35*, 1712 – 1715; (e) Cram, D. J.; Lam, P. Y.-S.; Ho, S. P. *J. Am. Chem. Soc.* **1986**, *108*, 839 – 841; (f) Mattei, P.; Diederich, F. *Helv. Chim. Acta* **1997**, *80*, 1555 – 1588.

An interesting application could be the kinetic resolution of racemic compounds with industrial interest, as it is shown in Figure 78.

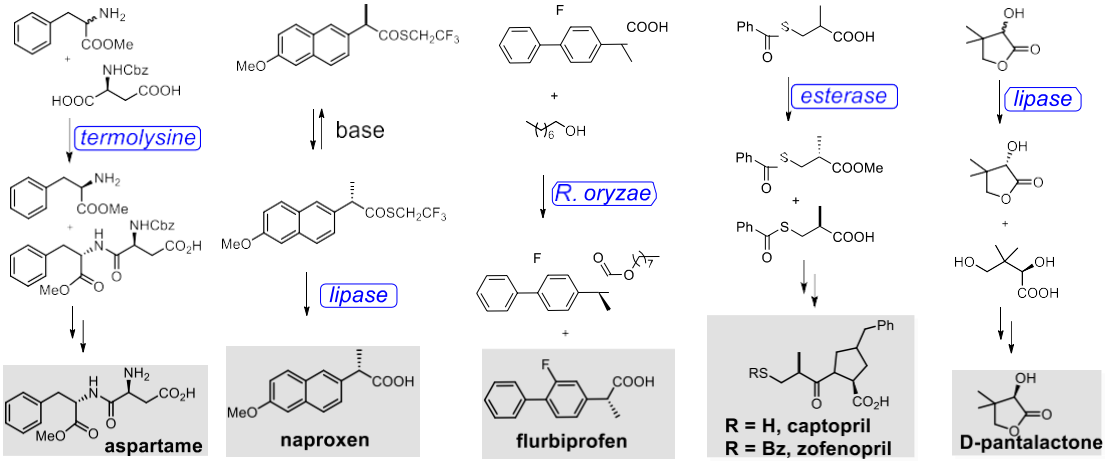

Figure 78. *Selected examples of possible reactions which could be catalysed with artificial hydrolases in the obtention of enantiopure compounds with industrial production.*

A rational understanding of the geometry of the active center of esterases and peptidases, based on the analysis of the X-ray structure of the enzymes, could be a promising starting point to design a truly enzyme mimic. The synthesis and testing of small molecules which try to mimic the catalytic groups of the active center of hydrolases could shed some light on the importance of the geometry in which the catalytic groups are organized to achieve high levels of catalysis.

2.2.2. Chymotrypsin and *N*-terminal hydrolases: Active center studies

Chymotrypsin

One of the most studied hydrolases is chymotrypsin (EC 3.4.21.1), a digestive enzyme responsible for peptide hydrolysis. The X-ray diffraction structure of chymotrypsin and, more specifically, the analysis of the X-ray structure of the active center in the presence of intermediate analogues covalently attached, as allowed us to understand the reaction mechanism of this enzyme.

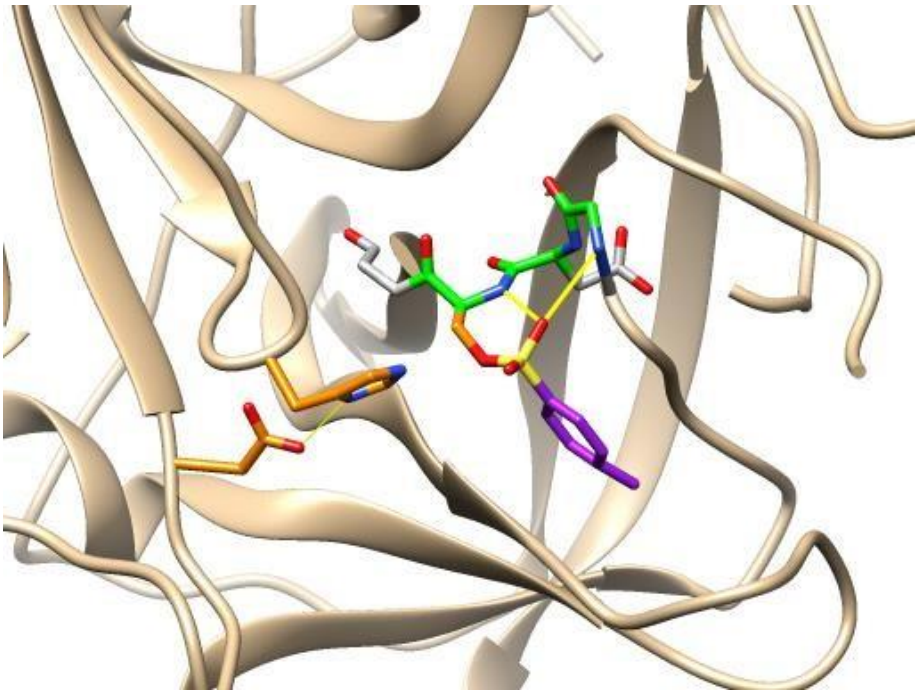

Figure 79. *X-ray diffraction structure of the tetrahedral intermediate analogue O-tosyl-α-chymotrypsin (PDB ID: 2CHA).*

Chymotrypsin active center consists of three different regions which, combined, confers the enzyme its catalytic properties: **catalytic triad**, **oxyanion hole** and **hydrophobic pocket**, as it is shown in Figure 80.

Catalytic triad is formed by serine **195**, histidine **57** and aspartic acid **102**. Serine **195** provides the hydroxyl group which will form a new O-C bond with the peptidic bond prone to be hydrolysed. Histidine **57** increases the nucleophilicity of the OH group by hydrogen bonding the OH with its imidazole ring. At the same time, the basicity of the imidazole is raised by hydrogen bonding with the side chain carboxylate of aspartic acid **102**. In this way, a hydrogen bond network is established with the goal of enhancing the hydroxyl group's nucleophilic properties.

The **oxyanion hole** is formed by glycine **193**, aspartic acid **194** and serine **195**, and provides two N-H bonds which form two hydrogen bonds with the substrate carbonyl group which is going to be hydrolysed. These two hydrogen bonds become stronger in the transition state of the reaction, where the carbonyl group acquires negative charge, and contribute to the stabilisation of the tetrahedral intermediate, according to Pauling hypothesis.[124]

The **hydrophobic pocket** is formed by a region of the enzyme in which hydrophobic amino acids predominate. This part of the enzyme helps to select the peptide bond which is going to

[124] Pauling, L. *Nature* **1948**, *161*, 707 – 709.

be hydrolysed, and which requires the presence of an amino acid with a hydrophobic aromatic side chain, such as tryptophan, tyrosine or phenylalanine. Hydrophobic effect justifies amino acids association in the binding pocket.

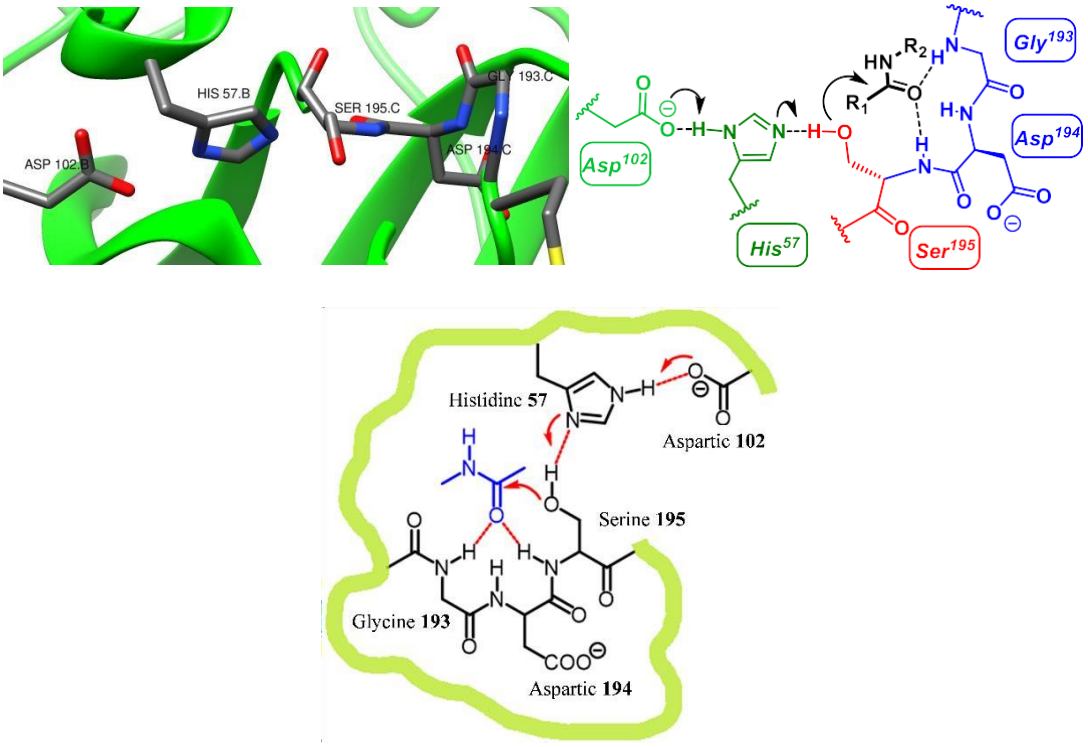

Figure 80. *Active center of bovine γ-chymotrypsin (PDB: 1AB9) (above) and schematic active center of chymotrypsin, showing the catalytic triad and the oxyanion hole (bottom).*

This complex machinery in chymotrypsin accelerates the reaction rate up to 10^{10} times.[125] Directed mutagenesis studies have been reported to evaluate the contribution of each amino acid of the active center in the catalytic reaction.[126] The replacement of serine 195 by alanine[127]

[125] Hedstrom, L. *Chem. Rev.* **2002**, *102*, 4501 – 4523.
[126] (a) Henderson, R.; *Mol*, J. *Biol.* **1970**, *54*, 341 – 354; (b) Robertus, J. D.; Kraut, J.; Alden, R. A.; Birktoft, J. J. *Biochemistry* **1972**, *11*, 4293 – 4303. (c) Bryan, P.; Pantoliano, M. W.; Quill, S. G.; Hsiao, H. Y.; Poulos, T. *Proc. Natl. Acad. Sci. USA* **1986**, *83*, 3743 – 3745; (d) Craik, C. S.; Roczniak, S.; Largman, C.; Rutter, W. J. *Science* **1987**, *237*, 909 – 913; (e) Sprang, S.; Standing, T.; Fletterick, R. J.; Stroud, R. M; Finer-Moore, J. N. H. Xuong, R. Hamlin *Science* **1987**, *237*, 905 – 909; (f) Carter, P.; Wells J. A. *Proteins: Struct.Funct. Genet*. **1990**, *7*, 335 – 342; (g) Corey, D. R.; Craik, C. S. *J*. Am. *Chem. Soc*. **1992**, *114*, 1784 – 1794; (h) Szeltner Z.; Rea, D.; Juhász, T.; Renner, V.; Mucsi, Z.; Orosz, G.; Fülöp, V.; Polgár, L. *J. Biol. Chem.* **2002**, *277*, 44597 – 44605.
[127] Corey, D. R.; Craik, C. S. *J. Am. Chem. Soc.* **1992**, *114*, 1784 – 1790.

reduced the reaction rate by a factor of 10^6. An acceleration rate of 10^4 remains due to the presence of the oxyanion hole, which is still available to bind and stabilize both substrate and tetrahedral intermediate. Substitution of aspartic acid 102 or histidine 57 by alanine reduces the reaction rate by a factor of around 10^4.[128] This implies that the hydrogen bond network of the catalytic triad is very important to enhance the nucleophilicity of the serine hydroxyl group.

N-terminal hydrolases

N-terminal hydrolases are another kind of hydrolytic enzymes which hydrolyse peptide bond in proteins. These enzymes replace the catalytic triad from chymotrypsin-like enzymes by only one *N*-terminal amino acid (usually serine, threonine or cysteine) in its active center, and the oxyanion hole is formed by two amino acids (glycine is usually one of them). Figure 81 shows the X-ray structure of the active center of human aspartylglucosaminidase (PDB ID: 1APY).

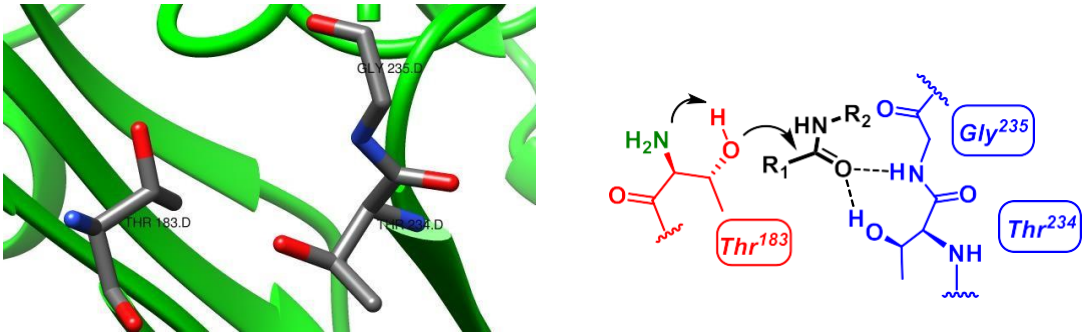

Figure 81. *Active center of human aspartylglucosaminidase (PDB: 1APY).*

2.2.3. Catalytic mechanism of hydrolytic enzymes

In spite of the differences in their active center, the hydrolysis mechanism of peptide bonds is similar for both chymotrypsin and *N*-terminal hydrolases. This mechanism can be divided in two different steps: generation of the acyl-enzyme **iv** by reaction between the enzyme and the substrate (Figure 82, **i** → **iv**) and subsequent hydrolysis of the acyl-enzyme by water (Figure 82, **iv** → **i**) to regenerate the free enzyme. The overall reaction includes the hydrolysis of the peptide bond to the corresponding amine and carboxylic acid.

[128] (a) Henderson, R. *J. Mol. Biol.* **1970**, *54*, 341 – 354. (b) Robertus, J. D.; Kraut, J.; Alden, R. A.; Birktoft, J. J. *Biochemistry* **1972**, *11*, 4293 – 4303.

- In the first half-cycle, the substrate is placed in the enzyme's active center, where two linear NH hydrogen bonds bind the amide carbonyl group (**ii**). The hydroxyl group reacts with the carbonyl carbon and form the first tetrahedral intermediate (**iii**). The negatively charged oxygen atom is stabilized by the NHs and the basic nitrogen atom from imidazole or the terminal NH_2 abstract the proton from the hydroxyl group. This intermediate evolves to the acyl enzyme (**iv**), the nitrogen transfers the proton to the leaving group (amine from the amide bond) and the carbonyl group is regenerated.

- In the second half-cycle, a water molecule is associated in the active center, near to the acyl-enzyme (**v**), and reacts to form the second tetrahedral intermediate (**vi**). The base transfers the proton from the water to the hydroxyl group, regenerating the free enzyme (**i**) and completing the hydrolysis of the peptide bond.

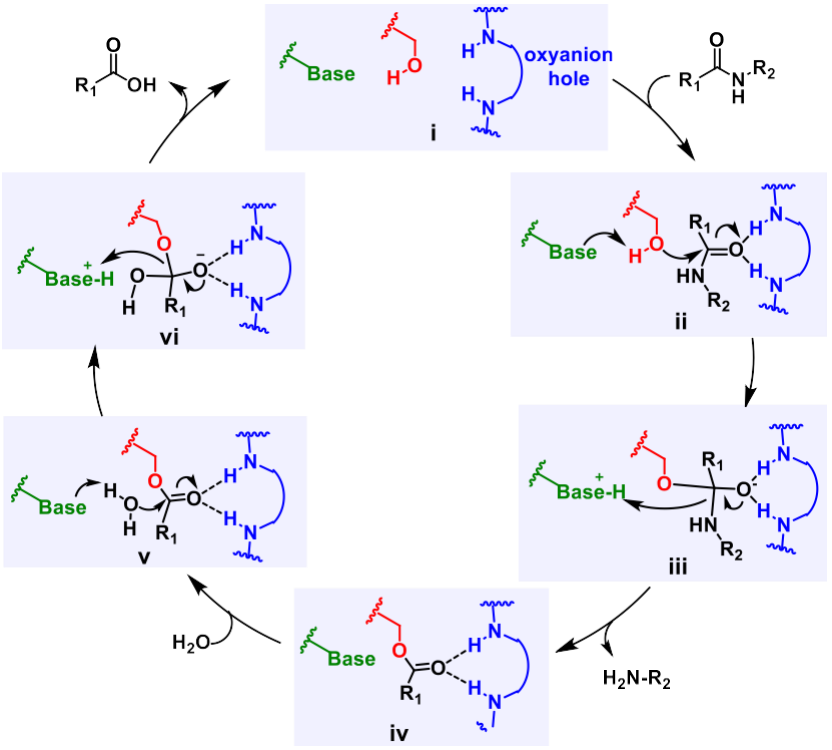

Figure 82. *Catalytic mechanism of hydrolytic enzymes.*

2.2.4. State-of-the-art. Hydrolytic enzyme mimics in the literature

Chemists have tried to mimic hydrolases for a long time. Especially remarkable are hydrolytic enzyme mimics contributions of Lehn in enantioselective thiolysis reactions[129] as well as Breslow[130] and Cram[131] in the hydrolysis of nitrophenyl esters, with reaction rates increases up to $7.5x10^5$ and 10^{11}, respectively. While most of these enzyme models rely on the formation of inclusion complexes of activated esters inside cyclodextrins, cucurbiturils, cavitands and other macrocycles,[130,132] artificial enzymes which try to mimic the geometry of the catalytic triad of serine or cysteine proteases are much scarcer.

One of the reasons is their challenging synthesis: each of the reactive groups in the active site corresponds to different domains of the protein backbone chain and are only brought together when the protein folds in its tertiary structure. Ema & Sakai[133] and Schafmeister[134] have reported small-molecule enzyme mimics able to simulate the catalytic triad of hydrolytic enzymes. Although large acceleration rates were obtained, their systems are limited to highly activated vinyl trifluoroacetate esters. Several research groups have tried to mimic the tridimensional arrangement of the catalytic groups in chymotrypsin by using polymer imprinting techniques[135] or by attaching the catalytic groups onto polymeric materials[136] or

---

[129] Lehn, J.; Sirlin, C. *J. Chem. Soc., Chem. Commun.* **1978**, 949 – 951.

[130] (a) Breslow, R.; Dong, S. D. *Chem. Rev.* **1998**, *98*, 1997 – 2011. (b) Trainor, G. L.; Breslow, R. *J. Am. Chem. Soc.* **1981**, *103*, 154 – 158. (c) Breslow, R.; Trainor, G.; Ueno, A. *J. Am. Chem. Soc.* **1983**, *105*, 2739 – 2744

[131] (a) Cram, D. J. *Angew Chem. Int. Ed. Engl.* **1988**, *27*, 1009 – 1020. (b) Cram, D. J.; Katz, H. E. *J. Am. Chem. Soc.* **1983**, *105*, 135 – 137. (c) Cram, D. J.; Lam, P. Y.-S.; Ho, S. P. *Ann. N. Y. Acad. Sci.* **1986**, *471*, 22 – 40. (d) Cram, D. J.; Katz, H. E.; Dicker, I. B. *J. Am. Chem. Soc.* **1984**, *106*, 4987 – 5000. (e) Cram, D. J.; Lam, P. Y.; Ho, S. P. *J. Am. Chem. Soc.* **1986**, *108*, 839 – 841.

[132] (a) Yuan, D. Q.; Kitagawa, Y.; Aoyama, K.; Douke, T.; Fukudome, M.; Fujita, K. *Angew. Chem. Int. Ed.* **2007**, *46*, 5024 – 5027. (b) Jiang, L.; Liu, Z.; Liang, Z.; Gao, Y. *Biorg. Med. Chem.* **2005**, *13*, 3673 – 3680. (c) Tabushi, I. *Acc. Chem. Res.* **1982**, *15*, 66 – 72. (d) Klöck, C.; Dsouza, R. N.; Nau, W. M. *Org. Lett.* **2009**, *11*, 2595 – 2598. (e) Purse, B. W.; Rebek, J. *Proc. Nat. Acad. Sci. U.S.A.* **2005**, *102*, 10777 – 10782. (f) Soberats, B.; Sanna, E.; Martorell, G.; Rotger, C.; Costa, A. *Org. Lett.* **2014**, *16*, 840 – 843.

[133] Ema, T.; Tanida, D.; Matsukawa, T.; Sakai, T. *Chem. Commun.* **2008**, 957 – 959.

[134] Kheirabadi, M.; Çelebi-Ölçüm, N.; Parker, M. F. L.; Zhao, Q.; Kiss, G.; Houk, K. N.; Schafmeister, C. E. *J. Am. Chem. Soc.* **2012**, *134*, 18345 – 18353.

[135] (a) Chen, L.; Xu, S.; Li, J. *Chem. Soc. Rev.* **2011**, *40*, 2922 – 2942. (b) Li, S.; Turner, A. P. F. *Molecularly Imprinted Catalysts: Principles, Syntheses, and Applications*; Elsevier: Amsterdam, 2015; pp 34 – 41. (c) Wulff, G. *Chem. Rev.* **2002**, *102*, 1 – 28. (d) Chen, L.; Wang, X.; Lu, W.; Wu, X.; Li, J. *Chem. Soc. Rev.* **2016**, *45*, 2137 – 211. (e) Mathew, D.; Thomas, B.; Devaky, K. S. *React. Funct. Polym.* **2018**, *124*, 121 – 128.

[136] (a) Nothling, M. D.; Ganesan, A.; Condic-Jurkic, K.; Pressly, E.; Davalos, A.; Gotrik, M. R.; Xiao, Z.; Khoshdel, E.; Hawker, C. J.; O'Mara, M. L.; Coote, M. L.; Connal, L. A. *Chem* **2017**, *2*, 732 – 745. (b) Delort, E.; Darbre, T.; Reymond, J.-L. *J. Am. Chem. Soc.* **2004**, *126*, 15642 – 15643. (c) Uhlich, N. A.; Darbre, T.; Reymond, J.-L. *Org. Biomol. Chem.* **2011**, *9*, 7071 – 7084. (d) Maillard, N.; Biswas, R.; Darbre, T.; Reymond, J.-L. *ACS Comb. Sci.* **2011**, *13*, 310 – 320. (e) Javor, S.; Reymond, J. L. *J. Org. Chem.* **2009**, *74*, 3665 – 3674. (f) Clouet, A.; Darbre, T.; Reymond, J. L. *Adv. Synth. Catal.* **2004**, *346*, 1195 – 1204.

micelles,[137] however, results are still not optimized enough to be applicable in industry. Connal has recently highlighted the state-of-the-art of synthetic catalysts inspired by hydrolytic enzymes which is still far to reproduce reactions of native enzymes on esters, amides and proteins under mild conditions.[138]

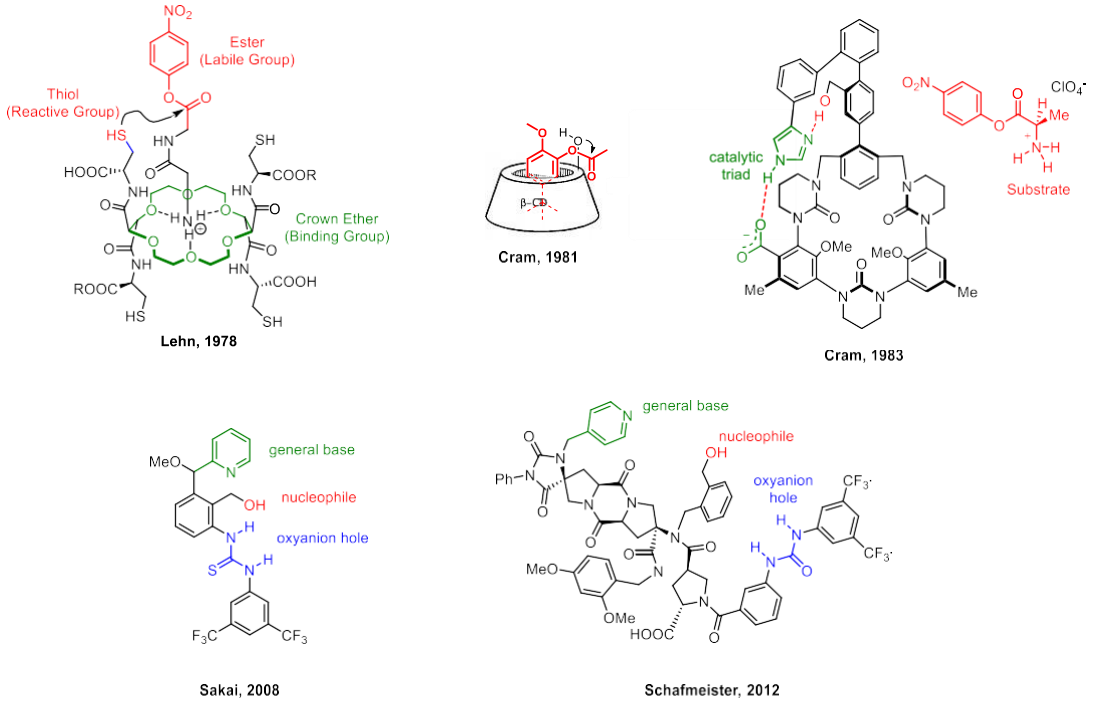

Figure 83. *Hydrolase enzyme mimics selection.*

The key factors to design a hydrolytic organocatalyst able to mimic the active center of serine-proteases is the correct arrangement of the reactive groups, the tetrahedral intermediate stabilization in the oxyanion-hole and the substrate association. Wessjohann and Zhu[139] tested several aminoalcohols in the acylation reaction with butyric anhydride. As it is shown in figure 16, the three-dimensional arrangement between the hydroxyl group and the amine is important to have good catalytic activity. According to Wessjohann and Zhu, 1,2-aminoalcohols in a propane skeleton offered the best results.

---

[137] (a) Nothling, M. D.; Xiao, Z.; Hill, N. S.; Blyth, M. T.; Bhaskaran, A.; Sani, M.-A.; Espinosa-Gomez, A.; Ngov, K.; White, J.; Buscher, T.; Separovic, F.; O'Mara, M. L; Coote, M. L.; Connal, L. A. *Sci. Adv.* **2020**, *6*, eaaz0404. (b) Hu, L.; Zhao, Y. *Helv. Chim. Acta* **2017**, *100*, e1700147. (c) Tonellato, U. *J. Chem. Soc., Perkin Trans. 2* **1977**, *6*, 821 – 827.

[138] Nothling, M. D.; Xiao, Z.; Bhaskaran, A.; Blyth, M. T.; Bennett, C.; Coote, M. L.; Connal, L. A. *ACS Catal.* **2019**, *9*, 168 – 187.

[139] Wessjohann, L. A.; Zhu, M. *Adv. Synth. Catal.* **2008**, *350*, 107 – 112.

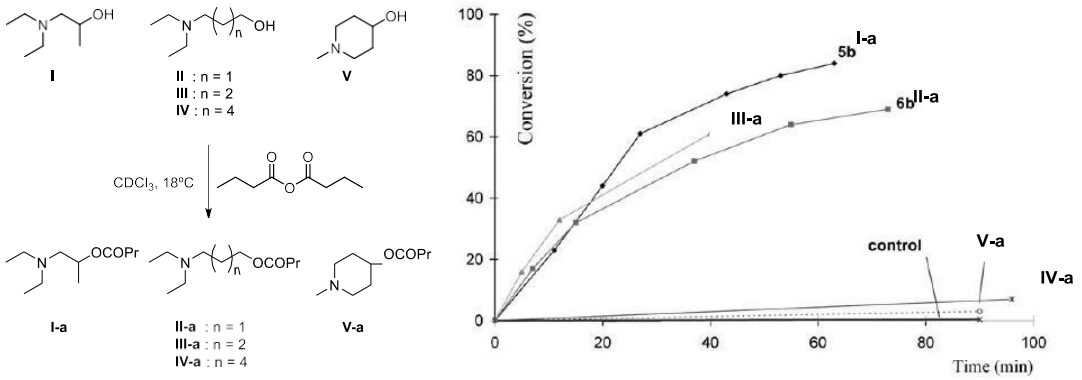

Figure 84. *Several aminoalcohols reported by Wessjohann and Zhu for acylation reactions.*

In conclusion, a hydrolytic organocatalyst which mimics the active center of chymotrypsin and *N*-terminal hydrolases should contain:

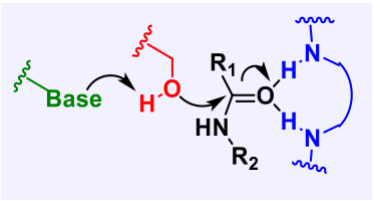

- A basic nitrogen to transport the proton from the nucleophile to the leaving group, through general basic catalysis.
- A nucleophilic hydroxyl group, able to react with the substrate *via* nucleophilic catalysis.
- An oxyanion-hole unit with the role of associating the carbonyl group from the acyl enzyme and the substrate; and also able to bind and stabilise the tetrahedral intermediate of the reaction.

2.3. Hydrolases mimics in our research group. Previous work

Several aminoalcohols have been developed in our research group where different spacers were decorated with an alcohol and a pyrrolidine, emulating the nucleophilic hydroxyl group and the basic amine of hydrolases, respectively.

We have studied the influence of the scaffold where hydroxyl group and amine are attached as well as the different geometry of each catalyst. To test their catalytic properties, acetylated catalysts were obtained and deacylation reaction was performed using neat deuterated methanol. By recording ^{1}H NMR spectra at different times and integration of the starting material and product signals is it possible to measure the conversion of the acylated and

deacylated catalyst over time, from which the half-life can be estimated (further explanation on experimental section, page 290).

Jorge García[140] reported several aminoalcohols with 2 and 3 carbon atoms between the hydroxyl group and the amine (Figure 85). Apparently, the introduction of a *n*-butyl chain (VII) in position C-2 of the 1,3-aminoalcohol scaffold was able to reduce the half-life of the reaction by a factor of 7. Interestingly, the introduction of hindered groups such as *t*-butyl (VIII) and trityl (**IX**) groups on catalyst **VI**, reduced the half-life 35 and 120 times! respectively. The more conformational restricted the catalysts are, the faster the methanolysis reaction takes place.

In catalyst **X**, where the distance between hydroxyl and amino group is only two carbon atoms, it was observed that the location where the hindered group was placed affects the reaction rate of the methanolysis. When a phenyl group was introduced in amine alpha carbon (**XI**) the half-life was reduced 2 times, whereas the introduction of the phenyl ring in the hydroxyl alpha carbon (**XII**) reduced the half-life 4.5 times. If the functional groups were placed in the equatorial positions of a cyclohexane ring, the half-life was reduced 10 times *versus* catalyst **X** (Figure 85).

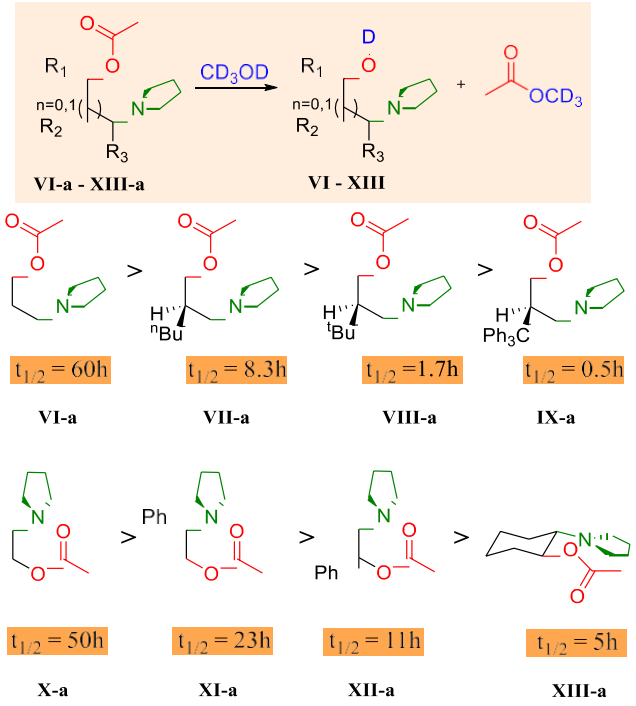

Figure 85. *Several aminoalcohols developed in our group.*[140]

[140] Martín García, J. Trabajo de Fin de Grado, **2017**, Universidad de Salamanca.

As catalyst **VII** – **IX** showed the best results, these scaffolds were considered as the catalytic triad starting point in the design of an artificial hydrolase. Then, oxyanion-hole mimics were attached to the amino alcohol skeleton. Ureas were first considered because they provide two directional NH bonds able to stablish two hydrogen bonds with the acetate carbonyl group. However, the incorporation of these oxyanion-hole units in catalysts **V** – **IX** did not improve the reaction rate of the methanolysis reaction. We believe that the flexibility of the skeleton allows the urea to hydrogen bond the pyrrolidne group, which is a better hydrogen bond acceptor than the acetate (Figure 86).

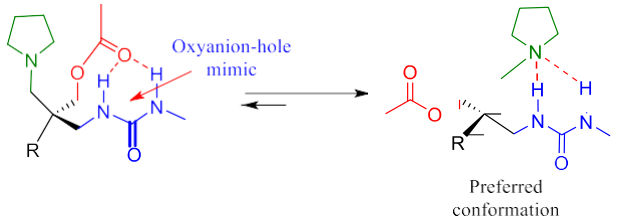

Figure 86. *Non-productive conformation in a 1,3-aminoalcohol functionalised with a urea as oxyanion hole mimic.*

To avoid the interaction between the pyrrolidine and the oxyanion hole, Sara del Mazo[141] designed a more rigid oxyanion-hole unit based on a chromane skeleton. This molecule should reduce the number of non-productive conformations and speed up the reaction rate of the methanolysis. However, in this case a half-life of 20 hours was obtained.

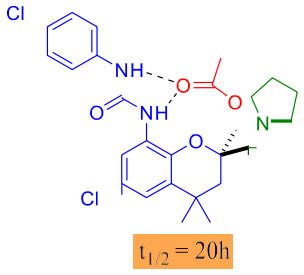

XIV-a

Figure 87. *Acetylated organocatalyst* **XIV-a** *with an oxyanion-hole unit based on a chromane skeleton.*[141]

As it is possible that in catalyst **XIV** the pyrrolidine is still able to form intramolecular hydrogen bonds with urea, catalyst **XIII** based on a cyclohexane ring was employed instead of catalyst **VI** as starting building block for organocatalyst synthesis.

It was observed that the location of the NH which mimics the oxyanion hole affects enormously the half-life of the reaction. The half-life improved 14.5 times *versus* catalyst **XIII** when the amide was in axial position and *trans* to the hydroxyl group (**XV**) but no

[141] del Mazo Borrego, S. Trabajo de Fin de Grado, **2016**, Universidad de Salamanca.

improvement was observed when the amide was placed in equatorial position and *cis* to the alcohol (**XVI**). When a more acidic NH was included in catalyst **XVII** using a bis-trifluoromethylaniline amide, the half-life was reduced 2 times *versus* catalyst **XVI** (Figure 20).

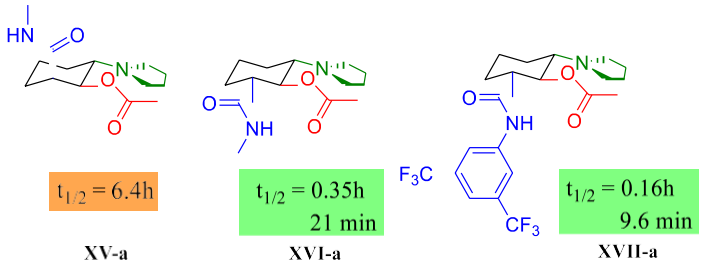

Figure 88. *Acetylated catalyst* **XIII** *derivatives* **XVI-a**, **XVI-a** *and* **XVII-a**, *where a methylamide and bis-trifluoromethylaniline mimics the enzyme oxyanion hole.*[140]

Cis epoxide was obtained in the reaction between the cyclohexene derivative and *m*-CPBA. The amide NH establishes a hydrogen bond with one of the *m*-CPBA peroxide oxygens and directs the epoxidation to the same face where the amide is positioned. Epoxide ring opening with pyrrolidine afforded catalyst **XV**, but isomerization of the amide α-carbon afforded a 1:1 mixture of **XV** and **XVI**.

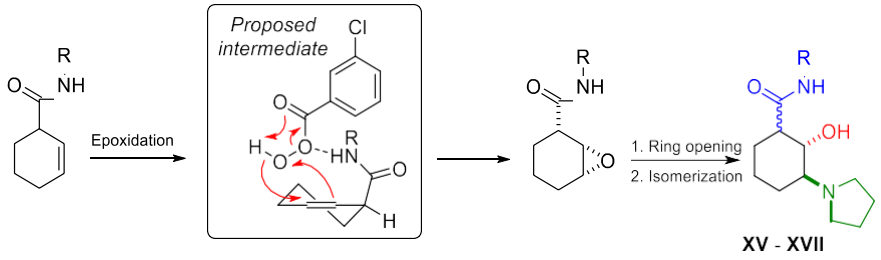

Figure 89. *General procedure to obtain catalyst* **XV** – **XVII**, *based on cyclohexane ring.*

To get rid of the stereoselectivity issues, Antonio Santos[142] and Ignacio Izquierdo[143] included a second NH group donor into the cyclohexane ring. Santos used two methylamides to set up the oxyanion hole unit, and the half-life was reduced to 7.5 min, 2.8 times better than catalyst **XVI**. Izquierdo designed an organocatalyst with more acidic NHs using bis-trifluoromethylaniline amides but, surprisingly, the expected catalyst was not obtained, even though the synthetic step to open the epoxide was the same used by Santos. Analysis of the ^{1}H NMR spectrum as well as X-ray diffraction analysis studies revealed the formation of compound **XXIII** (Figure 21).

[142] Santos Antón, A. Trabajo de Fin de Grado, **2018**, *Universidad de Salamanca.*
[143] Izquierdo Sánchez, I. Trabajo de Fin de Grado, **2018**, *Universidad de Salamanca.*

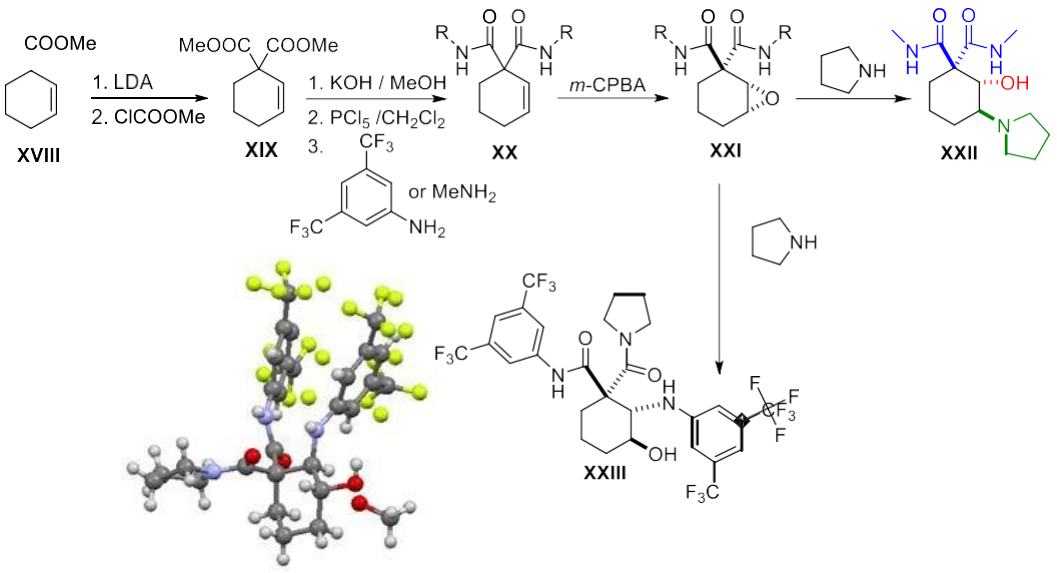

Figure 90. *Synthesis of catalyst* **XXII** *with two methylamides as oxyanion-hole unit. Catalyst with two bis-trifluoromethylanilines was not obtained because of the rearrangement with the pyrrolidine. X-ray diffraction structure of compound* **XXIII**.

We believe that the bis-trifluoromethylaniline NH is acidic enough to be deprotonated with pyrrolidine. Then, the amide anion attacks the epoxide, forming a β-lactam. Thereafter, the excess of pyrrolidine aminolyse the 4-member ring. The X-ray diffraction studies confirmed the relative stereochemistry of the functional groups. The pyrrolidinamide and the aniline are in *cis* configuration, which can be explained with the opening of the proposed β-lactam intermediate.

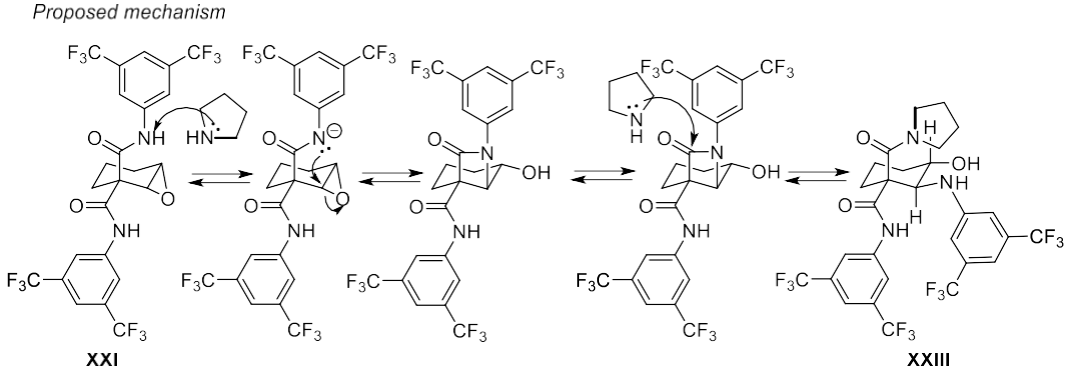

Figure 91. *Proposed mechanism to obtain compound* **XVIII**, *according to the stereochemistry observed.*

To avoid the β-lactam formation, compound **XXIX** was synthesized. In this case, epoxidation takes place in both faces of the double bond, so the epoxide opening led to a 1:1 mixture of compounds **XXVII** and **XXVIII**, which was easily separated washing with 2M aqueous HCl. Methanolysis of compound **XXIX** acetate gave a half-life of 8.9 min, which is similar to the value obtained with two methylamides. This result shows that the incorporation of a more acidic NH does not improve the methanolysis rate, probably because the geometry of the catalyst is not the ideal to stablish a strong hydrogen bond with the acetate carbonyl group.

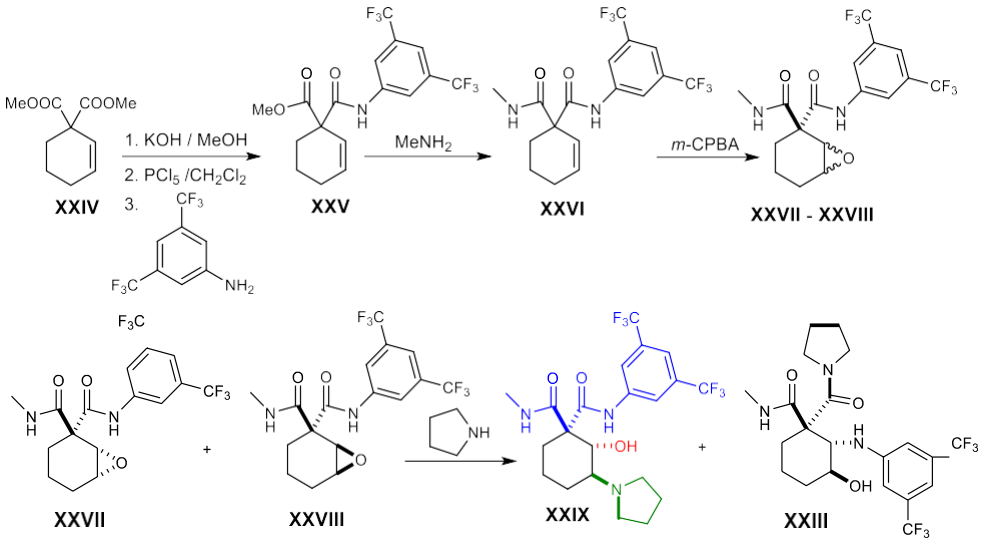

Figure 92. *Synthesis of catalyst* **XXIX** *with methylamide and bis-trifluoromethylamide as oxyanion-hole unit, which was obtained as a 1:1 mixture with compound* **XXIII**.

According to the results obtained in the research group, it should be possible to improve the catalytic performance of the catalysts by designing small molecules which place the catalytic groups with the adequate geometry. The oxyanion-hole unit should stablish two strong hydrogen bonds with the carbonyl oxygen while the base and hydroxyl group are positioned at the right distance between them to increase the nucleophilicity of the hydroxyl group and to favour the proton transfer from the nucleophile to the leaving group. The catalysts screened in the research group to date, although they show acceptable catalytic activity, do not possess the perfect geometry to favour these interactions, and a large margin for improvement is still possible.

Chapter 2 – Methods and Results

3. Methods and Results

3.1. Configuration between amino and hydroxyl group. Organocatalysts 5, 11 and 16. First generation organocatalysts

As explained in the Introduction, an organocatalyst that mimics the geometry of the active centre of hydrolytic enzymes, such as chymotrypsin and *N*-terminal hydrolases, shouldinclude: an amine, a hydroxyl group and an oxyanion-hole unit. In our research group, a seriesof catalysts with these characteristics have been studied, and the best results have been obtained with catalyst **XVI** (Figure 93), based on a cyclohexane scaffold.

However, the synthesis of compound **XVI** was troublesome: controlling the all-*trans* stereochemistry was a hard task. While the epoxidation with *m*-CPBA was directed by an intermolecular hydrogen bond between the NH of the precursor and the peracid as shown in the introduction (Figure 89), the epoxidation took place on the same face of the amide, yielding the *cis* epoxide. The α-isomerization of the carbonyl group resulted in the mixture of epimers **XV** and **XVI**, from which the half-life of each catalyst was obtained following the methodology explained in the experimental section.

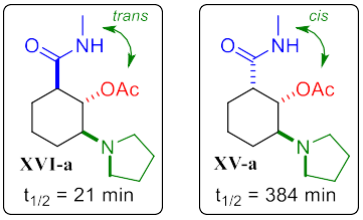

Figure 93. *Synthesis of catalysts* **XVI-a** *(trans) and* **XV-a** *(cis) with their corresponding half-life for the methanolysis reactions.*

Several structures have been proposed to avoid these synthetic problems and improve the catalytic properties of the organocatalysts.

First, we tried to mimic the active centre of chymotrypsin, where the hydroxyl group and the oxyanion hole are separated by two carbon atoms. However, the three-dimensional geometry of the catalytic triad is more difficult to mimic, since the hydroxyl group, the imidazole ring, and the aspartate belong to different amino acids which are far away in the primary structure of the protein but get closer when the protein folds to get the appropriate secondary and tertiary structures.

Alternatively, there is a family of hydrolytic enzymes where the hydroxyl group and the amine are on the same *N*-terminal amino acid and are separated by two carbon atoms. In these enzymes, the terminal amine of the protein backbone plays the role of the imidazole and the aspartate. By imitating this configuration, the problem of mimicking the chymotrypsin's catalytic triad could be simplified. In *N*-terminal hydrolases a secondary alcohol from threonine behaves as the nucleophilic hydroxyl group.

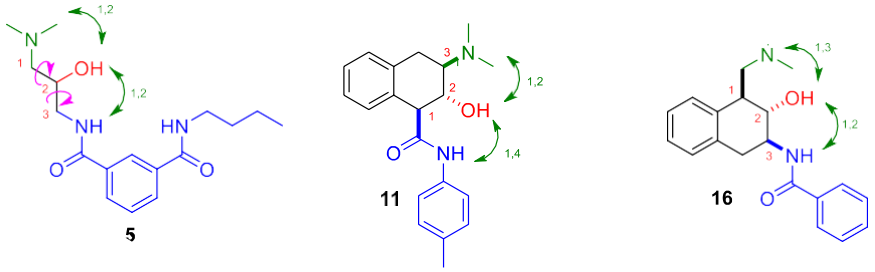

Figure 94. *Overview of different configurations between the functional groups. Structures of catalysts* **5**, **11** and **16**.

We started our study using catalyst **5** (Figure 94). Catalyst **5** perfectly combines features of both chymotrypsin and *N*-terminal hydrolases, with all functional groups separated by two carbon atoms. The *trans*-1,2-aminoalcohol can be readily obtained by nucleophilic attack of the desired amine to an epoxide, as shown in the Introduction. In this compound the methylene groups have free rotation so there are no stereochemical problems.

Catalyst **5** has also an isophthalic acid moiety, with two NH groups and an aromatic CH that can also behave as a hydrogen bond donor. This group has been successfully used in the literature as an oxyanion hole mimic.[144] However, rotations along the carbonyl carbon and the aromatic ring will generate non-productive conformations, which can affect negatively to the catalytic performance of compound **5**. Also, the amine and hydroxyl groups are placed on a scaffold with many possible conformations in which the functional groups can have many conformations, and some of them will not have the geometric requirements to catalyse the reaction.

In order to avoid non-productive conformations and at the same time keep the catalytic groups at the right distance, a more rigid cyclohexane skeleton was included in the catalysts' structures with distances of two and three carbon atoms between the amine and the hydroxyl groups. Also, different ways to anchor the oxyanion-hole were studied. 1-Naphthylamine and 1-naphthoic acid were respectively used as building blocks for organocatalysts **11** and **16** (Figure 94). The aromatic ring provides rigidity to the molecules and makes the synthesis easier. The 1,2 aminoalcohol arrangement of catalyst **11** resembles the disposition of *N*-terminal hydrolases, but the geometry of the oxyanion hole unit is different. The disposition of the functional groups in organocatalyst **16** is more similar to the structure of chymotrypsin, with the hydroxyl group and the oxyanion hole separated by two carbon atoms. Although the hydroxyl group and the amine are separated by three carbon atoms, modelling studies suggested that the amine is perfectly positioned to transport the proton from the nucleophile to the leaving group.

---

[144] (a) Chen, H.; Weiner, W. S.; Hamilton, A. D. *Curr. Opin. Chem. Biol.* **1997**, 1, 458 – 466. (b) S.-K. Chang, A. D. Hamilton, *J. Am. Chem. Soc.* **1988**, *110*, 1318 – 1319. (c) F. García-Tellado, S. Goswami, S.-K. Chang, S. J. Geib, A. D. Hamilton, *J. Am. Chem. Soc.* **1990**, *112*, 7393 – 7394.

3.1.1. Catalyst 5

***Modelling studies of catalyst* 5**

Before carrying out the synthesis of the catalyst, we performed a modelling study to check that the proposed geometry was similar to the catalytic triad in natural hydrolases. In Figure 95 it is observed that the oxyanion hole provided by the isophthalic acid moiety is around 5.14 Å, which is a bit wider than the oxyanion hole of chymotrypsin. Also, the distance between the dimethylamino nitrogen and the OH is short enough (2.70 Å) to facilitate the proton transfer.

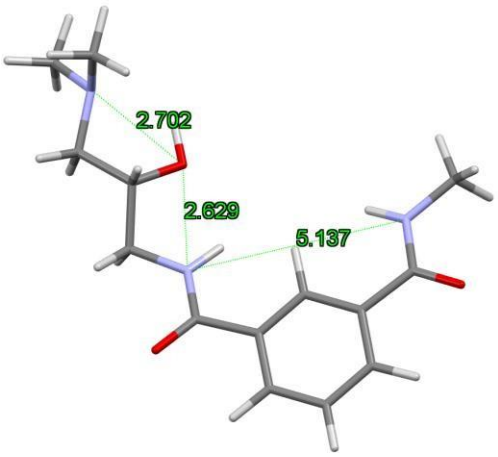

Figure 95. *DFT optimized (HF) structure for catalyst* **5**. *Butylamide was replaced by methylamide to reduce the calculation time.*

Catalyst* 5 *retrosynthesis

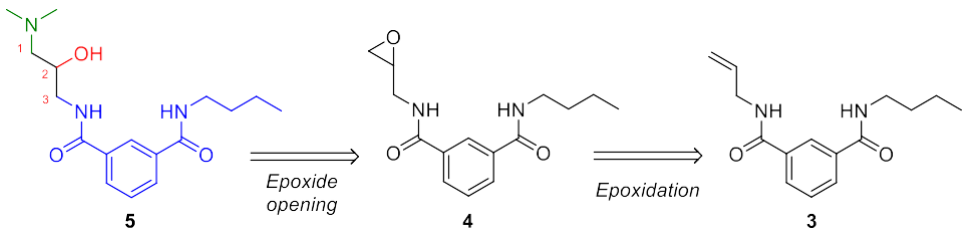

Figure 96. *Key intermediates in the retrosynthesis of catalyst* **5**.

The epoxidation of compound **3** and the subsequent ring opening with dimethylamine affords catalyst **5**.

Catalyst* 5 *synthesis

The synthesis of catalyst **5** began with the aminolysis of 3-(methoxycarbonyl)benzoic acid **1** with butylamine at room temperature overnight. Compound **2** has a carboxylic acid group prone to be linked to the aminoalcohol unit. The carboxylic acid was activated as the mixed anhydride with pivaloyl chloride (see Experimental Section, page 224) by reacting compound **2** with triethylamine and pivaloyl chloride. This anhydride was used without further purification in the reaction with allylamine to afford compound **3**.

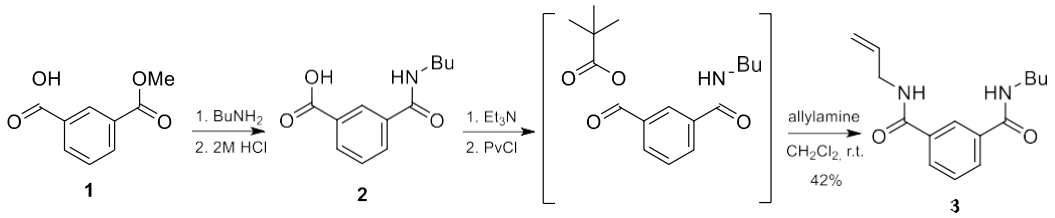

Figure 97. *Synthesis of compound* **3**.

The next step was the epoxidation of the double bond of compound **3** with *m*-CPBA. The progress of reaction was monitored by ^{1}H NMR taking small aliquots of the reaction mixture and removing the solvent under vacuum without heating the sample, to avoid a false positive while heating. Once the reaction was finished, the organic solvent was washed with a saturated aqueous solution of Na_2SO_3 and 4% Na_2CO_3 to remove the *m*-CPBA excess and 3-chlorobenzoic acid generated in the reaction, respectively.

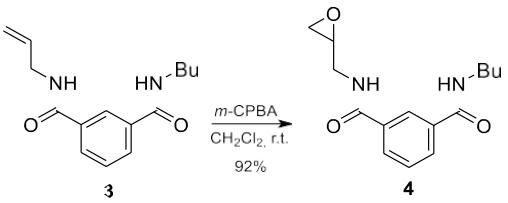

Figure 98. *Synthesis of the epoxide* **4**.

Purification of this epoxide by column chromatography using silica gel gave low yield of the epoxide **4**. An explanation for this behaviour might be the high reactivity of the epoxide in the silica gel, due to the presence of acid silanol groups in its surface. Isophthalic acid scaffold could also stabilize the oxygen atom in the ring opening reaction. Long reaction times are also undesirable because of the generation of 3-chlorobenzoic acid that acidifies the reaction conditions.

Since the ^{1}H NMR spectrum of crude epoxide **4** was almost clean, and this compound was unstable in silica gel, it was used without further purification in the next step. Thus, the epoxide was treated with 60% Me_2NH and heated to 85ºC, using a mixture of AcOH and THF as solvents. After one hour, the solvent was removed by low pressure distillation, the crude product was dissolved in EtOAc and the organic phase was washed with an aqueous solution

of 4% Na_2CO_3. Purification by column chromatography with silica gel afforded catalyst **5**. ^1H NMR spectrum showed an unexpected deshielding of the signals near to the amino group, which could be explained because catalyst **5** was obtained as the ammonium salt, due to the acidity of the silica gel.

In order to study the catalytic properties, the free amine was needed. Following the standard procedure explained in Experimental Section on page 224, the activated catalyst was obtained by washing a chloroform phase containing catalyst **5** with an aqueous solution of 5% NH_3. Apparently $NaHCO_3$ and Na_2CO_3 were not successful bases to generate the activated catalyst as they may be complexed by the oxyanion-hole.

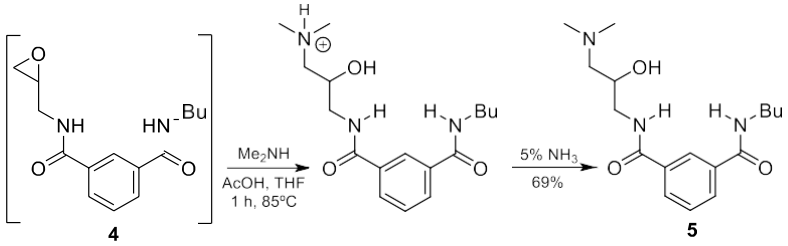

Figure 99. *Synthesis of catalyst* **5**.

Acetylated catalyst **5a** was obtained by treating catalyst **5** with acetic anhydride for 5 minutes, as explained in Experimental Section (page 224). The excess of acetic anhydride was removed by low pressure distillation and the crude product was stirred in a mixture of EtOAc and 5% Na_2CO_3 for 30 minutes. The most significant change in the ^1H NMR spectrum was the deshielding of H-2 protons from 3.86 – 3.65 ppm in the alcohol **5** to 5.06 ppm in the acetylated catalyst **5a**.

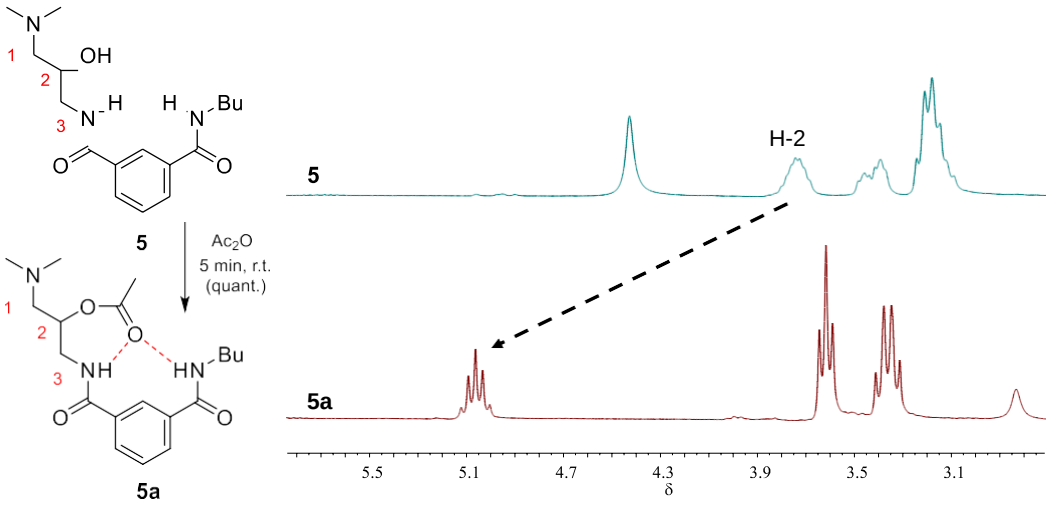

Figure 100. *Synthesis of acetylated catalyst* **5a** *(left) and* ^1H *NMR spectrum expansion (5.8 ppm – 2.7 ppm) showing the signals of the acetate (right).*

***Kinetic studies of catalyst* 5**

As explained in the Introduction, the study of the catalytic properties of these compounds began with the methanolysis of their acetates (Experimental Section, page 290). The acylation with strong acylating agents, such as acetic anhydride, is faster than deacetylation of the catalyst with deuterated methanol.

Following the methodology described in the Experimental Section (page 290), *ca.* 10 mg of acetylated catalyst **5a** were dissolved in neat deuterated methanol. Under these conditions, with a large excess of methanol, *pseudo*-first order aproximation could be applied, since the deuterated methanol concentration remains constant. ^{1}H NMR spectra were recorded at different times to study the reaction rate, and with the integration of the ^{1}H signals from **5a** and **5**, molar fractions (X) of each compound at different times were obtained. Plotting Ln [X_{5a}] versus time gave a straight line from which half-life ($t_{1/2}$) of the methanolysis reaction was obtained.

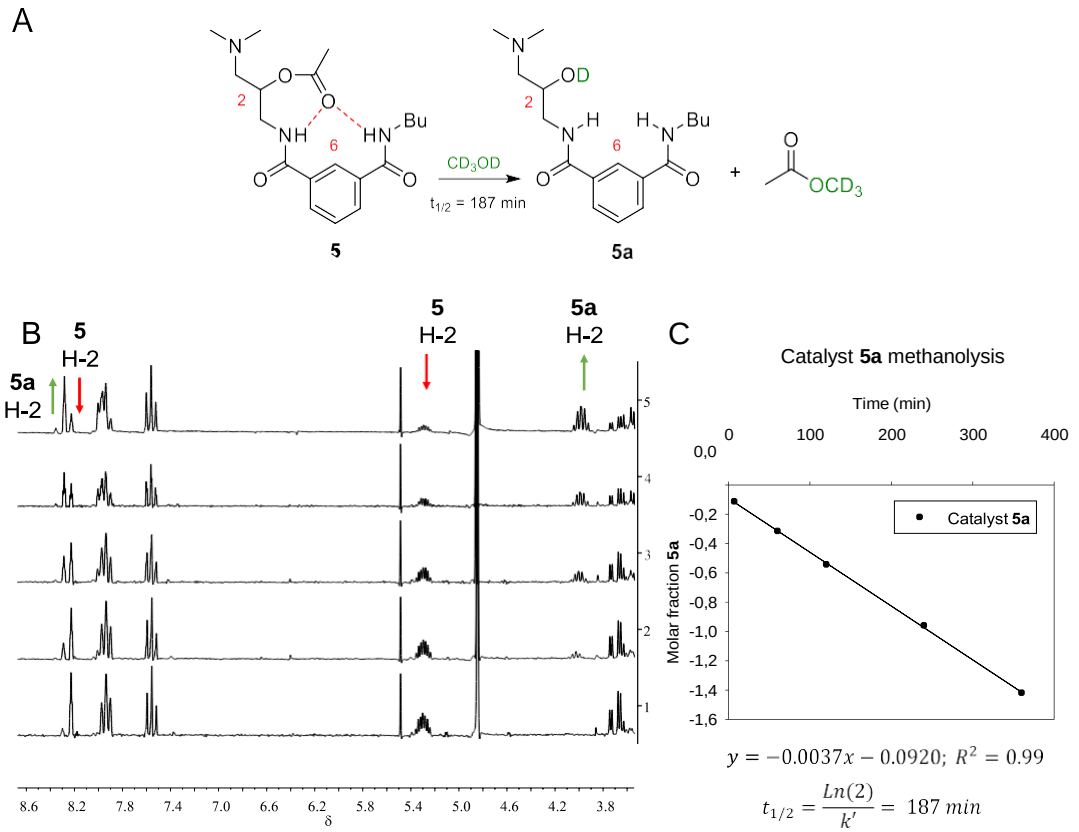

Figure 101. *(A) Methanolysis reaction of acetylated catalyst* **5a**. *(B) ^{1}H NMR spectra (8.60 ppm – 3.6 ppm) for* **5a** *methanolysis at 7 (1), 60 (2), 120 (3), 240 (4) and 360 (5) minutes. (C) Plotting of Ln[***5a***] vs time.*

According to the kinetic experiments, deacetylation of **5a** took place with a half-life of 187 min. This result agrees with catalysts previously reported in the Introduction, where non-

productive conformations in the catalysts structure allows the establishment of intramolecular hydrogen bonds between the dimethylamine and the oxyanion-hole which hampers the catalyst activity (Figure 102)

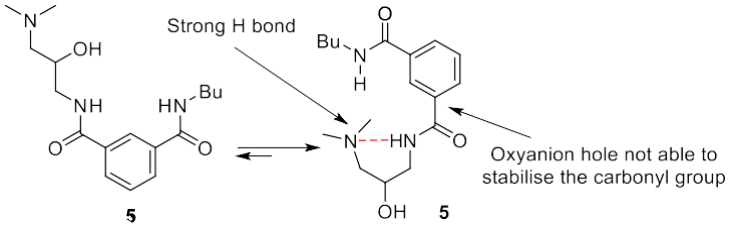

Figure 102. *Non-productive conformation in catalyst* **5**.

Although this kind of intramolecular hydrogen bond could not be formed in neat deuterated methanol, because the methanol makes a stronger hydrogen bond with the amine, in a transesterification reaction these conformations are problematic, because the reduction of the amount of the alcohol under the reaction conditions could allow the establishment of the intramolecular hydrogen bond. Also, if the oxyanion hole is not able to stabilize the carbonyl group in the acylation step, the reaction does not take place.

3.1.2. Catalyst 11

***Modelling studies of catalyst* 11**

To avoid the non-productive conformations in catalyst **5**, a rigid tetrahydronaphthalene skeleton was considered. Modelling studies showed that a equatorial disposition of thecatalytic groups keep a short distance between the dimethylamino nitrogen and the OH (2.69 Å), which is necessary to transport the proton between the OH and the base.

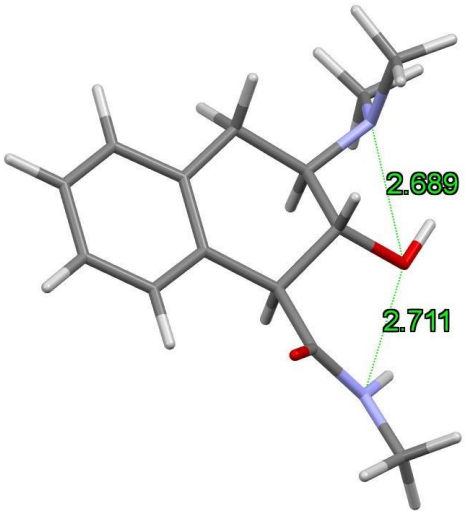

Figure 103. *DFT optimized (HF) structure for catalyst* **11**.

Catalyst* 11 *retrosynthesis

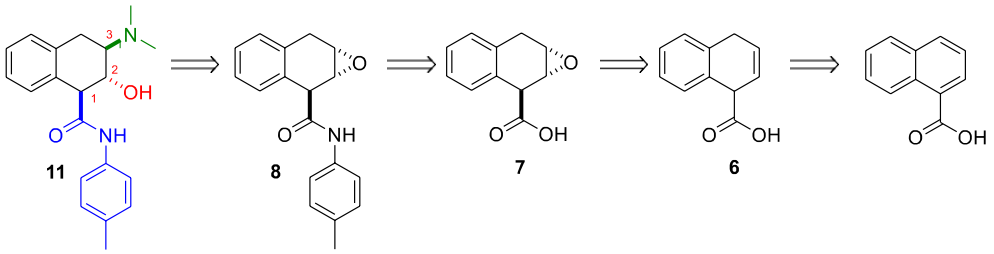

Figure 104. *Key intermediates in the retrosynthesis of catalyst* **11**.

Catalyst **11**, based on a 1-naphthoic acid moiety, maintains the *N*-terminal hydrolases 1,2-aminoalcohol arrangement, but the oxyanion-hole unit differs from that of chymotrypsin. In this case the oxyanion-hole unit is linked through the carboxylic acid at C–1 on the naphthalene ring.

Catalyst* 11 *synthesis

The synthesis of catalyst **11** began with the Birch reduction of commercial 1-naphthoic acid as described in the literature,[145] with 1 eq. of sodium in liquid ammonia at -78ºC. Tetrahydrofuran was added as cosolvent to afford a 50% w/v solution with 1-naphthoic acid, because the ammonium salt of 1-naphthoic acid formed was not soluble in neat liquid ammonia. Then, ammonia gas was condensed, and sodium was added in portions at -78ºC. The reaction was stirred at -33ºC until all the metal was dissolved and was warmed to -15ºC to remove almost all the ammonia. Temperature should not rise up to -10ºC to avoid isomerization of the alkene under the basic conditions. The reaction mixture was added over ice with 2M HCl, and the 12M HCl was added until a white solid crash out, corresponding to alkene **6**.

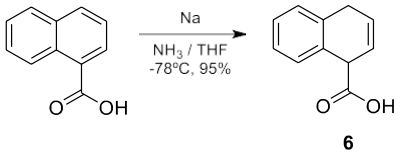

Figure 105. *Birch reduction of 1-naphthoic acid to afford alkene* **6**.

Since the epoxidation of either the carboxamide or the carboxylic acid yielded the *cis* epoxide, due to the formation of an intermolecular hydrogen bond which directs the epoxidizing agent to the same face of the carboxylic moiety (as shown in the Introduction), it was necessary to find conditions to avoid this interaction. Our first option was to deprotonate

[145] Weitz, I.S; Rabinovitz, M. *Journal of the Chemical Society* **1993**, *1*, 117 – 120.

the acid, so it could not interact with *m*-CPBA, but the sodium salt of compound **6** was not soluble in chloroform where the peracid is soluble. It was necessary to find an epoxidating agent soluble in water, where the sodium salt of compound **6** is soluble.

Even though hydrogen peroxide could be used, Oxone®, sulfuric acid peracid, was the best option for this reaction to proceed. Oxone® is the trade name of the triple salt $2xKHSO_5 \cdot KHSO_4 \cdot K_2SO_4$. It contains 50% mol of the epoxidating agent and 25% of potassium monohydrogensulfate and 25% of potassium sulfate. As the potassium monohydrogensulfate could act as an acid, it needs to be quenched first with Na_2CO_3 to avoid the precipitation of **6** in water. Also, the change in the pH has to be controlled during the reaction, because potassium monohydrogen sulfate is continuously generated under the reaction conditions. In this scenario, the negative charge of the carboxylate repels the negative charge of the persulfate and the reaction is directed to the opposite face of the carboxylate, as shown in Figure 106.

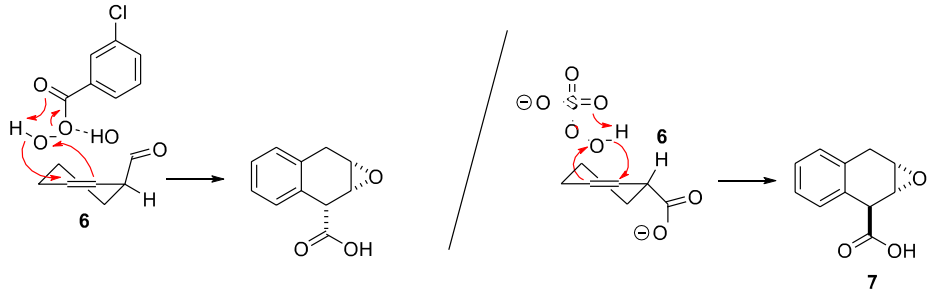

Figure 106. *Expected reactivity between alkene* **6** *and m*-CPBA *(left) and sodium salt of compound* **6** *with Oxone® (right).*

A 1:1 mixture of *cis* and *trans* isomers were obtained when a small excess of Na_2CO_3 was used in the reaction. This is probably due to the presence of low quantities of carboxylic acid **6** in equilibrium with the carboxylate, that binds the persulfate, leading to the *cis* epoxidation, as occurs in the epoxidation of amides with *m*-CPBA. Only with strong basic conditions the selectivity rises up to 4:1. Although several purifications were attempted to separate the *trans* isomer from the *cis* isomer, compound **7** could never be recovered, so the 4:1 mixture of *trans* and *cis* epoxides was used without further purification.

Then, the epoxide was opened with aqueous 20% NH_3 solution. Since the ammonium carboxylate formed in the reaction between ammonia and epoxide **7** was soluble in water, this reaction was carried out in water in a high-pressure reactor at 80ºC. ^{1}H NMR spectrum confirmed the ring-opening and the presence of a hydroxyl group attached to a CH at 4.00 ppm. However, the shape of its signal was not the expected triplet but a double double doublet, which indicated the presence of three vicinal protons instead of the two neighbours required for the hydroxyl group at C–2. This can be explained if the dimethylamine reacts in C–2, leading to the *trans*-aminoalcohol and leaving the carboxylic acid in the equatorial position, as shown in Figure 107.

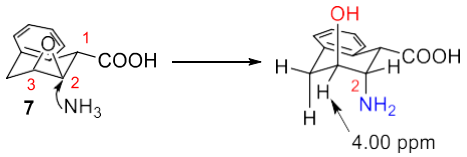

Figure 107. *Epoxide ring opening in compound* **7** *with ammonia.*

Since the carboxylate did not allow the ring-opening with the desired regiochemistry, toluidinamide **8** was synthesized. As the epoxide of compound **7** may not be stable under acidic conditions, common reagents such as $SOCl_2$ or PCl_5 were avoided to prepare the acid chloride. Thus, the carboxylic acid of compound **7** was activated through the mixed pivaloyl anhydride using triethylamine and pivaloyl chloride as reagents. Thereafter, the reaction of this anhydride with toluidine afforded the amide **8**.

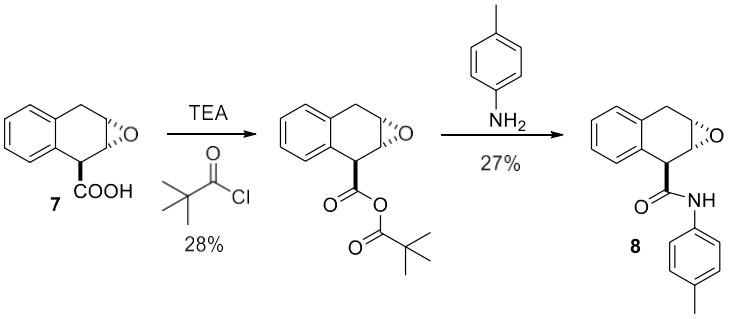

Figure 108. *Synthesis of toluidinamide* **8**.

Then, compound **8** was treated with an aqueous solution of 60% Me_2NH and MeOH as solvent at 60ºC. However, after distillation of the solvent and the excess of Me_2NH, the ^1H NMR spectrum showed no amine in the structure. Instead, a doublet at 6.01 ppm confirmed the allylic rearrangement of the epoxide under the basic reaction conditions which abstracts the acidic H–1, which is activated by both the aromatic ring and the carboxylic group.

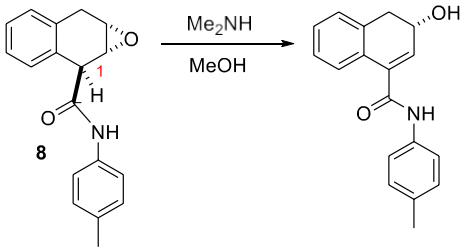

Figure 109. *Reaction of compound* **8** *with* Me_2NH.

In order to avoid the rearrangement, less basic sodium azide was used. While the pK_a of dimethylamine is 10.7, that of the azide is only 4.8, so the desired epoxide opening should be favoured at expenses of the allylic rearrangement. The reaction was carried out with sodium azide in propionic acid at 80ºC for 1 hour. The use of propionic acid instead of acetic acid was due to its lower pK_a: while the pK_a of acetic acid is 4.75 and protonates to some extent sodium

azide to generate hydrazoic acid, the higher 4.87 pK_a of propionic acid will generate a smaller hydrazoic acid concentration. Hydrazoic acid is toxic and undesired in the reaction.

Figure 110 shows how the reaction takes place in order to obtain the desired all-equatorial disposition. The hindered carboxamide **8** prevents the nucleophilic attack in C–2, so the azide prefers to react with the less populated conformation in which the amide stands in the axial position. In this conformation the azide attacks the C–3 carbon to yield the axial azide, which is the only stereochemically allowed concerted ring opening.

Once the reaction has taken place, the conformation changes from the axial disposition to the more stable equatorial disposition.

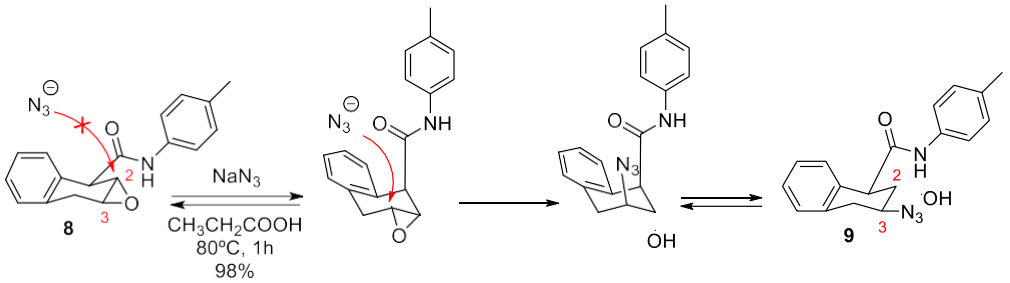

Figure 110. *Ring opening of epoxide* **8** *of with* NaN_3.

Once the desired stereochemistry in compound **9** was achieved, it was easy to obtain catalyst **11**. The reduction of the azide **9** to the amine **10** was carried out with H–2 in EtOAc using Pd/C as catalyst. Thereafter, the reductive alkylation of the amine with formaldehyde and sodium cyanoborohydride yielded catalyst **11**.

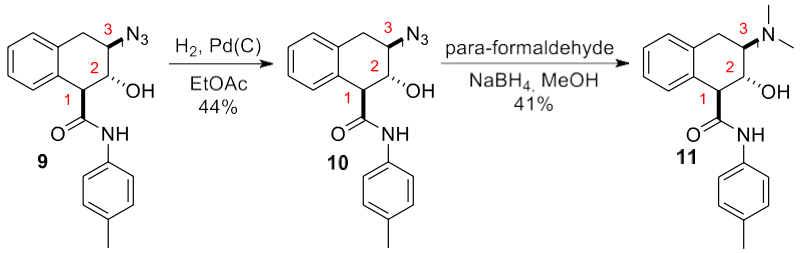

Figure 111. *Synthesis of catalyst* **11**.

The ^{1}H NMR spectrum of the aminoalcohol **11** matched the structure that modelling studies predicted. The equatorial configuration was confirmed by the signal at 4.24 ppm of H–2, with coupling constants of 10 Hz. This high coupling constant is due to the presence of two axial protons H–1 and H–3, which are geminal to the axial proton H–2. The ^{1}H NMR spectrum confirms that the groups in catalyst **11** are in equatorial positions.

Acetylated catalyst **11a** was obtained treating catalyst **11** with acetic anhydride, as it was explained in the Experimental Section (page 224).

^{1}H NMR spectrum showed the signal of the acetate at 2.29 ppm, and the expected deshielding of H–2 from 4.24 to 5.61 ppm. Again, the most significant feature was the shape of the signal of H–2. The original triplet in compound **11**, with a coupling constant of 10 Hz, became a doublet with J = 4 Hz in **11a**. Even though electron-withdrawing groups could reduce the coupling constant,[146] it is highly probable a change in the benzocyclohexane conformation. The strong intramolecular hydrogen bond between the dimethylamine group and the carboxamide (Figure 112) may explain the preference for the all-axial conformation.

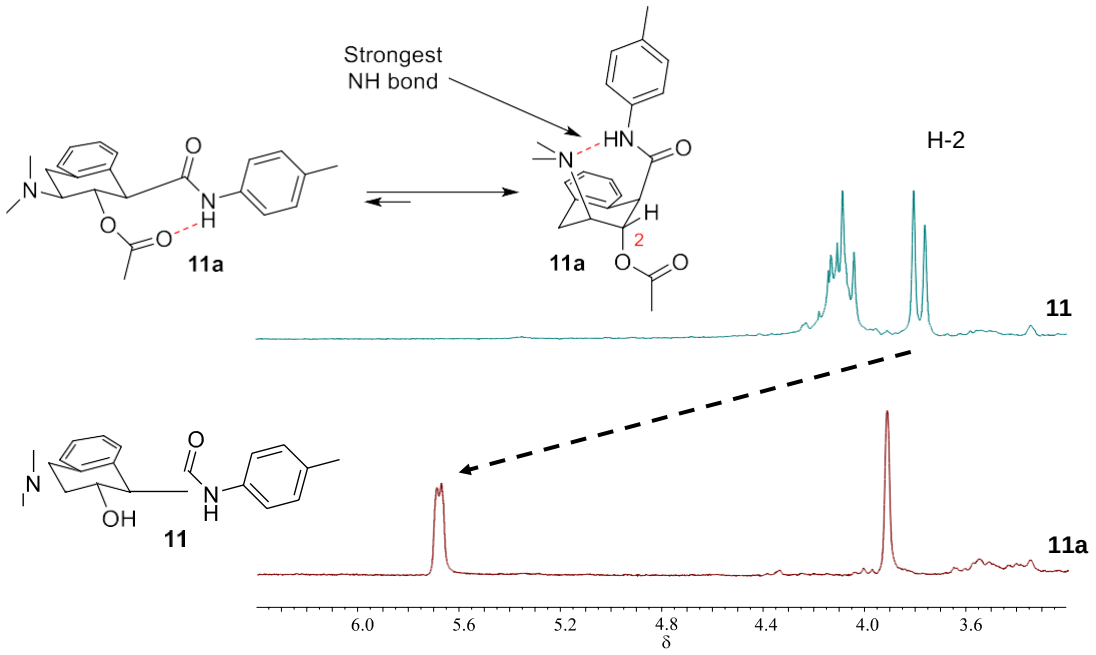

Figure 112. *^{1}H NMR spectrum (6.3 – 3.3 ppm) showing the signals of catalyst* **11** *and* **11a**, *where the conformational change explains the small coupling constant between H-1 and H-2.*

Kinetic studies of catalyst 11

Even though the conformation is not the ideal one to achieve catalysis, methanolysis reaction of the acetylated catalyst **11a** was studied. Following the methodology described in the Experimental Section (page 290), *ca.* 10 mg of acetylated catalyst **11a** were dissolved in neat deuterated methanol and ^{1}H NMR spectra were recorded at different times. Surprisingly, the conformation returned to all-equatorial positions in neat deuterated methanol, as showed the broad shape of the H–2 signal. This can be explained because the methanol makes its own

[146] Clayden, J.; Greeves, N.; Warren, S; Wothers, P. *Organic Chemistry*. 1st ed.; Oxford University Press: New York, **2001**, *1*, 268 – 269.

hydrogen bonds with both the catalyst **11a** amine and the amide NH, which are stronger than the intramolecular H-bond.

According to kinetic experiments, deacetylation reaction of catalyst **11a** with neat deuterated methanol took place with a half-life of 165 min. However, this time was longer than expected, as the catalyst should have an appropriate conformation in neat deuterated methanol which leaves the functional groups with the right geometry to catalyse the reaction.

3.1.3. Synthesis of catalyst 16

***Modelling studies of catalyst* 16**

To avoid the intramolecular hydrogen bond, in this catalyst the amine group is placed away from the oxyanion-hole unit and is separated three carbon atoms from the hydroxyl group. Even though this is not the structure of *N*-terminal hydrolases, Moody *et al.* have reported a mechanism for *N*-terminal hydrolases in which one molecule of water participates in the transport of the hydrogen from the hydroxyl group to the leaving group,[147] avoiding the strain of the four-membered cycle. Catalyst **16** is based on the same tetrahydronaphthalene moiety as catalyst **11**, but the catalytic groups are placed in a different disposition to obtain the desired geometry. In this case, the amino from the oxyanion-hole unit and the hydroxyl group have the chymotrypsin's disposition. Modelling studies showed that the equatorial disposition of the functional groups keeps the short distance between dimethylamino nitrogen and the OH despite being separated by three carbon atoms (2.72 Å).

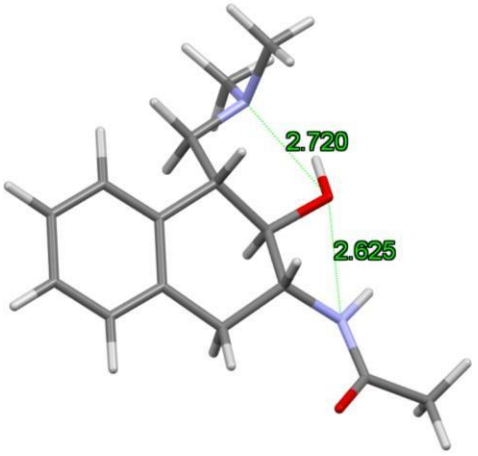

Figure 113. *DFT optimized (HF) structure for catalyst* **16**.

[147] Duggleby, H. J.; Tolley, S. P.; Hill, C. P.; Dodson, E. J.; Dodson, G.; Moody, P. C. E. *Nature* **1995**, *373*, 264 – 268.

Catalyst* 16 *retrosynthesis

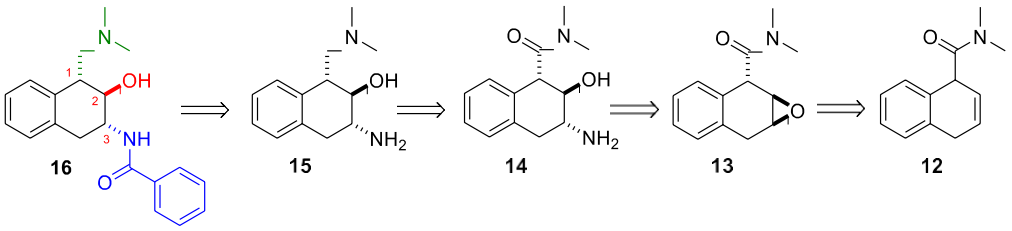

Figure 114. *Key intermediates in the retrosynthesis of organocatalyst* **16**.

Catalyst* 16 *synthesis

The synthesis of catalyst **16** began with the Birch reduction of 1-naphthoic acid to yield acid **6**. The activation of compound **6** *via* acid chloride using PCl_5, described on the Experimental Section (page 224), and the reaction with aqueous 60% Me_2NH solution in the biphasic Schotten-Baumann conditions (Experimental Section, page 224) afforded amide **12**. Basically, the acid chloride was dissolved in EtOAc and added dropwise over a biphasic mixture of the amine in EtOAc and a saturated aqueous solution of Na_2CO_3. The presence of the basic media quenches the HCl formed in the reaction, which would reduce the reactivity of the amine by protonating the nitrogen atom. After decantation and low pressure distillation of the organic solvent, the amide **12** was obtained as a brown oil. Proton signals corresponding to the alkene were observed at 6.23 – 5.97 ppm, as well as two different singlets at 3.04 and 3.05 ppm for each methyl group of the dimethylamide.

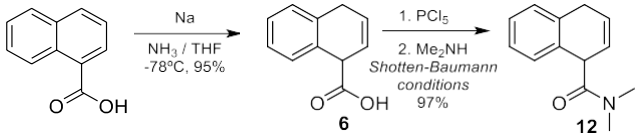

Figure 115. *Synthesis of dimethylamide* **12**.

The next reaction was the epoxidation of alkene **12** with *m*-CPBA in dichloromethane. In this case, no intermolecular hydrogen bond with *m*-CPBA is possible; also due to the hindrance between the amide and the oxidizing agent, the epoxidation takes place preferentially in the opposite face of the amide. Again, a 4:1 mixture of *trans:cis* epoxides was obtained. This time the *trans*-epoxide **13** could be purified from the mixture by crystallization in Et_2O.

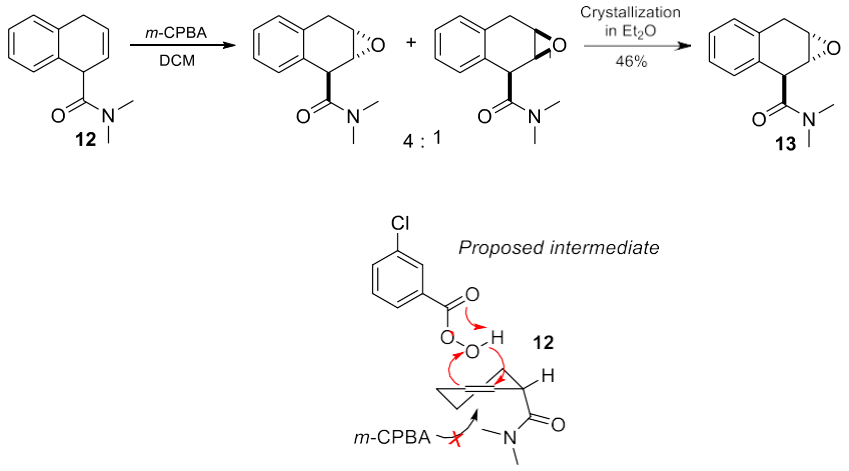

Figure 116. *Epoxidation of compound* **12** *with m-CPBA.*

Then, the epoxide was treated with an aqueous 20% NH_3 solution in MeOH at 80ºC in a high-pressure reactor for one hour. Under these basic conditions, the main product of the reaction was the allylic alcohol corresponding to the epoxide rearrangement *via* E1 elimination, due to the abstraction of H–1 proton by the amine, as it happened in catalyst **11**. But in this case, the analysis of the ^1H NMR spectrum showed small signals corresponding with the expected nucleophilic attack at C–3, which yields the desired epoxide opening.

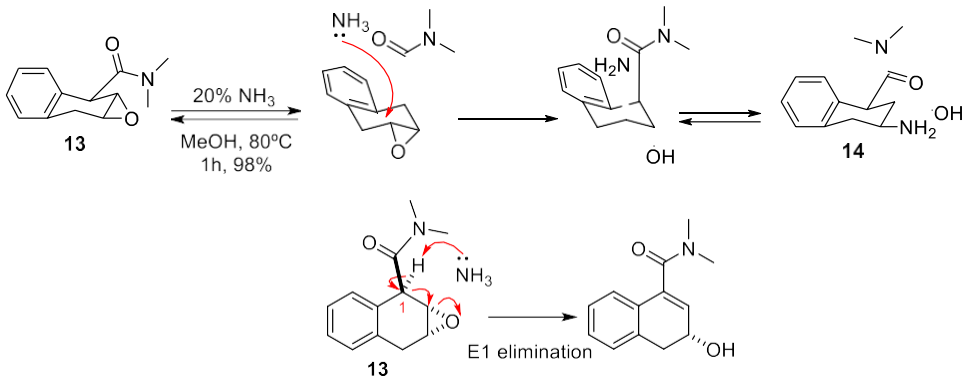

Figure 117. *Epoxide ring opening of compound* **13** *with NH_3, and allylic rearrangement to afford the allylic alcohol via E1 elimination.*

In order to disfavour the allylic rearrangement, less basic conditions were employed. NH_4Cl was used as the proton source, making a buffer with ammonia where it reacts with the epoxide and the NH_4Cl protonates the leaving group. Despite the buffer conditions, a small amount of the allyl alcohol was still observed in the crude reaction product. Isolation of compound **14** was easy since **14** has a free amine while the allyl alcohol is neutral. Thus, after extraction with 2M HCl and subsequent basification, concentration of the aqueous phase and extraction with 10% MeOH in $CHCl_3$ afforded the pure amine **14**. The allylic alcohol remained in the organic phase as it is not soluble in water. The *trans*-stereochemistry between the functional

groups was confirmed in the ^{1}H NMR spectrum with the triplet of H–2 at 4.10 ppm, and a coupling constant of J = 9.5 Hz.

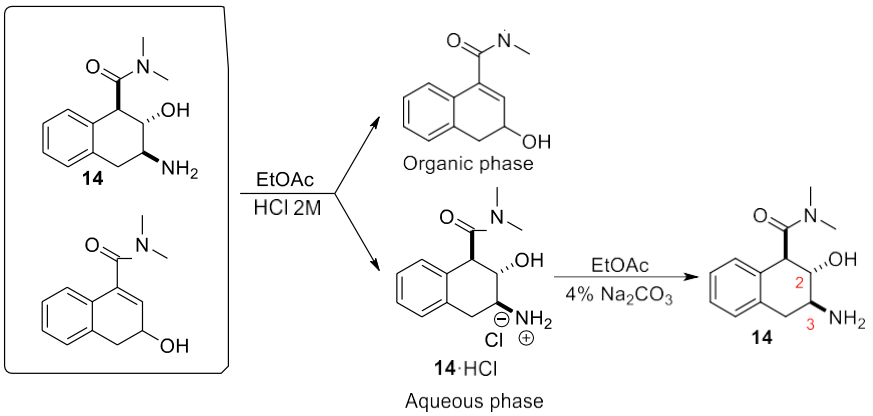

Figure 118. *Purification of compound* **14**.

The following reaction was the reduction of amide **14** to the dimethylamine. This transformation was carried out under standard conditions with $LiAlH_4$ in Et_2O. Compound **14** was dissolved in THF and added dropwise over a vigorously stirred mixture of $LiAlH_4$ in Et_2O. Once the reaction was completed, excess of $LiAlH_4$ was quenched following a standard procedure from the literature. Solvent low pressure distillation afforded amine **15** as a brown oil, which was used without further purification in the next reaction.

The last step was the introduction of the oxyanion-hole mimic unit. As in catalyst **11**, this unit was formed by a single NH group. Compound **15** was reacted with benzoyl chloride using Schotten-Baumann conditions, where the acid chloride was added dropwise over a biphasic mixture of the amine dissolved in EtOAc and a saturated aqueous Na_2CO_3 solution. Catalyst **16** was obtained after decantation, evaporation of the organic solvent and purification with a silica gel column chromatography. Finally, the compound obtained from the column was treated with an aqueous 5% NH_3 solution in order to deprotonate the amine.

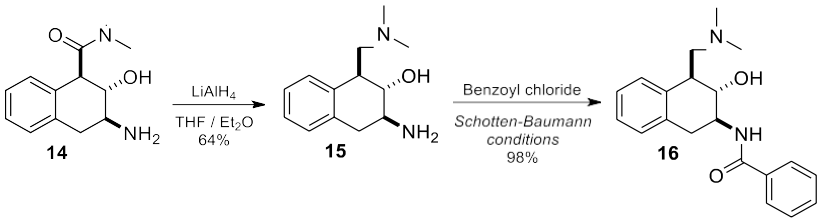

Figure 119. *Reduction of compound* **14** *and reaction with benzoyl chloride to afford catalyst* **16**.

The ^{1}H NMR spectrum showed the triplet of H–2 at 3.93 ppm with a coupling constant of J = 9.5 Hz, and the multiplet H–3 at 4.08 – 4.29 ppm. Furthermore, both methyl groups of dimethylamine are downfield and appear as a singlet at 2.38 ppm.

Acetylated catalyst **16a** was obtained by treating catalyst **16** with acetic anhydride as it was explained in the Experimental Section (page 224). ^{1}H NMR showed the signal for the acetate at 2.04 ppm, and the expected deshielding of H–2 from 3.93 to 5.28 ppm with J = 5.2 and 7.5 Hz. In this catalyst there is not a huge conformational change as in catalyst **11**, but the coupling constant shows that the catalyst should have a half chair conformation. twisted-boat conformation.

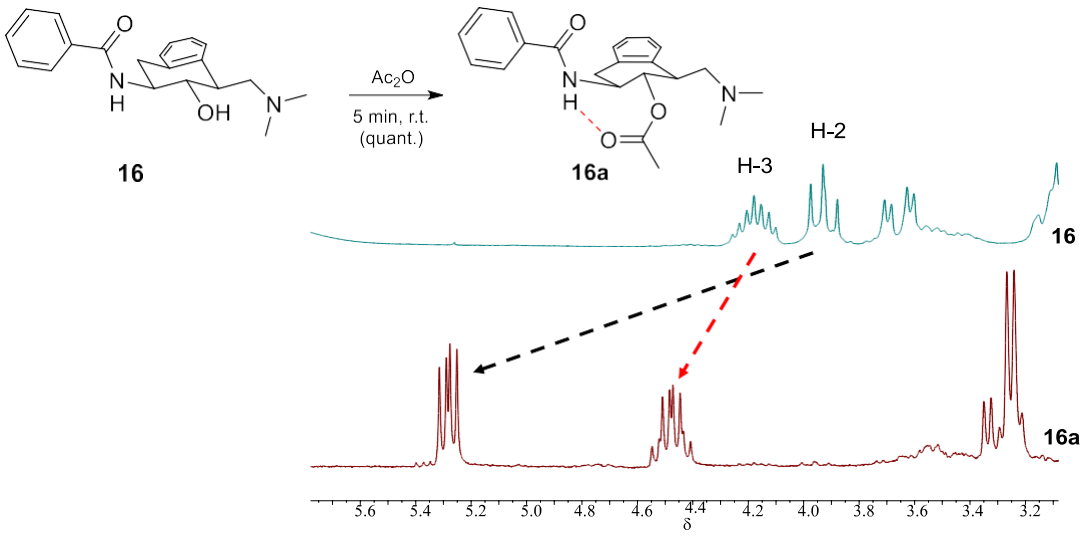

Figure 120. *Synthesis of acetylated catalyst* **16a** *and* ^{1}*H NMR spectrum (5.70 ppm – 3.10 ppm) showing the deshielding of H-2and the slight change in the coupling constant.*

Kinetic studies of catalyst **16**

Then, methanolysis reaction of compound **16a** was performed. Following the methodology described in the Experimental Section (page 290), *ca.* 10 mg of acetylated catalyst **16a** was dissolved in neat deuterated methanol and ^{1}H NMR spectra were recorded. According to the kinetic experiments, deacetylation reaction of catalyst **16a** in neat deuterated methanol took place with a half-life of 87 min. This result is 1.9 times better than the half-life obtained with catalyst **11**. Also, the acylated catalyst maintains the conformation during acylation and deacylation reactions.

Additionally, the structure of catalyst **16** is more attractive to introduce modifications in the oxyanion hole than the previous ones because it can use compound **15**, which mimics the catalytic triad, as intermediate. Building from this, the introduction of the oxyanion hole unit is straightforward by amide coupling, so more oxyanion holes can be easily tested.

3.1.4. Summary and conclusions for organocatalysts 5, 11 and 16

The three catalysts that we have synthesized mimic the catalytic triad (tertiary amine with a secondary alcohol) and oxyanion hole (amide NH) of natural hydrolases.

Despite of the presence of two NHs as oxyanion-hole unit, the free rotations of the methylene groups in the catalytic triad backbone reduced the half-life only to 187 min.

The substitution of this backbone for a more rigid tetrahydronaphthalene skeleton reduced the half-life only 22 minutes when compared with catalyst 5. However, it needs to be noted that catalyst **11** does not have the same number of carbons between the OH and the oxyanion-hole NH that chymotrypsin has. Furthermore, due to the conformational change in the acetylated **11a** in non-coordinating solvents, the acylation step was more difficult since the acylated product is less stable than the starting material.

Interestingly, the substitution of the 1,2-aminoalcohol for a 1,3-diaminoalcohol scaffold in catalyst **16** boosted the reaction rate and a half-life of 87 minutes was measured. Catalyst **16** has the same 1,2 configuration between the OH and the oxyanion-hole NH as chymotrypsin. The presence of the methylene group between the nitrogen and the OH allows the proton transport from the nucleophile to the leaving group.

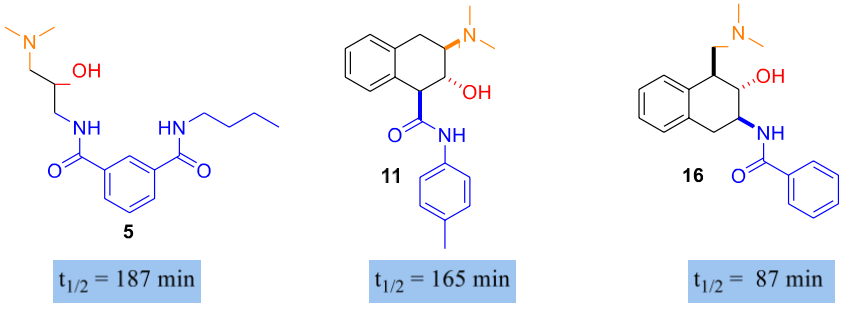

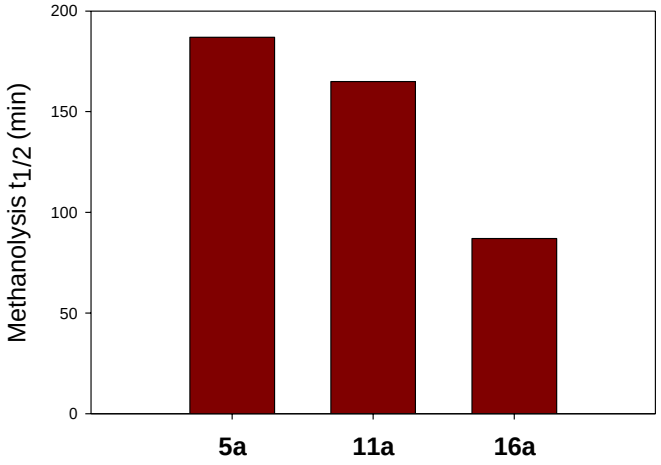

Figure 121. *Half-life for catalyst* **5a**, **11a** *and* **16a** *methanolysis reaction.*

3.2. Improved version of catalyst 16: Catalysts 21, 22, 25 and 29

The best arrangement of functional groups so far was founded in catalyst **16**, as it was shown in the previous section. This catalyst combines features of both chymotrypsin and *N*-terminal hydrolases, and it is a good starting point to improve its kinetic properties.

To do so, we started by designing a library of oxyanion-hole subunits that could be attached to the catalytic moiety **15**. Isophthalic acid, which has been employed successfully as oxyanion-hole mimic previously,[144] was first considered to improve the association of the carbonyl group of the acylated catalysts, and to stabilise the tetrahedral intermediate of the reaction. In Figure 122, several catalysts are proposed.

Also, dimethylamine was replaced by a more basic pyrrolidine in order to increase the catalytic performance.

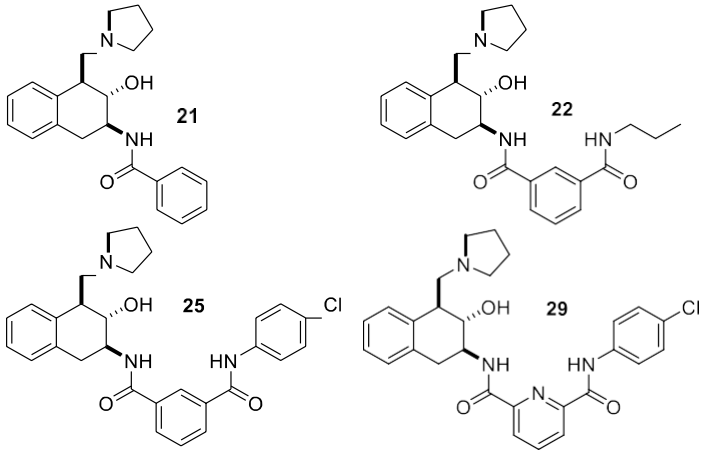

Figure 122. *Organocatalysts **21**, **22**, **25** and **29**.*

3.2.1. Catalyst 21

Catalyst* 21 *synthesis

The synthesis of this compound is similar to catalyst **16**. Pyrrolidinamide **17** was obtained by the reaction of the acid chloride of compound **8** and pyrrolidine using Schotten-Baumann conditions. The epoxidation of this compound with *m*-CPBA afforded a mixture of 6.4:1 *trans*:cis epoxide **18**, probably because the pyrrolidine is more bulky than dimethylamine. The crystallization of epoxide **18** in diethylether afforded the desired intermediate **18**.

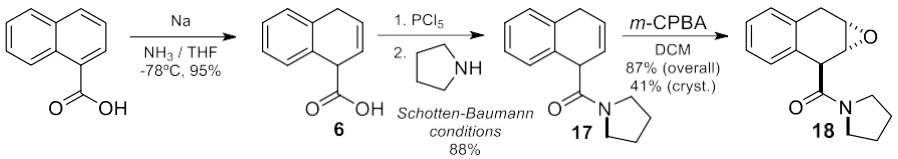

Figure 123. *Synthesis of epoxide **18** from 1-naphthoic acid.*

The reaction of the mixture of epoxides **18** with ammonia led to a mixture of compound **19** and the allylic alcohol, due to the allylic rearrangement of the epoxide under basic conditions. However, we realised that only the *cis* epoxide **18** was able to produce the allylic rearrangement by E2 elimination, because the leaving group (oxygen from epoxide) and the acidic H–1 are in *anti* positions.

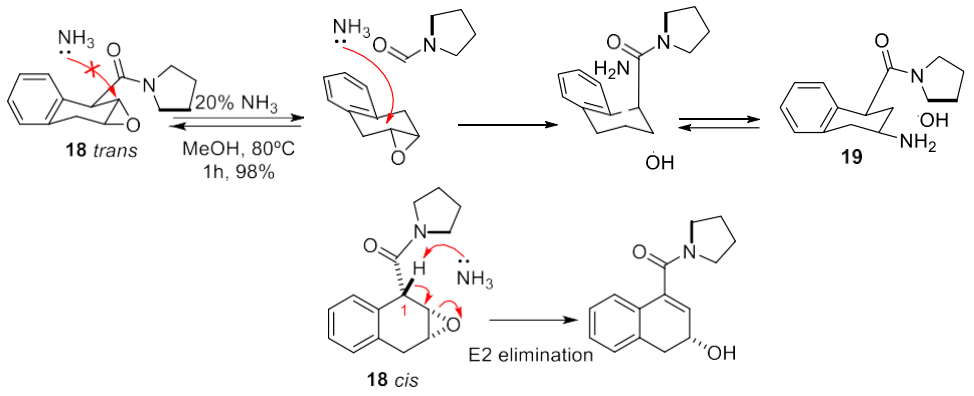

Figure 124. *Synthesis of aminoalcohol* **19** *from the mixture of epoxides* **18**.

Purification of compound **19** from the crude reaction mixture was carried out as in the case of compound **15**, extracting compound **19** as the hydrochloride to an aqueous phase. Basification with Na_2CO_3, concentration of this phase and extraction with 10% MeOH in $CDCl_3$ yielded the desired compound **19**. The yield of the reaction, using the mixture of epoxides, was 42 %.

The reduction of the pyrrolidinamide was carried out with $LiAlH_4$ following the same procedure shown before in the synthesis of **16**. A solution of compound **19** in THF was added dropwise over a vigorously stirred mixture of $LiAlH_4$ in diethylether, and the reaction was performed as in the reduction of compound **14**. Compound **20** was obtained as a yellowish oil and was used in the next step without further purification. This compound contains all the features of the catalytic triad and allows to link different oxyanion-hole mimics directly *via* amide formation.

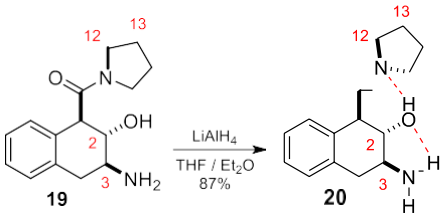

Figure 125. *Synthesis of compound* **20**.

The most interesting fact in the ^1H NMR spectrum of this compound was the change in the pyrrolidine signals. In the amide **19**, H–12 signals are different due to the geometry of the amide: one is close to the carbonyl group and the other one is close to the hydroxyl group (4.06

– 3.96 and 3.61 – 3.45 ppm). In catalyst **20**, these signals were shielded to 2.89 – 2.70 and 2.69 – 2.49 ppm. The difference between H–12 protons is due to the intramolecular H-bond between the amine and the alcohol, so the protons near to the alcohol are deshielded from the protons that go away from the hydroxyl group. H–2 is at 3.53 ppm with coupling constants of 9.4 and 6.7 Hz, so the cyclohexane ring must have a twisted boat conformation, due to the strong H-bond between the pyrrolidine and the alcohol.

To validate our model, we firstly introduced a simple aromatic acid chloride to provide the NH of the oxyanion hole. Schotten-Baumann conditions were used in the coupling between compound **20** and benzoyl chloride. The organic phase was separated and distilled under low pressure. Catalyst **21** was purified by column chromatography over silica gel and activated with 5% NH_3 solution.

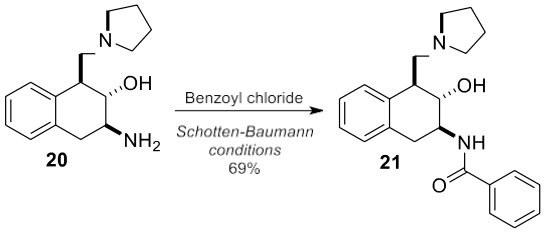

Figure 126. *Synthesis of catalyst* **21**.

The acetylated catalyst **21a** was obtained by treating catalyst **21** with acetic anhydride as it was explained in the Experimental Section (page 224). ^{1}H NMR spectrum showed the signal for the acetate at 2.04 ppm, and the expected deshielding of H–2 from 3.97 to 5.37 ppm, showing again the change in the coupling constant, from 10.4 and 8.1 Hz in the alcohol of **21** to 7.7 and 5.0 Hz in the acylated catalyst **21a**, so we think that the compound has a twisted-boat conformation in $CDCl_3$ as happened with catalyst **16a**. Pyrrolidine protons were shielded around 0.6 ppm in H–12 and 0.2 ppm in H–13.

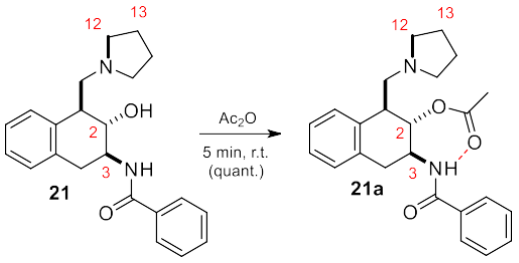

Figure 127. *Synthesis of acetylated catalyst* **21a**.

***Kinetic studies of catalyst* 21**

Methanolysis reaction of catalyst **21a** was performed. Following the methodology described in the Experimental Section (page 290), *ca.* 10 mg of acetylated catalyst **21a** were dissolved in neat deuterated methanol and ^{1}H NMR spectra were recorded over time. According to kinetic experiments, deacetylation reaction of catalyst **21a** in neat deuterated methanol took place with a half-life of 17 min. This result is 5 times better than the half-life obtained with catalyst **16**, so we can conclude that the change of the dimethylamine for the more basic pyrrolidine improved the kinetic performance.

3.2.2. Catalyst 22

Encouraged by the result obtained in the previous section, we decided to study other oxyanion hole mimics to reduce the half-life of the reaction. It is well known that chymotrypsin and *N*-terminal hydrolases stablish two linear NH bonds with the carbonyl group of the acylated enzyme. Furthermore, these NH bonds stabilise the tetrahedral intermediate of the reaction. Trying to mimic this feature from the enzymes, a second NH group was placed in the oxyanion-hole unit using an isophthalic acid moiety as scaffold.

Catalyst* 22 *synthesis

Acid **2** was activated *via* acid chloride using PCl_5 in DCM to obtain the corresponding acid chloride, which was used without further purification in the synthesis of catalyst **22** applying Schotten-Baumann conditions. This acid chloride was dissolved in EtOAc and was added dropwise over a mixture of compound **20** dissolved in EtOAc and a saturated aqueous Na_2CO_3 solution. After separation and purification with a column chromatography using silica gel, catalyst **22** was activated with 5% NH_3.

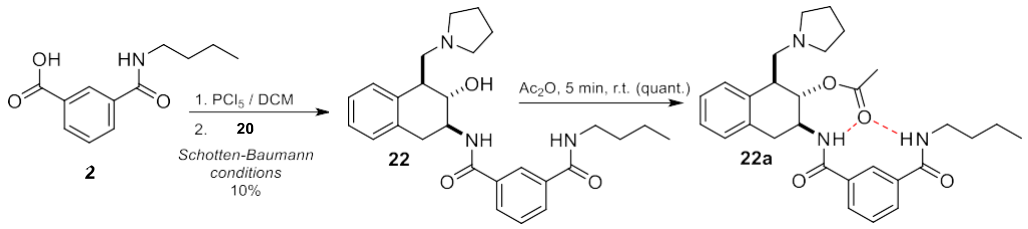

Figure 128. *Synthesis of catalyst* **22**.

Acetylated catalyst **22a** was obtained by treating catalyst **22** with acetic anhydride as it was explained in the Experimental Section (page 224).^{1}H NMR spectrum showed the signal for the acetate at 2.04 ppm, and the expected deshielding of H–2 from 3.97 to 5.39 ppm, as well as the change in the coupling constants from 9.2 and 10.9 Hz of the alcohol in **22** to 4.8 and 7.3 Hz of the acylated catalyst **22a**.

***Kinetic studies for catalyst* 22**

The methanolysis reaction of catalyst **22a** was performed following the methodology described in the Experimental Section (page 290). *ca.* 10 mg of acetylated catalyst **22a** was dissolved in neat deuterated methanol and ^{1}H NMR spectra were recorded over time. According to the kinetic experiments, deacetylation reaction of catalyst **22a** in neat deuterated methanol took place with a half-life of 12 min. This result is 1.4 times better than the half-life obtained with catalyst **21**. Even though the second NH group forms presumably a NH bond with the acetate which stabilises the tetrahedral intermediate of the reaction and reduces the half-life of the methanolysis, we expected a higher increase in the reactivity.

3.2.3. Catalyst 25

To improve the reactivity of catalyst **22**, we envisioned that increasing the acidity of the second NH in the oxyanion hole should enhance the stabilization of the tetrahedral intermediate of the acyl-catalyst. The acidity character of this NH can be easily increased replacing the butylamine by an aromatic amine bearing electron-withdrawing substituents as in *p*-chloroaniline.

Catalyst* 25 *synthesis

The synthesis of the oxyanion-hole unit began with the activation of the acid **1** with PCl_5 to yield the acid chloride. The reaction of this acid chloride with *p*-chloroaniline using Schotten-Baumann conditions afforded amide **23** as a white solid. In order to attach compound**20**, the methyl ester was hydrolysed refluxed with NaOH in a ternary mixture of MeOH / TFH / H_2O (1:1:1). Upon addition of 2M HCl, compound **24** crashed out as a white solid.

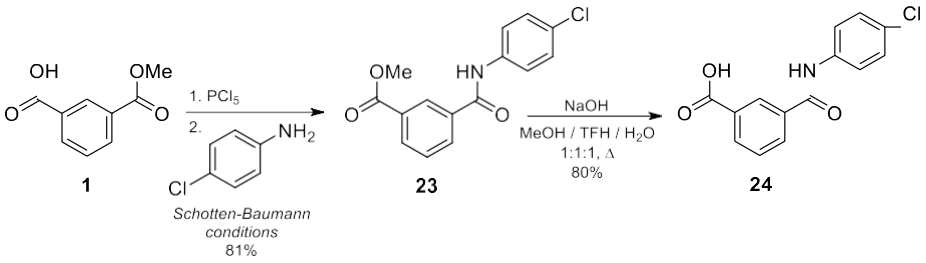

Figure 129. *Synthesis of oxyanion-hole unit* **24**.

Following the same procedure described in the previous sections, acid chloride activation of compound **24** using PCl_5 and reaction with compound **20** under Schotten-Baumann conditions afforded catalyst **25** after purification over silica gel and activation with and aqueous 5% NH_3 solution. ^{1}H NMR spectrum showed the expected double doublet of H–2 at 4.09 ppm, with J = 10.2 and 8.2 Hz.

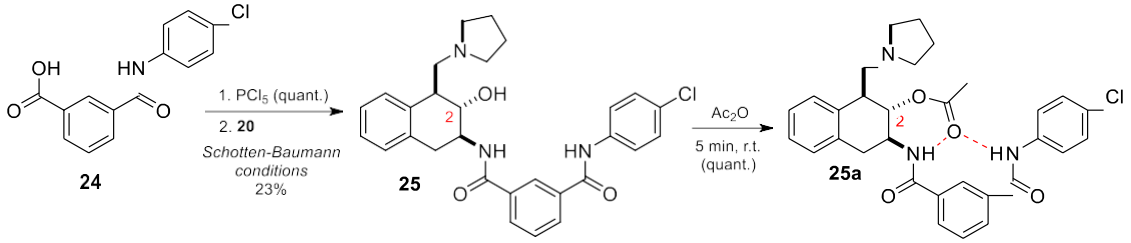

Figure 130. *Synthesis of catalyst* **25** *and acetylated catalyst* **25a**.

Acetylated catalyst **25a** was obtained by treating catalyst **25** with acetic anhydride as it was explained in the Experimental Section (page 224). ^{1}H NMR spectrum showed the signal for the acetate at 2.02 ppm, and the expected deshielding of H–2 from 4.09 to 5.31 ppm, with J = 7.2 and 4.7 Hz.

Kinetic studies of catalyst 25

Then, the methanolysis reaction of catalyst **25a** was performed. Following the methodology described in the Experimental Section (page 290). *ca.* 10 mg of acetylated catalyst **25a** was dissolved in neat deuterated methanol and ^{1}H NMR spectra were recorded over time. According to the kinetic experiments, deacetylation reaction of catalyst **25a** in neat deuterated methanol took place with a half-life of 15 min. Surprisingly, this result is worse than the half-life obtained for catalyst **22**, where the second NH is generated by a less acidic butylamide. It is well known that more acidic NH bonds improve the association in supramolecular receptors,[148] so this result exposes that, probably, the distance between the carbonyl group and/or the tetrahedral intermediate and the second NH is further than we were expecting initially, and likely, a dimer of the catalyst generates stronger hydrogen bonds between itself that the hydrogen bonds with the acetate.

3.2.4. Catalyst 29

In order to know if the problem is the long distance of the second NH with the carbonyl group, which makes unviable to improve the stabilization of the oxygen, the isophthalic acid moiety was changed by a pyridine dicarboxylic acid scaffold, which has been also employed in oxyanion-hole mimics.[149] As the C–N distance in the pyridine is shorter than the C–C

[148] Fuentes de Arriba, A. F.; Turiel, M. G.; Simón, L.; Sanz, F.; Boyero, J. F.; Muñiz, F. M.; Morán, J. R.; Alcázar, V. *Org. Biomol. Chem.* **2011**, *9*, 8321 – 8327.
[149] (a) C. A. Hunter, D. H. Purvis, *Angew. Chem. Int. Ed. Engl.* **1992**, *31*, 792 – 795; *Angew. Chem.* **1992**, *104*, 779 – 782; (b) H. Adams, F. J. Carver, C. A. Hunter, N. J. Osborne, *Chem. Commun.* **1996**, 2529 – 2530; (c) F. J. Carver, C. A. Hunter, R. J. Shannon, *J. Chem. Soc., Chem. Commun.*, **1994**, 1277 – 1280.

distance in the isophthalic acid aromatic ring, the second NH group will be closer to the active centre.

Modelling studies of both isophthalic and pyridine rings showed the shorter C–N distance (1.32 Å) in the pyridine than the C–C distance in the isophthalic acid (1.38 Å) (Figure 131). Therefore, a shorter distance of 3.07 Å between the second NH and the oxygen from the carbonyl group is now expected in the pyridine in comparison with the 3.46 Å in the isophthalic moiety. Besides, the distance between both nitrogen atoms from the NH groups is 5.02 Å and 4.61 Å (Figure 131).

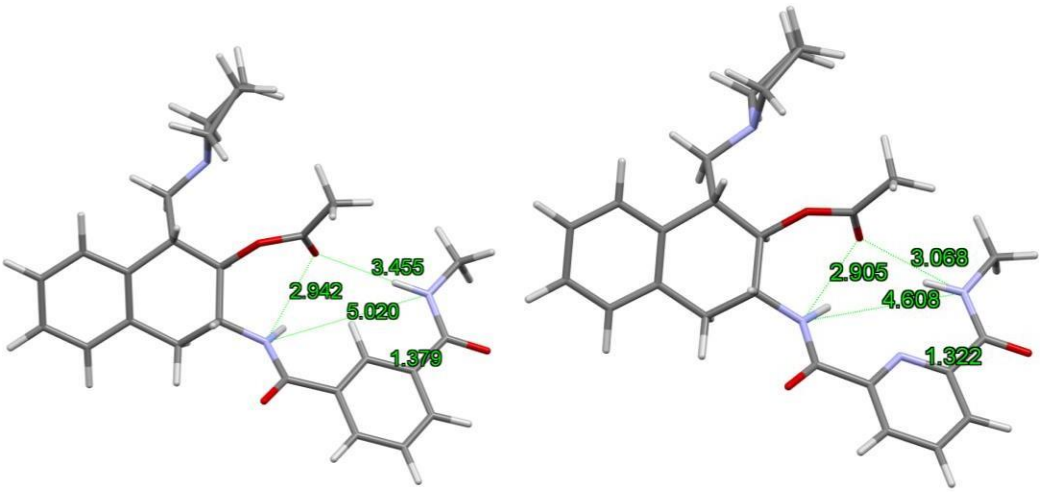

Figure 131. *DFT optimized (HF) structures for compounds **25a** (left) and **29a** (right). Methylamide was used in both cases to reduce the calculation time.*

The synthesis of the oxyanion hole is similar to the isophthalic acid moiety. 6-(methoxycarbonyl)picolinic acid **26** was activated *via* acid chloride with PCl_5, and it was used without further purification in the following reaction. Amide **27** was obtained by combining the acid chloride of **26** with *p*-chloroaniline using Schotten-Baumann conditions. The hydrolysis of the ester with KOH in MeOH afforded the corresponding acid **28** as a white solid after the addition of 2M HCl.

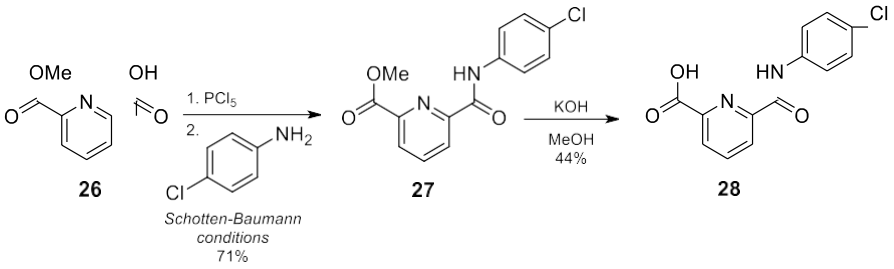

Figure 132. *Synthesis of oxyanion-hole unit* **28**.

Activation *via* acid chloride of compound **28** with PCl_5 and reaction with compound **20** under Schotten-Baumann conditions afforded catalyst **29** after purification over silica gel and activation with 5% NH_3. ^1H NMR spectrum showed the double doublet of H–2 at 4.10 ppm, with J = 8.6 and 10.4 Hz.

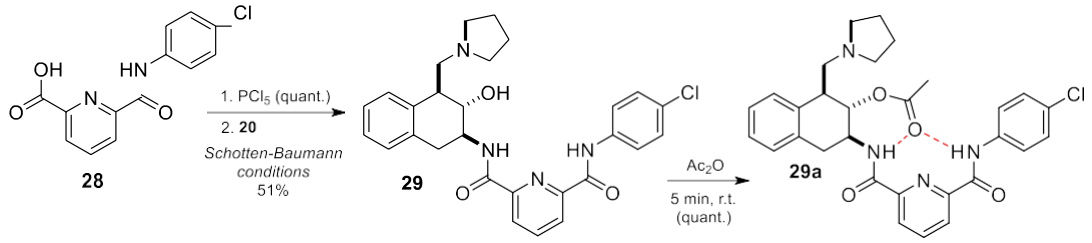

Figure 133. *Synthesis of catalyst* **29**.

Acetylated catalyst **29a** was obtained by treating catalyst **29** with acetic anhydride as it was explained in the Experimental Section (page 290). ^1H NMR spectrum showed the signal for the acetate at 2.07 ppm, and the expected deshielding of H–2 from 4.10 to 5.54 ppm, but now there was no such a big change in the coupling constants (10.4 and 8.6 Hz in the alcohol to 11.2 and 7.7 Hz in the acetate).

One interesting fact of this catalyst was the deshielding of the second NH–22, from 9.97 ppm in the alcohol **29** to 10.31 ppm in the acetylated catalyst **29a**. This can be explained if the distance between the NH and the carbonyl group is now shorter and makes a stronger hydrogen bond. In contrast, this effect was not observed in catalyst **25**, in which this NH is placed further.

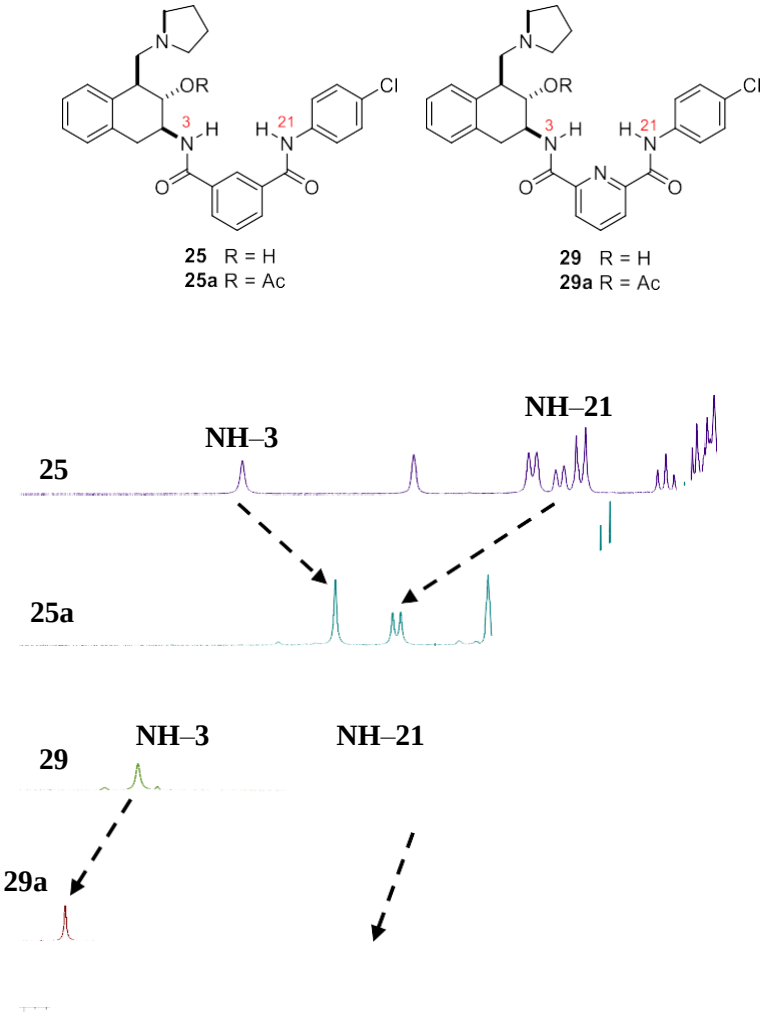

Figure 134. *^{1}H NMR spectra (10.4 – 6.6 ppm) showing the movement of NHs signals of catalyst **25** and **29** after acetylation.*

Kinetic studies of catalyst* 29 *– Methanolysis reaction

Then the methanolysis reaction of catalyst **29a** was studied. Following the methodology described in the Experimental Section (page 290), *ca.* 10 mg of acetylated catalyst **29a** were dissolved in neat deuterated methanol and ^{1}H NMR spectra were recorded over time. According to the kinetic experiments, deacetylation reaction of catalyst **29a** in neat deuterated methanol took place with a half-life of only 3.7 min. This result indicates that the second NH was too far from the carbonyl oxygen and/or the tetrahedral intermediate in catalyst **25** and much closer in catalyst **29**.

Encouraged with this result, we decided to study the behaviour of catalyst **29** in transesterification reactions.

Kinetic studies for catalyst* 29 *– Transesterification reaction

Since compound **29** was the best catalyst synthesized so far, it was used to study the transesterification of vinyl acetate with methanol.

Vinyl acetate and MeOH (1.6:1) were mixed in an NMR tube and catalyst **29** (<1 mol%) was added at 20ºC. The reaction progress was followed by ^{1}H NMR using external D_2O in a Shigemi NMR tube to lock the spectrometer. Integration of the starting material and product signals allowed us to calculate the concentration of starting material and products. Plotting molar fraction of vinyl acetate and methyl acetate *vs* time was used to calculate the reaction rate and a half-life of 68 hours was obtained. The same conditions were performed without catalyst **29** and monitored by ^{1}H NMR, but in this case no reaction was observed.

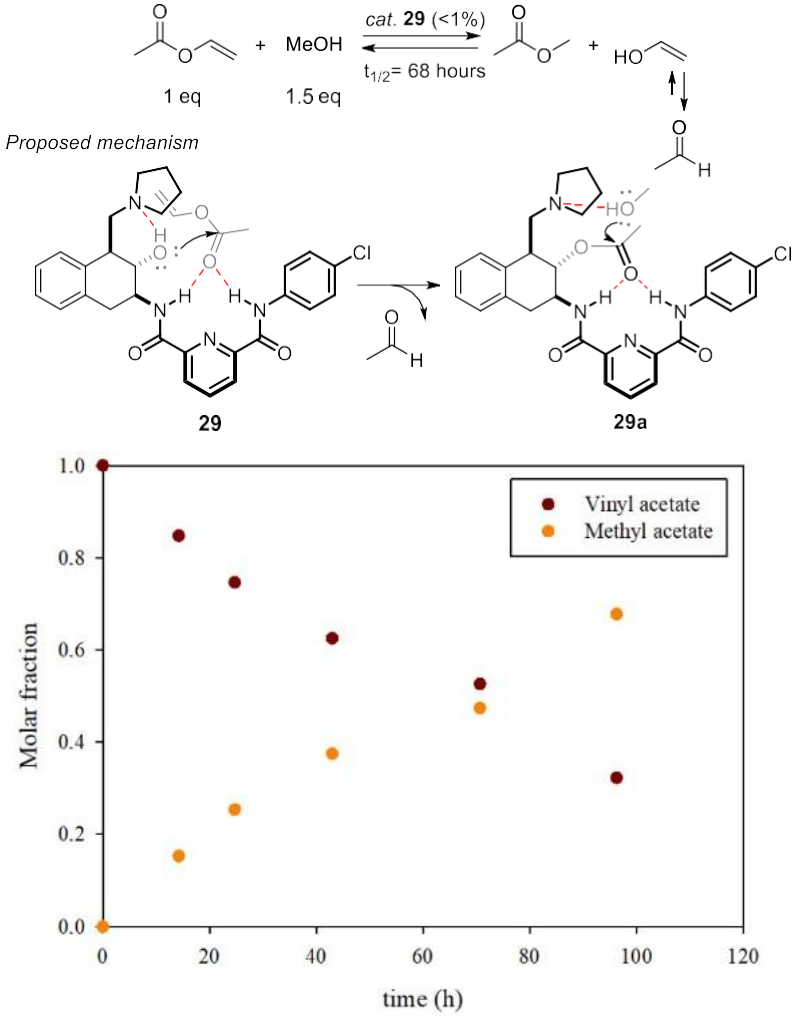

Figure 135. *General reaction and proposed mechanism for the transesterification reaction between vinyl acetate and MeOH catalysed with* **29** *(above) and molar fraction of vinyl acetate and methyl acetate vs time ploting (bottom)*

Even though this result was good, we expected a lower half-life for this reaction. Since the methanolysis study showed a half-life of only 3.7 min, the limiting step should be the acetylation of the catalyst. In order to better understand this first step, a ^{1}H NMR titration between catalyst **29** and EtOAc was performed to study the binding properties of catalyst **29** for EtOAc.

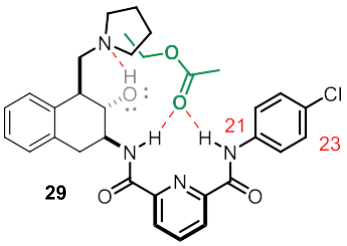

Figure 136. *Putative complex between* **29** *and EtOAc.*

Experimentally, 1.3 mg ($2.6\text{x}10^{-3}$ mmol) of catalyst **29** were dissolved into 400 μL of $CDCl_3$ and pure EtOAc was successively added to the reaction mixture, registering a ^{1}H NMR spectrum after each addition at 20ºC. Plotting H-21 and H-23 shifts of catalyst **29** *vs* the equivalents of EtOAc added gave an association constant of 0.79 M^{-1} with 6.1% of error. Titration analysis was performed with Bindfit software available on Internet.[150]

This low association constant shows that the main problem of catalyst **29** is the low affinity for the ester. This result indicates that the amount of the complex needed for the reaction to happen is very low, and the reaction rate, being proportional to the amount of this associate, is slower than expected.

Modelling studies of catalyst 29 *– Tetrahedral intermediate and ground state*

In order to improve the catalytic performance of the catalyst, several modelling studies of the tetrahedral intermediate and ground state of catalyst **29** were carried out to better understand the geometry of the key steps. Selected studies are shown below (see experimental section for further information, page 302).

[150] Supramolecular.org: http://app.supramolecular.org/bindfit/

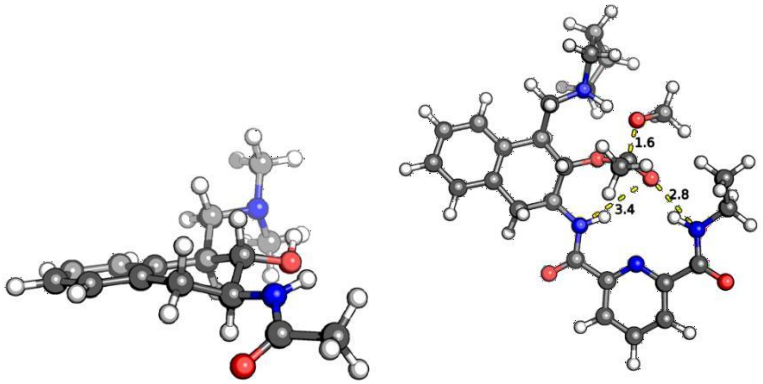

Figure 137. *Most stable conformation of a simplified model of catalyst **29** showing the equatorial arrangement of the catalytic groups (left) and calculated geometry of the transition state structure for the methanolysis reaction of compound* **29a** (right). *Selected distances between heteroatoms are depicted in angstroms (Å).*

As it can be seen in Figure 137 (left), the tetrahydronaphthalene skeleton has a half-chair conformation in which all the catalytic groups have a *pseudo*-equatorial configuration. Two hydrogen bonds are stablished between the amino and hydroxyl groups, and between the hydroxyl group and the oxyanion-hole NH. These hydrogen bond network creates a rigid scaffold which difficult the half-chair conformational change.

However, in the transition state model of Figure 137 (right) it is shown that the distances between the oxyanion-hole NHs and the carbonyl oxygen atom are a bit longer than expected (3.4 and 2.8 Å). Thus, a narrower oxyanion-hole mimic would be desirable to improve the catalytic performance.

Structural studies for catalyst* 29 *– NMR spectroscopy

HSQC spectrum of catalyst **29** confirmed the presence of diastereotopic protons in the tetrahydronaphthalene skeleton due to the rigidity induced by the hydrogen bonds between the catalytic groups. The biggest change was observed between H-4 double doublets at 3.70 and 2.90 ppm, where the carboxamide carbonyl oxygen deshielded only one of them. Interestingly, pyrrolidine H-12 appeared at 2.70 and 2.90 ppm, for the protons which are close to the OH.

COSY spectrum corroborated the proposed geometry for catalyst **29**. H-12 signals at 2.70 and 2.90 ppm from pyrrolidine are coupled with H-13 signal at 1.90 ppm. Another interesting feature is the cross peak observed between H-3 and H-4a which is more intense than the cross peak between H-3 and H-4b, which can be confirmed with the values adopted by the *J* coupling constants and corroborates the half-chair conformation and the rigid structure.

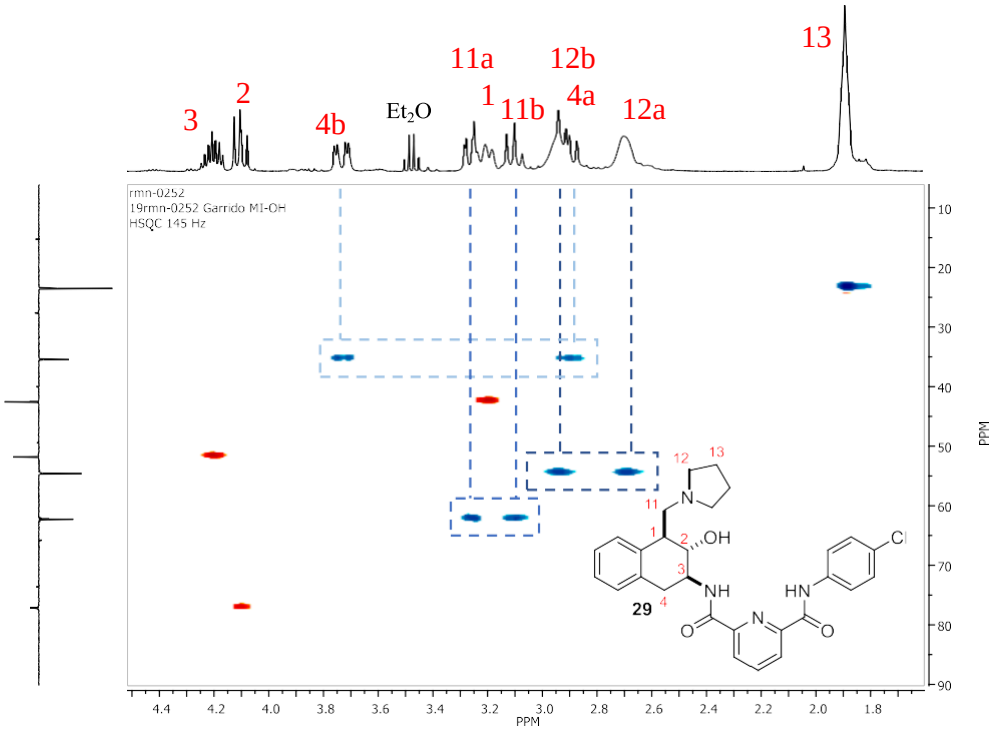

Figure 138. *HSQC experiment for catalyst* **29**.

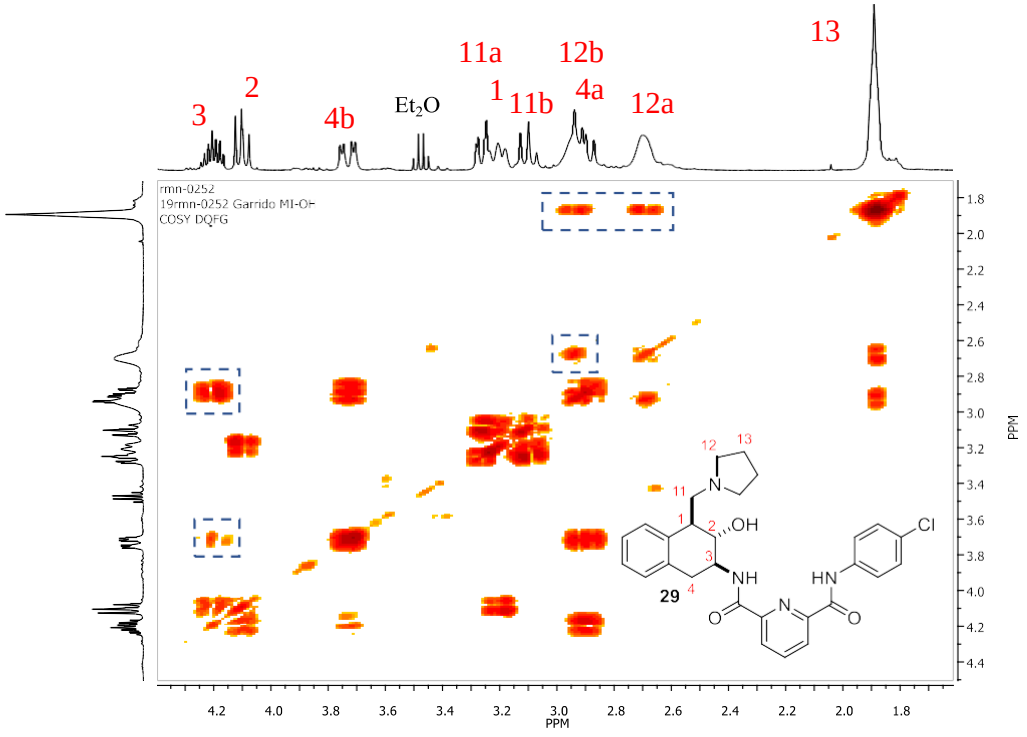

Figure 139. *COSY experiment for catalyst* **29**.

***Structural studies for catalyst* 29 *– Crystallographic studies for tetrahedral intermediate analogue* 29b**

As it has been explained in the Introduction, most of the X-ray structures of enzymes are crystallized with an inhibitor in their active centre which mimics the intermediate of the reaction that they catalyse. In trypsin-like hydrolytic enzymes, tosyl and phosphonate groups have been used as tetrahedral intermediate analogues.

Therefore, to show that catalyst **29** possesses a well-preorganized polar environment complementary to the transition state, its reaction with a transition state-mimic phenylphosphonic acid chloride was performed (Figure 140). Compound **29b** was confirmed by MS, showing the molecular ion $[M+H]^+$ at m/z = 645.2.

First, NMR studies were carried out. DMSO-d_6 was employed but the ^{1}H NMR spectrum was broad. This could be due to the zwitterionic feature, as it has both acid and amino groups in its structure. The presence of charges in the compound and a relatively big apolar structure makes micelles in the polar solvent, where the apolar region goes inside the micelle and the pulse relaxation is lost. As the compound was not soluble in $CDCl_3$, 5% CD_3OD in $CDCl_3$ was employed. In these conditions, better quality spectrum could be obtained. H–2 Signal was in common acetylated region, as well as the change in the signal shape due to the coupling constant with the phosphorous.

To increase our knowledge about the structure of catalyst **29**, we tried to crystallise it in order to obtain its X-ray structure. Pleasingly, X-ray quality crystals of the product were obtained from slow evaporation of a dichloromethane/methanol solution.

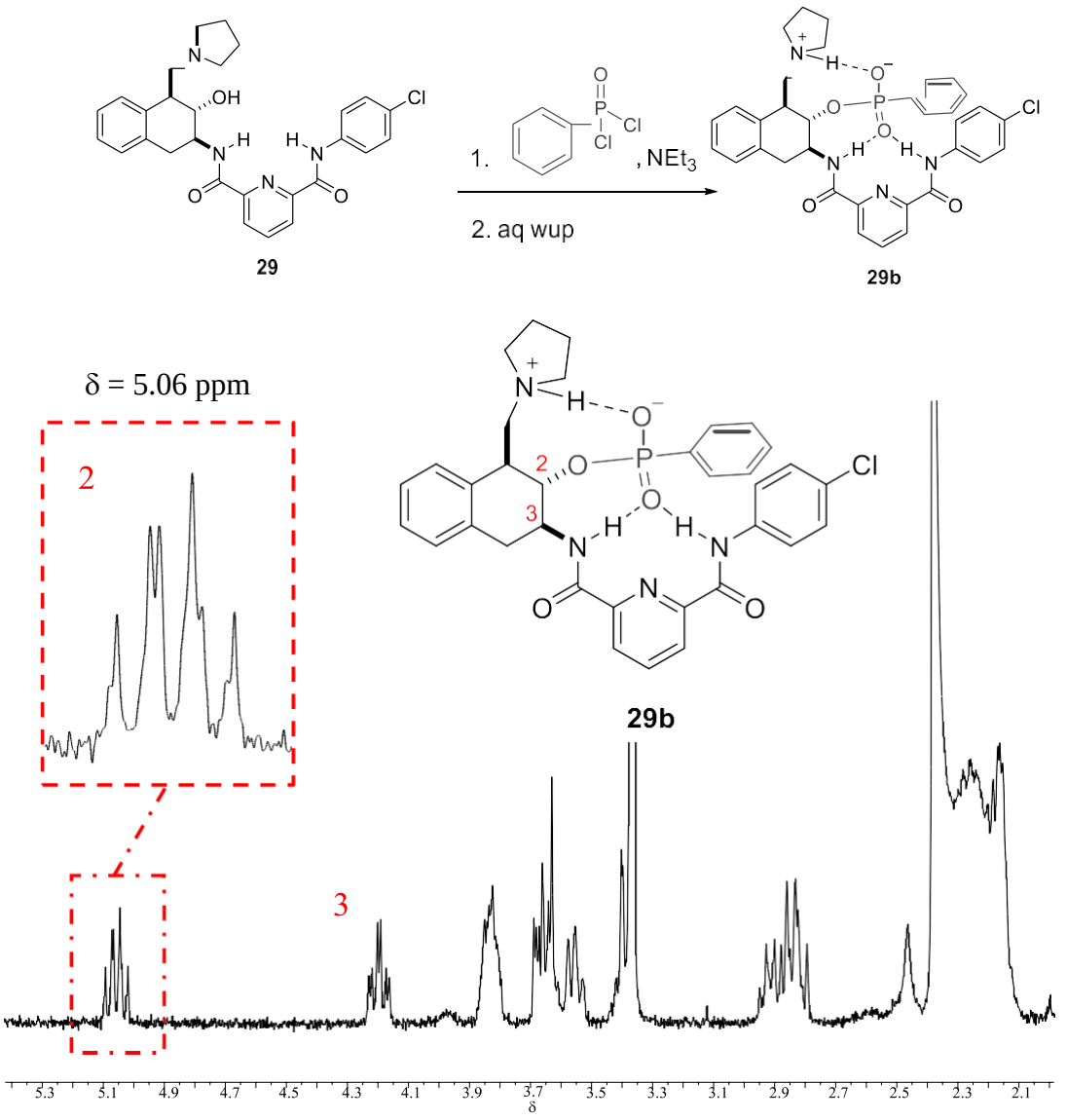

Figure 140. *Reaction of compound* **29** *with phenylphosphonic acid chloride (above) and* ^{1}H *NMR spectrum for catalyst* **29** *in 5% CD_3OD in $CDCl_3$, showing the common deshielding of H–2 in acylated catalysts and the coupling constant between the phosphorous and H–2 (bottom).*

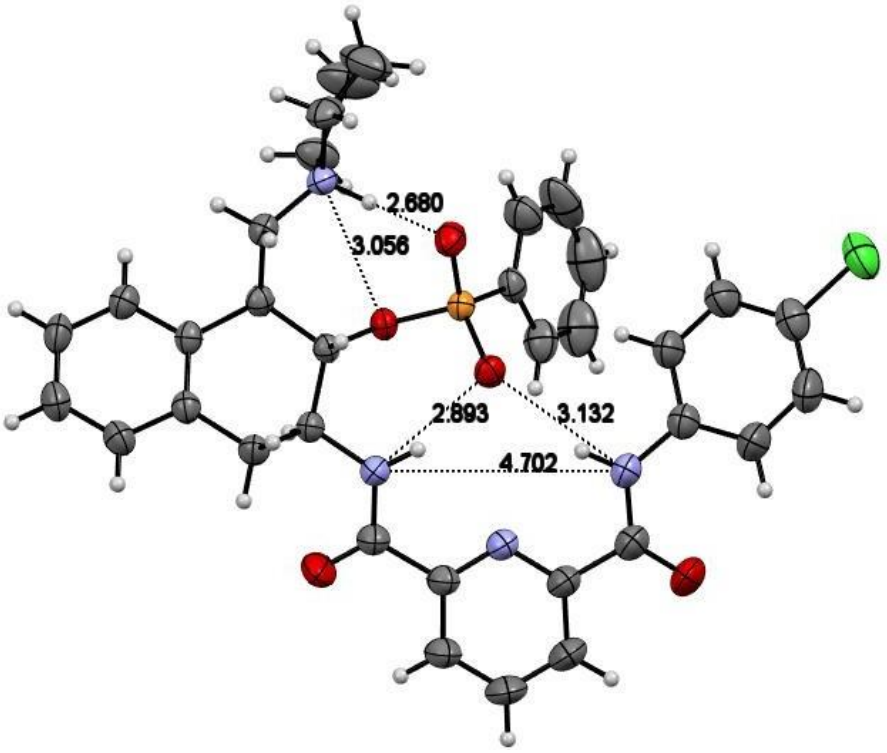

Figure 141. *X-ray diffraction structure of compound* **29b**. *Selected distances between heteroatoms are depicted in angstroms (Å).*

The single-crystal X-ray diffraction analysis showed a perfect fit of the phosphonate group inside the catalyst **29** oxyanion-hole (Figure 141). The phosphoryl oxygen which mimics the negatively charged oxygen of the transition state establishes two H-bonds of 2.89 and 3.13 Å with the pyridine aliphatic and aromatic NHs, respectively. The pyridine oxyanion hole showed a 4.70 Å distance between both NHs, which is in good agreement with natural oxyanion-holes.[151]

The shortest hydrogen bond with only 2.68 Å is set between the pyrrolidinium group and one of the phosphate oxygen atoms. Both phosphoryl oxygen showed similar O–P distances of 1.49 – 1.50 Å, which can be explained with a negatively charged phosphonate group, which contributes to the short pyrrolidinium H-bond.

One of the most attractive features of the structure is the similar distance established between the pyrrolidinium group with both the phosphonoester oxygen (3.06 Å) and the

[151] (a) Simón, L.; Goodman, J. M. *Org. Biomol. Chem.* **2012**, *10*, 1905 – 1913. (b) Simón, L.; Goodman, J. M. *J. Org. Chem.* **2010**, *75*, 1831 – 1840.

phosphoryl oxygen (2.68 Å) which may be a key factor to transport the proton from the nucleophile to the leaving group.

The conclusions obtained from the X-ray structure of compound **29b** agree with the observations detected in solution by ^{1}H NMR, which revealed the deshielding of the oxyanion-hole NHs upon acetylation of the catalyst. This implies that the acetate carbonyl group is hydrogen bonded by the oxyanion-hole NHs in a similar way as the phosphonate group which mimics the transition state of the reaction.

Tetrahedral intermediate analogue* 29b *comparison with natural chymotrypsin

To prove the similarity between catalyst **29** and the active site of a natural hydrolase, single-crystal X-ray diffraction structure of compound **29b** was superimposed with the active center of a chymotrypsin phosphate (Figure 142, PDB 1GCD). The phosphate group was fixed for both compounds, which allowed us to compare the geometry of the catalytic groups in the synthetic catalyst and the enzyme.

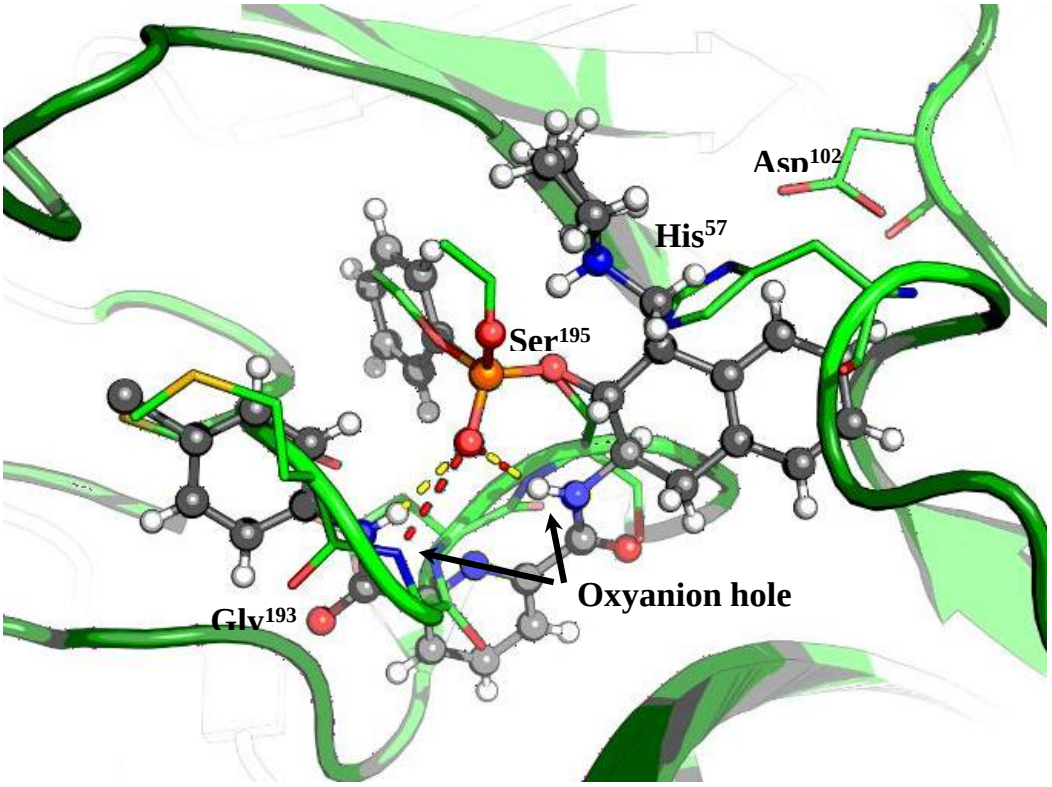

Figure 142. *Superimposition of the crystal structure of chymotrypsin phosphate (ribbon model) and compound* **29b** *(ball-and-stick model) in which the phosphate group is fixed for both compounds. Hydrogen bonds between the oxyanion hole NHs and the phosphate oxygen are depicted as red-dashed lines for chymotrypsin phosphate and yellow-dashed lines for compound* **29b**.

As can be observed in figure 53, the geometry of compound **29b** is fairly similar to the active center of chymotrypsin, with the exception of the basic group, probably because the chymotrypsin phosphate is a neutral compound, which prevents the proximity of the imidazole ring due to the lack of hydrogen bonding, while in compound **29b** a strong hydrogen bond is set between pyrrolidinium and phosphate groups. A better fit is obtained for the oxyanion-hole, with 2.90 Å distance between the phosphoryl oxygen and both the NH of Ser^{195} and catalyst **7** NH. The second H-bond of the oxyanion-hole between Gly^{193} and the phosphoryl oxygen is slightly shorter in chymotrypsin. The rigid pyridinedicarboxamide spacer, with a 4.70 Å distance between both NHs, is probably responsible for this fact, since in chymotrypsin, the oxyanion-hole distance between the NHs is around 4.30 Å.

3.2.5. Summary and conclusions for catalysts 21, 22, 25 and 29

The substitution of the dimethylamino group for the more basic pyrrolidine in catalyst **21** reduced the half-life 5 times. The incorporation of an additional hydrogen bond donor in the isophthalic oxyanion-hole mimic lowered the half-life to 12 minutes. However, increasing the NH acidity did not improve the reaction rate, probably because the second NH bond is too far away from the carbonyl group to stablish a strong hydrogen bond.

The substitution of the isophthalic oxyanion-hole mimic by a pyridinedicarboxylic acid scaffold allowed to reduce the oxyanion-hole size which reduced the half-life to only 3.7 minutes. This confirms that an oxyanion-hole mimic which gets the second NH closer would allow to improve the catalytic performance.

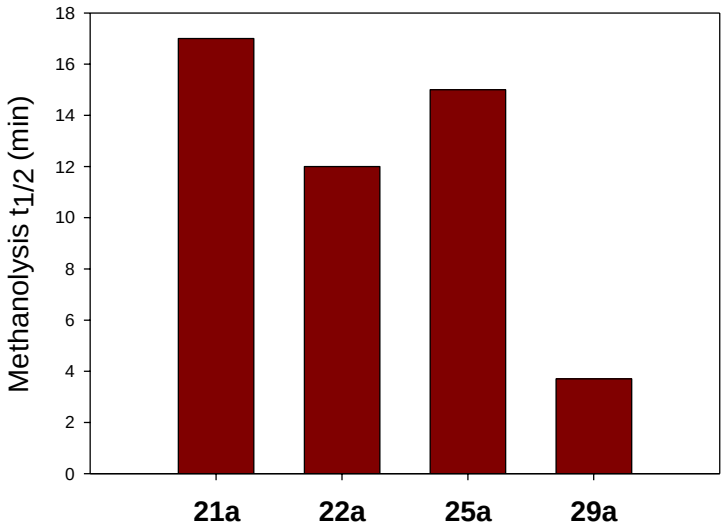

Figure 143. *Half-life for catalyst* **21a**, **22a**, **25a** *and* **29a** *methanolysis reaction.*

SUMMARY – 1st Generation organocatalysts.

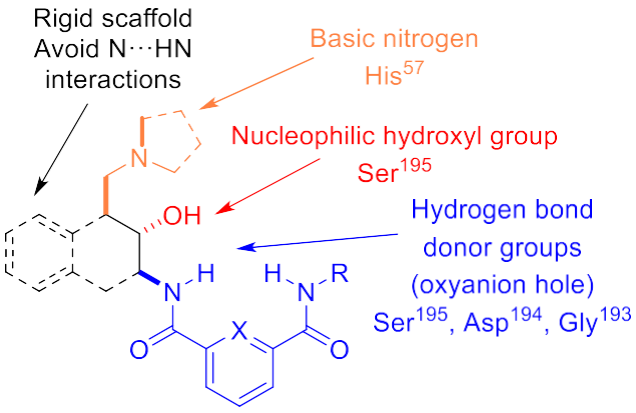

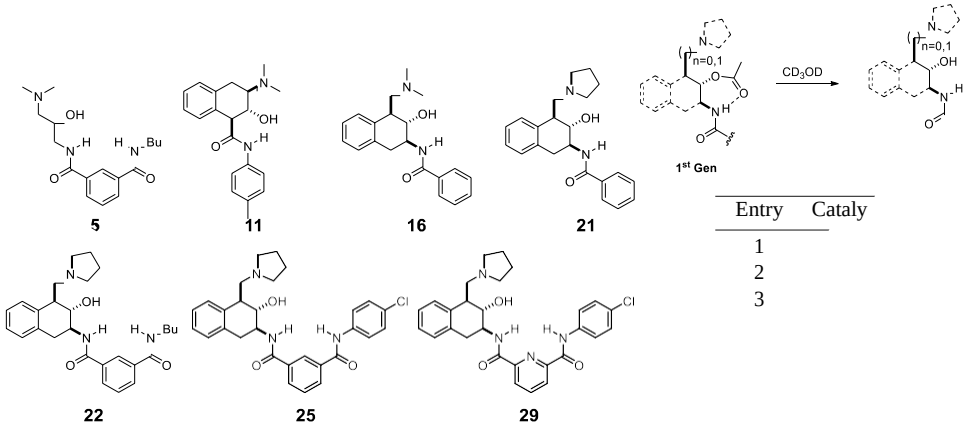

Entry	Cataly
1	
2	
3	

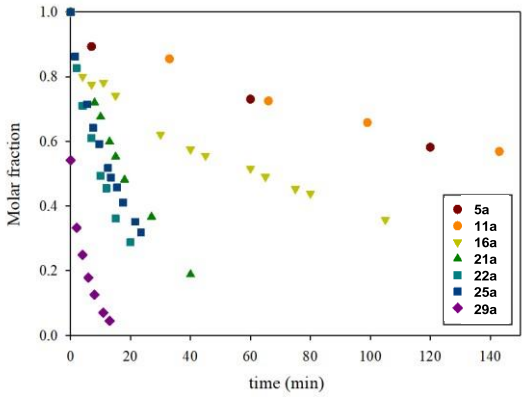

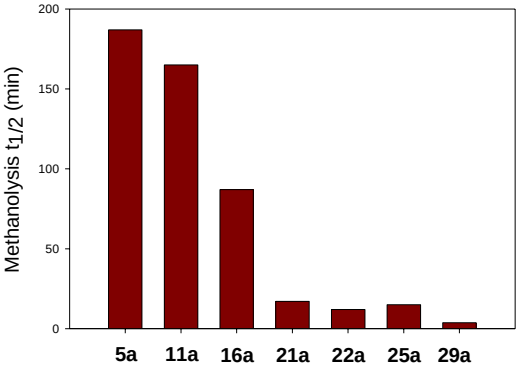

3.3. Oxyanion-hole improvement: Second generation organocatalysts

3.3.1. Narrow and adjustable oxyanion hole.

Even though the acylation step is still a challenge, catalyst **29** showed the best kinetic properties so far. The 1,3 arrangement between the pyrrolidine and the hydroxyl group allows the pyrrolidine to transfer the proton in both acylation and deacylation steps from the hydroxyl group to the leaving group. To improve the kinetic properties of the catalysts even more, a better oxyanion-hole unit should be attached in order to increase the stabilization of the carbonyl group from the acylating agent and the acyl-enzyme, and also the negatively charged oxygen which is generated in the tetrahedral intermediate.

Several oxyanion-hole models, based on xanthone, xanthene, chromane, chromenone, benzofuran and carbazole, among others (shown in Figure 144), have been studied previously in our group. All these structures have at least 2 NHs able to bind a carbonyl or an anion in their cavity, emulating the oxyanion hole of chymotrypsin formed by serine 195, aspartic acid 194 and glycine 193. They have been used as organocatalysts for Michael addition reactions, azlactone ring-opening, amino acid recognition or anion binding, among others.[152]

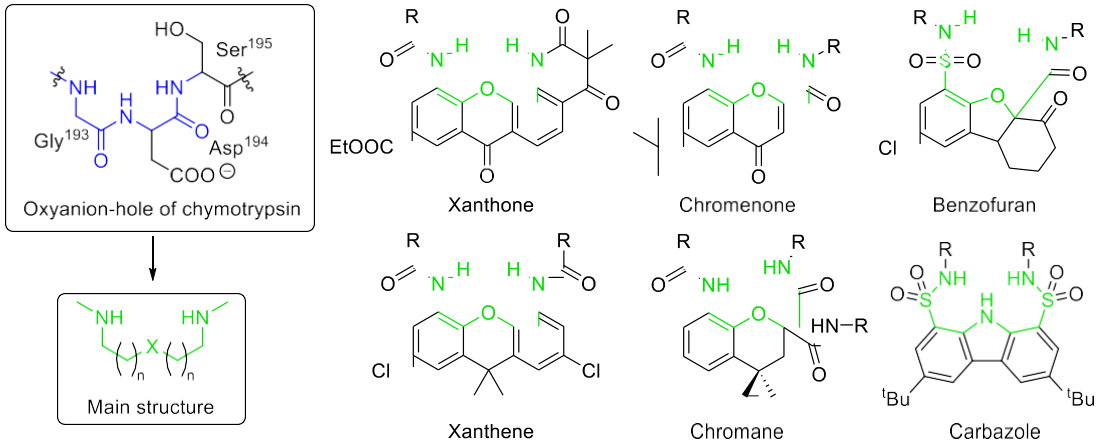

Figure 144. *Oxyanion-hole mimics based on xanthone, xanthene, chromane, chromenone, benzofuran and carbazole scaffolds.*[152]

[152] (a) Fuentes de Arriba, A. F.; Rubio, O. H.; Simón, L.; Alcázar, V. Monleón, L. M.; Sanz, F.; Morán, J. R. *Tetrahedron: Asymmetry* **2017**, *28*, 819 – 823. (b) Simón, L.; Muñiz, F. M.; Fuentes de Arriba, A. L.; Alcázar, V.; Raposo, C.; Morán, J. R. *OBC* **2010**, *8*, 1763 – 1768. (c) Rubio, O. H.; del Mazo, S.; Monleón, L. M.; Simón, L.; Temprano, A. G.; Morán, J. R. *OBC* **2017**, *15*, 4571 – 4578 (d) Blázquez, M. T.; Muñiz, F. M.; Saez, S.; Simón, L. M.; Alonso, A.; Raposo, C.; Lithgow, A.; Alcázar, V.; Morán, J. R. *Heterocycles* **2006**, *69*, 73 – 81. (e) Rubio, O. H.; Taouil, R.; Muniz, F. M.; Monleón, L. M.; Simón, L.; Sanz, F.; Morán, J. R. *OBC* **2017**, *15*, 477 – 485.

Although the previous skeletons try to mimic the oxyanion-hole geometry of natural hydrolases, modelling studies have shown that attaching the aminoalcohol **20** did not provide a promising geometry to associate the carbonyl group form the substrate.

In this work, oxyanion-hole mimics based on 2-naphthoic acid were studied. This scaffold has a more-rigid structure than the isophthalic acid moiety, and it can be decorated with appropriate binding groups such as amides and sulfonamides in order to enhance the association with the substrates.

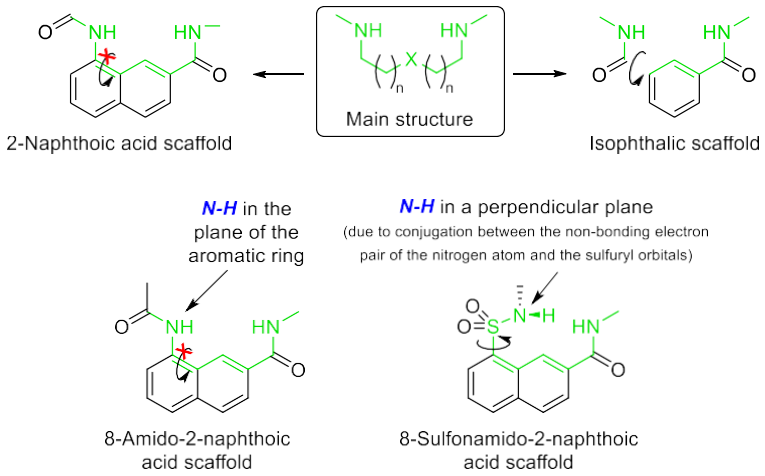

Figure 145. *Main structure of the oxyanion-hole mimics studied in our group (centre) and structural comparison with 2-naphthoic acid and isophthalic acid scaffolds.*

Modelling studies have been carried out with different oxyanion-hole mimics based on isophthalic acid, 8-amino-2-naphthoic acid and 8-sulfonamido-2-naphthoic acid moieties (Figure 146). The oxyanion-hole cavity distance in the isophthalic acid structure is 5.14 Å, and both NHs distances with the carbonylic oxygen are around 3.20 Å. These results can be improved with the 2-naphthoic acid moiety. The oxyanion-hole distance in the compound with the amide in C–8 is 4.92 Å, and the distance between the second NH and the carbonylic oxygen from the guest is 3.55 Å. In the sulfonamide derivative, the NHs distance is also 4.91 Å, but the distance between the second NH ant the oxygen is only 3.05 Å.

Consequently, sulfonamide at C–8 was selected to set up the second NH in the oxyanion-hole unit instead of the aromatic amide. Even though this configuration is not the same as chymotrypsin's oxyanion-hole, the sulfonamide group places its NH closer to the NH of the amide than the aromatic amide at C–8. Besides, the oxyanion-hole cavity distance could be modified because the C–S bond can rotate, which is one on the main principles in enzyme catalysis: a preorganized polar environment complementary with the guest transition state, and

which is mainly obtained through H-bonds and the active centre could modify its structure to fit both ground-state and transition state.[153]

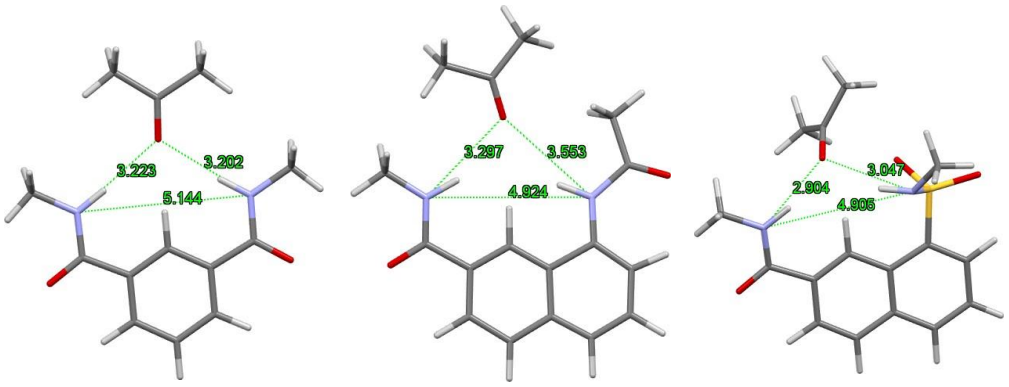

Figure 146. *Modelling studies of different oxyanion-hole mimics based on isophthalic acid (left), 8-amino-2-naphthoic acid (centre) and 8-sulfonamido-2-naphthoic acid (right).*

3.3.2. Catalyst 33

***Modelling studies of catalyst* 33**

To prove our hypothesis, we performed a modelling study of an 8-sulfonamide-2-naphthoic acid oxyanion-hole mimic attached to molecule **20** (Figure 147). An acetate group was linked to the OH to have a better estimation of the distances between the oxyanion-hole NHs and the carbonyl group which is going to be hydrolysed.

The study showed that the distance between the NHs is consistent with the previous results (4.62 Å) and get closer to the average oxyanion-hole distance of natural hydrolases (4.3 Å).[151] This result demonstrates the sulfonamide NH ability to get closer to the guest through rotation around the C–S bond. Also, it is observed that the distance between the sulfonamide NH and the carbonyl group is shorter (2.88 Å) than the same distance in carboxamide-based oxyanion-hole mimics (3.46 and 3.07 Å for **25a** and **29a**, respectively, Figure 131).

[153] (a) Schutz, C. N.; Warshel, A. *Proteins: Struct., Funct., Bioinf.* **2004**, *55*, 711 – 723.

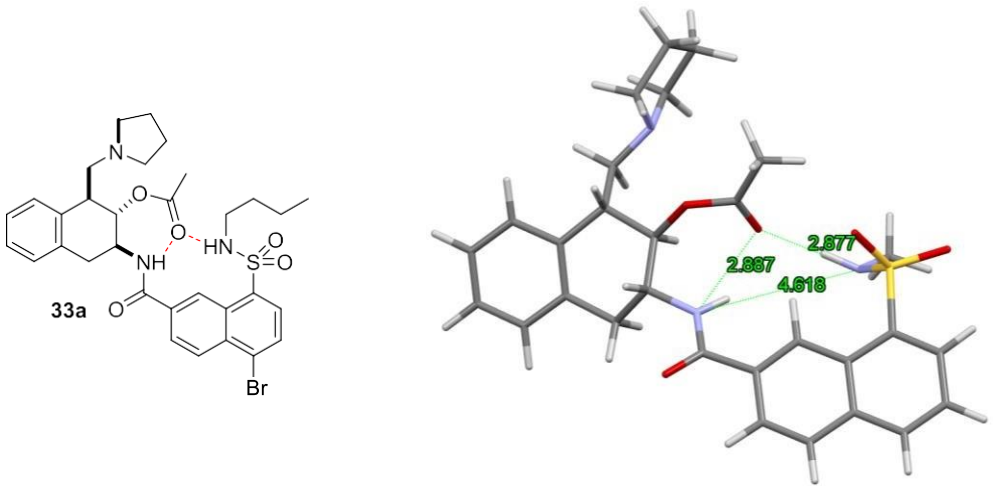

Figure 147. *Proposed structure (left) for catalyst* **33** *and DFT optimized (HF) structure (right) for catalyst* **33a** *(butylsulfonamide was replaced by methylsulfonamide toreduce the calculation time).*

Catalyst* 33 *synthesis

According to the literature, chlorosulfonation of aromatic rings with neat chlorosulfonic acid is a common process to obtain the corresponding chlorosulfonated derivatives. It is necessary to add an excess of chlorosulfonic acid since the first reaction generates the sulfonic acid, which is then transformed into the sulfonyl chloride in the presence of excess of chlorosulfonic acid. In compound **30** (synthesised in Chapter 1), C–6 and C–8 are reactive in electrophilic aromatic substitution due to the presence of the activating bromine atom. However, C–8 is the most reactive one because it is also in *peri* position.[154] Thus, 5-bromo-2-naphthoic acid **30** was dissolved in neat chlorosulfonic acid affording 5-bromo-8-chlorosulfonyl-2-naphthoic acid **31**. Work out was carried out after addition of the crude reaction mixture over water at 0ºC and filtering the crystalline compound. The yield, below 35%, was low probably due to the formation of sulfonic acids that remain in the aqueous phase. Extraction with ethyl acetate of the aqueous phase provided complex mixtures.

Then, compound **30** was dissolved in neat butylamine which acts as nucleophile and also as auxiliary base to quench the HCl generated in the sulfonamide synthesis. After 5 minutes, the reaction was added to an aqueous 2M HCl solution to remove the excess of butylamine

[154] (a) Carey, F. A.; Giuliano, R. M. *Organic Chemistry* 10th ed. McGraw Hill, **2017**. (b) Kartitzky, A. R.; Kim, M. S.; Fedoseyenko, D.; Widyan, K.; Sikin, M.; Francisco, M. *Tetrahedron* **2009**, *65*, 1111 – 1114.

and protonate the carboxylic acid. Sulfonamide **31** was obtained as a white solid after extraction with EtOAc.

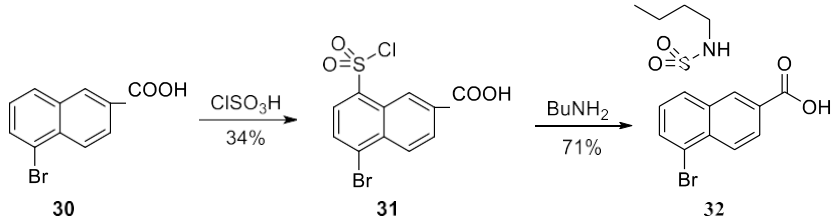

Figure 148. *Chlorosulfonation of compound* **30** *and synthesis of sulfonamide* **32**.

In the next step, acid **32** was activated using PCl_5 to obtain the acid chloride of **32**. This compound was employed in the coupling with amine **20** to obtain catalyst **33** using Schotten-Baumann conditions. Catalyst **33** was obtained after column chromatography purification over silica gel and treatment with 5% aqueous NH_3, following the same procedure made with the previous catalysts. ^{1}H NMR spectrum showed the triplet of H–2 at 4.21 ppm with J = 9.6 Hz.

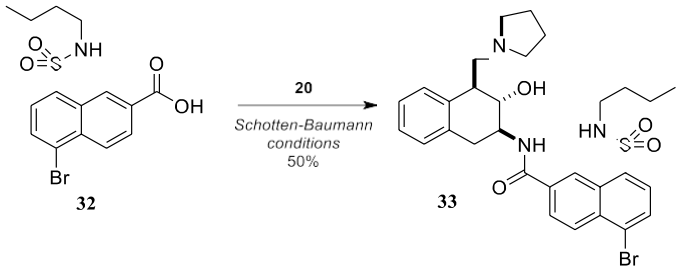

Figure 149. *Synthesis of catalyst* **33**.

Interestingly, catalyst **33** showed different reactivity in the acylation reaction. While the first generation catalysts could only be acetylated with strong acylating agents such as acetic anhydride, the acylated catalyst **33a** was obtained with EtOAc at reflux for 1 hour. To the best of our knowledge this is a remarkable result since it is the first time that an enzyme mimic is acylated with a non-activated ester.

In order to reduce the reaction time to obtain the acylated catalyst, more reactive vinyl acetate was used instead. Vinyl acetate reacts with the OH of catalyst **33** (as explained in the transesterification reaction between vinyl acetate and MeOH with catalyst **29**) to generate the acetylated catalyst **33a** in only 5 min at room temperature. Vinyl alcohol, which rapidly undergoes tautomerization to acetaldehyde, was obtained as a by-product but it could be removed easily by low pressure distillation.

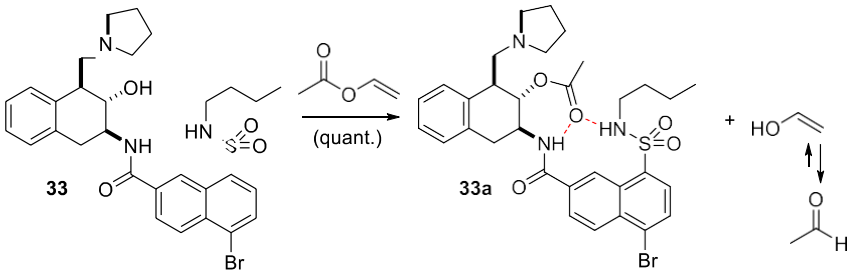

Figure 150. *Reaction of catalyst* **33** *with vinyl acetate to obtain acylated catalyst* **33a**.

^{1}H NMR spectrum showed the signal for the acetate at 2.24 ppm, and the expected deshielding of H–2 from 4.21 to 5.43 ppm with J = 10.2 and 6.9 Hz. The coupling constants showed that this catalyst should present a twisted-chair conformation, as previously reported for other catalysts.

***Kinetic studies of catalyst* 33**

The methanolysis reaction of catalyst **33a** was performed following the methodology described in the Experimental Section (page 290). *ca.* 10 mg of acetylated catalyst **33a** was dissolved in neat deuterated methanol and ^{1}H NMR spectra were recorded over time. According to the kinetic experiments, deacetylation of catalyst **33a** under these conditions took place with a half-life of 3.47 min. This result is similar to catalyst **29** (3.7 min) where the oxyanion-hole mimic based on picolinic acid has a chloroaniline in the second NH. A more accurate comparison is established with catalyst **22** (half-life of 15 min), where the second NH is formed by a butylamide in an isophthalic acid moiety. This represents a 4.3 times increase in the methanolysis rate of catalyst **33**.

Therefore, we can conclude that the more adjustable oxyanion-hole mimic based on 8-sulfonamido-2-naphthoic acid supposes an improvement in the kinetic properties (both acylation and deacylation reactions) of catalyst **33**.

3.3.3. NH acidity studies. Catalysts 35, 37 and 39

As it has been shown in the modelling studies of catalyst **33**, the second NH of the oxyanion-hole is placed closer to the carbonylic oxygen of the acetate in catalyst **33a**. It is expected that increasing the acidity of this NH should improve the reactivity of the catalyst. Therefore, catalysts **35**, **37** and **39** were proposed to study this effect, where aromatic *N*,*N*-dimethyl-*p*-phenylendiamine (electron-donating group), toluidine (weak electron-donating group) and *p*-chloroaniline (electron-withdrawing group) were used to modify the acidity of the NHs (Figure 10).

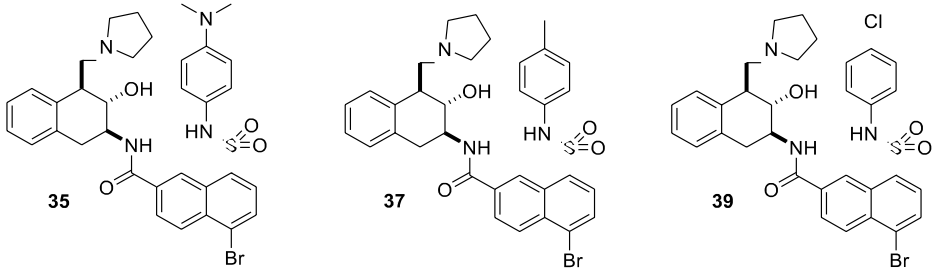

Figure 151. *Proposed catalysts* **35**, **37** *and* **39**.

Catalysts* 35, 37 *and* 39 *syntheses

The synthesis of the oxyanion-hole mimics **34**, **36** and **38** was carried out by the reaction of chlorosulfonyl compound **31** with the corresponding amines. *N*,*N*-dimethylaniline was used as the solvent and auxiliary base in the synthesis of compounds **35** and **36** since these amines are solids.

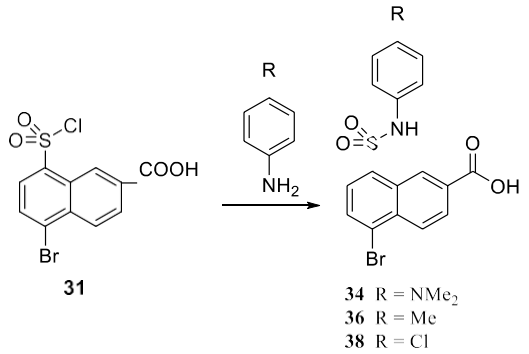

Figure 152. *Synthesis of compounds* **34**, **36** *and* **38**.

Attempts to obtain compound **34** acid chloride, followed by treatment with the amine **20** failed, probably due to the basicity of the dimethylamino group. As catalyst **35** could not be obtained in this reaction, DCC was used as the coupling agent between acid **34** and amine **20**. After column chromatography purification over silica gel and activation with aqueous 5% NH_3 solution, catalyst **35** was obtained.

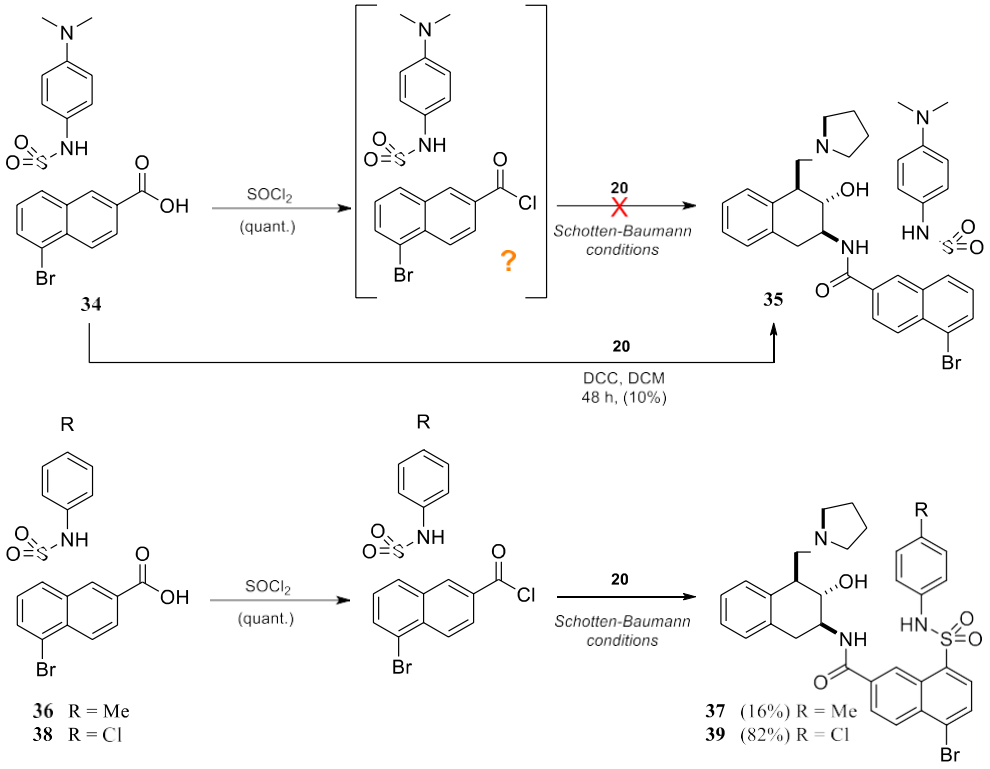

Figure 153. *Synthesis of catalysts* **35**, **37** *and* **39**.

Acid chlorides of **36** and **37** were obtained using $SOCl_2$, and subsequent reaction with amine **20** was carried out under Schotten-Baumann conditions. Good yields of catalyst **37** and **39** could be obtained using these conditions.

^{1}H NMR spectra showed the expected triplet of H–2 at 4.21, 4.26 and 4.32 ppm for **35**, **37** and **39** respectively, as well as the large coupling constant corresponding to all-axial hydrogens in the cyclohexane ring.

Acylated catalysts **35a**, **37a** and **39a** were obtained by treating the corresponding catalyst with vinyl acetate as it was explained in the Experimental Section (page 225). ^{1}H NMR spectra showed the signal for the acetate at 2.18, 2.27 and 2.31 ppm, respectively, and the expected deshielding of H–2 from 4.21, 4.26 and 4.32 ppm to 5.47, 5.50 and 5.51 ppm. As the second NH set up a stronger hydrogen bond with the carbonyl oxygen of the acetate, the signals in the ^{1}H NMR spectra are deshielded according to the increased acidity. This result agrees with modelling studies, which place the second NH much closer to the carbonyl group of the acetate than in the case of the catalysts based on an isophthalic or a picolinic acid moiety.

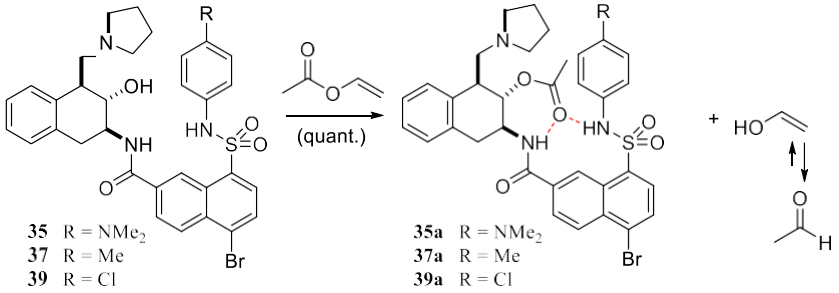

Figure 154. *Synthesis of acylated catalysts* **35a**, **37a** *and* **39a**.

***Kinetic studies for catalysts* 35, 37 *and* 39**

In the first experiment, the methanolysis reaction of catalyst **35a** was performed in neat deuterated methanol following the standard methodology applied before. However, the first ^{1}H NMR spectrum recorded just after dissolving compound **35a** in CD_3OD showed the reaction almost finished. This was also the case for **33a**, whose methanolysis is so fast that it is very difficult to record any spectrum before the reaction is finished at this concentration and temperature.

In order to reduce the reaction speed and being able to study the methanolysis reaction, a solution of 5% CD_3OD in $CDCl_3$ was employed in all the experiments. Also, instead of measuring absolute half-lives, this time competitive kinetics were run using **33a** as the reference. As the half-life for **33a** methanolysis has already been measured, competitive kinetics against **33a** should render more accurate data from which the absolute half-life for each catalyst can be estimated.

Following the standard methodology described in the Experimental Section (page 290), 10 mg *ca.* of the desired acetylated catalyst and *ca.* 10 mg of acetylated catalyst **33a** as reference were dissolved in 600 μL of a 5% CD_3OD in $CDCl_3$ solution and ^{1}H NMR spectra were recorded periodically at 20ºC. Despite the reduction in the total amount of deuterated methanol, *pseudo*-first order approximation was applied to study the reaction.

The results obtained in these experiments are very interesting. Catalyst **35**, bearing an aromatic NH, reacted 1.54 times faster than catalyst **33**, where the second NH is settled by an aliphatic amine. By comparing the results obtained with **35a**, **37a** and **39a**, the more acid the second NH is, the faster the reaction.

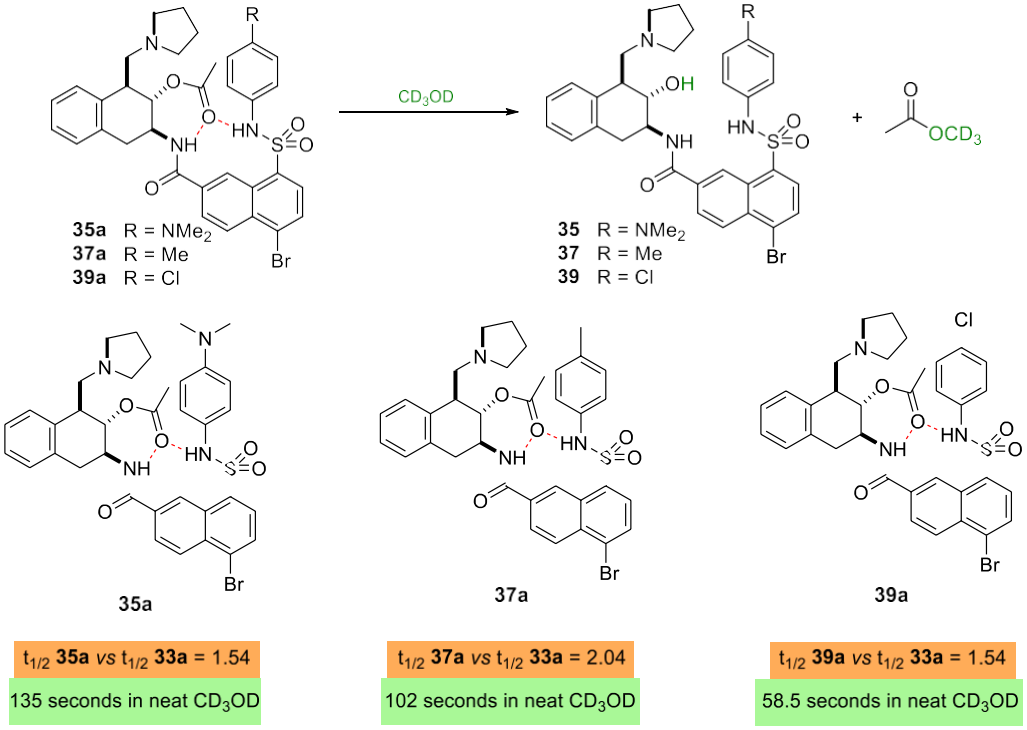

Figure 155. *Methanolysis studies of acylated catalysts* **35a**, **37a** *and* **39a**.

Thus, methanolysis of catalyst **37a** is 2.04 times faster than that of catalyst **33a**. If the aromatic ring has an electron-donating group, such as dimethylamine from catalyst **35**, either acyl-catalyst or tetrahedral intermediate are less stabilised than in catalyst **37**. Catalyst **39**, as opposed to catalyst **35**, has an electron-withdrawing group which stabilised better either the acyl-catalyst or the tetrahedral intermediate, so the reaction is 3.56 times faster than with catalyst **33a** and 1.75 times faster than with catalyst **37a**.

Structural studies of catalyst 35 – *Tetrahedral intermediate analogue* 35b

Following a similar strategy for crystallization as the methodology described for **29b**, 3-nitrophenylphosphonic acid dichloride was chosen to prepare a transition state mimic of the hydrolytic process. The reaction of this compound with the catalyst **35** afforded the transition state analogue **35b**, from which it was possible to obtained X-ray quality crystals. Hopefully, charge-transfer between the electron-rich dimethylamino and the electron-deficient nitro-aromatic ring should increase the possibilities of obtaining good crystals.

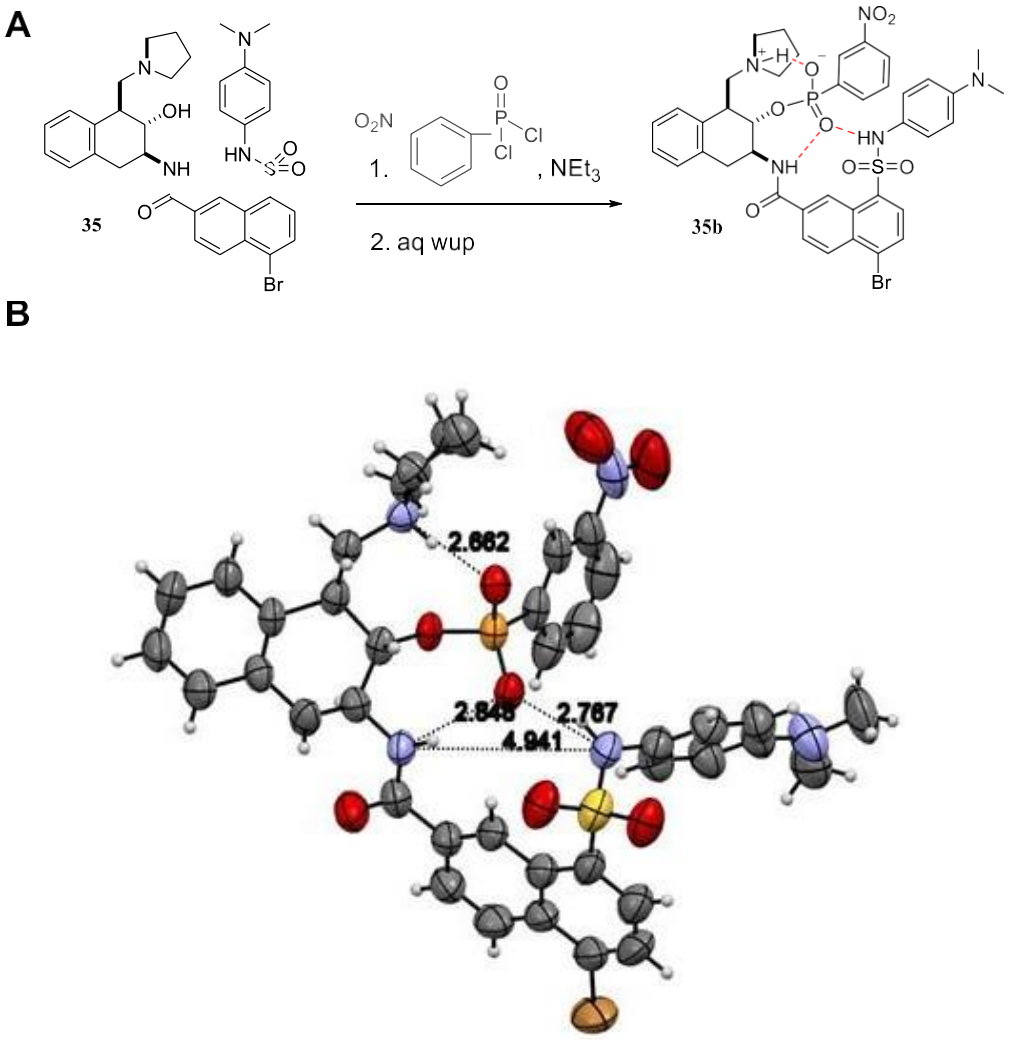

Figure 156. *(A) Reaction of compound* **35** *with 3-nitrophenylphosphonic acid chloride. (B) X-ray diffraction structure of compound* **35b**. *Selected distances between heteroatoms are depicted in angstroms (Å).*

The single-crystal X-ray diffraction analysis showed a perfect fit of the phosphonate group inside the oxyanion-hole of catalyst **35** (Figure 156). Many structural features of compound **35b** are similar to the X-ray structure of tetrahedral analogue **29b**: The shortest hydrogen bond with only 2.67 Å is set between the pyrrolidinium group and one of the phosphate oxygen atoms. Both the phosphoryl oxygens showed similar O−P distances of 1.49 Å, which can be explained with a negatively charged phosphonate group. Also, the similar distance established between the pyrrolidinium group with both the phosphonoester oxygens (3.15 Å) and the phosphoryl oxygen (2.66 Å) are the key factor to transport the proton from the nucleophile to the leaving group.

Nonetheless, the most interesting results are uncovered by the differences among picoline and 8-sulfonamide-2-naphthoic acid structures. The phosphoryl oxygen which mimics the negatively charged oxygen of the transition state establishes two hydrogen bonds of 2.85 and 2.77 Å with the 2-naphthoic aliphatic and aromatic NHs, respectively. Both hydrogen bonds are shorter than the distances showed for the same atoms in **29a** (2.89 Å and 3.13 Å).

The 8-sulfonamido-2-naphthoic acid oxyanion hole revealed a 4.94 Å distance between both NHs. Even though this distance is higher than in the tetrahedral analogue **29b**, the NH distance settled with the phosphoryl oxygen is shorter, which explains the increase in the reactivity.

The conclusions obtained from the X-ray structure of compound **35b** agree with the observations detected in ^{1}H NMR methanolysis studies, which revealed the deshielding of the oxyanion-hole NHs and the acetate signals upon acetylation of the catalyst. This implies that the acetate carbonyl group is hydrogen bonded by the oxyanion-hole in a similar way as the phosphonate group which mimics the reaction transition state.

3.4. Hydrogen bond network. Third generation organocatalysts

In the previous section the methanolysis reaction of acetate **39a** took place in only 10.7 minutes! using 5% CD_3OD in $CDCl_3$ solution. Extrapolation to neat deuterated methanol afforded 58.5 seconds.

According to the reaction rates of natural enzymes, this result could be improved up to 10^{10} acceleration in the rate constant. X-ray diffraction studies of the inhibited O-phosphonated-α-chymotrypsin (PDB: 1GCD) shows an interesting fact: the oxyanion hole, which stabilises the tetrahedral intermediate analogue with two linear NH groups from the enzyme backbone, is in turn stabilised by a second hydrogen bond network. These hydrogen bonds increase the strength of the hydrogen bonds formed between the oxygen of the tetrahedral intermediate mimics and the NHs of the oxyanion hole. This feature will be applied to our oxyanion-hole mimics where new hydrogen bond donor groups will be introduced in order to bond the carbonyl and sulfuryl bonds.

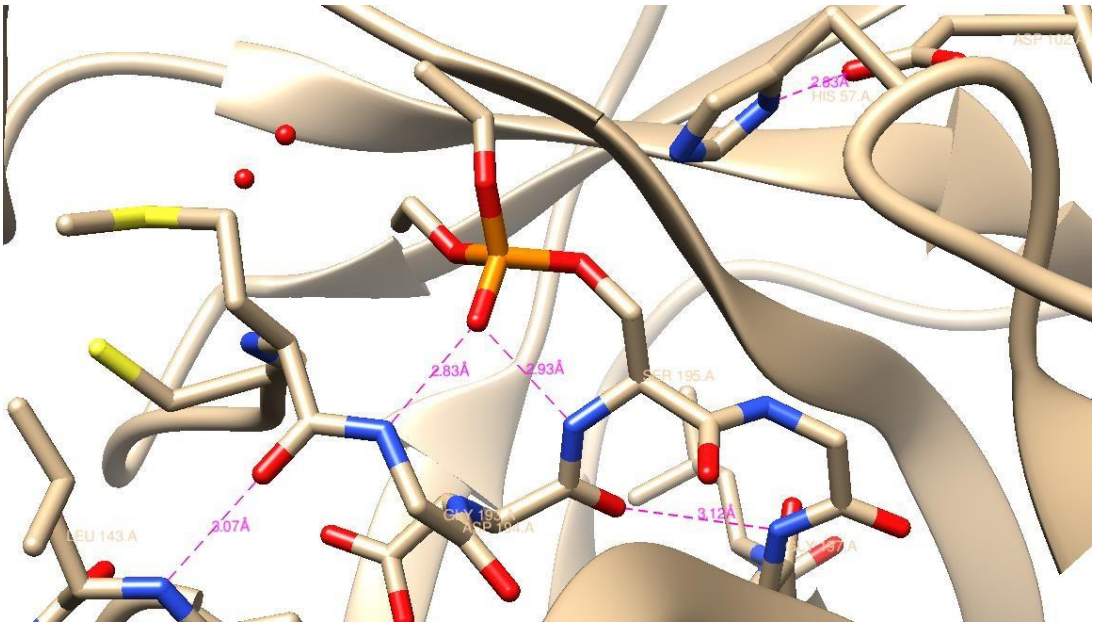

Figure 157. *X-ray structure of O-phosphonated-α-chymotrypsin (PDB: 1GCD), showing a second network of hydrogen bonds.*

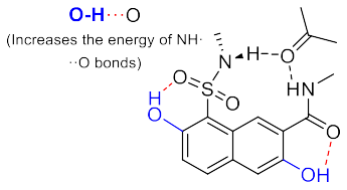

Figure 158. *Model of oxyanion-hole mimic bearing a 2nd hydrogen bond network.*

The use of an auxiliary hydrogen bond network has already been reported in the literature by Davis, Gale, Quesada and co-workes,[155] who studied the anion binding properties of two receptors based on isophthalic acid and dihydroxyisophthalic acid moieties. As it can be seen in Figure 159, the association constant between different anions and receptor **XXXI** is higher than K_{ass} with receptor **XXX** due to pre-organisation (the NHs are directed towards the cavity) and stronger hydrogen bonds settled between the anion and receptor **XXX**.

[155] Santacroce, P. V.; avis, J. T.; Light, M. E.; Gale, P. A.; Iglesias-Sánchez, J. C.; Prados, P.; Quesada, R. *J. Am. Chem. Soc.* **2007**, *129*, 1886 – 1887.

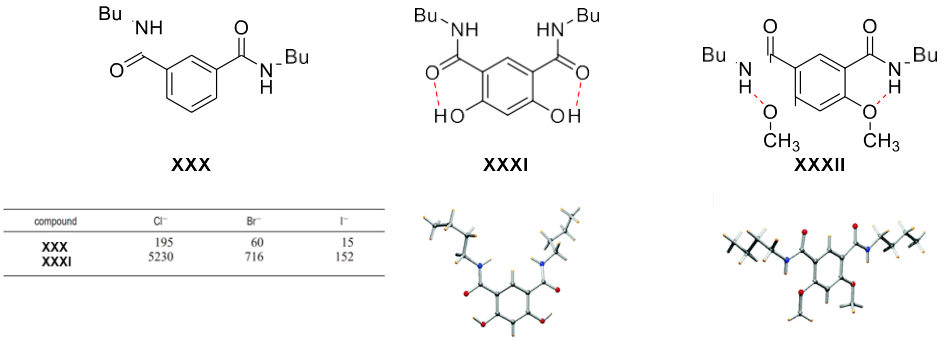

Figure 159. *Receptors* **XXX**, **XXXI** *and* **XXXII** *for anion transport across biological membranes, where receptor* **XXXI** *has two extra OH bonds which preorganised the structure and makes the NHs bond stronger.*[155]

In our experience, a competitive titration between receptor **XXXIII** and **XXXIV** with trioctylphosphine oxide as oxyanion hole mimic showed an increase up to 100 times in the competitive titration with trioctylphosphine (Figure 160).

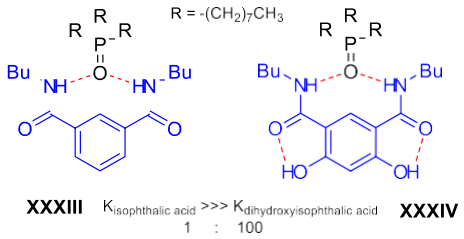

Figure 160. *Competitive titration between receptors* **XXXIII** *and* **XXXIV** *with trioctylphosphine oxide.*

Following this hypothesis, catalysts **44** and **48** in which the oxyanion-hole unit was decorated with one and two extra hydrogen bonds,respectively, able to establish a second hydrogen bond network, have been proposed.

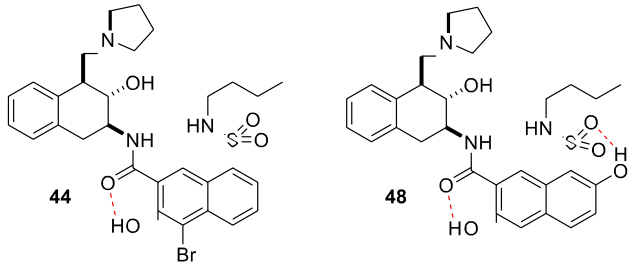

Figure 161. *Proposed catalysts* **44** *and* **48** *with a second hydrogen bond network configured by one and two extra H-bonds, respectively.*

Catalyst* 44 *and* 48 *syntheses

Oxyanion-hole mimic **43** was synthesized from commercially available 3-hydroxy-2-naphthoic acid (Figure 162). Before introducing the sulfonic acid in C–8, it is necessary to block C–8, because the most reactive position in an electrophilic aromatic substitution is *ortho* to the hydroxyl group (C–4). Our first proposal was the introduction of a bromine atom in C–**4.** Thus, bromination of 3-hydroxy-2-naphthoic acid with Br_2 in AcOH at reflux afforded the desired compound as a white solid after adding the reaction mixture over water. However, direct chlorosulfonation of 4-bromo-3-hydroxy-2-naphthoic acid in neat chlorosulfonic acid did not yield the expected compound, but the chlorosulfonation at C–5.

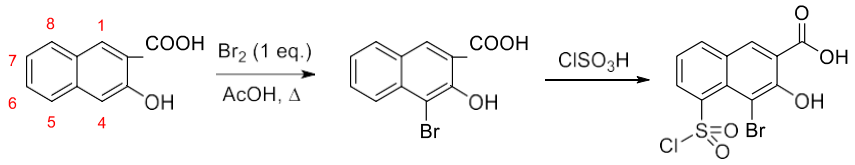

Figure 162. *Bromination of 3-hydroxy-2-naphthoic acid and subsequent chlorosulfonation.*

To overcome this issue, bromination of 3-hydroxy-2-naphthoic acid with an excess of Br_2 was carried out. The first bromine atom reacts in C–4 but, surprisingly, the second bromine atom reacts in C–7, yielding compound **40**. This fact was confirmed by ^{1}H NMR, where H–8 at 8.32 ppm appears as a doublet with a coupling constant of J = 2 Hz with H–6 in *meta* position.

Direct chlorosulfonation of compound **40** (Figure 163) did not provide the expected product. However, the preparation of the acid chloride *in situ* made the chlorosulfonation possible. Thus, compound **40** direct chlorosulfonation in neat chlorosulfonic acid was carried out in the presence of phosphorous pentachloride to facilitate the halogenation of the carboxylic acid. The bromine at C–7 favours the reaction in *ortho* and *para* positions, but C–8 is more reactive because it is *peri*. Under these conditions, compound **41** was obtained as a greenish solid after workup over ice.

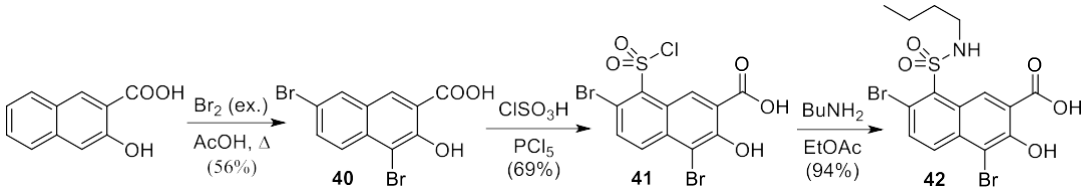

Figure 163. *Synthesis of compound* **40** *by double bromination of 3-hydroxy-2-naphthoic acid, chlorosulfonation to obtain compound* **41** *and synthesis of compound* **42**.

The aminolysis of compound **41** with butylamine in EtOAc afforded compound **42** in good yield after washing the organic phase with 2M HCl to get rid of the excess of butylamine.

Bromine atom at C–4 might not affect deeply the catalytic properties, even though it might make the intramolecular H-bond between the aromatic phenol with the amide carbonyl oxygen

slightly stronger. On the other hand, the bromine atom at C–7 might affect the conformation of the sulfonamide. To avoid these possible problems, reduction of both C–Br bonds was studied with different reducing reagents, such as Zn in AcOH and $SnCl_2$.

Surprisingly, compound **42** showed different reactivity with these two reagents: while $ZnCl_2$ reduced only the C–Br bond at C–4, Zn in AcOH reduced selectively the C–Br bond in C–7. The difference in reactivity can be explained according to the different electronic properties for both C–Br bonds. C–Br bond at C–4 is attached near to the aromatic OH which increases C–Br HOMO orbital energy, so its oxidative addition to Sn^{2+} is favoured instead of the electronic reduction by metal Zn. In contrast, C–Br bond at C–7 is attached near the electron-withdrawing sulfonamide which reduces C–Br LUMO orbital energy, so electronic reduction is favoured. In our case, the reaction was carried out with Zn in AcOH at 60ºC following a standard procedure previously developed in our research group.[156]

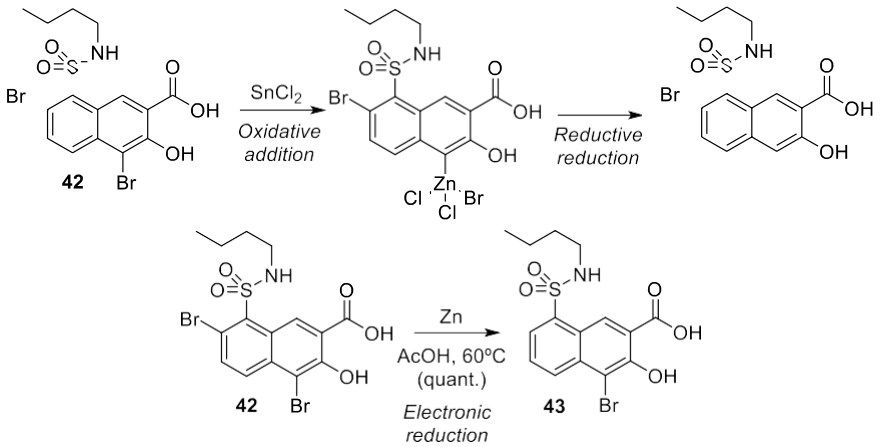

Figure 164. *Regioselective reduction of compound* **42** *using* $ZnCl_2$ *and Zn / AcOH.*

Further reduction of compound **43** could be carried out, but for the purpose of this study only C–Br bond at C–7 was removed. The reaction of acid **43** with $SOCl_2$ at reflux yielded the corresponding acid chloride quantitatively after removing the $SOCl_2$ under reduced pressure. Schotten-Baumann conditions were used for the coupling between compound **20** and the acid chloride of compound **43**. The organic phase was separated and distilled under low pressure. Catalyst **44** was purified by column chromatography over silica gel and activated with 5% NH_3 solution. ^{1}H NMR spectrum showed the expected triplet at 4.01 ppm with J = 10.0 Hz, and the double triplet at 4.37 ppm of the H–3 acylated with the oxyanion-hole unit.

[156] Gacho Temprano, A. Trabajo de Grado, **2016**, *Universidad de Salamanca*.

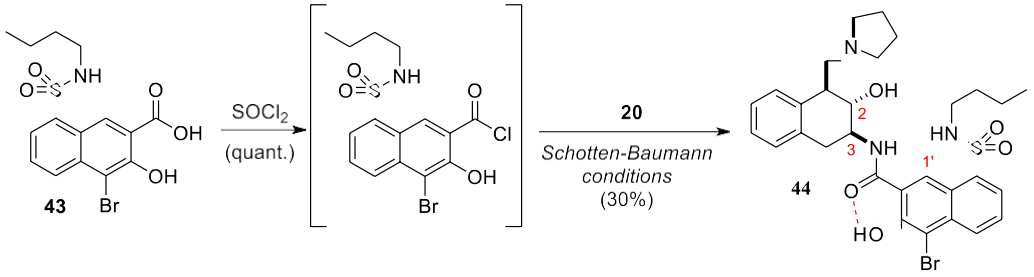

Figure 165. *Synthesis of catalyst* **44***.*

The synthesis of catalyst **48** began with non-expensive commercially available sodium 3-hydroxy-7-methoxy-2-naphthoate (Figure 166). This compound has an aromatic methoxy group at C–7, but demethylation has already been described using different methodologies.[157] First, this compound was suspended into DCM at 0ºC and neat chlorosulfonic acid was added carefully (the first reaction is the protonation of the carboxylate which is strongly exothermic). Once the reaction was completed, workup over ice gave compound **45** as a greenish solid, and additional extraction of the aqueous phase with more DCM afforded an additional portion of compound **45**. Reaction of the sulfonyl chloride **45** with butylamine in ethyl acetate yielded the sulfonamide **46**.

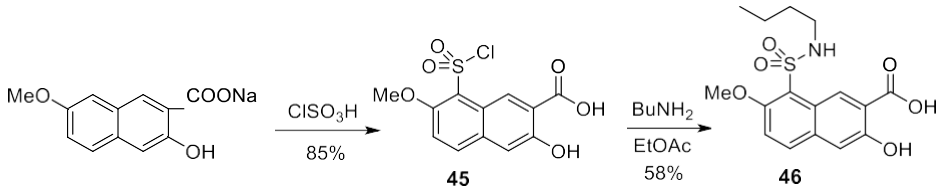

Figure 166. *Synthesis of chlorosulfonyl derivative* **45** *and sulfonamide* **46***.*

According to literature, methoxy groups could be transformed into the corresponding hydroxy groups with Na_2S in a Kraft-like process, in which lignine from wood was hydrolysed with Na_2S in basic conditions to produce wood pulp.[158] Direct demethylation of 3-hydroxy-7-methoxy-2-naphthoic acid could not be carried out using these conditions, so it was necessary the presence of the electron-withdrawing sulfonamide.

Compound **46** and $Na_2S{\cdot}9H_2O$ were dissolved in DMF and the reaction mixture was heated at 120ºC for 16 hours. The analysis by ^1H NMR of an aliquot of the reaction showed that the reaction had proceeded up to 50% conversion. The addition of more $Na_2S{\cdot}9H_2O$ and heating for another 16 hours was not enough to drive the reaction to completion. One explanation to this behaviour is the elimination of volatile H_2S generated by Na_2S with water. Since the H_2S

[157] Dong, S.; Herng, T.; Gopalakrishna, T.; Phan, H.; Lim, Z.; Hu, P.; Webster, R.; Ding, J.; Chi, C. *Angew. Chem. Int. Ed.* **2016**, *55*, 9316 – 9320.
[158] Kraft process: Gierer, J. *Wood Sci. Technol.* **1980**, *14*, 241 – 266.

is volatile it was removed from the reaction mixture under the reaction conditions, so according with Le Châtelier's principle, all Na_2S was removed. To avoid the removal of H_2S, the reaction was carried out in a closed reaction vessel. After 20 hours, the reaction was poured over an aqueous solution of 5% AcOH and compound **47** was obtained as a light brown solid.

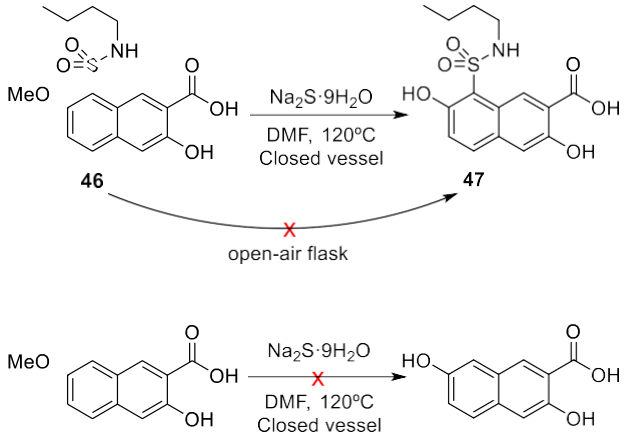

Figure 167. *Demethylation of compound* **46** *with* $Na_2S·9H_2O$ *(above) and attempts to direct demethylation of 3-hydroxy-7-methoxy-2-naphthoic acid.*

Catalyst **48** was synthesized according to the procedure described for catalyst **44**. Carboxylic acid **47** was activated with $SOCl_2$ and the acid chloride obtained was treated with amine **20** under Schotten-Baumann conditions. The crude reaction mixture was purified over silica gel and activated with 5% NH_3 to obtain catalyst **48**. ^{1}H NMR signals matched with the desired compound (H–2 at 4.00 ppm and H–3 at 4.33 ppm).

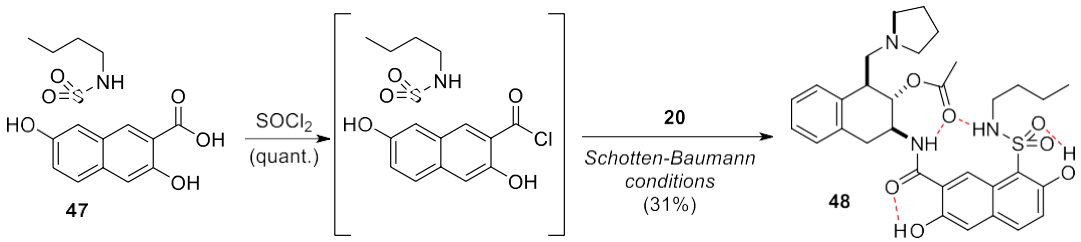

Figure 168. *Synthesis of catalyst* **48**.

Acylated catalysts **44a** and **48a** were obtained by treating the corresponding catalysts with vinyl acetate as it is explained in the Experimental Section. ^{1}H NMR spectra showed the signal for the acetate at 2.19 ppm in both compounds, and the expected deshielding of H–2 from 4.01 and 4.00 ppm to 5.53 and 5.45 ppm, respectively.

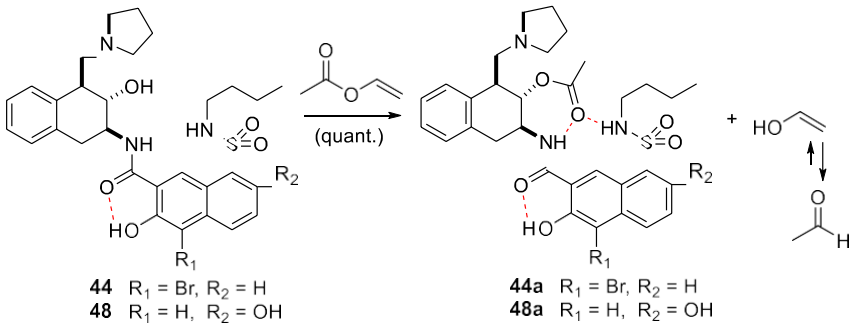

Figure 169. *Synthesis of acylated catalysts* **44a** *and* **48a**.

Kinetic studies for catalysts 44 *and* 48

Following the procedure described for catalysts **35**, **37** and **39**, the methanolysis reaction of **44a** and **48a** was studied with a 5% CD_3OD in $CDCl_3$ solution, according to the standard procedure described in the Experimental Section (page 290). *ca.* 10 mg of the desired acetylated catalyst and *ca.* 10 mg of acetylated catalyst **33a** as reference were dissolved into 600 μL of a 5% CD_3OD in $CDCl_3$ solution and ^1H NMR spectra were recorded periodically at 20ºC.

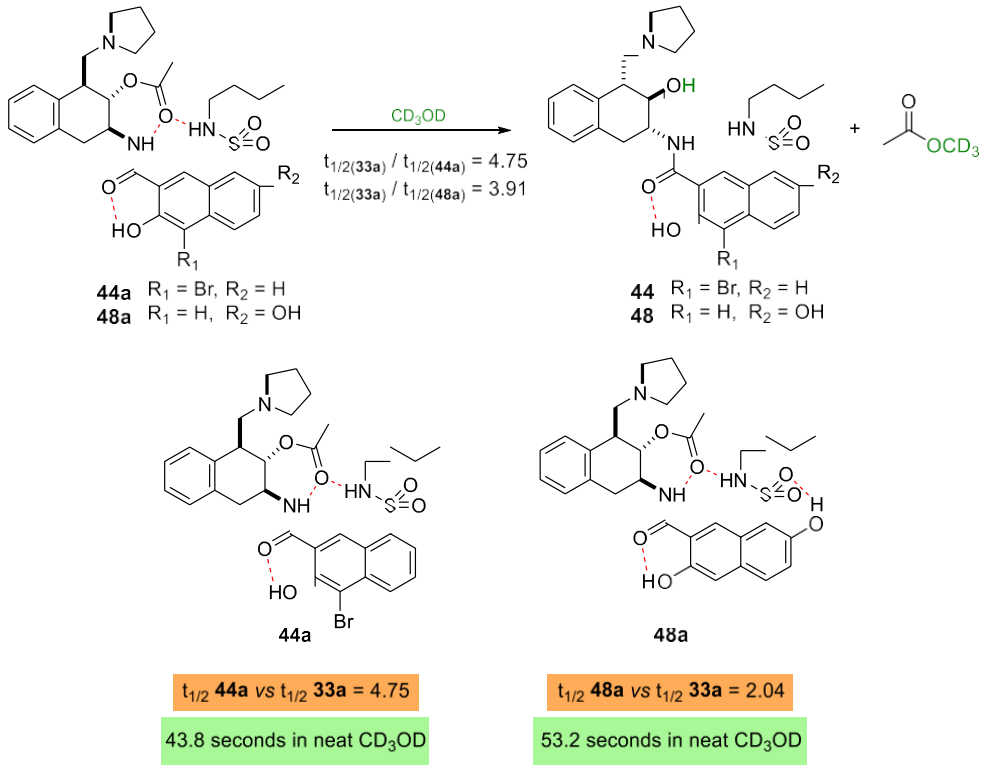

Figure 170. *Methanolysis studies of acylated catalysts* **44a** *and* **48a**.

The results showed that the methanolysis of catalyst **44a** was 4.75 times faster than that of catalyst **33a**. The introduction of one extra hydrogen bond between the oxygen of the carboxamide and the OH improved the catalytic properties. Strikingly, the presence of two OH···O bonds in catalyst **48a** improved only 3.91 times the methanolysis reaction rate. Probably, the electronegative bromine atom attached in C–4, makes a stronger hydrogen bond in catalyst **44**.

Anyway, both results are better than the reaction times obtained with the best first generation organocatalyst **39a**, where the second NH has a chlorophenyl group.

3.4.1. NH acidity studies. Catalysts 52, 56, 60 and 61

In order to test the influence of the acidity of the NH attached to the sulfonamide in the methanolysis reaction rate, catalysts **52**, **56** and **60** were synthesized (Figure 171). Also, catalyst **61** was prepared in order to test the effect of the OH at C–7 in the absence of Br in C–4 and compare it with catalyst **44**.

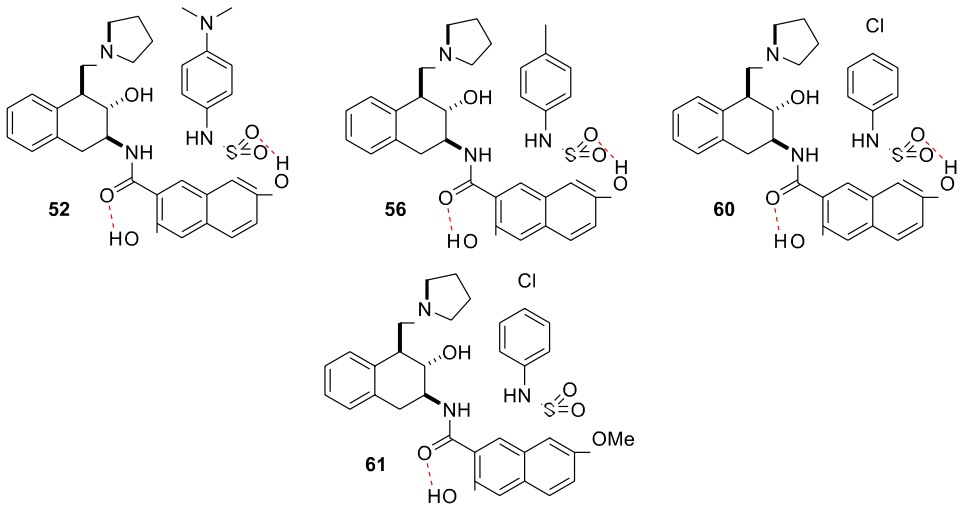

Figure 171. *Proposed catalysts* **52**, **56**, **60** *and* **61**.

Catalyst 52, 56, 60 *and* 61 *syntheses*

The synthesis of the oxyanion-hole mimics **50**, **54**, **57** and **58** was carried out by the reaction of chlorosulfonyl compound **45** and the corresponding amine. *N*,*N*-dimethylaniline was used as solvent and auxiliary base in the synthesis of compounds **53** and **57** since these amines are solids. Thereafter, demethylation was carried out following the procedure described above.

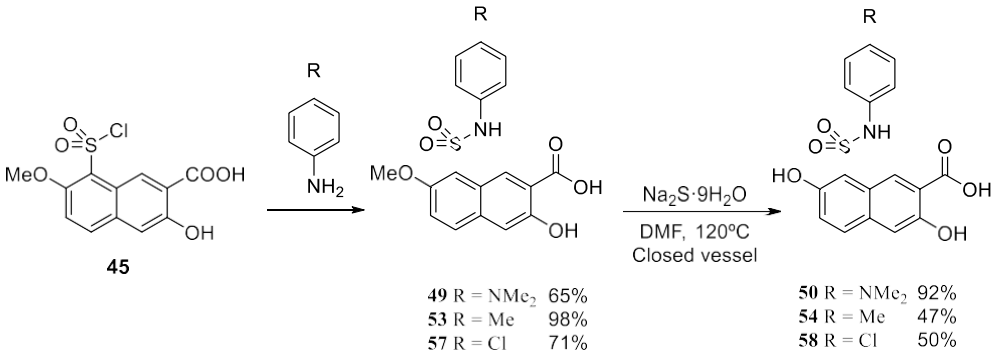

Figure 172. *Synthesis of oxyanion-hole mimics* **50**, **54**, **57** *and* **58**.

We first used compound **54** to optimise the reaction conditions of the coupling with amine **20**. Compound **54** acid chloride was obtained using $SOCl_2$ as described before, but the coupling with amine **20** under Schotten-Baumann conditions did not afford the desired catalyst **56.** Other conditions, such as EtOAc and an auxiliar base (TEA and *N*,*N*-dimethylaniline, among others), were attempted without positive results.

To confirm that the acid chloride obtained in the previous reaction was in good shape, it was dissolved in neat *n*-butylamine to afford the corresponding butylamide. The excess of butylamine was removed by low pressure distillation and the crude reaction product was washed with 2M HCl. The ^{1}H NMR spectrum confirmed the presence of the amide in good yield.

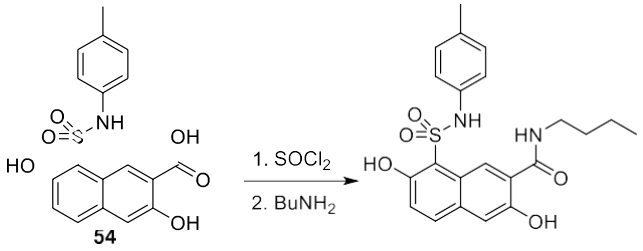

Figure 173. *Study of the amide synthesis in compound* **54**.

However, when the reaction was repeated using Schotten-Baumann conditions with one equivalent of butylamine, complicated mixtures were obtained. We concluded that the problem was not the reactivity of the amine but its consumption in other reactions, because using a large excess of the amine provided the desired product. We hypothesised an intermediate, showed in Figure 174, where the phenolic OHs react with $SOCl_2$ to explain the lack of reactivity with amine **20**.

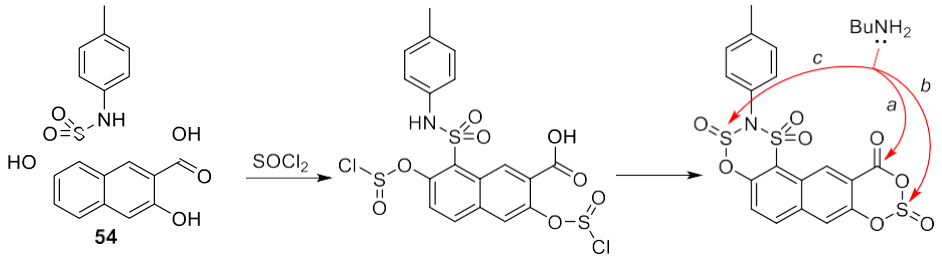

Figure 174. *Cyclic compound to explain the lack of reactivity in the carboxyl group.*

It is well known that $SOCl_2$ reacts violently with water and alcohols, so it would be expected that both aromatic OH groups react with $SOCl_2$ forming the corresponding chlorosulfites. These intermediates may react with the sulfonamide or the carboxylic acid to generate the respective cycles. While the use of a large excess of butylamine could allow to break the cycles and obtain the desired product, this would not be the case with just one equivalent of the amine.

To avoid this problem, aromatic OHs were protected as acetates. The reaction of compounds **50**, **54** and **58** with acetic anhydride and H_2SO_4 as catalyst provided the desired acetates at the phenolic positions, but one more acetate was observed in the ^{1}H NMR spectrum which corresponded to the sulfonamide NH acylation. Sometimes **51**, **55** and **59** acetyl mixed anhydride were obtained, and they were hydrolysed with MeOH in DCM. With all OHs and NH properly protected as acetates, the acid chloride was synthesized using standard conditions with either $SOCl_2$ or PCl_5, as shown in Figure 175.

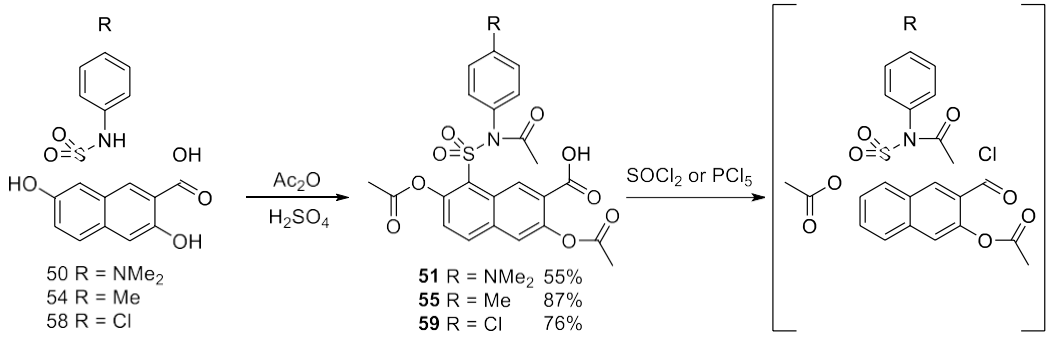

Figure 175. *Synthesis of compounds* **51**, **55** *and* **59** *and their acid chlorides.*

Then, acid chlorides of compounds **51**, **55** and **59** reacted with amine **20** in DCM, using *N*,*N*-dimethylaniline as auxiliary base to quench the hydrochloric acid generated in the reaction, yielding the corresponding amide. The last step was the hydrolysis of the 3 acetates with NaOH in MeOH. Catalysts **52**, **56** and **60** were obtained after work up with AcOH, solvent elimination, purification over silica gel and activating with 5% NH_3.

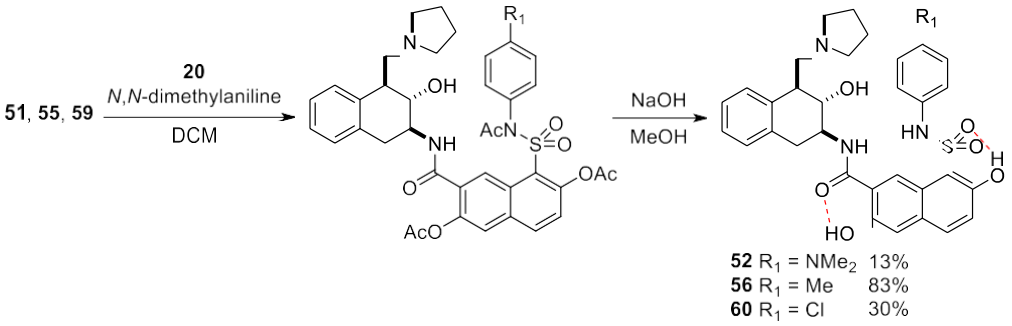

Figure 176. *Synthesis of catalysts* **52**, **56** *and* **60**.

In order to study the effect of the extra OH bond in C–7, catalyst **61** was prepared. after treating the acid **55** with $SOCl_2$ to obtain the acid chloride, and subsequent reaction with amine **20** under Schotten-Baumann conditions.

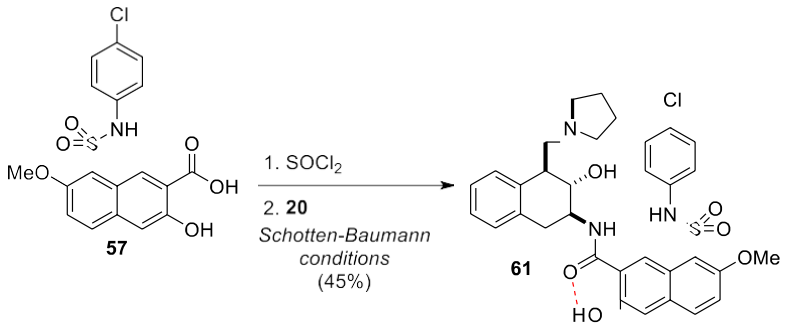

Figure 177. *Proposed catalyst* **61** *with only one extra OH bond.*

Table 3. *Chemical shifts of H-2 before and after acetylation of catalysts* **52**, **56**, **60** *and* **61**.

Entry	Compound	H-2 (OH) / ppm	H-2 (OAc) / ppm
1	**52**	4.16 – 4.02	5.66 – 5.52
2	**56**	4.38 – 4.26	6.04 – 5.76
3	**60**	4.15 – 4.07	6.36 – 6.26
4	**61**	4.30	5.55

Acylated catalysts **52a**, **56a**, **60a** and **61a** were obtained by treating the corresponding catalyst with vinyl acetate as it was explained before. ^{1}H NMR spectra showed the same behaviour observed with 2nd generation organocatalysts. The hydrogen bonding of the carbonyl group to more acidic NHs caused a more pronounced deshielding of the H–2 signal.

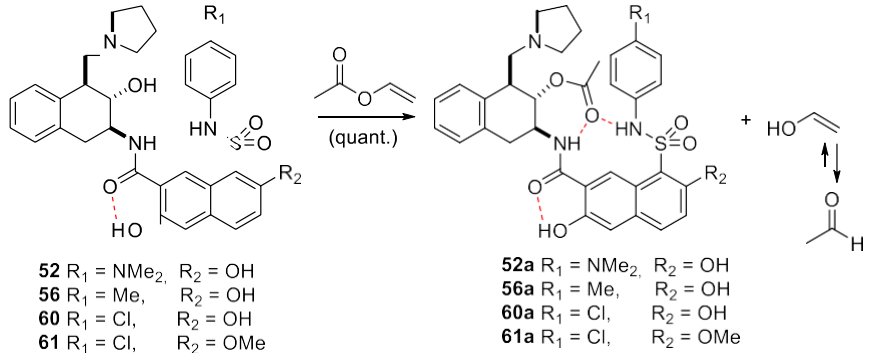

Figure 178. *Synthesis of acylated catalysts* **51a**, **54a**, **57a** *and* **58a**.

***Kinetic studies of catalysts* 52, 56, 60 *and* 61**

As in previous section, the methanolysis of **51a** **54a**, **57a** and **58a** was studied with a 5% CD_3OD in $CDCl_3$ solution, following the standard procedure described in the Experimental Section (page 290). *ca.* 10 mg of the desired acetylated catalyst and *ca.* 10 mg of acetylated catalyst **33a** as reference were dissolved into 600 μL of a 5% CD_3OD in $CDCl_3$ solution and ^1H NMR spectra were recorded periodically at 20ºC.

As it happened with catalyst 2nd generation, **56a** with an aromatic NH from the toluidine (weak electron-donating group), catalysed the reaction 7.97 times faster than **33a** and 2.04 times faster than **48a**, in which the second NH is substituted by an aliphatic amine. It can be observed how, the more acid the second NH is, the faster the reaction. Catalyst **52a** with the dimethylamino group (electron-donating group) increases the reactivity up to 6.99 times than catalyst **33a** but 1.14 times slower than **54a**. Catalyst **60** with the chloroaniline (electron-withdrawing group) improves the reaction up to 12.46 times than catalyst **33a** and 1.56 times than catalyst **56a**.

As expected, catalyst **61a** is worse than its homologous **60a**. Surprisingly, it is 1.72 times worse than **48a**, where the second one is settled by an aliphatic amine, and even 2.10 times worse than **44a**, in which there is only one extra OH bond. This can be explained due to the bromine electronegativity in compound **44a**, and the steric hindrance in catalyst **60a**.

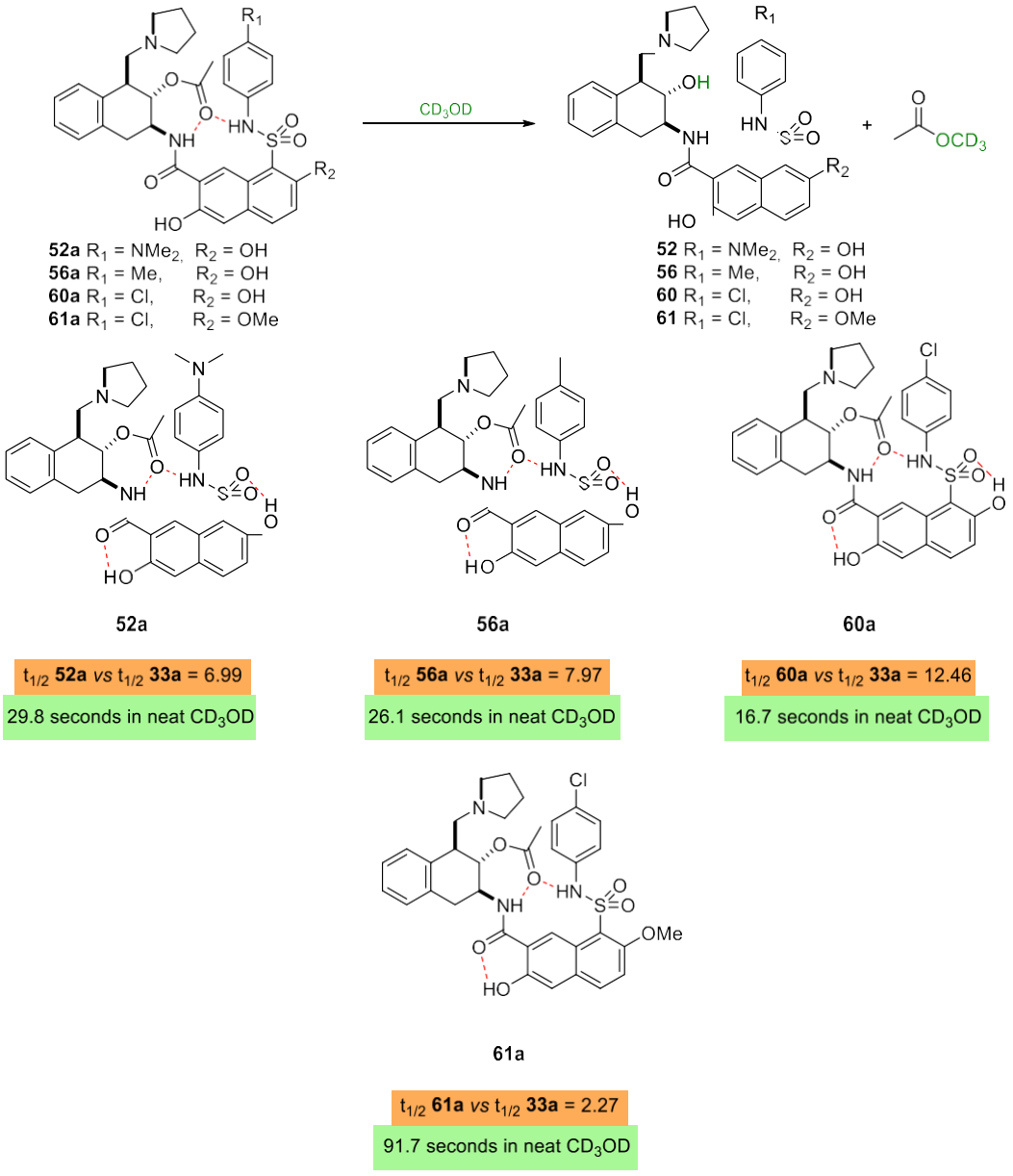

Figure 179. *Methanolysis studies of acylated catalysts* **52a**, **56a**, **60a** *and* **61a**.

SUMMARY – 2nd and 3rd Generation organocatalysts.

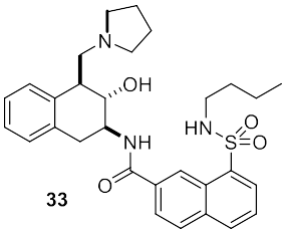

33

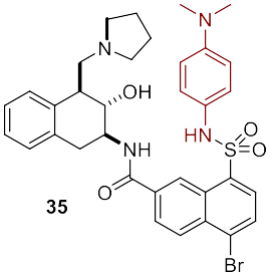

35

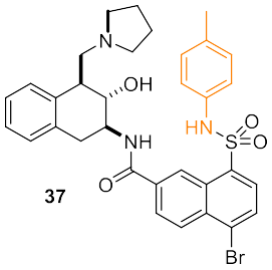

37

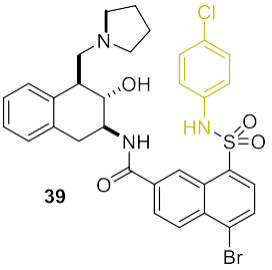

39

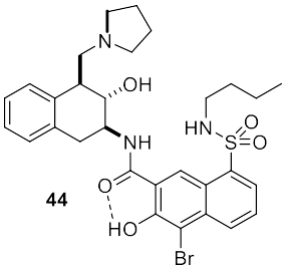

44

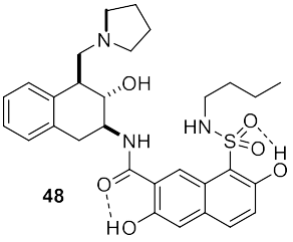

48

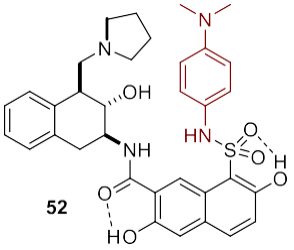

52

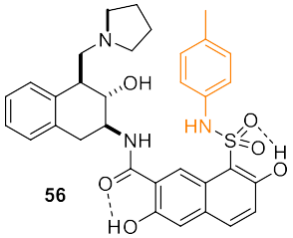

56

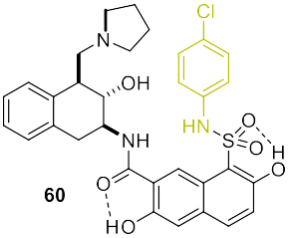

60

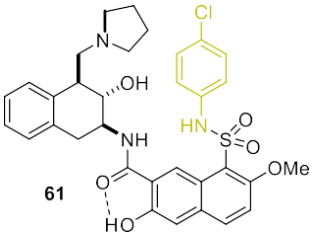

61

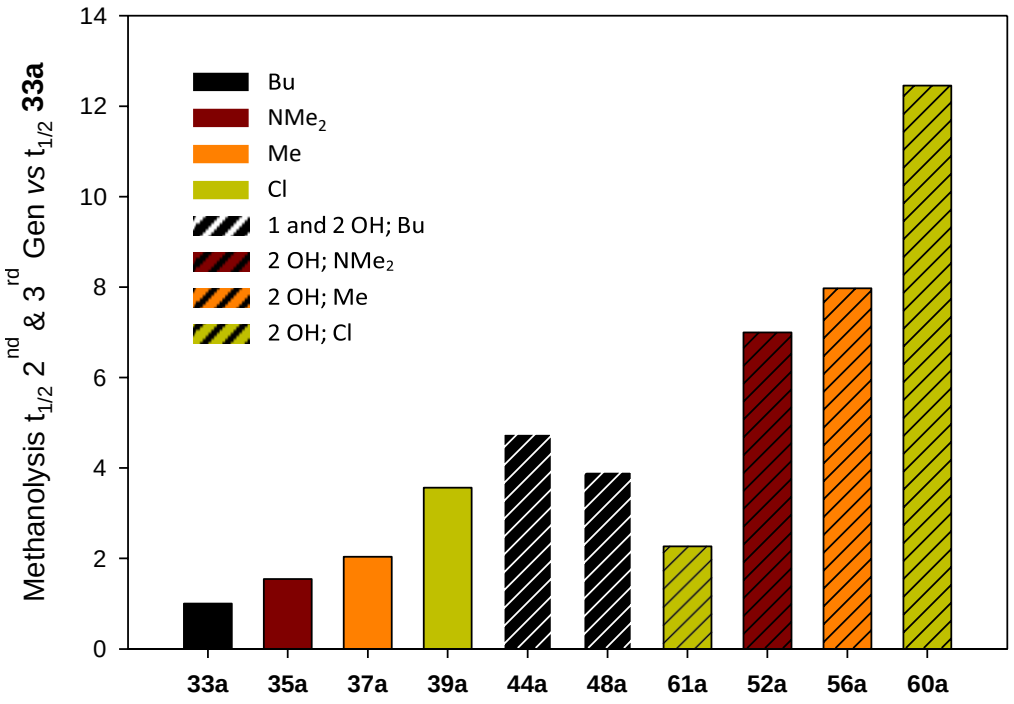

Figure 180. *Methanolysis studies for 2nd and 3rd generation catalysts (2nd & 3rd Gen).*

33a	1									
35a	1.54	1								
37a	2.04	1.32	1							
39a	3.56	2.31	1.75	1						
44a	4.75	3.08	2.33	1.33	1					
48a	3.92	2.54	1.92	1.10	0.82	1				
52a	6.99	4.53	3.43	1.96	1.47	1.79	1			
56a	7.97	5.17	3.91	2.24	1.68	2.04	1.14	1		
60a	12.45	8.07	6.11	3.50	2.62	3.18	1.78	1.56	1	
61a	2.27	1.47	1.11	0.64	0.48	0.58	0.32	0.28	0.18	1
	33a	**35a**	**37a**	**39a**	**44a**	**48a**	**52a**	**56a**	**60a**	**61a**

Figure 181. *Graph showing the increase in the reaction rate between the different 2nd and 3rd generation catalysts. For a correct understanding, the graph shows how much faster are the catalysts on the left versus the catalysts on the bottom.*

3.5. Kinetic studies for catalyst 5, 39 and 60

As the half-life of catalyst **33** in neat methanol was 3.47 min, a reaction rate acceleration of 12.46 for catalyst **60** means that the half-life should be 0.28 min. Considering that the half-life of uncatalyzed ethyl acetate hydrolysis in water is 150 years,[159] it can be calculated a reaction rate boost of $2.8 \cdot 10^8$, a value which is quite close to the 10^{10} acceleration factor found in chymotrypsin.[160]

Remarkably, while first generation catalysts required acetic anhydride for its acetylation, second and third generation catalysts were acetylated at room temperature by dissolving them in vinyl acetate for a few minutes.

More interestingly, second and third generation were acetylated using a non-activated ester as ethyl acetate. Although the reaction was sluggish at room temperature (Table 4), it could be accelerated by refluxing the solution.

Table 4. *Acetylation of catalyst* **29**, **39** *and* **60** *with ethyl acetate.*

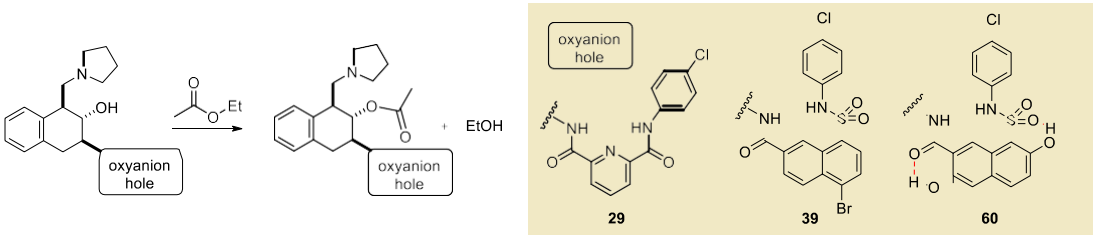

Entry	Catalyst	Conversion after 24 h at rt (%)[b]	Conversion after 30 min at 82ºC (%)[b]
1	**29**	Traces[a]	traces
2	**39**	30	28
3	**60**	17[a]	46

[a] The catalyst was not completely soluble in the reaction media. [a] The catalyst (0.1 mmol) was dissolved in EtOAc (0.05M) for 24 hours. Then it was heated at 82ºC in a closed vial for 30 minutes. Conversions were determined by ^{1}H NMR integration.

Also, second and third generation catalysts were able to catalyse the transesterification of ethyl acetate with methanol at room temperature. Although the conversion was low after 63 hours, it could be observed how catalyst **11** provided the best results, with a 3.6% conversion and 8.9 of turnover number.

[159] Kirby, A. J.; Hollfelder, F. From Enzyme Models to Model Enzymes. RSCPublishing: Cambridge, UK **2009**.
[160] Carter, P.; Wells, J. A. *Nature* **1988**, *332*, 564 – 568.

Table 5. *Transesterification of ethyl acetate with methanol catalysed by* **29**, **39** *and* **60**.

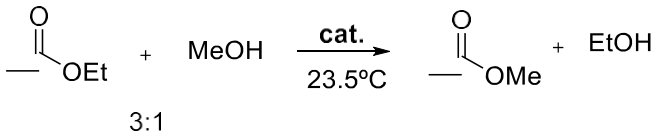

Entry	Catalyst	Conversion (%)[a]	TON
1	**29**	0.7	1.7
2	**39**	2.6	6.2
3	**60**	3.6	8.9

[a] Catalyst **12**, **5** and **11** (0.4 mol%, 0.025M) were dissolved in a 3:1 mixture of ethyl acetate/methanol. The reaction was left at 23.5 ºC for 63 hours. Conversion was determined by ^{1}H NMR integration. TON: Turnover number.

We believe that the presence of residual water in the reaction media hydrolysed EtOAc (catalysed by **39** or **60**) and generated AcOH, which protonated the catalyst pyrrolidine and inactivated them. Aqueous Na_2CO_3 addition to the reaction media to neutralise AcOH did not solve completely this problem, probably because it occupies the oxyanion-hole cavity.

3.6. Summary and conclusions for 2nd and 3rd generation catalysts (2nd & 3rd Gen.)

Modelling studies suggested that changing the piridinedicarboxylic acid oxyanion-hole mimic by a sulfonamide in 2-naphthoic acid C-8 would get the second NH closer to the carbonyl group. This prediction was confirmed experimentally in catalyst **33**. We believe that the free rotation of the C–S allows the sulfonamide to adapt the oxyanion hole to the guest size in the different reaction steps.

Pleasingly, increasing the second NH acidity allowed to increase the reaction rate (2nd generation catalysts). Also, the incorporation of a second hydrogen bond network which stabilizes the oxyanion hole carbonyl and sulfuryl oxygens boosted the half-life up to 16 seconds (catalyst **60**) in neat deuterated methanol (3rd generation catalysts).

While the 1st generation catalysts required acetic anhydride to get acetylated, 2nd and 3rd generation catalysts were acetylated with vinyl acetate at room temperature and ethyl acetate under reflux. 2nd and 3rd generation were also acetylated with non-activated ethyl acetate at room temperature but required longer reaction times.

Catalysts **39** and **60** were able to transesterificate non-activated ethyl acetate with methanol at room temperature but conversions are low. Anyway, results are remarkable, because, to the best of our knowledge this is the best time that a hydrolase mimic is able to catalyse the transesterification of a non-activated ester, at room temperature under neutral conditions.

3.7. Improve association constant. Oxyanion-hole models 64, 67 and 69

The catalysts developed in the last chapter, although they have shown a good catalytic performance, still lack a good association constant for the substrate. The association constant between catalyst **56** and ethyl acetate in $CDCl_3$ could not be measured by ^1H NMR titration. ^1H NMR of catalyst **56** showed broad signals which did not sharp even after the addition of three equivalents of EtOAc. We believe that a kind of dimer causes the broad signals as the addition of AcOH or tetraethylammonium chloride (TEAC) transforms the broad signals into sharp signals (Figure 182).

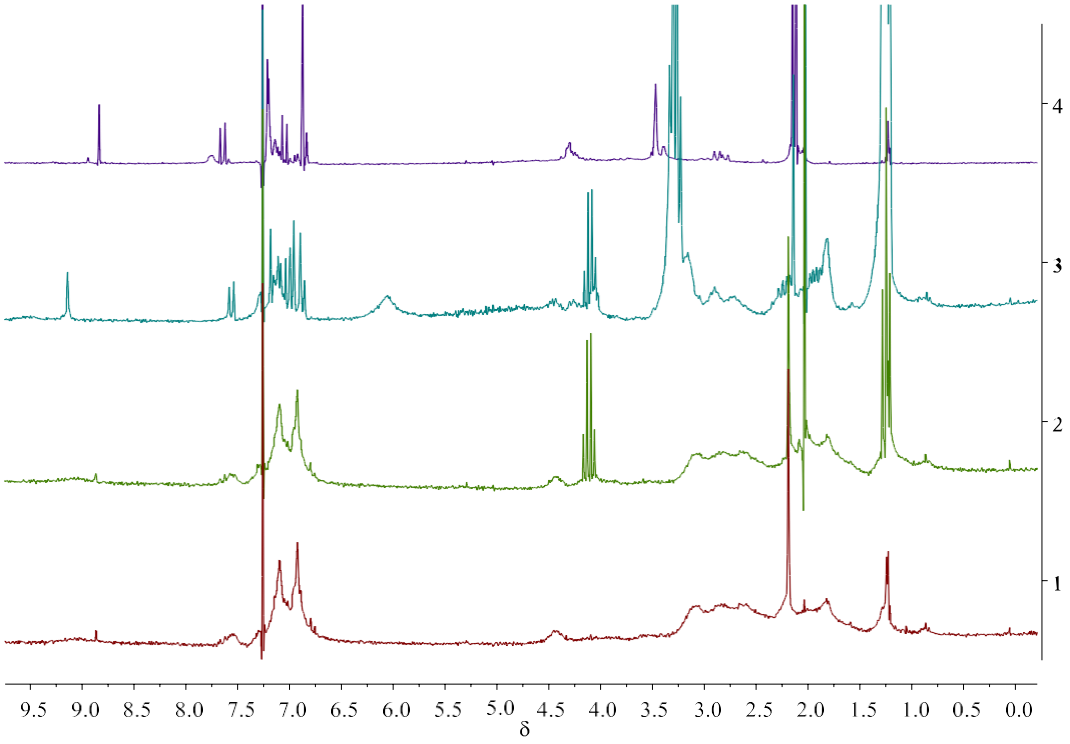

Figure 182. *Catalyst* **56** *^1H NMR spectra (9.5 –0.0 ppm) before (1) and after the addition of EtOAc (2), EtOAc and TEAC (3) and AcOH (4).*

In our opinion, increasing the association constant between the ester and the catalyst should break the putative dimer and be the boost that our synthetic hydrolase needs to compete with natural hydrolases. By forming a strong associate between the catalyst and the ester, the entropy of the reaction is reduced and the attack of the hydroxyl group to the ester carbonyl group should be facilitated.

In order to test our hypothesis, we decided to synthesise as series of oxyanion-hole mimics based on the 8-sulfonamido-2-naphthoic acid skeleton which had shown good results in the previous chapter and include electron rich aromatic amines in their structure. These groups should stablish π-π stacking interactions with aromatic esters decorated with electron

withdrawing groups. In fact, if the complementarity between the receptor and the ester is good enough, charge-transfer complexes should be visible with the naked eye.

By comparing these new oxyanion-hole mimics with the receptors synthesised in the previous chapter, we should be able to test the influence of the π-π stacking interactions in the reaction rate and confirm if a better association constant between the catalyst and the substrate is able to increase the reaction rate.

One of the advantages of the oxyanion-hole mimic receptor based on the 2-naphtoic acid skeleton with a sulfonamide in C–8 is that the cleft is dynamic, and the NH provided by the sulfonamide can adapt to the size of the guest because there is some free rotation around the C–S bond. This contrast with receptors in which the C–8 is decorated with an amide. In this case, the cleft tends to have a planar conformation because in this way all the groups are stabilised by resonance.

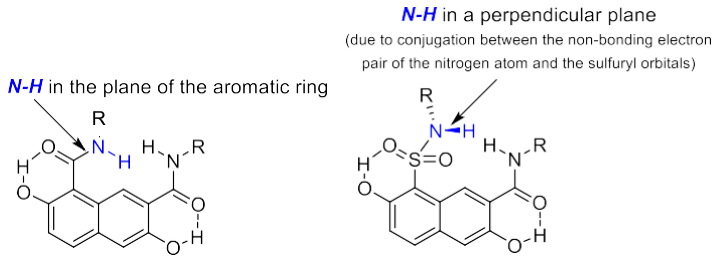

Figure 183. *Oxyanion-hole based on 8-sulfonamido-2-naphthoic acid.*

As it was shown in the previous chapter, the OH groups in C–3 and C–7 stablish two intramolecular hydrogen bonds with the carboxamide in C–2 and sulfonamide in C–8 in the right conformation to direct the NHs towards the cleft. Also, these hydrogen bonds become stronger when a negatively charged oxygen (such as the carbonyl oxygen in the transition state) is associated by the cleft. This negatively charged oxygen will stablish a stronger hydrogen bond with the carboxamide and sulfonamide NHs, leaving a partially negative carboxamide and sulfonamide carbonyl groups, which will also strength the phenolic OH bonds. In this way, four hydrogen bonds (two intramolecular and two intermolecular with the guest) should become stronger in the transition state, reducing in this way the activation energy of the reaction.

3.7.1. Receptor 64

We started our study with the synthesis of receptor **64** (Figure 184). Direct chlorosulfonation of 3,7-hydroxy-2-naphthoic acid with excess of chlorosulfonic acid in dichloromethane yielded compound **62** in good yield. Then, it was reacted with bis(trifluoromethyl)aniline to generate sulfonamide **63**. This amine is often used to increase the acid character of NHs, which should favour the formation of a strong associate. Next, *p*-

dimethylamino aniline was coupled with the carboxylic acid at C–2, yielding receptor **64** in good yield. We expected that this electron-rich amine could increase the association constant with the electron-deficient aromatic guest by additional stabilization *via* charge-transfer interactions.

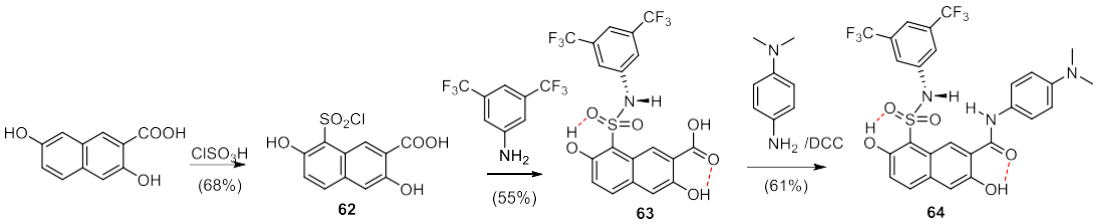

Figure 184. *Synthesis of receptor* **64**.

Pleasingly, X-ray quality crystals of receptor **64** were obtained by slow evaporation from methanol. The obtention of X-ray crystals is very important because it allow us to know if the receptor fulfil the geometric requirements necessary to associate the guest.

The X-ray structure of receptor **64** shows a molecule of methanol forming two hydrogen bonds of 2.83 Å and 2.87 Å with the NHs that constitute the oxyanion hole of the receptor. The size of the oxyanion hole (4.73 Å) is close to the average oxyanion-hole distance found in many hydrolases.[151] As expected, two short intramolecular hydrogen bonds were observed between the phenolic OH in C–2 and the carboxamide (2.55 Å) and between the phenolic OH in C–7 and the sulfonamide (2.59 Å).

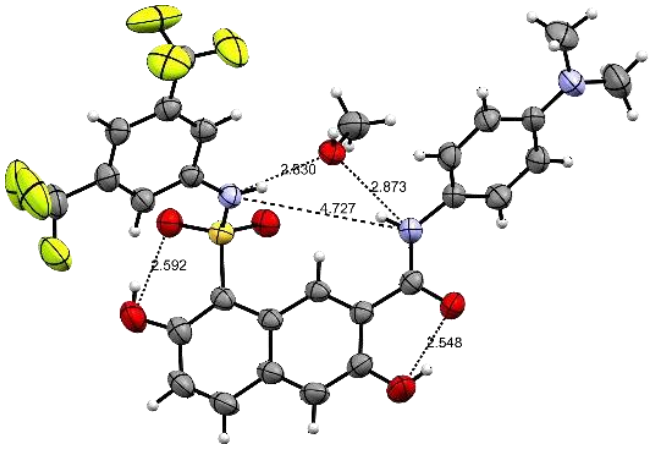

Figure 185. *Crystal structure of the complex between receptor* **64** *and methanol. Selected distances between heavy atoms [Å]: intramolecular H-bonds: 2.592(4) and 2.548(4); width oxyanion hole NH-NH: 4.727(4); intermolecular H-bonds with methanol: 2.830(4) and 2.873(4).*

Then, the ability of receptor **64** to associate carbonyl groups and alcohols was studied. Electron-deficient aromatic guests such as methyl 3,5-dinitrobenzoate, 3,5-dinitrobenzyl alcohol and 3,5-dinitrobenzamide were chosen. However, neither of them were able to significantly shift the receptor protons even after the addition of 6 equivalents of the guest. In order to understand this surprising lack of binding, modelling studies were performed (Figure 186). According to the calculations, the receptor stablishes a strong dimer stabilised by up to 4 intermolecular hydrogen bonds, with one of the sulfonamide oxygens of one molecule setting two strong hydrogen bonds with the NHs of another molecule of the receptor.

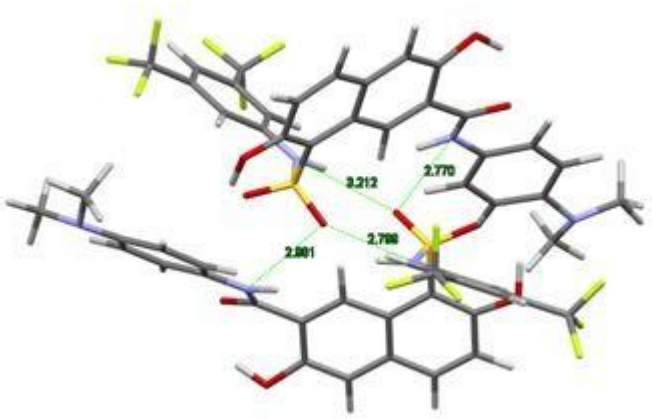

Figure 186. *DFT optimized (HF) structure for dimer of receptor* **64**.

To confirm the formation of a dimer, ^{1}H NMR titration was performed and showed a dimerization constant of 15 M^{-1} in $CDCl_3$.

3.7.2. Receptor 67

To avoid this problem, bis(trifluoromethyl)aniline was substituted by 1-naphthylamine. This aniline provides a less acidic NH, which should disfavour the formation of a strong dimer. Also, the presence of a larger aromatic sheet may favour the formation of π-π stacking interactions with the guest while providing steric bulk and a conformational rigid compound. In addition, 2-amino-6-methylpyridine, widely used by Hamilton[161] and Diederich,[162] was

[161] (a) Chang, S.-K.; Hamilton, A. D. *J. Am. Chem. Soc.* **1988**, *110*, 1318 – 1319. (b) García-Tellado, F.; Goswami, S.; Chang, S.-K.; Geib, S. J.; Hamilton, A. D. *J. Am. Chem. Soc.* **1990**, *112*, 7393 – 7394.
[162] (a) Lustenberger, P.; Martinborough, E.; Denti, T. M.; Diederich, F. *J. Chem. Soc. Perkin Trans. 2* **1998**, 747 – 762. (b) Cuntze, J.; Diederich, F. *Helv. Chim. Acta* **1997**, *80*, 897 – 911. (c) Owens, L.; Thilgen, C.; Knobler, C.; Diederich, F. *Helv. Chim. Acta* **1993**, *76*, 2757 – 2774. (d) Montero, V. A.; Tomlinson, L.; Houk, K. N.; Diederich, F. *Tetrahedron Lett.* **1991**, *32*, 5309 – 5312.

attached to the carboxylic acid in order to increase the number of hydrogen bonds with the guest and facilitate its association.

The synthesis of this receptor initially followed the same methodology employed for receptor **64**. However, the coupling between the carboxylic acid and 2-amino-6-methylpyridine failed under the reaction conditions employed before (DCC). HBTU also failed to provide the desired receptor and it was not possible to prepare the acid chloride, either with $COCl_2$, $SOCl_2$ or PCl_5.

Thus, the synthetic route was modified (Figure 187). First, 2,7-hidroxynaphtoic acid was esterified in methanol under Fischer conditions to yield the ester, which was chlorosulfonated following the reaction conditions employed for the synthesis of receptor **64**. The introduction of the 1-naphthylamine took place in good yield. Finally, the aminolysis of the ester with the anion of 2-amino-6-methylpyridine (generated with BuLi in THF) afforded the desiredreceptor **67**.

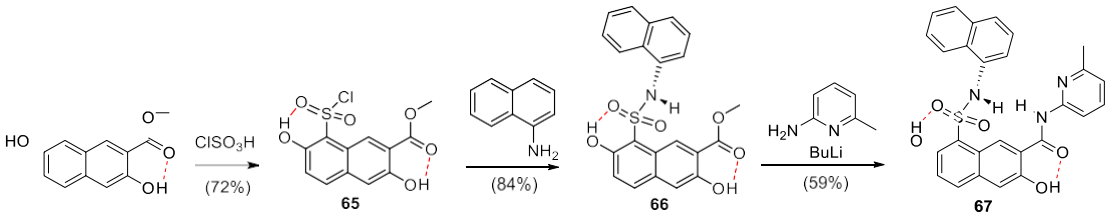

Figure 187. *Synthesis of receptor* **67**.

Again, it was possible to obtain X-ray quality crystals from 1% AcOH solution in MeOH (Figure 188). Surprisingly, the X-ray structure did not show a molecule of acetic acid in the cleft (which should be favoured in the presence of the pyridine ring) but a molecule of MeOH. It is also remarkably that the aminopyridine ring is rotated 180º respect to its previous position in receptor **64**, is such a way that the NH from the carboxamide acts as hydrogen bond donor (2.69 Å) towards the phenolic OH of C–3 instead of pointing to the interior of the cleft. The phenolic OH in C–7 keeps forming a short intramolecular hydrogen bond of 2.59 Å with one of the sulfonamide oxygens. The methanol molecule inside the cleft behaves as hydrogen bond donor with the carboxamide carbonyl group (2.68 Å) and hydrogen bond acceptor from the sulfonamide NH (2.90 Å).

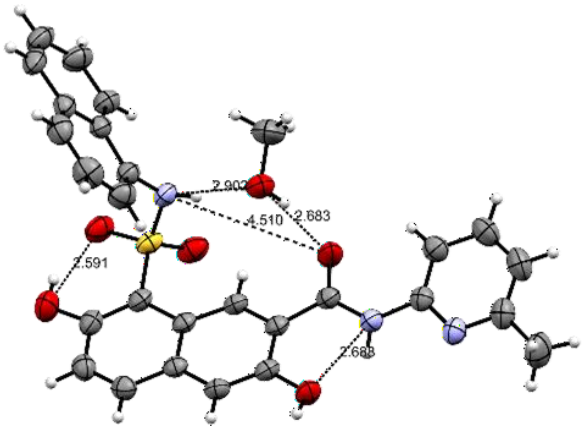

Figure 188. *Crystal structure of the complex between receptor* **67** *and methanol. Selected distances between heavy atoms [Å]: intramolecular H-bonds: 2.591(2) and 2.688(2); width oxyanion hole $NH_{sulfonamide}$-$CO_{carboxamide}$: 4.510(2); intermolecular H-bonds with methanol: 2.902(2) and 2.683(2).*

However, crystallization of receptor **67** from glacial acetic acid yielded the complex with a molecule of acetic acid inside the cleft (Figure 189). The carbonyl group of acetic acid stablishes two hydrogen bonds of 2.82 Å and 2.90 Å with the sulfonamide and carboxamide NHs, respectively. In this case, the phenolic OH in C–3 behaves as hydrogen bond donor and stablishes a short intramolecular hydrogen bond of 2.59 Å with the carboxamide carbonyl group, while the OH in C–7 forms an intramolecular hydrogen bond of 2.56 Å with one of the sulfonamide oxygen atoms. In this way, both NHs are directed towards the inner part of the cleft, forming an oxyanion hole of 5.08 Å, a bit wider than the oxyanion hole of receptor **64**. This is not surprising, as sp^2 oxygen is less basic than sp^3, and forms weaker and larger hydrogen bonds than the methanol oxygen.

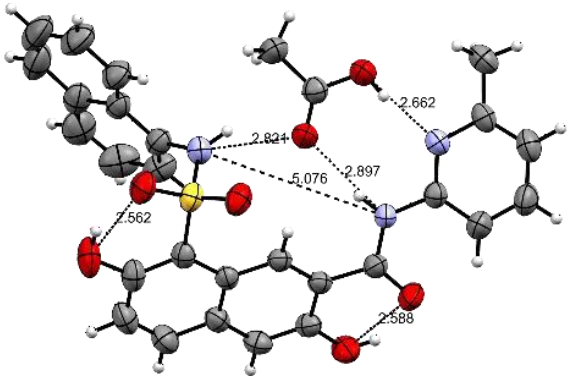

Figure 189. *Crystal structure of the complex between receptor* **67** *and acetic acid. Selected distances between heavy atoms [Å]: intramolecular H-bonds: 2.562(3) and 2.588(2); width oxyanion hole NH-NH: 5.076(2); intermolecular H-bonds with acetic acid: $NH_{sulfonamide}$ 2.821(2); $NH_{carboxamide}$ 2.897(2); $N_{pyridine}$ 2.662(2).*

Then, association constants between receptor **67** and different guests were measured by ^{1}H NMR titrations. Acetic acid showed a K_{ass} of $6.7 \cdot 10^3$ M^{-1} in $CDCl_3$ (at 20ºC), which is quite acceptable taking into account that single amidopyridine complexes possess association constants in the double digit range. Also, the geometry in solution seems similar to the geometry in the solid state. Addition of increasing amounts of acetic acid to a solution of receptor **67** in $CDCl_3$ caused the deshielding of H–1 from 9.13 ppm to 9.33 ppm (due to its proximity with the acetic acid carboxyl in the complex) as well as the deshielding of the pyridine protons. Also, the methyl group from acetic acid is shielded in the complex (it appears at 1.6 ppm) because is placed in the shielding cone of the naphtylamine aromatic ring, as it is also observed in the X-ray structure.

Unfortunately, no charge transfer complex was observed after titration of receptor **67** with electron-deficient 3,5-dinitro- and 2,4,6-trinitrobenzoic acids.

3.7.3. Receptor 69

At this point, a new design was considered. DFT calculations showed that the introduction of the 2-methyl-6-aminopyridine scaffold in the sulfonamide and a more flexible dimethylamino benzylamine fragment in the carboxamide should generate an oxyanion hole mimic prone to associate electron deficient aromatic benzoic acid while stablishing a charge transfer complex with the benzylamine aromatic ring (Figure 190).

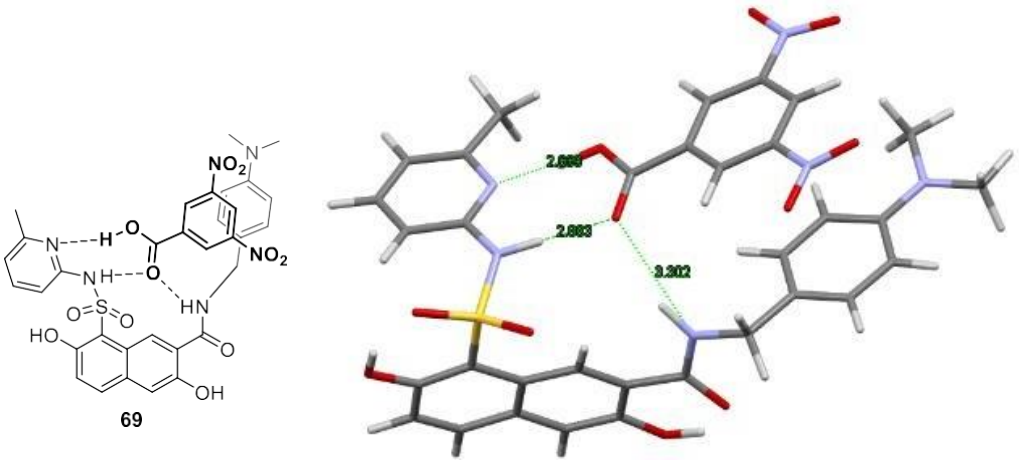

69

Figure 190. *DFT optimized (HF) structure for the associate between receptor* **69** *and 3,5-dinitrobenzoic acid, showing H-bonds and π–π interactions.*

The synthesis of this receptor followed the same methodology developed for receptor **67**. Starting from chlorosulfonated intermediate **65**, reaction with 2-amino-6-methylpyridine yielded compound **68**, which was aminolised with p-dimethylaminobenzylamine at 70ºC. Receptor **69** was obtained in good yield.

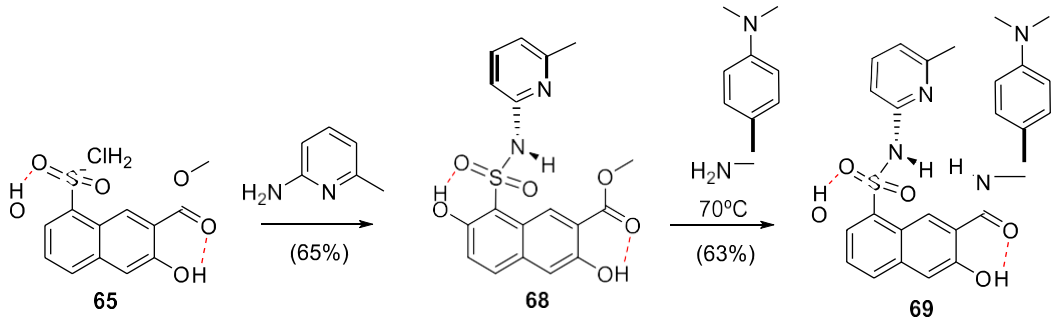

Figure 191. *Synthesis of receptor* **69**.

Dilution experiments performed with receptor **69** between $6.32 \cdot 10^{-2}$ M and $1.23 \cdot 10^{-4}$ M showed a dimerisation constant of 44 M^{-1}after ^{1}H NMR titration in $CDCl_3$. In spite of this fact, receptor **69** showed a good association constant for 3,5-dinitrobenzoic acid ($K_{ass} = 3.4 \cdot 10^4$ M^{-1}). The protons shifts corroborated the formation of the complex with the expected geometry: the protons of the dimethylbenzylamine ring shielded due to the proximity of the dinitrobenzoic acid ring and the pyridine protons were deshielded due to the association of the carboxylic acid. ROESY experiments confirmed the proximity between dinitrobenzoyl and the dimethylbenzylamine rings.

The contribution of the charge transfer complex to the association constant was confirmed with a ^{1}H NMR titration with benzoic acid. In this case, a $K_{ass} = 6.3 \cdot 10^2$ M^{-1} was obtained. However, the lower acidity of benzoic acid ($pK_a = 4.1$)[163] *versus* 3,5-dinitrobenzoic acid ($pK_a = 2.82$) could explain the low association constant obtained for benzoic acid.

A high association constant of $K_{ass} = 8.1 \cdot 10^4$ M^{-1} was obtained with 2,4,6-trinitrobenzoic acid as guest. Also, a red colour was observed after addition of the guest, which could be explained with the formation of a charge transfer complex. In fact, the absorbance spectrum of receptor **69** showed the appearance of a charge transfer band around 500 nm upon addition of 2,4,6-trinitrobenzoic acid.

[163] Jover, J.; Bosque, R.; Sales, J. *QSAR Comb. Sci.* **2008**, *27*, 563 – 581.

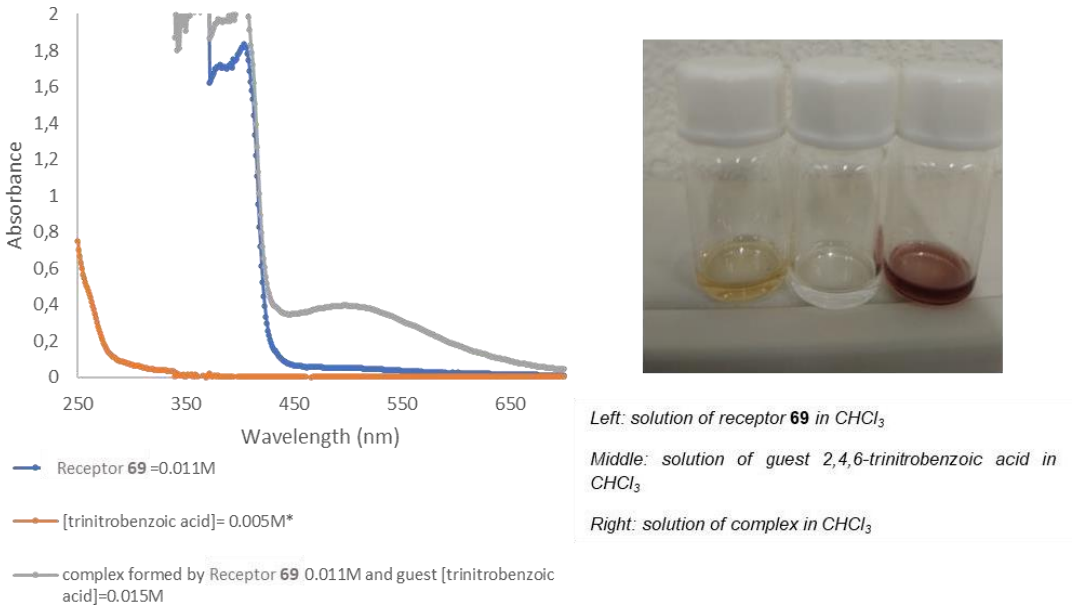

Figure 192. *(Left) Absorbance spectrum of the receptor* **69***, 2,4,6-trinitrobenzoic acid and the complex formed between them. (Right) Vials containing a solution of receptor* **69***, 2,4,6-trinitrobenzoic acid and the complex between receptor* **69** *and 2,4,6-trinitrobenzoic acid in* $CDCl_3$.

Then we considered other electron deficient aromatic compounds as guests lacking the benzoic acid functional groups. We hypothesised that the combination of the hydrogen bonds provided by the oxyanion hole and the charge transfer complex formation with the electron-rich benzylamine should be enough to associate the guest.

First titration with methyl 3,5-dinitrobenzoate showed very small shifts for the protons of the receptor upon addition of increasing amounts of the guest. Instead, 3,5-dinitrobenzyl alcohol showed a stronger charge transfer complex, and an association constant of K_{ass} = 23 M^{-1} could be measured. More basic 3,5-dinitrobenzamide provided a stronger association constant of K_{ass} = 298 M^{-1}. This guest is able to form up to three hydrogen bonds with the receptor, increasing in this way the extent of the association when compared with the corresponding alcohol and ester.

In the case of both the 3,5-dinitrobenzyl alcohol and 3,5-dinitrobenzamide it is observed the deshielding of the NHs and the pyridine signals as well as the shielding of the dimethylbenzylamine protons due to the proximity of the dinitrobenzoyl aromatic ring.

These results are summarised in Table 6.

Table 6. *Binding constants determined from NMR titrations in $CDCl_3$ at 20ºC.*

Entry	Receptor	Guest	logK_{ass}
1	**64**	[a]	1.18
2	**67**	acetic acid	3.83 ± 0.03
3	**69**	[a]	1.64
4	**69**	3,5-dinitrobenzoic acid	4.53 ± 0.14
5	**69**	benzoic acid	2.79 ± 0.02
6	**69**	2,4,6-trinitrobenzoic acid	4.91 ± 0.40
7	**69**	3,5-dinitrobenzyl alcohol	1.36 ± 0.02
8	**69**	3,5-dinitrobenzamide	2.47 ± 0.01

[a] Self-association constants through dilution experiments.

3.7.4. Summary and conclusions for oxyanion-hole mimics 64, 67 and 69

These results show that these kinds of receptors have a great tendency to form dimers, and probably this fact is preventing the acylation of the hydrolase mimics developed in the previous chapter to happen at higher speed.

As a future plan, in order to increase the acylation reaction rate, it would be necessary to design new receptors which avoid the formation of dimers.

Chapter 2 –Conclusions

4. Conclusions

The following conclusions are extracted from this chapter:

- First, second and third generation of organocatalysts were synthesised and fully characterised.

- Modelling studies for different geometries between the functional groups were performed to find the best catalyst candidates.

- Kinetic studies of the methanolysis reaction with first generation acetylated catalysts showed:

  - A rigid skeleton based on a tetrahydronaphthalene structure is required to provide fast reaction rates.

  - A separation of three carbon atoms between the dimethylamino and the OH groups was better than a separation of two carbon atoms.

  - Increasing the basicity of the amino group improved the reaction rates.

  - The presence of an oxyanion-hole mimic in the catalyst structure reduced the reaction half-life. The shorter the oxyanion hole, the faster the methanolysis was.

- Kinetic studies of the methanolysis reaction with second generation acetylated catalysts showed:

  - The incorporation of an 8-sulfonamide-2-naphthoic acid oxyanion-hole mimic into the catalysts structure improve the reaction rates. X-ray diffraction studies showed a shorter distance between the sulfonamide NH and the oxygen guest than in the case of the first generation catalysts.

  - Increasing the acidity of the second sulfonamide NH reduced the reaction half-life.

- Kinetic studies of the methanolysis reaction with third generation acetylated catalysts showed:

  - The presence of a secondary hydrogen bond network stabilised the negatively-charged oxygen generated in the methanolysis tetrahedral intermediate.

  - Reaction rates were increased up to $2.8 \cdot 10^8$ *versus* the non-catalysed ethyl acetate hydrolysis.

  - Catalyst **60** was able to promote the methanolysis of ethyl acetate at room temperature. To the best of our knowledge, this is the first time that a artificial hydrolase is able to catalyse the transesterification of a non-activated ester at room temperature under neutral conditions.

- Receptors **64**, **67** and **69** showed that the sulfonamide incorporation in the oxyanion-hole unit promotes the formation of dimers which hamper the substrate association.

Chapter 2 – Experimental Section

5. Experimental Section

5.1. Materials and instrumentation

Reagents

Reagents were purchased and used without further purification unless otherwise noted. The solvents used were purified and dried following the standard methods.[164]

Purification of reaction crudes

Reactions were monitored by analytical thin layer chromatography (TLC) using pre-coated aluminium-backed plates (0.2 mm silica gel 60 F_{254}, Merck®) and visualized by UV light (254 or 365 nm) or different stains such as $KMnO_4$, iodine or phosphomolybdic acid. Compounds purification was performed using silica gel column chromatography (Chromagel 60A SdS. C.C. 70-200 μm) with solvent mixtures with increasing polarity as eluents and crystallization in different solvent mixtures.

Melting Points (m.p.)

Melting points were measured in a Leica Galen III microscope and were reported in ºC.

IR spectroscopy

IR spectra were recorded using a Nicolet IR100 with NaCl crystals as films or with Nujol slurry for solids.

NMR spectroscopy

^1H and ^{13}C NMR spectra were recorded at room temperature using Bruker models WP-200-SY, Varian Mercury 200 MHz (200 MHz to ^1H and 50 MHz to ^{13}C) and Bruker Advance NEO 400 MHz with a Prodigy CPPBBO BB-H&F z-gradient cryo-probe (400 MHz to ^1H and 100 MHz to ^{13}C) spectrometers. Chemical shifts were reported in parts per million (ppm) to the nearest 0.01 ppm for ^1H and to the nearest 0.1 ppm for ^{13}C, with TMS or the solvent signal as an internal standard using reported shifts (^1H/^{13}C): deuterated chloroform $CDCl_3$ 7.26/77.2 ppm, dimethylsulfoxide DMSO-d_6 2.49/39.5 ppm or methanol CD_3OD-d_4 3.3/49.0 ppm and tetramethylsilane TMS 0.00 ppm.[165] Coupling constants (*J*) were reported in Hertz. The following abbreviations were used to explain the multiplicities: s, singlet; d, doublet; t, triplet; q, quartet; quin, quintet; sext, sextet; m, multiplet; br, broad.

Mass spectrometry

Mass spectra were recorded on a quadrupole-TOF Applied Biosystems QSTAR XL and Waters ZQ 4000 spectrometers using electrospray ionization (ESI) or electronic impact (EI).

---

[164] Armarego, W. L. F.; Perrin, D. D. Purification of Laboratory Chemicals; 3rd ed.; Pergamon Press: Oxford, **1988**.
[165] Gottlieb, H. E.; Kotlyar, V.; Nudelman, A. *J. Org. Chem.* **1997**, *62*, 7512–7515.

X ray diffraction studies

X-ray diffraction structures were measured in a Bruker Kappa Apex II with a CCD detector diffractometer. Data were collected at 298(2) K using Cu K_α radiation (λ = 1.54178 Å) and ω scan technique and were corrected for Lorentz and polarization effects.

A series of narrow frames data were collected with a scan width of 0.5º in ω and an exposure time of 10 s per frame. The data were integrated with SAINT[166] to a resolution of 0.78 Å using a narrow-frame algorithm. Data were corrected for absorption effects using the multi-scan method using SADABS.[167]

Subsequent structure solution and refinement were carried out with SHELXT and SHELXL, respectively.[168] Scattering factors were taken from the International Tables for Crystallography.[169] In the crystals for the associate between receptor **64** and methanol, hydrogen atoms attached to N1 and N2 were located in a difference Fourier map and the rest of the hydrogen atoms were positioned geometrically. In both receptor **67** associates, all hydrogen atoms were placed in calculated positions. Mercury 4.2.0 program was used for analysis and molecular and crystal structures drawings preparation.[170]

^{1}H NMR titration experiments

A typical procedure for ^{1}H NMR titrations is described. A receptor solution (3.5 mM, 0.8 mL) in $CDCl_3$ was prepared and a volume of 400 μL was added to a standard NMR tube. The ^{1}H NMR spectrum of the sample was recorded at 298 K. A solution of the guest (0.05 M) was prepared by dissolving the exact amount of the salt in the remaining solution (0.4 mL) of the receptor. Aliquots of this solution were then added to the NMR tube, mixing well after each addition, and recording the corresponding ^{1}H NMR spectrum. The concentration of the receptor was thus kept constant during the titration as the guest solution also contained the receptor at its initial concentration. During the course of the titration, some proton signals of the receptor are shifted and these chemical shifts (δ ppm) were plotted against the guest concentrations. The titration curve thus obtained or binding isotherm is fitted to a mathematical model and the association constant (K_a) was calculated using a Monte Carlo nonlinear curve-fitting method.

---

[166] SAINT-NT Version 6.0, Madison, Wisconsin, USA: Bruker–AXS, **2001**.
[167] SADABS 2008/1, L. Krause, R. Herbst-Irmer, G. M. Sheldrick, D. Stalke. *J. Appl. Crystallogr*. **2015**, *48*, 3–10.
[168] (a) SHELXTL 2014/4, G. M. Sheldrick, *Acta Cryst. A* **2015**, *71*, 3-8, (b) SHELXTL 2014/7, G. M. Sheldrick, *Acta Cryst. A* **2015**, *71*, 3–8
[169] U. Shmueli, ed. International Tables for Crystallography. New York: Springer; **2006**.
[170] C. F. Macrae, P. R. Edgington, P. McCabe, E. Pidcock, G. P. Shields, R. Taylor, M. Towler, J. J. Van de Streek, *J. Appl. Cryst.* **2006**, *39*, 453–457.

The binding constant analysis has been performed using the software developed by Dr. C. Raposo (Universidad de Salamanca) and the website supramolecular.org (http://app.supramolecular.org/bindfit/). Good agreement has been observed with both sofwares.

Modelling studies

Theorical studies were carried out using GAMESS interface of Chem3D 19.1 software[171] using the semiempirical method AM1 and theorical Hartree-Fock calculations.

Further calculations were made using Gaussian16 software[172] The M06-2X DFT functional[173] combined with 6-31G(d,p) basis set[174] was employed, along with the GD3 empirical dispersion correction.[175] Gibbs free energy was calculated on the optimized structures using the Quasy rigid rotor harmonic oscillator approximation implemented in Goodvibes.[176] Molecular graphics were prepared using *Pymol*.[177]

---

[171] G. M. J. Barca, C. Bertoni, L.Carrington, D. Datta, N. De Silva, J. E. Deustua, D. G. Fedorov, J. R. Gour, A. O. Gunina, E. Guidez, T. Harville, S. Irle, J. Ivanic, K. Kowalski, S. S. Leang, H. Li, W. Li, J. J. Lutz, I. Magoulas, J. Mato, V. Mironov, H. Nakata, B. Q. Pham, P. Piecuch, D. Poole, S. R. Pruitt, A. P. Rendell, L. B. Roskop, K. Ruedenberg, T. Sattasathuchana, M. W. Schmidt, J. Shen, L. Slipchenko, M. Sosonkina, V. Sundriyal, A. Tiwari, J. L. Galvez Vallejo, B. Westheimer, M. Włoch, P. Xu, F. Zahariev, M. S. Gordon, *J. Chem. Phys.* **2020**, *152*, 154102.

[172] Frisch, M. J.; Trucks, G. W.; Schlegel, H. B.; Scuseria, G. E.; Robb, M. A.; Cheeseman, J. R.; Scalmani, G.; Barone, V.; Petersson, G. A.; Nakatsuji, H.; Li, X.; Caricato, M.; Marenich, A. V.; Bloino, J.; Janesko, B. G.; Gomperts, R.; Mennucci, B.; Hratchian, H. P.; Ortiz, J. V.; Izmaylov, A. F.; Sonnenberg, J. L.; Williams; Ding, F.; Lipparini, F.; Egidi, F.; Goings, J.; Peng, B.; Petrone, A.; Henderson, T.; Ranasinghe, D.; Zakrzewski, V. G.; Gao, J.; Rega, N.; Zheng, G.; Liang, W.; Hada, M.; Ehara, M.; Toyota, K.; Fukuda, R.; Hasegawa, J.; Ishida, M.; Nakajima, T.; Honda, Y.; Kitao, O.; Nakai, H.; Vreven, T.; Throssell, K.; Montgomery Jr, J. A.; Peralta, J. E.; Ogliaro, F.; Bearpark, M. J.; Heyd, J. J.; Brothers, E. N.; Kudin, K. N.; Staroverov, V. N.; Keith, T. A.; Kobayashi, R.; Normand, J.; Raghavachari, K.; Rendell, A. P.; Burant, J. C.; Iyengar, S. S.; Tomasi, J.; Cossi, M.; Millam, J. M.; Klene, M.; Adamo, C.; Cammi, R.; Ochterski, J. W.; Martin, R. L.; Morokuma, K.; Farkas, O.; Foresman, J. B.; Fox, D. J. *Gaussian 16 Rev. B.01*, Wallingford, CT, **2016**.

[173] (a) Zhao, Y.; Truhlar, D. G., *Acc. Chem. Res.* **2008**, *41*, 157–167. (b) Zhao, Y.; Truhlar, D. *Theor. Chem. Account.* **2008**, *120*, 215–241. (c) Zhao, H.; Truhlar, D. G., *Theor. Chem. Acta* **2007**, *120*, 215–241.

[174] (a) Hariharan, P. C.; Pople, J. A. *Theor. Chem. Acc.* **1973**, *28*, 213–222. (b) Francl, M. M.; Pietro, W. J.; Hehre, W. J.; Binkley, J. S.; DeFrees, D. J.; Pople, J. A.; Gordon, M. S. *J. Chem. Phys.* **1982**, *77*, 3654–3665.

[175] Grimme, S.; Antony, J.; Ehrlich, S.; Krieg, H. *J. Chem. Phys.* **2010**, *132*, 154104.

[176] (a) Grimme, S. *Chem. Eur. J.* **2012**, *18*, 9955–9964. (b) Funes-Ardoiz, I.; Paton, R. S. (**2016**) GoodVibes v3.0.1. http://doi.org/10.5281/zenodo.595246.

[177] The PyMOL Molecular Graphics System, Version 1.8 Schrödinger, LLC.

5.2. General Procedures

1. Acid activation using pivaloyl anhydride

To a 10% w/v acid solution (1.0 mmol) in DCM triethylamine (1.1 mmol) was added and the reaction mixture was concentrated under reduced pressure at room temperature. The residue was dissolved in DCM (10% w/v) and pivaloyl chloride (1.0 mmol) was added to the solution. After 5 min stirring, the reaction mixture was concentrated under reduced pressure. The residue was dissolved in EtOAc (50 mL), washed with brine (2x20 mL) and a 4% Na_2CO_3 aqueous solution (2x20 mL). The organic solvent was dried over anhydrous Na_2SO_4 and concentrated under reduced pressure to give the title compound. The pivalic acid mixed anhydride was used in the following step without further purification.

2. Acid activation using PCl_5

The acid (1.0 mmol) was slowly added to a 10% w/v PCl_5 solution (1.1 mmol) in DCM and the reaction was stirred for 30 minutes. The reaction mixture was concentrated under reduced pressure and the crude product was used in the next step without further purification.

3. Acid activation using $SOCl_2$

A 10% w/v acid solution (1.0 mmol) in $SOCl_2$ was refluxed for 1 hour. $SOCl_2$ was removed under reduced pressure to give the acid chloride which was used in the following step without further purification.

4. Amide synthesis using Schotten-Baumann conditions

A 10% w/v acid chloride solution (1 mmol) in EtOAc was added to a mixture of the corresponding amine (1.0 mmol) in EtOAc (10% w/v) and a saturated solution of Na_2CO_3 (25% of the total amount of EtOAc). After 10 minutes, the aqueous phase was removed, the organic layer was washed with brine (2x20 mL), dried over anhydrous Na_2SO_4 and the organic solvent was concentrated under reduced pressure. The residue was purified in a silica gel chromatography.

5. Catalyst activation with aqueous 5% NH_3

Catalysts appeared partially protonated after silica gel column chromatography purification, which could negatively bias their catalytic activity. In order to free the amine group, the catalyst was dissolved in EtOAc and washed with 5% NH_3 v/v aqueous solution. The organic phase was dried over anhydrous Na_2SO_4 and concentrated under reduced pressure to yield the activated catalyst. Apparently $NaHCO_3$ and Na_2CO_3 were not successful bases to generate the activated catalyst as they may be complexed by the oxyanion-hole.

6. Catalyst acetylation using acetic anhydride

The required catalyst (*ca.* 10 mg) was dissolved in the minimum amount of aceticanhydride (*ca.* 500 μL) and the reaction mixture was stirred for 5 minutes. Then, the excess ofacetic anhydride was removed in vacuo and the residue was dissolved in EtOAc (20 mL). 5

mL of a saturated solution of Na_2CO_3 were added and the mixture was vigorously stirred for 2 hours. Thereafter, the aqueous phase was removed, and the organic phase was dried over anhydrous Na_2SO_4 and concentrated in vacuo to afford the desired compound quantitatively.

7. Catalyst acetylation using vinyl acetate

The required catalyst (*ca.* 10 mg) was dissolved in the minimum amount of vinyl acetate (*ca.* 500 μL) and the reaction mixture was stirred for 5 minutes. Then, the excess of vinyl acetate was removed in vacuo to afford the desired compound quantitatively.

5.3. Synthetic details and characterization

N^1-Allyl-N^3-butylisophthalamide (3)

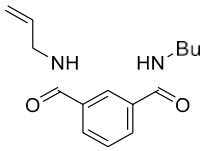

3

Following the *General Procedure 1 for acid activation using pivaloyl anhydride* described on page 224, the reaction between 3-(butylcarbamoyl)benzoic acid (2.5 g, 11.3 mmol),[178] Et_3N (3.5 mL, 25.1 mmol) and pivaloyl chloride (3.0 mL, 24.5 mmol) gave 3-(butylcarbamoyl)benzoic pivalic anhydride which was used in the next step without further purification.

The 3-(butylcarbamoyl)benzoic pivalic anhydride obtained in the previous step was added to a solution of allylamine (2.5 mL, 33.4 mmol) in DCM (25 ml) and stirred for 5 min, then the reaction mixture was washed with HCl 2 M (2x20 mL) and aqueous 4% Na_2CO_3 (2x20 mL). The organic phase was dried over anhydrous Na_2SO_4 and concentrated under reduced pressure. The residue was purified by column chromatography on silica gel using 50% EtOAc in DCM yielding compound **3** (1.25 g, 42%) as a yellowish oil.

m.p.: oily compound.

IR (thin film, υ in cm^{-1}): 3299, 3066, 2962, 2916, 2858, 1645, 1547, 1485, 1439, 1301, 1175, 1145, 1083, 996, 918, 821, 736.

^{1}H NMR (200 MHz, $CDCl_3$) δ 8.26 (s, 1H), 7.87 (d, *J* = 7.0 Hz, 2H), 7.33 (t, *J* = 7.0 Hz, 1H, NH), 7.16 (br t, NH), 5.89 – 5.64 (m, 1H), 5.09 (d, *J* = 19.0 Hz, 1H), 5.02 (d, *J* = 11.0 Hz, 1H), 3.91 (t, *J* = 5.5 Hz, 2H), 3.28 (q, *J* = 7.0 Hz, 2H), 1.16 – 1.54 (m, 4H), 0.81 (t, *J* = 7.1 Hz, 3H).

^{13}C NMR (50 MHz, $CDCl_3$) δ 167.1 (C), 166.9 (C), 134.9 (C), 134.5 (C), 133.8 (CH), 130.2 (CH), 130.1 (CH), 128.8 (CH), 125.4 (CH), 116.5 (CH_2), 42.5 (CH_2), 39.9 (CH_2), 31.5 (CH_2), 20.1 (CH_2), 13.7 (CH_3).

MS (ESI+): Calculated for $C_{15}H_{21}N_2O_2$ $[M+H]^+$ 261.2, found 261.1.

[178] Oliva, A. I.; Simón, L.; Muñiz, F. M.; Sanz, F.; Morán, J. R. *Tetrahedron* **2004**, *60*, 3755–3762.

N^1-Butyl-N^3-(3-(dimethylamino)-2-hydroxypropyl)isophthalamide (catalyst 5)

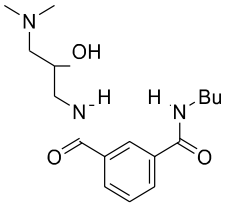

5

Compound **3** (700 mg, 2.7 mmol) was dissolved in DCM (7 mL) and *m*-CPBA 70% (1.4 g, 5.7 mmol) was added. After 3 hours, 50 mL of DCM were added and the organic phase was washed with an aqueous saturated solution of Na_2SO_3 (2x20 mL) and Na_2CO_3 4% (2x20 mL), dried over anhydrous Na_2SO_4 and concentrated under reduced pressure to afford epoxide **4** (680 mg 92 %), which was used without further purification in the following step.

Epoxide **4** (680 mg, 2.5 mmol) was dissolved in an aqueous Me_2NH solution (15 mL, 60 %). AcOH (1 mL) and THF (1 mL) were added and the reaction mixture was heated at 85ºC for one hour. The solvent was concentrated under reduced pressure and the residue was purified by silica gel chromatography using MeOH as eluent and activated following the *General Procedure 5 for catalyst activation with NH_3*, described on page 224, affording catalyst **5** (550 mg, 69 %) as a yellowish oil.

m.p.: oily compound.

IR (thin film, υ in cm^{-1}): 3312, 3081, 2936, 2858, 2832, 2774, 1645, 1535, 1463, 1301, 1113, 1041, 918, 723.

^{1}H NMR (200 MHz, $CDCl_3$) δ 8.13 (s, 1H), 7.82 (br t, NH), 7.80 (d, *J* = 7.5 Hz, 1H), 7.73 (d, *J* = 7.5 Hz, 1H), 7.42 (br t, NH), 7.20 (t, *J* = 7.5 Hz, 1H), 4.43 (br s, OH), 3.86 – 3.65 (m, 1H), 3.52 – 3.34 (m, 1H), 3.20 (q, *J* = 7.2 Hz, 2H), 3.28 – 3.06 (m, 1H), 2.31 – 1.98 (m, 2H), 2.08 (s, 6H), 1.48 – 1.28 (m, 2H), 1.17 (sext, *J* = 7.2 Hz, 2H), 0.73 (t, *J* = 7.2 Hz, 3H).

^{13}C NMR (50 MHz, $CDCl_3$) δ 167.3 (C), 167.0 (C), 134.7 (C), 134.2 (C), 130.0 (CH), 129.8 (CH), 128.4 (CH), 125.4 (CH), 66.7 (CH), 62.9 (CH_2), 45.5 (2 CH_3), 44.4 (CH_2), 39.8 (CH_2), 31.4 (CH_2), 20.0 (CH_2), 13.6 (CH_3).

HRMS (ESI+): Calculated for $C_{17}H_{28}N_3O_3$ $[M+H]^+$ 322.2125, found 322.2133.

1-(3-(Butylcarbamoyl)benzamido)-3-(dimethylamino)propan-2-yl acetate (catalyst 5a)

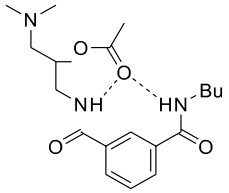

5a

Following the *General Procedure 6 for catalyst acetylation using acetic anhydride* described on page 224, the reaction of catalyst **5** (10 mg, 0.03 mmol) with 500 μL of acetic anhydride gave 10 mg (quant.) of **5a** as an oily compound.

m.p.: oily compound.

IR (thin-film, υ in cm^{-1}): 3312, 3072, 2955, 2925, 2871, 2826, 2774, 1742, 1651, 1541, 1476, 1376, 1229, 1048. 717.

^{1}H NMR (200 MHz, $CDCl_3$) δ 8.14 (s, 1H), 7.95 (br t, NH), 7.87 (d, *J* = 7.8 Hz, 1H), 7.81 (d, *J* = 7.8 Hz, 1H), 7.39 (t, *J* = 7.8 Hz, 1H), 6.75 (br t, NH), 5.06 (quin, *J* = 6.0 Hz, 1H), 3.62 (t, *J* = 6.0 Hz, 2H), 3.36 (q, *J* = 6.5 Hz, 2H), 2.59 – 2.42 (m, 2H), 2.26 (s, 6H), 2.01 (s, 3H), 1.63 – 1.44 (m, 2H), 1.33 (sext, *J* = 7.2 Hz, 2H), 0.88 (t, *J* = 7.2 Hz, 3H).

^{13}C NMR (50 MHz, $CDCl_3$) δ 170.9 (C), 166.8 (2 C), 135.1 (C), 134.6 (C), 130.1 (CH), 129.6 (CH), 128.8 (CH), 125.4 (CH), 69.8 (CH), 61.5 (CH_2), 46.2 (2 CH_3), 43.2 (CH_2), 40.0 (CH_2), 31.7 (CH_2), 21.2 (CH_3), 20.2 (CH_2), 13.8 (CH_3).

MS (ESI+): Calculated for $C_{19}H_{30}N_3O_4$ $[M+H]^+$ 364.2, found 364.3

1,4-Dihydronaphthalene-1-carboxylic acid (6)

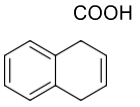

6

Following the procedure described in the literature,[179] a 250 mL three-necked flask was fitted with a septum and an inlet tube for ammonia gas. A solution of 1-naphthoic acid (20.0

[179] (a) Marshall, J. L.; Folsom, T. K. *J. Org. Chem.* **1971**, *36*, 2011–2014. (b) Marshall, J. L.; Ihrig A. M.; Jenkins, P. N. *J. Org. Chem.* **1972**, *37*, 1863–1863. (c) Rabideau, P. W.; Burkholder, E. G.; Yates, M. J. *Synth. Commun.* **1980**, *10*, 627–632. (d) Murthy, A. R.; Sundar, N. S.; Subba Rao, G. S. R. *Tetrahedron* **1982**, *38*, 2831–2836. (e) Yoshimi, Y.; Ishie, A.; Oda, H.; Moriguchi, Y.; Kanezaki, H.; Nakaya, Y.; Katsuno, K.; Itou, T.; Inagaki, S.; Morita, T.; Hatanaka, M. *Tetrahedron Lett.* **2008**, *49*, 3400–3404.

g, 0.11 mol) in 40 mL of THF was added into the flask and the solution was cooled down to -78ºC. Ammonia (40 mL) gas was condensed in the solution and then sodium (6.0 g, 0.23 mol) was added in portions at -78ºC for 15 minutes. The reaction was stirred for 1 hour at -33ºC until all the alkali metal was dissolved. The inlet tube was slowly removed, and the mixture was warmed to -15ºC while stirring, leaving the flask opened until most ammonia had evaporated. The reaction mixture was carefully added into a 1000 mL Erlenmeyer flask with a mixture of ice (250 g) and aqueous HCl (30 mL, 12 M). 30 mL more of HCl 12 M were added and the precipitate was filtered affording compound **6** (19.2 g, 95%) as a white solid.

^{1}H NMR (200 MHz, $CDCl_3$) δ 7.31 – 7.15 (m, 4H). 6.24 – 6.15 (m, 1H), 6.04 – 5.94 (m, 1H), 4.44 (q, *J* = 4.0 Hz, 1H), 3.54 (dq, *J* = 4.0, 21.0 Hz, 1H), 3.37 (dt, *J* = 4.0, 21.0 Hz, 1H).

All spectral properties match with those described in the literature.[179]

1a,2,7,7a-Tetrahydronaphtho[2,3-*b*]oxirene-2-carboxylic acid (7)

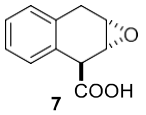

7

Compound **6** (5.0 g, 0.03 mol) and Na_2CO_3 (10 g, 0.09 mol) were dissolved in water (100 mL) in a 500 mL round-bottom flask. Then, a mixture of Oxone® (30.0 g, 0.2 mol) and Na_2CO_3 (21.0 g, 0.2 mol) was slowly added in portions into the flask for 1 hour. The mixture was transferred into a 1000 mL Erlenmeyer flask and cooled down to 0ºC. HCl 2 M was added with vigorously stirring until pH =1-2. The aqueous phase was extracted with EtOAc (3x50 mL) at 0ºC. Combined organic phases were dried over anhydrous Na_2SO_4 and filtered. The solvent was concentrated under reduced pressure affording compound **7** (1.8 g, 30%, 4:1 *trans*/*cis* mixture) as a yellowish oil, which was used in the next step without further purification.

^{1}H NMR (200 MHz, $CDCl_3$) δ 7.30 – 7.04 (m, 4H), 4.36 (d, *J* = 2.0 Hz, 1H), 3.75 – 3.51 (m, 2H), 3.40 – 3.20 (m, 2H).

_N_-(_p_-Tolyl)-1a,2,7,7a-tetrahydronaphtho[2,3-_b_]oxirene-2-carboxamide (8)

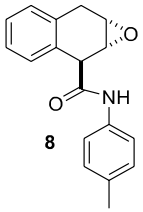

8

Following the *General Procedure 1 for acid activation using pivaloyl anhydride* described on page 224, the reaction between compound **7** (1.8 g, 9.0 mmol), triethylamine (954 mg, 9.0 mmol) and pivaloyl chloride (1.2 g, 9.0 mmol) gave the pivaloyl anhydride of compound **7** (700 mg, 28%) as an oily compound, which was used in the next step without further purification.

The pivaloyl anhydride of compound **7** (700 mg, 2.55 mmol) and *p*-toluidine (965 mg, 9.0 mmol) were dissolved in EtOAc (10 mL). After 10 minutes, Et_2O was added and the precipitate was filtered off yielding compound **8** (680 mg, 27%) as a white solid.

m.p.: 168 – 170ºC.

IR (nujol, υ in cm^{-1}): 3300, 2915, 2845, 1660, 1600, 1352, 820, 756.

^{1}H NMR (200 MHz, $CDCl_3$) δ 7.50 (br s, NH), 7.33 – 7.11 (m, 6H), 7.06 (d, *J* = 8.2 Hz, 2H), 4.27 (d, *J* = 2.4 Hz, 1H), 3.80 (dd, *J* = 2.4, 4.2 Hz, 1H), 3.63 – 3.52 (m, 1H), 3.48 – 3.19 (m, 2H), 2.29 (s, 3H).

^{13}C NMR (50 MHz, $CDCl_3$) δ 168.8 (C), 134.8 (C), 134.6 (C), 132.7 (C), 130.4 (C), 130.2 (CH), 129.8 (CH), 129.5 (2 CH), 128.6 (CH), 127.5 (CH), 120.3 (2 CH), 53.6 (CH), 51.4 (CH), 49.9 (CH), 30.1 (CH_2), 20.9 (CH_3).

MS (ESI+): Calculated for $C_{18}H_{17}NO_2Na$ $[M+Na]^+$ 302.1, found 302.1.

3-Azido-2-hydroxy-_N_-(_p_-tolyl)-1,2,3,4-tetrahydronaphthalene-1-carboxamide (9)

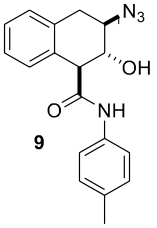

9

A compound **8** solution (680 mg, 2.0 mmol) and sodium azide (5.0 g, 80.0 mmol) in propionic acid (25 mL) and water (5 mL) was heated at 80ºC for 1 hour. Water (50 mL) was added and the precipitated was filtered off. Compound **9** (630 mg, 98%) was obtained as a white solid.

m.p.: 133 – 137ºC.

IR (nujol, υ in cm^{-1}): 3312, 2961, 2851, 2338, 2118, 1644, 1520, 1450, 1378, 1073, 820.

^{1}H NMR (200 MHz, CD_3OD) δ 7.52 (d, *J* = 8.4 Hz, 2H), 7.20 – 7.06 (m, 6H), 4.19 (t, *J* = 9.5 Hz, 1H), 3.90 (d, *J* = 9.5 Hz, 1H), 3.67 (ddd, *J* = 11.6, 9.5 and 5.5Hz, 1H), 3.10 (dd; *J* = 16.3 and 5.5 Hz, 1H), 2.79 (dd, *J* = 16.3 and 11.6 Hz, 1H), 2.30 (s, 3H).

^{13}C NMR (50 MHz, CD_3OD) δ 173.8 (C), 137.0 (C), 135.2 (2 C), 134.7 (C), 130.2 (2 CH), 129.9 (CH), 128.4 (CH), 128.3 (CH), 127.9 (CH), 121.6 (2 CH), 74.8 (CH), 64.2 (CH), 57.7 (CH), 35.6 (CH_2), 21.0 (CH_3).

MS (ESI+): Calculated for $C_{18}H_{19}N_4O_2$ $[M+H]^+$ 323.2, found 323.2.

3-Amino-2-hydroxy-*N*-(*p*-tolyl)-1,2,3,4-tetrahydronaphthalene-1-carboxamide (10)

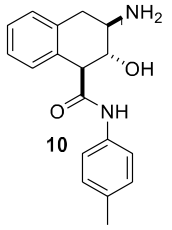

10

Pd/C 5% (220 mg, 2.1 mmol) was added to a compound **9** solution (530 mg, 1.6 mmol) in EtOAc (10 mL) and the reaction mixture was connected to a hydrogenator with H_2 (4 atm). After stirring the reaction mixture for 24 hours, Pd/C was filtered off, and the organic solvent was concentrated under reduced pressure. Compound **10** (200 mg, 44%) was obtained as a white solid.

m.p.: 188 – 190ºC.

IR (nujol, υ in cm^{-1}): 3600 (broad), 3279, 2929, 2851, 1660, 1530, 1372, 1050.

^{1}H NMR (200 MHz, CD_3OD) δ 7.53 (d, *J* = 8.5 Hz, 2H), 7.18 – 7.08 (m, 6H), 3.96 (t, *J* = 9.2 Hz, 1H), 3.81 (d, *J* = 9.2 Hz, 1H), 3.15 – 2.87 (m, 2H), 2.76 (dd, *J* = 14.1 and 10.4 Hz, 1H), 2.30 (s, 3H).

^{13}C NMR (50 MHz, CD_3OD) δ 174.4 (C), 137.2 (C), 136.3 (C), 135.3 (C), 135.2 (C), 130.3 (2 CH), 129.8 (CH), 128.5 (CH), 128.1 (CH), 127.6 (CH), 121.6 (2 CH), 75.8 (CH), 58.0 (CH), 53.5 (CH), 37.6 (CH_2), 21.0 (CH_3).

MS (ESI+): Calculated for $C_{18}H_{21}N_2O_2$ $[M+H]^+$ 297.2, found 297.2.

3-(Dimethylamino)-2-hydroxy-N-(*p*-tolyl)-1,2,3,4-tetrahydronaphthalene-1-carboxamide (catalyst 11)

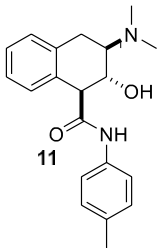

11

A compound **10** solution (200 mg, 0.7 mmol), paraformaldehyde (1.1 g, 40.0 mmol), acetic acid (440 mg, 7.3 mmol) and sodium cyanoborohydride (340 mg, 5.4 mmol) in 5 mL of MeOH was stirred for 1 hour. The reaction mixture was quenched with 1 mL of an aqueous saturated solution of Na_2CO_3 and diluted with EtOAc (50 mL). The organic phase was washed with an aqueous 4% Na_2CO_3solution (2x30 mL), dried over anhydrous Na_2SO_4 and filtered. The organic solvent was concentrated under reduced pressure and the residue activated following the *General Procedure 5 for catalyst activation with NH_3*, described on page 224, affording catalyst **11** (90 mg, 41%) as a white solid.

m.p.: 165 – 170ºC.

IR (nujol, υ in cm^{-1}): 3286, 2961, 1651, 1600, 1469, 1242, 820, 743.

^{1}H NMR (200 MHz, $CDCl_3$) δ 8.33 (br s, NH), 7.47 (d, *J* = 8.4 Hz, 2H), 7.23 – 7.04 (m, 4H), 7.06 (d, *J* = 8.4 Hz, 2H), 4.22 – 3.96 (m, 1H), 3.78 (d, *J* = 8.9 Hz, 1H), 2.87 – 2.65 (m, 3H), 2.35 (s, 6H), 2.30 (s, 3H).

^{13}C NMR (50 MHz, $CDCl_3$) δ 171.6 (C), 135.8 (C), 135.3 (C), 133.8 (C), 132.3 (C), 129.5 (CH), 129.4 (2 CH), 129.2 (CH), 127.2 (CH), 126.7 (CH), 120.2 (2 CH), 69.4 (CH), 64.6 (CH), 56.7 (CH), 40.4 (2 CH_3), 24.9 (CH_2), 21.0 (CH_3).

HRMS (ESI+): Calculated for $C_{20}H_{25}N_2O_2$ $[M+H]^+$ 325.1911, found 325.1914.

3-(Dimethylamino)-1-(p-tolylcarbamoyl)-1,2,3,4-tetrahydronaphthalen-2-yl acetate (catalyst 11a)

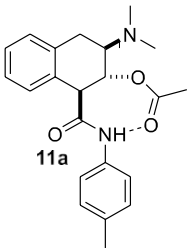

Following the *General Procedure 6 for catalyst acetylation* described on page 224, the reaction between catalyst **11** (10 mg, 0.03 mmol) and acetic anhydride (500 μL) yielded **11a** (11 mg, quant.).

m.p.: oily compound.

IR (nujol, υ in cm^{-1}): 3312, 2930, 1748, 1657, 1612, 1527, 1242, 1030, 814, 749.

^{1}H NMR (200 MHz, $CDCl_3$) δ 10.02 (br s, NH), 7.43 – 7.12 (m, 6H), 7.06 (d, *J* = 8.3 Hz, 2H), 5.68 (d, *J* = 3.6 Hz, 1H), 3.92 (s, 1H), 3.15 – 2.73 (m, 3H), 2.41 (s, 6H), 2.27 (s, 3H), 2.07 (s, 3H).

^{13}C NMR (50 MHz, $CDCl_3$) δ 170.4 (C), 169.9 (C), 136.3 (C), 133.5 (C), 132.7 (C), 132.0 (C), 129.5 (2 CH), 128.9 (CH), 128.5 (CH), 127.8 (CH), 127.5 (CH), 119.5 (2 CH), 69.2 (CH), 61.9 (CH), 54.3 (CH), 42.6 (2 CH_3), 27.8 (CH_2), 21.3 (CH_3), 21.0 (CH_3).

MS (ESI+): Calculated for $C_{22}H_{27}N_2O_3$ $[M+H]^+$ 367.2, found 367.3.

***N*,*N*-Dimethyl-1,4-dihydronaphthalene-1-carboxamide (12)**

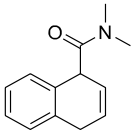

12

Following the *General Procedure 2 for acid activation using PCl_5* described on page 224, the reaction between compound **6** (8.6 g, 49.4 mmol) and PCl_5 (10.7 g, 51.4 mmol) in DCM (50 mL) afforded compound **6** acid chloride which was used in the next step without further purification.

Following the *General Procedure 4 for amide synthesis using Schotten-Baumann conditions* described on page 224, the reaction between compound **6** acid chloride and an aqueous solution of 60% dimethylamine (20 mL, 178.7 mmol) afforded compound **12** (9.6 g 97%) as a brown oil.

m.p.: oily compound.

IR (nujol, υ in cm^{-1}): 3033; 2929; 1645; 1489; 1443; 1405; 1262; 1132; 1061; 1028; 866; 756; 648.

^{1}H NMR (400 MHz, $CDCl_3$) δ 7.33 – 7.22 (m, 3H), 7.18 (d, *J* = 7.2 Hz, 1H), 6.23 – 6.12 (m, 1H), 6.07 – 5.97 (m, 1H), 4.81 (q, *J* = 5.4 Hz, 1H), 3.68 – 3.56 (m, 1H), 3.55 – 3.43 (m, 1H), 3.05 (s, 3H), 3.04 (s, 3H).

^{13}C NMR (100 MHz, $CDCl_3$) δ 172.6 (C), 133.7 (C), 132.1 (C), 128.7 (CH), 127.4 (CH), 126.9 (CH), 126.8 (CH), 126.5 (CH), 123.4 (CH), 46.5 (CH), 37.3 (CH_3), 36.4 (CH_3), 29.9 (CH_2).

HRMS (ESI+): Calculated for $C_{13}H_{16}NO$ $[M+H]^+$ 202.1226, found 202.1219.

_N,N_-Dimethyl-1a,2,7,7a-tetrahydronaphtho[2,3-_b_]oxirene-2-carboxamide (13)

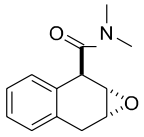

13

m-CPBA (13.0 g, 52.8 mmol) was added to a compound **12** solution (9.6 g, 47.8 mmol) in DCM (50 mL) and the reaction mixture was stirred for 16 hours at room temperature. The solvent was concentrated under reduced pressure at 0ºC. The residue was dissolved in 100 mL of EtOAc and the organic phase was washed with an aqueous solution of 5% Na_2SO_3 (2x25 mL) and with an aqueous solution of 4% Na_2CO_3 (2x25 mL). The combined organic extracts were dried over anhydrous Na_2SO_4, filtered and concentrated under reduced pressure and the residue was crystallized in Et_2O affording compound **13** (4.8 g 46 %) as a white solid.

m.p.: 99 – 101ºC.

IR (nujol, υ in cm^{-1}): 2923, 2852, 1651, 1249, 1126, 976, 827, 756.

^{1}H NMR (400 MHz, DMSO-d_6) δ 7.21 – 7.09 (m, 3H), 7.07 (d, *J* = 7.3 Hz, 1H), 4.81 (d, *J* = 1.7 Hz, 1H), 3.51 – 3.47 (m, 1H), 3.47 – 3.43 (m, 1H), 3.33 (d, *J* = 17.3 Hz, 1H), 3.33 (s, 3H), 3.14 (d, *J* = 17.3 Hz, 1H), 2.82 (s, 3H).

^{13}C NMR (100 MHz, DMSO-d_6) δ 170.2 (C), 133.6 (C), 132.9 (C), 129.1 (CH), 128.8 (CH), 126.9 (CH), 126.1 (CH), 52.5 (CH), 50.7 (CH), 42.9 (CH), 37.6 (CH_2), 35.3 (CH_3), 29.9 (CH_3).

HRMS (ESI+): Calculated for $C_{13}H_{16}NO_2$ $[M+H]^+$ 218.1176, found 218.1173.

3-Amino-2-hydroxy-*N*,*N*-dimethyl-1,2,3,4-tetrahydronaphthalene-1-carboxamide (14)

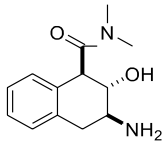

14

An aqueous 20% NH_3 solution (6 mL, 70.6 mmol) was added to a compound **13** solution (2.0 g, 9.2 mmol) and NH_4Cl (1.0 g, 19.8 mmol) in MeOH (10 mL) and was heated at 80ºC for 16 hours in a closed flask. The organic solvent was concentrated under reduced pressure and aqueous HCl (5 mL 2M) and EtOAc (20 mL) were added to the residue. The aqueous phase was washed with EtOAc (2x30 mL) and then solid Na_2CO_3 was added with vigorous stirring to the aqueous phase until pH 11-12. Due to compound **14** hydrophilicity, the aqueous phase was concentrated under reduced pressure in order to decrease the water volume to 5 mL. The aqueous phase was extracted with a solution of 10% MeOH in $CHCl_3$ (3x30 mL) and the organic phase was dried over anhydrous Na_2SO_4, filtered and concentrated under reduced pressure affording compound **14** (1.37 g, 64 %) of as a brown oil.

m.p.: oily compound.

IR (thin-film, υ in cm^{-1}): 3338 (broad), 2923, 2852, 1618, 1457, 1379, 1126, 1061, 743.

^{1}H NMR (400 MHz, DMSO-d_6) δ 7.12 – 7.10 (m, 3H), 6.81 (d, J =8.5 Hz, 1H), 4.38 (d, J = 9.5 Hz, 1H,), 4.10 (t, J = 9.5 Hz, 1H), 3.40 (dt, J = 11.2 and 5.4 Hz, 1H), 3.22 (s, 3H), 3.25 – 3.15 (m, 1H), 3.01 (dd, J = 16.0 and 11.2 Hz, 1H), 2.97 (s, 3H).

^{13}C NMR (100 MHz, DMSO-d_6) δ 172.4 (C), 134.6 (C), 132.9 (C), 128.5 (CH), 127.0 (CH), 126.7 (CH), 126.6 (CH), 70.4 (CH), 51.5 (CH), 48.9 (CH), 37.8 (CH_3), 35.5 (CH_3), 32.6 (CH_2).

HRMS (ESI+): Calculated for $C_{13}H_{19}N_2O_2$ $[M+H]^+$ 235.1441, found 235.1433.

***N*-(4-((Dimethylamino)methyl)-3-hydroxy-1,2,3,4-tetrahydronaphthalen-2-yl)benzamide (catalyst 16)**

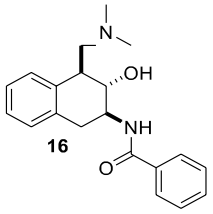

16

A compound **14** solution (500 mg, 2.1 mmol) in THF (2 mL) was added dropwise over a suspension of $LiAlH_4$ (400 mg, 10.5 mmol) in Et_2O (20 mL) under Argon atmosphere at 0ºC

with vigorous stirring. Once the addition was finished, the reaction mixture was stirred for 16 hours at room temperature. Water (400 μL) and an aqueous solution of NaOH (400 μL 15%), followed by more water (1,2mL) were successively added dropwise to the reaction mixture at 0ºC. After warming up to room temperature, the reaction mixture was dried over anhydrous Na_2SO_4, filtered and concentrated under reduced pressure affording amine **15** (420 mg 87%) as a yellowish oil which was used without further purification in the following reaction.

Following the *General Procedure 3 for amide synthesis using Schotten-Baumann conditions* described on page 224, the reaction between compound **15** (420 mg, 1.9 mmol) and benzoyl chloride (250 μL, 2.1 mmol) afforded catalyst **16** (600 mg, (98 %) as a brown oil after activation following *General Procedure 5 for catalyst activation with NH_3*, described on page 224.

m.p.: oily compound.

IR (nujol, υ in cm^{-1}): 3319, 3059, 2936, 2845, 2780, 1651, 1547, 1469, 1326, 1041, 917, 742.

^{1}H NMR (200 MHz, $CDCl_3$) δ 7.82 (d, *J* = 8.1 Hz, 2H), 7.51 – 7.32 (m, 3H), 7.27 – 7.04 (m, 4H), 6.92 (br d, NH), 4.29 – 4.08 (m, 1H), 3.93 (t, *J* = 9.6 Hz, 1H), 3.66 (dd, *J* = 16.2 and 4.9 Hz, 1H), 3.21 – 2.98 (m, 2H), 3.90 – 2.62 (m, 2H), 2.38 (s, 6H).

^{13}C NMR (50 MHz, $CDCl_3$) δ 168.2 (C), 135.0 (C), 134.9 (C), 134.4 (C), 131.3 (CH), 129.6 (CH), 128.4 (2 CH), 127.1 (2 CH), 126.8 (CH), 126.4 (2 CH), 77.4 (CH), 66.4 (CH_2), 51.9 (CH), 45.9 (2 CH_3), 41.9 (CH), 35.7 (CH_2).

HRMS (ESI+): Calculated for $C_{20}H_{25}N_2O_2$ $[M+H]^+$ 325.1911, found 325.1916.

3-Benzamido-1-((dimethylamino)methyl)-1,2,3,4-tetrahydronaphthalen-2-yl acetate (catalyst 16a)

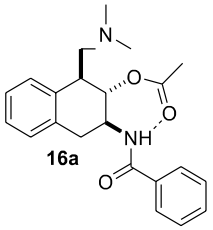

16a

Following the *General Procedure 6 for catalyst acetylation using acetic anhydride* described on page 224, the reaction between catalyst **16** (10 mg, 0.03 mmol) and 500 μL of acetic anhydride yielded **16a** (12 mg, quant.) as a brown oil.

m.p.: oily compound.

IR (nujol, υ in cm^{-1}): 3332, 3059, 2942, 2826, 2754, 1742, 1651, 1547, 1489, 1372, 1242, 1041, 917, 736.

^{1}H NMR (200 MHz, $CDCl_3$) δ 8.31 (br d, *J* = 8.0 Hz, NH), 7.74 (dd, *J* = 7.9 and 1.6 Hz, 2H), 7.50 – 7.30 (m, 4H), 7.23 – 7.05 (m, 3H), 5.28 (dd, *J* = 7.5 and 5.2 Hz, 1H), 4.56 – 4.36 (m, 1H), 3.30 (dd, *J* = 16.4 and 5.2 Hz, 1H), 3.34 – 3.22 (m, 1H), 2.95 (dd, *J* = 16.4 and 7.7 Hz, 1H), 2.74 (dd, *J* = 13.0 and 5.2 Hz, 1H), 2.60 (dd, *J* = 13.0 and 6.2 Hz, 1H), 2.13 (s, 6H), 2.04, (s, 3H).

^{13}C NMR (50 MHz, $CDCl_3$) δ 171.9 (C), 167.5 (C), 135.7 (C), 134.8 (C), 133.9 (C), 131.4 (CH), 129.3 (CH), 128.5 (2 CH), 128.3 (CH), 127.1 (2 CH), 126.7 (CH), 126.6 (CH), 74.9 (CH), 64.8 (CH_2), 48.8 (CH), 46.6 (2 CH_3), 42.8 (CH), 33.6 (CH_2), 21.3 (CH_3).

MS (ESI+): Calculated for $C_{22}H_{27}N_2O_3$ $[M+H]^+$ 367.2, found 367.2.

(1,4-Dihydronaphthalen-1-yl)(pyrrolidin-1-yl)methanone (17)

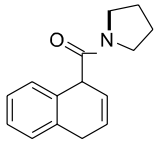

17

Following the *General Procedure 2 for acid activation using PCl_5* described on page 224, the reaction between compound **6** (14.0 g, 80.4 mmol) and PCl_5 (17.5 g, 84.0 mmol) in DCM (50 mL) afforded compound **6** acid chloride which was used in the next step without further purification.

Following the *General Procedure 4 for amide synthesis using Schotten-Baumann conditions* described on page 224, the reaction of compound **6** acid chloride obtained in the previous step with pyrrolidine (15 mL, 183.0 mol) afforded compound **17** (16.1g,88%) as a brown oil.

m.p.: oily compound.

IR (nujol, υ in cm^{-1}): 3027, 2962, 2871, 2819, 1632, 1424, 756.

^{1}H NMR (400 MHz, $CDCl_3$) δ 7.23 – 7.05 (m, 4H), 6.17 – 6.04 (m, 1H), 5.97 – 5.84 (m, 1H), 4.64 – 4.58 (m, 1H), 3.56 – 3.42 (m, 5H), 3.20 – 3.01 (m, 1H), 1.93 – 1.73 (m, 4H).

^{13}C NMR (100 MHz, $CDCl_3$) δ 171.2 (C), 134.1 (C), 132.7 (C), 128.7 (CH), 127.7 (CH), 127.1 (CH), 127.0 (CH), 126.6 (CH), 123.2 (CH), 48.0 (CH), 46.7 (CH_2), 46.1 (CH_2), 30.0 (CH_2), 26.5 (CH_2), 24.0 (CH_2).

HRMS (ESI+): Calculated for $C_{15}H_{18}NO$ $[M+H]^+$ 228.1383, found 228.1395

Pyrrolidin-1-yl(1a,2,7,7a-tetrahydronaphtho[2,3-*b*]oxiren-2-yl)methanone (18)

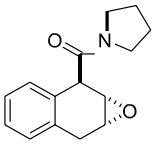

18

m-CPBA 70% (6.5 g, 26.4 mmol) was added to a compound **17** solution (6.0 g, 26.4 mmol) in DCM (50 mL) and the reaction mixture was stirred for 16 hours. The organic solvent was concentrated under reduced pressure at 0ºC. The crude reaction mixture was dissolved in EtOAc (100 mL) and washed with an aqueous solution of 5% Na_2SO_3 (2x25 mL) and with an aqueous solution of 4% Na_2CO_3 (2x25 mL). The combined organic extracts were dried over anhydrous Na_2SO_4, filtered and concentrated under reduced pressure affording 5.6 g (87%) of a 6.4:1 *trans*/*cis* mixture, which was purified by crystallization in Et_2O affording compound **18** (2.6 g, 41%) as a white solid.

m.p.: 120 – 123ºC.

IR (nujol, υ in cm^{-1}): 2960, 2929, 2856, 1625, 1456, 1418, 983, 821, 749.

^{1}H NMR (200 MHz, $CDCl_3$) δ 7.29 – 6.96 (m, 4H), 4.52 (d, *J* = 1.7 Hz, 1H), 3.99 – 3.70 (m, 2H), 3.71 – 3.40 (m, 5H), 3.26 (dd, *J* = 2.4, 17.5 Hz, 1H), 2.25 – 1.79 (m, 4H).

^{13}C NMR (50 MHz, $CDCl_3$) δ 169.7 (C), 133.4 (C), 131.7 (C), 130.0 (CH), 128.8 (CH), 127.8 (CH), 126.7 (CH), 53.6 (CH), 52.0 (CH), 47.6 (CH_2), 46.7 (CH), 46.3 (CH_2), 30.5 (CH_2), 26.5 (CH_2), 24.4 (CH_2).

HRMS (ESI+): Calculated for $C_{15}H_{18}NO_2$ $[M+H]^+$ 244.1332, found 244.1349.

(3-Amino-2-hydroxy-1,2,3,4-tetrahydronaphthalen-1-yl)(pyrrolidin-1-yl)methanone (19)

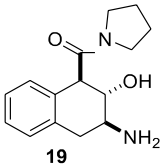

19

An aqueous 20% NH_3 solution (20 mL, 68.8 mmol) was added to a solution of compound **23** 6.4:1 *trans*/*cis* mixture (5.6 g, 23.0 mmol) and NH_4Cl (3.0 g, 56.1 mmol) in MeOH (50 mL) and the resulting mixture was heated at 80ºC for 16 hours in a closed flask. The organic solvent was concentrated under reduced pressure and the residue was treated with aqueous HCl 2M (5mL) and EtOAc (20 mL). The aqueous phase was washed with EtOAc (2x30 mL) and then solid Na_2CO_3 was added with vigorous stirring to the aqueous phase until pH 11-12. Due to the hydrophilicity of compound **19**, the aqueous phase was concentrated under reducedpressure in order to decrease the amount of solvent to 5 mL. The aqueous phase was extractedwith a solution of 10% MeOH in $CHCl_3$ (3x30 mL) and the organic phase was dried over anhydrous Na_2SO_4, filtered and concentrated under reduced pressure affording compound **19** (2.5 g, 42%) as a brown oil.

m.p.: oily compound.

IR (nujol, υ in cm^{-1}): 3377 (broad), 2955, 2916, 2858, 1619, 1450, 1366.

^{1}H NMR (400 MHz, $CDCl_3$) δ 7.11 – 6.99 (m, 3H), 6.83 – 6.78 (m, 1H), 4.06 – 3.96 (m, 2H), 3.80 – 3.72 (m, 1H), 3.61 – 3.45 (m, 3H), 3.16 – 3.07 (m, 1H), 3.03 (dd, *J* = 16.1 and 5.3 Hz, 1H), 2.76 (dd, *J* = 16.1 and 11.5 Hz, 1H), 2.00 – 1.78 (m, 4H).

^{13}C NMR (100 MHz, $CDCl_3$) δ 172.5 (C), 134.8 (C), 133.9 (C), 129.0 (CH), 127.0 (CH), 126.8 (CH), 126.7 (CH), 73.7 (CH), 52.8 (CH), 52.4 (CH), 47.6 (CH_2), 46.3 (CH_2), 36.6 (CH_2), 26.1 (CH_2), 24.6 (CH_2).

HRMS (ESI+): Calculated for $C_{15}H_{21}N_2O_2$ $[M+H]^+$ 261.1598, found 261.1524.

3-Amino-1-(pyrrolidin-1-ylmethyl)-1,2,3,4-tetrahydronaphthalen-2-ol (20)

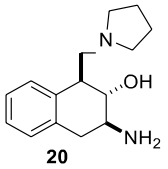

20

A compound **19** solution (2.0 g, 7.7 mmol) in THF (3 mL) was added dropwise over a stirred suspension of $LiAlH_4$ (1.6 g, 42.1 mmol) in Et_2O (80 mL) under Argon atmosphere at 0ºC. Once the addition was finished, the reaction mixture was stirred for 16 hours at room temperature. 1.6 mL of water, 1.6 mL of an aqueous solution of 15% NaOH and 4.8 mL of water were successively added dropwise into the reaction mixture at 0ºC. After warming up to room temperature, the reaction mixture was dried over anhydrous Na_2SO_4, filtered and concentrated under reduced pressure affording compound **20** (1.75 g, 87%) as a yellowish oil.

m.p.: oily compound.

IR (nujol, υ in cm^{-1}): 3351, 3273, 2923, 1638, 1606, 1489, 1456, 743.

^1H NMR (200 MHz, $CDCl_3$) δ 7.28 – 7.18 (m, 1H), 7.18 – 7.06 (m, 3H), 3.53 (dd, *J* = 9.4 and 6.7 Hz, 1H), 3.16 – 2.89 (m, 4H), 2.89 – 2.70 (m, 3H), 2.69 – 2.49 (m, 3H), 1.88 – 1.74 (m, 4H).

^{13}C NMR (50 MHz, $CDCl_3$) δ135.5 (2 C), 129.2 (CH), 126.5 (CH), 126.5 (CH), 126.2 (CH), 81.4 (CH), 62.8 (CH_2), 54.7 (2 CH_2), 51.9 (CH), 42.8 (CH), 38.0 (CH_2), 23.6 (2 CH_2).

HRMS (ESI+): Calculated for $C_{15}H_{23}N_2O$ $[M+H]^+$ 247.1805, found 247.1821

***N*-(3-Hydroxy-4-(pyrrolidin-1-ylmethyl)-1,2,3,4-tetrahydronaphthalen-2-yl)benzamide (catalyst 21)**

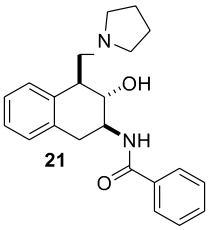

21

Following the *General Procedure 4 for amide synthesis using Schotten-Baumann conditions* described on page 224, the reaction between compound **20** (260 mg, 1.0 mmol) and benzoyl chloride (130 μL, 1.1 mmol) yielded catalyst **21** (240 mg, 69 %) as a brown oil after activation following the *General Procedure 5 for catalyst activation with NH_3*, described on page 224.

m.p.: oily compound.

IR (thin film, υ in cm^{-1}): 3312, 3066, 2968, 2813, 1638, 1540, 1482, 1307, 1119, 1047, 917, 730.

^{1}H NMR (200 MHz, $CDCl_3$) δ 7.85 (dd, *J* = 7.9 and 1.7 Hz, 2H), 7.54 – 7.33 (m, 3H), 7.29 – 7.07 (m, 4H), 6.88 (br d, *J* = 4.5 Hz, NH), 4.27 – 4.08 (m, 1H), 3.97 (dd, *J* = 10.4 and 8.1 Hz, 1H), 3.69 (dd, *J* = 16.2 and 4.9 Hz, 1H), 3.27 – 3.05 (m, 3H), 3.01 – 2.60 (m, 5H), 1.79 – 1.91 (m, 4H).

^{13}C NMR (50 MHz, $CDCl_3$) δ 168.2 (C), 135.1 (C), 134.9 (C), 134.5 (C), 131.4 (CH), 129.7 (CH), 128.5 (2 CH), 127.2 (2 CH), 126.9 (CH), 126.5 (CH), 126.4 (CH), 76.9 (CH), 62.5 (CH_2), 54.8 (2 CH_2), 52.1 (CH), 43.0 (CH), 35.8 (CH_2), 23.6 (2 CH_2).

HRMS (ESI+): Calculated for $C_{22}H_{27}N_2O_2$ $[M+H]^+$ 351.2067, found 351.2066.

3-Benzamido-1-(pyrrolidin-1-ylmethyl)-1,2,3,4-tetrahydronaphthalen-2-yl acetate (catalyst 21a)

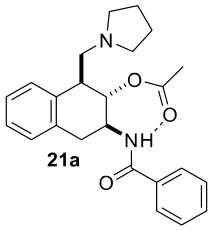

21a

Following the *General Procedure 6 for catalyst acetylation using acetic anhydride* described on page 224, the reaction of catalyst **21** (140 mg, 0.4 mmol) with 500 μL of acetic anhydride yielded compound **21a** (140 mg, 89 %) as a brown oil.

m.p.: oily compound.

IR (nujol, υ in cm^{-1}): 3331, 3072, 2955, 2929, 2793, 1735, 1664, 1554, 1242, 1028, 924, 730.

^{1}H NMR (200 MHz, $CDCl_3$) δ 8.13 (br d, *J* = 8.0 Hz, NH), 7.72 (dd, *J* = 7.8 and 1.7 Hz, 2H), 7.52 – 7.26 (m, 3H), 7.21 – 7.03 (m, 4H), 5.37 (dd, *J* = 7.7 and 5.0 Hz, 1H), 4.46 (qd, *J* = 7.7 and 5.3 Hz, 1H), 3.31 (dd, *J* = 16.4 and 5.2 Hz, 1H), 3.39 – 3.26 (m, 1H), 3.01 – 2.88 (m, 2H), 2.79 (dd, *J* = 12.8 and 6.7 Hz, 1H), 2.52 – 2.40 (m, 2H), 2.39 – 2.27 (m, 2H), 2.04 (s, 3H), 1.64 – 1.51 (m, 4H).

^{13}C NMR (50 MHz, $CDCl_3$) δ 172.0 (C), 167.8 (C), 135.9 (C), 135.0 (C), 134.0 (C), 131.4 (CH), 129.2 (CH), 128.5 (2 CH), 128.4 (CH), 127.1 (2 CH), 126.7 (CH), 126.5 (CH), 75.1 (CH), 61.6 (CH_2), 55.2 (2 CH_2), 49.1 (CH), 43.5 (CH), 33.8 (CH_2), 23.7 (2 CH_2), 21.3 (CH_3).

MS (ESI+): Calculated for $C_{24}H_{29}N_2O_3$ $[M+H]^+$ 393.2, found 393.2.

N^1-Butyl-N^3-(3-hydroxy-4-(pyrrolidin-1-ylmethyl)-1,2,3,4-tetrahydronaphthalen-2-yl)isophthalamide (catalyst 22)

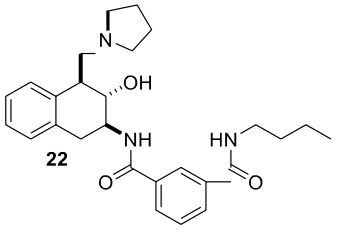

22

Following the *General Procedure 4 for amide synthesis using Schotten-Baumann conditions* described on page 224, the reaction between compound **20** (111 mg, 0.5 mmol) and the compound **2** acid chloride (100 mg, 0.4 mmol) yielded the crude catalyst **22**. Purification was carried out on a silica gel column chromatography using MeOH/NH_3 as eluent. Activation following the *General Procedure 5 for catalyst activation with NH_3*, as described on page 224 was performed to yield catalyst **22** (20.2 mg, 10 %) as a brown oil.

m.p.: oily compound.

IR (thin layer, υ in cm^{-1}): 3312, 3066, 2962, 2936, 2858, 2806, 1645, 1547, 1313, 1132, 1048, 905, 730.

^{1}H NMR (200 MHz, $CDCl_3$) δ 8.19 (s, 1H), 7.88 (dd, *J* = 7.7 and 3.9 Hz, 2H), 7.38 (t, *J* = 7.7 Hz, 1H), 7.30 – 7.01 (m, 4H, NH), 6.79 (br t, *J* = 5.3 Hz, NH), 4.37 – 4.13 (m, 1H), 3.97 (dd, *J* = 10.9 and 9.2 Hz, 1H), 3.61 – 3.31 (m, 3H), 3.25 – 2.95 (m, 3H), 2.94 – 2.68 (m, 3H), 2.68 – 2.47 (m, 2H), 1.90 – 1.69 (m, 4H), 1.66 – 1.44 (m, 2H), 1.35 (quin, *J* = 7.2 Hz, 2H), 0.91 (t, *J* = 7.2 Hz, 3H).

^{13}C NMR (50 MHz, $CDCl_3$) δ 167.3 (C), 167.0 (C), 135.2 (C), 134.7 (C), 134.7 (C), 134.5 (C), 130.4 (CH), 129.9 (CH), 129.5 (CH), 128.8 (CH), 126.9 (CH), 126.5 (CH), 126.5 (CH), 125.1 (CH), 77.4 (CH), 62.7 (CH_2), 54.7 (2 CH_2), 51.8 (CH), 43.0 (CH), 40.0 (CH_2), 35.9 (CH_2), 31.8 (CH_2), 23.6 (2 CH_2), 20.3 (CH_2), 13.9 (CH_3).

HRMS (ESI+): Calculated for $C_{27}H_{36}N_3O_3$ $[M+H]^+$ 450.2751, found 450.2756.

3-(3-(Butylcarbamoyl)benzamido)-1-(pyrrolidin-1-ylmethyl)-1,2,3,4-tetrahydronaphthalen-2-yl acetate (catalyst 22a)

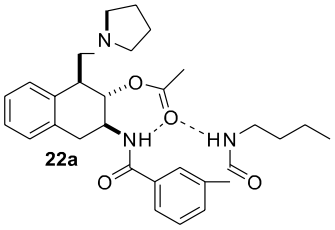

22a

Following the *General Procedure 6 for catalyst acetylation using acetic anhydride* described on page 224, the reaction of catalyst **22** (10 mg, 0.02 mmol) with acetic anhydride (500 μL) yielded compound **22a** (11 mg, quant.) of as a brown oil.

m.p.: oily compound.

IR (nujol, υ in cm^{-1}): 3312, 3053, 2962, 2923, 2858, 2780, 1729, 1651, 1541, 1242, 1139, 1028, 911, 743.

^{1}H NMR (200 MHz, $CDCl_3$) δ 8.48 (br d, *J* = 5.4 Hz, NH), 8.09 (t, *J* = 1.6 Hz, 1H), 7.97 (dt, *J* = 8.1 and 1.6 Hz, 1H), 7.76 (dt, *J* = 8.1 and 1.6 Hz, 1H), 7.45 (t, *J* = 7.7 Hz, 1H), 7.35 – 7.25 (m, 1H), 7.23 – 7.04 (m, 3H), 6.45 (br t, *J* = 5.4 Hz, NH), 5.36 (dd, *J* = 7.3 and 4.8 Hz, 1H), 4.54 – 4.34 (m, 1H), 3.52 – 3.37 (m, 3H), 3.36 – 3.19 (m, 1H), 3.04 – 2.87 (m, 2H), 2.78 (dd, *J* = 12.9 and 6.7 Hz, 1H), 2.53 – 2.37 (m, 2H), 2.36 – 2.21 (m, 2H), 2.04 (s, 3H), 1.65 – 1.31 (m, 8H), 0.94 (t, *J* = 7.2 Hz, 3H).

^{13}C NMR (50 MHz, $CDCl_3$) δ 172.0 (C), 167.2 (C), 166.6 (C), 135.7 (C), 135.3 (C), 135.2 (C), 133.8 (C), 130.5 (CH), 129.5 (CH), 129.2 (CH), 129.0 (CH), 128.5 (CH), 126.8 (CH), 126.6 (CH), 125.3 (CH), 75.2 (CH), 61.6 (CH_2), 55.2 (2 CH_2), 49.1 (CH), 43.5 (CH), 40.0 (CH_2), 33.5 (CH_2), 31.8 (CH_2), 23.6 (2 CH_2), 21.4 (CH_3), 20.3 (CH_2), 13.9 (CH_3).

MS (ESI+): Calculated for $C_{29}H_{38}N_3O_4$: $[M+H]^+$ 492.3, found 492.3.

Methyl 3-((4-chlorophenyl)carbamoyl)benzoate (23)

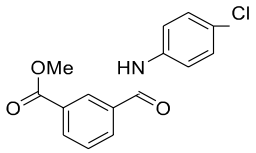

23

Following the *General Procedure 2 for acid activation using PCl_5* described on page 224, the reaction between 3-(methoxycarbonyl)benzoic acid (0.8 g, 4.5 mmol) and PCl_5 (2.0 g, 9.6 mmol) in DCM (20 mL) yielded compound **1** acid chloride, which was used in the next step without further purification.

Following the *General Procedure 4 for amide synthesis using Schotten-Baumann conditions* described on page 224, the reaction between compound **1** acid chloride and *p*-chloroaniline (1.0 g, 7.8 mmol) yielded compound **23** (1.0 g, 81%) as a white solid.

m.p.: 143 – 145ºC.

IR (nujol, υ in cm^{-1}): 3293, 1729, 1658, 1599, 1515, 1242, 827.

^{1}H NMR (200 MHz, DMSO-d_6) δ 10.57 (br s, NH), 8.53 (t, *J* = 1.7 Hz, 1H), 8.23 (d, *J* = 7.8 Hz, 1H), 8.15 (d, *J* = 7.8 Hz, 1H), 7.83 (d, *J* = 8.8 Hz, 2H), 7.68 (t, *J* = 7.8 Hz, 1H), 7.41 (d, *J* = 8.8 Hz, 2H), 3.90 (s, 3H).

^{13}C NMR (50 MHz, DMSO-d_6) δ 165.7 (C), 164.6 (C), 137.9 (C), 135.2 (C), 132.4 (CH), 132.1 (CH), 129.9 (C), 129.0 (CH), 128.5 (2 CH), 128.4 (CH), 127.5 (C), 122.0 (2 CH), 52.4 (CH_3).

MS (ESI+): Calculated for $C_{15}H_{13}ClNO_3$ $[M+H]^+$ 290.1, found 290.0.

3-((4-Chlorophenyl)carbamoyl)benzoic acid (24)

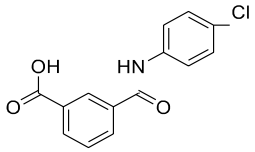

24

A **23** solution (1.0 g, 3.5 mmol) and NaOH (0.3 g, 7.5 mmol) in 60 mL THF:MeOH:H_2O (1:1:1) was refluxed for 2 hours. The reaction mixture was concentrated under reduced pressure and the residue was added over 10 mL of an HCl aqueous 12 M solution, yielding a precipitate which was filtered under reduced pressure. Compound **24** (760 mg, 80%) was obtained as a white solid.

m.p.: > 230ºC.

IR (nujol, υ in cm^{-1}): 3280, 1697, 1638, 1586, 1515, 1457, 1113, 944, 827, 704.

^{1}H NMR (200 MHz, DMSO-d_6) δ 10.57 (br s, NH), 8.54 (s, 1H), 8.19 (d, *J* = 8.0 Hz, 1H), 8.15 (d, *J* = 8.0 Hz, 1H), 7.84 (d, *J* = 8.8 Hz, 2H), 7.66 (t, *J* = 8.0 Hz, 1H), 7.41 (d, *J* = 8.8 Hz, 2H).

^{13}C NMR (50 MHz, DMSO-d_6) δ 166.8 (C), 164.9 (C), 138.0 (C), 135.1 (C), 132.3 (CH), 132.1 (CH), 131.1 (C), 128.9 (CH), 128.6 (3 CH), 127.5 (C), 122.0 (2 CH).

MS (ESI-): Calculated for $C_{14}H_9ClNO_3$ $[M-H]^-$ 274.1, found 273.9.

N^1-(4-Chlorophenyl)-N^3-(3-hydroxy-4-(pyrrolidin-1-ylmethyl)-1,2,3,4-tetrahydronaphthalen-2-yl)isophthalamide (catalyst 25)

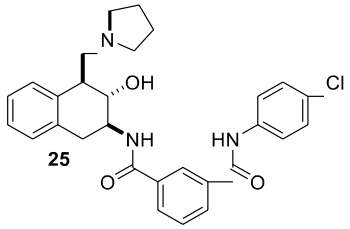

Following the *General Procedure 2 for acid activation using PCl_5* described on page 224, the reaction between compound **24** (400 mg, 1.5 mmol) and PCl_5 (400 mg, 1.9 mmol) in 10 mL of DCM gave 450 mg (quant.) of the acid chloride of **24**, which was used in the next step without further purification.

Following the *General Procedure 4 for amide synthesis using Schotten-Baumann conditions* described on page 224, the reaction between compound **24** acid chloride (450 mg, 1.5 mmol) and compound **20** (300 mg, 1.2 mmol) yielded de crude catalyst **25**. Purification over silica gel column chromatography using MeOH as eluent and activation following the *General Procedure 5 for catalyst activation with NH_3*, described on page 224, afforded the pure catalyst **25** (140 mg, 23 %) as a brown oil.

m.p.: oily compound.

IR (thin layer, υ in cm^{-1}): 3293, 3066, 2936, 1658, 1534, 1489, 1405, 1314, 1249, 1093, 918, 834, 723.

^{1}H NMR (200 MHz, $CDCl_3$) δ 9.38 (br s, NH), 8.57 (s, 1H), 8.01 (d, *J* = 7.8 Hz, NH), 7.89 (d, *J* = 7.8 Hz, 1H), 7.79 (d, *J* = 8.8 Hz, 2H), 7.39 (t, *J* = 7.8 Hz, 1H), 7.26 – 7.00 (m, 6H), 4.47 – 4.26 (m, 1H), 4.09 (dd, *J* = 10.2 and 8.2 Hz, 1H), 3.33 (dd, *J* = 16.2 and 5.0 Hz, 1H), 3.25 – 2.95 (m, 3H), 2.95 – 2.67 (m, 5H), 1.96 – 1.71 (m, 4H).

^{13}C NMR (50 MHz, $CDCl_3$) δ 167.3 (C), 165.7 (C), 137.4 (C), 135.2 (C), 134.8 (C), 134.1 (C), 133.5 (C), 131.5 (CH), 131.1 (CH), 129.7 (CH), 129.2 (C), 129.2 (CH), 129.0 (2 CH), 127.3 (CH), 126.8 (CH), 126.4 (CH), 124.9 (CH), 121.9 (2 CH), 76.7 (CH), 62.1 (CH_2), 54.8 (2 CH_2), 51.9 (CH), 42.8 (CH), 35.8 (CH_2), 23.6 (2 CH_2).

HRMS (ESI+): Calculated for $C_{29}H_{31}ClN_3O_3$ $[M+H]^+$ 504.2048, found 504.2052.

3-(3-((4-Chlorophenyl)carbamoyl)benzamido)-1-(pyrrolidin-1-ylmethyl)-1,2,3,4-tetrahydronaphthalen-2-yl acetate (catalyst 25a)

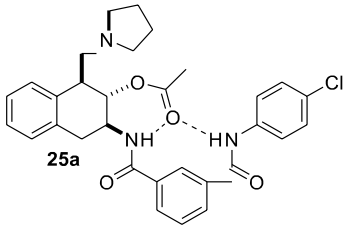

25a

Following the *General Procedure 6 for catalyst acetylation using acetic anhydride* described on page 224, the reaction of catalyst **25** (60 mg, 0.1 mmol) with acetic anhydride (500 μL) yielded compound **25a** (65 mg, quant) as a brown oil.

m.p.: oily compound.

IR (nujol, υ in cm^{-1}): 3299, 2962, 2806, 1736, 1651, 1535, 1314, 1242, 905, 834, 736.

^{1}H NMR (200 MHz, $CDCl_3$) δ 8.94 (br s, NH), 8.65 (br d, *J* = 7.5 Hz, NH), 8.22 (s, 1H), 8.02 (d, *J* = 7.8 Hz, 1H), 7.74 (d, *J* = 7.8 Hz, 1H), 7.67 (d, *J* = 8.9 Hz, 2H), 7.42 (t, *J* = 7.8 Hz, 1H), 7.27 (d, *J* = 8.9 Hz, 2H), 7.34 – 7.11 (m, 3H), 7.08 – 6.96 (m, 1H), 5.31 (dd, *J* = 7.2 and 4.7 Hz, 1H), 4.44 – 4.24 (m, 1H), 3.27 – 3.09 (m, 2H), 2.98 – 2.81 (m, 2H), 2.75 (dd, *J* = 12.9 and 6.6 Hz, 1H), 2.48 – 2.32 (m, 2H), 2.33 – 2.17 (m, 2H), 2.02 (s, 3H), 1.57 – 1.43 (m, 4H).

^{13}C NMR (50 MHz, $CDCl_3$) δ 172.0 (C), 167.3 (C), 165.1 (C), 136.9 (C), 135.5 (C), 135.3 (C), 135.1 (C), 133.5 (C), 130.9 (CH), 130.1 (CH), 129.5 (C), 129.2 (CH), 129.1 (CH), 129.1 (2 CH), 128.5 (CH), 126.8 (CH), 126.7 (CH), 125.6 (CH), 121.7 (2 CH), 75.2 (CH), 61.6 (CH_2), 55.2 (2 CH_2), 49.0 (CH), 43.4 (CH), 33.4 (CH_2), 23.6 (2 CH_2), 21.4 (CH_3).

MS (ESI+): Calculated for $C_{31}H_{33}ClN_3O_4$ $[M+H]^+$ 546.2, found 546.2.

Methyl 6-((4-chlorophenyl)carbamoyl)picolinate (27)

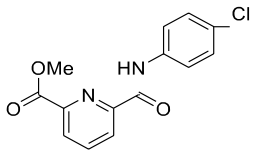

27

Following the *General Procedure 2 for acid activation using PCl_5* described on page 224, the reaction between 3-(methoxycarbonyl)picolinic acid **26** (4.4 g, 24.3 mmol) and PCl_5 (5.5 g, 26.4 mmol) in DCM (50mL) yielded compound **26** acid chloride, which was used in the next step without further purification.

Following the *General Procedure 4 for amide synthesis using Schotten-Baumann conditions* described on page 224, the reaction between compound **26** acid chloride with *p*-chloroaniline (3.1 g, 24.3 mmol) yielded compound **27** (5.0 g, 71%) of as a white solid.

m.p.: 112 – 114ºC.

IR (nujol, υ in cm^{-1}): 3494, 3228, 1736, 1677, 1599, 1534, 1249, 834, 718, 664.

^{1}H NMR (200 MHz, DMSO-d_6) δ 10.51 (br s, NH), 8.36 – 8.20 (m, 3H), 7.89 (d, *J* = 8.9 Hz, 2H), 7.43 (d, *J* = 8.9 Hz, 2H), 3.96 (s, 3H).

^{13}C NMR (50 MHz, DMSO-d_6) δ 164.6 (C), 162.3 (C), 150.4 (C), 146.6 (C), 139.6 (CH), 137.0 (C), 128.6 (2 CH), 127.9 (C), 127.5 (CH), 125.8 (CH), 122.0 (2 CH), 52.8 (CH_3).

MS (ESI+): Calculated for $C_{14}H_{12}ClN_2O_3$ $[M+H]^+$ 291.1, found 291.0.

6-((4-Chlorophenyl)carbamoyl)picolinic acid (28)

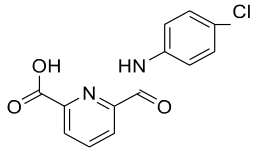

28

A solution of **27** (1.0 g, 3.4 mmol) in MeOH (20 ml) was added over a solution of KOH (0.3 g, 5.4 mmol) in MeOH (10 mL) and 2 mL of H_2O and the reaction mixture was refluxed for 20 minutes. Then, the solvents were concentrated under reduced pressure and the crude reaction mixture was treated with aqueous 12M HCl (10 mL) yielding a precipitate which was filtered under reduced pressure. Compound **28** (420 mg, 44%) was obtained as a white solid.

m.p.: 197 – 199ºC.

IR (nujol, υ in cm^{-1}): 3552, 3474, 3384, 3280, 1697, 1658, 1599, 1534, 1288, 1242, 1087, 847, 730.

^{1}H NMR (200 MHz, DMSO-d_6) δ 11.00 (br s, NH), 8.45 – 8.18 (m, 3H), 7.89 (d, *J* = 8.9 Hz, 2H), 7.46 (d, *J* = 8.9 Hz, 2H).

^{13}C NMR (50 MHz, DMSO-d_6) δ 164.8 (C), 161.6 (C), 149.0 (C), 146.3 (C), 140.2 (CH), 137.0 (C), 128.7 (2 CH), 128.5 (C), 127.1 (CH), 125.9 (CH), 122.3 (2 CH).

MS (ESI-): Calculated for $C_{13}H_8ClN_2O_3$ $[M-H]^-$ 275.0, found 274.9. Calculated for $C_{12}H_8ClN_2O_1$ $[M-H-CO_2]^-$ 231.0, found 230.9.

N^2-(4-Chlorophenyl)-N^6-(3-hydroxy-4-(pyrrolidin-1-ylmethyl)-1,2,3,4-tetrahydronaphthalen-2-yl)pyridine-2,6-dicarboxamide (catalyst 29)

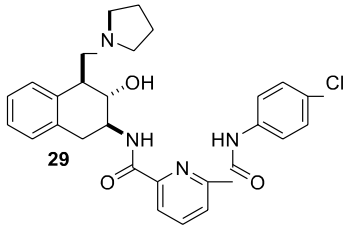

Following the *General Procedure 1 for acid activation using pivaloyl anhydride* described on page 224, the reaction between compound **28** (260 mg, 0.9 mmol), triethylamine (0.5 mL, 3.6 mmol) and pivaloyl chloride (1.0 mL, 8.2 mmol) yielded compound **28** mixed pivaloyl anhydride, which was used in the next step without further purification.

The compound **28** mixed anhydride was added to a solution of compound **20** (240 mg, 1.0 mmol) in 5 mL of EtOAc and was stirred for 5 minutes. The organic phase was washed with a saturated aqueous Na_2CO_3solution (5 mL) and concentrated under reduced pressure. The residue was purified by silica gel column chromatography using MeOH as eluent and activated following the *General Procedure 5 for catalyst activation with NH_3*, described on page 224, affording compound **29** (250 mg, 51%) of as a white solid.

m.p.: 193 – 197ºC.

IR (nujol, υ in cm^{-1}): 3325, 3293, 1690, 1651, 1528.

^{1}H NMR (400 MHz, $CDCl_3$) δ 9.97 (br s, NH), 8.63 (br d, *J* =3.9 Hz, NH), 8.38 (d, *J* = 7.8 Hz, 1H), 8.35 (d, *J* = 7.8 Hz, 1H), 8.04 (t, *J* = 7.8 Hz, 1H), 7.70 (d, *J* =8.7 Hz, 2H), 7.30 (d, *J* = 8.7 Hz, 2H), 7.23 – 7.10 (m, 4H), 4.25 – 4.15 (m, 1H), 4.10 (dd, *J* = 10.4 and 8.6 Hz, 1H), 3.73 (dd, *J* = 16.2 and 4.8 Hz, 1H), 3.31 – 3.16 (m, 2H), 3.10 (t, *J* = 11.2 Hz, 1H), 3.00 – 2.92 (m, 2H), 2.90 (dd, *J* = 16.2 and 11.2 Hz, 1H), 2.76 and 2.65 (m, 2H), 1.95 – 1.81 (m, 4H).

^{13}C NMR (100 MHz, $CDCl_3$) δ 164.0 (C), 161.6 (C), 149.3 (C), 148.6 (C), 139.4 (CH), 136.3 (C), 134.8 (C), 134.3 (C), 129.8 (C), 129.8 (CH), 129.1 (2 CH), 127.1 (CH), 126.7 (CH), 126.6 (CH), 125.3 (CH), 125.1 (CH), 121.9 (2 CH), 77.4 (CH), 62.5 (CH_2), 54.8 (2 CH_2), 52.0 (CH), 42.7 (CH), 35.6 (CH_2), 23.7 (2 CH_2).

HRMS (ESI+): Calculated for $C_{28}H_{30}ClN_4O_3$ $[M+H]^+$ 505.2001, found 505.1983

6-((4-Chlorophenyl)carbamoyl)picolinamido-1-(pyrrolidin-1-ylmethyl)-1,2,3,4-tetrahydronaphthalen-2-yl acetate (catalyst 29a)

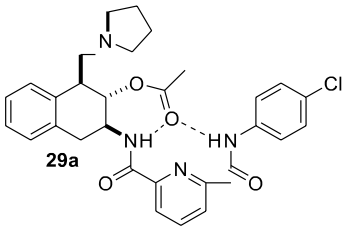

Following the *General Procedure 6 for catalyst acetylation* described on page 224, the reaction of catalyst **29** (100 mg, 0.2 mmol) with 500 μL of acetic anhydride gave compound **29a** (105 mg, quant.) as a white solid.

m.p.: 192 – 196ºC.

IR (nujol, υ in cm^{-1}): 3312, 1735, 1696, 1645, 1521.

^{1}H NMR (400 MHz, $CDCl_3$) δ 10.31 (br s, NH), 8.85 (br d, *J* = 6.8 Hz, NH), 8.47 (dd, *J* = 7.7 and 1.1 Hz, 1H), 8.36 (dd, *J* = 7.7 and 1.1 Hz, 1H), 8.09 (t, *J* = 7.7 Hz, 1H), 8.09 (d, *J* = 8.9 Hz, 2H), 7.46 (d, *J* = 7.5 Hz, 1H), 7.36 (d, *J* = 8.9 Hz, 2H), 7.29 – 7.10 (m, 3H), 5.54 (dd, *J* = 11.2 and 7.7 Hz, 1H), 4.34 (ddt, *J* = 11.5, 7.0 and 4.6 Hz, 1H), 3.47 – 3.33 (m, 2H), 2.90 (dd, *J* = 12.5 and 5.5 Hz, 1H), 2.85 (dd, *J* = 14.3 and 10.8 Hz, 1H), 2.76 (dd, *J* = 12.5 and 7.0 Hz, 1H), 2.63 – 2.53 (m, 2H), 2.53 – 2.43 (m, 2H), 2.07 (s, 3H), 1.84 – 1.71 (m, 4H).

^{13}C NMR (100 MHz, $CDCl_3$) δ 174.4 (C), 163.7 (C), 161.9 (C), 149.1 (C), 148.8 (C), 139.4 (CH), 137.1 (C), 136.9 (C), 133.8 (C), 129.5 (C), 129.0 (2 CH), 129.0 (CH), 128.3 (CH), 126.9 (CH), 126.7 (CH), 125.5 (CH), 125.0 (CH), 121.8 (2 CH), 76.5 (CH), 61.9 (CH_2), 54.8 (2 CH_2), 52.1 (CH), 43.6 (CH), 35.2 (CH_2), 24.0 (2 CH_2), 21.5 (CH_3).

HRMS (ESI+): Calculated for $C_{30}H_{32}ClN_4O_4$ $[M+H]^+$ 547.2107, found 547.2094.

3-(6-((4-Chlorophenyl)carbamoyl)picolinamido)-1-(pyrrolidin-1-ylmethyl)-1,2,3,4-tetrahydronaphthalen-2-yl hydrogen phenylphosphonate (tetrahedral analogue 29b)

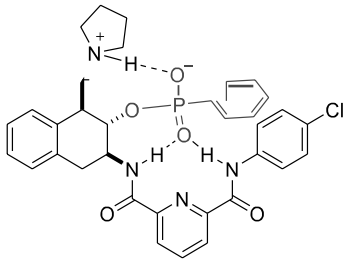

29b

Following the literature,[180] phenyl phosphonic acid (400 mg, 2.5 mmol) was dissolved in DCM (10 mL) and DMF (10 μL). A solution of oxalyl chloride (800 μL, 9.5 mmol) in DCM (5 mL) was added and the reaction mixture was refluxed for 1 hour under Argon atmosphere. The solvent was concentrated under reduced pressure and the obtained phenyl phosphonic dichloride was used without further purification.

The phosphonic dichloride prepared in the previous step (100 mg, 0.5 mmol) was added to a catalyst **29** solution (150 mg, 0.3 mmol) and triethylamine (1 mL, 7.3 mmol) in DCM (1.5 mL). After 5 minutes, the solvent was concentrated under reduced pressure, the residue was dissolved in a 20% H_2O solution in THF (5 mL) and the mixture was refluxed for 5 minutes. The reaction mixture was concentrated under reduce pressure, EtOAc was added to the aqueous phase and the solid was filtered off. Compound **29b** (20 mg, 10 %) was obtained as a white solid.

^{1}H NMR (400 MHz, 5% CD_3OD in $CDCl_3$) δ 8.42 (dt, *J* = 7.8 and 1.4 Hz, 1H), 8.35 (dt, *J* = 7.8 and 1.3 Hz, 1H), 8.05 (t, *J* = 7.8 Hz, 1H), 7.73 (d, *J* = 9.1 Hz, 2H), 7.67 – 7.60 (m, 2H), 7.24 – 7.08 (m, 9H), 5.12 – 4.99 (m, 1H), 4.20 (dt, *J* = 11.0 and 3.9 Hz, 1H), 3.90 – 3.78 (m, 2H), 3.72 – 3.49 (m, 3H), 3.42 – 3.36 (m, 1H), 2.99 – 2.77 (m, 3H), 2.33 – 2.09 (m, 4H).

^{13}C NMR (100 MHz, 5% CD_3OD in $CDCl_3$) δ 165.1 (C), 162.9 (C), 149.6 (C), 149.1 (C), 138.8 (CH), 137.0 (C), 135.6 (2 C), 133.5 (C), 130.6 (d, *J* = 283 Hz, C), 131.3 (CH), 131.0 (d, *J* = 10 Hz, 2 CH), 130.3 (CH), 128.4 (2 CH), 128.2 (d, *J* = 14 Hz, 2 CH), 127.9 (CH), 127.1 (CH), 127.0 (CH), 125.5 (CH), 124.7 (CH), 123.3 (2 CH), 74.3 (d, *J* = 5 Hz, CH), 62.1 (CH_2), 56.0 (CH_2), 52.9 (CH_2), 52.0 (CH), 43.6 (d, *J* = 5 Hz, CH), 35.0 (CH_2), 23.4 (CH_2), 23.1 (CH_2).

MS (ESI+): Calculated for $C_{34}H_{35}ClN_4O_5P$ $[M+H]^+$ 645.2, found 645.2.

[180] Rogers, R. S. *Tetrahedron Lett.* **1992**, *33*, 7473–7474.

5-Bromo-2-naphthoic acid (30)

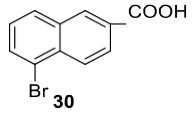

30

To a 2-naphthoic acid solution (11.0 g, 63.9 mmol) in 98% H_2SO_4 (80 mL) at 0ºC, NaBr (4.0 g, 38.9 mmol) was added in portions for 15 minutes. The resulting reaction mixture was stirred under these conditions for one hour and the solid was collected by filtration under reduced pressure and recrystallized in 100 mL of 20% MeOH in DCM. Compound **30** (3.14 g, 32 %) was obtained as a white solid.

m.p.: >230ºC

IR (nujol, υ in cm^{-1}): 1677, 1625, 1554, 1492, 1339, 1301, 1197, 970, 924, 775.

^{1}H NMR (400 MHz, DMSO-d6) δ 8.66 (s, 1H), 8.20 (d, *J* = 8.5 Hz, 1H), 8.18 (d, *J* = 7.5 Hz, 2H), 8.13 (dd, *J* = 8.5, 1.5 Hz, 1H), 8.00 (d, *J* = 7.5 Hz, 1H), 7.52 (t, *J* = 7.5 Hz, 1H).

^{13}C NMR (100 MHz, DMSO-d6) δ 167.0 (C), 133.6 (C), 133.0 (C), 132.3 (CH), 131.1 (CH), 129.7 (CH), 129.1 (C), 127.6 (CH), 127.0 (CH), 126.8 (CH), 121.6 (C).

HRMS (ESI-): Calculated for $C_{11}H_6{}^{79}BrO_2$ $[M-H]^-$ 248.9556, found 248.9555.

5-Bromo-8-(chlorosulfonyl)-2-naphthoic acid (31)

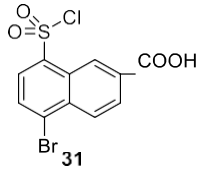

31

Compound **30** (2.0 g, 8.0 mmol) was added to HSO_3Cl (10 mL, 150.2 mmol) at 0ºC and the thus obtained reaction mixture was stirred under these conditions for one hour. Then, the reaction was warmed to 70ºC for 20 minutes, cooled down to room temperature and added to ice (100 g). Compound **31** 2.50 g (90 %) was obtained as a white solid by filtration under reduced pressure.

^{1}H NMR (400 MHz, DMSO-d_6) δ 9.62 (s, 1H), 8.24 (d, *J* = 8.8 Hz, 1H), 8.12 (dd, *J* = 8.8, 1.6 Hz, 1H), 7.97 (d, *J* = 7.8 Hz, 1H), 7.92 (d, *J* = 7.8 Hz, 1H).

5-Bromo-8-(*N*-butylsulfamoyl)-2-naphthoic acid (32)

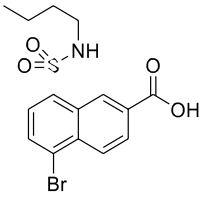

32

Compound **31** (200 mg, 0.6 mmol) was added to butylamine (5 mL, 50.6 mmol). After 5 minutes, the reaction was added to an aqueous 2M HCl solution (40 mL) and extracted with EtOAc (2x30 mL). The organic phase was dried over anhydrous Na_2SO_4, filtered and the solvent was removed under reduced pressure. Compound **32** (156 mg, 71 %) was obtained as a white solid.

m.p.: 174 – 176ºC

IR (nujol, υ in cm^{-1}): 2942, 1697, 1625, 1560, 1515, 1294, 1262, 1200, 1158, 1087, 1041, 950, 898, 840, 762, 639.

^{1}H NMR (400 MHz, DMSO-d_6) δ 9.42 (d, *J* = 1.5 Hz, 1H), 8.40 (d, *J* = 8.9 Hz, 1H), 8.25 (dd, *J* = 8.9, 1.5 Hz, 1H), 8.18 (d, *J* = 7.9 Hz, 1H), 8.17 (br t, *J* = 6.0 Hz, NH), 8.05 (d, *J* = 7.9 Hz, 1H), 2.85 (q, *J* = 6.9 Hz, 2H), 1.32 (quin, *J* = 7.3 Hz, 2H), 1.15 (hex, *J* = 7.3 Hz, 2H), 0.70 (t, *J* = 7.3 Hz, 3H).

^{13}C NMR (100 MHz, DMSO-d6) δ 166.8 (C), 137.6 (C), 133.7 (C), 131.1 (CH), 130.7 (C), 129.0 (CH), 128.2 (C), 128.1 (CH), 127.9 (CH), 127.9 (CH), 127.4 (C), 42.3 (CH_2), 31.2 (CH_2), 19.1 (CH_2), 13.3 (CH_3).

HRMS (ESI-): Calculated for $C_{15}H_{15}{}^{79}BrNO_4S$ $[M-H]^-$ 383.9910, found 383.9912.

5-Bromo-8-(*N*-butylsulfamoyl)-*N*-(-3-hydroxy-4-(pyrrolidin-1-ylmethyl)-1,2,3,4-tetrahydro-naphthalen-2-yl)-2-naphthamide (catalyst 33)

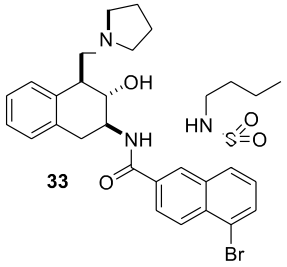

33

Compound **32** (150 mg, 0.39 mmol) was refluxed in $SOCl_2$ (5 mL) for 30 minutes and stirred at room temperature for 2 hours. Then, it was concentrated under reduced pressure to

yield the compound **32** acid chloride (quant.), which was used in the next step without further purification.

The acid chloride of **36** (157 mg, 0.39 mmol) was dissolved in EtOAc (10 mL) and was added over a stirred solution of amine **20** (110 mg, 0.45 mmol) in a mixture of 10 mL EtOAc and 10 mL of an aqueous 4% Na_2CO_3 saturated solution. The acid chloride reaction flask was washed with more of EtOAc (4 mL) and added over the reaction mixture. The reaction mixture was transferred to a separatory funnel. The aqueous phase was extracted with EtOAc, the organic phase was washed with brine, dried over anhydrous Na_2SO_4, filtrated and concentrated under reduced pressure. The crude reaction mixture was purified by silica gel column chromatography using mixtures of MeOH in EtOAc (1-20%) as eluent, yielding compound **33** The compound was then activated following the *General Procedure 5 for catalyst activation with NH_3*, described on page 224, affording catalyst **33** (120 mg, 50%).

m.p.: glassy compound

IR (film, υ in cm^{-1}): 3260, 3072, 2962, 2923, 2858, 1658, 1547, 1495, 1450, 1327, 1203, 1152, 905, 736.

^{1}H NMR (400 MHz, $CDCl_3$) δ 9.06 (d, *J* = 1.1 Hz, 1H), 8.14 (d, *J* = 7.9 Hz, 1H), 8.09 – 8.00 (m, 2H), 7.93 (d, *J* = 7.9 Hz, 1H), 7.45 (br d, *J* = 8.0 Hz, NH), 7.34 – 7.28 (m, 1H), 7.23 – 7.13 (m, 2H), 7.12 – 7.06 (m, 1H), 4.46 – 4.33 (m, 1H), 4.21 (t, *J* = 9.6 Hz, 1H), 3.33 (dd, *J* = 16.1, 4.8 Hz, 1H), 3.27 – 3.17 (m, 2H), 3.10 – 2.84 (m, 6H), 2.69 – 2.55 (m, 2H), 1.95 – 1.81 (m, 4H), 1.48 (quin, *J* = 7.4 Hz, 3H), 1.28 (hex, *J* = 7.4 Hz, 2H), 0.77 (t, *J* = 7.4 Hz, 3H).

^{13}C NMR (100 MHz, $CDCl_3$) δ 166.8 (C), 136.2 (C), 134.8 (C), 134.6 (C), 134.0 (C), 133.6 (C), 130.3 (CH), 129.9 (CH), 129.5 (CH), 128.9 (C), 128.6 (CH), 128.5 (C), 127.0 (CH), 126.8 (CH), 126.7 (2 CH), 123.3 (CH), 77.4 (CH), 62.8 (CH_2), 54.9 (2 CH_2), 51.7 (CH), 43.5 (CH), 43.0 (CH_2), 35.9 (CH_2), 32.3 (CH_2), 23.6 (2 CH_2), 19.9 (CH_2), 13.7 (CH_3).

HRMS (ESI+): Calculated for $C_{30}H_{37}{}^{79}BrN_3O_4S$ $[M+H]^+$ 614.1683, found 614.1677.

3-(5-Bromo-8-(*N*-butylsulfamoyl)-2-naphthamido)-1-(pyrrolidin-1-ylmethyl)-1,2,3,4-tetra-hydronaphthalen-2-yl acetate (catalyst 33a)

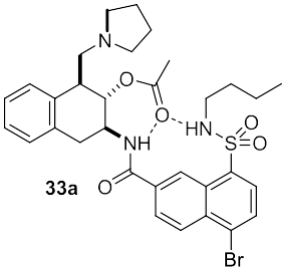

33a

Following the *General Procedure 7 for catalyst acetylation using vinyl acetate* described on page 225, the reaction of catalyst **33** (20 mg, 0.03 mmol) with 500 μL of vinyl acetate gave compound **33a** (16 mg,76 %) as a yellowish oil.

^{1}H NMR (400 MHz, $CDCl_3$) δ 8.77 (s, 1H), 8.45 (d, *J* = 8.8 Hz, 1H), 8.18 (d, *J* = 7.9 Hz, 1H), 8.17 (dd, *J* = 8.8, 1.6 Hz, 1H), 7.94 (d, *J* = 7.9 Hz, 1H), 7.57 (br s, NH), 7.38 (d, *J* = 7.3 Hz, 1H), 7.25 – 7.11 (m, 3H), 6.84 (br s, NH), 5.43 (dd, *J* = 10.2, 6.9 Hz, 1H), 4.46 – 4.35 (m, 1H), 3.44 (dd, *J* = 15.7, 4.6 Hz, 1H), 3.37 (dd, *J* = 12.6, 6.7 Hz, 1H), 3.03 – 2.92 (m, 1H), 2.92 – 2.73 (m, 4H), 2.60 – 2.49 (m, 2H), 2.50 – 2.39 (m, 2H), 2.24 (s, 3H), 1.76 – 1.66 (m, 4H), 1.43 (m, 2H), 1.25 (quin, *J* = 7.6 Hz, 2H), 0.78 (t, *J* = 7.3 Hz, 3H).

^{13}C NMR (100 MHz, $CDCl_3$) δ 175.6 (C), 167.0 (C), 136.4 (2 C), 134.9 (C), 134.1 (C), 133.8 (C), 130.8 (CH), 130.2 (CH), 129.3 (CH), 129.2 (C), 129.0 (CH), 128.6 (C), 128.2 (CH), 127.2 (CH), 126.9 (CH), 126.8 (CH), 122.9 (CH), 77.0 (CH), 62.1 (CH_2), 54.8 (2 CH_2), 51.9 (CH), 43.8 (CH), 42.7 (CH_2), 34.7 (CH_2), 31.9 (CH_2), 23.9 (2 CH_2), 21.6 (CH_3), 19.8 (CH_2), 13.6 (CH_3).

5-Bromo-8-(*N*-(4-dimethylamino)phenyl)sulfamoyl)-2-naphthoic acid (34)

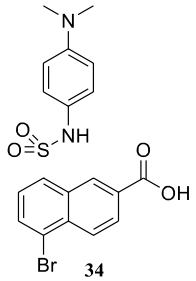

34

Compound **31** (122 mg, 0.35 mmol) and *N*,*N*-dimethyl-*p*-phenylenediamine (78 mg, 0.57 mmol) were mixed in EtOAc (630 μL). The reaction mixture was stirred until a precipitate showed up. Then, the solvent was evaporated under reduced pressure, the crude product was suspended in MeOH-H_2O and the precipitate was collected by filtration yielding compound **34** (50 mg, 32%) which was used without further purification in the next reaction.

m.p.: 214 – 216ºC

IR (nujol, υ in cm^{-1}): 2929, 1690, 1612, 1554, 1521, 1346, 1292, 1246, 1200, 1152, 1048, 989, 905, 847, 756, 697, 639.

^{1}H NMR (400 MHz, DMSO-d_6) δ 10.23 (s, 1H), 9.38 (s, 1H), 8.37 (d, *J* = 8.9 Hz, 1H), 8.23 (dd, *J* = 8.9, 1.4 Hz, 1H), 8.12 (d, *J* = 8.0 Hz, 1H), 7.97 (d, *J* = 8.0 Hz, 1H), 6.75 (d, *J* = 7.9 Hz, 2H), 6.54 (d, *J* = 7.9 Hz, 2H), 2.78 (s, 6H).

^{13}C NMR (100 MHz, DMSO-d_6) δ 166.8 (C), 148.0 (C, broad), 145.7 (C), 136.6 (C), 133.5 (C), 130.9 (CH), 130.8 (C), 130.2 (CH), 128.4 (C), 128.0 (CH), 127.9 (CH), 127.9 (C), 127.8 (CH), 124.3 (2 CH, broad), 113.1 (2 CH, broad), 40.4 (2 CH_3).

HRMS (ESI+): Calculated for $C_{19}H_{18}{}^{79}BrN_2O_4S$ $[M+H]^+$ 449.0166, found 449.0157.

5-Bromo-8-(*N*-(4-(dimethylamino)phenyl)sulfamoyl)-*N*-(-3-hydroxy-4-(pyrrolidin-1-ylmethyl)-1,2,3,4-tetrahydronaphthalen-2-yl)-2-naphthamide (catalyst 35)

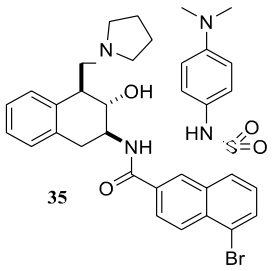

35

The acid **34** (200 mg, 0.45 mmol), amine **20** (110 mg, 0.44 mmol) and DCC (92 mg, 0.45 mmol) were dissolved in DCM (2.5 mL) and left overnight. A ^{1}H NMR spectrum of an aliquot of the reaction mixture showed that the reaction was not finished, therefore more amine **20** (70 mg, 0.28 mmol) was added and the reaction was left overnight again. Next day, ^{1}H NMR analysis showed that the reaction was finished and after silica gel column chromatography using mixtures of MeOH in DCM (0-1.2%) as eluent, compound **35** (30 mg, 10%) was obtained. The compound was activated following the *General Procedure 5 for catalyst activation with NH_3*, described on page 224, affording catalyst **35** (15 mg) as a yellowish oil.

m.p.: glassy compound

IR (film, υ in cm^{-1}): 3306, 3085, 2968, 2929, 2845, 1651, 1547, 1521, 1320, 1145, 944, 749.

^{1}H NMR (400 MHz, $CDCl_3$) δ 9.25 (s, 1H), 8.13 (d, *J* = 8.8 Hz, 1H), 7.98 (br d, *J* = 5.8 Hz, NH), 7.86 (d, *J* = 8.8 Hz, 1H), 7.86 (d, *J* = 7.9 Hz, 1H), 7.72 (d, *J* = 7.9 Hz, 1H), 7.31 – 7.23 (m, 1H), 7.20 – 7.09 (m, 2H), 7.06 (d, *J* = 6.1 Hz, 1H), 6.77 (d, *J* = 9.0 Hz, 2H), 6.38 (d, *J* = 9.0 Hz, 2H), 4.42 – 4.29 (m, 1H), 4.21 (t, *J* = 9.4 Hz, 1H), 3.41 (dd, *J* = 16.1, 4.8 Hz, 1H), 3.26

– 3.09 (m, 2H), 3.09 – 2.98 (m, 1H), 2.90 (dd, *J* = 16.0, 11.4 Hz, 1H), 2.85 – 2.75 (m, 2H), 2.79 (s, 6H), 2.60 – 2.52 (m, 2H), 1.84 – 1.73 (m, 4H).

^{13}C NMR (100 MHz, $CDCl_3$) δ 167.6 (C), 149.1 (C), 135.5 (C), 135.0 (C), 134.8 (C), 134.7 (C), 133.5 (C), 131.1 (CH), 129.9 (CH), 129.9 (CH), 129.3 (CH), 129.1 (C), 128.5 (C), 128.5 (CH), 126.9 (CH), 126.8 (2 CH), 126.5 (CH), 126.0 (CH), 124.6 (C), 124.0 (CH), 112.7 (2 CH), 76.5 (CH), 62.4 (CH_2), 54.9 (2 CH_2), 52.2 (CH), 43.8 (CH), 40.6 (2 CH_3), 35.9 (CH_2), 23.6 (2 CH_2).

HRMS (ESI+): Calculated for $C_{34}H_{38}{}^{79}BrN_4O_4S$ $[M+H]^+$ 677.1792, found 677.1789.

3-(5-Bromo-8-(*N*-(4-(dimethylamino)phenyl)sulfamoyl)-2-naphthamido)-1-(pyrrolidin-1-ylmethyl)-1,2,3,4-tetrahydronaphthalen-2-yl acetate (catalyst 35a)

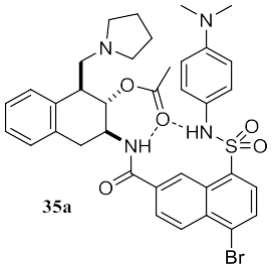

35a

Following the *General Procedure 7 for Catalyst acetylation using vinyl acetate* described on page 225, the reaction of catalyst **35** (15 mg, 0.02 mmol) with 500 μL of vinyl acetate yielded compound **35a** (16 mg, quant.) as a yellowish oil.

^{1}H NMR (400 MHz, $CDCl_3$) δ 8.96 (s, 1H), 8.45 (d, *J* = 8.9 Hz, 1H), 8.22 (dd, *J* = 8.9, 1.5 Hz, 1H), 7.99 (d, *J* = 7.9 Hz, 1H), 7.80 (d, *J* = 7.9 Hz, 1H), 7.74 (br d, *J* = 7.6 Hz, NH), 7.38 (d, *J* = 7.2 Hz, 1H), 7.25 – 7.11 (m, 3H), 6.80 (d, *J* = 9.0 Hz, 2H), 6.45 (d, *J* = 9.0 Hz, 2H), 5.47 (dd, *J* = 10.3, 6.9 Hz, 1H), 4.50 – 4.37 (m, 1H), 3.42 (dd, *J* = 15.7, 4.5 Hz, 1H), 3.38 (dd, *J* = 12.9, 6.6 Hz, 1H), 2.90 (dd, *J* = 15.9, 12.5 Hz, 1H), 2.83 (s, 6H), 2.85 – 2.76 (m, 2H), 2.60 – 2.49 (m, 2H), 2.49 – 2.40 (m, 2H), 2.18 (s, 3H), 1.77 – 1.66 (m, 4H).

^{13}C NMR (100 MHz, $CDCl_3$) δ 175.8 (C), 166.7 (C), 149.2 (C), 136.3 (C), 135.8 (C), 134.8 (C), 133.9 (C), 133.9 (C), 131.6 (CH), 130.2 (CH), 129.3 (CH), 129.3 (C), 129.0 (CH), 128.7 (C), 128.3 (CH), 127.2 (CH), 126.9 (CH), 126.8 (CH), 126.0 (2 CH), 124.4 (C), 122.8 (CH), 112.8 (2 CH), 77.4 (CH), 62.2 (CH_2), 54.9 (2 CH_2), 52.0 (CH), 43.8 (CH), 40.6 (2 CH_3), 34.8 (CH_2), 23.8 (2 CH_2), 21.7 (CH_3).

3-(5-Bromo-8-(*N*-(4-(dimethylamino)phenyl)sulfamoyl)-2-naphthamido)-1-(pyrrolidin-1-ylmethyl)-1,2,3,4-tetrahydronaphthalen-2-yl hydrogen (3-nitrophenyl)phosphonate (tetrahedral analogue 35b)

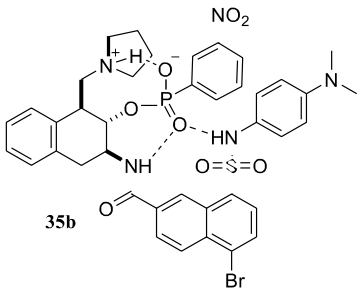

35b

Compound **35b** was prepared following the procedure described in the literature.[181]

5-Bromo-8-(*N*-(*p*-tolyl)sulfamoyl)-2-naphthoic acid (36)

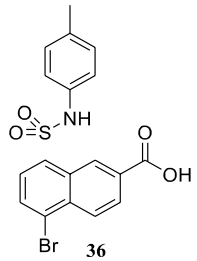

36

Compound **36** was prepared following the same procedure described for the synthesis of compound **34**.

m.p.: 200 – 205ºc

IR (nujol, υ in cm^{-1}): 2916, 1690, 1619, 1560, 1508, 1333, 1301, 1262, 1200, 1145, 937, 900, 847, 756, 692, 631.

^{1}H NMR (400 MHz, DMSO-d_6) δ 10.71 (s, 1H), 9.39 (s, 1H), 8.36 (d, *J* = 8.9 Hz, 1H), 8.23 (dd, *J* = 8.9, 1.4 Hz, 1H), 8.13 (d, *J* = 8.0 Hz, 1H), 8.04 (d, *J* = 8.0 Hz, 1H), 6.96 (d, *J* = 8.2 Hz, 2H), 6.88 (d, *J* = 8.2 Hz, 2H), 2.13 (s, 3H).

^{13}C NMR (100 MHz, DMSO-d_6) δ 166.8 (C), 136.3 (C), 134.5 (C), 133.6 (C), 133.5 (C), 130.9 (CH), 130.9 (C), 130.1 (CH), 129.6 (2 CH), 128.2 (C), 128.2 (C), 128.2 (CH), 128.0 (CH), 127.5 (CH), 120.8 (2 CH), 20.3 (CH_3).

HRMS (ESI-): Calculated for $C_{18}H_{13}{}^{79}BrNO_4S$ $[M-H]^-$ 417.9754, found 417.9754.

[181] Garrido-González, J. J.; Simón, L.; Sanz, F.; Morán, J. R.; Fuentes de Arriba, Á. L. *ACS Catal.* **2020**, *10*, 11162-11170.

5-Bromo-*N*-(3-hydroxy-4-(pyrrolidin-1-ylmethyl)-1,2,3,4-tetrahydronaphthalen-2-yl)-8-(*N*-(*p*-tolyl)sulfamoyl)-2-naphthamide (catalyst 37)

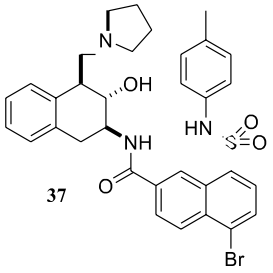

37

Compound **36** (278 mg, 0.66 mmol) was refluxed in $SOCl_2$ (6 mL) for 30 minutes and stirred at room temperature for 2 hours. Then, it was concentrated under reduced pressure to yield the compound **36** acid chloride, which was used in the next step without further purification.

The acid chloride of **36** (311 mg, 0.87 mmol) was dissolved in EtOAc (4 mL) and was added over a stirred solution of amine **20** (270 mg, 1.1 mmol) in a mixture of 4 mL EtOAc and 8 mL of an aqueous $NaHCO_3$ saturated solution. The acid chloride reaction flask was washed with more of EtOAc (4 mL) and added over the reaction mixture. After 90 minutes a solid appeared in the reaction mixture and DCM (5 mL) was added. The reaction mixture wasstirred 30 minutes more and then was transferred to a separatory funnel. The aqueous phase was extracted with EtOAc, the organic phase was washed with brine, dried over anhydrous Na_2SO_4, filtrated and concentrated under reduced pressure. The crude reaction mixture was purified by silica gel column chromatography using mixtures of MeOH in EtOAc (1-20%) aseluent, yielding compound **37 (**90 mg, 16 %). The compound was then activated following the*General Procedure 5 for catalyst activation with NH_3*, described on page 224, affording 62 mg of catalyst **37**.

m.p.: glassy compound

IR (film, υ in cm^{-1}): 3351, 3286, 3092, 2968, 2923, 2858, 1645, 1547, 1508, 1456, 1333, 1158, 1054, 924, 749.

^{1}H NMR (400 MHz, $CDCl_3$) δ 9.20 (s, 1H), 8.01 (d, *J* = 8.0 Hz, 1H), 7.97 (d, *J* = 8.9 Hz, 1H), 7.93 (br d, *J* = 6.0 Hz, NH), 7.85 (d, *J* = 8.9 Hz, 1H), 7.76 (d, *J* = 8.0 Hz, 1H), 7.34 (d, *J* = 6.9 Hz, 1H), 7.22 – 7.11 (m, 2H), 7.08 (d, *J* = 6.7 Hz, 1H), 6.87 (d, *J* = 8.9 Hz, 2H), 6.84 (d, *J* = 8.9 Hz, 2H), 4.43 – 4.32 (m, 1H), 4.26 (dd, *J* = 10.2, 8.2 Hz, 1H), 3.43 (dd, *J* = 16.0, 4.7 Hz, 1H), 3.24 – 3.12 (m, 2H), 3.03 (dd, *J* = 12.7, 11.0 Hz, 1H), 2.91 (dd, *J* = 16.0, 11.0 Hz, 1H), 2.83 – 2.73 (m, 2H), 2.66 – 2.53 (m, 2H), 2.14 (s, 3H), 1.81 – 1.70 (m, *J* = 23.1 Hz, 4H).

^{13}C NMR (100 MHz, $CDCl_3$) δ 167.7 (C), 135.7 (C), 135.1 (C), 134.9 (C), 134.7 (C), 134.7 (C), 133.7 (C), 133.4 (C), 131.4 (CH), 130.0 (CH), 129.8 (2 CH), 129.4 (C), 129.3 (CH), 128.3

(C), 128.3 (CH), 127.1 (CH), 126.8 (CH), 126.6 (CH), 126.6 (CH), 123.9 (CH), 121.8 (2 CH), 75.7 (CH), 62.0 (CH_2), 54.9 (2 CH_2), 52.7 (CH), 44.6 (CH), 36.0 (CH_2), 23.6 (2 CH_2), 20.9 (CH_3).

HRMS (ESI+): Calculated for $C_{33}H_{35}^{79}BrN_3O_4S$ $[M+H]^+$ 648.1526, found 648.1520.

3-(5-Bromo-8-(*N*-(*p*-tolyl)sulfamoyl)-2-naphthamido)-1-(pyrrolidin-1-ylmethyl)-1,2,3,4-tetrahydronaphthalen-2-yl acetate (catalyst 37a)

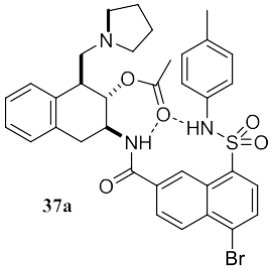

37a

Following the *General Procedure 7 for catalyst acetylation using vinyl acetate* described on page 225, the reaction of catalyst **37** (20 mg, 0.03 mmol) with 500 μL of vinyl acetate gave compound **37a** (21 mg, quant.) as a yellowish oil.

^{1}H NMR (400 MHz, $CDCl_3$) δ 8.89 (s, 1H), 8.41 (d, *J* = 8.8 Hz, 1H), 8.17 (dd, *J* = 8.8, 1.5 Hz, 1H), 8.13 (d, *J* = 8.0 Hz, 1H), 7.85 (d, *J* = 8.0 Hz, 1H), 7.68 (br d, *J* = 5.7 Hz, NH), 7.38 (d, *J* = 7.4 Hz, 1H), 7.25 – 7.09 (m, 3H), 6.94 (d, *J* = 8.7 Hz, 2H), 6.91 (d, *J* = 8.7 Hz, 2H), 5.50 (dd, *J* = 10.5, 6.9 Hz, 1H), 4.48 – 4.37 (m, 1H), 3.45 (dd, *J* = 15.7, 4.5 Hz, 1H), 3.39 (dd, *J* = 12.6, 6.7 Hz, 1H), 2.94 – 2.83 (m, 2H), 2.79 (dd, *J* = 12.4, 7.7 Hz, 1H), 2.62 – 2.51 (m, 2H), 2.50 – 2.40 (m, 2H), 2.27 (s, 3H), 2.20 (s, 3H), 1.78 – 1.67 (m, 4H).

^{13}C NMR (100 MHz, $CDCl_3$) δ 176.2 (C), 166.8 (C), 136.3 (C), 135.5 (C), 135.0 (2 C), 134.0 (C), 133.9 (C), 133.8 (C), 131.7 (CH), 130.1 (CH), 129.9 (2 CH), 129.8 (C), 129.4 (CH), 129.0 (CH), 128.6 (C), 128.2 (CH), 127.3 (CH), 126.9 (CH), 126.8 (CH), 122.6 (CH), 121.4 (2 CH), 77.3 (CH), 62.3 (CH_2), 54.9 (2 CH_2), 52.1 (CH), 43.8 (CH), 34.7 (CH_2), 23.9 (2 CH_2), 21.8 (CH_3), 20.9 (CH_3).

5-Bromo-8-(N-(4-chlorophenyl)sulfamoyl)-2-naphthoic acid (38)

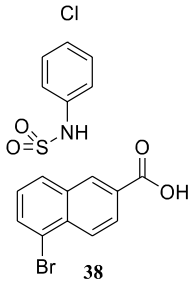

38

Compound **31** (200 mg, 0.63 mmol) and *p*-chloroaniline (97 mg, 0.76 mmol) were mixed with *N,N'*-dimethylaniline (1 mL). The reaction mixture was stirred for 3 hours. Then, it was added over a 30 mL of aqueous 4% HCl, extracted with EtOAC, washed with aqueous 4% HCl, dried over anhydrous Na_2SO_4, filtered and evaporated under reduced pressure. Then, the crude was triturated in DCM, collected by filtration and washed with DCM, yielding compound **38** (134 mg, 48%) which was used without further purification in the next reaction.

m.p.: >230ºC

IR (nujol, υ in cm^{-1}): 1690, 1632, 1567, 1495, 1340, 1301, 1262, 1203, 1145, 1093, 931, 847, 749, 730, 692, 646.

^{1}H NMR (400 MHz, DMSO-d_6) δ 11.06 (s, 1H), 9.37 (s, 1H), 8.38 (d, *J* = 8.8 Hz, 1H), 8.24 (dd, *J* = 8.8, 1.3 Hz, 1H), 8.15 (d, *J* = 8.0 Hz, 1H), 8.08 (d, *J* = 8.0 Hz, 1H), 7.24 (d, *J* = 8.8 Hz, 2H), 7.03 (d, *J* = 8.8 Hz, 2H).

^{13}C NMR (100 MHz, DMSO-d_6) δ 166.7 (C), 136.2 (C), 135.9 (C), 133.6 (C), 131.1 (C), 131.0 (CH), 130.3 (CH), 129.2 (2 CH), 128.5 (C), 128.4 (C), 128.3 (CH), 128.1 (CH), 128.0 (C), 127.2 (CH), 121.8 (2 CH).

HRMS (ESI-): Calculated for $C_{17}H_{10}{}^{79}Br^{35}ClNO_4S$ $[M-H]^-$ 437.9207, found 437.9209.

5-Bromo-8-(*N*-(4-chlorophenyl)sulfamoyl)-*N*-(3-hydroxy-4-(pyrrolidin-1-ylmethyl)-1,2,3,4-tetrahydronaphthalen-2-yl)-2-naphthamide (catalyst 39)

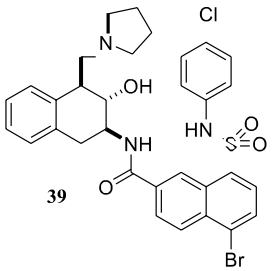

39

Compound **38** (96 mg, 0.22 mmol) was refluxed in $SOCl_2$ (5 mL) for 45 minutes. Then, it was cooled down to room temperature and evaporated under reduced pressure to yield the acid chloride of **38** quantitatively, which was used in the next step without further purification.

The compound **38** acid chloride (100 mg, 0.22 mmol) was dissolved in EtOAc (2.2 mL) and added over a stirred solution of amine **20** (78 mg, 0.32 mmol) in a mixture of 5.5 mL EtOAc and 5.5 mL of an aqueous saturated solution of Na_2CO_3. The acid chloride reaction flask was washed with more EtOAc (2.25 mL) and added over the reaction mixture. After 50 minutes the aqueous phase was extracted with EtOAc, dried over anhydrous Na_2SO_4, filtered and concentrated under reduced pressure. The crude reaction mixture was purified by silica gel column chromatography using mixtures of MeOH in EtOAc (0-25%) as eluent, yielding compound **39** (120 mg, 82 %). The compound was activated following the *General Procedure 5 for catalyst activation with NH_3*, described on page 224, affording catalyst **39** (50 mg).

m.p.: glassy compound

IR (film, υ in cm^{-1}): 3416, 3098, 2981, 2929, 2852, 1651, 1560, 1482, 1333, 1288, 1171, 1106, 918, 834, 736.

^{1}H NMR (400 MHz, $CDCl_3$) δ 9.19 (s, 1H), 8.09 (br s, NH), 8.02 (d, *J* = 8.0 Hz, 1H), 7.89 (d, *J* = 7.2 Hz, 1H), 7.81 – 7.74 (m, 1H), 7.78 (d, *J* = 8.0 Hz, 1H), 7.34 (d, *J* = 7.0 Hz, 1H), 7.18 (t, *J* = 7.0 Hz, 1H) 7.14 (t, *J* = 7.0 Hz, 1H), 7.05 (d, *J* = 7.0 Hz, 1H), 6.97 (d, *J* = 8.6 Hz, 2H), 6.93 (d, *J* = 8.6 Hz, 2H), 4.47 – 4.33 (m, 1H), 4.32 (dd, *J* = 10.0, 8.3 Hz, 1H), 3.36 (dd, *J* = 15.7, 4.2 Hz, 1H), 3.26 – 3.11 (m, 2H), 3.03 (dd, *J* = 12.0, 9.9 Hz, 1H), 2.93 (dd, *J* = 15.7, 12.0 Hz, 1H), 2.82 – 2.72 (m, 2H), 2.66 – 2.55 (m, 2H), 1.73 (s, 4H).

^{13}C NMR (100 MHz, $CDCl_3$) δ 167.8 (C), 135.7 (2 C), 135.0 (C), 134.6 (C), 134.5 (C), 133.3 (C), 131.3 (CH), 130.1 (C), 130.0 (CH), 129.6 (C), 129.3 (2 CH), 129.2 (CH), 128.2 (CH), 128.1 (C), 127.3 (CH), 126.8 (CH), 126.7 (CH), 126.4 (CH), 124.0 (CH), 122.4 (2 CH), 75.4 (CH), 61.9 (CH_2), 54.9 (2 CH_2), 52.7 (CH), 44.9 (CH), 35.9 (CH_2), 23.6 (2 CH_2).

HRMS (ESI+): Calculated for $C_{32}H_{32}{}^{79}Br^{35}ClN_3O_4S$ $[M+H]^+$ 668.0980, found 668.0971.

3-(5-Bromo-8-(*N*-(4-chlorophenyl)sulfamoyl)-2-naphthamido)-1-(pyrrolidin-1-ylmethyl)-1,2,3,4-tetrahydronaphthalen-2-yl acetate (catalyst 39a)

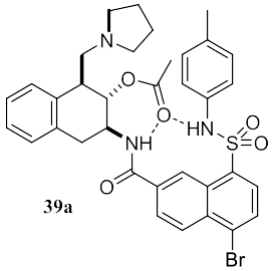

39a

Following the *General Procedure 7 for catalyst acetylation using vinyl acetate* described on page 225, the reaction of catalyst **39** (30 mg, 0.05 mmol) with 500 μL of vinyl acetate gave compound **39a** (32 mg, quant.) as a yellowish oil.

^{1}H NMR (400 MHz, $CDCl_3$) δ 8.84 (s, 1H), 8.42 (d, *J* = 8.8 Hz, 1H), 8.16 (d, *J* = 8.8 Hz, 1H), 8.16 (d, *J* = 8.0 Hz, 2H), 7.89 (d, *J* = 8.0 Hz, 1H), 7.67 (br s, NH), 7.37 (d, *J* = 7.3 Hz, 1H), 7.24 – 7.08 (m, 4H), 7.00 (d, *J* = 7.8 Hz, 2H), 5.51 (t, *J* = 8.0 Hz, 1H), 4.49 – 4.34 (m, 1H), 3.55 – 3.34 (m, 2H), 2.96 – 2.76 (m, 3H), 2.64 – 2.53 (m, 2H), 2.53 – 2.42 (m, 2H), 2.31 (s, 3H), 1.80 – 1.69 (m, 4H).

^{13}C NMR (100 MHz, $CDCl_3$) δ 176.6 (C), 166.9 (C), 136.1 (C), 135.3 (C), 135.2 (C), 135.0 (C), 134.0 (C), 133.7 (C), 131.8 (CH), 130.2 (C), 130.2 (C), 130.1 (CH), 129.5 (2 CH), 129.0 (CH), 128.5 (C), 128.2 (CH), 127.4 (CH), 127.0 (CH), 126.9 (CH), 126.8 (CH), 122.4 (CH), 121.7 (2 CH), 77.4 (CH), 62.3 (CH_2), 54.9 (2 CH_2), 52.1 (CH), 43.8 (CH), 34.7 (CH_2), 23.8 (2 CH_2), 21.9 (CH_3).

4,7-Dibromo-3-hydroxy-2-naphthoic acid (40)

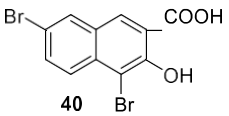

40

3-Hydroxy-2-naphthoic acid (20.4 g, 108.6 mmol) was dissolved in acetic acid and heated to reflux under stirring. When the solid is completely dissolved, bromine (14.5 mL, 282.9 mmol) was added dropwise and the reaction is stirred under reflux for 2 hours. Then the reaction mixture was added over water, the solid is collected by filtration, washed with water and purified by recrystallization in acetic acid, yielding compound **40** (21 g, 56%).

m.p.: >230ºC

IR (nujol, υ in cm^{-1}): 3246, 1671, 1615, 1327, 1281, 1197, 1152, 1067, 931, 808, 749, 632.

^{1}H NMR (400 MHz, DMSO-d_6) δ 8.60 (s, 1H), 8.36 (d, *J* = 2.0 Hz, 1H), 7.94 (d, *J* = 9.1 Hz, 1H), 7.80 (dd, *J* = 9.1, 2.0 Hz, 1H).

^{13}C NMR (100 MHz, DMSO-d_6) δ 171.2 (C), 153.8 (C), 133.7 (C), 133.4 (CH), 131.6 (CH), 131.5 (CH), 128.2 (C), 127.1 (CH), 117.4 (C), 116.4 (C), 105.5 (C).

HRMS (ESI-): Calculated for $C_{11}H_5{}^{79}Br^{81}BrO_3$ $[M-H]^-$ 344.8590, found 344.8589.

4,7-Dibromo-8-(chlorosulfonyl)-3-hydroxy-2-naphthoic acid (41)

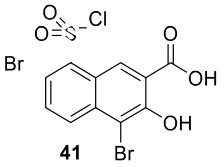

41

Compound **40** (340 mg, 0.98 mmol) was dissolved in chlorosulfonic acid (8 mL) and PCl_5 (300 mg, 1.44 mmol) was added. The reaction mixture was heated at 79ºC form 30 minutes and then cooled down to room temperature and added over ice. The precipitate was collected by filtration yielding compound **41** (300 mg, 69%) as a yellow solid. This compound was used in the next step without further purification.

^{1}H NMR (400 MHz, DMSO-d_6) δ 10.17 (s, 1H), 7.92 (d, *J* = 9.1 Hz, 1H), 7.83 (d, *J* = 9.1 Hz, 1H).

4,7-Dibromo-8-(*N*-butylsulfamoyl)-3-hydroxy-2-naphthoic acid (42)

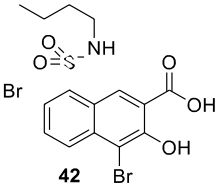

42

Butylamine (5 mL, 50.6 mmol) was added over a stirred solution of compound **41** (300 mg, 0.67 mmol) in EtOAc (50 mL). After 30 minutes the reaction mixture was transferred to a separatory funnel and washed with an 5% HCl aqueous solution, dried over anhydrous Na_2SO_4, filtered and concentrated under reduced pressure yielding compound **42** (302 mg, 94%) as a yellow solid, which was used in the next step without further purification.

m.p.: 218 – 222ºC

IR (neat, υ in cm^{-1}): 3448, 3280, 2910, 2845, 1677, 1346, 1288, 1158, 1106, 970.

^{1}H NMR (400 MHz, DMSO-d_6) δ 9.89 (s, 1H), 8.20 (d, J = 9.2 Hz, 1H), 8.18 (br t, J = 5.7 Hz, NH), 8.02 (d, J = 9.2 Hz, 1H), 2.87 (q, J = 7.3 Hz, 2H), 1.30 (quin, J = 7.3 Hz, 2H), 1.14 (hex, J = 7.3 Hz, 2H), 0.69 (t, J = 7.3 Hz, 3H).

^{13}C NMR (100 MHz, DMSO-d_6) δ 171.2 (C), 154.2 (C), 137.2 (C), 136.6 (CH), 135.1 (C), 130.7 (CH), 129.8 (CH), 125.0 (C), 120.0 (C), 116.9 (C), 106.5 (C), 42.0 (CH_2), 31.0 (CH_2), 19.1 (CH_2), 13.3 (CH_3).

HRMS (ESI-): Calculated for $C_{15}H_{14}{}^{79}Br^{81}BrNO_5S$ $[M-H]^-$ 479.8944, found 479.8944.

4-Bromo-8-(*N*-butylsulfamoyl)-3-hydroxy-2-naphthoic acid (43)

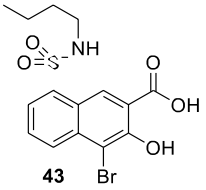

43

Zn (70 g, 1.1 mol) was added over a compound **42** solution (280 mg, 0.58 mmol) in acetic acid (25 mL). The reaction mixture was heated at 60ºC for 30 minutes. Then, it was cooled down to room temperature and the precipitate was filtered. The filtrate was concentrated under reduced pressure yielding compound **43** (270 mg, quant.) as a yellow solid which was used in the next step without further purification.

m.p.: 178 – 180ºC

IR (neat, υ in cm^{-1}): 3552, 3299, 3182, 2949, 2923, 2865, 1671, 1489, 1417, 1313, 1126, 1108, 985, 862, 800.

^{1}H NMR (400 MHz, DMSO-d_6) δ 9.41 (s, 1H), 8.36 (dd, J = 8.6, 0.9 Hz, 1H), 8.06 (br t, J = 5.7 Hz, NH), 8.02 (dd, J = 7.3, 0.9 Hz, 1H), 7.83 (dd, J = 8.6, 7.3 Hz, 1H), 2.85 (q, J = 7.2 Hz, 2H), 1.32 (quin, J = 7.2 Hz, 2H), 1.17 (hex, J = 7.2 Hz, 2H), 0.72 (t, J = 7.2 Hz, 3H).

^{13}C NMR (100 MHz, DMSO-d_6) δ 171.2 (C), 154.3 (C), 138.2 (C), 136.0 (C), 130.3 (CH), 129.1 (CH), 128.9 (CH), 126.3 (CH), 121.7 (C), 116.9 (C), 106.6 (C), 42.3 (CH_2), 31.3 (CH_2), 19.1 (CH_2), 13.4 (CH_3).

HRMS (ESI+): Calculated for $C_{15}H_{16}{}^{79}BrNO_5SNa$ $[M+Na]^+$ 423.9825, found 423.9819.

4-Bromo-8-(*N*-butylsulfamoyl)-3-hydroxy-*N*-(3-hydroxy-4-(pyrrolidin-1-ylmethyl)-1,2,3,4-tetrahydronaphthalen-2-yl)-2-naphthamide (catalyst 44)

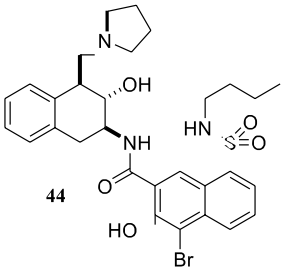

44

Compound **43** (250 mg, 0.62 mmol) was refluxed in $SOCl_2$ (7 mL) for 25 minutes and then concentrated under reduced pressure to yield compound **43** acid chloride, which was used in the next step without further purification.

A solution of amine **20** (175 mg, 0.71 mmol) in EtOAc (20 mL) was added over compound **43** acid chloride (220 mg, 0.52 mmol) in EtOAc (15 mL) with a saturated $NaHCO_3$ aqueous solution (10 mL). The reaction mixture was stirred for 1 hour and then transferred to a separatory funnel. The organic phase was added over anhydrous Na_2SO_4, filtered and concentrated under reduced pressure. The crude reaction mixture was purified by silica gel column chromatography using 2.5% MeOH in DCM as eluent, yielding catalyst **44** (100 mg, 30 %) as a yellow solid. Compound **44** (30 mg) was then activated following the *General Procedure 5 for catalyst activation with NH_3*, described on page 224, affording 9 mg of catalyst **44**.

m.p.: glassy compound

IR (film, υ in cm^{-1}): 3228, 3072, 2962, 2923, 2865, 1625, 1580, 1469.

^{1}H NMR (400 MHz, CD_3OD) δ 9.19 (s, 1H), 8.27 (d, *J* = 8.7 Hz, 1H), 7.83 (dd, *J* = 7.2, 1.0 Hz, 1H), 7.47 (dd, *J* = 8.7, 7.2 Hz, 1H), 7.36 (d, *J* = 7.0 Hz, 1H), 7.24 – 7.13 (m, 3H), 4.37 (dt, *J* = 10.0, 5.0 Hz, 1H), 4.01 (t, *J* = 10.0 Hz, 1H), 3.73 – 3.63 (m, 1H), 3.51 – 3.41 (m, 1H), 3.41 – 3.33 (m, 4H), 3.22 (dd, *J* = 16.2, 4.8 Hz, 1H), 2.95 (dd, *J* = 15.8, 11.4 Hz, 1H), 2.78 (dt, *J* = 6.9, 1.8 Hz, 2H), 2.10 – 1.99 (m, 4H), 1.36 – 1.11 (m, 4H), 0.71 (t, *J* = 7.3 Hz, 3H).

^{13}C NMR (100 MHz, CD_3OD) δ 170.8 (C), 163.8 (C), 138.1 (C), 137.9 (C), 136.2 (C), 134.8 (C), 131.6 (CH), 130.3 (CH), 128.3 (CH), 128.2 (CH), 127.9 (CH), 127.4 (CH), 127.1 (CH), 125.6 (CH), 125.1 (C), 120.1 (C), 112.9 (C), 77.3 (CH), 62.4 (CH_2), 56.3 (2 CH_2), 52.8 (CH), 44.7 (CH), 43.6 (CH_2), 36.4 (CH_2), 32.7 (CH_2), 24.2 (2 CH_2), 20.6 (CH_2), 13.8 (CH_3).

HRMS (ESI+): Calculated for $C_{30}H37^{79}BrN_3O_5S$ $[M+H]^+$ 630.1632, found 630.1627.

3-(4-Bromo-8-(*N*-butylsulfamoyl)-3-hydroxy-2-naphthamido)-1-(pyrrolidin-1-ylmethyl)-1,2,3,4-tetrahydronaphthalen-2-yl acetate (catalyst 44a)

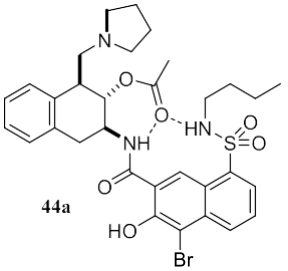

44a

Following the *General Procedure 7 for catalyst acetylation using vinyl acetate* described on page 225, the catalyst **44** reaction (9 mg, 0.01 mmol) with 500 μL of vinyl acetate gave compound **44a** (10.1 mg, quant.) as a yellowish oil.

^{1}H NMR (400 MHz, $CDCl_3$) δ 8.77 (s, 1H), 8.46 (d, *J* = 8.6 Hz, 1H), 8.20 (d, *J* = 7.1 Hz, 1H), 7.65 (dd, *J* = 8.6, 7.1 Hz, 1H), 7.35 (d, *J* = 7.2 Hz, 1H), 7.25 – 7.13 (m, 3H), 6.89 (br d, *J* = 7.4 Hz, NH), 5.53 (dd, *J* = 9.3, 7.3 Hz, 1H), 4.38 (dt, *J* = 11.3, 4.4 Hz, 1H), 3.49 – 3.24 (m, 3H), 3.01 – 2.78 (m, 4H), 2.68 – 2.58 (m, 2H), 2.58 – 2.43 (m, 2H), 2.19 (s, 3H), 1.84 – 1.70 (m, 4H), 1.45 – 1.34 (m, 2H), 1.29 – 1.16 (m, 2H), 0.77 (t, *J* = 7.3 Hz, 3H).

^{13}C NMR (100 MHz, $CDCl_3$) δ 175.5 (C), 169.4 (C), 154.7 (C), 136.8 (C), 136.4 (C), 135.9 (C), 133.6 (C), 131.6 (CH), 129.1 (CH), 128.7 (CH), 128.2 (CH), 128.0 (CH), 127.2 (CH), 127.1 (CH), 123.3 (CH), 122.0 (C), 118.3 (C), 109.1 (C), 77.4 (CH), 61.9 (CH_2), 54.9 (2 CH_2), 52.4 (CH), 43.8 (CH), 42.7 (CH_2), 34.3 (CH_2), 31.9 (CH_2), 23.8 (2 CH_2), 21.6 (CH_3), 19.8 (CH_2), 13.6 (CH_3).

8-(Chlorosulfonyl)-3-hydroxy-7-methoxy-2-naphthoic acid (45)

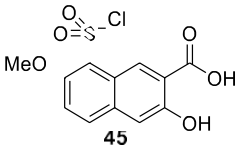

45

Sodium 3-hydroxy-7-methoxy-2-naphthoate (5.0 g, 20.8 mmol) was suspended in DCM (30 mL) at 0ºC and chlorosulfonic acid (15 mL, 225.3 mmol) was added dropwise with stirring. After 1 hour the reaction was poured slowly (very exothermic) over ice. EtOAc was added and the organic phase was separated, dried over anhydrous Na_2SO_4, filtrated and evaporated under reduced pressure yielding compound **62** (5.6 g, 85 %) as a green solid which was used without further purification in the next reaction.

^{1}H NMR (400 MHz, DMSO-d_6) δ 9.93 (s, 1H), 7.75 (d, J = 9.1 Hz, 1H), 7.42 (d, J = 9.1 Hz, 1H), 7.22 (s, 1H), 3.82 (s, 3H).

8-(*N*-Butylsulfamoyl)-3-hydroxy-7-methoxy-2-naphthoic acid (46)

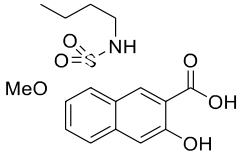

46

Compound **45** (390 mg, 1.29 mmol) was added portion wise over $BuNH_2$ (4.5 mL) at 0ºC. The reaction mixture was stirred for 30 minutes. Then, it was added over 50 mL of an aqueous 4% HCl solution with ice. The precipitate was collected by filtration yielding compound **46** (255 mg, 58%) as a brown solid which was used without further purification in the next reaction.

m.p.: >230ºC

IR (nujol, υ in cm^{-1}): 3306, 2929, 1677, 1606, 1521, 1333, 1262, 1165, 1126, 989, 911, 860, 795, 754, 671.

^{1}H NMR (400 MHz, DMSO-d_6) δ 9.71 (s, 1H), 8.06 (d, J = 9.3 Hz, 1H), 7.66 (d, J = 9.3 Hz, 1H), 7.39 (s, 1H), 7.36 (br t, J = 6.0 Hz, NH), 4.03 (s, 3H), 2.78 (q, J = 7.3 Hz, 2H), 1.35 (quin, J = 7.3 Hz, 2H), 1.21 (hex, J = 7.3 Hz, 2H), 0.75 (t, J = 7.3 Hz, 3H).

^{13}C NMR (100 MHz, DMSO-d_6) δ 171.6 (C), 154.4 (C), 154.4 (C), 133.2 (C), 133.2 (CH), 128.8 (CH), 123.6 (C), 121.5 (C), 117.6 (CH), 116.9 (C), 112.0 (CH), 57.2 (CH_3), 42.4 (CH_2), 31.0 (CH_2), 19.3 (CH_2), 13.5 (CH_3).

HRMS (ESI-): Calculated for $C_{16}H_{18}NO_6S$ $[M-H]^-$ 352.0860, found 352.0858.

8-(*N*-Butylsulfamoyl)-3,7-dihydroxy-2-naphthoic acid (47)

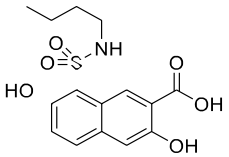

47

Compound **47** was prepared following the same procedure as compound **50**.

m.p.: 200 – 203ºC

IR (nujol, υ in cm^{-1}): 3280, 2942, 1690, 1619, 1567, 1534, 1405, 1197, 1145, 1100, 1077, 931, 866, 801, 723, 684.

^{1}H NMR (400 MHz, DMSO-d_6) δ 10.84 (br s, Ar-OH), 9.32 (s, 1H), 7.93 (d, *J* = 9.0 Hz, 1H), 7.77 (br t, *J* = 6.0 Hz, NH), 7.36 (s, 1H), 7.28 (d, *J* = 9.0 Hz, 1H), 2.80 (q, *J* = 7.2 Hz, 2H), 1.31 (quin, *J* = 7.2 Hz, 2H), 1.15 (hex, *J* = 7.2 Hz, 2H), 0.69 (t, *J* = 7.2 Hz, 3H).

^{13}C NMR (101 MHz, DMSO-d_6) δ 171.6 (C), 154.6 (C), 154.2 (C), 133.7 (CH), 133.0 (C), 127.8 (CH), 122.6 (C), 122.5 (CH), 116.4 (C), 115.1 (C), 112.7 (CH), 42.0 (CH_2), 30.8 (CH_2), 19.1 (CH_2), 13.4 (CH_3).

HRMS (ESI+): Calculated for $C_{15}H_{17}NO_6SNa$ $[M+Na]^+$ 362.0669, found 362.0665.

8-(*N*-Butylsulfamoyl)-3,7-dihydroxy-*N*-(3-hydroxy-4-(pyrrolidin-1-ylmethyl)-1,2,3,4-tetrahydronaphthalen-2-yl)-2-naphthamide (catalyst 48)

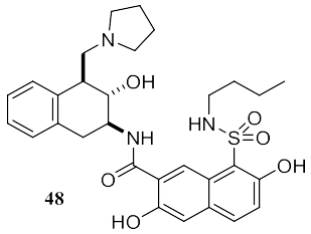

48

Compound **47** (235 mg, 0.69 mmol) was refluxed in $SOCl_2$ (5 mL) for 20 minutes and then concentrated under reduced pressure to yield compound **47** acid chloride, which was used in the next step without further purification.

The compound **47** acid chloride (302 mg, 0.69 mmol) was dissolved in 4 mL of EtOAc and added over a stirred solution of amine **20** (180 mg, 0.73 mmol) in a mixture of 3 mL EtOAc and 6 mL of an aqueous saturated solution of $NaHCO_3$. The acid chloride reaction flask was washed with 1 mL more of EtOAc and added over the reaction mixture. After 45 minutes the aqueous phase was extracted with EtOAc, dried over anhydrous Na_2SO_4, filtered and concentrated under reduced pressure. The crude reaction mixture was purified by silica gel column chromatography using mixtures of MeOH in EtOAc (0-20%) as eluent, yielding compound **48** (120 mg, 31 %). This compound was then activated following the *General Procedure 5 for catalyst activation with NH_3*, described on page 224, affording catalyst **48** (93 mg).

m.p.: glassy compound

IR (film, υ in cm^{-1}): 3072, 2988, 2916, 2858, 1651, 1573, 1463, 1392, 1346, 1249, 1119, 937, 873, 743.

^{1}H NMR (400 MHz, CD_3OD) δ 8.98 (s, 1H), 7.73 (d, *J* = 9.1 Hz, 1H), 7.34 (d, *J* = 7.0 Hz, 1H), 7.19 (s, 1H), 7.25 – 7.08 (m, 3H), 7.08 (d, *J* = 9.1 Hz, 1H), 4.33 (dt, *J* = 10.4, 5.0 Hz, 1H), 4.00 (dd, *J* = 9.8, 7.7 Hz, 1H), 3.42 (d, *J* = 9.1 Hz, 1H), 3.28 – 3.14 (m, 3H), 3.11 – 3.01 (m, 2H), 3.00 – 2.94 (m, 2H), 2.89 (dd, *J* = 16.0, 11.0 Hz, 1H), 2.78 (dt, *J* = 6.9, 1.5 Hz, 2H), 1.96 – 1.86 (m, 4H), 1.37 – 1.26 (m, 2H), 1.24 – 1.12 (m, 2H), 0.72 (t, *J* = 7.3 Hz, 3H).

^{13}C NMR (100 MHz, CD_3OD) δ 170.3 (C), 157.2 (2 C), 135.9 (C), 135.6 (C), 134.9 (CH), 133.9 (C), 130.1 (CH), 128.2 (CH), 128.0 (CH), 127.8 (CH), 126.6 (CH), 123.3 (CH), 123.0 (C), 122.9 (C), 115.2 (CH), 113.8 (C), 77.0 (CH), 62.6 (CH_2), 55.9 (2 CH_2), 52.9 (CH), 45.0 (CH), 43.3 (CH_2), 36.1 (CH_2), 32.3 (CH_2), 24.3 (2 CH_2), 20.7 (CH_2), 13.8 (CH_3).

HRMS (ESI+): Calculated for $C_{30}H_{38}N_3O_5S$ $[M+H]^+$ 568.2476, found 568.2467.

3-(8-(*N*-Butylsulfamoyl)-3,7-dihydroxy-2-naphthamido)-1-(pyrrolidin-1-ylmethyl)-1,2,3,4-tetrahydronaphthalen-2-yl acetate (catalyst 48a)

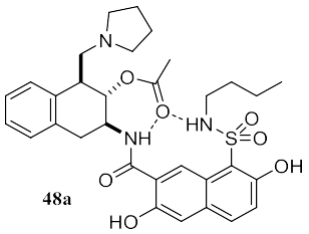

48a

Following the *General Procedure 7 for catalyst acetylation using vinyl acetate* described on page 225, the reaction of catalyst **48** (16 mg, 0.03 mmol) with 500 μL of vinyl acetate gave compound **48a** (17.2 mg, quant.) as a yellowish oil.

^{1}H NMR (400 MHz, $CDCl_3$) δ 8.39 (s, 1H), 7.72 (d, *J* = 9.1 Hz, 1H), 7.34 (d, *J* = 7.2 Hz, 1H), 7.24 (s, 1H), 7.23 – 7.09 (m, 3H), 7.13 (d, *J* = 9.1 Hz, 1H), 5.45 (dd, *J* = 9.2, 7.8 Hz, 1H), 4.32 (dt, *J* = 11.3, 4.3 Hz, 1H), 3.42 (dd, *J* = 15.6, 4.3 Hz, 1H), 3.35 (dd, *J* = 12.8, 6.9 Hz, 1H), 2.98 – 2.89 (m, 2H), 2.89 – 2.72 (m, 3H), 2.62 – 2.52 (m, 2H), 2.52 – 2.41 (m, 2H), 2.19 (s, 3H), 1.79 – 1.66 (m, 4H), 1.48 – 1.36 (m, 2H), 1.31 – 1.15 (m, 2H), 0.76 (t, *J* = 7.3 Hz, 3H).

^{13}C NMR (100 MHz, $CDCl_3$) δ 175.9 (C), 169.9 (C), 156.5 (C), 155.9 (C), 136.2 (C), 134.4 (CH), 133.6 (C), 133.1 (C), 129.0 (CH), 128.2 (CH), 127.1 (CH), 126.9 (CH), 123.1 (CH), 122.0 (C), 121.9 (CH), 118.2 (C), 114.5 (CH), 111.9 (C), 77.4 (CH), 62.1 (CH_2), 54.8 (2 CH_2), 52.3 (CH), 43.8 (CH), 42.4 (CH_2), 34.6 (CH_2), 31.6 (CH_2), 23.9 (2 CH_2), 21.7 (CH_3), 19.8 (CH_2), 13.6 (CH_3).

8-(*N*-(4-(Dimethylamino)phenyl)sulfamoyl)-3-hydroxy-7-methoxy-2-naphthoic acid (49)

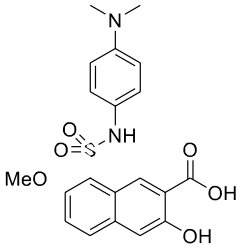

49

Compound **45** (625 mg, 1.97 mmol) was added over a solution of *N*,*N*-dimethyl-*p*-phenylenediamine (875 mg, 6.42 mmol) in 20 mL EtOAc. The reaction mixture was stirred for 1 hour, then the solvent was evaporated under reduced pressure and the crude product was suspended in MeOH and added over 44 mL of an aqueous 10% AcOH solution. The precipitate was collected by filtration and dried in an oven for 3 hours at 70 ºC, yielding compound **49** (531 mg, 65%) which was used without further purification in the next reaction.

m.p.: >230ºC

IR (nujol, υ in cm^{-1}): 3273, 2929, 1677, 1607, 1554, 1515, 1327, 1262, 1152, 1093, 1054, 976, 911, 866, 814, 730, 684.

^{1}H NMR (400 MHz, DMSO-d_6) δ 9.70 (br s, NH), 9.49 (s, 1H), 8.02 (d, *J* = 9.2 Hz, 1H), 7.63 (d, *J* = 9.2 Hz, 1H), 7.33 (s, 1H), 6.92 (d, *J* = 7.9 Hz, 2H), 6.51 (d, *J* = 7.9 Hz, 2H), 4.08 (s, 3H), 2.73 (s, 6H).

^{13}C NMR (101 MHz, DMSO-d_6) δ 171.5 (C), 154.9 (C), 154.4 (C), 147.7 (C), 133.7 (CH), 133.0 (C), 128.4 (CH), 126.5 (C), 124.1 (C), 123.1 (2 CH), 120.0 (C), 117.2 (C), 117.1 (CH), 112.7 (2 CH), 112.0 (CH), 57.1 (CH_3), 40.2 (2 CH_3).

HRMS (ESI-): Calculated for $C_{20}H_{19}N_2O_6S$ $[M-H]^-$ 415.0969, found 415.0969.

8-(*N*-(4-(Dimethylamino)phenyl)sulfamoyl)-3,7-dihydroxy-2-naphthoic acid (50)

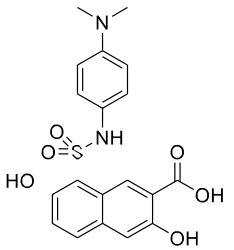

50

Compound **49** (531 mg, 1.28 mmol) was dissolved in 5 mL of DMF and $Na_2S{\cdot}9H_2O$ (1.54 g, 6.41 mmol) was added portion wise. The reaction mixture was heated at 120ºC under stirring

for 20 hours in a closed reaction vessel. Then, the reaction mixture was cooled down to room temperature and added over 100 mL of a 5% AcOH aqueous solution. The solid which appeared was filtrated under vacuum and dried overnight yielding compound **50** (475 mg, 92%) as a light brown solid.

m.p.: 150 – 153ºC

IR (nujol, υ in cm^{-1}): 3228, 2923, 1664, 1606, 1573, 1515, 1223, 1113, 1022, 944, 877, 840, 730, 677.

^{1}H NMR (400 MHz, DMSO-d_6) δ 10.93 (br s, Ar-OH), 9.74 (br s, NH), 9.37 (s, 1H), 7.87 (d, *J* = 9.0 Hz, 1H), 7.31 (s, 1H), 7.22 (d, *J* = 9.0 Hz, 1H), 6.82 (d, *J* = 8.9 Hz, 2H), 6.49 (d, *J* = 8.9 Hz, 2H), 2.75 (s, 6H).

^{13}C NMR (100 MHz, DMSO-d_6) δ 171.5 (C), 154.6 (C), 154.5 (C), 148.2 (C), 133.8 (CH), 132.7 (C), 127.6 (CH), 125.6 (C), 124.2 (2 CH), 123.1 (C), 122.2 (CH), 116.7 (C), 114.8 (C), 112.6 (3 CH), 40.2 (2 CH_3).

HRMS (ESI-): Calculated for $C_{19}H_{17}N_2O_6S$ $[M-H]^-$ 401.0812, found 401.0812.

3,7-Diacetoxy-8-(*N*-acetyl-*N*-(4-(dimethylamino)phenyl)sulfamoyl)-2-naphthoic acid (51)

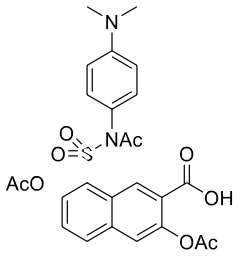

51

Compound **50** (95 mg, 0.24 mmol) was suspended in a mixture of 2 mL of Ac_2O and 0.5 mL of DMF with 3 drops of 95% H_2SO_4. The reaction mixture was stirred at 60 ºC until the solution became homogenous. Then, it was added over water and extracted with EtOAc twice. The organic phase was dried over anhydrous Na_2SO_4, filtrated and concentrated under reduced pressure. ^{1}H NMR showed the presence of some amount of the mixed anhydride of carboxylic acid. Then, MeOH (10 mL) was added and the reaction mixture was heated at 65ºC for 3 hours. Afterwards, it was evaporated under reduced pressure to yield compound **51** (70 mg, 55%), which was used in the next step without further purification.

8-(*N*-(4-(Dimethylamino)phenyl)sulfamoyl)-3,7-dihydroxy-*N*-(3-hydroxy-4-(pyrrolidin-1-ylmethyl)-1,2,3,4-tetrahydronaphthalen-2-yl)-2-naphthamide (catalyst 52)

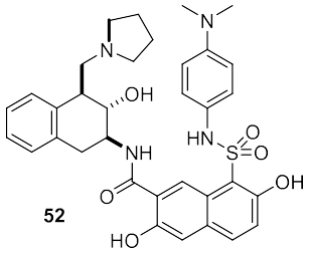

52

Compound **51** (110 mg, 0.21 mmol) was dissolved in DCM (5 mL) and PCl_5 (76 mg, 0.37 mmol) was added. The reaction mixture was stirred at room temperature for 5 minutes and then evaporated to dryness to yield compound **51** acid chloride quantitatively, which was used in the next step without further purification.

The acid chloride of **51** (63 mg, 0.12 mmol) was dissolved in 2 mL of DCM and added over a stirred solution of amine **20** (56 mg, 0.23 mmol) in a solution of *N,N'*-dimethylaniline (30 μL, 0.24 mmol) in 3 mL of DCM. The reaction flask with the acid chloride was washed with 1 mL of DCM and added over the reaction mixture solution. After 10 minutes a ^{1}H NMR spectrum of an aliquot of the reaction mixture showed that the reaction was finished and the solvent was evaporated.

In order to hydrolyse the acetyl groups, 5 mL of MeOH were added to the reaction flask followed by NaOH (130 mg, 3.25 mmol). The reaction mixture was stirred for 2.5 hours, then quenched with 0.4 mL of AcOH and evaporated to dryness. The crude reaction mixture was purified by silica gel column chromatography using mixtures of MeOH in DCM (0-7%) as eluent yielding compound **51** (10 mg, 13 %). The compound was activated following *General Procedure 5 for catalyst activation with NH_3*, described on page 224, affording 10 mg of catalyst **52**.

m.p.: glassy compound

IR (film, υ in cm^{-1}): 3221, 3053, 2923, 2852, 1651, 1456, 1405, 1113, 957, 743.

^{1}H NMR (400 MHz, 5% CD_3OD in $CDCl_3$) δ 8.81 (s, 1H), 7.59 (d, *J* = 9.0 Hz, 1H), 7.23 – 7.04 (m, 5H), 6.91 (d, *J* = 9.0 Hz, 1H), 6.71 (d, *J* = 8.5 Hz, 2H), 6.40 (d, *J* = 8.5 Hz, 2H), 4.42 (dt, *J* = 11.1, 5.0 Hz, 1H), 4.16 – 4.02 (m, 1H), 3.33 – 2.81 (m, 9H), 2.78 (s, 6H), 1.97 – 1.74 (m, 4H).

^{13}C NMR (100 MHz, 5% CD_3OD in $CDCl_3$) δ 170.5 (C), 156.5 (C), 149.3 (C), 134.8 (C), 134.7 (C), 134.3 (CH), 133.7 (C), 133.7 (C), 132.7 (C), 129.5 (CH), 127.1 (CH), 126.6 (CH), 126.4 (CH), 125.8 (2 CH), 124.3 (C), 122.7 (CH), 122.4 (CH), 121.6 (C), 114.5 (CH), 112.8 (2 CH), 111.3 (C), 77.4 (CH), 62.2 (CH_2), 54.8 (2 CH_2), 51.3 (CH), 42.9 (CH), 40.6 (2 CH_3), 35.3 (CH_2), 23.5 (2 CH_2).

HRMS (ESI+): Calculated for $C_{34}H_{39}N_4O_6S$ $[M+H]^+$ 631.2585, found 631.2584.

3-(8-(*N*-(4-(Dimethylamino)phenyl)sulfamoyl)-3,7-dihydroxy-2-naphthamido)-1-(pyrrolidin-1-ylmethyl)-1,2,3,4-tetrahydronaphthalen-2-yl acetate (catalyst 52a)

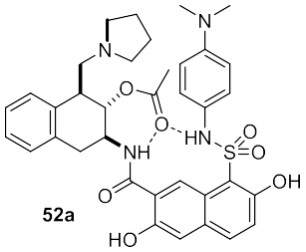

52a

Following the *General Procedure 7 for catalyst acetylation using vinyl acetate* described on page 225, the reaction of catalyst **52** (10 mg, 0.02 mmol) with 500 μL of vinyl acetate gave compound **52a** (10.7 mg, quant.) as a yellowish oil.

^{1}H NMR (400 MHz, $CDCl_3$) δ 8.64 (s, 1H), 7.68 (d, *J* = 9.1 Hz, 1H), 7.34 (d, *J* = 7.3 Hz, 1H), 7.28 (s, 1H), 7.24 – 7.13 (m, 3H), 7.00 (d, *J* = 9.1 Hz, 1H), 6.77 (d, *J* = 8.8 Hz, 2H), 6.45 (d, *J* = 8.8 Hz, 2H), 5.66 – 5.52 (m, 1H), 4.49 – 4.36 (m, 1H), 3.47 – 3.33 (m, 3H), 3.05 – 2.88 (m, 2H), 2.85 (s, 6H), 2.72 – 2.40 (m, 4H), 2.07 (s, 3H), 1.84 – 1.70 (m, 4H).

^{13}C NMR (100 MHz, $CDCl_3$) δ 169.9 (C), 156.9 (C), 156.1 (C), 149.6 (C), 134.4 (CH), 134.0 (C), 133.0 (C), 129.1 (CH), 128.1 (CH), 127.1 (CH), 126.7 (CH), 125.1 (C), 123.5 (C), 123.0 (CH), 122.0 (2 CH), 118.0 (C), 114.6 (CH), 112.7 (2 CH), 111.6 (C), 77.4 (CH), 55.0 (CH_2), 52.0 (CH), 43.9 (CH), 40.6 (2 CH_3), 34.5 (CH_2), 29.8 (CH_2), 23.7 (2 CH_2), 14.3 (CH_3).

3-Hydroxy-7-methoxy-8-(*N*-(*p*-tolyl)sulfamoyl)-2-naphthoic acid (53)

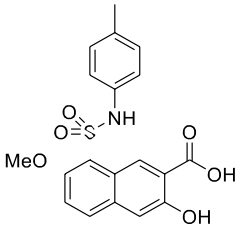

53

Compound **45** (300 mg, 0.95 mmol) was mixed with *p*-toluidine (200 mg, 1.87 mmol) in 2 mL of *N*,*N'*-dimethylaniline The reaction mixture was stirred for 1 hour, then 2 mL of EtOAc were added to solubilize the precipitate. The organic solvent was evaporated under reduced pressure, the crude was dissolved in MeOH and added over an aqueous solution of 4% HCl. The precipitate was collected by filtration. The solid was suspended in DCM and filtered again,

yielding compound **53** (360 mg, 98%) which was used without further purification in the next reaction.

m.p.: >230ºC

IR (nujol, υ in cm^{-1}): 3267, 2929, 1664, 1619, 1521, 1327, 1249, 1152, 976, 911, 866, 808, 723, 697, 615.

^{1}H NMR (400 MHz, DMSO-d_6) δ 9.96 (br s, NH), 9.74 (s, 1H), 8.02 (d, *J* = 9.3 Hz, 1H), 7.58 (d, *J* = 9.3 Hz, 1H), 7.36 (s, 1H), 6.97 (d, *J* = 8.5 Hz, 2H), 6.92 (d, *J* = 8.5 Hz, 2H), 4.01 (s, 3H), 2.09 (s, 3H).

^{13}C NMR (100 MHz, DMSO-d_6) δ 171.5 (C), 155.1 (C), 154.4 (C), 135.3 (C), 134.0 (CH), 134.0 (C), 133.0 (C), 132.8 (C), 129.4 (2 CH), 128.2 (CH), 124.1 (C), 119.6 (2 CH), 117.2 (CH), 117.2 (C), 112.2 (CH), 57.2 (CH_3), 20.2 (CH_3).

HRMS (ESI-): Calculated for $C_{19}H_{16}NO_6S$ $[M-H]^-$ 386.0703, found 386.0703.

3,7-Dihydroxy-8-(*N*-(*p*-tolyl)sulfamoyl)-2-naphthoic acid (54)

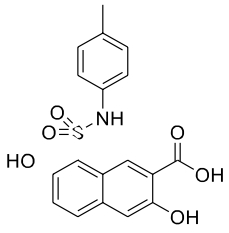

54

Compound **53** (154 mg, 0.40 mmol) was dissolved in DMF (1.5 mL) and $Na_2S{\cdot}9H_2O$ (354 mg, 1.47 mmol) was added portion wise. The reaction was stirred at 120 ºC for 14.5 hours in a closed reaction vessel. Then, it was cooled down to room temperature and added over an aqueous solution of HCl 2M. The aqueous phase was extracted with EtOAc (x2), washed with water (x2), dried over anhydrous Na_2SO_4, filtered and evaporated under reduced pressure. The crude was suspended in DCM and the precipitate was collected by filtration under vacuum, yielding compound **54** (70 mg, 47%) which was used without further purification in the next reaction.

m.p.: 224 – 226ºC

IR (nujol, υ in cm^{-1}): 3293, 2910, 1684, 1619, 1521, 1275, 1216, 1132, 1035, 937, 866, 801, 723, 665.

^{1}H NMR (400 MHz, DMSO-d_6) δ 11.08 (br s, Ar-OH), 10.12 (br s, NH), 9.46 (s, 1H), 7.87 (d, *J* = 9.2 Hz, 1H), 7.31 (s, 1H), 7.22 (d, *J* = 9.2 Hz, 1H), 6.94 (s, 4H), 2.11 (s, 3H).

^{13}C NMR (100 MHz, DMSO-d_6) δ 171.5 (C), 154.7 (C), 154.4 (C), 135.0 (C), 133.9 (CH), 133.1 (C), 132.7 (C), 129.4 (2 CH), 127.5 (CH), 123.3 (C), 122.2 (CH), 120.3 (2 CH), 116.7 (C), 115.1 (C), 112.7 (CH), 20.2 (CH_3).

HRMS (ESI-): Calculated for $C_{18}H_{14}NO_6S$ $[M-H]^-$ 372.0547, found 372.0546.

3,7-Diacetoxy-8-(*N*-acetyl-*N*-(*p*-tolyl)sulfamoyl)-2-naphthoic acid (55)

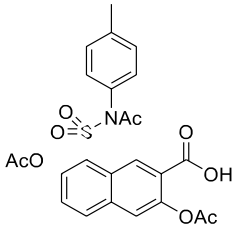

55

Compound **54** (470 mg, 1.26 mmol) was suspended in Ac_2O (7 mL) and 2 drops of 95% H_2SO_4 were added. The reaction mixture was stirred until the solution became homogenous. Then it was added over of water (50 mL) and filtered under vacuum, yielding compound **55** (548 mg, 87%) which was used without further purification in the next step.

3,7-Dihydroxy-*N*-(3-hydroxy-4-(pyrrolidin-1-ylmethyl)-1,2,3,4-tetrahydronaphthalen-2-yl)-8-(*N*-(*p*-tolyl)sulfamoyl)-2-naphthamide (catalyst 56)

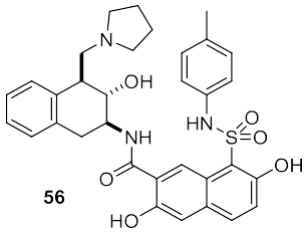

56

Compound **55** (112 mg, 0.22 mmol) was dissolved in $SOCl_2$ (2 mL) and refluxed until the solution became homogenous. Then it was evaporated under reduced pressure to yield compound **55** acid chloride quantitatively, which was used in the next step without further purification

The compound **55** acid chloride (116 mg, 0.22 mmol) was dissolved in DCM (3 mL) and added over a stirred solution of amine **20** (117 mg, 0.48 mmol) and *N,N'*-dimethylaniline (56 μL, 0.44 mmol) in DCM. (4 mL) The reaction flask with the acid chloride was washed with 2 mL of DCM and added over the reaction mixture solution.

The acetyl groups were hydrolised with NaOH in MeOH and then it was neutralised with AcOH. After filtration and purification by column chromatography, catalyst **56** was obtained (110 mg, 83%). 12 mg of compound **56** were activated following the *General Procedure 5 for*

catalyst activation with NH_3, described on page 224, affording the acid free catalyst **56** (12 mg, 9%).

m.p.: glassy compound

IR (film, υ in cm^{-1}):3234, 3014, 2916, 2832, 1651, 1580, 1405, 1210, 1113, 756.

^{1}H NMR (400 MHz, 5% CD_3OD in $CDCl_3$) δ 8.92 (s, 1H), 7.71 (d, *J* = 9.0 Hz, 1H), 7.36 (s, 1H), 7.31 – 7.16 (m, 4H and NH), 7.06 (d, *J* = 9.0 Hz, 1H), 6.98 (d, *J* = 8.1 Hz, 2H), 6.91 (d, *J* = 8.1 Hz, 2H), 4.53 (dt, *J* = 11.0, 4.7 Hz, 1H), 4.38 – 4.26 (m, 1H), 3.53 – 2.98 (m, 9H), 2.24 (s, 3H), 2.15 – 2.00 (m, 4H).

^{13}C NMR (100 MHz, 5% CD_3OD in $CDCl_3$) δ 170.3 (C), 156.6 (C), 135.2 (C), 135.1 (C), 134.6 (CH), 133.5 (C), 133.0 (C), 132.7 (C), 129.8 (2 CH), 129.7 (CH), 127.4 (CH), 126.8 (CH), 126.5 (CH), 122.7 (CH), 122.4 (CH), 122.0 (2 CH), 121.7 (C), 114.5 (CH), 111.3 (C), 77.4 (CH), 61.9 (CH_2), 55.1 (2 CH_2), 51.4 (CH), 43.0 (CH), 35.2 (CH_2), 23.3 (2 CH_2), 20.8 (CH_3).

HRMS (ESI+): Calculated for $C_{33}H_{36}N_3O_6S$ $[M+H]^+$ 602.7255, found 602.2312.

3-(3,7-Dihydroxy-8-(*N*-(*p*-tolyl)sulfamoyl)-2-naphthamido)-1-(pyrrolidin-1-ylmethyl)-1,2,3,4-tetrahydronaphthalen-2-yl acetate (catalyst 56a)

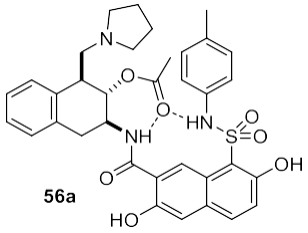

56a

Following the *General Procedure 7 for catalyst acetylation using vinyl acetate* described on page 225, the reaction of catalyst **56** (12 mg, 0.02 mmol) with 500 μL of vinyl acetate gave compound **56a** (12.8 mg, quant.) as a yellowish oil.

^{1}H NMR (400 MHz, $CDCl_3$) δ 10.37 (br s, OH), 8.73 (s, 1H), 7.67 (d, *J* = 9.1 Hz, 1H), 7.25 (s, 1H), 7.28 – 7.17 (m, 4H), 7.03 (d, *J* = 9.1 Hz, 1H), 6.94 (d, *J* = 8.0 Hz, 2H), 6.89 (d, *J* = 8.0 Hz, 2H), 6.04 – 5.76 (m, 1H), 4.57 – 4.42 (m, 1H), 3.67 – 2.52 (m, 9H), 2.20 (s, 3H), 2.12 (s, 3H), 2.02 – 1.81 (m, 4H).

^{13}C NMR (100 MHz, $CDCl_3$) δ 170.2 (C), 156.9 (C), 156.2 (C), 135.5 (C), 135.5 (C), 134.7 (CH), 133.5 (C), 133.0 (C), 129.9 (2 CH), 129.8 (CH), 129.4 (CH), 128.1 (CH), 127.5 (CH), 122.8 (CH), 122.3 (2 CH), 121.9 (C), 121.8 (C), 121.1 (C), 118.3 (C), 114.6 (2 CH), 111.6

(C), 77.4 (CH), 61.8 (CH_2), 55.2 (2 CH_2), 51.7 (CH), 44.3 (CH), 34.0 (CH_2), 23.5 (2 CH_2), 21.5 (CH_3), 21.0 (CH_3).

8-(*N*-(4-Chlorophenyl)sulfamoyl)-3-hydroxy-7-methoxy-2-naphthoic acid (57)

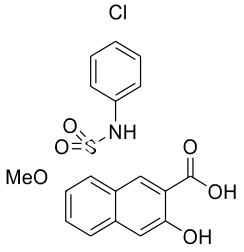

57

Compound **45** (680 mg, 2.15 mmol) was added over a solution of *p*-chloroaniline (450 mg, 3.53 mmol) in 2 mL of *N*,*N'*-dimethylaniline. The reaction mixture was stirred for 1 hour, then added over 40 mL of a 4% HCl aqueous solution. The flask was washed with MeOH and the precipitate was collected by filtration, yielding compound **57** (625 mg, 71%), which was used without further purification in the next step.

m.p.: >230ºC

IR (nujol, υ in cm^{-1}): 3260, 1671, 1612, 1515, 1340, 1262, 1158, 1093, 970, 918, 877, 814, 723, 678.

^{1}H NMR (400 MHz, DMSO-d_6) δ 10.34 (br s, NH), 9.72 (s, 1H), 8.05 (d, *J* = 9.3 Hz, 1H), 7.58 (d, *J* = 9.3 Hz, 1H), 7.38 (s, 1H), 7.20 (d, *J* = 8.8 Hz, 2H), 7.08 (d, *J* = 8.8 Hz, 2H), 3.97 (s, 3H).

^{13}C NMR (100 MHz, DMSO-d_6) δ 171.4 (C), 155.1 (C), 154.52 (C), 137.1 (C), 134.3 (CH), 133.0 (C), 129.0 (2 CH), 128.1 (CH), 127.5 (C), 123.9 (C), 120.4 (2 CH), 119.2 (C), 117.4 (C), 117.2 (CH), 112.4 (CH), 57.2 (CH_3).

HRMS (ESI-): Calculated for $C_{18}H_{13}{}^{35}ClNO_6S$ $[M-H]^-$ 406.0157, found 406.0156.

8-(*N*-(4-Chlorophenyl)sulfamoyl)-3,7-dihydroxy-2-naphthoic acid (58)

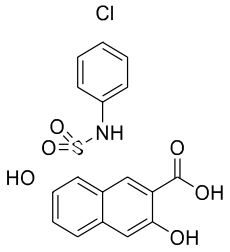

58

Compound **57** (145 mg, 0.36 mmol) was dissolved in 1.5 mL of DMF and $Na_2S·9H_2O$ (708 mg, 2.95 mmol) was added portion wise. The reaction mixture was heated at 120ºC under stirring for 24 hours in a closed reaction vessel. Analysis of an aliquot by ^{1}H NMR showed that the reaction was not finished (probably due to old-wet Na_2S). More $Na_2S·9H_2O$ was added (714 mg, 2.97 mmol) and the reaction mixture was heated at 120ºC under stirring for 3 days. Then, it was cooled down to room temperature and added over 100 mL of an aqueous solution of 4% HCl. The aqueous phase was extracted with EtOAc twice, washed with water twice, dissolved in MeOH and added over water. The solid was filtered under vacuum yielding compound **58** (70 mg, 50%).

m.p.: 190 – 193ºC

IR (nujol, υ in cm^{-1}): 3312, 1664, 1619, 1521, 1314, 1262, 1203, 1132, 1031, 937, 877, 821, 723, 678.

^{1}H NMR (400 MHz, DMSO-d_6) δ 11.22 (br s, Ar-OH), 10.41 (br s, NH), 9.50 (s, 1H), 7.87 (d, *J* = 9.2 Hz, 1H), 7.32 (s, 1H), 7.24 – 7.18 (m, 3H), 7.06 (d, *J* = 8.8 Hz, 2H).

^{13}C NMR (100 MHz, DMSO-d_6) δ 171.5 (C), 154.6 (C), 154.5 (C), 137.0 (C), 134.1 (CH), 132.6 (C), 128.9 (2 CH), 127.6 (C), 127.4 (CH), 123.5 (C), 122.0 (CH), 120.8 (2 CH), 116.8 (C), 115.3 (C), 112.7 (CH).

HRMS (ESI-): Calculated for $C_{17}H_{11}{}^{35}ClNO_6S$ $[M-H]^-$ 392.0001, found 392.0001.

3,7-Diacetoxy-8-(*N*-acetyl-*N*-(4-chlorophenyl)sulfamoyl)-2-naphthoic acid (59)

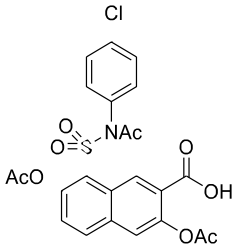

59

Compound **58** (190 mg, 0.48 mmol) was dissolved in Ac_2O (5 mL) and 3 drops of 95% H_2SO_4 were added. The reaction mixture was stirred for 2 hours at room temperature and then added over ice and water and extracted with EtOAc twice. The organic phase was dried over anhydrous Na_2SO_4, filtered, and concentrated under reduced pressure to yield compound **59** (190 mg, 76 %), which was used in the next step without further purification.

8-(*N*-(4-Chlorophenyl)sulfamoyl)-3,7-dihydroxy-*N*-(3-hydroxy-4-(pyrrolidin-1-ylmethyl)-1,2,3,4-tetrahydronaphthalen-2-yl)-2-naphthamide (catalyst 60)

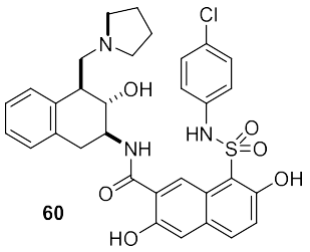

60

Compound **59** (190 mg, 0.37 mmol) was dissolved in DCM (13 mL) and PCl_5 (172 mg, 0.83 mmol) was added portion wise. The reaction mixture was stirred for 15 minutes at room temperature and then concentrated under reduced pressure to yield the acid chloride of compound **59** quantitatively, which was used in the next step without further purification.

The compound **59** acid chloride (199 mg, 0.37 mmol) was dissolved in DCM (3 mL) and added over a stirred solution of amine **20** (115 mg, 0.47 mmol) and *N*,*N'*-dimethylaniline (100 μL, 0.79 mmol) in DCM (10 mL). The acid chloride reaction flask was washed with 2 mL more of DCM and added over the reaction mixture. After 30 minutes, a ^{1}H NMR spectrum of an aliquot of the reaction mixture showed some starting material and more amine **20** (17 mg, 0.069 mmol) was added. The reaction mixture was stirred 75 minutes more and then the solvent was evaporated.

To hydrolyse the acetyl groups, 10 mL of MeOH were added to the reaction flask followed by NaOH (110 mg, 2.75 mmol). The reaction mixture was stirred for 15 minutes, neutralized with AcOH and evaporated under reduced pressure. Azeotropic distillation with toluene in the rotary evaporator was performed to eliminate the excess of AcOH. The crude reaction

productwas purified by silica gel column chromatography using mixtures of MeOH in EtOAc (0-40%) as eluent, yielding compound **60** (70 mg, 30 %). This compound was then activated following the *General Procedure 5 for catalyst activation with NH_3*, described on page 224, affording 59 mg of catalyst **60**.

m.p.: glassy compound

IR (film, υ in cm^{-1}):3221, 3053, 3000, 2988, 2923, 1664, 1482, 1418, 119, 617.

^{1}H NMR (400 MHz, 5% CD_3OD in $CDCl_3$) δ 8.79 (s, 1H), 7.60 (d, *J* = 9.2 Hz, 1H), 7.20 – 7.06 (m, 5H), 7.03 (d, *J* = 8.6 Hz, 2H), 6.98 (d, *J* = 9.2 Hz, 1H), 6.86 (d, *J* = 8.6 Hz, 2H), 4.38 (dt, *J* = 11.2, 4.8 Hz, 1H), 4.15 – 4.07 (m, 1H), 3.39 – 2.80 (m, 9H), 2.05 – 1.90 (m, 4H).

^{13}C NMR (100 MHz, $CDCl_3$) δ 170.3 (C), 156.8 (C), 156.5 (C), 156.3 (C), 135.5 (C), 135.0 (C), 134.8 (CH), 133.1 (C), 132.8 (C), 130.2 (C), 129.7 (CH), 129.3 (2 CH), 127.3 (CH), 126.8 (CH), 126.6 (CH), 122.4 (2 CH), 122.2 (2 CH), 121.2 (C), 114.8 (CH), 110.9 (C), 74.6 (CH), 62.0 (CH_2), 55.0 (2 CH_2), 51.5 (CH), 43.0 (CH), 35.2 (CH_2), 23.3 (2 CH_2).

HRMS (ESI+): Calculated for $C_{32}H_{33}^{35}ClN_3O_6S$ $[M+H]^+$ 622.1773, found 622.1768.

3-(8-(*N*-(4-Chlorophenyl)sulfamoyl)-3-hydroxy-7-methoxy-2-naphthamido)-1-(pyrrolidin-1-ylmethyl)-1,2,3,4-tetrahydronaphthalen-2-yl acetate (catalyst 60a)

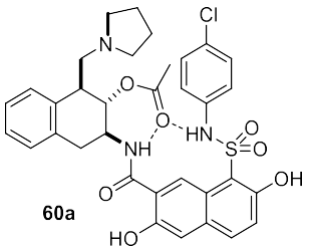

60a

Following the *General Procedure 7 for catalyst acetylation using vinyl acetate* described on page 225, the reaction of catalyst **60** (20 mg, 0.03 mmol) with 500 μL of vinyl acetate gave compound **60a** (21.4 mg, quant.) as a yellowish oil.

^{1}H NMR (400 MHz, $CDCl_3$) δ 10.48 (br s, OH), 8.78 (s, 1H), 7.69 (d, *J* = 9.1 Hz, 1H), 7.34 – 7.20 (m, 5H), 7.10 (d, *J* = 8.6 Hz, 2H), 7.07 (d, *J* = 9.1 Hz, 1H), 6.99 (d, *J* = 8.6 Hz, 2H), 6.36 – 6.26 (m, 1H), 4.75 – 4.55 (m, 1H), 3.84 – 3.72 (m, 1H), 3.65 – 3.33 (m, 4H), 3.31 – 3.18 (m, 1H), 3.09 – 2.93 (m, 1H), 2.96 – 2.75 (m, 2H), 2.12 (s, 3H), 2.10 – 1.96 (m, 4H).

^{13}C NMR (100 MHz, $CDCl_3$) δ 170.4 (C), 157.1 (C), 156.4 (C), 135.9 (C), 135.8 (C), 135.6 (C), 134.8 (CH), 133.5 (C), 132.9 (C), 129.9 (CH), 129.3 (2 CH), 128.4 (C), 128.0 (CH), 127.5 (CH), 127.3 (CH), 122.7 (CH), 122.3 (CH), 122.1 (2 CH), 121.8 (C), 118.3 (C), 114.5 (CH),

111.3 (C), 77.4 (CH), 60.7 (CH_2), 56.3 (2 CH_2), 50.1 (CH), 44.4 (CH), 34.0 (CH_2), 23.2 (2 CH_2), 21.3 (CH_3).

8-(*N*-(4-Chlorophenyl)sulfamoyl)-3-hydroxy-*N*-(3-hydroxy-4-(pyrrolidin-1-ylmethyl)-1,2,3,4-tetrahydronaphthalen-2-yl)-7-methoxy-2-naphthamide (61)

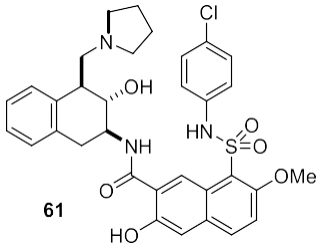

61

Compound **57** (195 mg, 0.48 mmol) was refluxed in $SOCl_2$ (2.5 mL) for 30 minutes. Then, it was cooled down to room temperature and evaporated under reduced pressure to yield compound **57** acid chloride quantitatively, which was used in the next step without further purification.

The acid chloride of **57** (204 mg, 0.48 mmol) was dissolved in 3 mL of EtOAc and 1 mL of DCM and added over a stirred mixture of amine **20** (117 mg, 0.47 mmol) in 4 mL of EtOAc and 4 mL of a saturated aqueous solution of $NaHCO_3$. The flask with the acid chloride was washed with 3 mL EtOAc and 2 mL of DCM and added over the reaction mixture. A precipitate was formed. THF and DCM were added to dissolve it fruitlessly. The reaction mixture was stirred for 21.5 hours, then transferred to a separatory funnel. The aqueous phase was extracted first with EtOAc and then with DCM. The organic phases were combined, dried over anhydrous Na_2SO_4, filtered, and evaporated under reduced pressure. The crude product was purified by silica gel chromatography column with mixtures of MeOH in EtOAc (0-25%) yielding compound **61** (134 mg, 45%). The compound was activated following the *General Procedure 5 for catalyst activation with NH_3*, described on page 224, affording 129 mg of catalyst **61**.

m.p.: glassy compound

IR (film, υ in cm^{-1}): 3323, 2962, 2929, 1651, 918, 834, 730.

^{1}H NMR (400 MHz, $CDCl_3$) δ 9.29 (br s, OH), 8.26 (s, 1H), 7.37 (d, *J* = 7.0 Hz, 1H), 7.25 – 7.10 (m, 3H), 6.98 (d, *J* = 8.8 Hz, 2H), 6.97 (s, 1H), 6.96 (d, *J* = 7.0 Hz, 2H), 6.88 (d, *J* = 8.8 Hz, 2H), 4.50 (m, 1H), 4.30 (dd, *J* = 10.1, 8.7 Hz, 1H), 3.85 (s, 3H), 3.40 (dd, *J* = 16.4, 5.0 Hz, 1H), 3.37 – 3.27 (m, 2H), 3.21 (t, *J* = 12.6 Hz, 1H), 3.08 – 2.94 (m, 3H), 2.87 – 2.71 (m, 2H), 1.86 – 1.68 (m, 4H).

^{13}C NMR (100 MHz, $CDCl_3$) δ 171.0 (C), 154.9 (C), 154.0 (C), 136.5 (C), 134.9 (C), 133.9 (C), 133.4 (CH), 132.2 (C), 129.6 (CH), 129.1 (2 CH), 129.1 (C), 127.2 (CH), 126.7 (CH),

126.4 (CH), 125.7 (CH), 124.0 (C), 120.2 (2 CH), 119.5 (C), 118.6 (C), 114.5 (CH), 112.1 (CH), 77.4 (CH), 62.3 (CH_2), 56.7 (CH_3), 54.9 (2 CH_2), 51.7 (CH), 43.2 (CH), 36.2 (CH_2), 23.5 (2 CH_2).

HRMS (ESI+): Calculated for $C_{33}H_{35}^{35}ClN_3O_6S$ $[M+H]^+$ 636.1930, found 636.1923.

3-(8-(*N*-(4-Chlorophenyl)sulfamoyl)-3-hydroxy-7-methoxy-2-naphthamido)-1-(pyrrolidin-1-ylmethyl)-1,2,3,4-tetrahydronaphthalen-2-yl acetate (61a)

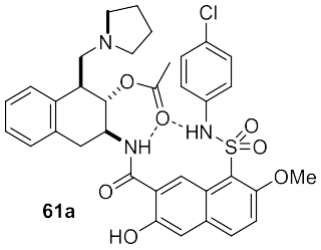

61a

Following the *General Procedure 7 for catalyst acetylation using vinyl acetate* described on page 225, the reaction of catalyst **61** (30 mg, 0.05 mmol) with 500 μL of vinyl acetate gave 32.0 mg (quant.) of compound **61a** as a yellowish oil.

^{1}H NMR (400 MHz, $CDCl_3$) δ 9.20 (s, 1H), 7.78 (d, *J* = 9.2 Hz, 1H), 7.39 (d, *J* = 7.0 Hz, 1H), 7.21 (m, 5H), 7.10 (d, *J* = 9.5 Hz, 2H), 7.07 (d, *J* = 9.5 Hz, 2H), 5.55 (dd, *J* = 8.2, 6.5 Hz, 1H), 4.46 (dt, *J* = 9.6, 4.9 Hz, 1H), 4.07 (s, 3H), 3.35 (dd, *J* = 14.1, 6.2 Hz, 2H), 3.04 (dd, *J* = 15.9, 10.1 Hz, 1H), 2.97 (dd, *J* = 12.5, 4.4 Hz, 1H), 2.89 – 2.79 (m, 1H), 2.65 – 2.49 (m, 2H), 2.49 – 2.37 (m, 2H), 2.14 (s, 3H), 1.69 – 1.58 (m, 4H).

^{13}C NMR (100 MHz, $CDCl_3$) δ 173.1 (C), 170.2 (C), 155.8 (C), 155.6 (C), 135.9 (C), 134.5 (CH), 133.7 (C), 133.1 (C), 130.3 (C), 129.3 (2 CH), 129.3 (C), 129.1 (CH), 128.4 (CH), 126.9 (CH), 126.9 (CH), 124.1 (C), 123.9 (CH), 122.1 (2 CH), 120.5 (C), 119.9 (C), 116.6 (CH), 113.2 (CH), 77.4 (CH), 61.6 (CH_2), 58.1 (CH_3), 55.0 (2 CH_2), 50.8 (CH), 43.8 (CH), 34.0 (CH_2), 23.7 (2 CH_2), 21.4 (CH_3).

8-(Chlorosulfonyl)-3,7-dihydroxy-2-naphthoic acid (62)

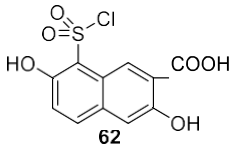

62

3,7-dihydroxy-2-naphthoic acid (2.0 g, 9.8 mmol) was suspended in DCM (8 mL) at room temperature and chlorosulfonic acid (15 mL, 225.3 mmol) was added dropwise with stirring. After 20 minutes the reaction was diluted with 50 mL of DCM and poured slowly (very

exothermic) over 100 mL of DCM with 40 g of ice. Separation of the organic phase, drying with anhydrous sodium sulfate and evaporation under reduced pressure yielded the compound **62** (2.0 g, 68 %) as a green solid which was used without further purification in the next reaction.

m.p.: > 230 ºC.

IR (nujol, υ in cm^{-1}): 3299, 1671, 1606, 1281, 1210, 1126, 873, 717.

^{1}H NMR (400 MHz, DMSO-d_6) δ 9.28 (s, 1H), 7.65 (d, *J* = 9.0 Hz, 1H), 7.21 (s, 1H), 7.07 (d, *J* = 9.0 Hz, 1H).

^{13}C NMR (100 MHz, DMSO- d_6) δ 172.1 (C), 154.0 (C), 150.6 (C), 132.7 (C), 130.3 (CH), 129.8 (CH), 123.6 (C), 123.0 (CH), 121.6 (C), 114.9 (C), 111.5 (CH).

HRMS (ESI-): Calculated for $C_{11}H_7O_7S$ [M hydrolysed-H]$^-$ 282.9918, found 282.9919.

8-(*N*-(3,5-Bis(trifluoromethyl)phenyl)sulfamoyl)-3,7-dihydroxy-2-naphthoic acid (63)

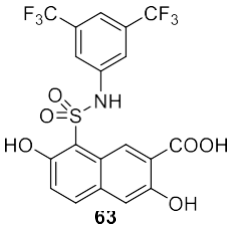

63

Compound **62** (500 mg, 1.7 mmol) was dissolved in bis(trifluoromethyl)aniline (2 mL, 12.8 mmol) and the mixture was heated to 70ºC under argon atmosphere for 10 minutes. The reaction mixture was partitioned with 20 mL of EtOAc and 40 mL of an aqueous solution of 4% Na_2CO_3. The aqueous layer was acidified with 5 mL of 35% HCl, and the precipitate generated was filtered. The recrystallization of the solid in MeOH afforded compound **63** (450 mg, 55 %) as a yellowish solid.

m.p.: 214 – 217 ºC.

IR (nujol, υ in cm^{-1}): 3247, 1671, 1624, 1532, 1417, 1313, 1278, 1198, 1170, 1123, 1013, 978, 933, 875, 796, 725, 699, 672.

^{1}H NMR (400 MHz, CD_3OD) δ 9.32 (s, 1H), 7.78 (d, *J* = 9.2 Hz, 1H), 7.53 (s, 2H), 7.51 (s, 1H), 7.19 (s, 1H), 7.13 (d, *J* = 9.2 Hz, 1H).

^{13}C NMR (100 MHz, CD_3OD) δ 173.1 (C), 157.5 (C), 157.3 (C), 141.2 (C), 136.4 (CH), 135.0 (C), 133.5 (q, *J* = 33 Hz, 2 C), 128.6 (CH), 124.3 (q, *J* = 272 Hz, 2 C), 123.8 (C), 123.3 (CH), 120.7 (q, *J* = 3.0 Hz, 2 CH), 118.1 (quin, *J* = 3.0 Hz, CH), 117.2 (C), 114.3 (CH), 114.1 (C).

HRMS (ESI-): Calculated for $C_{19}H_{10}F_6NO_6S$ $[M-H]^-$ 494.0139, found 494.0139.

8-(*N*-(3,5-Bis(trifluoromethyl)phenyl)sulfamoyl)-*N*-(4-(dimethylamino)phenyl)-3,7-dihydroxy-2-naphthamide (receptor 64)

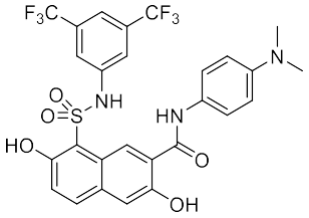

64

The acid **63** (200 mg, 0.4 mmol) and *N*,*N*-dimethyl-*p*-phenylendiamine (55 mg, 0.4 mmol) were dissolved in 1 mL of DCM to yield a clear solution. DCC (83 mg, 0.4 mmol) was added and the reaction was allowed to stand at room temperature for 1 hour. The crude reaction mixture was purified by column chromatography over silica gel, eluting with EtOAc in DCM mixtures of increasing polarity (starting with 5%, the deep yellow fraction was collected). Recrystallization from MeOH afforded receptor **64** (150 mg, 61 %) as an orange-yellowish solid.

m.p.: 138 – 140 ºC.

IR (nujol, υ in cm^{-1}): 3265, 2922, 1650, 1619, 1586, 1528, 1414, 1308, 1277, 1222, 1171, 1136, 1019, 978, 933, 872, 839, 807, 784, 740, 676.

^{1}H NMR (400 MHz, DMSO-d_6) δ 11.25 (broad s, OH, NH), 11.11 (broad s, OH), 10.30 (broad s, NH), 9.36 (s, 1H), 7.89 (d, *J* = 9.0 Hz, 1H), 7.64 (broad s, 2H), 7.60 (d, *J* = 8.7 Hz, 2H), 7.59 (broad s, 1H), 7.30 (s, 1H), 7.17 (d, *J* = 9.0 Hz, 1H), 6.77 (d, *J* = 8.7 Hz, 2H), 2.89 (s, 6H).

^{13}C NMR (100 MHz, DMSO-d_6) δ 163.8 (C), 154.9 (C), 151.2 (C), 147.3 (C), 140.9 (C), 134.4 (CH), 130.9 (q, *J* = 32.9 Hz, 2 C), 130.7 (C), 128.6 (C), 125.9 (CH), 125.0 (C), 124.0 (C), 123.0 (q, *J* = 272.9 Hz, 2 C), 121.5 (2 CH), 120.5 (CH), 117.6 (broad s, 2 CH), 115.6 (broad s, CH), 114.7 (C), 112.8 (2 CH), 112.3 (CH), 40.5 (2 CH_3).

HRMS (ESI+): Calculated for $C_{27}H_{22}F_6N_3O_5S$ $[M+H]^+$ 614.1179, found 614.1171.

Methyl 8-(chlorosulfonyl)-3,7-dihydroxy-2-naphthoate (65)

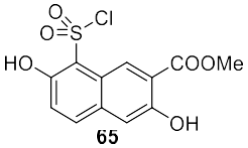

65

Methyl 3,7-dihydroxy-2-naphthoate (2.0 g, 9.2 mmol) was suspended in DCM (8 mL) at room temperature and chlorosulfonic acid (15 mL, 225.3 mmol) was added dropwise with stirring. After 20 minutes the reaction was diluted with 50 mL of DCM and poured slowly (very exothermic) over 100 mL of DCM with 40 g of ice. Separation of the organic phase, drying with anhydrous sodium sulfate and evaporation under reduced pressure yielded the compound **65** (2.1 g, 72 %) as a green solid which was used without further purification in the next reaction.

m.p.: 112 ºC.

IR (nujol, υ in cm^{-1}): 3338, 1684, 1625, 1547, 1521, 1327, 1268, 1223, 1139, 1074, 924, 873, 795, 736.

^{1}H NMR (400 MHz, $CDCl_3$) δ 10.55 (broad s, OH), 9.72 (broad s, OH), 9.11 (s, 1H), 7.81 (d, *J* = 9.1 Hz, 1H), 7.26 (s, 1H), 7.12 (d, *J* = 9.1 Hz, 1H), 4.01 (s, 3H).

^{13}C NMR (100 MHz, $CDCl_3$) δ 170.1 (C), 156.9 (C), 155.7 (C), 138.0 (CH), 133.8 (C), 126.6 (CH), 123.2 (CH), 120.6 (C), 118.7 (C), 116.2 (C), 114.6 (CH), 53.3 (CH_3).

HRMS (ESI-): Calculated for $C_{12}H_9O_7S$ [M hydrolysed-H]$^-$ 297.0074, found 297.0075.

Methyl 3,7-dihydroxy-8-(*N*-(naphthalen-1-yl)sulfamoyl)-2-naphthoate (66)

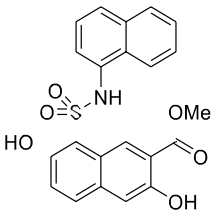

66

Freshly sublimed 1-naphthylamine (1,0 g, 7.0 mmol) was dissolved in 1 mL of DCM. Then, compound **65** (400 mg, 1.3 mmol) was added and the mixture was heated at 60ºC under argon atmosphere for 10 minutes. Thereafter, the organic solvent was evaporated under reduced pressure and the crude reaction mixture was purified by column chromatography over silica gel, eluting with DCM in hexane mixtures of increasing polarity (starting with 80%, the deep yellow fraction was collected). Compound **66** (450 mg, 84 %) was obtained as a pale-brown solid.

m.p.: 190 ºC.

IR (nujol, υ in cm^{-1}): 3323, 3191, 2924, 2855, 1676, 1620, 1558, 1523, 1346, 1292, 1260, 1211, 1144, 1123, 1088, 1015, 945, 867, 834, 776, 705, 679.

^{1}H NMR (400 MHz, $CDCl_3$) δ 10.43 (broad s, OH), 10.04 (broad s, OH), 9.09 (s, 1H), 7.81 (d, *J* = 8.5 Hz, 1H), 7.76 (d, *J* = 7.5 Hz, 1H), 7.70 (d, *J* = 8.5 Hz, 1H), 7.68 (d, *J* = 9.2 Hz, 1H), 7.42 (t, *J* = 7.5 Hz, 1H), 7.31 (t, *J* = 7.5 Hz, 1H), 7.25 (t, *J* = 8.5 Hz, 1H), 7.23 (s, 1H), 7.18 (broad s, NH), 7.08 (d, *J* = 7.5 Hz, 1H), 7.03 (d, *J* = 9.2 Hz, 1H), 3.94 (s, 3H).

^{13}C NMR (100 MHz, $CDCl_3$) δ 170.1 (C), 156.9 (C), 155.9 (C), 135.2 (CH), 134.4 (C), 133.9 (C), 130.4 (C), 129.9 (C), 128.5 (CH), 128.4 (CH), 127.0 (CH), 126.8 (CH), 126.6 (CH), 125.3 (CH), 124.3 (CH), 123.6 (CH), 122.0 (C), 121.9 (CH), 115.3 (C), 114.1 (CH), 111.8 (C), 53.0 (CH_3).

HRMS (ESI+): Calculated for $C_{22}H_{18}NO_6S$ $[M+H]^+$ 424.0849, found 424.0842.

3,7-Dihydroxy-*N*-(6-methylpyridin-2-yl)-8-(*N*-(naphthalen-1-yl)sulfamoyl)-2-naphthamide (receptor 67)

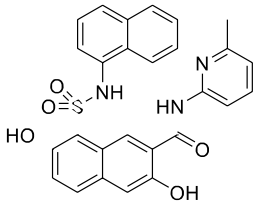

67

n-Butyllithium 1.6 M in hexane (2.5 mL, 4.0 mmol) was added to a solution of 2-amino-6-methylpyridine (400 mg, 3.7 mmol) in 10 mL of dry THF at -80ºC under argon atmosphere. Thereafter, ester **66** (100 mg, 0,24 mmol) in 4 mL of THF was added and the reaction mixture was warmed to room temperature for 1 hour. After this time, the organic solvent was evaporated under reduced pressure and then 20 mL of an aqueous solution of 5% acetic acid and 20 mL of EtOAc were added. The organic phase was separated, dried over anhydrous sodium sulfate and evaporated under reduced pressure affording an oily compound, which was treated with Et_2O to crystallize receptor **67** (70 mg, 59 %) as a pale-green solid.

m.p.: 225 ºC.

IR (nujol, υ in cm^{-1}): 3276, 2923, 2854, 1664, 1606, 1563, 1541, 1412, 1333, 1274, 1215, 1144, 1117, 935, 872, 776, 725, 687, 653.

^{1}H NMR (400 MHz, $CDCl_3$:CD_3OD 95:5) δ 9.40 (s, 1H), 8.45 (d, *J* = 7.9 Hz, 1H), 8.36 (d, *J* = 8.4 Hz, 1H), 8.01 (d, *J* = 8.0 Hz, 1H), 8.00 (t, *J* = 8.0 Hz, 1H), 7.94 (d, *J* = 6.0 Hz, 1H), 7.92

(d, *J* = 6.0 Hz, 1H), 7.66 (t, *J* = 7.5 Hz, 1H), 7.6 (t, *J* = 7.5 Hz, 1H), 7.56 (s, 1H), 7.47 (t, *J* = 8.0 Hz, 1H), 7.31 – 7.21 (m, 3H), 2.76 (s, 3H).

^{13}C NMR (100 MHz, $CDCl_3$) δ 168.4 (C), 156.6 (2 C), 155.8 (C), 150.4 (C), 140.0 (CH), 134.5 (CH), 134.4 (C), 133.4 (C), 131.2 (C), 130.3 (C), 128.3 (CH), 128.0 (CH), 126.6 (CH), 126.5 (CH), 125.5 (CH), 123.4 (CH), 123.4 (CH), 123.3 (CH), 122.5 (CH), 122.2 (C), 120.3 (CH), 118.2 (C), 115.0 (CH), 112.7 (CH), 112.4 (C), 23.8 (CH_3).

HRMS (ESI+): Calculated for $C_{27}H_{22}N_3O_5S$ $[M + H]^+$ 500.1275, found 500.1267.

Methyl 3,7-dihydroxy-8-(*N*-(6-methylpyridin-2-yl)sulfamoyl)-2-naphthoate (68)

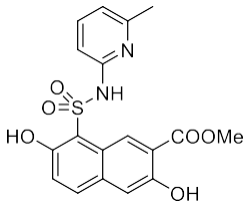

68

Compound **65** (250 mg, 0.8 mmol) was added to a round-bottom flask with melted 2-amino-6-methylpyridine (500 mg, 4.6 mmol) at 70ºC under argon atmosphere, and the reaction was kept at this temperature for 1 hour. After this time, the reaction mixture was poured over 20 mL of an aqueous solution of 5% acetic acid and the resulting precipitate was collected affording compound **68** (200 mg, 65 %) as a pale-green solid.

m.p.: 201 – 203 ºC.

IR (nujol, υ in cm^{-1}): 2917, 1684, 1618, 1518, 1223, 1160, 1125, 1091, 1056, 1012, 928, 856, 789, 724, 674.

^{1}H NMR (400 MHz, $CDCl_3$) δ 10.36 (broad s, OH), 9.20 (s, 1H), 7.68 (d, *J* = 9.1 Hz, 1H), 7.57 (t, *J* = 8.0 Hz, 1H), 7.20 (s, 1H), 7.18 (d, *J* = 9.1 Hz, 1H), 6.92 (d, *J* = 8.0 Hz, 1H), 6.53 (d, *J* = 8.0 Hz, 1H), 3.64 (s, 3H), 2.44 (s, 3H).

^{13}C NMR (100 MHz, $CDCl_3$) δ 170.4 (C), 155.5 (C), 155.2 (C), 155.1 (C), 148.9 (C), 143.3 (CH), 134.0 (C), 133.8 (CH), 128.3 (CH), 123.7 (CH), 122.6 (C), 115.4 (C), 115.0 (C), 113.8 (CH), 113.4 (CH), 113.3 (CH), 52.5 (CH_3), 20.1 (CH_3).

HRMS (ESI+): Calculated for $C_{18}H_{17}N_2O_6S$ $[M+H]^+$ 389.0802, found 389.0795.

_N_-(4-(Dimethylamino)benzyl)-3,7-dihydroxy-8-(_N_-(6-methylpyridin-2-yl)sulfamoyl)-2-naphthamide (receptor 69)

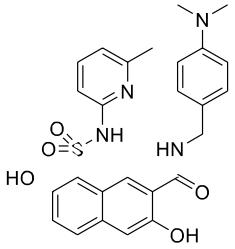

69

Ester **68** (100 mg, 0.26 mmol) was dissolved in freshly distilled 4-(dimethylamino)benzylamine (1 g, 6.7 mmol) at 70ºC under strict oxygen exclusion. After 1 hour, 20 mL of an aqueous solution of 5% acetic acid were added to the reaction mixture, and the resulting precipitate was filtered off affording receptor **69** (82 mg, 63 %) as a pale-brown solid.

m.p.: 129 ºC.

IR (nujol, υ in cm^{-1}): 3358, 2923, 2854, 1721, 1613, 1525, 1270, 1223, 1177, 1097, 1060, 1013, 973, 932, 861, 813, 786, 739, 666.

^{1}H NMR (400 MHz, $CDCl_3$) δ 8.90 (s, 1H), 8.33 (broad s, NH), 7.67 (d, *J* = 9.0 Hz, 1H), 7.47 (t, *J* = 8.0 Hz, 1H), 7.21 (s, 1H), 7.14 (d, *J* = 9.0 Hz, 1H), 7.06 (d, *J* = 8.0 Hz, 2H), 6.80 (d, *J* = 8.0 Hz, 1H), 6.50 – 6.37 (m, 3H), 4.44 (s, 2H), 2.79 (s, 6H), 2.27 (s, 3H).

^{13}C NMR (100 MHz, $CDCl_3$) δ 169.8 (C), 156.3 (C), 154.9 (C), 154.9 (C), 149.9 (C), 148.8 (C), 143.4 (CH), 133.7 (CH), 133.0 (C), 129.1 (2 CH), 125.6 (C), 123.6 (CH), 122.7 (CH), 122.3 (C), 118.2 (C), 115.0 (C), 114.0 (CH), 113.3 (CH), 113.2 (CH), 112.5 (2 CH), 43.3 (CH_2), 40.6 (2 CH_3), 19.9 (CH_3).

HRMS (ESI+): Calculated for $C_{26}H_{27}N_4O_5S$ $[M+H]^+$ 507.1697, found 507.1693.

5.4. Kinetic studies

5.4.1. Methanolysis studies

To test the hydrolytic activity, the methanolysis rates of the acetylated catalysts were measured. The reaction progress was followed by integration of the product ^{1}H NMR signals and those of the starting material in the corresponding spectra. Two different methodologies were employed.

***1st Generation of organocatalysts* (5, 11, 16, 21, 22, 25, 29)**

The acetylated catalyst (10 mg). was dissolved in CD_3OD (400 μL) and the ^{1}H NMR spectra were recorded periodically at 20ºC. Under these conditions, CD_3OD concentration can be considered constant, and *pseudo*-first order conditions can be applied.

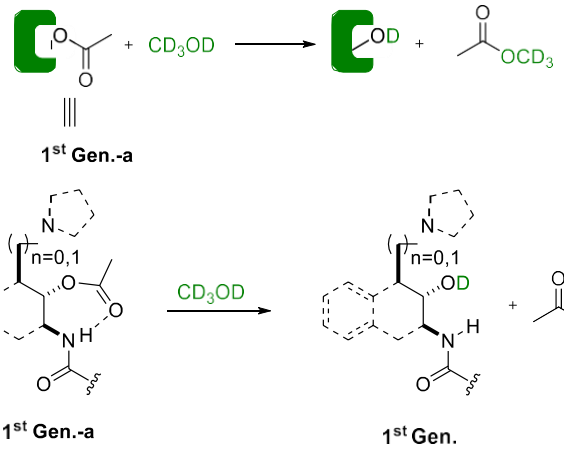

Kinetic studies for the first generation catalysts are freely available at:
https://pubs.acs.org/doi/suppl/10.1021/acscatal.0c02121/suppl_file/cs0c02121_si_001.pdf

***2nd – 3rd Generation of organocatalysts* (33, 35, 37, 39, 44, 48, 52, 56, 60, 61)**

10 mg *ca.* of the desired acetylated catalyst and 10 mg *ca.* of acetylated catalyst **33a** as reference (in order to obtain more accurate results) were dissolved in a 5% CD_3OD in $CDCl_3$ solution (600 μL) and ^{1}H NMR spectra were recorded periodically at 20ºC. Despite the reduction in the total amount of deuterated methanol, *pseudo*-first order approximation is still suitable to study the reaction kinetics.

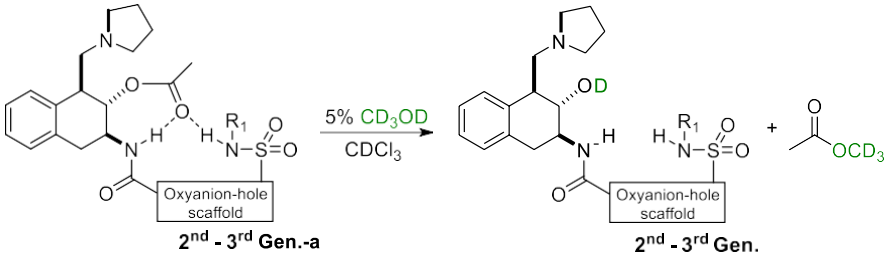

The following equation was employed:

$$v = -\frac{\partial[\boldsymbol{X_{C\_a}}]}{\partial t} = k[\boldsymbol{X_{C\_a}}]^m[CD_3OD]^n = k'[\boldsymbol{X_{C\_a}}]$$

$$m = n = 1\ ;\ [CD_3OD] = \text{constant}\ (pseudo - \text{first order conditions})$$

$$\int_{[\boldsymbol{X_{C\_a}}]_0}^{[\boldsymbol{X_{C\_a}}]} \frac{\partial[\boldsymbol{X_{C\_a}}]}{[\boldsymbol{X_{C\_a}}]} = -k' \int_{t_0}^{t} \partial t$$

$$Ln[\boldsymbol{X_{C\_a}}] - Ln[\boldsymbol{X_{C\_a}}]_0 = -k't$$

$$Ln\,[\boldsymbol{X_{C\_a}}] = Ln\,[\boldsymbol{X_{C\_a}}]_0 - k't \rightarrow t_{1/2} = \frac{Ln\,[2]}{k'}$$

Equation S1. *General formula for methanolysis studies (*$X_{\mathbf{C\_a}}$ *molar fraction of acetylated organocatalysts).*

From Equation S1, plotting $Ln[X_{C\_a}]$ *versus* time should give a straight line. From the slope of this line k' can be obtained, and consequently the $t_{1/2}$ of methanolysis of **C_a**. The concentration of starting material and product were calculated as molar fraction (X) by integration of suitable signals for both acylated and deacylated catalyst. For 2nd and 3rd generation of organocatalysts, **C_a** was normalized with the $t_{1/2}$ of acetylated catalyst **33a**.

Methanolysis results – 1st generation organocatalysts

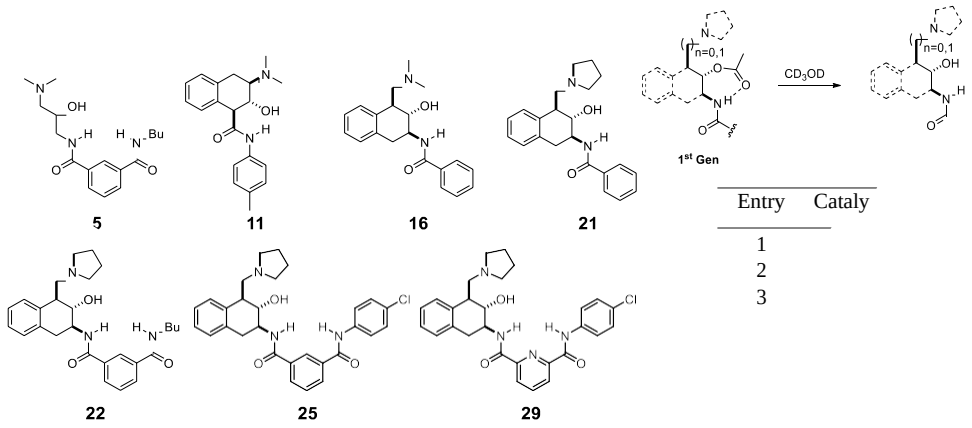

Entry	Cataly
1	
2	
3	

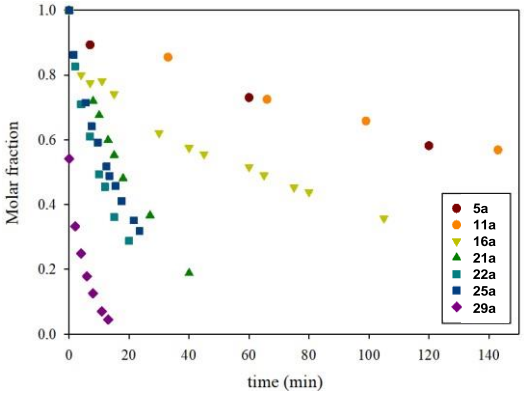

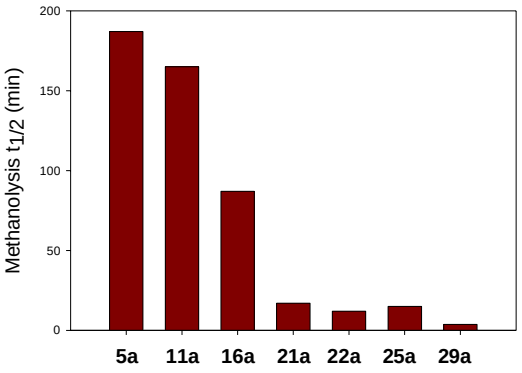

Kinetic studies for the first generation catalysts are freely available at:
https://pubs.acs.org/doi/suppl/10.1021/acscatal.0c02121/suppl_file/cs0c02121_si_001.pdf

Methanolysis results – 2nd and 3rd generation organocatalysts

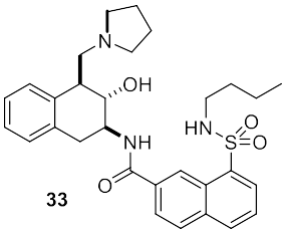

33

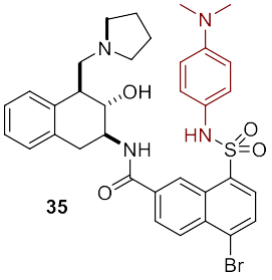

35

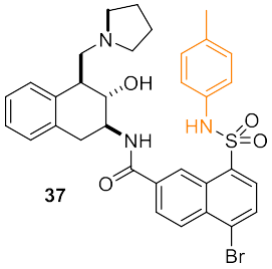

37

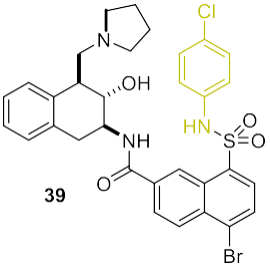

39

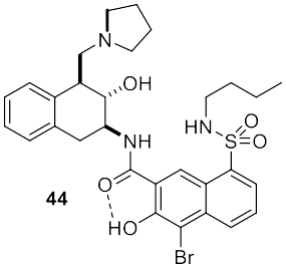

44

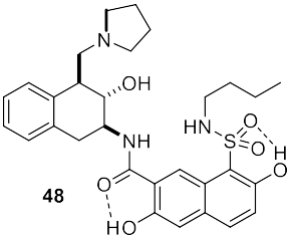

48

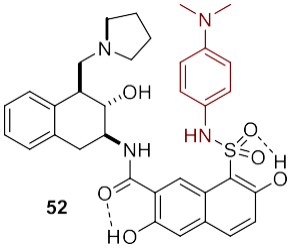

52

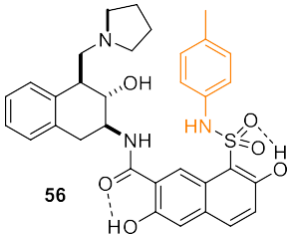

56

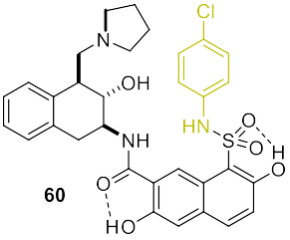

60

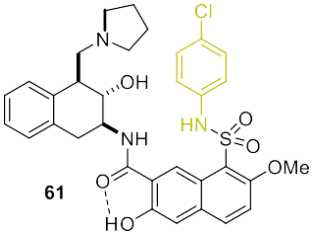

61

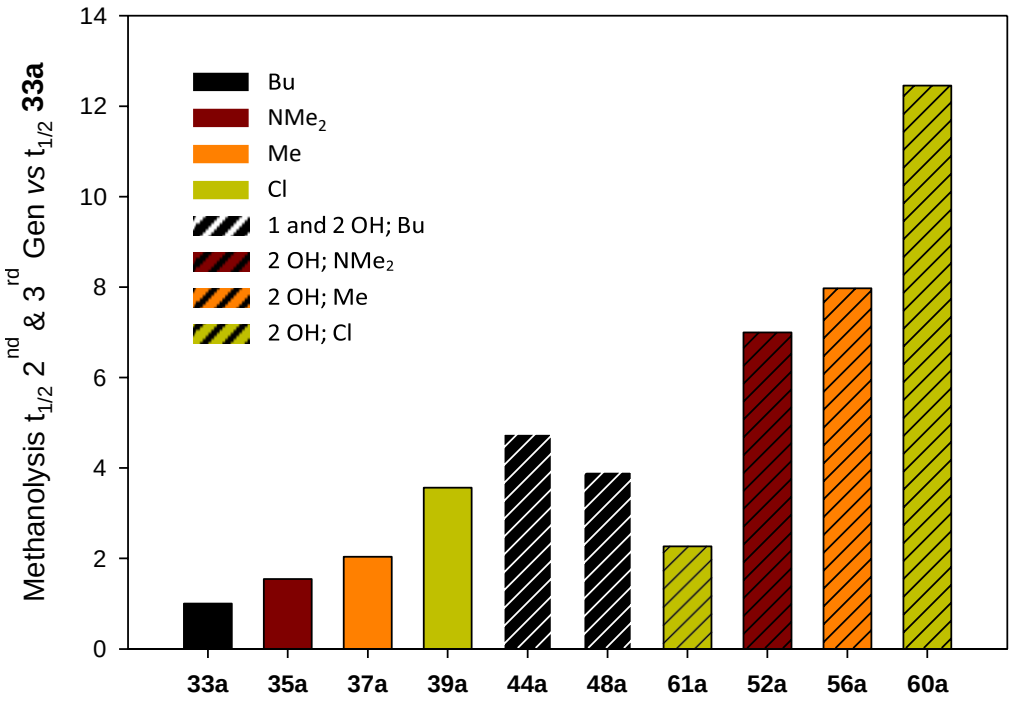

Figure 193. *Methanolysis studies for 2nd and 3rd generation catalysts (2nd & 3rd Gen).*

33a	1									
35a	1.54	1								
37a	2.04	1.32	1							
39a	3.56	2.31	1.75	1						
44a	4.75	3.08	2.33	1.33	1					
48a	3.92	2.54	1.92	1.10	0.82	1				
52a	6.99	4.53	3.43	1.96	1.47	1.79	1			
56a	7.97	5.17	3.91	2.24	1.68	2.04	1.14	1		
60a	12.45	8.07	6.11	3.50	2.62	3.18	1.78	1.56	1	
61a	2.27	1.47	1.11	0.64	0.48	0.58	0.32	0.28	0.18	1
	33a	**35a**	**37a**	**39a**	**44a**	**48a**	**52a**	**56a**	**60a**	**61a**

Figure 194. *Graph showing the increase in the reaction rate between the different 2nd and 3rd generation catalysts.*

Graphs below represent plotting of Ln[X_{C_a}] *versus* time for the catalysts.

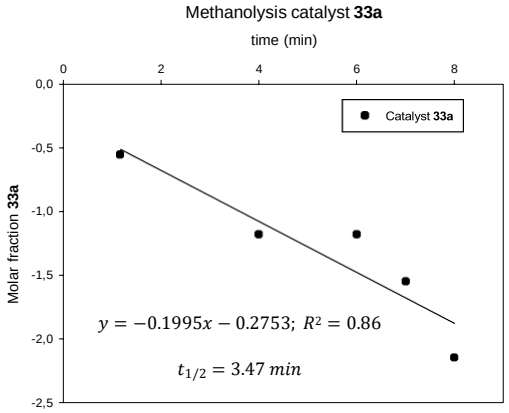

Plotting of Ln[X_{33a}] *vs* time.

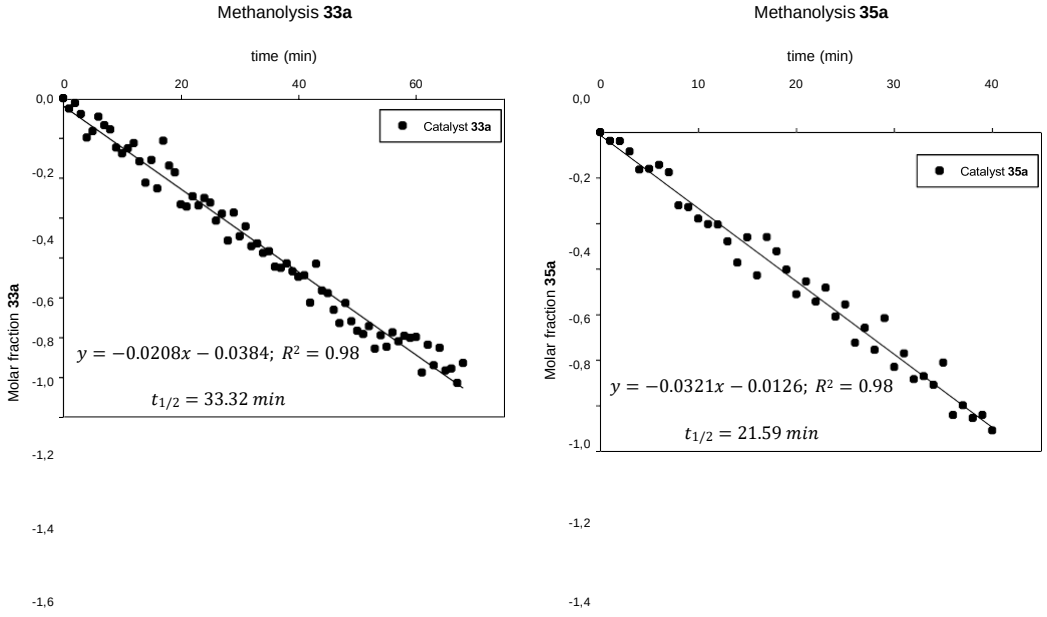

Plotting of Ln[X_{33a}] *vs* time (left) and Ln[X_{35a}] *vs* time (right).

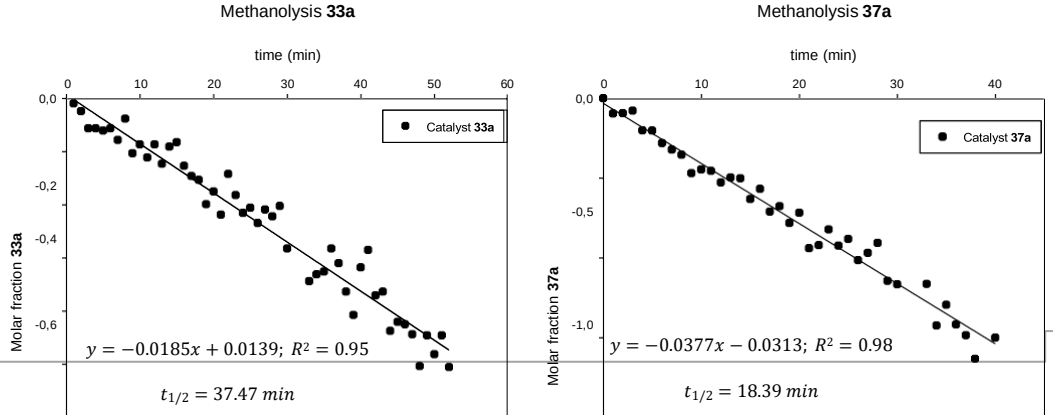

-0,8

-1,0

-1,2

-1,5

-2,0

Plotting of Ln[X_{33a}] *vs* time (left) and Ln[X_{37a}] *vs* time (right).

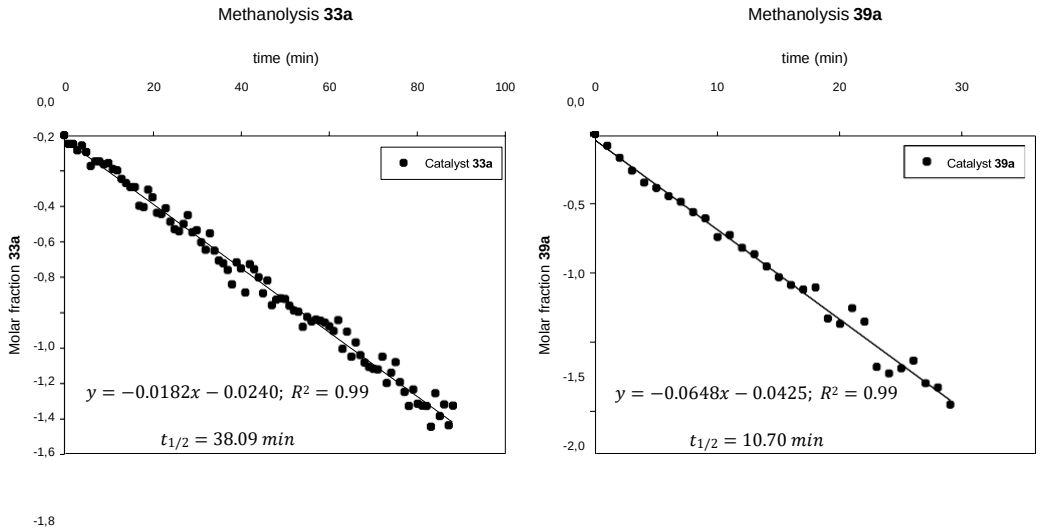

Plotting of Ln[X_{33a}] *vs* time (left) and Ln[X_{39a}] *vs* time (right).

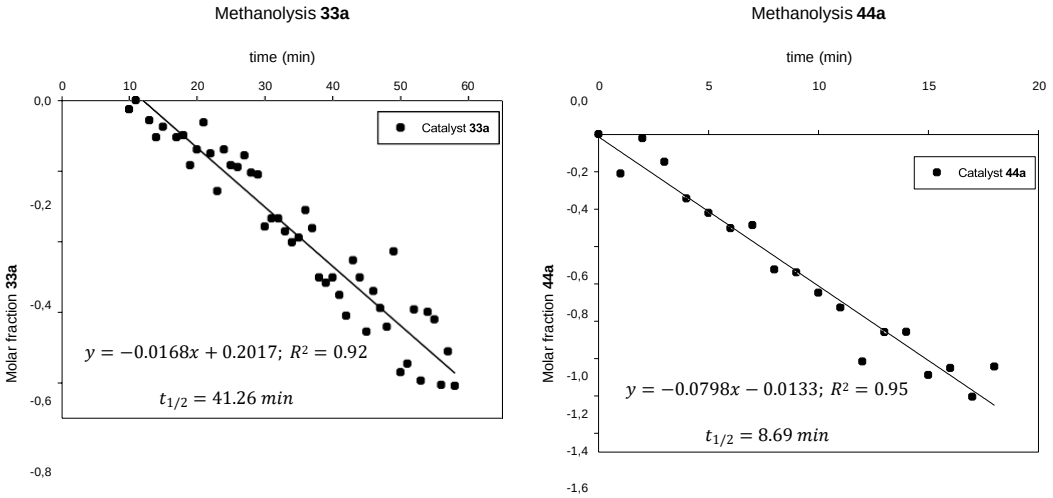

Plotting of Ln[X_{33a}] *vs* time (left) and Ln[X_{44a}] *vs* time (right).

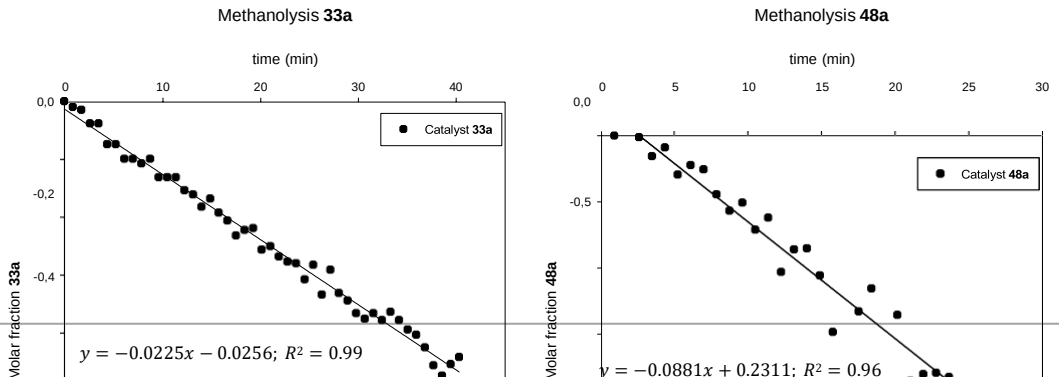

-0,6

-0,8

-1,0

-1,0

-1,5

-2,0

Plotting of Ln[X_{33a}] *vs* time (left) and Ln[X_{48a}] *vs* time (right).

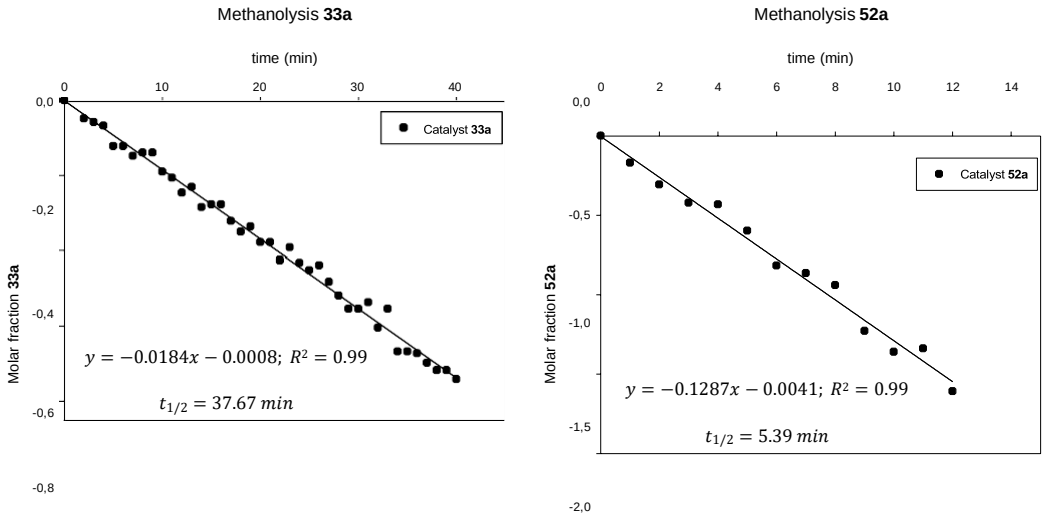

Plotting of Ln[X_{33a}] *vs* time (left) and Ln[X_{52a}] *vs* time (right).

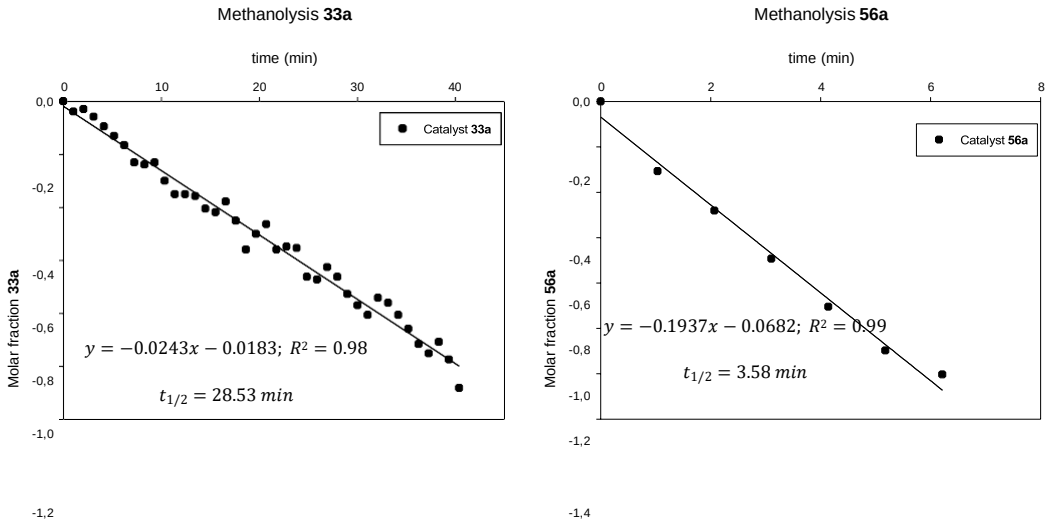

Plotting of Ln[X_{33a}] *vs* time (left) and Ln[X_{56a}] *vs* time (right).

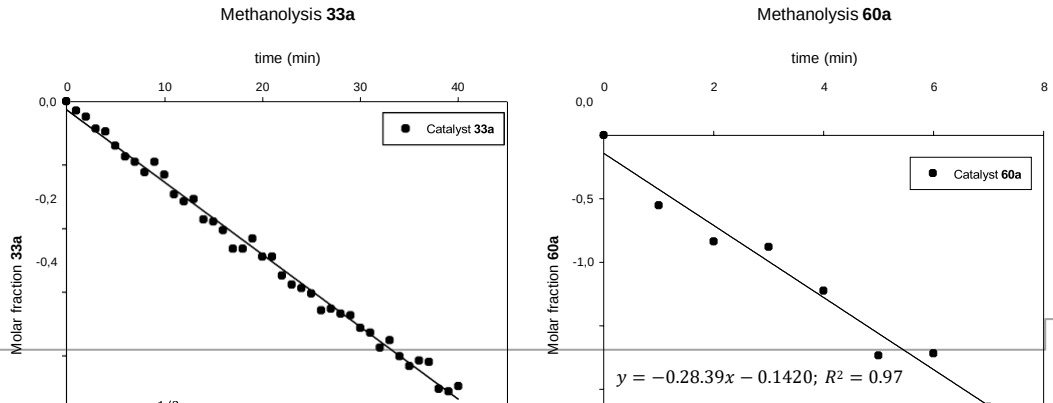

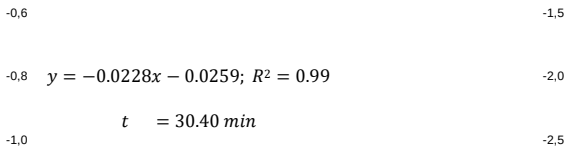
-0,6
-0,8
-1,0
-1,5
-2,0
-2,5
$y = -0.0228x - 0.0259;\ R^2 = 0.99$
$t = 30.40\ min$

Plotting of Ln[$X_{\mathbf{33a}}$] *vs* time (left) and Ln[$X_{\mathbf{60a}}$] *vs* time (right).

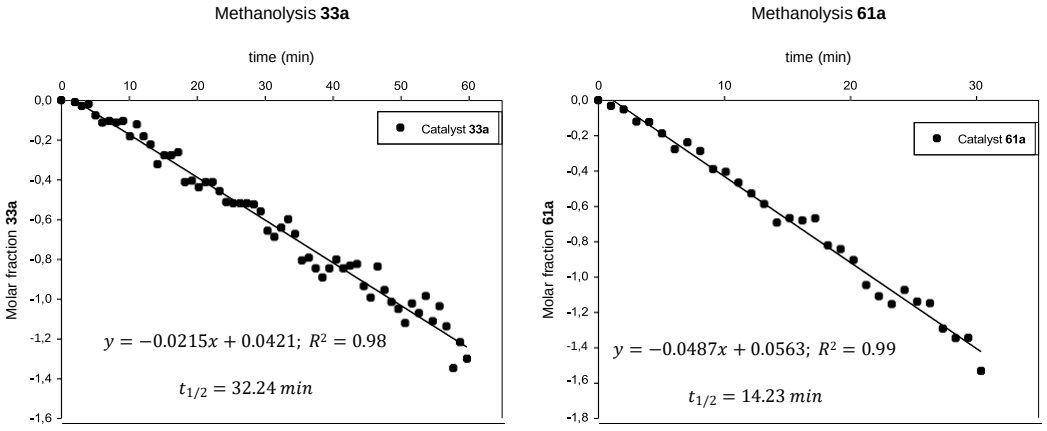

Plotting of Ln[$X_{\mathbf{33a}}$] *vs* time (left) and Ln[$X_{\mathbf{61a}}$] *vs* time (right).

5.4.2. Transesterification Studies

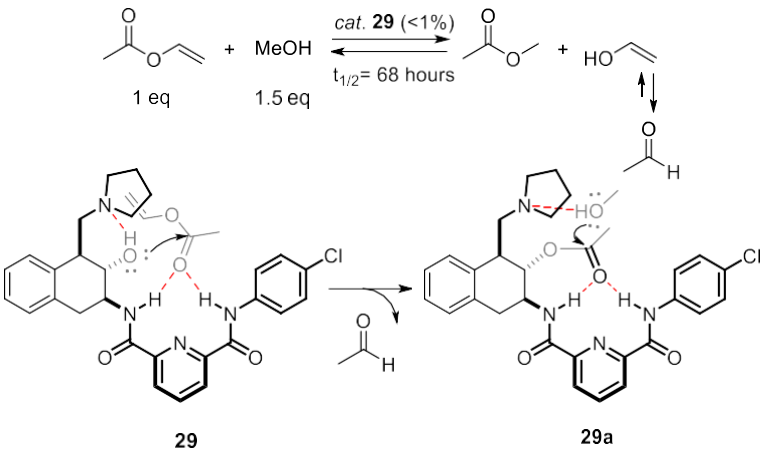

Figure 195. *General reaction (above) and proposed mechanism for the transesterification reaction between vinyl acetate and MeOH catalysed with* **29**.

Vinyl acetate (290 μL, 3.2 mmol) and MeOH (210 μL, 5.2 mmol) were mixed in an NMR tube and catalyst **29** (10 mg, $2.0x10^{-3}$ mmol, <1 mol%) was added at 20ºC. The reaction progress was followed by ^{1}H NMR using external D_2O in a Shigemi NMR tube to lock the spectrometer. Integration of the starting material and product signals was used to calculate the concentration of starting material and products. Plotting molar fraction of vinyl acetate and methyl acetate *vs* time was used to calculate the reaction rate and a half-life of 68 hours was obtained.

The same conditions were performed without catalyst **29** and monitored by ^{1}H NMR. No reaction was observed.

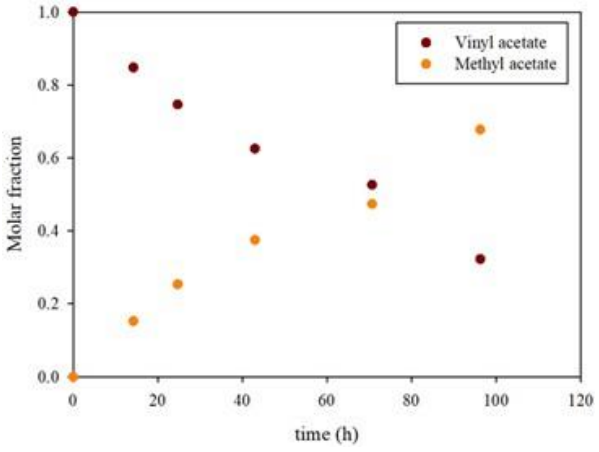

Figure 196. *Transesterification reaction of vinyl acetate with MeOH catalysed with* **29**.

5.5. Titration studies

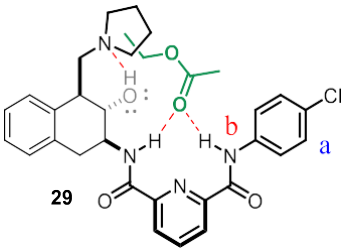

Figure 198. *Associate between* **29** *and EtOAc.*

To test the catalyst **29** ability to form an associate with the substrate, a titration between catalyst **29** and EtOAc was performed and followed by ^{1}H NMR. Catalyst **29** (1.3 mg, 2.6x10^{-3} mmol) was dissolved in 400 μL of $CDCl_3$ and pure EtOAc was successively added to the reaction mixture, registering successive ^{1}H NMR spectra after each addition at 20ºC. Plotting the shifts of protons a and b of catalyst **29** against the equivalents of EtOAc added gave an association constant of 0.79 M^{-1} with 6.1% error.

Titration analysis was performed with Bindfit.

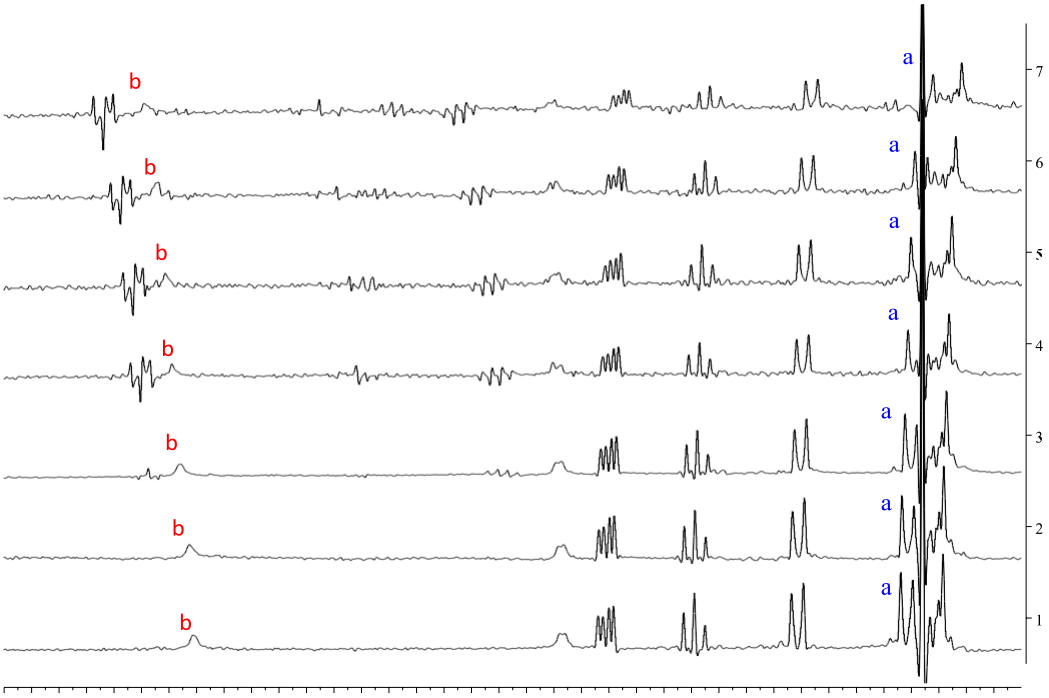

Figure 199. *^{1}H NMR (7.1-10.5 ppm) spectra of* **29** *in $CDCl_3$ with (1) 0 eq, (2) 8 eq, (3) 20 eq, (4) 39 eq, (5) 57 eq, (6) 76 eq and (7) 128 eq of EtOAc.*

Table 7. *Titration of catalyst* **29** *with EtOAc.*

EtOAc/μL	EtOAc eq.	δ_a	δ_b
0	0	7.3391	9.9123
2	8	7.3350	9.9254
5	20	7.3237	9.9598
10	39	7.3125	9.9881
15	57	7.3017	10.0140
20	76	7.2867	10.0460
35	128	7.2535	10.0880

$$k = 0.79 \text{ x } 1/\text{mol} \cdot \text{L}^{-1}$$

$$k_{error} = 6.1\ \%$$

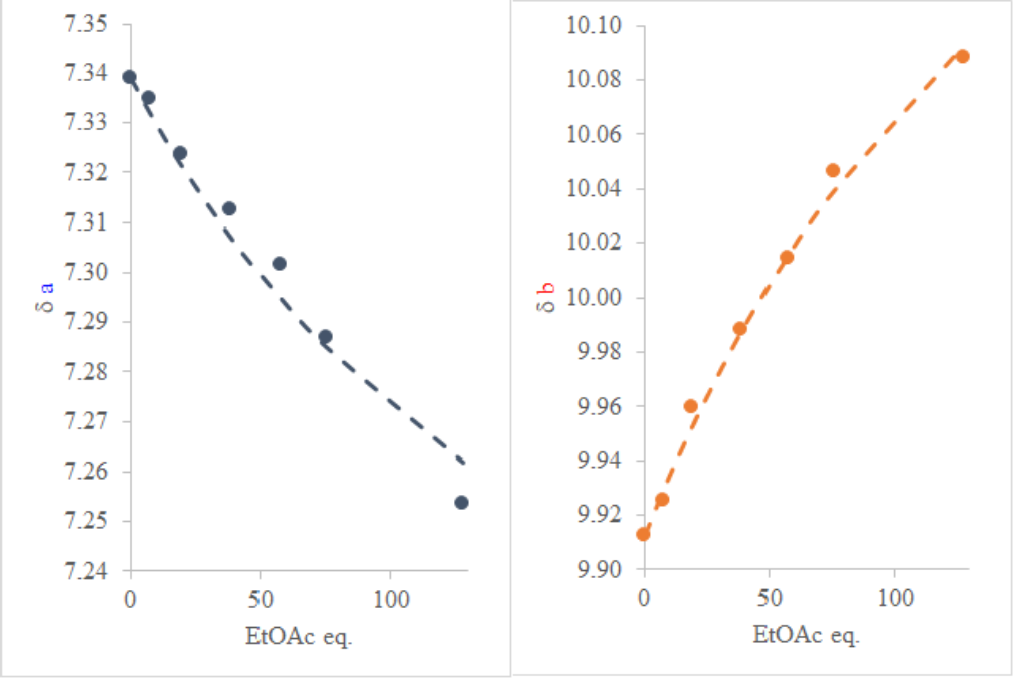

Figure 200. *Titration of catalyst* **29** *with EtOAc.*

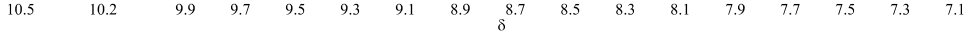

Titration studies for receptors **64**, **67** and **69** are freely available at: *https://chemistry-europe.onlinelibrary.wiley.com/action/downloadSupplement?doi=10.1002%2Fchem.202102137&file=chem202102137-sup-0001-misc_information.pdf*

5.6. Computational studies

For the conformational analysis of the **Catalyst model 1st-Gen**, different conformations were considered rotating the amide C8-N13 bond and the C11-N12 bonds, as well as equatorial and axial arrangement of these groups

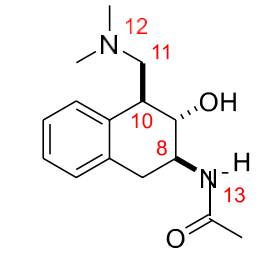

Catalyst model 1st-Gen

Conformation	Relative Gibbs free energy (kcal/mol)
Conf 1 (equatorial)	0.0
Conf 2 (equatorial)	3.0
Conf 3 (equatorial)	2.4
Conf 4 (equatorial)	5.5
Conf 5 (axial)	4.6
Conf 6 (axial)	5.6
Conf 7 (axial)	5.2

Conf 1

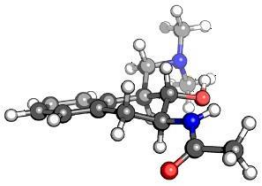

Conf 2

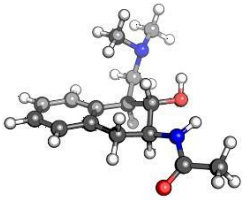

Conf 3

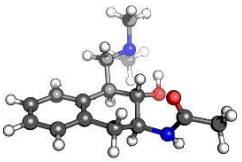

Conf 4

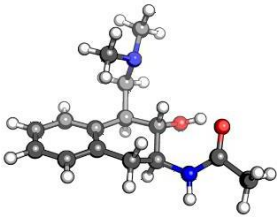

Conf 5

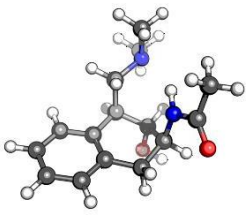

Conf 6

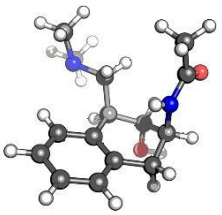

Conf 7

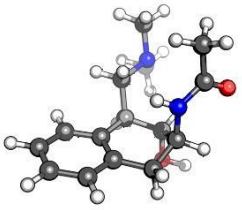

The geometry of the TS structure corresponding to the methanolysis of the acetylated catalyst was calculated with the same level of theory. The structure shows a single imaginary frequency.

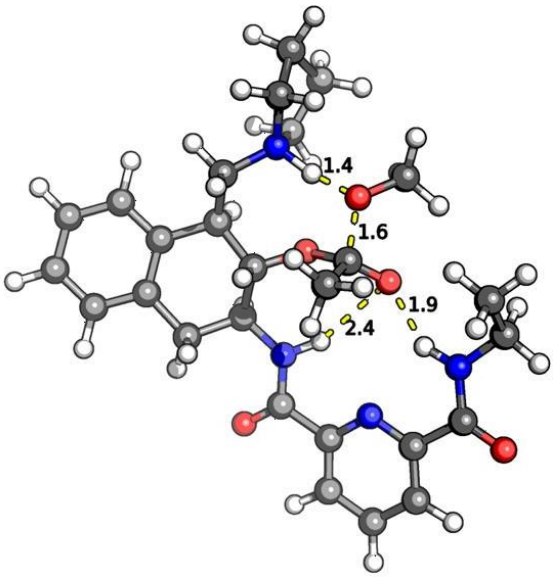

Computational studies coordinates are freely available at:
https://pubs.acs.org/doi/suppl/10.1021/acscatal.0c02121/suppl_file/cs0c02121_si_001.pdf

Annex I – Final compounds list

Chapter 1 – Supramolecular receptors

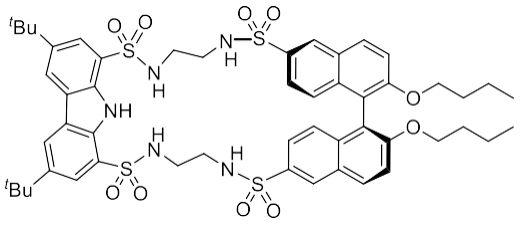

(*S*)-**2**

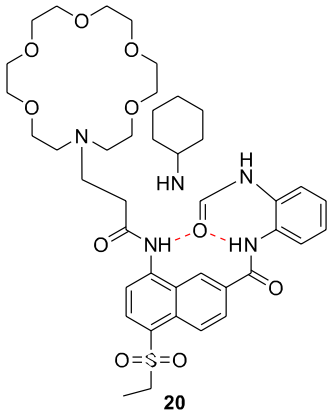

20

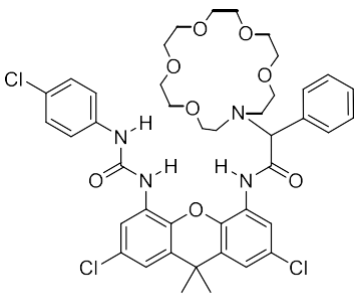

28

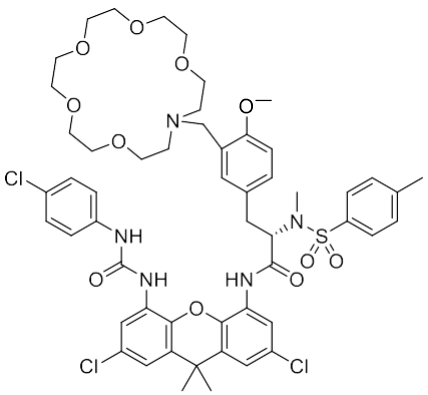

38

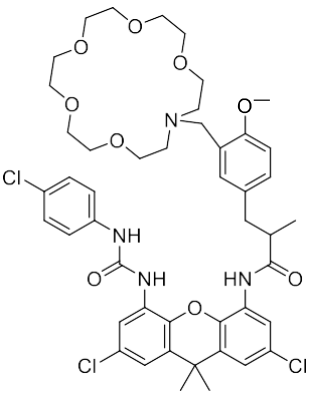

46

Chapter 2 – Organocatalysts

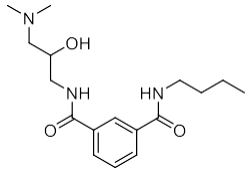

5

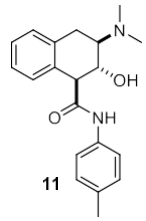

11

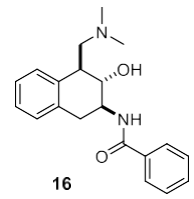

16

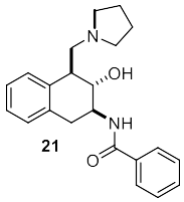

21

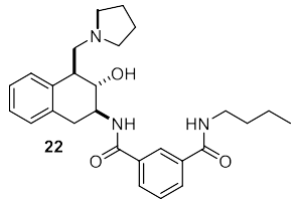

22

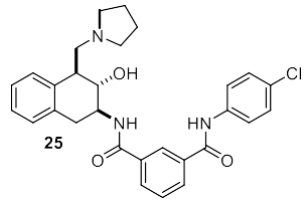

25

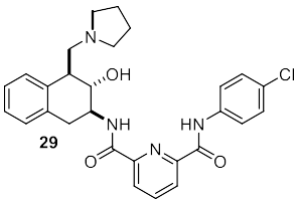

29

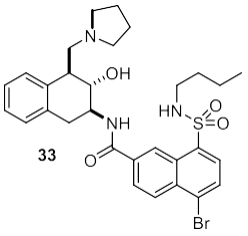

33

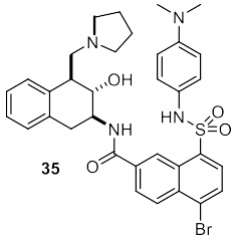

35

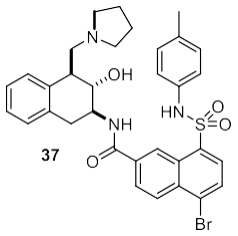

37

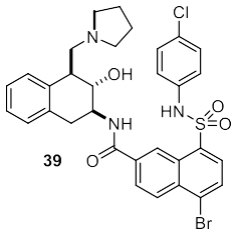

39

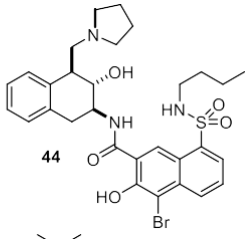

44

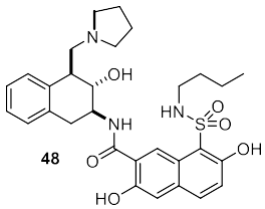

48

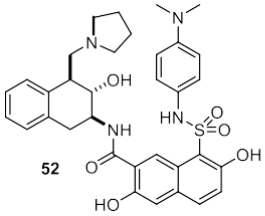

52

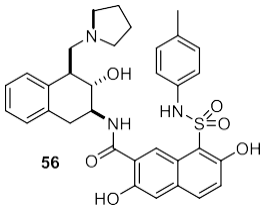

56

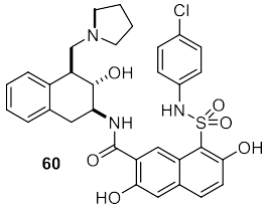

60

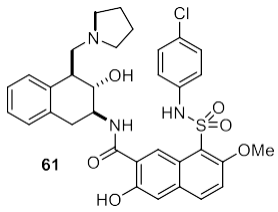

61

Chapter 2 – Oxyanion-hole mimics

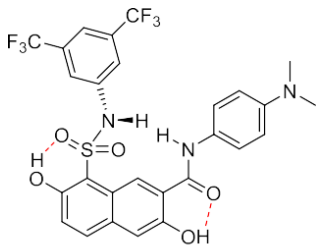

64

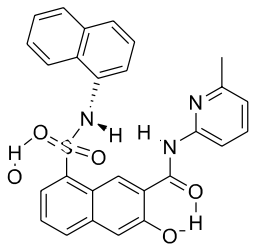

67

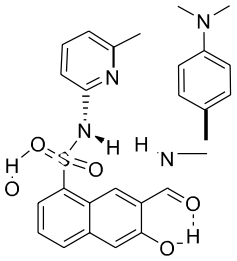

69

Annex II – Publications

OL | Organic Letters

pubs.acs.org/OrgLett Letter

Highly Enantioselective Extraction of Phenylglycine by a Chiral Macrocyclic Receptor Based on Supramolecular Interactions

María G. Turiel, José J. Garrido-González, Luis Simón, Francisca Sanz, Anna M. Lithgow, Joaquín R. Morán, Ángel L. Fuentes de Arriba,* and Victoria Alcázar*

Cite This: *Org. Lett.* 2020, 22, 867–872 Read Online

ACCESS | Metrics & More | Article Recommendations | Supporting Information

ABSTRACT: Using supramolecular interactions, a novel macrocyclic receptor is able to selectively extract zwitterionic phenylglycine from neutral aqueous solutions into chloroform with up to 91.8% *ee*. Modeling studies, nuclear magnetic resonance experiments, and X-ray diffraction analysis were carried out to explain the high enantioselectivity observed.

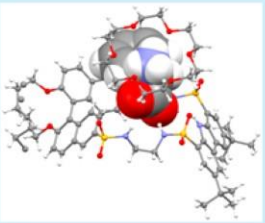

Enantiopure amino acids are important building blocks in pharmaceuticals, agrochemicals, and food and fragrance industries. Whereas L-amino acids are the components of proteins, D-enantiomers have found interesting applications in antibiotics, chemotherapeutics, immunosuppressives, deodorants, fluorescent markers of DNA, sweeteners, pesticides, and so on.[1] In fact 5% of the top 200 brand name drugs by retail sales in 2018 possessed a D-amino acid in their structure.[2]

Much of the industrial production of amino acids relies on fermentation processes, which usually require large volumes of water, large fermenter capacity, strict sterility, and costly methods for product recovery that boost the capital investment.[3] Attractive alternatives arise from asymmetric synthesis or simple racemic synthesis followed by a chiral resolution step. In the last several years, enantioselective liquid–liquid extraction has appeared as an attractive option because of its low energy consumption, recyclability, easy handling, and easy scalability.[4] This technique requires a chiral receptor that is able to transport one of the amino acid enantiomers from an aqueous phase to an organic phase (Figure 1A). However, this is a challenging task due to the ionic nature of zwitterionic amino acids that makes them highly hydrophilic and extremely soluble in aqueous solutions, thus increasing the energetic cost associated with their desolvation. Also, the receptor needs to be able to simultaneously associate the positively charged ammonium group and the negatively charged carboxylate group of the amino acids, which are arranged in a specific tridimensional disposition. All of these features increase the complexity of the receptor structure. Amino acid derivatization has been proposed as an option to facilitate the extraction; however, a further deprotection step that increases the cost of the process is required. To make it profitable, it would be more attractive to find a receptor that is able to directly extract zwitterionic amino acids from aqueous solutions with high selectivity. Crown ethers,[5] guanidiniums,[6] metal complexes,[7] lanthanide complexes,[8] and BINOL-carbonyl hosts[9] have been traditionally employed,[4] although most systems possess moderate operational selectivities (Figure 1B, selected examples for zwitterionic phenylglycine).

We have previously reported[10] a carbazole-based receptor **1** (Figure 1C) functionalized with two sulfonamide groups as H-bond sites for anion complexation. Whereas excellent affinities were obtained for halide anions ($K_a = 7.9 \times 10^6\ M^{-1}$ for Cl^- in $CHCl_3$), a strong decrease in binding was observed for oxyanions. This behavior, according to the X-ray structural analysis and modeling studies,[10] was attributed to the importance of the CH···X (halogen) interactions in the binding process and the steric hindrance and receptor conformational changes observed for oxyanion association. Trying to develop a more efficient synthetic host for oxyanions and eventually for zwitterionic amino acids, the macrocyclic structure **2** (Figure 1D) was designed with several improved features: (i) two more H-bond donor groups were added, (ii) the macrocyclic structure ensures a higher degree of preorganization, reducing the entropic cost of association,[11] (iii) a chiral binaphthyl unit enables the enantioselective

Received: December 6, 2019
Published: January 13, 2020

https://dx.doi.org/10.1021/acs.orglett.9b04379
Org. Lett. 2020, 22, 867–872

Organic Letters pubs.acs.org/OrgLett Letter

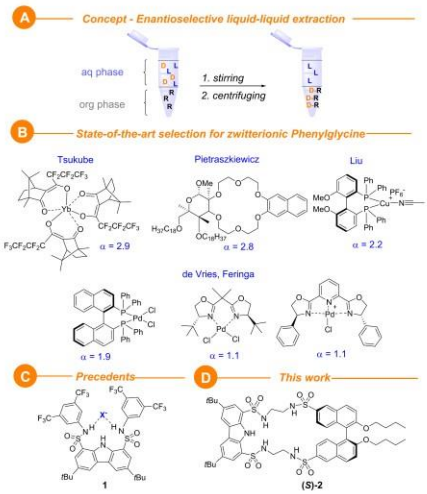

Figure 1. (A) Enantioselective liquid−liquid extraction concept (R = chiral receptor). (B) Selected chiral receptors and selectivities (α) for zwitterionic phenylglycine (Phg). (C) Precedents in the group for anion recognition with a carbazole scaffold. (D) Novel chiral macrocyclic receptor based on a carbazole-BINOL scaffold.

recognition of chiral anions, and (iv) the steric hindrance around the sulfonamide NH groups has been reduced, replacing the bis(trifluoromethyl)anilines by ethylenediamines. Thus anion binding can be expected in the hydrogen-bonding donor pocket of the preorganized receptor **2**, whereas the chiral BINOL building block should be able to preferentially select one of the enantiomers. Also, (i) sulfonamide-based carbazole receptors provide more acidic NH compounds than carboxamides and hence potentially stronger associates, (ii) they do not require transition metals, and (iii) their synthesis can be easily carried out on a multigram scale from inexpensive starting materials. Herein we report our findings.

The synthetic strategy for the preparation of compound **2** was a convergent synthesis where ring closure could be achieved by the simultaneous formation of two sulfonamide bonds. Whereas two different approaches were considered (disconnections *a* and *b*), as shown in Scheme 1a, route *a* afforded macrocycle **2** in higher yield (36 vs 25% in route *b*). As illustrated in Scheme 1b, starting from the readily available 3,6-di-*tert*-butyl-9*H*-carbazole **3**[12] and 2,2′-dihydroxy-1,1′-binaphthyl **4**,[13] the synthesis of **2** was straightforward, involving as key intermediates the disulfonyl dichlorides **5**[10] and **8**,[5c] previously synthesized by our group. Nuclear magnetic resonance (NMR) experiments were carried out to unambiguously assign the chemical shifts for protons, both in $CDCl_3$ and in DMSO-d_6 solvents (Figures S9−S18).

The anion binding affinity of racemic macrocycle **2** was explored and compared with acyclic receptor **1** by ^{1}H NMR titrations in $CDCl_3$ as solvent (Figures S19−S21). Halide and acetate anions were selected to compare with previous results obtained with receptor **1**.[10]

Scheme 1. (a) Synthetic Strategies Leading to Macrocycle **2** and (b) Synthesis of the Racemic Macrocycle **2** via Route *a*

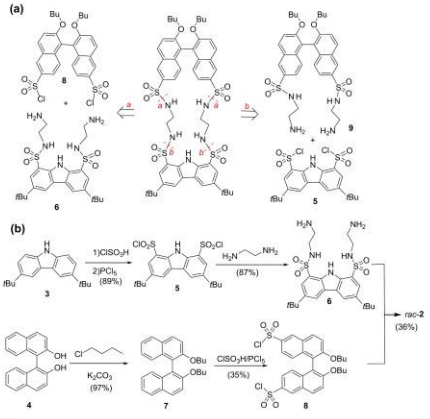

Whereas receptors **1** and **2** were found to display similar high affinities for halides (Table 1, entries 1 and 2), macrocycle

Table 1. Association Constants K_a (M^{-1}) for the Complexes Formed by Macrocycle 2 and Receptor 1 and Selected Anions (Added as Tetrabutyl or Tetraethylammonium Salts) at 298 K in $CDCl_3$[a]

entry	anion	receptor **1**	receptor **2**
1	Cl^-	7.9×10^6[b]	8.0×10^5[c]
2	I^-	4.2×10^5[b]	5.0×10^5[c]
3	AcO^-	[d]	2.8×10^5

[a]Errors estimated to be ≤10%. [b]Measured by fluorescence. [c]Measured by ^{1}H NMR competitive titration with receptor **1**. [d]Data could not be fitted to a binding model due to the possible deprotonation of receptor **1** by acetate.

2 was able to bind acetate with an association constant >10^5 M^{-1} (Table 1, entry 3). Thus the replacement of the bis(trifluoromethyl)aniline by ethylenediamine in the sulfonamide linkages proved to be effective to avoid deprotonation (previously observed for receptor **1**), resulting in acetate binding through H bonds.

Encouraged by these results, we next explored the association of amino acids in their zwitterionic form. Whereas macrocycle **2** combines an oxyanion hole moiety[14] for binding of carboxylates and a binaphthyl unit to impart chirality, ammonium binding was achieved using 18-*crown*-6 ether.[15] Thus the ability of this system to extract zwitterionic amino acids from aqueous solution into a chloroform phase was studied.[5c]

In a typical liquid−liquid extraction experiment, a saturated aqueous solution of the amino acid was added to a solution of macrocycle **2** and 18-*crown*-6 ether in $CDCl_3$, followed by vigorous stirring.^{1}H NMR analysis of the organic phase was used to estimate the extraction efficiency (Table 2, Figures S22−S34).

https://dx.doi.org/10.1021/acs.orglett.9b04379
Org. Lett. 2020, 22, 867−872

Table 2. Extraction of Zwitterionic Amino Acids from Aqueous Solution into $CDCl_3$ by a Combination of Macrocycle 2 and 18-*crown*-6 Ether

entry	amino acid[a]	extraction (%)[b]
1	D,L-alanine	
2	D,L-leucine	
3	D,L-phenylalanine	quant. (56.4% ee)[c]
4	D,L-phenylglycine	quant. (91.8% ee)[c]
5	D,L-serine	
6	D,L-tryptophan	
7	D,L-tyrosine	
8	D,L-valine	

[a]0.5 mL of an aqueous saturated solution of the amino acid was added to 0.5 mL of a $CDCl_3$ solution of **2** (1.15×10^{-2} M) and 18-*crown*-6 ether (2.65×10^{-2} M), followed by vigorous stirring and centrifugation. [b]Single extraction experiment; extraction percentages based on the macrocycle concentration in the organic phase and determined by the integration of the ^{1}H NMR signals. [c]Determined by HPLC when receptor (*S*)-**2** is used.

Macrocycle **2** proved to be highly selective for aromatic amino acids phenylglycine and phenylalanine, which were quantitatively extracted into $CDCl_3$ with a 1:1 macrocycle to amino acid binding stoichiometry (Figures S32, S36, and S38); the rest of the tested amino acids were not extracted to any measurable extent. Figure 2 displays the aromatic region of the ^{1}H NMR spectra of macrocycle **2** before (a) and after the extraction with a saturated solution of D-phenylglycine (b) and D-phenylalanine (c), where the appearance of the aromatic ring signals of both amino acids can be observed.

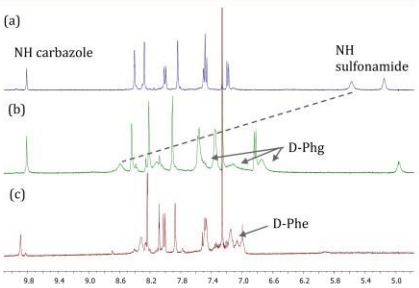

Figure 2. Partial ^{1}H NMR spectra of macrocycle (*S*)-**2** before (a) and after liquid−liquid extraction with a saturated solution of D-phenylglycine (b) and D-phenylalanine (c).

Amino acid recovery from the chloroform phase was easily achieved by removing the aqueous phase and washing the organic phase with one equivalent of potassium decanoate in water. 18-*crown*-6 ether traces were eliminated by washing the aqueous phase twice with chloroform (Figure S40).

The fact that among the natural amino acids tested, only phenylalanine was extracted could be used in the preparation of food supplements for the treatment of phenylketonuria.[16]

The observed selectivity in the extraction of the underivatized amino acids prompted us to prepare the enantiopure receptor (*S*)-**2** starting from (*S*)-2,2′-dihydroxy-1,1′-binaphthyl **4**.[17] While chiral macrocycle **2** was being synthesized, further evidence of enantioselective binding was obtained using a methodology our group has successfully applied for the resolution of racemic receptors.[5c,18] Conventional TLC plates were impregnated with a 1.5% aqueous solution of L-phenylglycine and the stoichiometric amount of 18-*crown*-6 ether and dried. Elution of the racemic macrocycle afforded two separated spots, corresponding to the diastereomeric complexes of L-phenylglycine with each enantiomer of racemic **2**. At the same time, the elution of (*S*)-**2** in TLC plates impregnated either with L-phenylglycine and D-phenylglycine clearly showed that a strong complex is formed with D-phenylglycine, affording a spot with a larger R_f value than the spot generated after elution in the L-phenylglycine-impregnated TLC (Figure S41).

These preliminary results were later confirmed by the liquid−liquid extraction experiments with the enantiopure macrocycle (*S*)-**2** and the racemic amino acids. To our delight, analysis by chiral HPLC showed a preference of macrocycle (*S*)-**2** for D-enantiomers, reaching 91.8% *ee* for phenylglycine (Table 2, entry 4) and 56.4% *ee* for phenylalanine (Table 2, entry 3). The selectivity obtained for zwitterionic phenylglycine (α = 11.2) is, to our knowledge, the best result for this amino acid obtained so far.

To understand the origin of this enantiodiscrimination, NMR studies were carried out on the diastereomeric complexes of receptor (*S*)-**2** with L- and D-phenylglycine in the presence of 18-*crown*-6 ether. The chemical shifts for selected protons are displayed in the SI (Table S1, Figures S33−S39) and show that the carbazole NH is not involved in the binding with the amino acid, whereas the carbazole sulfonamide NH compounds are shifted from 5.57 ppm to 8.59 and 8.43 ppm in the complexes, as expected when H bonds are formed (Figure 2). The very different chemical shifts for the *meta* protons of both enantiomers of phenylglycine in the complexes are remarkable and seem to indicate different geometries for the associates. This hypothesis was also corroborated by the ^{13}C NMR spectra of the two diastereomeric complexes, where differences in chemical shifts were observed for some of the macrocycle carbons (Figure S39).

X-ray crystallographic analysis turned out to be a powerful tool to clarify the geometry of the complexes. When an equimolecular mixture of racemic macrocycle **2**, racemic phenylglycine, and 18-*crown*-6 ether was dissolved in a chloroform/methanol solution, crystals of the ternary complexes 1:1:1 were obtained, with the configurations (*S*)-**2**·D-phenylglycine and (*R*)-**2**·L-phenylglycine (Figure 3, Figures S46−S48).

The X-ray structure shows that the carboxylate is bound to the macrocycle through three H bonds: two formed with both carbazole sulfonamides (Table S4, entries 1 and 2) and the third one formed with one of the binaphthyl sulfonamides (Table S4, entry 3). The fourth sulfonamide NH is not involved in the binding, pointing outside the cavity. As expected, the ammonium group is encapsulated by the crown ether, forming several H bonds. The crown ether is tilted toward the H atom in the amino acid to prevent steric interactions with the larger α-carbon substituents (Figure 3, bottom). In addition, two intramolecular H bonds are formed in the macrocycle between the carbazole NH and one of the oxygen atoms of the sulfonamide linked to the carbazole ring (2.450 and 2.466 Å).

https://dx.doi.org/10.1021/acs.orglett.9b04379
Org. Lett. 2020, 22, 867−872

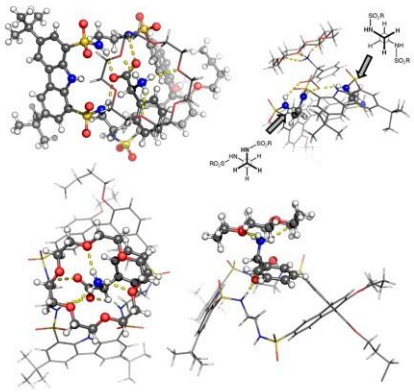

Figure 3. X-ray structure of the ternary complex (*S*)-**2**·D-phenylglycine·18-*crown*-6 ether with hydrogen bonds as yellow dotted lines. For clarity, the ternary complex is shown in two views: amino acid and macrocycle (above) and amino acid with crown ether (below). The dihedral angles of the ethylenediamine groups are shown in the top-right view.

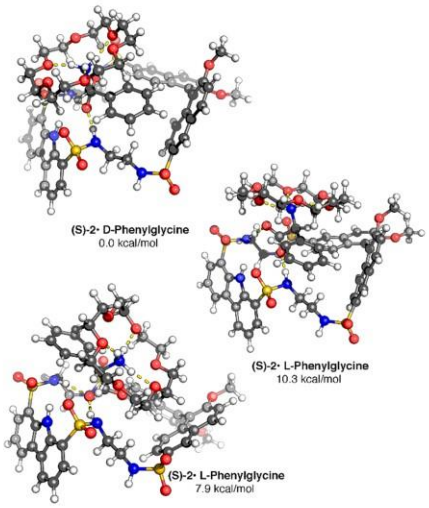

Figure 4. DFT-optimized structures for the complexes of (*S*)-**2** and phenylglycine.

The phenyl substituent is located in the gap left by the binaphthyl group; the conformation adopted by the nearest ethylenediamine (Figure 3, top-right), which directs the fourth NH out of the cavity, contributes to enlarge this gap. In addition, the upfield shift of the phenylglycine meta ^{1}H signals (6.74 ppm) in the (*S*)-**2**·D-phenylglycine complex can be attributed to the proximity of these protons to the binaphthyl aromatic sheet (Table S1).

Because no crystals were obtained for the weak complex, density functional theory (DFT) calculations were performed to explain the enantioselectivity (see details in the SI). The structure of the most stable (*S*)-**2**·D-phenylglycine complex (Figure 4) is similar to the X-ray structure. For the (*S*)-**2**·L-phenylglycine complex, two structures were found. The first one shows the carboxylate and the phenyl group occupying the same positions as in the strong complex, leading the H substituent (and the bulky crown ether that is tilted toward it) in the direction of the other binaphthyl sheet. Alternatively, the gap that is occupied by the phenyl group in the stronger complex can be used to accommodate the amino substituent bound to the crown ether. The latter structure is 2.4 kcal/mol more stable but is still highly destabilized with respect to the (*S*)-**2**·D-phenylglycine complex (7.9 kcal/mol). A similar study on the complexes with phenylalanine shows a smaller energy difference (4.5 kcal/mol).

In conclusion, we have shown that using supramolecular interactions, a new chiral macrocyclic receptor is able to selectively extract zwitterionic phenylglycine from aqueous solutions with high enantioselectivity. The X-ray diffraction and DFT studies analysis explained the high enantiodiscrimination observed and will be helpful to further improve the receptor design in the near future.

■ ASSOCIATED CONTENT

Supporting Information

The Supporting Information is available free of charge at https://pubs.acs.org/doi/10.1021/acs.orglett.9b04379.

Experimental procedures, spectroscopic data, NMR titrations and extraction experiments, HPLC chromatograms, ORTEP diagrams, X-ray crystal structure data, and modelization studies (PDF)

Accession Codes

CCDC 1441451 contains the supplementary crystallographic data for this paper. These data can be obtained free of charge via www.ccdc.cam.ac.uk/data_request/cif, or by emailing data_request@ccdc.cam.ac.uk, or by contacting The Cambridge Crystallographic Data Centre, 12 Union Road, Cambridge CB2 1EZ, UK; fax: +44 1223 336033.

■ AUTHOR INFORMATION

Corresponding Authors

Ángel L. Fuentes de Arriba − *University of Salamanca, Salamanca, Spain;* orcid.org/0000-0001-7424-8146; Email: angelfuentes@usal.es

Victoria Alcázar − *Polytechnical University of Madrid, Madrid, Spain;* orcid.org/0000-0002-1891-3209; Email: mariavictoria.alcazar@upm.es

Other Authors

María G. Turiel − *University of Salamanca, Salamanca, Spain*

José J. Garrido-González − *University of Salamanca, Salamanca, Spain*

https://dx.doi.org/10.1021/acs.orglett.9b04379
Org. Lett. 2020, 22, 867−872

Luis Simón − *University of Salamanca, Salamanca, Spain;* orcid.org/0000-0002-3781-0803
Francisca Sanz − *University of Salamanca, Salamanca, Spain*
Anna M. Lithgow − *University of Salamanca, Salamanca, Spain*
Joaquín R. Morán − *University of Salamanca, Salamanca, Spain*

Complete contact information is available at: https://pubs.acs.org/10.1021/acs.orglett.9b04379

Notes

The authors declare no competing financial interest.

■ ACKNOWLEDGMENTS

This work was supported by the Junta de Castilla y León (European Regional Development Fund-SA069P17), the University of Salamanca (Own Research Programs-KCEP/463AC01), and the MINECO (CTQ2017-87529-R), whose support is well appreciated. A.L.F.A. thanks the University of Salamanca for a postdoctoral fellowship, and J.J.G.-G. gratefully acknowledges USAL for a predoctoral grant. We thank Dr. C. Raposo and J. F. Boyero (Mass Spectrometry Service, University of Salamanca) for the mass spectra and chiral HPLC, A. López García and J. A. González Ramos (Computational Services, University of Salamanca) for IT support, and V. Obregón (Bio-Oils Huelva) for her support. We also acknowledge the employment of the University of Salamanca server housing service.

■ REFERENCES

(1) Martínez-Rodríguez, S.; Martínez-Gómez, A. I.; Rodríguez-Vico, F.; Clemente-Jiménez, J. M.; Las Heras-Vázquez, F. J. Natural Occurrence and Industrial Applications of D-Amino Acids: An Overview. *Chem. Biodiversity* **2010**, *7*, 1531−1548.

(2) (a) Top Pharmaceuticals Poster. https://njardarson.lab.arizona.edu/content/top-pharmaceuticals-poster, Njardarson group, November 2019. (b) McGrath, N.; Brichacek, M.; Njardarson, J. T. A Graphical Journey of Innovative Organic Architectures That Have Improved Our Lives. *J. Chem. Educ.* **2010**, *87*, 1348−1349.

(3) Sugimoto, M. Amino Acids, Production Processes. In *Encyclopedia of Industrial Biotechnology: Bioprocess, Bioseparation, and Cell Technology*; Flickinger, M. C., Ed.; John Wiley & Sons, 2010.

(4) Schuur, B.; Verkuijl, B. J. V.; Minnaard, A. J.; de Vries, J. G.; Heeres, H. J.; Feringa, B. L. Chiral separation by enantioselective liquid-liquid extraction. *Org. Biomol. Chem.* **2011**, *9*, 36−51.

(5) Selected examples: (a) Kozbia, M.; Pietraszkiewicz, M.; Pietraszkiewicz, O. Chiral Discrimination of Amino Acids by an Optically Active Crown Ether Studied by HPLC, Extraction and a Liquid Membrane Transport Experiments. *J. Inclusion Phenom. Mol. Recognit. Chem.* **1998**, *30*, 69−77. (b) Lingenfelter, D. S.; Helgeson, R. C.; Cram, D. J. Host-Guest Complexation. 23. High Chiral Recognition of Amino Acid and Ester Guests by Hosts Containing One Chiral Element. *J. Org. Chem.* **1981**, *46*, 393−406. (c) Hernández, J. V.; Oliva, A. I.; Simón, L.; Muñiz, F. M.; Grande, M.; Morán, J. R. Ternary enantioselective complexes from α-amino acids, 18-crown-6 ether and a macrocyclic xanthone-based receptor. *Tetrahedron Lett.* **2004**, *45*, 4831−4833.

(6) (a) Galan, A.; Andreu, D.; Echavarren, A.; Prados, P.; De Mendoza, J. A receptor for the enantioselective recognition of phenylalanine and tryptophan under neutral conditions. *J. Am. Chem. Soc.* **1992**, *114*, 1511−1512. (b) Blondeau, P.; Segura, M.; Pérez-Fernández, R.; de Mendoza, J. Molecular Recognition of Oxoanions Based on Guanidinium Receptors. *Chem. Soc. Rev.* **2007**, *36*, 198−210.

(7) (a) Verkuijl, B. J. V.; Minnaard, A. J.; de Vries, J. G.; Feringa, B. L. Chiral Separation of Underivatized Amino Acids by Reactive Extraction with Palladium-BINAP Complexes. *J. Org. Chem.* **2009**, *74*, 6526−6533. (b) Liu, X.; Ma, Y.; Cao, T.; Tan, D.; Wei, X.; Yang, J.; Yu, L. Enantioselective liquid-liquid extraction of amino acid enantiomers using (*S*)-MeO-BIPHEP-metal complexes as chiral extractants. *Sep. Purif. Technol.* **2019**, *211*, 189−197. (c) Verkuijl, B. J. V.; Schoonen, A. K.; Minnaard, A. J.; de Vries, J. G.; Feringa, B. L. The Use of *N*-Type Ligands in the Enantioselective Liquid−Liquid Extraction of Underivatized Amino Acids. *Eur. J. Org. Chem.* **2010**, *2010*, 5197−5202. (d) Zhu, Y.-Y.; Wu, X.-D.; Gu, S.-X.; Pu, L. Free Amino Acid Recognition: A Bisbinaphthyl-Based Fluorescent Probe with High Enantioselectivity. *J. Am. Chem. Soc.* **2019**, *141*, 175−181.

(8) Selected examples: Tsukube, H.; Uenishi, J.-i.; Kanatani, T.; Itoh, H.; Yonemitsu, O. Enantioselective binding and extraction of zwitterionic amino acids by chiral lanthanide complexes. *Chem. Commun.* **1996**, 477−478.

(9) Huang, H.; Nandhakumar, R.; Choi, M.; Su, Z.; Kim, K. M. Enantioselective Liquid−Liquid Extractions of Underivatized General Amino Acids with a Chiral Ketone Extractant. *J. Am. Chem. Soc.* **2013**, *135*, 2653−2658.

(10) Fuentes de Arriba, Á. L.; Turiel, M. G.; Simón, L.; Sanz, F.; Boyero, J. F.; Muñiz, F. M.; Morán, J. R.; Alcázar, V. Sulfonamide carbazole receptors for anion recognition. *Org. Biomol. Chem.* **2011**, *9*, 8321−8327.

(11) (a) Martí-Centelles, V.; Pandey, M. D.; Burguete, M. I.; Luis, S. V. Macrocyclization Reactions: The Importance of Conformational, Configurational, and Template-Induced Preorganization. *Chem. Rev.* **2015**, *115*, 8736−8834. (b) *Macrocyclic Chemistry. Current Trends and Future Perspectives*; Gloe, K., Ed.; Springer: Dordrecht, The Netherlands, 2005.

(12) Yang, X.; Lu, R.; Gai, F.; Xue, P.; Zhan, Y. Rigid dendritic gelators based on oligocarbazoles. *Chem. Commun.* **2010**, *46*, 1088−1090.

(13) Kyba, E. P.; Siegel, M. G.; Sousa, L. R.; Sogah, G. D.; Cram, D. J. Chiral, hinged, and functionalized multiheteromacrocycles. *J. Am. Chem. Soc.* **1973**, *95*, 2691−2692.

(14) (a) Simón, L.; Goodman, J. M. Hydrogen-bond stabilization in oxyanion holes: grand jeté to three dimensions. *Org. Biomol. Chem.* **2012**, *10*, 1905−1913. (b) Simón, L.; Goodman, J. M. Enzyme Catalysis by Hydrogen Bonds: The Balance between Transition State Binding and Substrate Binding in Oxyanion Holes. *J. Org. Chem.* **2010**, *75*, 1831−1840. (c) Simón, L.; Muñiz, F. M.; Fuentes de Arriba, Á.; Alcázar, V.; Raposo, C.; Morán, J. R. Synthesis of a chiral artificial receptor with catalytic activity in Michael additions and its chiral resolution by a new methodology. *Org. Biomol. Chem.* **2010**, *8*, 1763−1768. (d) Pihko, P.; Rapakko, S.; Wierenga, R. K. In *Hydrogen Bonding in Organic Synthesis*; Wiley-VCH Verlag GmbH & Co. KGaA, 2009; pp 43−71. (e) Muñiz, F. M.; Alcázar Montero, V.; Fuentes de Arriba, A. L.; Simón, L.; Raposo, C.; Morán, J. R. Thiourea versus the oxyanion hole as a double H-bond donor. *Tetrahedron Lett.* **2008**, *49*, 5050−5052. (f) Simón, L.; Muñiz, F. M.; Sáez, S.; Raposo, C.; Morán, J. R. Artificial enzymes for the enantioselective Michael-type addition of thiols combining basic catalysis with two- and three-pronged oxyanion hole mimics. *ARKIVOC* **2007**, *iv*, 47−64. (g) Simón, L.; Muñiz, F. M.; Sáez, S.; Raposo, C.; Morán, J. R. Enzyme Mimics for Michael Additions with Novel Proton Transport Groups. *Eur. J. Org. Chem.* **2007**, *2007*, 4821−4830.

(15) (a) Späth, A.; König, B. Molecular recognition of organic ammonium ions in solution using synthetic receptors. *Beilstein J. Org. Chem.* **2010**, *6*, No. 32. (b) Gokel, G. W.; Leevy, W. M.; Weber, M. E. Crown Ethers: Sensors for Ions and Molecular Scaffolds for Materials and Biological Models. *Chem. Rev.* **2004**, *104*, 2723−2750.

(16) Al Hafid, N.; Christodoulou, J. Phenylketonuria: a review of current and future treatments. *Transl. Pediatr.* **2015**, *4*, 304−317.

(17) Tanaka, K.; Okada, T.; Toda, F. Separation of the Enantiomers of 2,2′-Dihydroxy-1, 1′-binaphthyl and 10,10′-Dihydroxy-9,9′-biphe-

nanthryl by Complexation with *N*-Alkylcinchonidinium Halides. *Angew. Chem., Int. Ed. Engl.* **1993**, *32*, 1147−1148.
(18) (a) Temprano, Á. G.; Monleón, L. M.; Rubio, O. H.; Simón Rubio, L.; Pérez, A. B.; Sanz, F.; Morán, J. R. A highly selective receptor for zwitterionic proline. *Org. Biomol. Chem.* **2016**, *14*, 1325−1331. (b) Gómez Herrero, F.; Rubio, O. H.; Monleón, L. M.; Fuentes de Arriba, Á. L.; Simón Rubio, L.; Morán, J. R. A molecular receptor for zwitterionic phenylalanine. *Org. Biomol. Chem.* **2016**, *14*, 3906−3912. (c) de Juan Fernández, L.; Fuentes de Arriba, Á. L.; Monleón, L. M.; Rubio, O. H.; Alcázar Montero, V.; Simón Rubio, L.; Morán, J. R. An Enantioselective Benzofuran-Based Receptor for Dinitrobenzoyl-Substituted Amino Acids. *Eur. J. Org. Chem.* **2016**, *2016*, 1541−1547. (d) Fuentes de Arriba, Á. L.; Gómez Herrero, A.; Rubio, O. H.; Monleón, L. M.; Simón Rubio, L.; Alcázar, V.; Sanz, F.; Morán, J. R. Chiral recognition with a benzofuran receptor that mimics an oxyanion hole. *Org. Biomol. Chem.* **2015**, *13*, 493−501.

https://dx.doi.org/10.1021/acs.orglett.9b04379
Org. Lett. 2020, 22, 867−872

ACS Catalysis

pubs.acs.org/acscatalysis Research Article

An Enzyme Model Which Mimics Chymotrypsin and N-Terminal Hydrolases

José J. Garrido-González, Mª Mercedes Iglesias Aparicio, Miguel Martínez García, Luis Simón, Francisca Sanz, Joaquín R. Morán,* and Angel L. Fuentes de Arriba*

Cite This: ACS Catal. 2020, 10, 11162−11170 Read Online

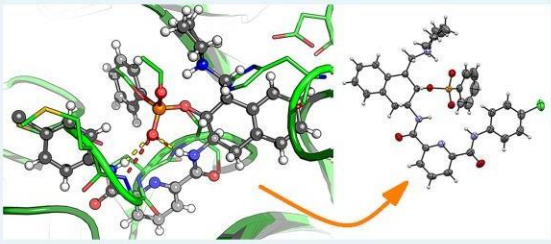

ABSTRACT: Enzymes are the most efficient and specific catalysts to date. Although they have been thoroughly studied for years, building a true enzyme mimic remains a challenging and necessary task. Here, we show how a three-dimensional geometry analysis of the key catalytic residues in natural hydrolases has been exploited to design and synthesize small-molecule artificial enzymes which mimic the active centers of chymotrypsin and N-terminal hydrolases. The optimized prototype catalyzes the methanolysis of the acyl enzyme mimic with a half-life of only 3.7 min at 20 °C, and it is also able to perform the transesterification of vinyl acetate at room temperature. DFT studies and X-ray diffraction analysis of the catalyst bound to a transition state analogue proves the similarity with the geometry of natural hydrolases.

KEYWORDS: *artificial hydrolase, enzyme mimic, chymotrypsin, N-terminal hydrolase, organocatalysis, hydrogen bond, oxyanion hole, transesterification*

INTRODUCTION

Enzymes are the only catalysts that operate in biochemistry; however, they have also found important applications in industry since, to date, many processes cannot be carried out economically with synthetic catalysts.[1] The highly selective 11-hydroxylation of 11-deoxycortisol to yield cortisol by 11-β-hydroxylase is a good example.[2]

In particular, hydrolytic enzymes, which are a family of more than 200 enzymes responsible for lipid, sugar, and peptide hydrolysis, have found important applications in fine chemical production, the food and detergent industry, paper manufacturing, chemical degradation processes, biomass conversion, and the pharma industry.[3] However, their low stability, high cost, and risk of denaturalization under extreme pH, temperature, or salt conditions make them tricky substances to work with. Hence, there is an increasing interest in developing artificial hydrolases for industrial, academic, and therapeutic purposes. Suh has recently outlined the importance of artificial proteases as new catalytic drugs[4] for amyloid diseases.[5]

Chemists have tried to mimic hydrolases for a long time. Especially remarkable are the contributions of Lehn in enantioselective thiolysis reactions[6] as well as those of Breslow[7] and Cram[8] in the hydrolysis of nitrophenyl esters, with reaction rate increases up to 7.5×10^5 and 10^{11}, respectively. While most of these enzyme models rely on the formation of inclusion complexes of activated esters inside cyclodextrins, cucurbiturils, cavitands, and other macrocycles,[7,9] artificial enzymes which try to mimic the geometry of the catalytic triad of serine or cysteine proteases are much scarcer. One of the reasons is their challenging synthesis: each of the reactive groups in the active site corresponds to different domains of the protein backbone chain and are only brought

Received: May 13, 2020
Revised: August 13, 2020
Published: August 31, 2020

https://dx.doi.org/10.1021/acscatal.0c02121
ACS Catal. 2020, 10, 11162−11170

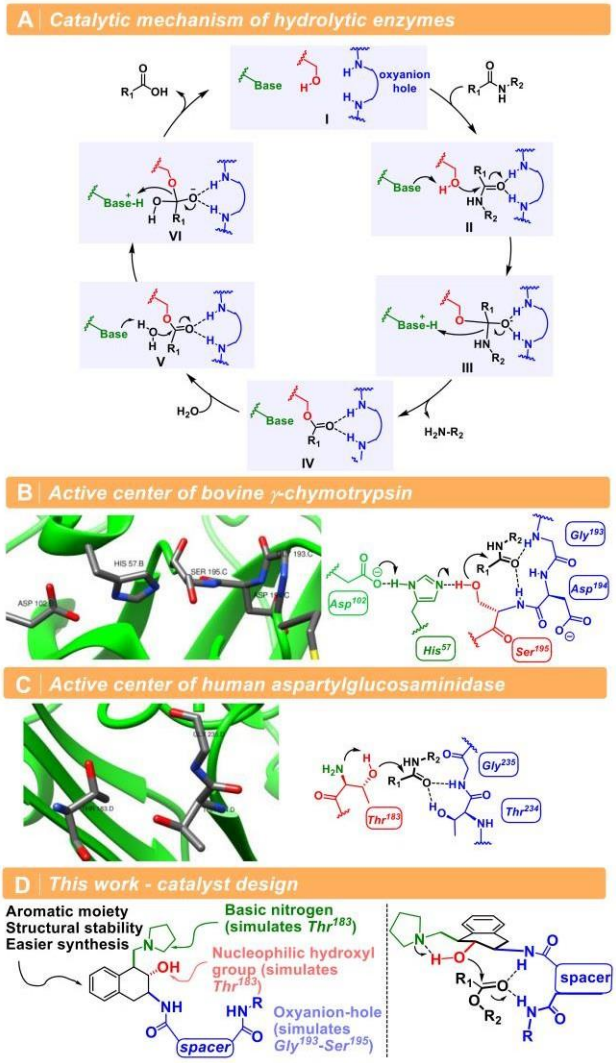

Figure 1. (A) General mechanism of hydrolytic enzymes. (B) Active center of *bovine γ-chymotrypsin* (PDB 1AB9). (C) Active center of human *aspartylglucosaminidase* (PDB 1APY). (D) Catalytic features of the hydrolase mimic designed in this work.

together when the protein folds in its tertiary structure (Figure 1B). Ema and Sakai[10] and Schafmeister[11] have reported small-molecule enzyme mimics able to simulate the catalytic triad of hydrolytic enzymes. Although large acceleration rates were obtained, their systems are limited to highly activated vinyl trifluoroacetate esters. Several research groups have tried to mimic the three-dimensional arrangement of the catalytic groups in chymotrypsin by using polymer imprinting

https://dx.doi.org/10.1021/acscatal.0c02121
ACS Catal. 2020, 10, 11162−11170

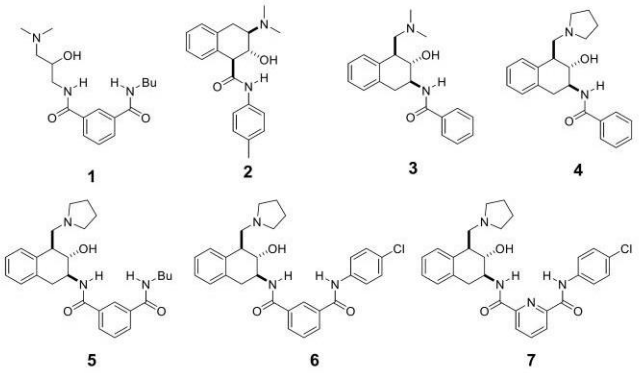

Figure 2. Hydrolase mimics synthesized in this work.

techniques[12] or by attaching the catalytic groups onto polymeric materials[13] or micelles;[14] however, the results are still not optimized enough to be applicable in industry. Connal has recently highlighted the state of the art of synthetic catalysts inspired by hydrolytic enzymes which is still far from reproducing reactions of native enzymes on esters, amides, and proteins under mild conditions.[15] In our opinion, a rational understanding of the geometry of the active center of hydrolytic enzymes, on the basis of an analysis of the X-ray structure of hydrolases, could be a promising starting point to design a true enzyme mimic. The synthesis and testing of small molecules which try to mimic the catalytic groups of the active center of hydrolases could shed some light on the importance of the geometry of the catalytic groups of the active site to achieve high levels of catalysis. Herein, we wish to report our findings.

Among all the different families of proteolytic enzymes, N-terminal hydrolases[16] are a superfamily of enzymes which lack the histidine−aspartate combination of the catalytic triad,[17] being replaced by a terminal $-NH_2$ group which stems from a terminal serine, threonine, or cysteine (Figure 1C). This fact makes them attractive candidates for the development of artificial enzymes, since the combination of a simple 1,2-amino alcohol with a suitable oxyanion hole could provide a decent enzyme mimic. Although one would expect the amino group to be protonated in aqueous solution, the protein environment reduces the pK_a of the α-amino group to a value close to histidine's first pK_a (6.2).[18] On the other hand, the usual hydrophobic pocket may not even be necessary, since chymotrypsin excludes water from the active center during its reactions.[19] According to Warshel, the main factor to explain enzymatic catalysis comes from a preorganized polar environment which is complementary with the guest transition state and which is mainly obtained through H bonds.[20] In fact, site-directed mutagenesis studies have shown that most of the catalytic activity of chymotrypsin (10^{10}) can be explained with the H bonds of the oxyanion hole (10^4) and the catalytic triad (10^6).[21] Therefore, a similar array of H bonds from a small synthetic molecule may provide catalysis comparable to that of natural enzymes.

RESULTS AND DISCUSSION

Kinetic and Computational Studies. Taking inspiration from natural chymotrypsin and N-terminal hydrolases, we synthesized enzyme mimic **1** (Figure 2, see the Supporting Information for its preparation). Catalyst **1** combines an oxyanion-hole mimic, based on an isophthalic acid moiety, a nucleophilic hydroxyl group, and a basic dimethylamine group. The isophthalic acid spacer, with two NHs and an aromatic C−H that can also behave as an H-bond donor, has been successfully used in the literature as an oxyanion-hole mimic.[22] The oxyanion hole and hydroxyl group are separated by two carbon atoms (as in the chymotrypsin catalytic triad; Figure 1B). Concurrently, we hope that the 1,2-amino alcohol moiety plays the same role as terminal threonine in N-terminal hydrolases, in which $-NH_2$ and $-OH$ groups are in a 1,2-disposition (Figure 1C). 1,2-Amino alcohols have already shown transacylation activity with activated esters.[23]

The classical mechanism of hydrolytic enzymes through the well-known catalytic triad requires an acylation step of a serine or cysteine residue (**II** → **IV**, Figure 1A) and subsequent hydrolysis of the acyl intermediate by H_2O (**IV** → **VI**, Figure 1A). It has been observed for both natural and artificial enzymes that the acylation step is faster than the acyl intermediate hydrolysis,[10,23,24] although these results may be biased, as most examples use activated esters as substrates, which possess a good leaving group that is not available for the second step. This difference in the reaction rates causes a lack of turnover,[25] as once the hydroxyl group of the enzyme mimic is acylated (**IV**, Figure 1A) it does not undergo further reaction.

To complement previous studies, we decided to tackle the *a priori*, more challenging acyl intermediate hydrolysis with enzyme mimic **1** (Figure 2). Hence, by aiming at the rate-limiting step of the mechanism, we should have a fast estimation of the possibilities of this scaffold to be used in hydrolysis or transesterification reactions. To test the catalytic activity of compound **1**, acetylation of its hydroxyl group was first performed in Ac_2O, and after isolation of acetylated catalyst **1**, it was transferred to an NMR tube and dissolved in deuterated methanol. Catalyst **1** was designed to be soluble in chloroform, which is a solvent that can mimic the hydrophobic

https://dx.doi.org/10.1021/acscatal.0c02121
ACS Catal. 2020, 10, 11162−11170

environment of the hydrolase active site. However, to speed up and simplify the study, as pseudo-first-order kinetics can be applied, deuterated methanol was used as the solvent and the deacetylation kinetics were followed by ^{1}H NMR at 20 °C.

According to kinetic experiments (see the Supporting Information), deacetylation of **1a** by CD_3OD took place with a half-life of 187 min (Table 1, entry 1). This result was slower than expected, as the biological conversion of ethyl acetate to ethanol takes place in only 5−10 min.[26] Probably, the free rotation of the methylene groups generates nonproductive conformations in the catalyst structure due to the establishment of intramolecular H bonds between the basic dimethylamine nitrogen and the oxyanion hole, which hamper catalyst activity.

Table 1. Half-Life (min) of the Methanolysis Reaction of Acetylated Catalysts 1a−7a

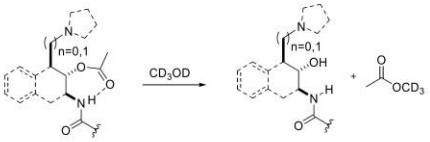

1a-7a **1-7**

entry	catalyst	$t_{1/2}$ (min)[a]
1	**1a**	187
2	**2a**	165
3	**3a**	87
4	**4a**	17
5	**5a**	12
6	**6a**	15
7	**7a**	3.7

[a]Ca. 10 mg of the acetylated catalyst **1a−7a** was dissolved in 400 μL of CD_3OD, and ^{1}H NMR spectra were recorded periodically at 20 °C. The half-life was determined by ^{1}H NMR integration.

Although Breslow and others have shown that more structural flexibility provided improved outcomes in enzyme mimics,[27] in this case it is necessary to anchor the different catalytic groups to a rigid scaffold in order to prevent nonproductive conformations. This is a challenging task, because if the distances between the different groups are not appropriate, the catalyst will not show any catalytic activity. After screening different possibilities, we chose a rigid template based on a dihydronaphthalene scaffold to anchor the basic group, nucleophilic hydroxyl group, and oxyanion-hole moiety (Figure 1D). The presence of the aromatic ring confers structural stability to the molecule and facilitates the synthesis.

With these premises in hand, catalyst **2** was prepared. For the sake of synthetic simplicity, the oxyanion-hole role was performed by a single NH. Under these conditions, a small reduction in the half-life of 20 min was observed in comparison with catalyst **1** (Table 1, entry 2).

Looking for alternative scaffolds, we envisaged a 1,3-amino alcohol geometry. Although this disposition differs from the 1,2-amino alcohol scaffold in N-terminal hydrolases, water molecules could be necessary in N-terminal hydrolases to transport the proton between $-NH_2$ and $-OH$ groups, preventing in this way the formation of a strained four-membered ring.[28] The greater distance between the hydroxyl and amino groups in a 1,3-amino alcohol arrangement could be a key aspect to circumvent this problem. An extensive conformational search for a model compound (see the Supporting Information) suggested that the equatorial disposition of all the catalytic groups, required to make the proton transport feasible, is the most stable conformation by more than 4.6 kcal/mol over the most stable axial disposition (Figure 3). This geometry provides a distance of 2.75 Å between OH and NH_2, which is close to the 2.92 Å between the same groups in N-terminal hydrolase human aspartylglucosaminidase or the 3.02 Å between OH and imidazole in bovine γ-chymotrypsin. In this enzyme one of the NHs in the oxyanion hole is 3.09 Å from the serine OH, while in the model of Figure 3 this distance is around 2.66 Å.

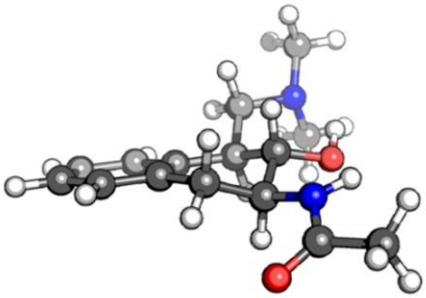

Figure 3. Most stable conformation of a model of catalysts **3**−**7** showing the equatorial arrangement of catalytic groups.

Thus, this motif was incorporated in catalyst **3**. Pleasingly, kinetic studies showed that the catalyst **3** skeleton is almost twice as good as that of catalyst **2**, with a half-life of 87 min (Table 1, entry 3).

Next, a series of modifications were introduced in the catalyst **3** structure to improve its catalytic activity. While the replacement of the dimethylamino group for a more basic pyrrolidine entailed a 5-fold decrease in half-life (Table 1, entry 4), the introduction of a second NH group via an isophthalic acid moiety to construct the oxyanion-hole motif allowed reducing the half-life to 12 min (Table 1, entry 5).

To our surprise, increasing the acidity of the second NH in the oxyanion hole of catalyst **6** did not reduce the reaction rate (Table 1, entry 6). Probably the rigidity of the dihydronaphthalene scaffold prevents the formation of the required short H bond between the acetate carbonyl group and the aromatic isophthalic NH, favoring the formation of some kind of dimer. Indeed, the ^{1}H NMR spectrum of **6a** showed a shielding of 0.4 ppm for the isophthalic NH in comparison with the same NH in free catalyst **6** (Figure 4).

To shorten the distance between this NH bond and the carbonyl group, an oxyanion-hole mimic with a shorter distance between both NHs was explored. In this regard, 2,6-pyridinedicarboxylic acid may be a reasonable choice, since aromatic C−N distances (1.33 Å) are shorter than aromatic C−C distances (1.39 Å), the pyridine nitrogen nonbonding lone pair should direct the NHs toward the cavity,[29] and also the pyridine ring should enhance the NH acidity. According to our expectations, catalyst **7** showed a stronger intramolecular

https://dx.doi.org/10.1021/acscatal.0c02121
ACS Catal. 2020, 10, 11162−11170

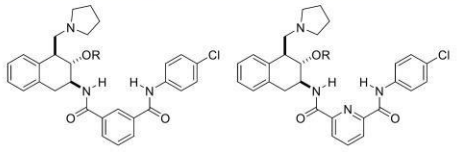

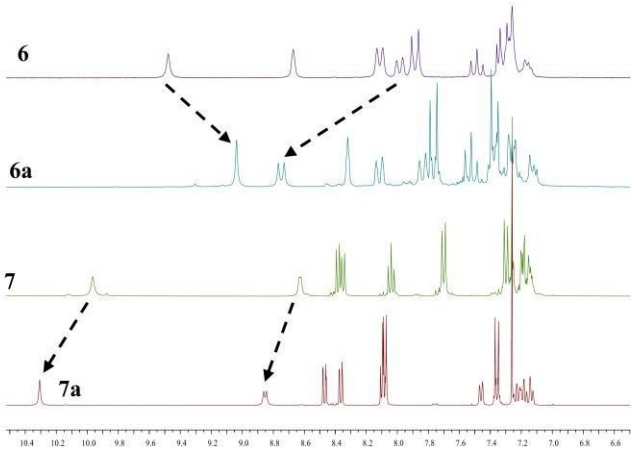

Figure 4. ^{1}H NMR spectra (6.6−10.4 ppm) showing the movement of NH signals of catalysts **6** and **7** after acetylation.

H bond between the acetate carbonyl group and the aromatic NH, which was deshielded by 0.34 ppm in the presence of the acetate group (Figure 4).

DFT studies of the reaction transition state supported this observation, showing a short H bond of 2.8 Å between the isophthalic NH and the carbonyl oxygen atom (Figure 5).

Kinetics studies corroborated this hypothesis, as the methanolysis of **7a** showed a half-life of only 3.7 min (Table 1, entry 7). Figure 6 collects the variation with time of the molar fraction of the acetylated catalysts **1**−**7** prepared in this study.

Transesterifications and Association Studies. Encouraged by this result, we next tested the ability of compound **7** to catalyze the transesterification of vinyl acetate. Interestingly, low catalyst loadings of **7** (<1 mol %) were enough to catalyze the transesterification between vinyl acetate and methanol with 50% conversion after 68 h at 20 °C (Figure 7). No reaction took place in the absence of catalyst after 100 h. Also, compound **7a** could be obtained after 3 days by mixing catalyst **7** in vinyl acetate, showing the participation of the acyl intermediate in the reaction mechanism. To our knowledge this is the first time that a small-molecule hydrolase mimic has been able to catalyze the transesterification of vinyl acetate.

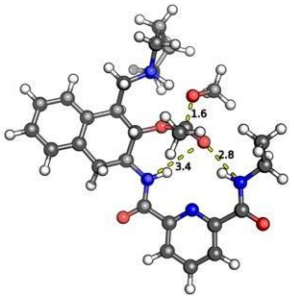

Figure 5. Calculated geometry of the transition state structure for the methanolysis reaction of compound **7a**. Selected distances between heteroatoms are depicted in angstroms.

Next, to prove the enzyme-like similarities of compound **7**, the association constant between catalyst **7** and EtOAc was measured by ^{1}H NMR titration in $CDCl_3$ at 20 °C. Successive

https://dx.doi.org/10.1021/acscatal.0c02121
ACS Catal. 2020, 10, 11162−11170

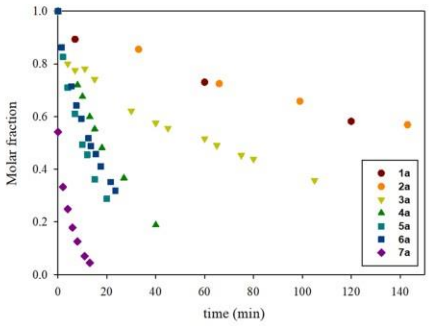

Figure 6. Time-dependent methanolysis of acetylated catalysts **1**−**7**.

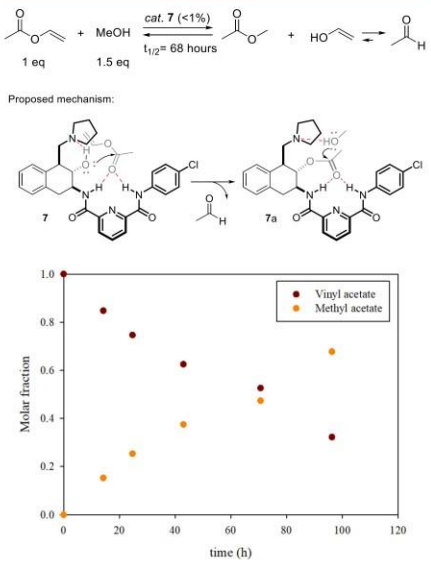

Figure 7. Time-dependent transesterification of vinyl acetate catalyzed with compound 7.

additions of ethyl acetate aliquots to a solution of catalyst **7** in $CDCl_3$ and plotting of the signal shifts vs equivalents of ethyl acetate gave an association constant of 0.79 M^{-1} (see the Supporting Information). This value could explain the still low reaction rate for transesterification reactions in comparison with deacetylation reactions.

X-ray Studies. In order to show that catalyst **7** possesses a well-preorganized polar environment complementary to the transition state, its reaction with the transition state mimic phenylphosphonic acid chloride was performed (Figure 8A). Pleasingly, X-ray-quality crystals of the product were obtained from slow evaporation of a dichloromethane/methanol solution.

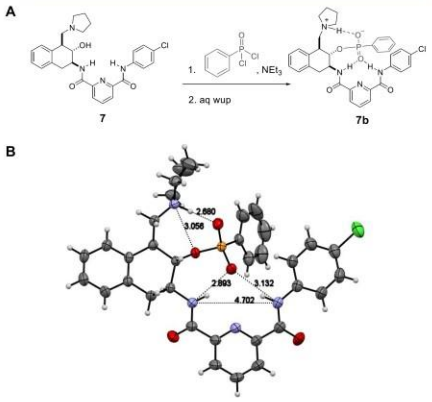

Figure 8. (A) Reaction of compound **7** with phenylphosphonic acid chloride. (B) X-ray diffraction structure of compound **7b**. Selected distances between heteroatoms are depicted in angstroms.

The single-crystal X-ray diffraction analysis showed a perfect fit of the phosphonate group inside the catalyst **7** oxyanion hole (Figure 8B). The phosphoryl oxygen which mimics the negatively charged oxygen of the transition state establishes two H bonds of 2.89 and 3.13 Å with the pyridine aliphatic and aromatic NHs, respectively. The pyridine oxyanion hole showed a 4.70 Å distance between both NHs, which is in good agreement with natural oxyanion holes.[30]

The shortest H bond of only 2.68 Å is set between the pyrrolidinium group and one of the phosphate oxygen atoms. Both phosphoryl oxygens showed similar O−P distances of 1.49−1.50 Å, which can be explained by a negatively charged phosphonate group, which contributes to the short pyrrolidinium H bond.

One of the most attractive features of the structure is the similar distances established between the pyrrolidinium group with both the phosphonoester oxygen (3.06 Å) and the phosphoryl oxygen (2.68 Å), which may be a key factor in transporting the proton from the nucleophile to the leaving group.

The conclusions obtained from the X-ray structure of compound **7b** agree with the observations detected in solution by ^{1}H NMR, which revealed the deshielding of the oxyanion-hole NHs upon acetylation of the catalysts. This implies that the acetate carbonyl group is hydrogen-bonded by the oxyanion-hole NHs in a way similar to that for the phosphonate group which mimics the transition state of the reaction.

Comparison with Natural Chymotrypsin. To prove the similarity of catalyst **7** with the active site of a natural hydrolase, the single-crystal X-ray diffraction structure of compound **7b** was superimposed with the active center of a chymotrypsin phosphate (PDB 1GCD) (Figure 9). The phosphate group was fixed for both compounds, which allowed

https://dx.doi.org/10.1021/acscatal.0c02121
ACS Catal. 2020, 10, 11162−11170

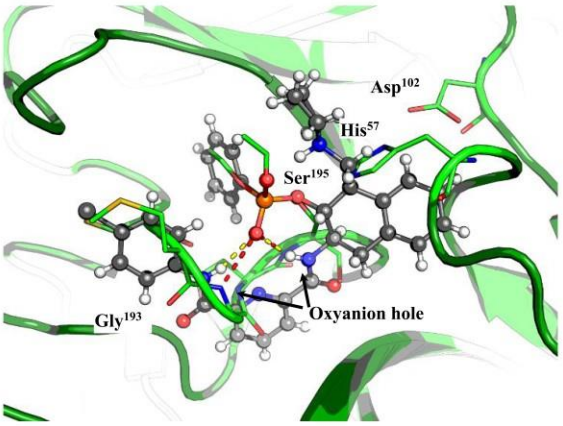

Figure 9. Superimposition of the crystal structure of chymotrypsin phosphate (ribbon model) and compound **7b** (ball and stick model), in which the phosphate group is fixed for both compounds. Hydrogen bonds between the oxyanion-hole NHs and the phosphate oxygen are depicted as red dashed lines for chymotrypsin phosphate and yellow dashed lines for compound **7b**.

a comparison of the geometry of the catalytic groups in the synthetic catalyst and the enzyme.

As can be observed in Figure 9, the geometry of compound **7b** is fairly similar to that of the active center of chymotrypsin, with the exception of the basic group, probably because the chymotrypsin phosphate is a neutral compound, which prevents the proximity of the imidazole ring due to the lack of hydrogen bonding, while in compound **7b** a strong H bond is set between pyrrolidinium and phosphate groups. A better fit is obtained for the oxyanion hole, with 2.90 Å distance between the phosphoryl oxygen and both the NH of Ser^{195} and the NH of catalyst **7**. The second H bond of the oxyanion hole between Gly^{193} and the phosphoryl oxygen is slightly shorter in chymotrypsin. The rigid pyridinedicarboxamide spacer, with a 4.70 Å distance between both NHs, is probably responsible for this fact, since in chymotrypsin, the oxyanion-hole distance between the NHs is around 4.30 Å.

■ CONCLUSIONS

In conclusion, a detailed analysis of the key amino acid residues responsible for catalysis in serine proteases and N-terminal hydrolases has allowed us to simulate their active center by using a rigid cyclohexane skeleton where the base, nucleophilic hydroxyl group, and oxyanion hole have been rationally positioned. This small-molecule artificial enzyme catalyzes the deacetylation of enzyme mimics in less than 10 min and the transesterification of vinyl acetate at room temperature. Investigations to extend this reactivity to peptide bonds is currently ongoing in our laboratory and will be reported in due course.

■ ASSOCIATED CONTENT

Supporting Information

The Supporting Information is available free of charge at https://pubs.acs.org/doi/10.1021/acscatal.0c02121.

Experimental procedures, spectroscopic data, NMR titrations, kinetic data, ORTEP diagrams, X-ray crystal structure data, and modelization studies (PDF)

Crystallographic data (CIF)

Accession Codes

CCDC 2031919 contains the supplementary crystallographic data for this paper. These data can be obtained free of charge via www.ccdc.cam.ac.uk/data_request/cif, or by emailing data_request@ccdc.cam.ac.uk, or by contacting The Cambridge Crystallographic Data Centre, 12 Union Road, Cambridge CB2 1EZ, UK; fax: +44 1223 336033.

■ AUTHOR INFORMATION

Corresponding Authors

Joaquín R. Morán − *Organic Chemistry Department, University of Salamanca, Salamanca E-37008, Spain*; Email: romoran@usal.es

Ángel L. Fuentes de Arriba − *Organic Chemistry Department, University of Salamanca, Salamanca E-37008, Spain*; orcid.org/0000-0001-7424-8146; Email: angelfuentes@usal.es

Authors

José J. Garrido-González − *Organic Chemistry Department, University of Salamanca, Salamanca E-37008, Spain*

M[a] Mercedes Iglesias Aparicio − *Organic Chemistry Department, University of Salamanca, Salamanca E-37008, Spain*

Miguel Martínez García − *Organic Chemistry Department, University of Salamanca, Salamanca E-37008, Spain*

Luis Simón − *Chemical Engineering Department, University of Salamanca, Salamanca E-37008, Spain*; orcid.org/0000-0002-3781-0803

Francisca Sanz − *X-Ray Diffraction Service, University of Salamanca, Salamanca E-37008, Spain*

Complete contact information is available at:

https://pubs.acs.org/10.1021/acscatal.0c02121

Author Contributions

The manuscript was written through contributions of all authors. All authors have given approval to the final version of the manuscript.

Notes

The authors declare no competing financial interest.

■ ACKNOWLEDGMENTS

This work was supported by Junta de Castilla y León (European Regional Development Fund-SA069P17), the University of Salamanca (Own Research Programs-KCEP/463AC01), MINECO (CTQ2017-87529-R), and Fundación Memoria de D. Samuel Solórzano Barruso (FS/8-2019). J.J.G.-G. and A.L.F.d.A. gratefully acknowledge the University of Salamanca for predoctoral and postdoctoral fellowships, respectively. We also thank the *NUCLEUS* platform at University of Salamanca, A. López García and J. A. González Ramos for IT support, V. Obregón from Bio-Oils Huelva, and the University of Salamanca server housing service.

■ DEDICATION

This article is dedicated to Professor Josefa Anaya on ocassion of her retirement.

■ REFERENCES

(1) (a) Drauz, K.; Gröger, H.; May, O. *Enzyme Catalysis in Organic Synthesis*, 3rd ed.; Wiley-VCH: Weinheim, Germany, 2012; p 3. (b) Kirk, O.; Borchert, T. V.; Fuglsang, C. C. Industrial Enzyme Applications. *Curr. Opin. Biotechnol.* **2002**, *13*, 345−351.

(2) Slater, L. B. Industry and Academy: The Synthesis of Steroids. *Hist. Stud. Phys. Biol. Sci.* **2000**, *30*, 443−480.

(3) Chapman, J.; Ismail, A. E.; Dinu, C. Z. Industrial Applications of Enzymes: Recent Advances, Techniques, and Outlooks. *Catalysts* **2018**, *8*, 238−264.

(4) Lee, T. Y.; Suh, J. Target-selective peptide-cleaving catalysts as a new paradigm in drug design. *Chem. Soc. Rev.* **2009**, *38*, 1949−1957.

(5) (a) Suh, J. Progress in Designing Artificial Proteases: A New Therapeutic Option for Amyloid Diseases. *Asian J. Org. Chem.* **2014**, *3*, 18−32. (b) Lee, T. Y.; Suh, J. *Pure Appl. Chem.* **2009**, *81*, 255−262.

(6) Lehn, J.; Sirlin, C. Molecular Catalysis: Enhanced Rates of Thiolysis with High Structural and Chiral Recognition in Complexes of a Reactive Macrocyclic Receptor Molecule. *J. Chem. Soc., Chem. Commun.* **1978**, 949−951.

(7) (a) Breslow, R.; Dong, S. D. Biomimetic Reactions Catalyzed by Cyclodextrins and Their Derivatives. *Chem. Rev.* **1998**, *98*, 1997−2011. (b) Trainor, G. L.; Breslow, R. High Acylation Rates and Enantioselectivity with Cyclodextrin Complexes of Rigid Substrates. *J. Am. Chem. Soc.* **1981**, *103*, 154−158. (c) Breslow, R.; Trainor, G.; Ueno, A. Optimization of Metallocene Substrates for 1-Cyclodextrin Reactions. *J. Am. Chem. Soc.* **1983**, *105*, 2739−2744.

(8) (a) Cram, D. J. The Design of Molecular Hosts, Guests, and Their Complexes. *Angew. Chem., Int. Ed. Engl.* **1988**, *27*, 1009−1020. (b) Cram, D. J.; Katz, H. E. An Incremental Approach to Hosts That Mimic Serine Proteases. *J. Am. Chem. Soc.* **1983**, *105*, 135−137. (c) Cram, D. J.; Lam, P. Y.-S.; Ho, S. P. Synthesis of a Partial Transacylase Mimic. *Ann. N. Y. Acad. Sci.* **1986**, *471*, 22−40. (d) Cram, D. J.; Katz, H. E.; Dicker, I. B. Host-Guest Complexation. 31. A Transacylase Partial Mimic. *J. Am. Chem. Soc.* **1984**, *106*, 4987−5000.

(9) (a) Yuan, D. Q.; Kitagawa, Y.; Aoyama, K.; Douke, T.; Fukudome, M.; Fujita, K. Imidazolyl Cyclodextrins: Artificial Serine Proteases Enabling Regiospecific Reactions. *Angew. Chem., Int. Ed.* **2007**, *46*, 5024−5027. (b) Jiang, L.; Liu, Z.; Liang, Z.; Gao, Y. An Artificial Aspartic Proteinase System. *Bioorg. Med. Chem.* **2005**, *13*, 3673−3680. (c) Tabushi, I. Cyclodextrin Catalysis as a Model for Enzyme Action. *Acc. Chem. Res.* **1982**, *15*, 66−72. (d) Klöck, C.; Dsouza, R. N.; Nau, W. M. Cucurbituril-Mediated Supramolecular Acid Catalysis. *Org. Lett.* **2009**, *11*, 2595−2598. (e) Purse, B. W.; Rebek, J. Functional Cavitands: Chemical Reactivity in Structured Environments. *Proc. Natl. Acad. Sci. U. S. A.* **2005**, *102*, 10777−10782. (f) Soberats, B.; Sanna, E.; Martorell, G.; Rotger, C.; Costa, A. Programmed Enzyme-Mimic Hydrolysis of a Choline Carbonate by a Metal-Free 2-Aminobenzimidazole-Based Cavitand. *Org. Lett.* **2014**, *16*, 840−843.

(10) Ema, T.; Tanida, D.; Matsukawa, T.; Sakai, T. Biomimetic Trifunctional Organocatalyst Showing a Great Acceleration for the Transesterification Between Vinyl Ester and Alcohol. *Chem. Commun.* **2008**, 957−959.

(11) Kheirabadi, M.; Çelebi-Ölçüm, N.; Parker, M. F. L.; Zhao, Q.; Kiss, G.; Houk, K. N.; Schafmeister, C. E. Spiroligozymes for Transesterifications: Design and Relationship of Structure to Activity. *J. Am. Chem. Soc.* **2012**, *134*, 18345−18353.

(12) (a) Chen, L.; Xu, S.; Li, J. Recent Advances in Molecular Imprinting Technology: Current Status, Challenges and Highlighted Applications. *Chem. Soc. Rev.* **2011**, *40*, 2922−2942. (b) Li, S.; Turner, A. P. F. *Molecularly Imprinted Catalysts: Principles, Syntheses, and Applications*; Elsevier: Amsterdam, 2015; pp 34−41. (c) Wulff, G. Enzyme-Like Catalysis by Molecularly Imprinted Polymers. *Chem. Rev.* **2002**, *102*, 1−28. (d) Chen, L.; Wang, X.; Lu, W.; Wu, X.; Li, J. Molecular Imprinting: Perspectives and Applications. *Chem. Soc. Rev.* **2016**, *45*, 2137−211. (e) Mathew, D.; Thomas, B.; Devaky, K. S. Biomimetic Recognition and Peptidase Activities of Transition State Analogue Imprinted Chymotrypsin Mimics. *React. Funct. Polym.* **2018**, *124*, 121−128.

(13) (a) Nothling, M. D.; Ganesan, A.; Condic-Jurkic, K.; Pressly, E.; Davalos, A.; Gotrik, M. R.; Xiao, Z.; Khoshdel, E.; Hawker, C. J.; O'Mara, M. L.; Coote, M. L.; Connal, L. A. Simple Design of an Enzyme-Inspired Supported Catalyst Based on a Catalytic Triad. *Chem.* **2017**, *2*, 732−745. (b) Delort, E.; Darbre, T.; Reymond, J.-L. A Strong Positive Dendritic Effect in a Peptide Dendrimer-Catalyzed Ester Hydrolysis Reaction. *J. Am. Chem. Soc.* **2004**, *126*, 15642−15643. (c) Uhlich, N. A.; Darbre, T.; Reymond, J.-L. Peptide Dendrimer Enzyme Models for ester hydrolysis and Aldolization Prepared by Convergent Thioether Ligation. *Org. Biomol. Chem.* **2011**, *9*, 7071−7084. (d) Maillard, N.; Biswas, R.; Darbre, T.; Reymond, J.-L. Combinatorial discovery of Peptide Dendrimer Enzyme Models Hydrolyzing Isobutyryl Fluorescein. *ACS Comb. Sci.* **2011**, *13*, 310−320. (e) Javor, S.; Reymond, J. L. Molecular dynamics and docking studies of single site esterase peptide dendrimers. *J. Org. Chem.* **2009**, *74*, 3665−3674. (f) Clouet, A.; Darbre, T.; Reymond, J. L. Esterolytic peptide dendrimers with a hydrophobic core and catalytic residues at the surface. *Adv. Synth. Catal.* **2004**, *346*, 1195−1204.

(14) (a) Nothling, M. D.; Xiao, Z.; Hill, N. S.; Blyth, M. T.; Bhaskaran, A.; Sani, M.-A.; Espinosa-Gomez, A.; Ngov, K.; White, J.; Buscher, T.; Separovic, F.; O'Mara, M. L.; Coote, M. L.; Connal, L. A. A multifunctional surfactant catalyst inspired by hydrolases. *Sci. Adv.* **2020**, *6*, No. eaaz0404. (b) Hu, L.; Zhao, Y. Cross-Linked Micelles with Enzyme-like Active Sites for Biomimetic Hydrolysis of Activated Esters. *Helv. Chim. Acta* **2017**, *100*, No. e1700147. (c) Tonellato, U. Functional Micellar Catalysis. Part 2. Ester Hydrolysis Promoted by Micelles Containing the Imidazole Ring and the Hydroxy-Group. *J. Chem. Soc., Perkin Trans. 2* **1977**, *6*, 821−827.

(15) Nothling, M. D.; Xiao, Z.; Bhaskaran, A.; Blyth, M. T.; Bennett, C.; Coote, M. L.; Connal, L. A. Synthetic Catalysts Inspired by Hydrolytic Enzymes. *ACS Catal.* **2019**, *9*, 168−187.

(16) (a) Oinonen, C.; Ruovinen, J. Structural comparison of Ntn-hydrolases. *Protein Sci.* **2000**, *9*, 2329−2337. (b) Zhiryakova, D.; Ivanov, I.; Ilieva, S.; Guncheva, M.; Galunsky, B.; Stambolieva, N. Do N-terminal nucleophile hydrolases indeed have a single amino acid catalytic center? Supporting amino acid residues at the active site of penicillin G acylase. *FEBS J.* **2009**, *276*, 2589−2598. (c) Ekici, O. D.; Paetzel, M.; Dalbey, R. E. Unconventional serine proteases: Variations

on the catalytic Ser/His/Asp triad configuration. *Protein Sci.* **2008**, *17*, 2023−2037. (d) Oinonen, C.; Tikkanen, R.; Rouvinen, J.; Peltonen, L. Three-dimensional structure of human lysosomal aspartylglucosaminidase. *Nat. Struct. Mol. Biol.* **1995**, *2*, 1102−1108.

(17) (a) Brannigan, J. A.; Dodson, G.; Duggleby, H. J.; Moody, P. C. E.; Smith, J. L.; Tomchick, D. R.; Murzin, A. G. A protein catalytic framework with an N-terminal nucleophiles capable of self-activation. *Nature* **1995**, *378*, 416−419. (b) Oinonen, C.; Rouvinen, J. *Protein Sci.* **2000**, *9*, 2329−2337.

(18) (a) Lee, Y. S.; Kim, H. W.; Park, S. S. The Role of -Amino Group of the N-terminal Serine of - Subunit for Enzyme Catalysis and Autoproteolytic Activation of Glutaryl 7-Aminocephalosporanic Acid Acylase. *J. Biol. Chem.* **2000**, *275*, 39200−39206. (b) Morillas, M.; Goble, M. L.; Virden, R. The kinetics of acylation and deacylation of penicillin acylase from Escherichia coli ATCC 11105: evidence for lowered pK_a values of groups near the catalytic centre. *Biochem. J.* **1999**, *338*, 235−239.

(19) Kirby, A. J.; Hollfelder, F. *From Enzyme Models to Model Enzymes*; RSC Publishing: Cambridge, U.K., 2009; p 4.

(20) Schutz, C. N.; Warshel, A. The low barrier hydrogen bond (LBHB) proposal revisited: The case of the Asp ··· His pair in serine proteases. *Proteins: Struct., Funct., Genet.* **2004**, *55*, 711−723.

(21) Hedstrom, L. Serie Protease Mechanism and Specificity. *Chem. Rev.* **2002**, *102*, 4501−4523.

(22) Chen, H.; Weiner, W. S.; Hamilton, A. D. Recognition of neutral species with synthetic receptors. *Curr. Opin. Chem. Biol.* **1997**, *1*, 458−466.

(23) Wayman, K. A.; Sammakia, T. O-Nucleophilic Amino Alcohol Acyl-Transfer Catalysts: The Effect of Acidity of the Hydroxyl Group on the Activity of the Catalyst. *Org. Lett.* **2003**, *5*, 4105−4108.

(24) (a) D'Souza, V. T.; Bender, M. L. Miniature organic models of enzymes. *Acc. Chem. Res.* **1987**, *20*, 146−152. (b) Breslow, R.; Nesnas, N. Burst kinetics and turnover in an esterase mimic. *Tetrahedron Lett.* **1999**, *40*, 3335−3338. (c) Fersht, A. *Structure and Mechanism in Protein Science, A Guide to Enzyme Catalysis and Protein Folding*, 2nd ed.; W. H. Freeman: New York, 1999; pp 218−231.

(25) Menger, F. M.; Whitesell, L. G. A protease mimic with turnover capabilities. *J. Am. Chem. Soc.* **1985**, *107*, 707−708.

(26) Estevan, C.; Vilanova, E. Ethyl Acetate. In *Encyclopedia of Toxicology*, 3rd ed.; Academic Press: London, 2014; pp 506−510.

(27) Breslow, R. Biomimetic Chemistry and Artificial Enzymes: Catalysis by Design. *Acc. Chem. Res.* **1995**, *28*, 146−153.

(28) Duggleby, H. J.; Tolley, S. P.; Hill, C. P.; Dodson, E. J.; Dodson, G.; Moody, P. C. E. Penicillin acylase has a single-amino-acid catalytic centre. *Nature* **1995**, *373*, 264−268.

(29) Marlin, D. S.; Olmstead, M. M.; Mascharak, P. K. Extended structures controlled by intramolecular and intermolecular hydrogen bonding: a case study with pyridine-2,6-dicarboxamide, 1,3-benzenedicarboxamide and *N,N′*-dimethyl-2,6-pyridinedicarboxamide. *J. Mol. Struct.* **2000**, *554*, 211−223.

(30) (a) Simón, L.; Goodman, J. M. Enzyme Catalysis by Hydrogen Bonds: The Balance between Transition State Binding and Substrate Binding in Oxyanion Holes. *J. Org. Chem.* **2010**, *75*, 1831−1840. (b) Simón, L.; Goodman, J. M. Hydrogen-bond stabilization in oxyanion holes: *grand jeté* to three dimensions. *Org. Biomol. Chem.* **2012**, *10*, 1905−1913.

https://dx.doi.org/10.1021/acscatal.0c02121
ACS Catal. 2020, 10, 11162−11170

Chemistry–A European Journal | Communication
doi.org/10.1002/chem.202102137
Chemistry Europe
European Chemical Societies Publishing

Special Collection

An Adjustable Cleft Based on an 8-Sulfonamide-2-Naphthoic Acid with Oxyanion Hole Geometry

José J. Garrido-González,[a] Irene Boya del Teso,[a] Ángel L. Fuentes de Arriba,[a] Francisca Sanz,[b] Eva M. Martín del Valle,[c] Joaquín R. Morán,[a] and Victoria Alcázar*[d]

Dedicated to François Diederich. We are so grateful to be part of the Diederich chemistry family: his contagious enthusiasm and inspiration will always guide us.

Abstract: Cleft type receptors showing the oxyanion hole motif have been prepared in a straightforward synthesis starting from the commercial 3,7-dihidroxy-2-naphthoic acid. The double H-bond donor pattern is achieved by the introduction of a sulfonamide group in the C-8 position of naphthalene and a carboxamide at the C-2 position. This cleft, for which the geometry resembles that of an oxyanion hole, is able to adjust to different guests, as shown by the analysis of the X-ray crystal structures of associates with methanol or acetic acid. Combination of hydrogen bonds and charge-transfer interactions led to further stabilization of the complexes, in which the electron-rich aromatic ring of the receptor was close in space to the electron-deficient dinitroaromatic guests. Modelling studies and bidimensional NMR experiments have been carried out to provide additional information.

The oxyanion hole is a well-established feature in enzyme catalysis.[1] Two strong linear H-bonds stabilize the transition state because the charged carbonyl oxygen undergoes stronger H-bonds than the neutral ground state, reducing therefore the transition state energy. In this sense, rigid, broad oxyanion holes may not be ideal for catalysis, since stronger H-bonds mean also shorter distances between H-bond donors and acceptors;[2] thus, an adjustable oxyanion hole would be better to increase the energy difference between ground and transition states. Conventional oxyanion hole mimics, as the classic isophthalic acid derivatives used extensively by Hamilton[3] or pyridine 2,6-dicarboxylic acid derivatives used by Hunter,[4] showed distances around 5 Å between the NHs, which is well suited for ground state association, as judged for the many published receptors.[5] To get a narrow oxyanion hole-like cleft, an amide and a sulfonamide groups have been placed over a naphthalene skeleton. Carboxamides and sulfonamides have very different geometries as H-bond donors; the need for conjugation of the nitrogen non-bonding electron pair with the sulfuryl orbitals in sulfonamides, directs the H-bond essentially in a nearly perpendicular direction to the carboxamide, as shown in Figure 1.

Placing the sulfonamide in the C-8 position on a 2-naphthoic acid amide skeleton, provides an ideal oxyanion hole with distances which are adaptable as a function of the C–S torsion, and can be as short as 4.7 Å. Also, the presence of the H-1 in the cleft may provide an additional H-bond (CH···O), which can further stabilize the guest in the complex. These carbon-oxygen hydrogen bonding are well reputed in the literature.[6]

Another feature in this cleft is the presence of the two phenol groups in positions C-3 and C-7, since they form intramolecular H-bonds which fix the carboxamide and sulfonamide conformations. This makes the cleft more rigid[7] and might improve catalysis since the negative charge on the carbonyl oxygen in the transition state would attract the

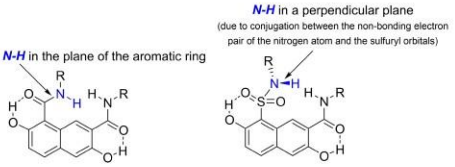

Figure 1. Different geometries between NH donors in the naphthalene skeleton: biscarboxamide cleft (left) and sulfonamide-carboxamide cleft (right).

[a] J. J. Garrido-González, I. Boya del Teso, Dr. Á. L. Fuentes de Arriba, Dr. J. R. Morán
Departamento de Química Orgánica
Universidad de Salamanca
Plaza de los Caídos s/n, Salamanca 37008, (Spain)

[b] Dr. F. Sanz
Servicio de Difracción de Rayos X
University of Salamanca
Plaza de los Caídos s/n, Salamanca 37008 (Spain)

[c] Dr. E. M. Martín del Valle
Departamento de Ingeniería Química
Universidad de Salamanca
Plaza de los Caídos s/n, Salamanca 37008 (Spain)

[d] Dr. V. Alcázar
Departamento de Ingeniería Química Industrial y del Medio Ambiente
Universidad Politécnica de Madrid
C/José Gutiérrez Abascal, 2, Madrid 28006 (Spain)
E-mail: mariavictoria.alcazar@upm.es

Supporting information for this article is available on the WWW under https://doi.org/10.1002/chem.202102137

Special Collection This article belongs to a Joint Special Collection dedicated to François Diederich.

Chemistry–A European Journal | Communication doi.org/10.1002/chem.202102137 | Chemistry Europe European Chemical Societies Publishing

carboxamide hydrogen, leaving therefore, a negative carboxamide carbonyl group which also strengthens the phenolic H-bond. The same reasoning may be valid for the sulfonamide sulfuryl group; thus, the four H-bonds in the complex (the two intramolecular and the two intermolecular with the guest) might be stronger in the transition state and a larger reduction of the transition state energy could be achieved.

Also, the presence of the two phenolic groups in the naphthalene skeleton showed a further benefit since they direct sulfonation in the 2-naphthoic acid to position C-8; therefore, chlorosulfonation of the commercially available 3,7-dihydroxy-2-naphthoic acid leads to the desired skeleton, as shown in Scheme 1.

To improve the binding properties of the cleft, a bis(trifluoromethyl)aniline was chosen as the sulfonamide substituent, since this group is known to increase the H-bonds strength.[8] The carboxamide was substituted with a *p*-dimethylamino aniline group. This electron-rich aromatic ring may provide additional stabilization of the complex due to charge transfer interactions with electron-deficient aromatic rings (Scheme 1).

Receptor **3** crystallizes well from methanol, yielding beautiful yellow crystals suitable for X-ray analysis (Figure 2).

The X-ray structure of receptor **3** was highly promising, showing the expected conformation for the sulfonamide, which is fixed with a short intramolecular H-bond (2.592 Å) same as for carboxamide (2.548 Å). The size of the oxyanion-hole, measured as the distance between the two nitrogen atoms is below 5 Å (4.727 Å), quite close to the average oxyanion-hole distance found in many enzymes.[10] The X-ray structure shows a

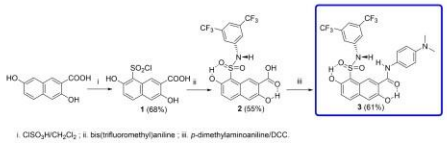

i. $ClSO_2H/CH_2Cl_2$; ii. bis(trifluoromethyl)aniline ; iii. *p*-dimethylaminoaniline/DCC

Scheme 1. Structure and preparation of receptor **3**.

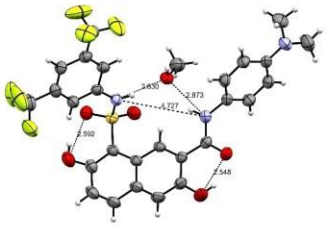

Figure 2. Crystal structure of the complex between receptor **3** and methanol.[9] Selected distances between heavy atoms [Å]: intramolecular H-bonds: 2.592(4) and 2.548(4); width oxyanion hole NH-NH: 4.727(4); intermolecular H-bonds with methanol: 2.830(4) and 2.873(4).

methanol molecule located inside the cleft, accepting two strong H-bonds from the receptor NHs, with 2.830 Å (sulfonamide NH) and 2.873 Å (carboxamide NH). This methanol molecule forms a third H-bond in the crystal (2.782 Å), acting as an H-bond donor with the carboxamide carbonyl group of a second molecule of receptor **3**. This provides an ideal surrounding for the methanol forming three strong H-bonds (Figure S29). Another remarkable feature of this structure is the large torsion angle that forms the *p*-dimethylamino aniline with the carboxamide carbonyl group (67°). This sacrifices a great amount of conjugation energy, but seems to be outweighed by the π-π stacking interaction between the dimethylamino aniline ring and the bis(trifluoromethyl)aniline of another molecule of receptor **3** (Figures S30–S31).

NMR titration experiments with this receptor evidenced a weak binding: firstly, compound **3** is only sparingly soluble in chloroform and, secondly it dimerizes in this solvent. Although dimerization studies showed a small constant of 15 M^{-1}, it was enough to discourage association of electron-deficient aromatic guests as methyl 3,5-dinitrobenzoate, 3,5-dinitrobenzyl alcohol or 3,5-dinitrobenzamide. In no case, significative shifts for the receptor **3** protons were observed upon addition of up to 6 equivalents of the corresponding guests. Modelling studies suggest for the dimer a structure stabilized by up to 4 intermolecular H-bonds, with one of the sulfonamide oxygens of one receptor setting 2 strong hydrogen bonds with the NHs of another molecule of receptor (Table S4).

Trying to improve the properties of this cleft, a larger aromatic sheet of 1-naphthylamine was included as the sulfonamide substituent. The steric bulk of the naphthylamine yielded a conformational rigid compound, since the *peri* CH proton has to be located between the nitrogen and the oxygen atoms of the sulfonamide. On the other hand, and to increase the number of hydrogen bonds, the widely used 2-amino-6-methylpyridine explored by Hamilton[3] and Diederich,[11] was installed as by an amide linkage in the carboxamide, yielding receptor **6**. The preparation of this compound is shown in Scheme 2.

While the reaction of the sulfonyl chloride **4** with 1-naphthylamine was straightforward, the introduction of the aminopyridine was quite challenging. It was not possible to prepare the acid chloride, either with oxalyl chloride, thionyl chloride or phosphorus pentachloride. Coupling the acid and the aminopyridine with HBTU or DCC also failed to produce the desired amide. Finally, it was possible to obtain the desired compound **6** by reacting the methyl ester **5** with a large excess of the aminopyridine anion in THF at room temperature.

Receptor **6** crystallizes from a methanol/acetic acid mixture (99/1) yielding suitable crystals for X-ray analysis. Surprisingly, the structure does not correspond to the expected acetic acid complex, but rather to receptor **6** with a methanol molecule in the cleft (Figure 3).

As expected, the naphthylamine *peri* CH proton is located between the sufonamide nitrogen and oxygen atoms, yielding a nitrogen atom with an almost completely loss of conjugation with the aromatic ring (torsion angle 86°, Figure S32). On the other side, the aminopyridine is almost coplanar with the

Chemistry–A European Journal | Communication doi.org/10.1002/chem.202102137 | Chemistry Europe European Chemical Societies Publishing

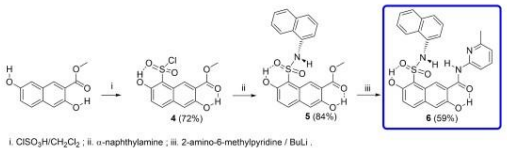

Scheme 2. Structure and preparation of receptor **6**.

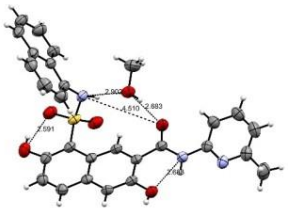

Figure 3. Crystal structure of the complex between receptor **6** and methanol.[12] Selected distances between heavy atoms [Å]: intramolecular H-bonds: 2.591(2) and 2.688(2); width oxyanion hole $NH_{sulfonamide}$-$CO_{carboxamide}$: 4.510(2); intermolecular H-bonds with methanol: 2.902(2) and 2.683(2).

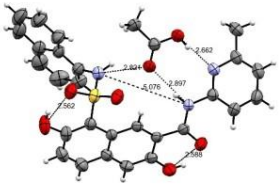

Figure 4. Crystal structure of the complex between receptor **6** and acetic acid.[13] Selected distances between heavy atoms [Å]: intramolecular H-bonds: 2.562(3) and 2.588(2); width oxyanion hole NH-NH: 5.076(2); intermolecular H-bonds with acetic acid: $NH_{sulfonamide}$ 2.821(2); $NH_{carboxamide}$ 2.897(2); $N_{pyridine}$ 2.662(2).

naphthalene backbone, with almost no loss of conjugation energy. Stacking in this complex is dominated by naphthalene pile up (Figure S33).

The most striking feature is the H-bond pattern of the methanol molecule in the cleft. In this case, the methanol acts both as an H-bond acceptor with the sulfonamide NH (2.902 Å) and as a donor with the carboxamide carbonyl group (2.684 Å). This leaves a narrow cleft of only 4.510 Å, in which the carboxamide is twisted 180° respect to its previous position in receptor **3**. Therefore, the intramolecular H-bond with the phenol at C-3 is now set with the amide NH as a donor. Since the phenolic oxygen is not a good H-bond acceptor, this H-bond is long for an intramolecular one (2.688 Å). This phenol group also acts as a donor, setting a H-bond with another methanol molecules with acts as the acceptor (2.757 Å, Figure S34). In this way, methanol forms again the three possible H-bonds.

Pleasingly, crystallization of receptor **6** from pure glacial acetic acid leaves the expected acetic acid associate (Figure 4).

X-ray analysis shows a cleft between the sulfonamide and carboxamide NHs larger than in receptor **3**, with 5.076 Å compared to the previous 4.727 Å for compound **3**. This is expected, since the acetic acid carbonyl forms weaker and larger H-bonds than the methanol oxygen. The differences in H-bond distances for sulfonamide and carboxamide NHs also corroborate that the cleft can adapt to the strength of the different H-bonds (Figures 2 and 4). The shortest H-bond corresponds, nevertheless, to the carboxyl proton and the basic pyridine nitrogen, with a distance of 2.662 Å. Interestingly, two more acetic acid molecules show up in this crystalline structure (Figure S35), with H-bonds between the oxygen atoms (2.658 Å and 2.642 Å) similar to the already reported for acetic acid dimers.[14]

To study the stability of the acetic acid complex, an NMR titration was carried out. Adding acetic acid to a $1.5 \cdot 10^{-3}$ M solution of receptor **6** in deuterochloroform induces large shifts in the receptor **6** signals; in particular, H-1 shifts from 9.126 ppm to 9.329 ppm showing its proximity with the acetic acid carboxyl in the complex. Deshielding of the pyridine protons also confirms the formation of the strong H-bond between the acid and the pyridine nitrogen. An association constant of $6.7 \cdot 10^{3}$ M was determined, which is a good result compared to single amidopyridine complexes in the range of hundreds. The geometry of the complex in solution seems to be similar to the one in the crystalline state, in which the acetic acid is over the naphthylamine ring; the shielding cone of this aromatic ring should produce an acetic acid methyl group absorbing upfield compared to the free acid. Indeed, a chemical shift of 1.6 ppm was estimated for this methyl group in the complex (Figure S21).

However, and despite the large aromatic sheet of receptor **6**, no charge transfer was achieved with electron-deficient aromatic compound as dinitro or trinitrobenzoic acids.

With the aim of combining H-bonds with charge-transfer effects in the associate, a new receptor was designed. The previous disappointing results obtained with the dimethylamino aniline fragment in receptor **3** suggested to include in the receptor a more flexible electron-rich aromatic unit for charge-transfer and a dimethylamino benzylamine fragment was chosen; rotation over the methylene bond might adjust the

Chemistry–A European Journal | Communication doi.org/10.1002/chem.202102137 | Chemistry Europe European Chemical Societies Publishing

geometry while maximizing charge-transfer effects with suitable guests (Scheme 3)

Receptor **8** is highly soluble in chloroform and initial qualitative experiments show the development of deep colours upon addition of electron-poor guests as 3,5-dinitrobenzoic or 2,4,6-trinitrobenzoic acids.

^{1}H NMR shifts of receptor **8** in chloroform strongly depends on the concentration, suggesting the presence of a dimer; dilution experiments changing receptor concentration from $6.32\cdot10^{-2}$ M to $1.23\cdot10^{-4}$ M afforded a self-association constant of $44M^{-1}$ (Figure S22). Despite dimer formation, receptor **8** is a good receptor for electron-deficient guests. As shown in Figure 5, the modelling study presents a good fit for the planar 3,5-dinitrobenozic acid and the receptor **8**, in which the electron-poor aromatic ring is nicely on top of the dimethylaniline fragment while three linear H-bonds are set.

^{1}H NMR titration with 3,5-dinitrobenzoic acid at constant concentration of the receptor ($2.47\cdot10^{-3}$ M) was performed and the shielding of the signals of the dimethylaniline aromatic protons evidenced the proximity of the dinitrobenzoyl aromatic group. On the other hand, all the pyridine signals were deshielded, as expected for the formation of strong H-bonds. An association constant of $K_a = 3.4\cdot10^{-4}$ M^{-1} was determined (Figures S23–S24).

^{1}H NMR bidimensional spectra allow the assignation of all the signals and ROESY, in particular, confirms the structure of the proposed associate with cross correlations among the dinitrobenzoyl and the dimethylaniline protons (Figure S13).

To assess the effect of the charge transfer, a titration with benzoic acid was carried out. Under similar conditions (constant concentration of receptor **8** of $3.3\cdot10^{-3}$ M) addition of benzoic acid developed no colour and an association constant of $6.3\cdot10^{2}\ -^{-1}$ was determined. Since 3,5-dinitrobenzoic acid ($pK_a = 2.82$) is stronger than benzoic acid ($pK_a = 4.21$)),[15] the decrease in association constant might also be attributed partially to this fact; but also, the small association constant with benzoic acid could also be explained because sulfonylamido pyridines show a worse behaviour than the corresponding carboxamido pyridines (Table 1).[16]

While the planar dinitrobenzoic acid fits well in this cleft, the association of 2,4,6-trinitrobenzoic acid is not so obvious since its geometry is completely different. A reddish colour was developed upon addition of the guest, due to the charge transfer; red colour generation due to proton transfer can be ruled out, since neither the trinitrobenzoate nor the amidopyridinium cation are coloured compounds. An X-ray study with diamino pyridine[17] shows the carboxylic acid forming an 80° angle with the aromatic ring. Nevertheless, the charge transfer effect also takes places with this host (Figure S27), probably because the benzylamine can rotate the methylene bond to get a reasonable overlap. A modelling study, showing this possibility is shown in the Figure 6.

Titration in chloroform solution yielded a high association constant $K_a = 8.1\cdot10^{4}$ M^{-1}. As in the case of dinitrobenzoic acid, all the signals of the complex could be assigned to the corresponding protons through bidimensional spectra.

The good results obtained with receptor **8** and nitrobenzoic acids encouraged us to test non-acid nitroaromatic compounds, hoping that the combination of the hydrogen bonds and charge transfer may allow significant association.

First attempt with methyl 3,5-dinitrobenzoate showed a low association constant. It develops a weak charge transfer band with very small shifts in the ^{1}H NMR signals. Plot of the signals

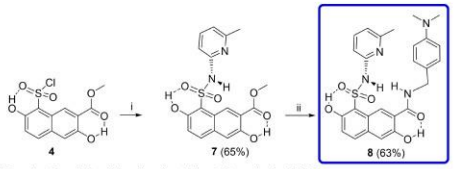

i. 2-amino-6-methylpyridine ; ii. *p*-dimethylaminobenzylamine/ 70°C .

Scheme 3. Structure and preparation of receptor **8**.

Table 1. Binding constants determined from NMR titrations in $CDCl_3$ at 20 °C.

Entry	Receptor	Guest	logK_a
1	**3**	[a]	1.18
2	**6**	Acetic acid	3.83 ± 0.03
3	**8**	[a]	1.64
4	**8**	3,5-dinitrobenzoic acid	4.53 ± 0.14
5	**8**	Benzoic acid	2.79 ± 0.02
6	**8**	2,4,6-trinitrobenzoic acid	4.91 ± 0.40
7	**8**	3,5-dinitrobenzyl alcohol	1.36 ± 0.02
8	**8**	3,5-dinitrobenzamide	2.47 ± 0.01

[a] Self-association constants through dilution experiments.

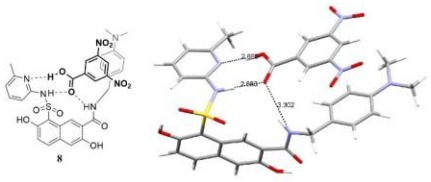

Figure 5. Modelling studies. Associate between receptor **8** and 3,5-dinitrobenzoic acid, showing H-bonds and π-π interactions.

Figure 6. Modelling studies. Associate between receptor **8** and 2,4,6-trinitrobenzoic acid, showing H-bonds and π-π interactions.

Chemistry–A European Journal | Communication doi.org/10.1002/chem.202102137 Chemistry Europe European Chemical Societies Publishing

yielded straight lines and therefore a conventional titration may provide very large errors. As shown in the X-ray studies, alcohols are better H-bond acceptors than esters and, indeed, dinitrobenzyl alcohol yields an increased colour in the complex and the association constant could be determined, $K_a = 23\ M^{-1}$. Finally, 3,5-dinitrobenzamide was also tested. This guest can form three H-bonds and therefore is better than the ester and the alcohol, yielding a $K_a = 298\ M^{-1}$. In both cases the expected deshielding of the NHs and the pyridine signals can be observed so as the shielding of the dimethylaniline protons due to the proximity of the dinitrobenzoyl aromatic ring.

In summary, placing a sulfonamide on the C-8 position of a 2-naphthamide affords an adjustable oxyanion hole which can adapt to carbonyl or alcohol oxygens as shown in X-ray studies. These X-ray studies show two possible geometries for the complex with methanol, one in which the receptor acts donating two H-bonds to the methanol molecule and another in which methanol also acts as the H-bond donor. The combination with aminopyridines allow good association with carboxylic acids, while combination with electron-rich aromatics, provide large association with electron-deficient aromatic acids or even association with non-acidic dinitroaromatic guests.

Acknowledgements

This work was supported by MICINN (PID2019-108994RB-I00), Junta de Castilla y León (European Regional Development Fund-SA069P17), RS2D company, the University of Salamanca (Own Research Programs-KCEP/463AC01 and 18K155/463AC01) and Fundación Memoria de D. Samuel Solórzano Barruso (FS/8-2019). JJGG is gratefully acknowledged to University of Salamanca for a predoctoral fellowship. IBT and ALFA thank the Spanish Government for a Collaboration Fellowship and a Beatriz Galindo Fellowship, respectively. We also thank NUCLEUS platform at University of Salamanca, especially Anna Lithgow (NMR Service) and César Raposo (MS Service). Virginia Obregón from Bio-Oils Huelva is gratefully acknowledged.

Conflict of Interest

The authors declare no conflict of interest.

Keywords: carboxylic acids · charge transfer · hydrogen bonds · molecular recognition · oxyanion hole

[1] a) A. Warshel, G. Narayszabo, F. Sussman, J. K. Hwang, *Biochemistry* **1989**, *28*, 3629–3637; b) P. Bryan, M. W. Pantoliano, S. G. Quill, H. Y. Hsiao, T. Poulos, *Proc. Natl. Acad. Sci. USA* **1986**, *83*, 3743–3745 ; c) D. M. Blow, *Acc. Chem. Res.* **1976**, *9*, 145–152; d) R. Henderson, *J. Mol. Biol.* **1968**, *35*, 143–164.
[2] a) W. W. Cleland, P. A. Frey, J. A. Gerlt, *J. Biol. Chem.* **1998**, *273*, 25529–25532; b) D. Herschlag, M. M. Pinney, *Biochemistry* **2018**, *57*, 3338–3352.
[3] a) S.-K. Chang, A. D. Hamilton, *J. Am. Chem. Soc.* **1988**, *110*, 1318–1319; b) F. García-Tellado, S. Goswami, S.-K. Chang, S. J. Geib, A. D. Hamilton, *J. Am. Chem. Soc.* **1990**, *112*, 7393–7394.
[4] a) C. A. Hunter, D. H. Purvis, *Angew. Chem. Int. Ed. Engl.* **1992**, *31*, 792–795; *Angew. Chem.* **1992**, *104*, 779–782; b) H. Adams, F. J. Carver, C. A. Hunter, N. J. Osborne, *Chem. Commun.* **1996**, 2529–2530; c) F. J. Carver, C. A. Hunter, R. J. Shannon, *J. Chem. Soc. Chem. Commun.* **1994**, 1277–1280.
[5] a) J. Dong, A. P. Davis, *Angew. Chem. Int. Ed.* **2021**, *60*, 8035–8048; *Angew. Chem.* **2021**, *133*, 8113–8126; b) N. H. Evans, C. E. Gell, M. J. G. Peach, *Org. Biomol. Chem.* **2016**, *14*, 7972–7981; c) C. Byrne, K. M. Houlihan, P. Devi, P. Jensen, P. J. Rutledge, *Molecules* **2014**, *19*, 20751–20767; d) S. C. Picot, B. R. Mullaney, P. D. Beer, *Chem. Eur. J.* **2012**, *18*, 6230–6237; e) A. J. Wilson, in *Supramolecular Chemistry: From Molecules to Nanomaterials* (Eds.: P. A. Gale, J. W. Steed), J. Wiley & Sons, **2012**, p. 1325; f) P. A. Gale, J. Garric, M. E. Light, B. A. McNally, B. D. Smith, *Chem. Commun.* **2007**, 1736–1738; g) S. R. Collinson, T. Gelbrich, M. B. Hursthouse, J. H. R. Tucker, *Chem. Commun.* **2001**, 555–556.
[6] S. Horowitz, R. C. Trievel, *J. Mol. Biol.* **2012**, *287*, 41576–41582.
[7] P. V. Santacroce, J. T. Davis, M. E. Light, P. A. Gale, J. C. Iglesias-Sánchez, P. Prados, R. Quesada, *J. Am. Chem. Soc.* **2007**, *129*, 1886–1887.
[8] a) A. L. Fuentes de Arriba, M. G. Turiel, L. Simón, F. Sanz, J. F. Boyero, F. M. Muniz, J. R. Morán, V. Alcázar, *Org. Biomol. Chem.* **2011**, *9*, 8321–8327; b) Z. Zhang, P. R. Schreiner, *Chem. Soc. Rev.* **2009**, *38*, 1187–1198; c) A. Wittkopp, P. R. Schreiner, *Chem. Eur. J.* **2003**, *9*, 407–414.
[9] Deposition Number(s) 2089810 (receptor **3** with methanol) contain(s) the supplementary crystallographic data for this paper. These data are provided free of charge by the joint Cambridge Crystallographic Data Centre and Fachinformationszentrum Karlsruhe Access Structures service.
[10] a) L. Simón, J. M. Goodman, *Org. Biomol. Chem.* **2012**, *10*, 1905–1913; b) L. Simón, J. M. Goodman, *J. Org. Chem.* **2010**, *75*, 1831–1840.
[11] a) P. Lustenberger, E. Martinborough, T. M. Denti, F. Diederich, *J. Chem. Soc. Perkin Trans. 2* **1998**, 747–762; b) J. Cuntze, F. Diederich, *Helv. Chim. Acta* **1997**, *80*, 897–911; c) L. Owens, C. Thilgen, C. Knobler, F. Diederich, *Helv. Chim. Acta* **1993**, *76*, 2757–2774; d) V. A. Montero, L. Tomlinson, K. N. Houk, F. Diederich, *Tetrahedron Lett.* **1991**, *32*, 5309–5312.
[12] Deposition Number(s) 2089806 (receptor **6** with methanol) contain(s) the supplementary crystallographic data for this paper. These data are provided free of charge by the joint Cambridge Crystallographic Data Centre and Fachinformationszentrum Karlsruhe Access Structures service.
[13] Deposition Number(s) 2089809 (receptor **6** with acetic acid) contain(s) the supplementary crystallographic data for this paper. These data are provided free of charge by the joint Cambridge Crystallographic Data Centre and Fachinformationszentrum Karlsruhe Access Structures service.
[14] O. Socha, M. Dracínský, *Molecules* **2020**, *25*, 2150.
[15] J. Jover, R. Bosque, J. Sales, *QSAR Comb. Sci.* **2008**, *27*, 563–581.
[16] a) F. Gómez Herrero, O. H. Rubio, L. M. Monleón, Á. L. Fuentes de Arriba, L. Simón, J. R. Morán, *Org. Biomol. Chem.* **2016**, *14*, 3906–3912; b) Á. L. Fuentes de Arriba, Á. Gómez Herrero, O. H. Rubio, L. M. Monleón, L. Simón, V. Alcázar, F. Sanz, J. R. Morán, *Org. Biomol. Chem.* **2015**, *13*, 493–501.
[17] G. Smith, R. C. Bott, A. D. Rae, A. C. Willis, *Aust. J. Chem.* **2000**, *53*, 531–534.

Manuscript received: June 15, 2021
Accepted manuscript online: August 15, 2021
Version of record online: September 27, 2021

Annex III – NMR Spectra

NMR spectra of already published compounds can be found freely available at:

Chapter 1

https://pubs.acs.org/doi/suppl/10.1021/acs.orglett.9b04379/suppl_file/ol9b04379_si_001.pdf

Chapter 2

https://pubs.acs.org/doi/suppl/10.1021/acscatal.0c02121/suppl_file/cs0c02121_si_001.pdf

https://chemistry-europe.onlinelibrary.wiley.com/action/downloadSupplement?doi=10.1002%2Fchem.202102137&file=chem202102137-sup-0001-misc_information.pdf

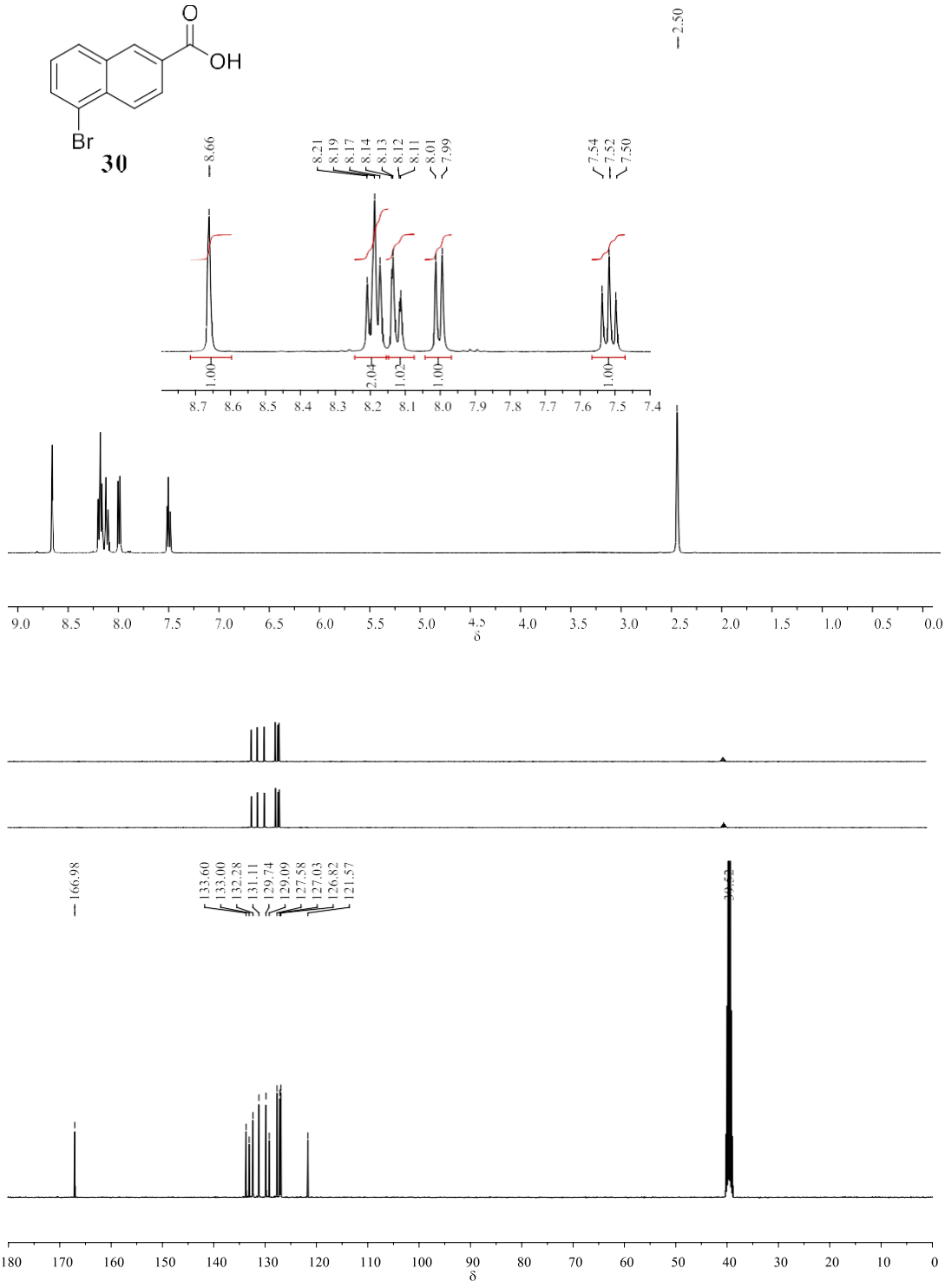

Figure S1. *^{1}H and ^{13}C NMR spectra of compound* **30** *in DMSO-d_6.*

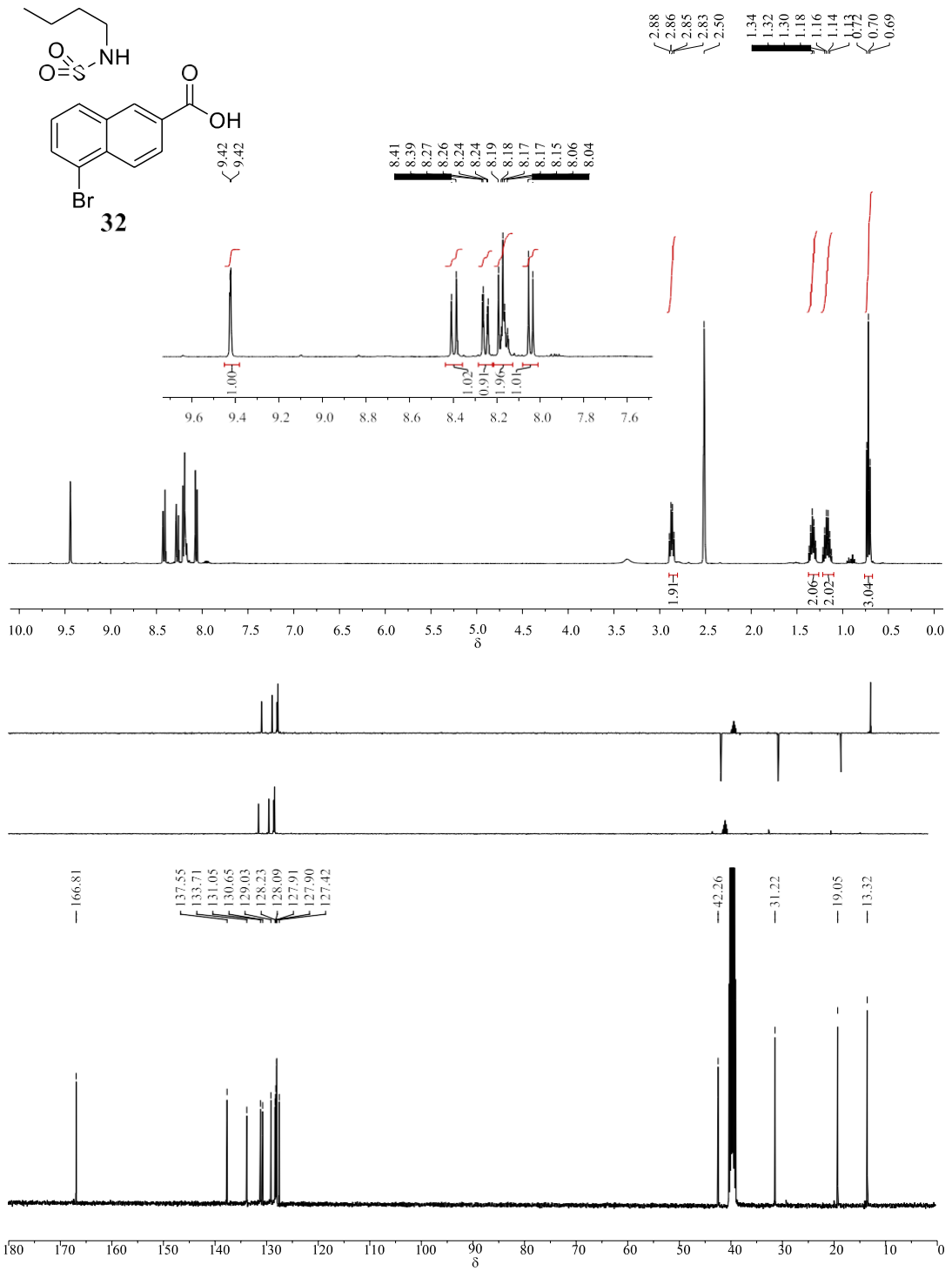

Figure S2. *^{1}H and ^{13}C NMR spectra of compound* **32** *in DMSO-d_6*

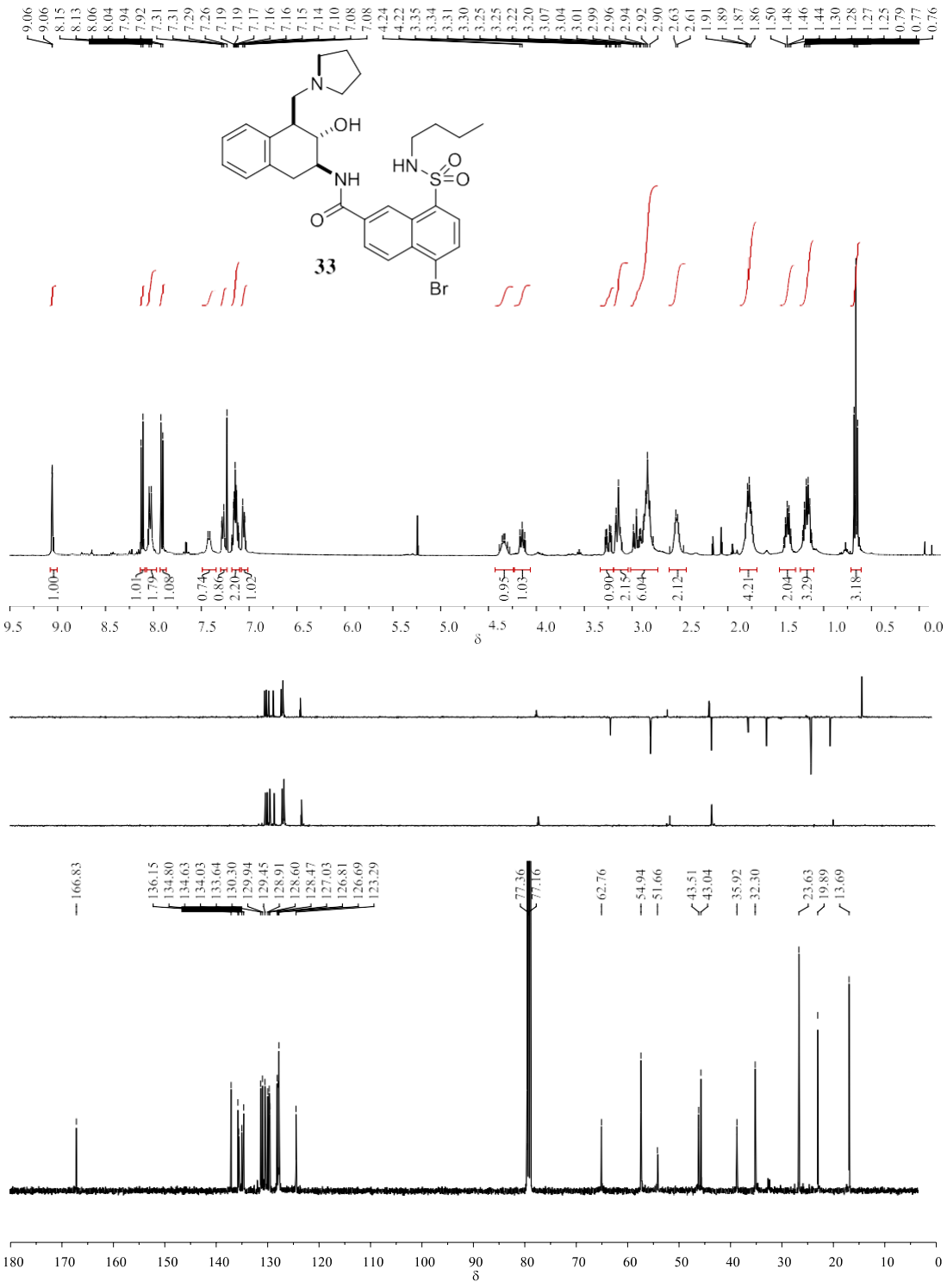

Figure S3. *^{1}H and ^{13}C NMR spectra of compound* **33** *in $CDCl_3$.*

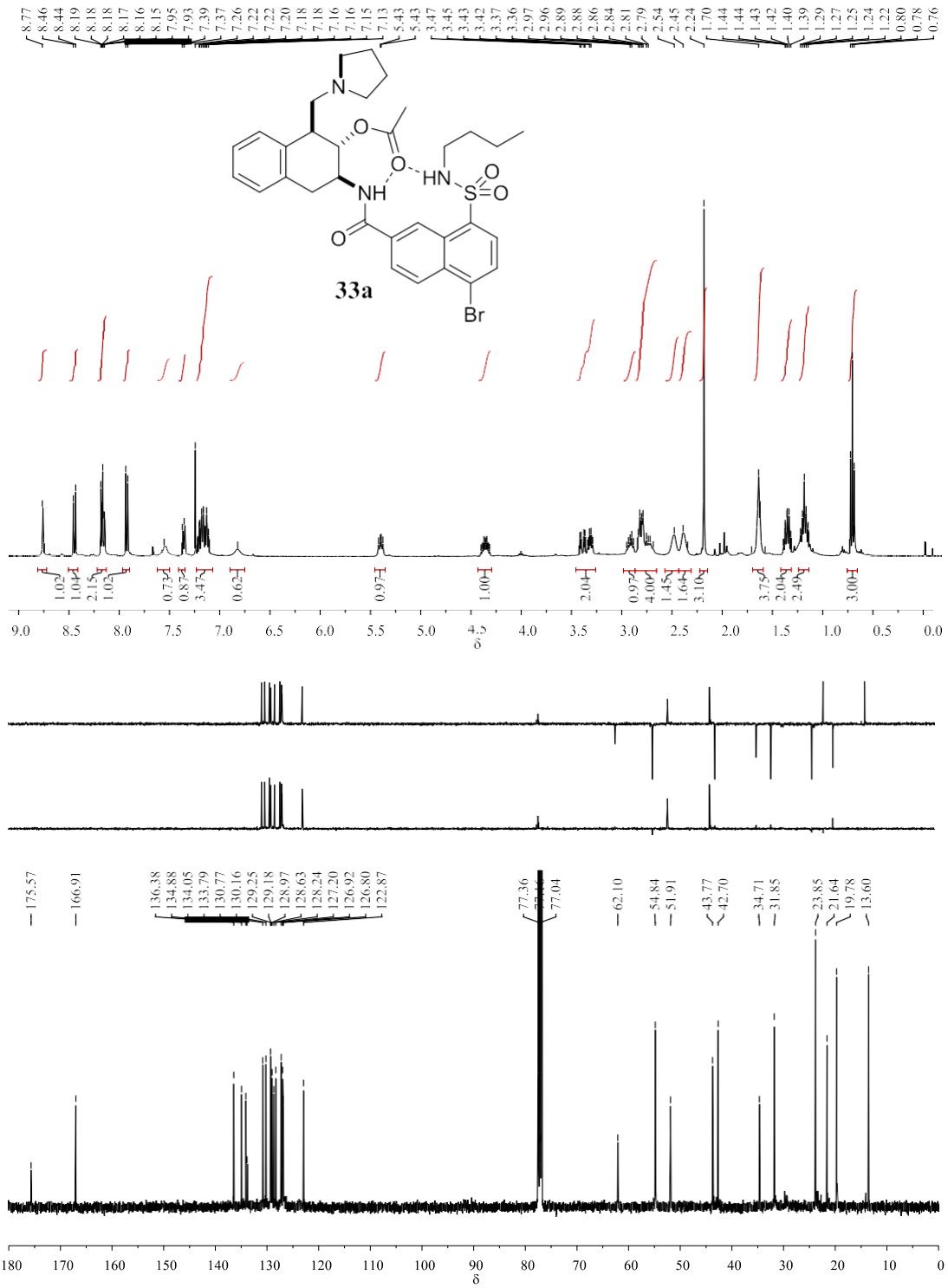

Figure S4. *^{1}H and ^{13}C NMR spectra of compound* **33a** *in $CDCl_3$.*

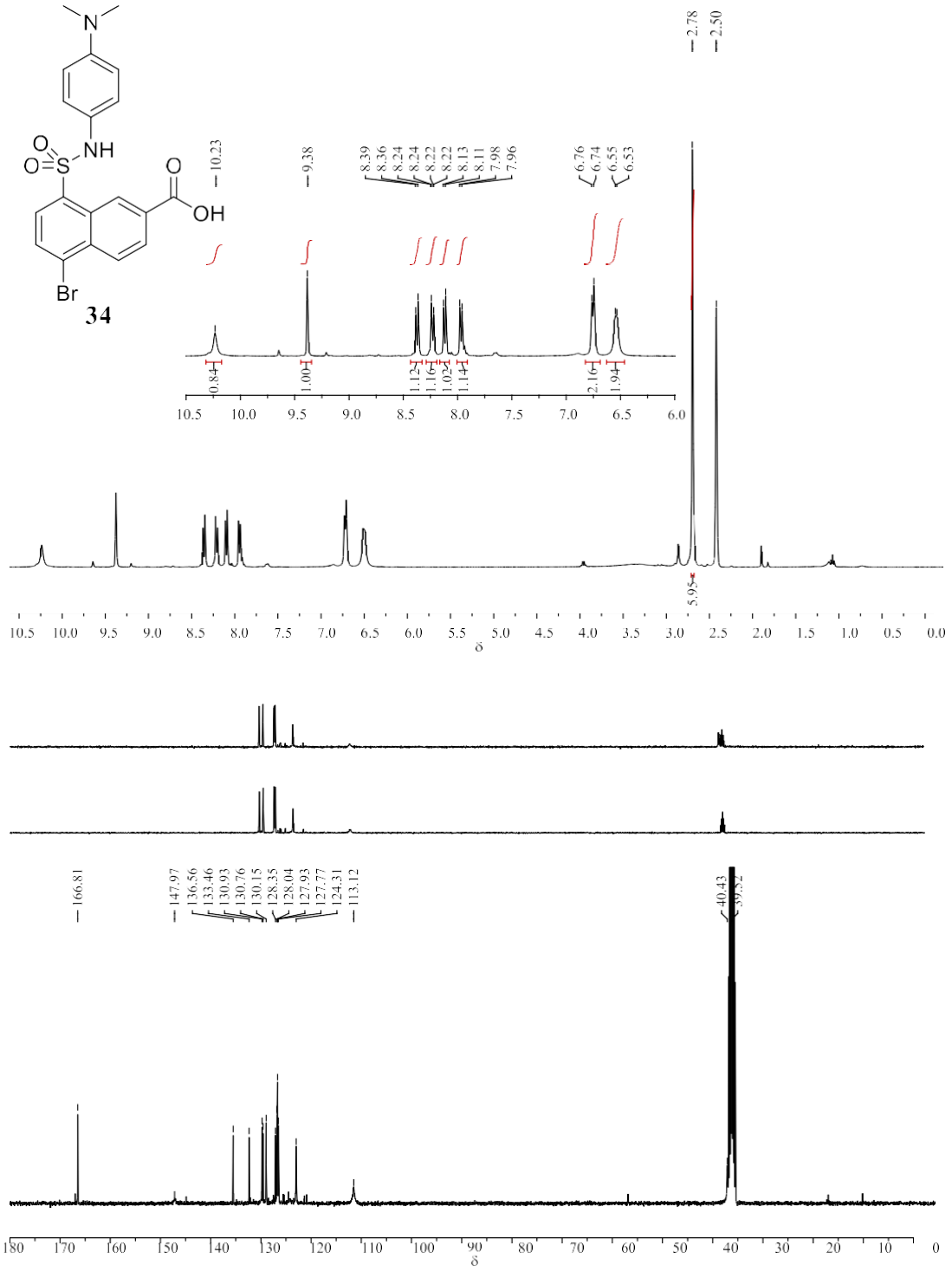

Figure S5. *^{1}H and ^{13}C NMR spectra of compound* **34** *in DMSO-d_6.*

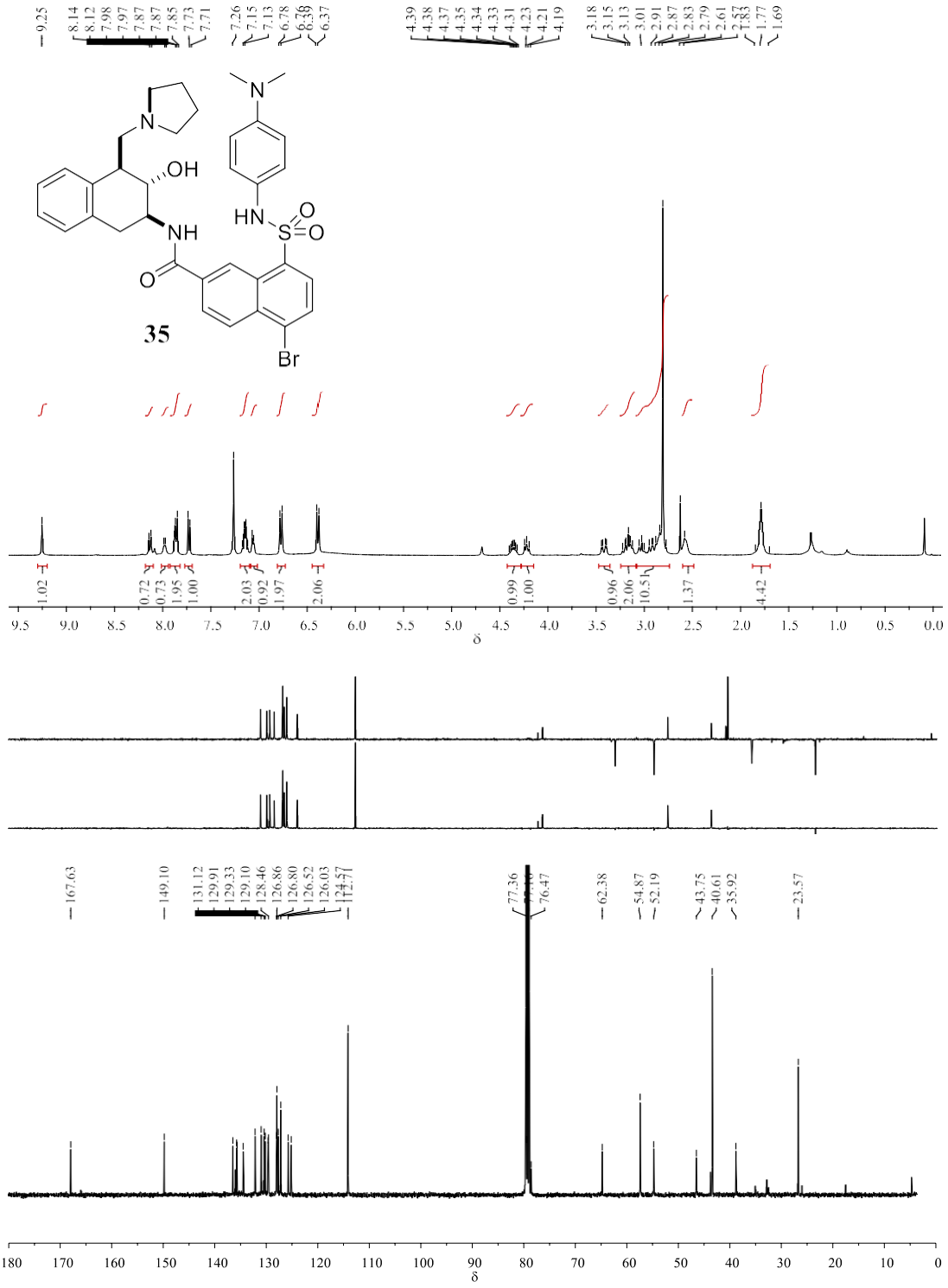

Figure S6. *^{1}H and ^{13}C NMR spectra of compound* **35** *in $CDCl_3$*

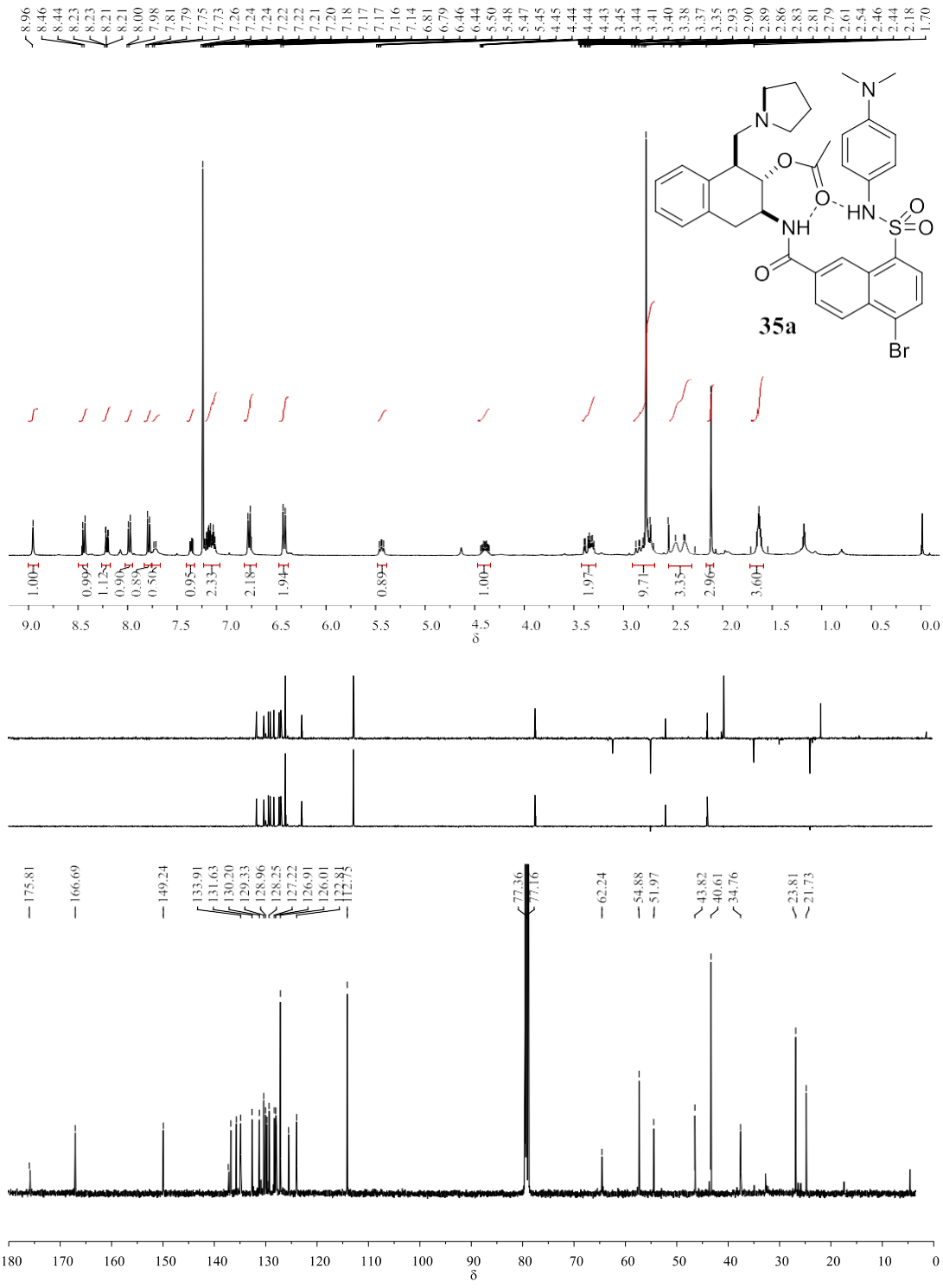

Figure S7. *^{1}H and ^{13}C NMR spectra of compound* **35a** *in $CDCl_3$*

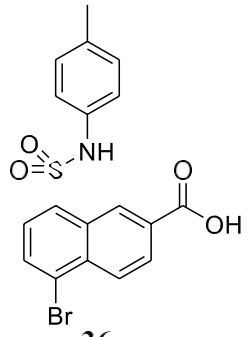

36

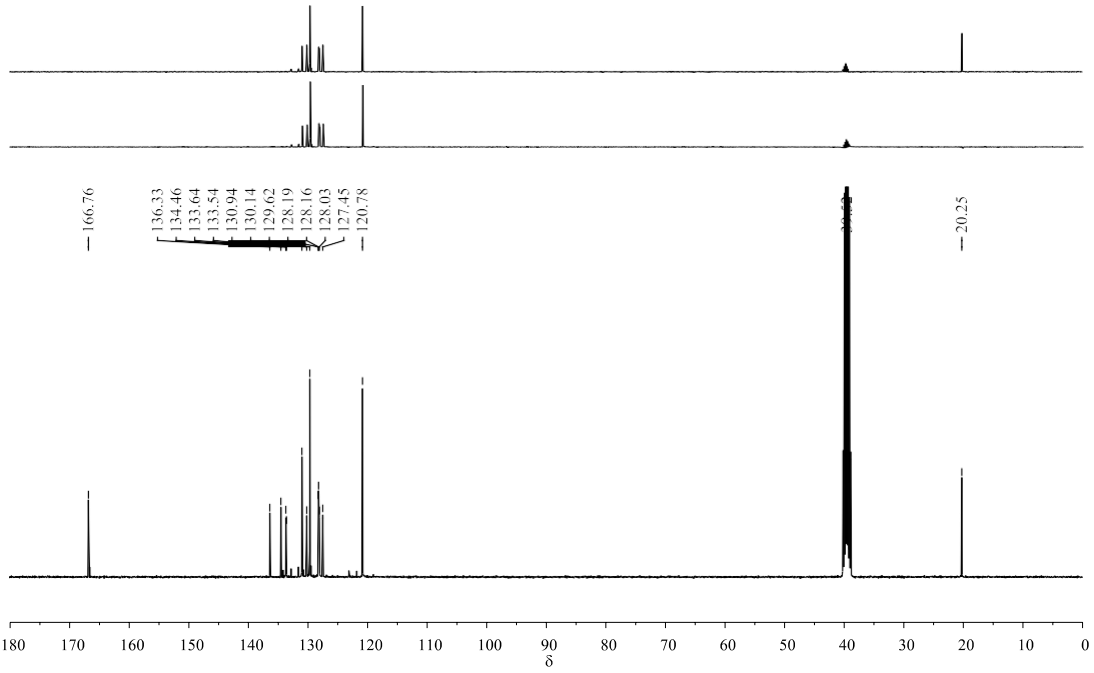

Figure S8. *^{1}H and ^{13}C NMR spectra of compound* **36** *in DMSO-d_6.*

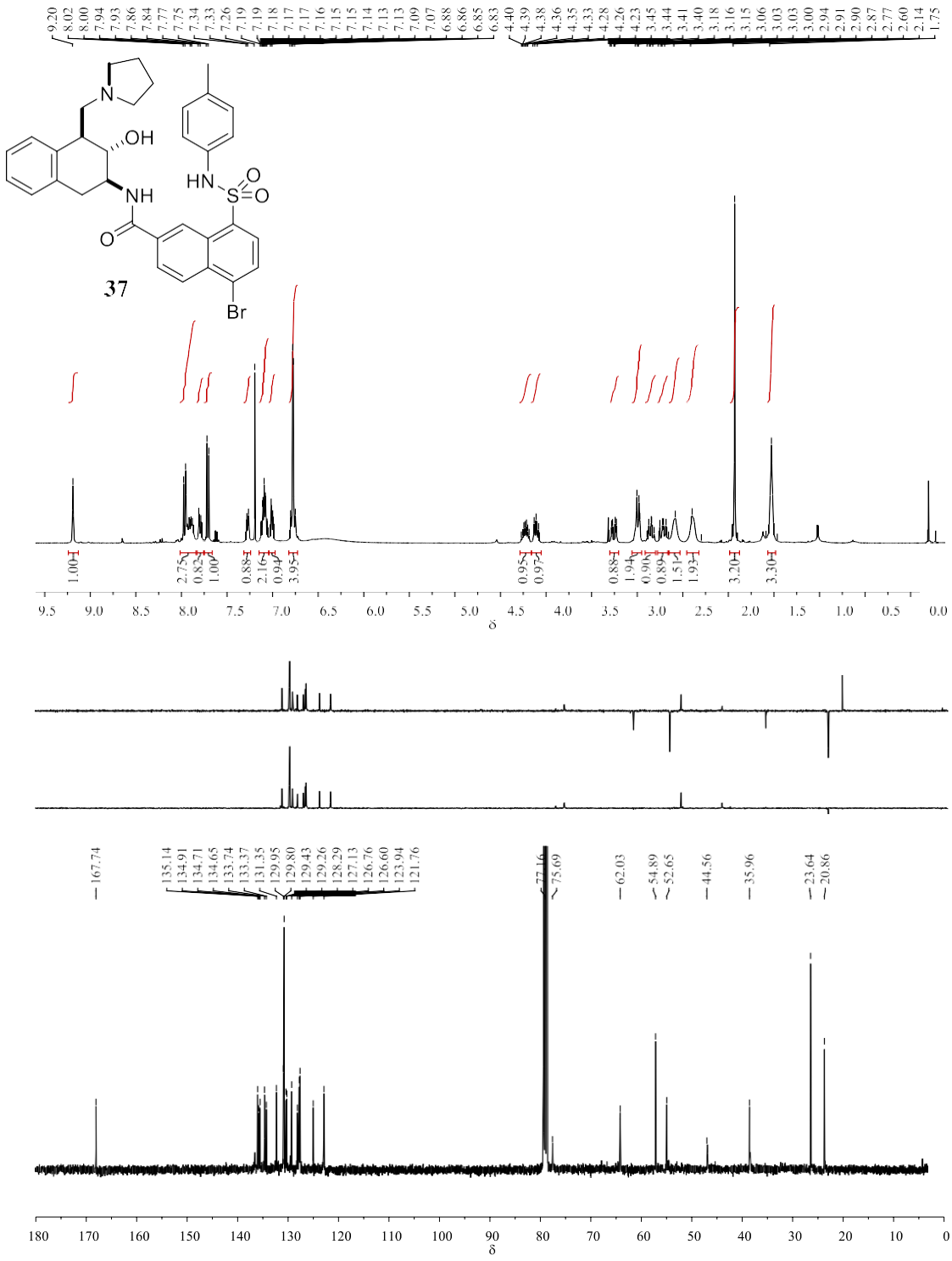

Figure S9. *^{1}H and ^{13}C NMR spectra of compound* **37** *in $CDCl_3$.*

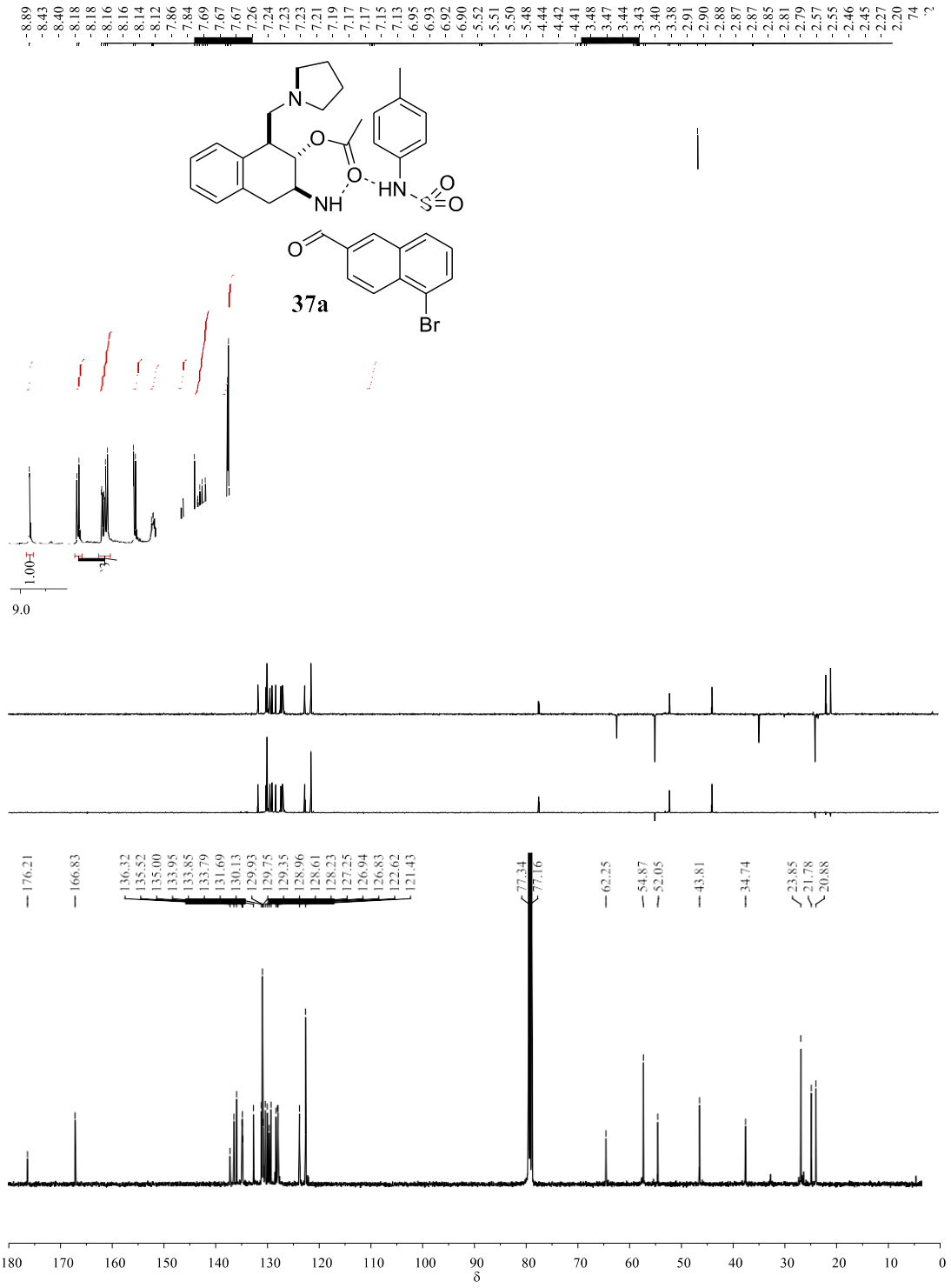

Figure S10. *^{1}H and ^{13}C NMR spectra of compound* **37a** *in $CDCl_3$.*

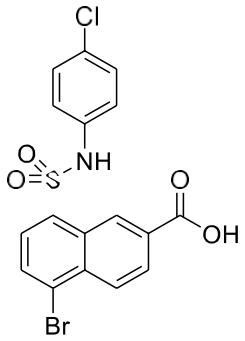

38

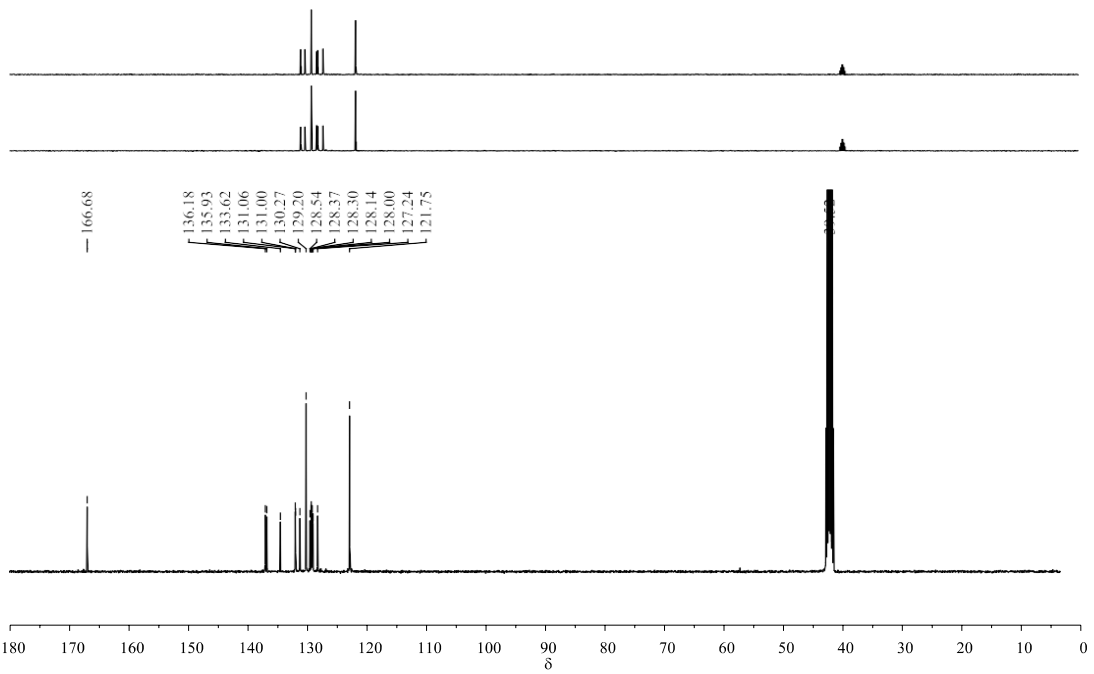

Figure S11. *^{1}H and ^{13}C NMR spectra of compound* **38** *in DMSO-d_6.*

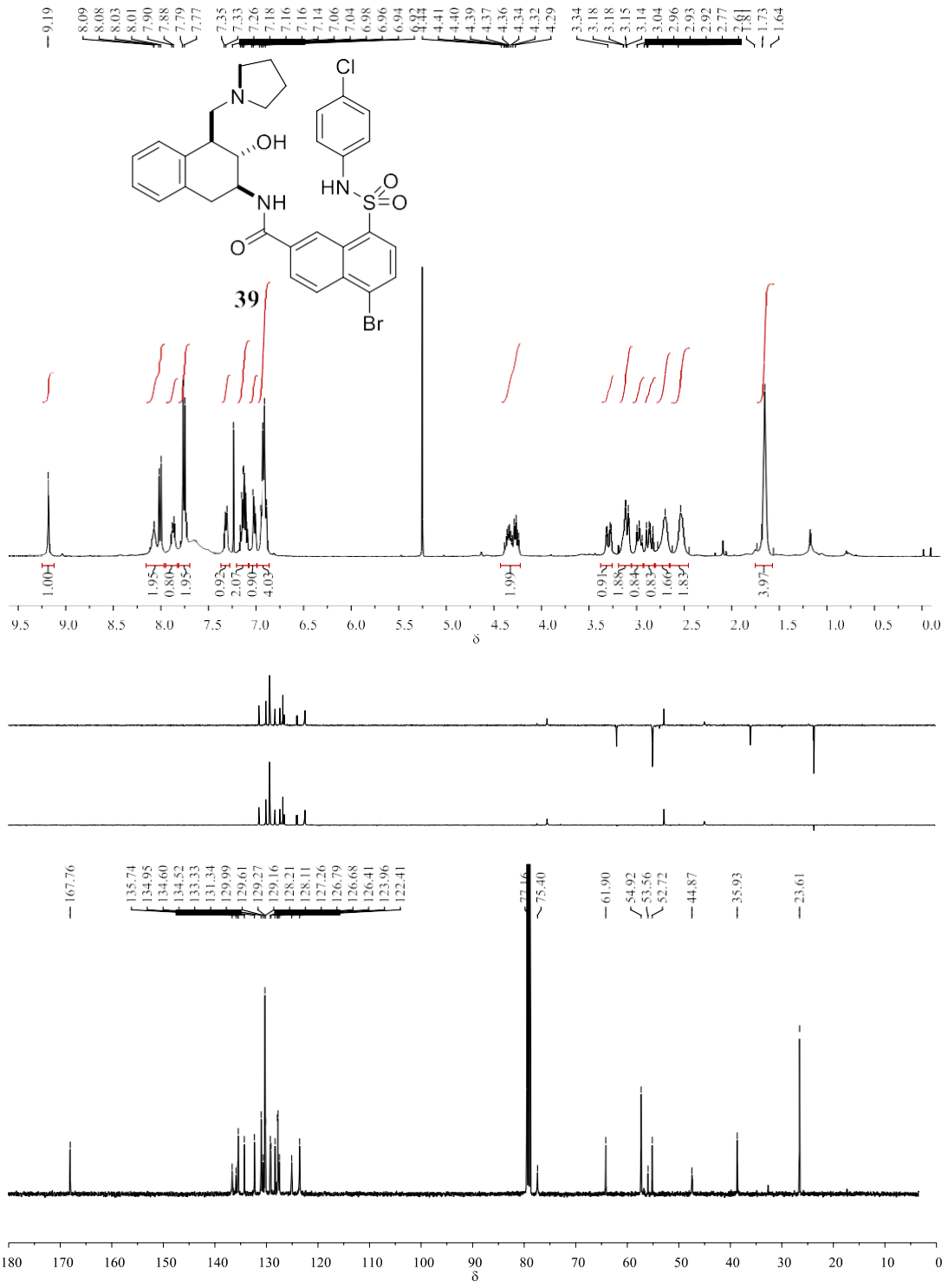

Figure S12. *^{1}H and ^{13}C NMR spectra of compound* **39** *in $CDCl_3$.*

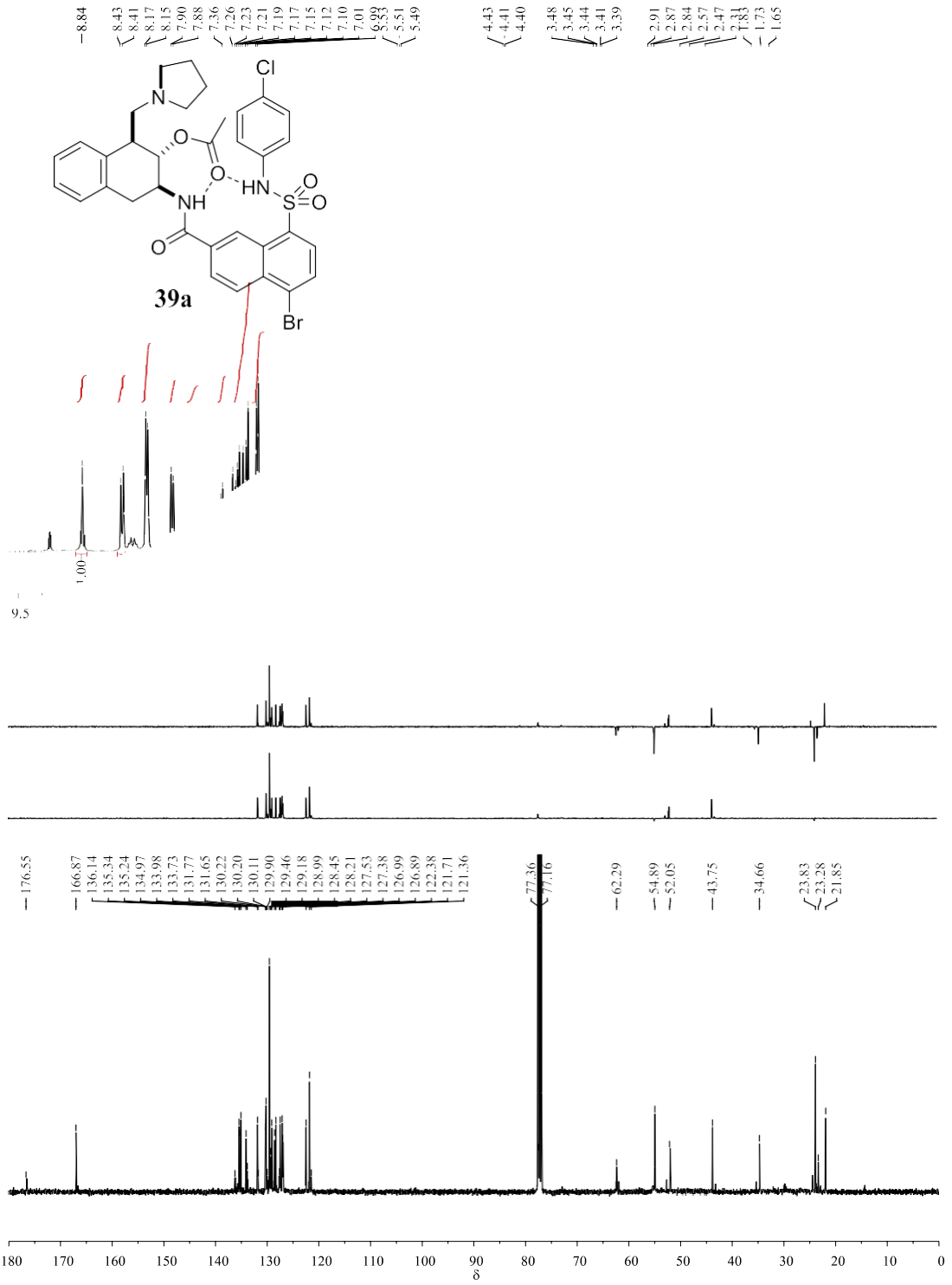

Figure S13. *^{1}H and ^{13}C NMR spectra of compound* **39a** *in $CDCl_3$.*

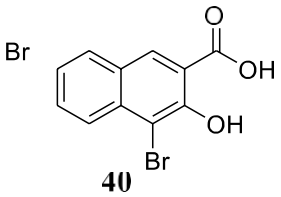

40

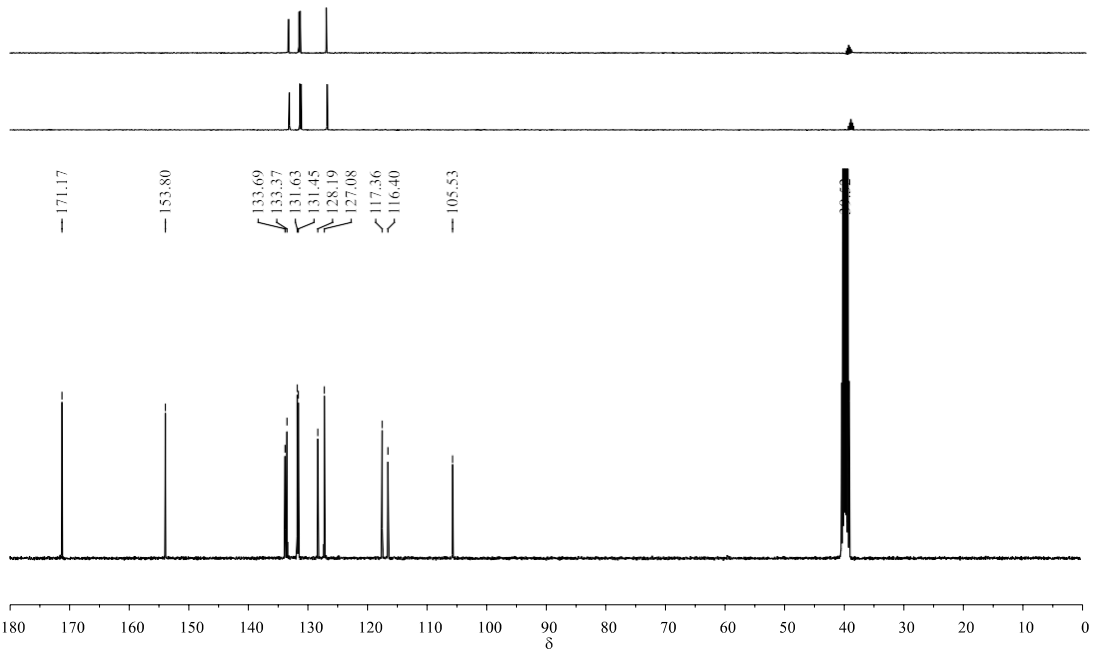

Figure S14. *^{1}H and ^{13}C NMR spectra of compound* **40** *in DMSO-d_6.*

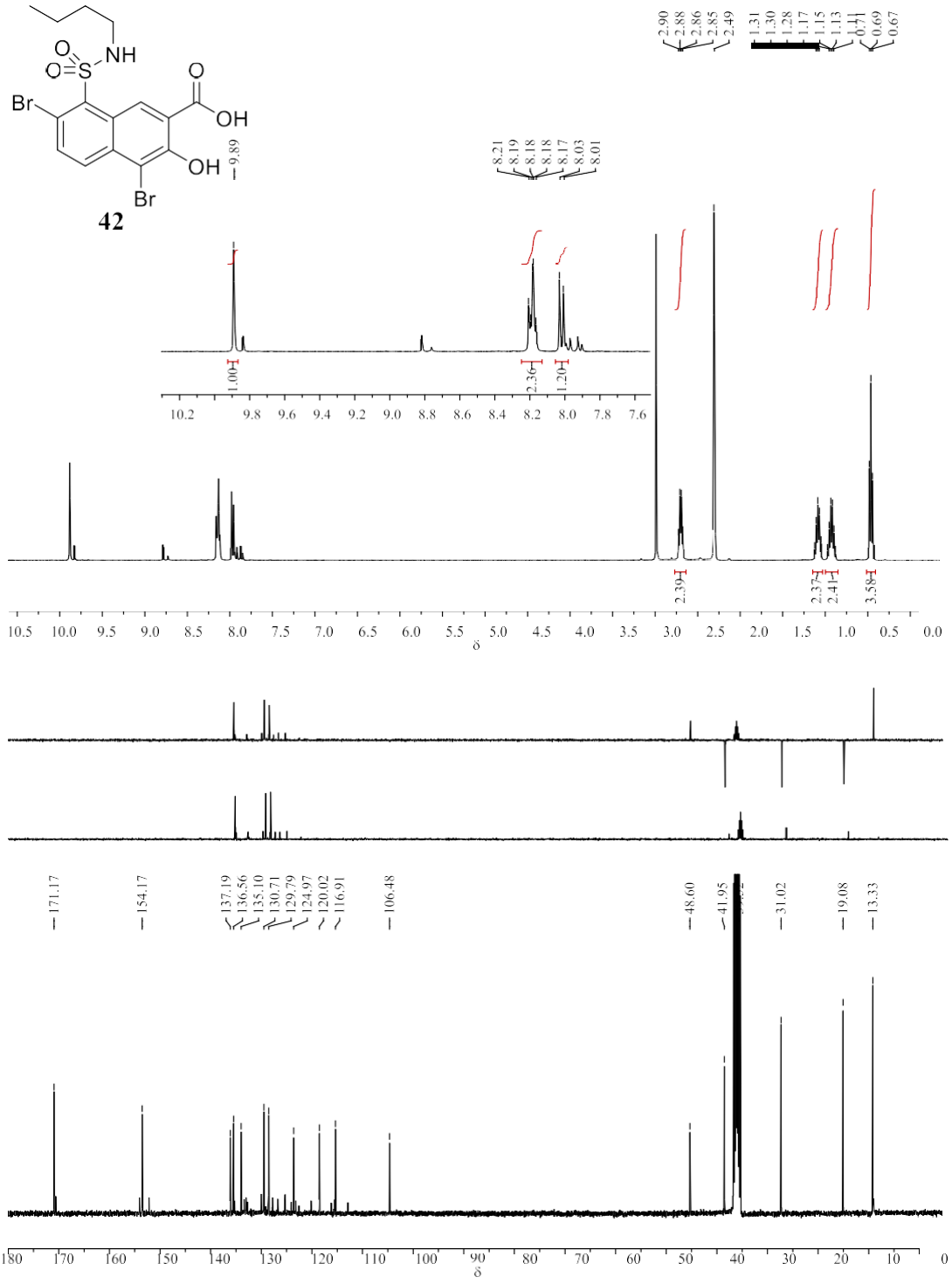

Figure S15. *^{1}H and ^{13}C NMR spectra of compound* **42** *in DMSO-d_6.*

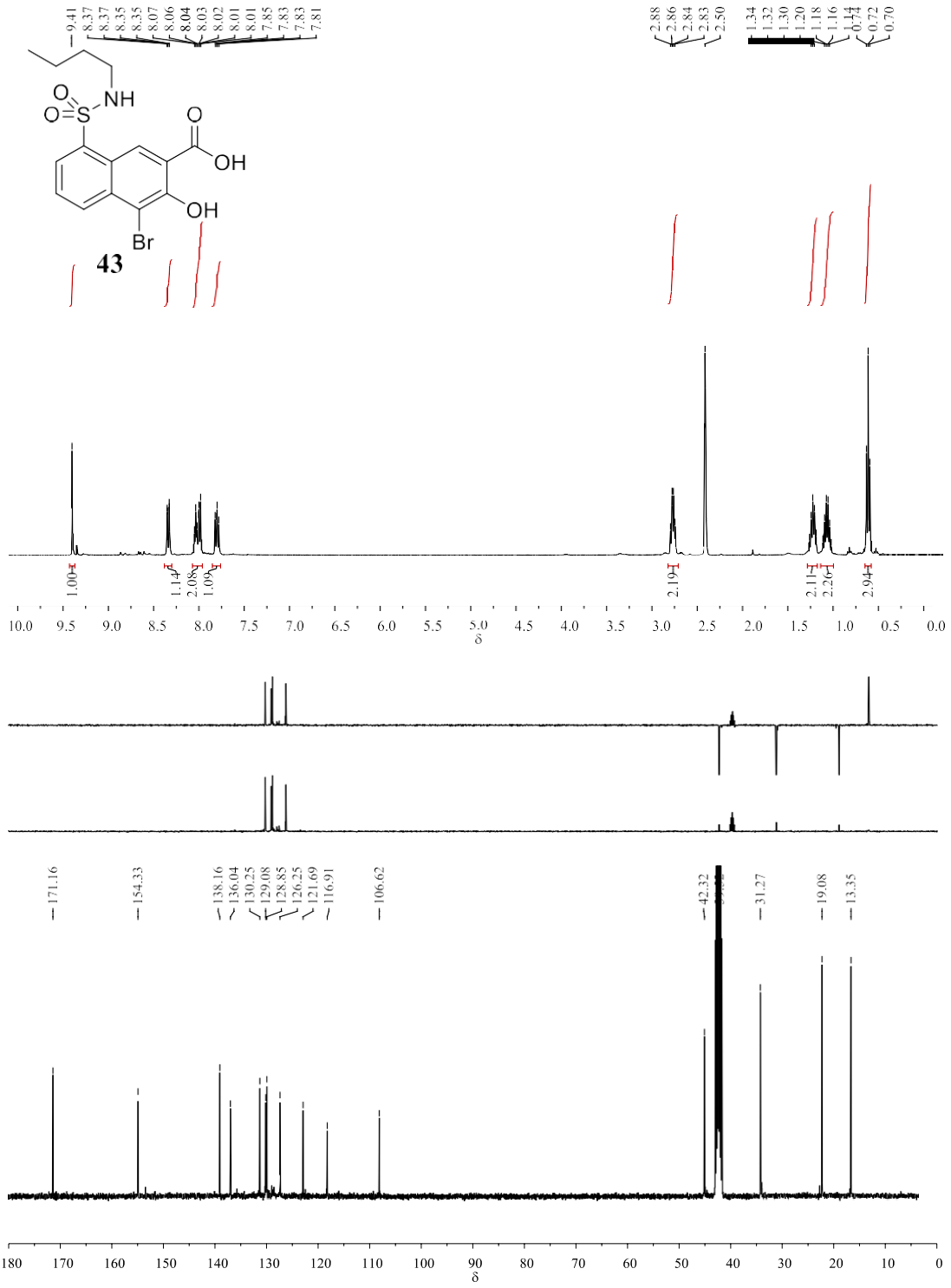

Figure S16. *^{1}H and ^{13}C NMR spectra of compound* **43** *in DMSO-d_6.*

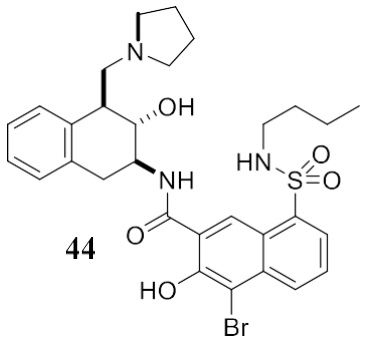
N
OH
NH
HN
S
O
O
O
HO
Br

44

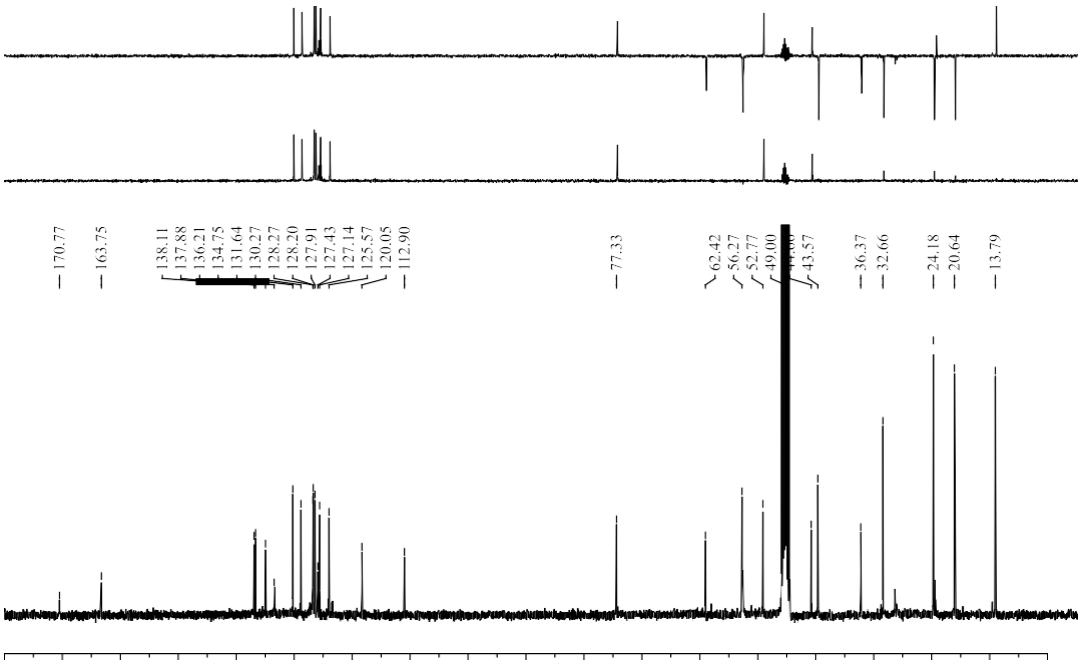
170.77
163.75
138.11
137.88
136.21
134.75
131.64
130.27
128.27
128.20
127.91
127.43
127.14
125.57
120.05
112.90
77.33
62.42
56.27
52.77
49.00
43.57
36.37
32.66
24.18
20.64
13.79

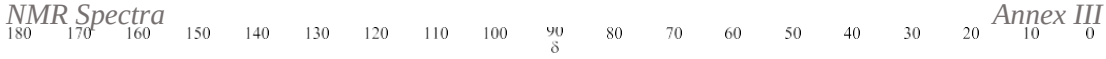

Figure S17. *^{1}H and ^{13}C NMR spectra of compound* **44** *in CD_3OD.*

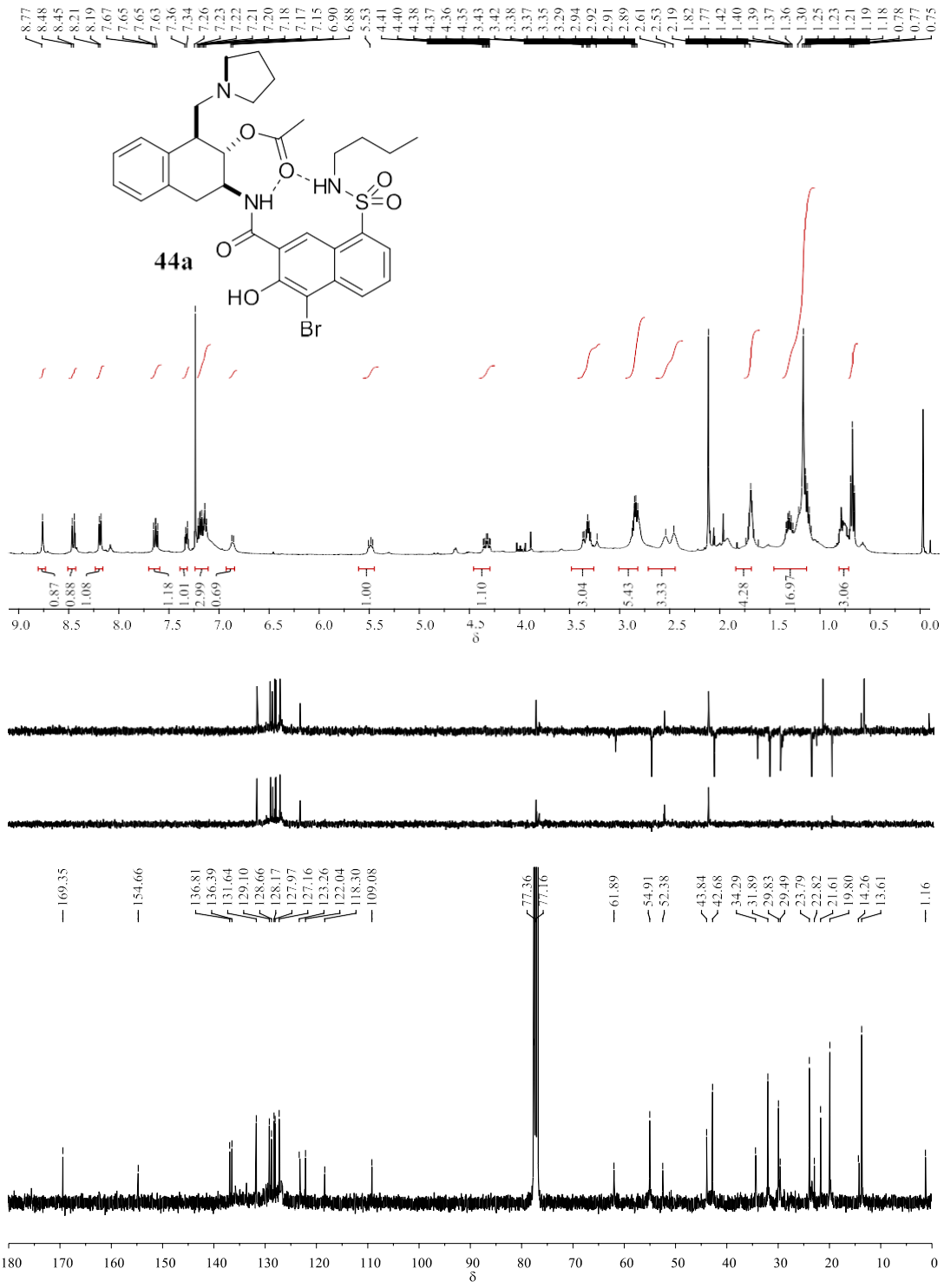

Figure S18. *^{1}H and ^{13}C NMR spectra of compound* **44a** *in $CDCl_3$.*

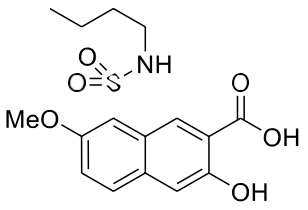
O
O=S
NH
O
MeO
OH
OH

46

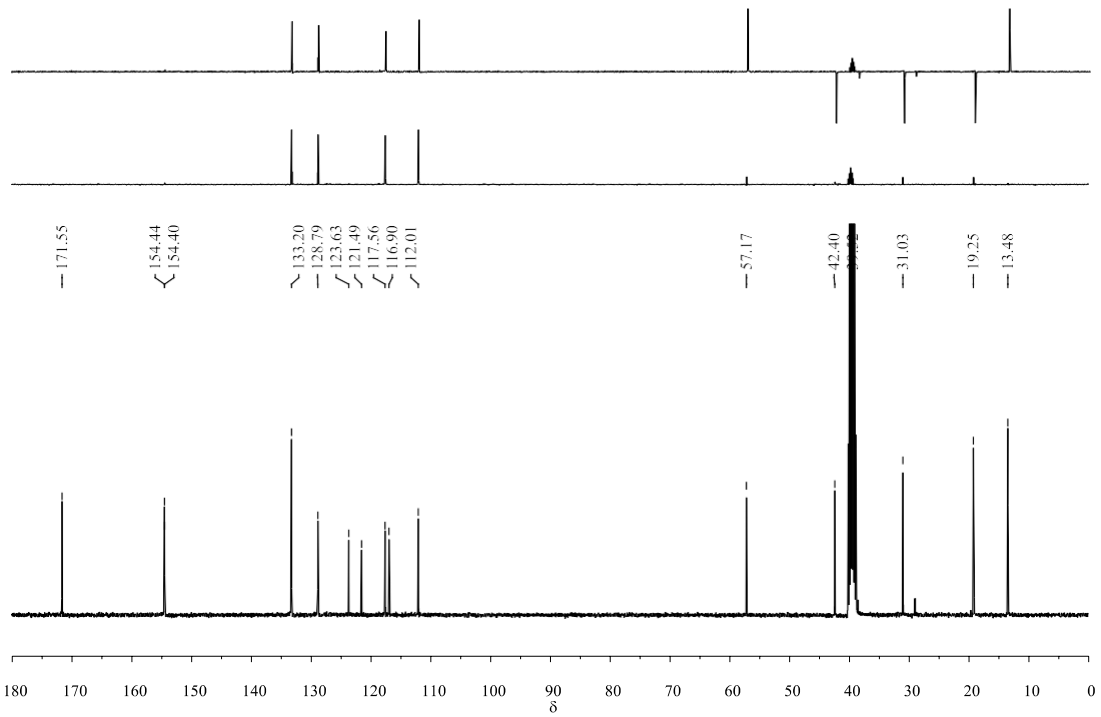
171.55
154.44
154.40
133.20
128.79
123.63
121.49
117.56
116.90
112.01
57.17
42.40
31.03
19.25
13.48
180
170
160
150
140
130
120
110
100
90
80
70
60
50
40
30
20
10
0
δ

Figure S19. *^{1}H and ^{13}C NMR spectra of compound* **46** *in DMSO-d_6.*

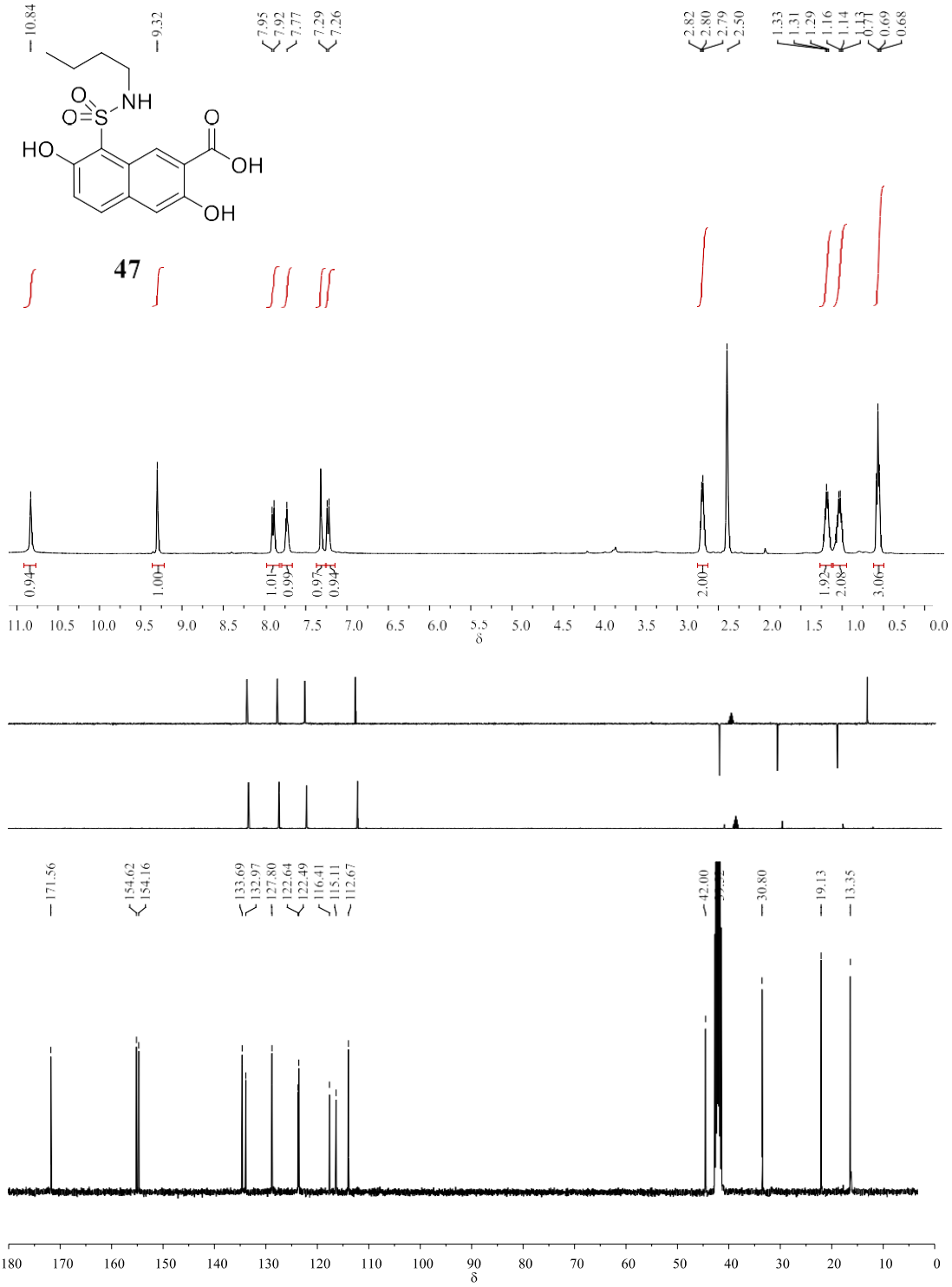

Figure S20. *^{1}H and ^{13}C NMR spectra of compound* **47** *in DMSO-d_6.*

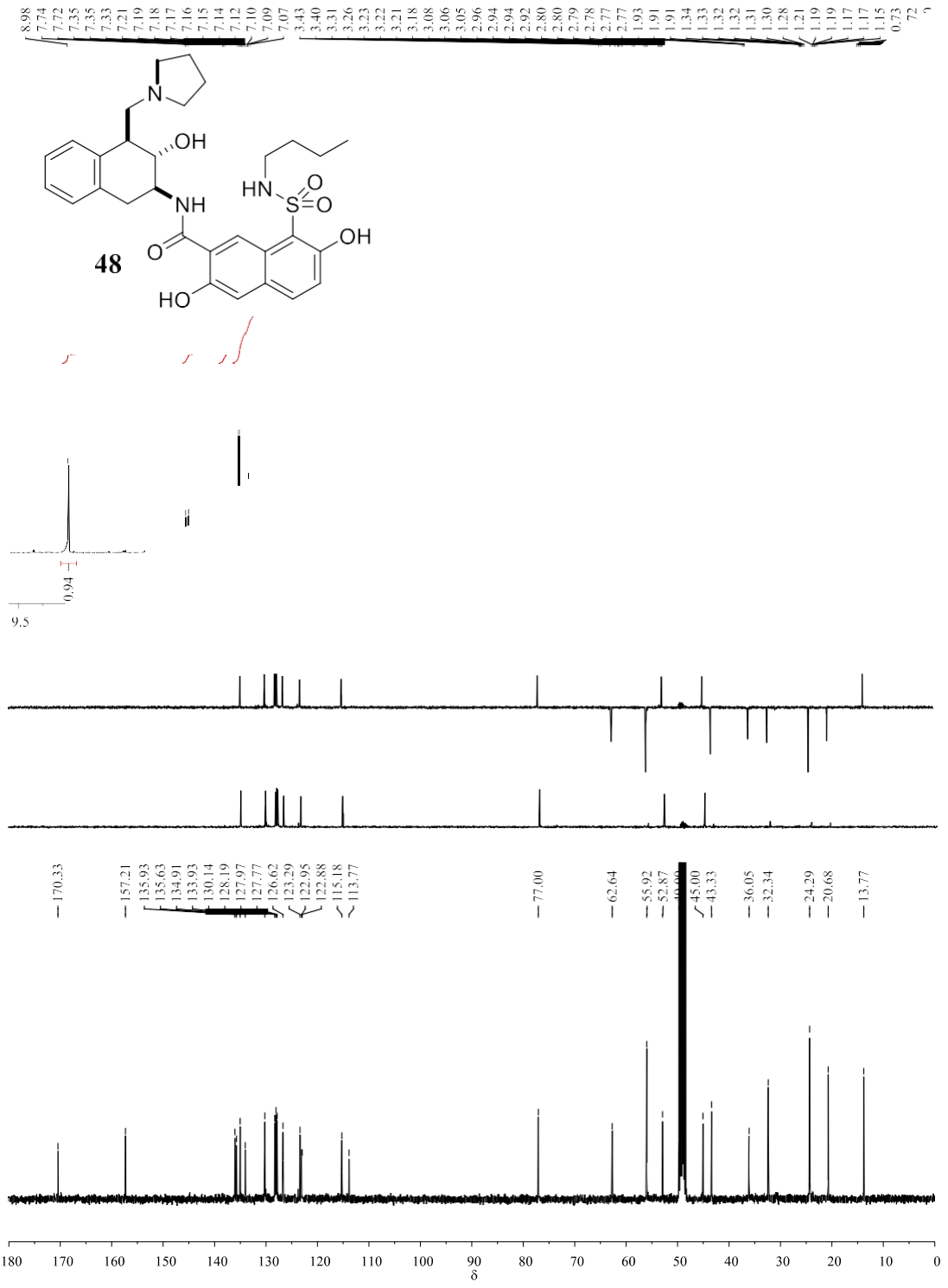

Figure S21. *^{1}H and ^{13}C NMR spectra of compound* **48** *in $CDCl_3$.*

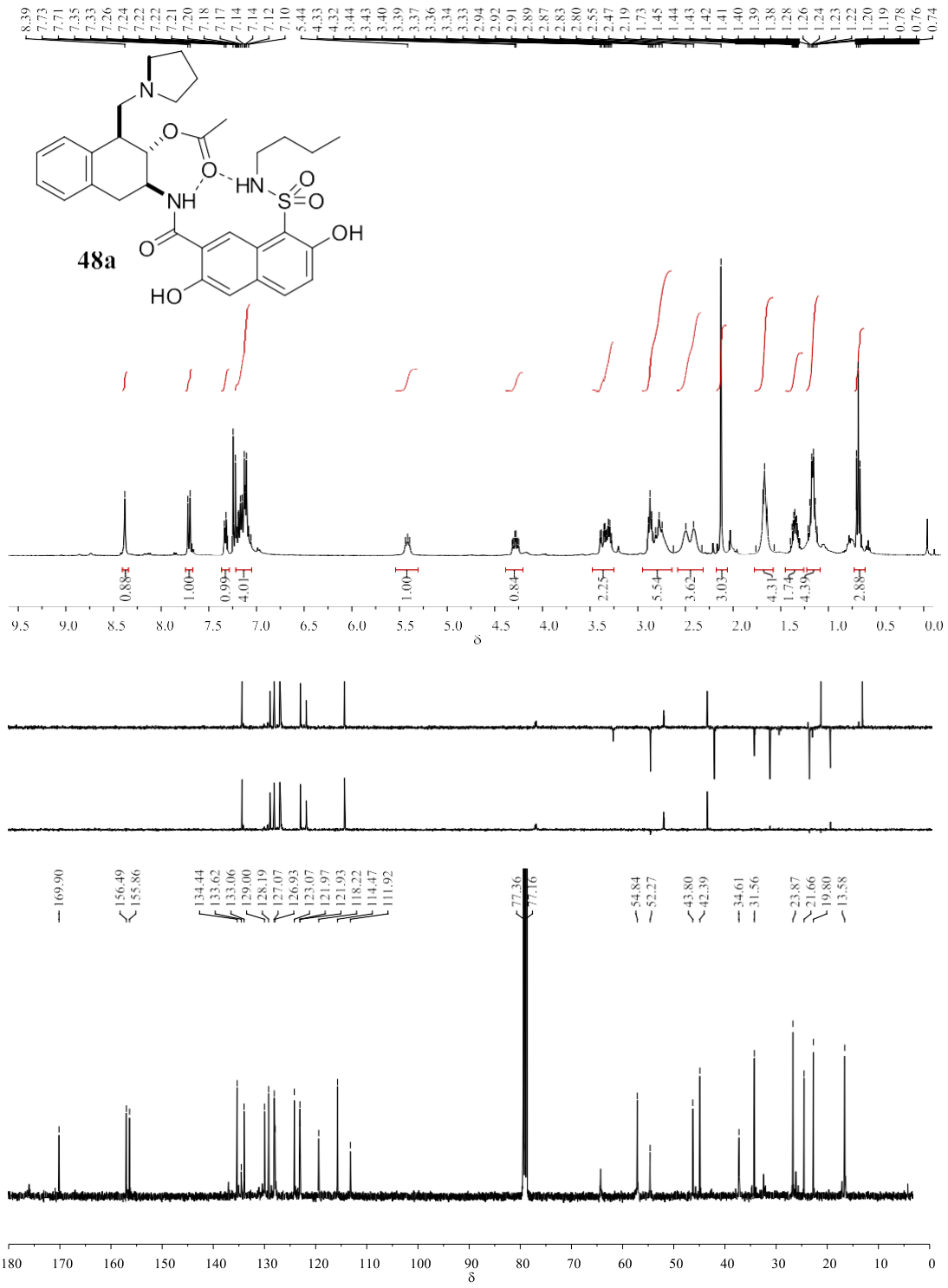

Figure S22. *^{1}H and ^{13}C NMR spectra of compound* **48a** *in $CDCl_3$.*

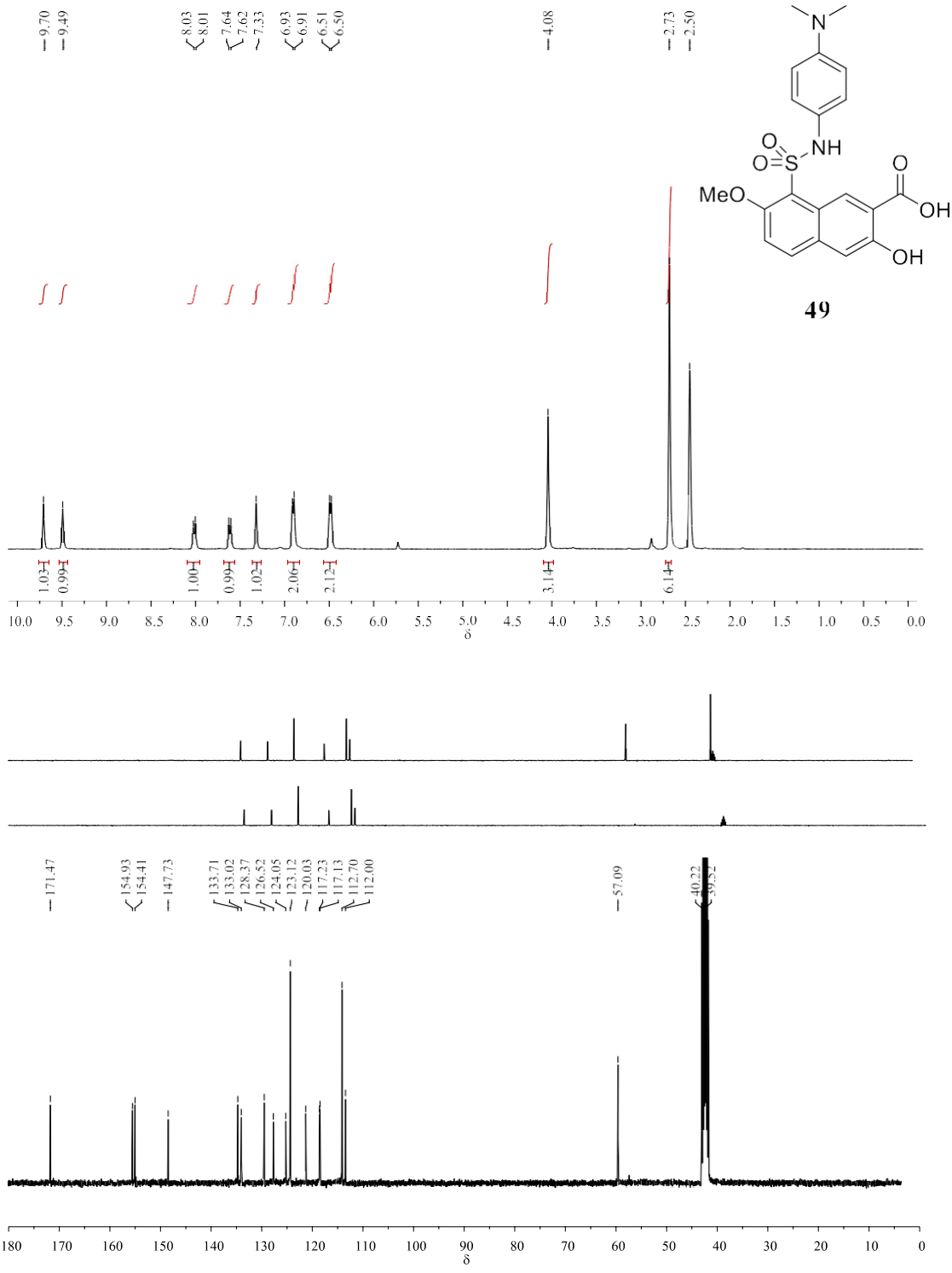

Figure S23. *^{1}H and ^{13}C NMR spectra of compound* **49** *in DMSO-d_6.*

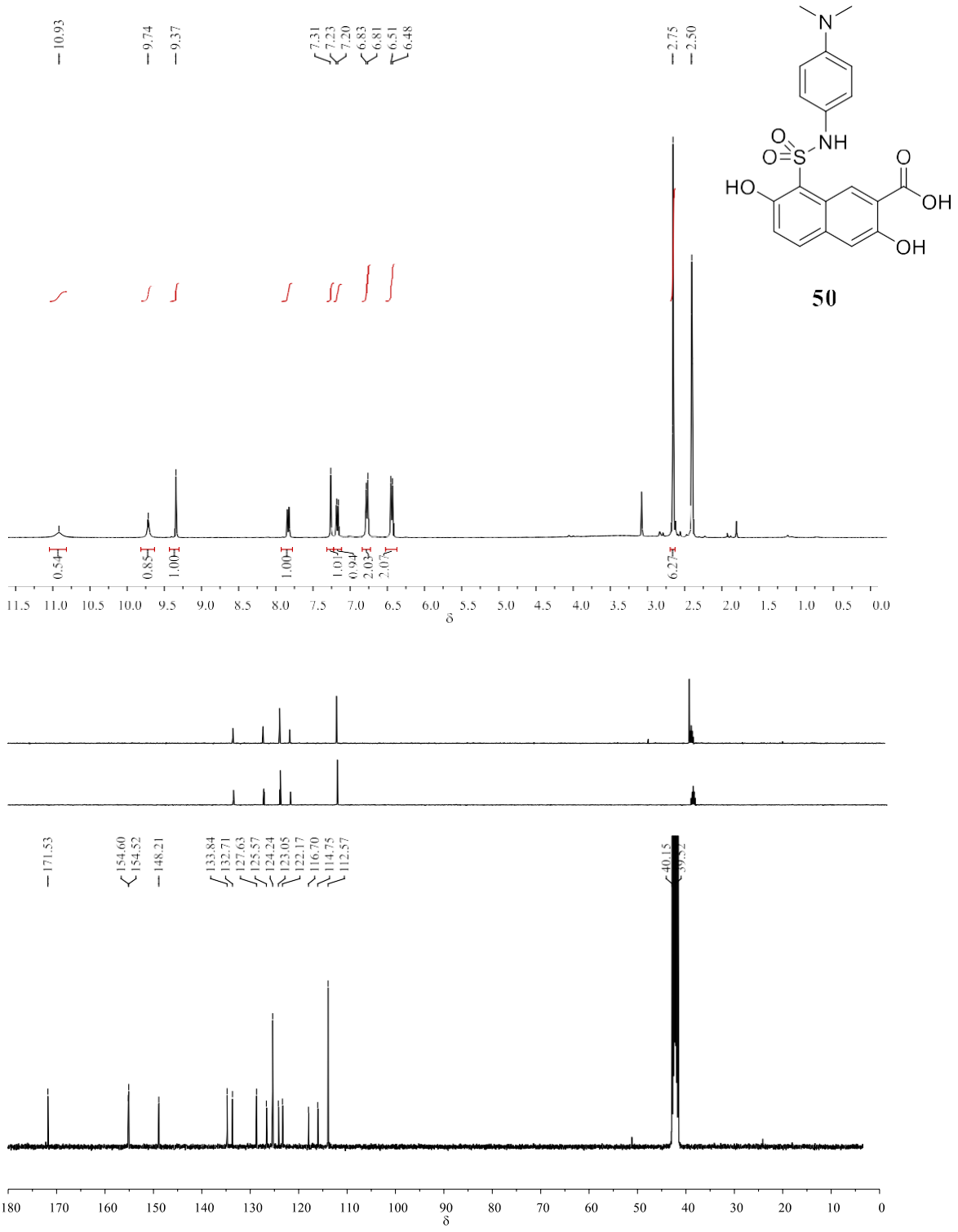

Figure S24. *^{1}H and ^{13}C NMR spectra of compound* **50** *in DMSO-d_6.*

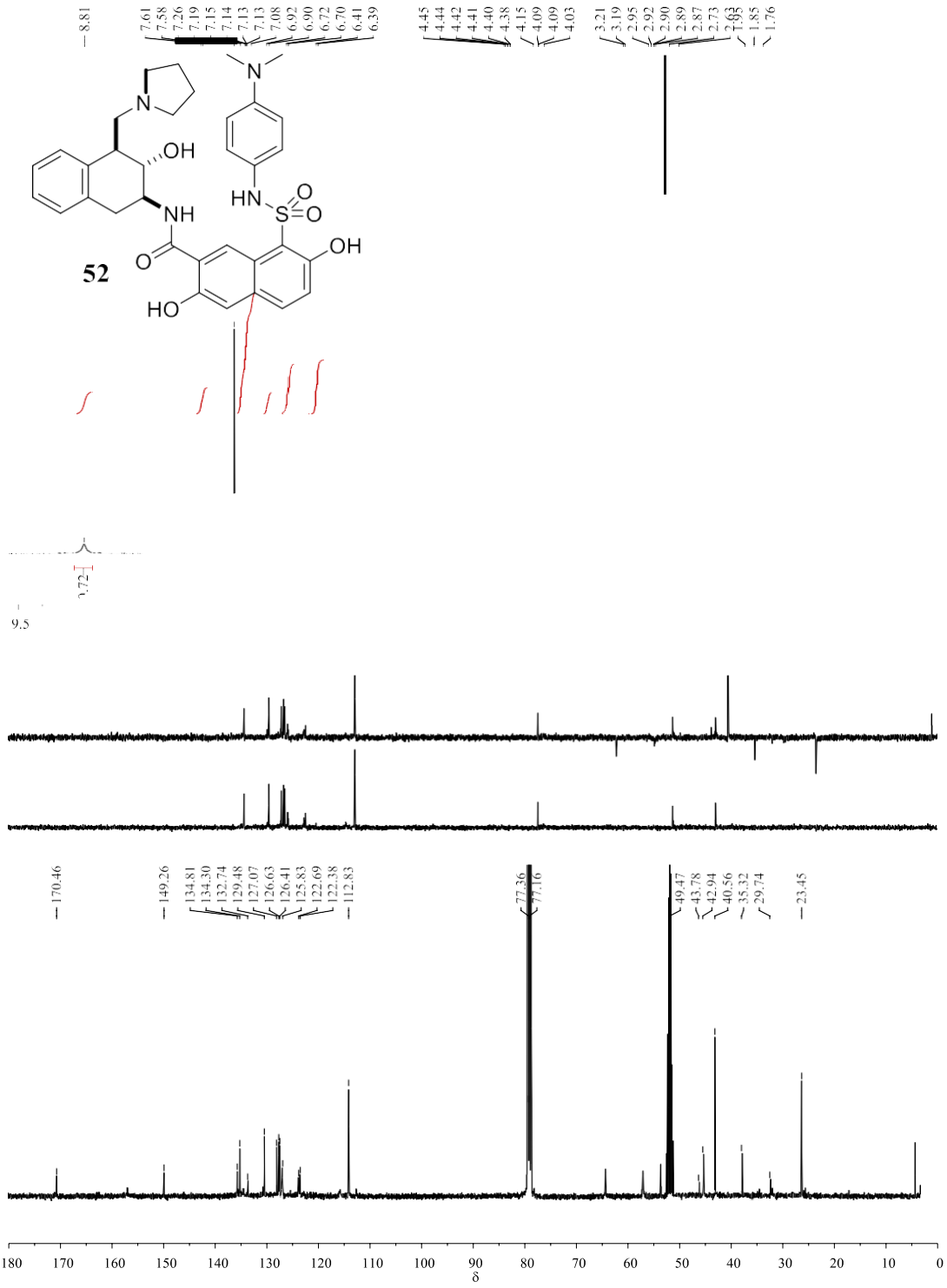

Figure S25. *^{1}H and ^{13}C NMR spectra of compound* **52** *in 5% CD_3OD in $CDCl_3$.*

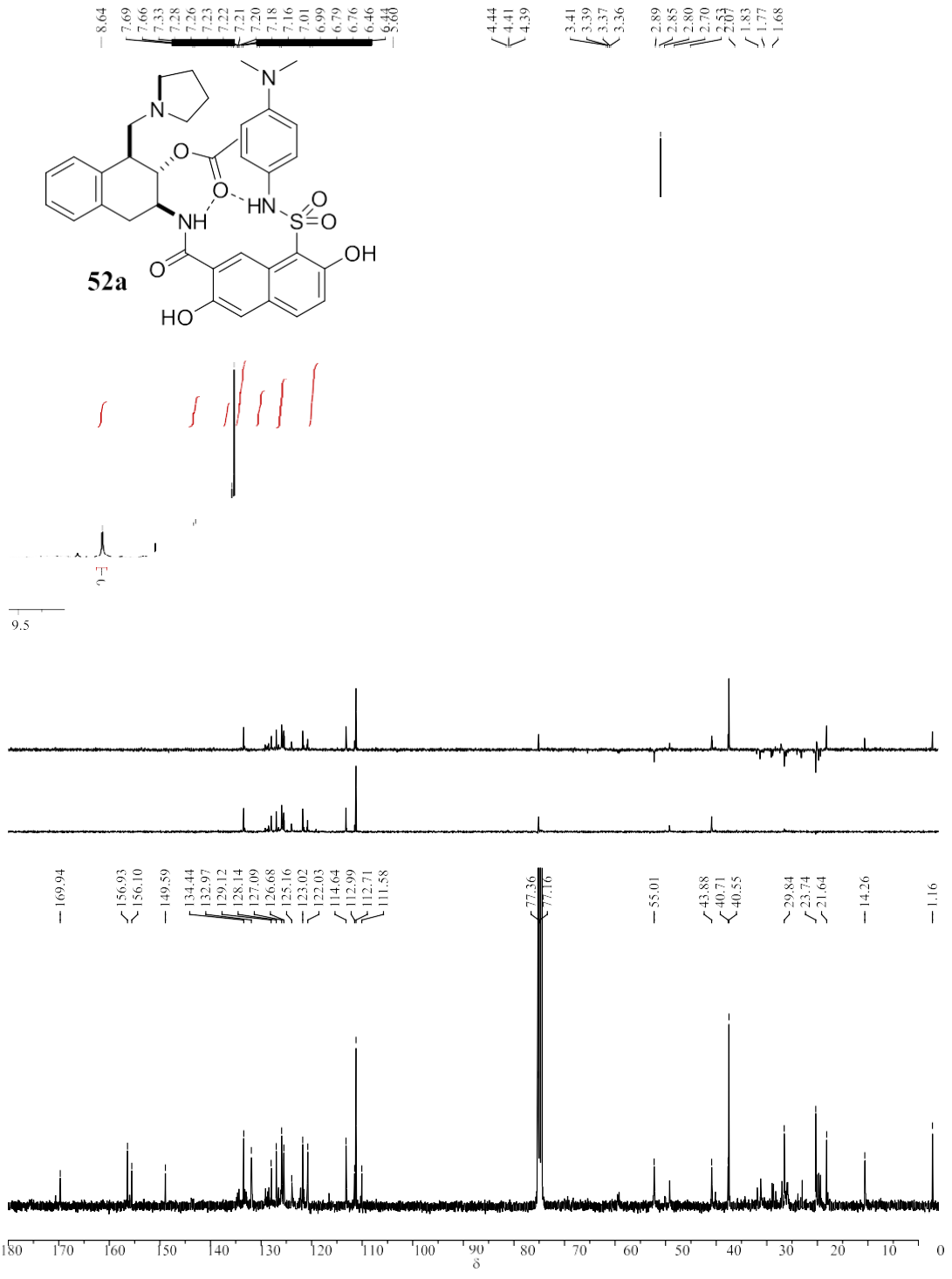
8.64
7.69
7.66
7.33
7.28
7.26
7.23
7.22
7.21
7.20
7.18
7.16
7.01
6.99
6.79
6.76
6.46
6.44
6.40
4.44
4.41
4.39
3.41
3.39
3.37
3.36
2.89
2.85
2.80
2.70
2.53
2.07
1.83
1.77
1.68
52a
9.5
169.94
156.93
156.10
149.59
134.44
132.97
129.12
128.14
127.09
126.68
125.16
123.02
122.03
114.64
112.99
112.71
111.58
77.36
77.16
55.01
43.88
40.71
40.55
29.84
23.74
21.64
14.26
1.16
δ

Figure S26. *^{1}H and ^{13}C NMR spectra of compound* **52a** *in $CDCl_3$.*

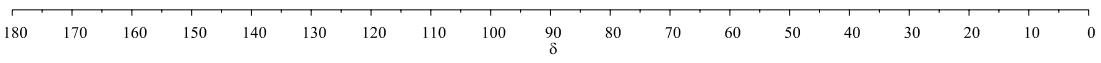

Figure S27. *^{1}H and ^{13}C NMR spectra of compound* **53** *in DMSO-d_6.*

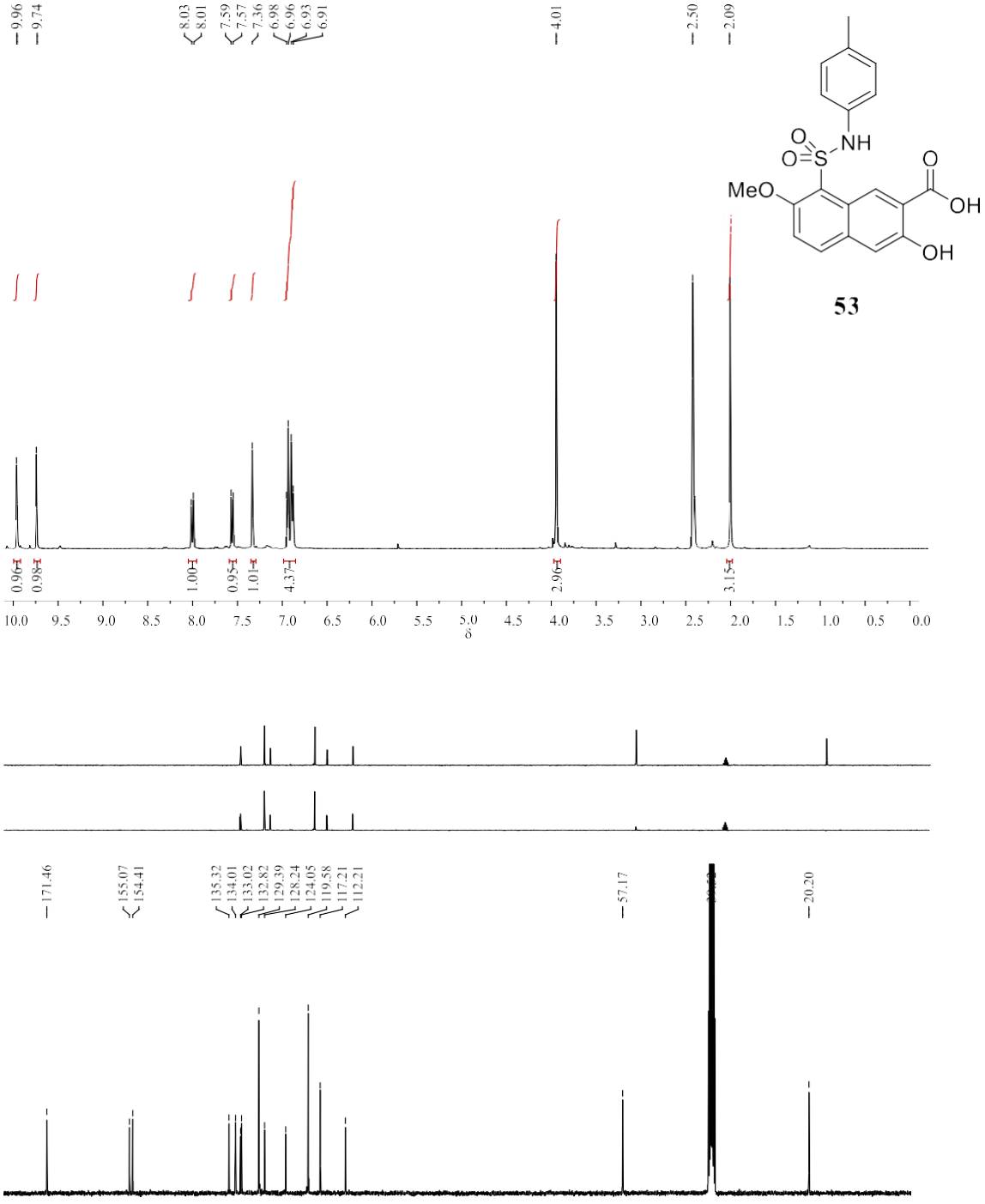
9.96
9.74
8.03
8.01
7.59
7.57
7.36
6.98
6.96
6.93
6.91
4.01
2.50
2.09
NH
O
S
MeO
OH
OH
53
0.96
0.98
1.00
0.95
1.01
4.37
2.96
3.15
δ
171.46
155.07
154.41
135.32
134.01
133.02
132.82
129.39
128.24
124.05
119.58
117.21
112.21
57.17
20.20

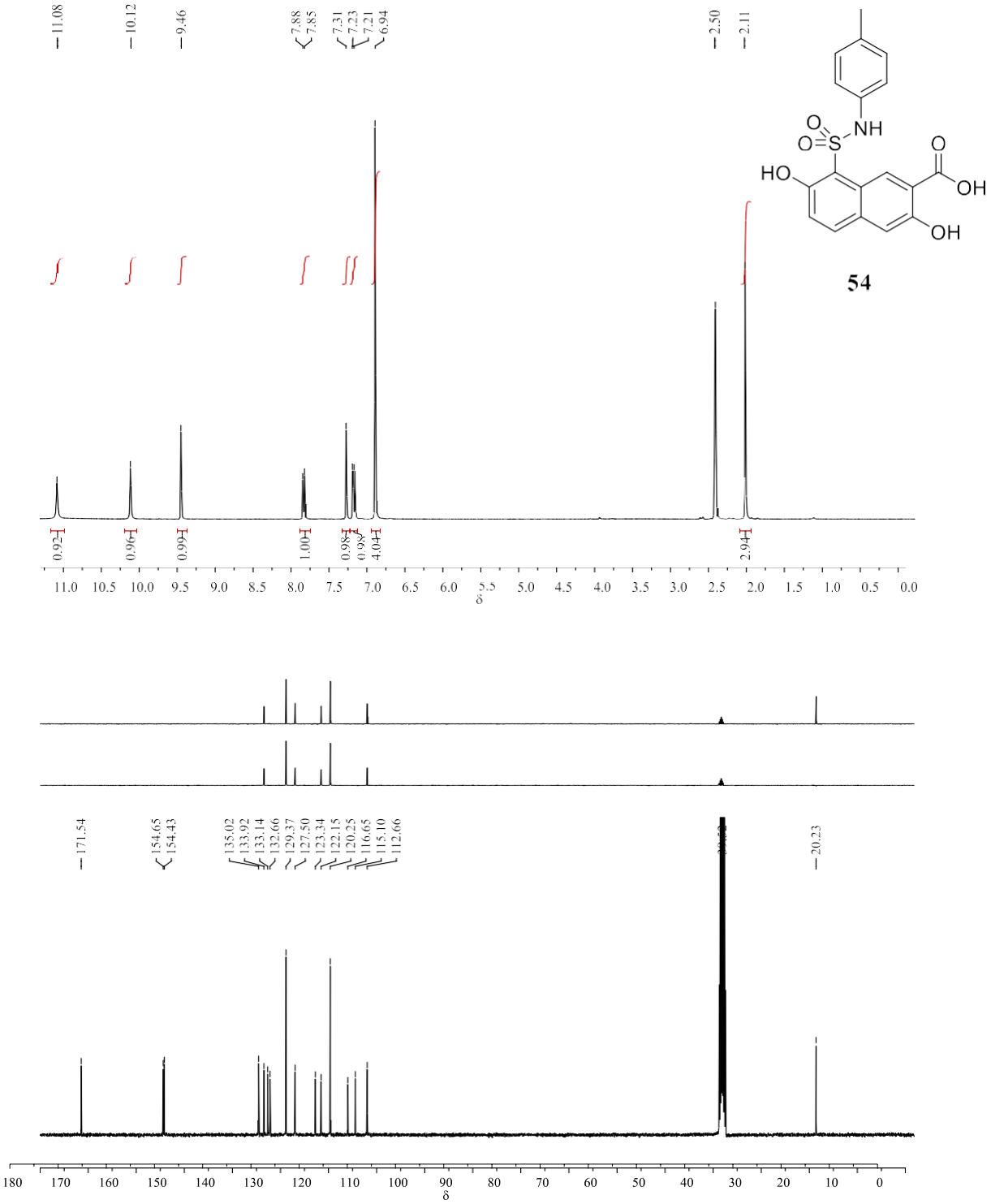

Figure S29. *^{1}H and ^{13}C NMR spectra of compound* **56** *in $CDCl_3$.*

Figure S28. *^{1}H and ^{13}C NMR spectra of compound* **54** *in DMSO-d_6.*

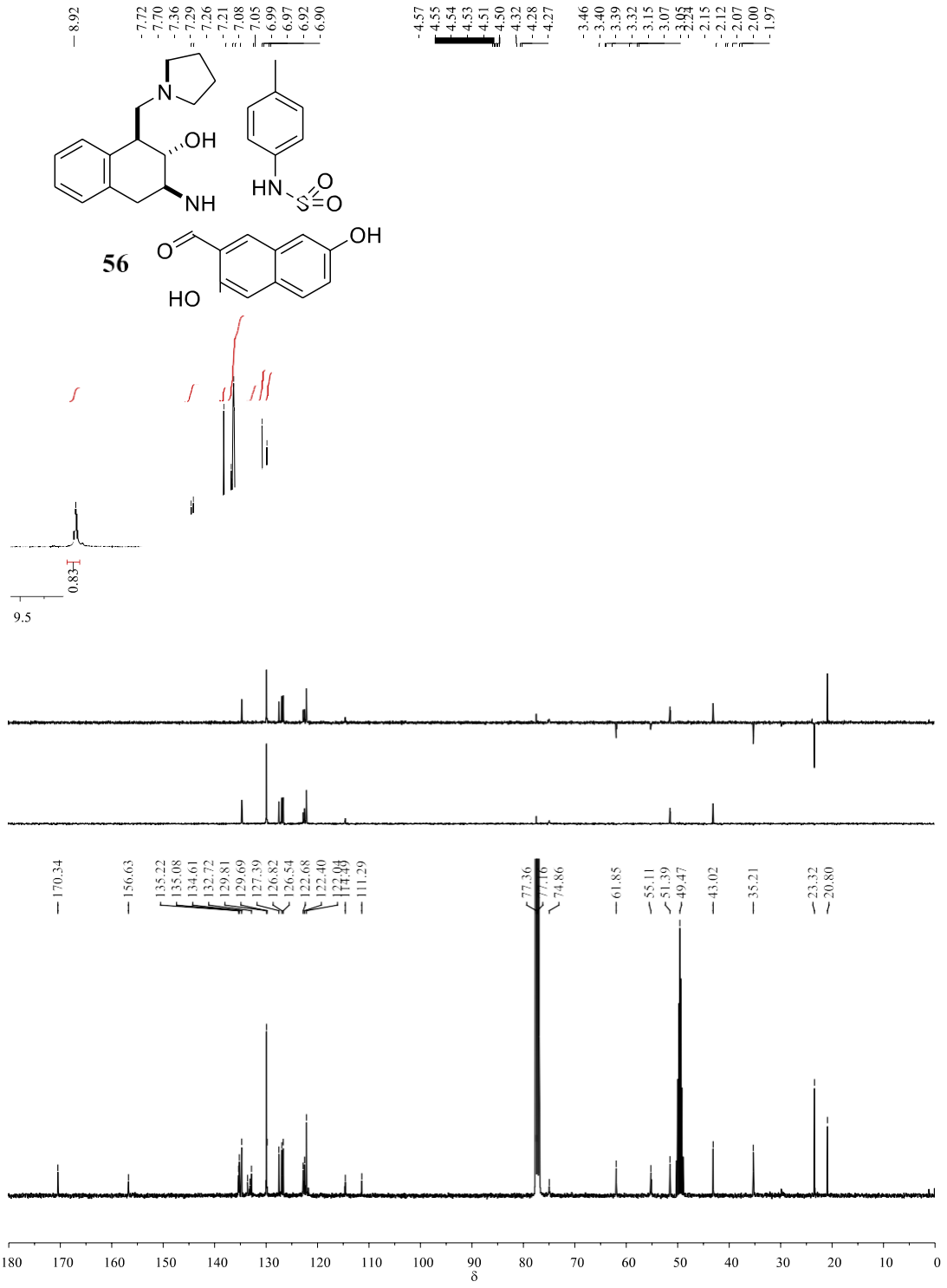

Figure S29. *^{1}H and ^{13}C NMR spectra of compound* **56** *in $CDCl_3$.*

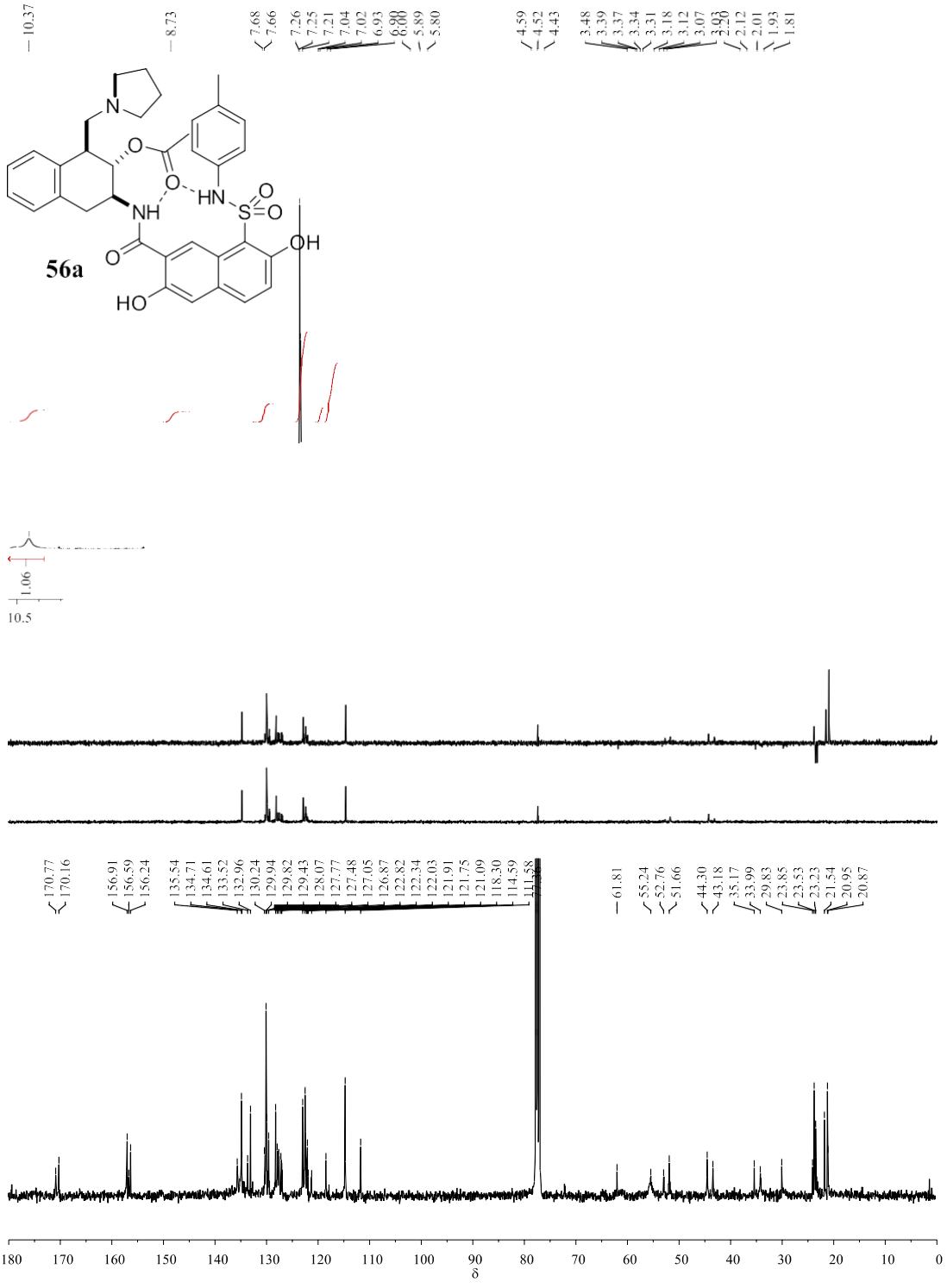

Figure S30. *^{1}H and ^{13}C NMR spectra of compound* **56a** *in $CDCl_3$.*

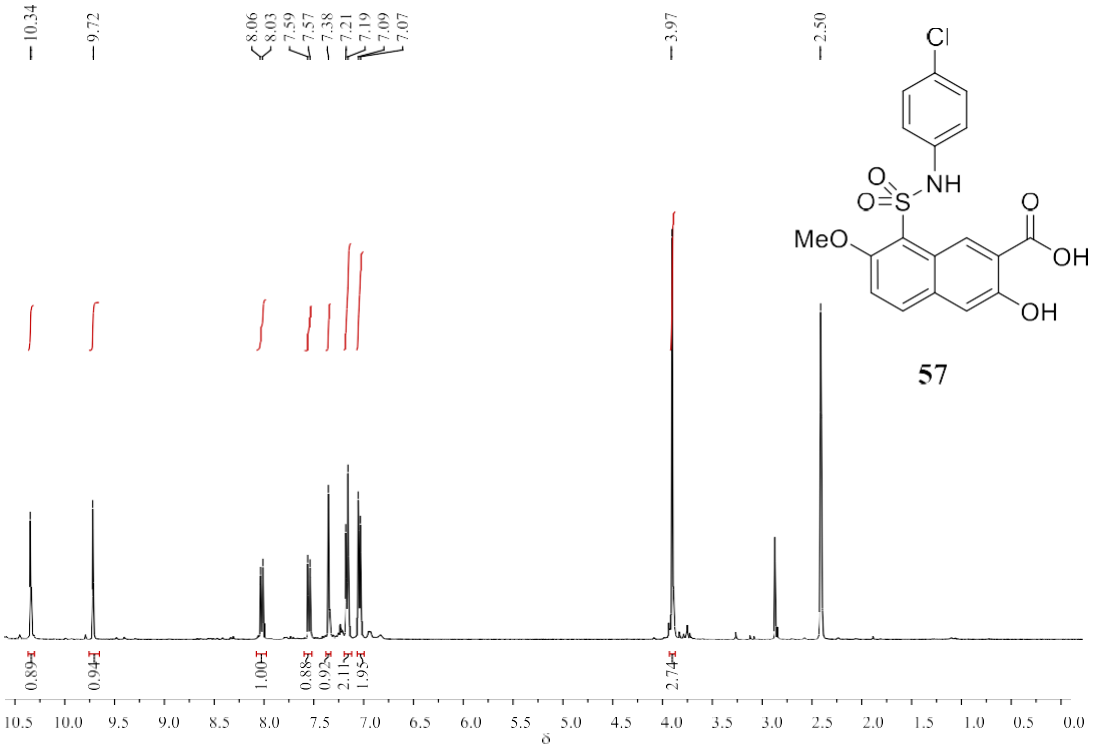
10.34
9.72
8.06
8.03
7.59
7.57
7.38
7.21
7.19
7.09
7.07
3.97
2.50
0.89
0.94
1.00
0.88
0.92
2.11
1.95
2.74
δ

Cl
NH
O
S
MeO
OH
OH

57

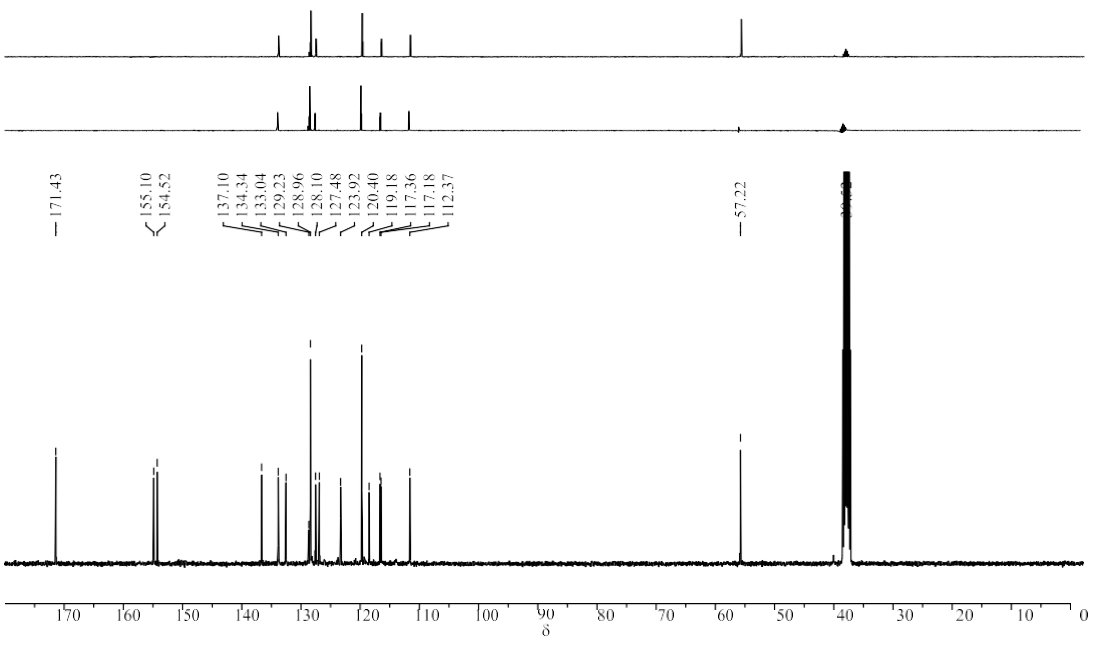
171.43
155.10
154.52
137.10
134.34
133.04
129.23
128.96
128.10
127.48
123.92
120.40
119.18
117.36
117.18
112.37
57.22
δ

Figure S31. *^{1}H and ^{13}C NMR spectra of compound* **57** *in DMSO-d_6.*

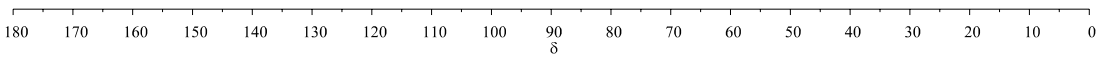

Figure S30. *^{1}H and ^{13}C NMR spectra of compound* **56a** *in $CDCl_3$.*

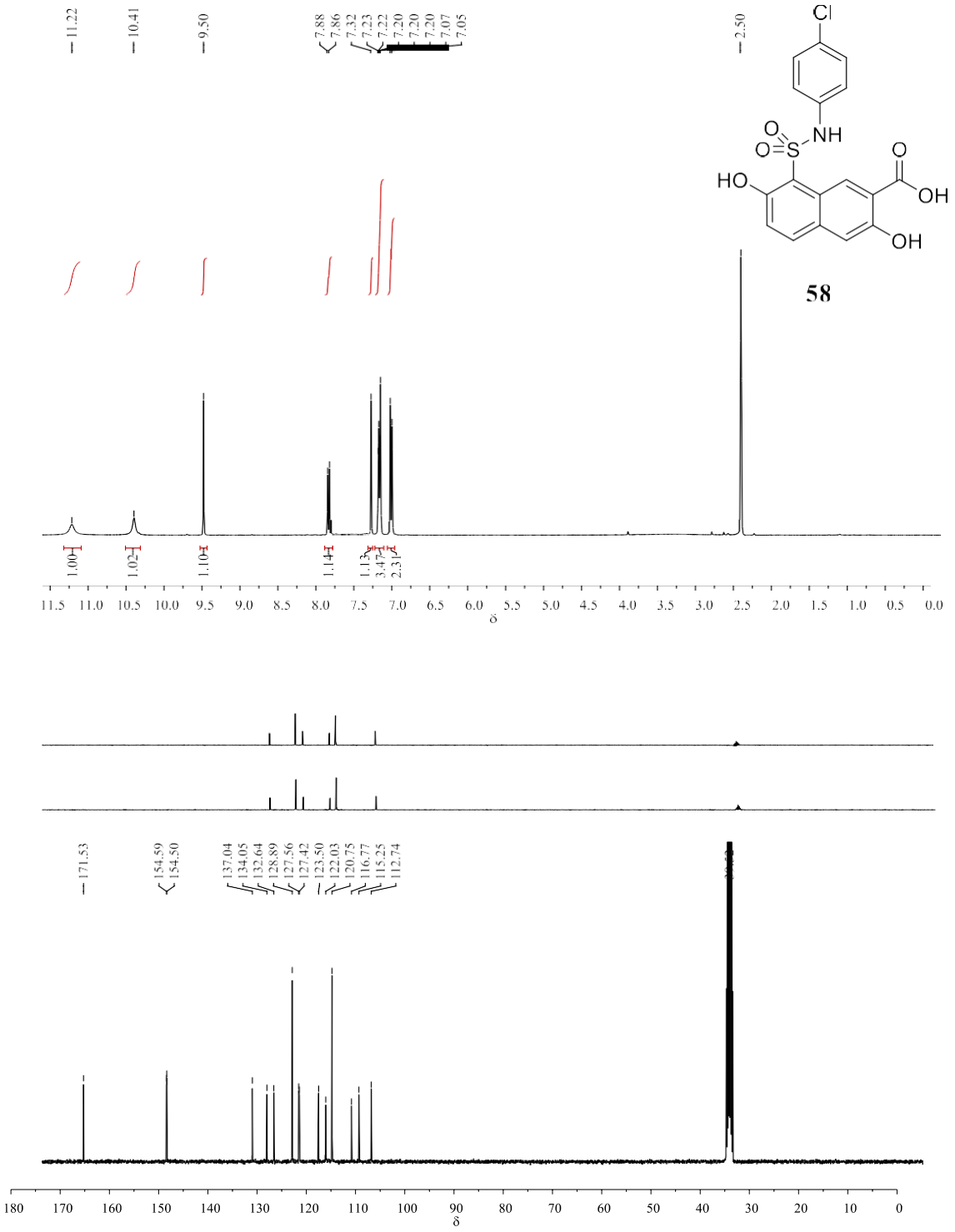

Figure S33. *^{1}H and ^{13}C NMR spectra of compound* **60** *in $CDCl_3$.*

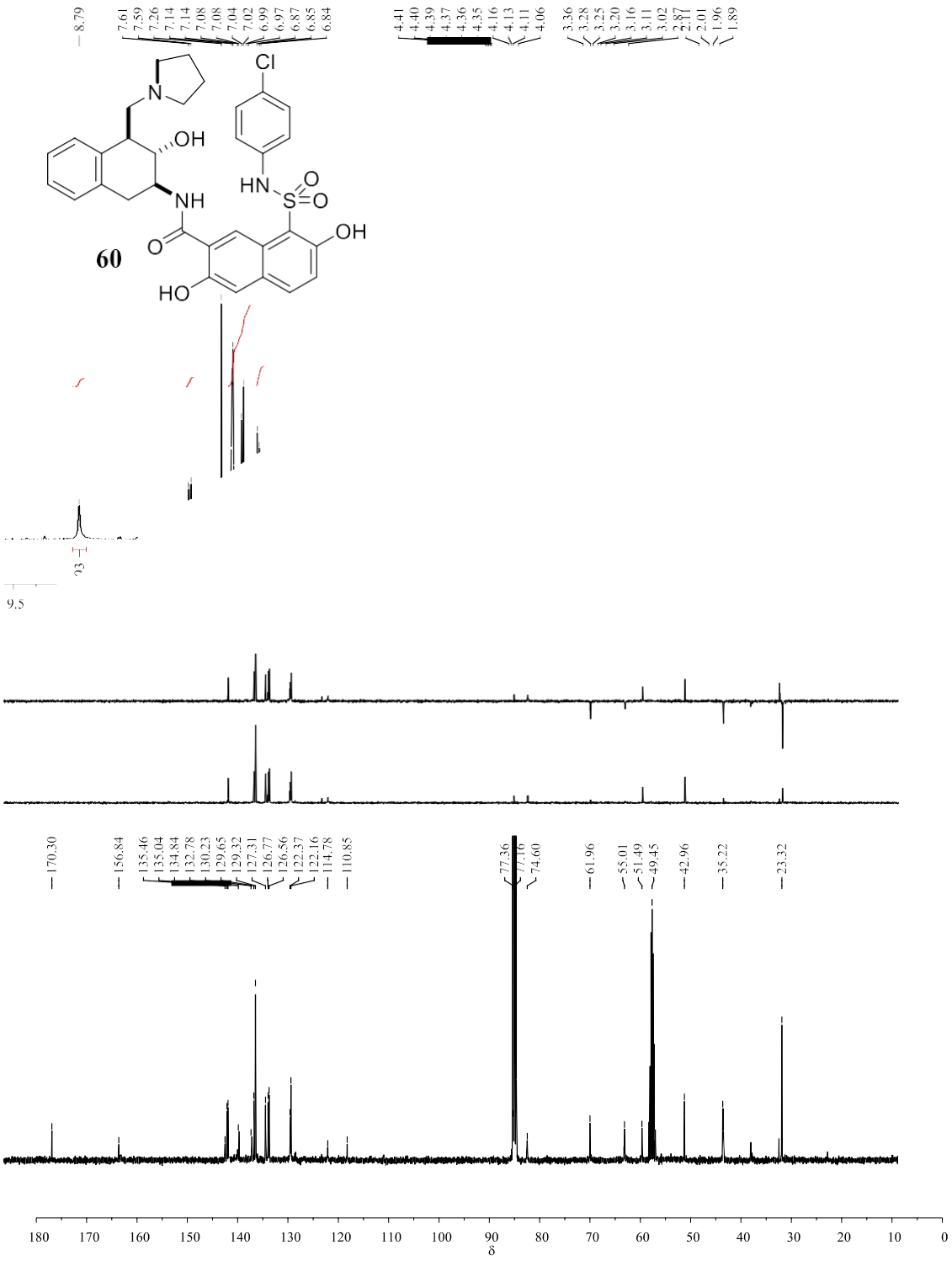

Figure S32. *^{1}H and ^{13}C NMR spectra of compound* **58** *in DMSO-d_6.*

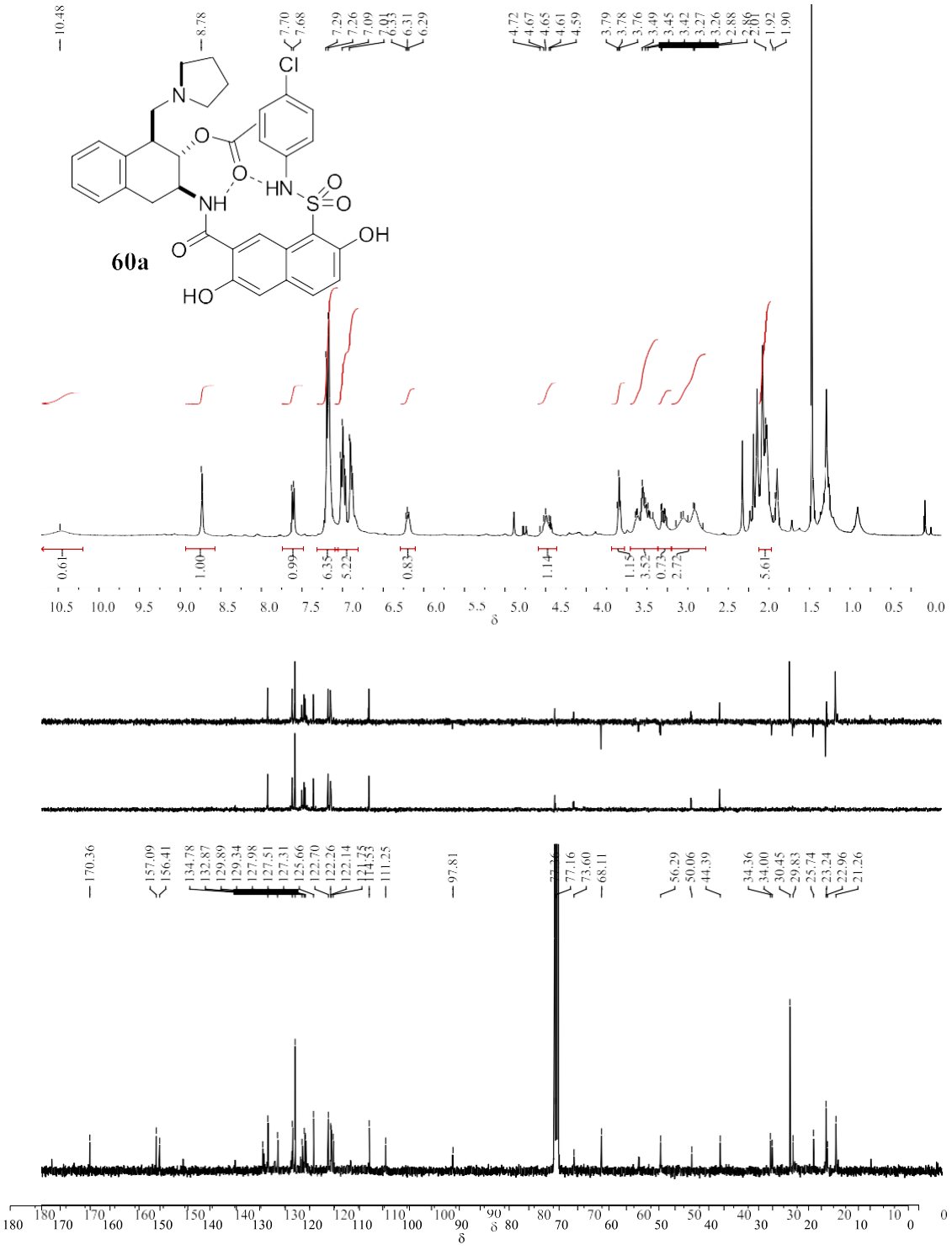

Figure S35. *^{1}H and ^{13}C NMR spectra of compound* **61** *in $CDCl_3$.*

Figure S34. *^{1}H and ^{13}C NMR spectra of compound* **60a** *in $CDCl_3$.*

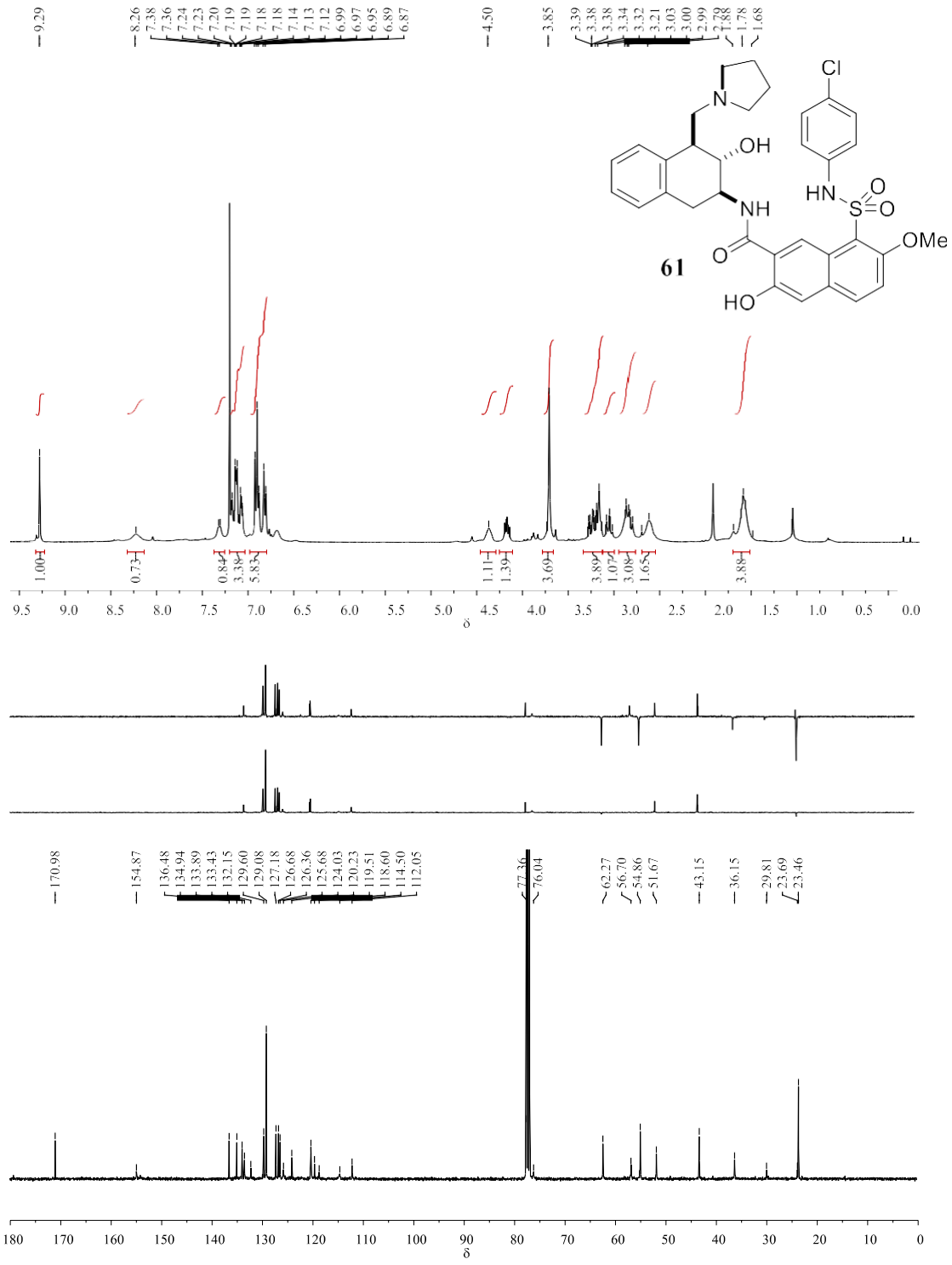

Figure S35. *^{1}H and ^{13}C NMR spectra of compound* **61** *in $CDCl_3$.*

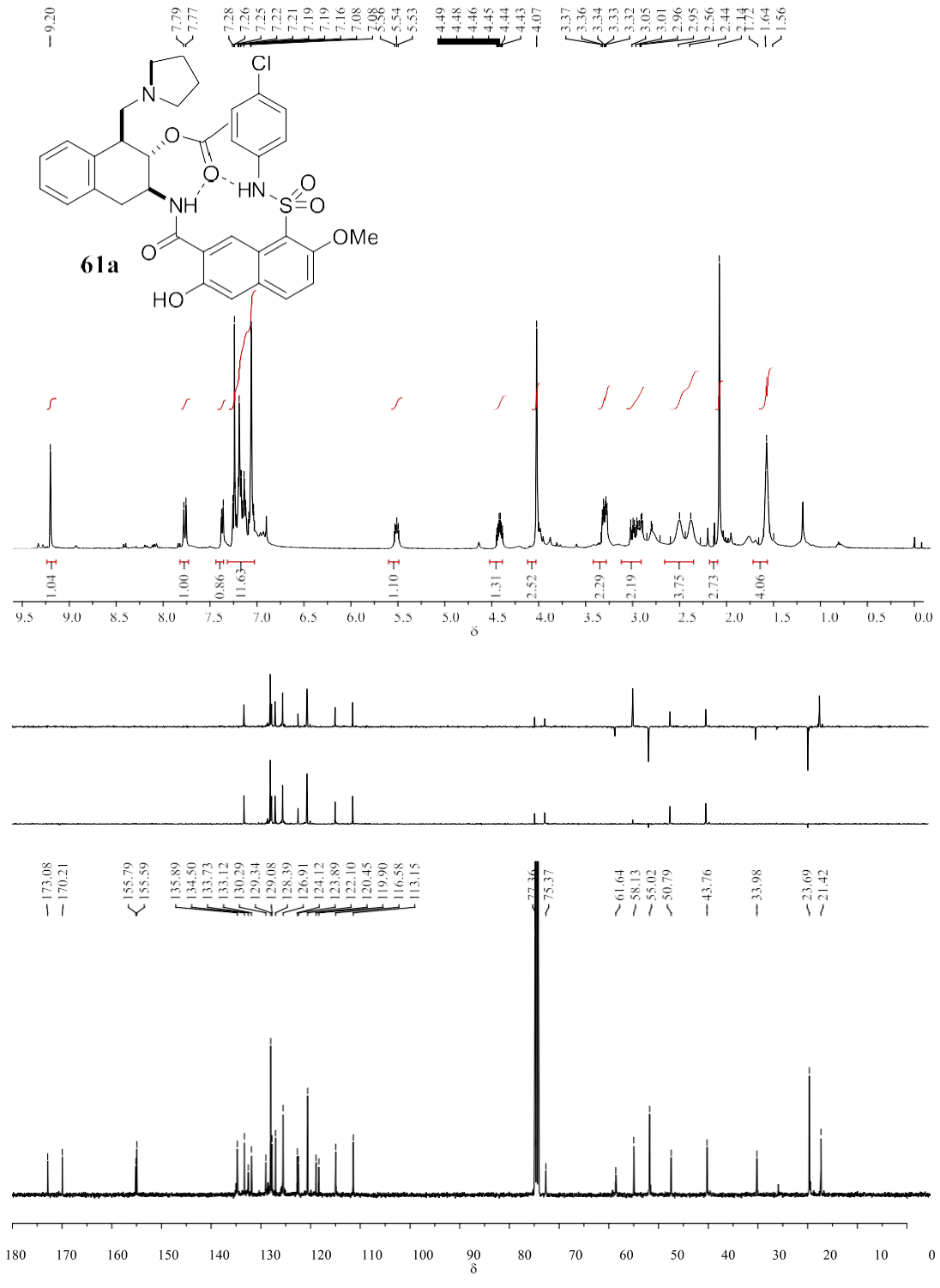
61a
Cl
N
O
O
HN
S
O
O
NH
OMe
O
HO
9.20
7.79
7.77
7.28
7.26
7.25
7.22
7.21
7.19
7.19
7.16
7.08
5.56
5.54
5.53
4.49
4.48
4.46
4.45
4.44
4.43
4.07
3.37
3.36
3.34
3.33
3.32
3.05
3.01
2.96
2.95
2.56
2.44
2.14
1.64
1.56
1.04
1.00
0.86
11.63
1.10
1.31
2.52
2.29
2.19
3.75
2.73
4.06
δ
173.08
170.21
155.79
155.59
135.89
134.50
133.73
133.12
130.29
129.34
129.08
128.39
126.91
124.12
123.89
122.10
120.45
119.90
116.58
113.15
77.36
75.37
61.64
58.13
55.02
50.79
43.76
33.98
23.69
21.42
δ

Figure S36. *^{1}H and ^{13}C NMR spectra of compound* **61a** *in $CDCl_3$.*

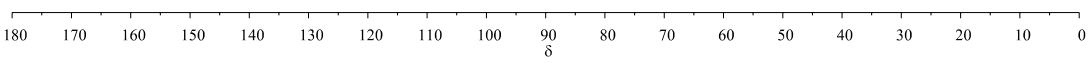

Figure S35. *^{1}H and ^{13}C NMR spectra of compound* **61** *in $CDCl_3$.*

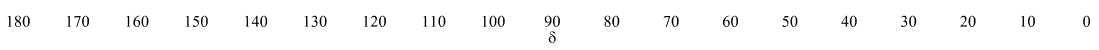
180 170 160 150 140 130 120 110 100 90 80 70 60 50 40 30 20 10 0
δ

Annex IV – Kinetic Studies

Kinetic studies of already published compounds can be found freely available at:

Chapter 2

https://pubs.acs.org/doi/suppl/10.1021/acscatal.0c02121/suppl_file/cs0c02121_si_001.pdf

https://chemistry-europe.onlinelibrary.wiley.com/action/downloadSupplement?doi=10.1002%2Fchem.202102137&file=chem202102137-sup-0001-misc_information.pdf

1. Methanolysis Studies

1. Kinetic Studies

Methanolysis results

Half-lives for the methanolysis reaction of 3rd generation catalyst in CD_3OD 5% $CDCl_3$.

Entry	Catalyst	$t_{1/2}$**33a**	$t_{1/2}$**C_a**	$\frac{t_{1/2}\mathbf{33a}}{t_{1/2}\mathbf{C\_a}}$
1	**33a**	3.47[a]	3.47[a]	1
2	**35a**	33.32	21.59	1.54
3	**37a**	37.47	18.39	2.04
4	**39a**	38.09	10.70	3.56
5	**44a**	41.26	8.69	4.75
6	**48a**	30.81	7.87	3.91
7	**52a**	37.67	5.39	6.99
8	**56a**	28.53	3.58	7.97
9	**61a**	32.24	14.23	2.27
10	**60a**	30.40	2.44	12.46

[a]Half-life measured in neat CD_3OD.

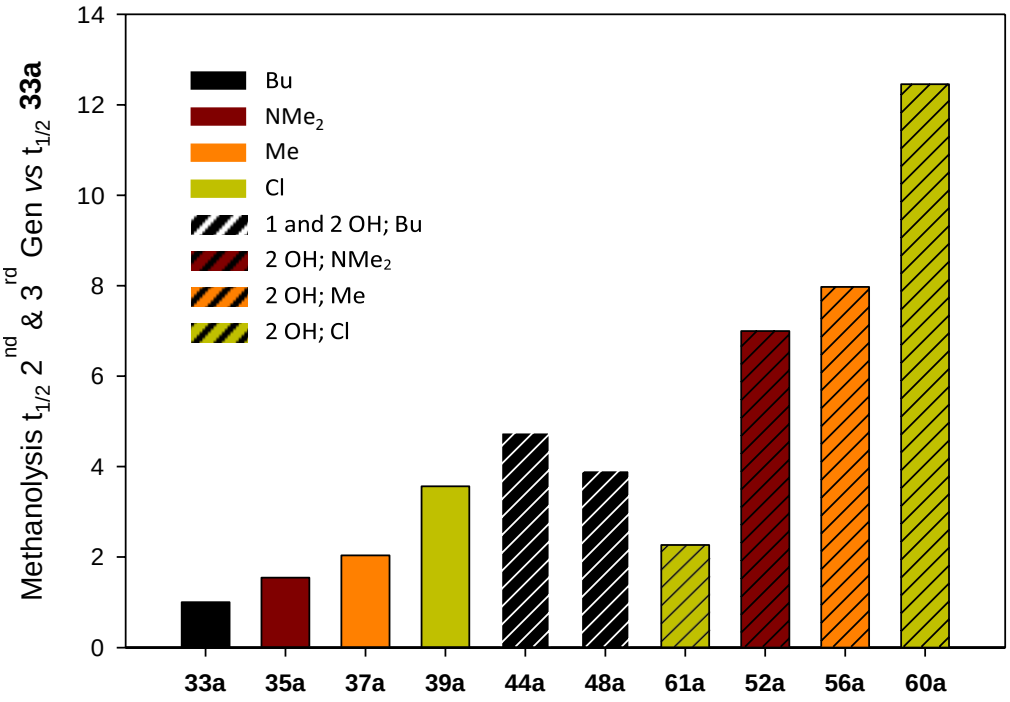

$t_{1/2}$ C_a vs $t_{1/2}$ **33a**.

Catalyst **33**

Methanolysis study was performed in neat CD_3OD. $1_{\mathbf{33}}$ and $1_{\mathbf{33a}}$ signals from the ^1H NMR spectra of 0 were integrated to calculate the molar fraction (X). All data are collected in 0 and plotting $Ln[X_{\mathbf{33a}}]$ *versus* time gave the equation shown in 0, from which the half-life was calculated:

Variation of molar fraction with time for methanolysis of **33a**.

Entry	Time[a]/min	X_{33a}	X_{33}	$Ln(X_{33a})$
1	1.1670	0.5747	0.4253	-0.5539
2	4.0000	0.3086	0.6914	-1.1756
3	6.0000	0.3086	0.6914	-1.1756
4	7.0000	0.2137	0.7863	-1.5433
5	8.0000	0.1167	0.8833	-2.1483

[a]Time relative to the first NMR measured.

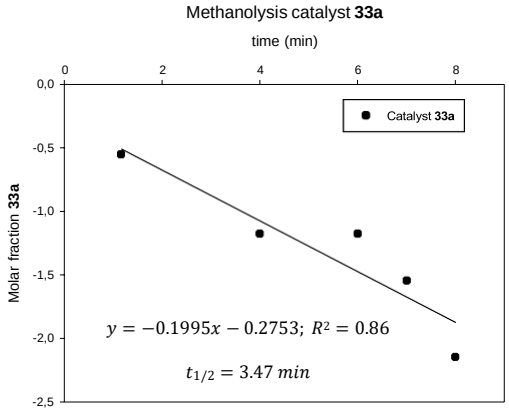

Plotting of $Ln[X_{33a}]$ vs time.

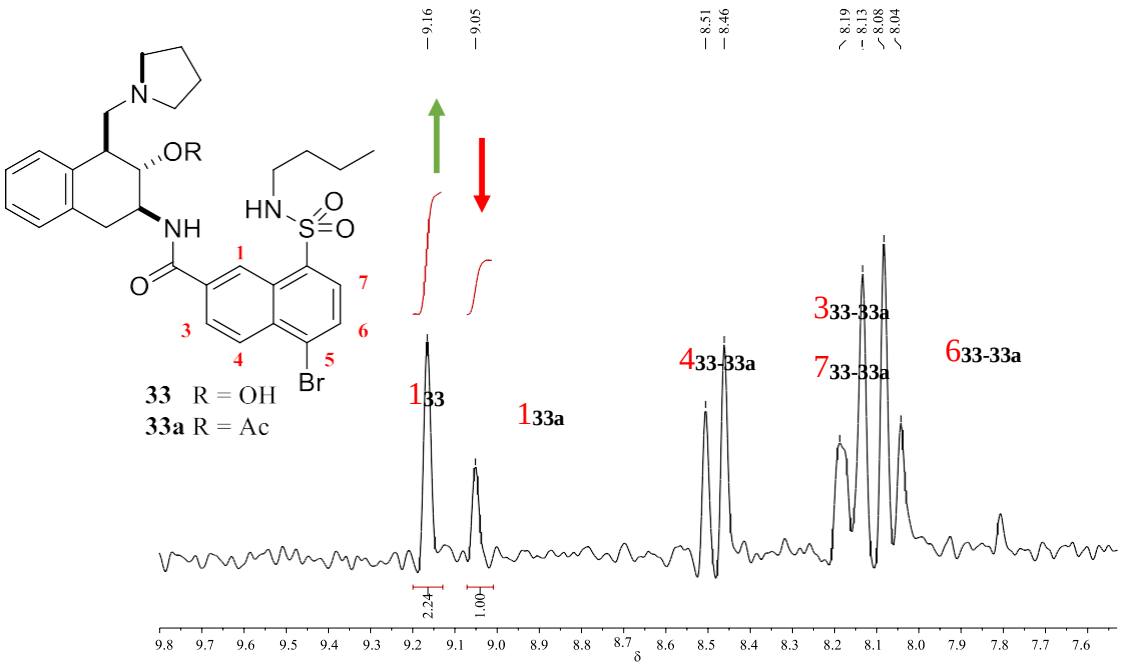

*^1H NMR spectra (7.6-9.8 ppm) for methanolysis of **33a** at 4 min in neat CD_3OD.*

Catalyst **35**

1_{35}, 1_{35a}, 1_{33} and 1_{33a} signals from the ^{1}H NMR spectra of 0 were integrated to calculate the molar fraction (X). All data are collected in 0 and 0; plotting Ln[$X_{33a-35a}$] *versus* time gave the equation shown in 0 from which the half-life was calculated:

Variation of molar fraction with time for methanolysis of **33a**.

Entry	Time[a]/min	X_{33a}	X_{33}	Ln(X_{33a})	Entry	Time[a]/min	X_{33a}	X_{33}	Ln(X_{33a})
1	0	1.0000	0.0000	0.0000	36	35	0.4642	0.5358	-0.7675
2	1	0.9494	0.0506	-0.0520	37	36	0.4294	0.5706	-0.8454
3	2	0.9763	0.0237	-0.0240	38	37	0.4267	0.5733	-0.8516
4	3	0.9238	0.0762	-0.0792	39	38	0.4367	0.5633	-0.8286
5	4	0.8208	0.1792	-0.1974	40	39	0.4198	0.5802	-0.8680
6	5	0.8479	0.1521	-0.1650	41	40	0.4081	0.5919	-0.8961
7	6	0.9116	0.0884	-0.0926	42	41	0.4114	0.5886	-0.8882
8	7	0.8730	0.1270	-0.1358	43	42	0.3585	0.6415	-1.0259
9	8	0.8549	0.1451	-0.1568	44	43	0.4357	0.5643	-0.8307
10	9	0.7805	0.2195	-0.2479	45	44	0.3810	0.6190	-0.9650
11	10	0.7575	0.2425	-0.2777	46	45	0.3761	0.6239	-0.9778
12	11	0.7775	0.2225	-0.2517	47	46	0.3458	0.6542	-1.0618
13	12	0.7986	0.2014	-0.2249	48	47	0.3236	0.6764	-1.1283
14	13	0.7281	0.2719	-0.3173	49	48	0.3578	0.6422	-1.0277
15	14	0.6542	0.3458	-0.4244	50	49	0.3267	0.6733	-1.1188
16	15	0.7333	0.2667	-0.3102	51	50	0.3114	0.6886	-1.1668
17	16	0.6360	0.3640	-0.4525	52	51	0.3063	0.6937	-1.1832
18	17	0.8080	0.1920	-0.2132	53	52	0.3186	0.6814	-1.1439
19	18	0.7130	0.2870	-0.3383	54	53	0.2847	0.7153	-1.2563
20	19	0.6892	0.3108	-0.3723	55	54	0.3045	0.6955	-1.1892
21	20	0.5871	0.4129	-0.5325	56	55	0.2875	0.7125	-1.2466
22	21	0.5805	0.4195	-0.5439	57	56	0.3090	0.6910	-1.1743
23	22	0.6115	0.3885	-0.4919	58	57	0.2953	0.7047	-1.2197
24	23	0.5838	0.4162	-0.5382	59	58	0.3036	0.6964	-1.1921
25	24	0.6061	0.3939	-0.5007	60	59	0.3005	0.6995	-1.2024
26	25	0.5922	0.4078	-0.5240	61	60	0.3018	0.6982	-1.1980
27	26	0.5409	0.4591	-0.6145	62	61	0.2526	0.7474	-1.3759
28	27	0.5600	0.4400	-0.5798	63	62	0.2903	0.7097	-1.2367
29	28	0.4895	0.5105	-0.7143	64	63	0.2619	0.7381	-1.3397
30	29	0.5631	0.4369	-0.5744	65	64	0.2859	0.7141	-1.2521
31	30	0.5002	0.4998	-0.6927	66	65	0.2551	0.7449	-1.3660
32	31	0.5257	0.4743	-0.6430	67	66	0.2577	0.7423	-1.3561
33	32	0.4760	0.5240	-0.7424	68	67	0.2397	0.7603	-1.4284
34	33	0.4827	0.5173	-0.7284	69	68	0.2650	0.7350	-1.3282
35	34	0.4600	0.5400	-0.7764					

[a]Time relative to the first NMR measured.

Variation of molar fraction with time for methanolysis of **35a**.

Entry	Time[a]/min	X_{35a}	X_{35}	$Ln(X_{35a})$
1	0	1.0000	0.0000	0.0000
2	1	0.9629	0.0371	-0.0378
3	2	0.9618	0.0382	-0.0389
4	3	0.9189	0.0811	-0.0846
5	4	0.8485	0.1515	-0.1643
6	5	0.8516	0.1484	-0.1607
7	6	0.8667	0.1333	-0.1431
8	7	0.8385	0.1615	-0.1761
9	8	0.7255	0.2745	-0.3209
10	9	0.7199	0.2801	-0.3287
11	10	0.6843	0.3157	-0.3794
12	11	0.6681	0.3319	-0.4032
13	12	0.6666	0.3334	-0.4055
14	13	0.6193	0.3807	-0.4791
15	14	0.5642	0.4358	-0.5723
16	15	0.6308	0.3692	-0.4608
17	16	0.5337	0.4663	-0.6280
18	17	0.6312	0.3688	-0.4601
19	18	0.5930	0.4070	-0.5226
20	19	0.5470	0.4530	-0.6034
21	20	0.4912	0.5088	-0.7109
22	21	0.5194	0.4806	-0.6551
23	22	0.4755	0.5245	-0.7435
24	23	0.5054	0.4946	-0.6825
25	24	0.4451	0.5549	-0.8094
26	25	0.4696	0.5304	-0.7559
27	26	0.3969	0.6031	-0.9241
28	27	0.4236	0.5764	-0.8590
29	28	0.3848	0.6152	-0.9551
30	29	0.4421	0.5579	-0.8163
31	30	0.3567	0.6433	-1.0309
32	31	0.3788	0.6212	-0.9708
33	32	0.3382	0.6618	-1.0840
34	33	0.3427	0.6573	-1.0710
35	34	0.3299	0.6701	-1.1089
36	35	0.3638	0.6362	-1.0111
37	36	0.2890	0.7110	-1.2414
38	37	0.3016	0.6984	-1.1985
39	38	0.2851	0.7149	-1.2549
40	39	0.2891	0.7109	-1.2410
41	40	0.2701	0.7299	-1.3091

[a]Time relative to the first NMR measured.

Plotting of $Ln[X_{33a}]$ vs time (left) and $Ln[X_{35a}]$ vs time (right).

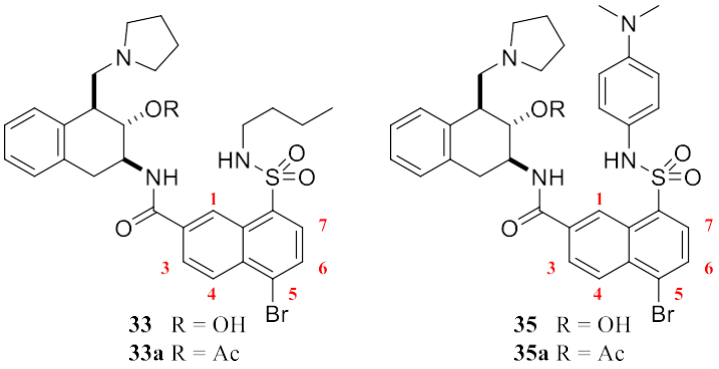

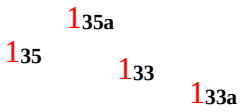

*^{1}H NMR spectra (7.4-9.8 ppm) for methanolysis of **33a** and **35a** at 21 min relative to the first NMR measured in CD_3OD 5% in $CDCl_3$.*

Catalyst **37**

1_{37}, 1_{37a}, 1_{33} and 1_{33a} signals from the ^{1}H NMR spectra of 0 were integrated to calculate the molar fraction (X). All data are collected in 0 and 0; plotting Ln[$X_{33a-37a}$] *versus* time gave the equation shown in 0 from which the half-life was calculated:

Variation of molar fraction with time for methanolysis of **33a**.

Entry	Time[a]/min	X_{33a}	X_{33}	Ln(X_{33a})
1	1	0.9804	0.0196	-0.0198
2	2	0.9524	0.0476	-0.0488
3	3	0.8929	0.1071	-0.1133
4	4	0.8929	0.1071	-0.1133
5	5	0.8850	0.1150	-0.1222
6	6	0.8929	0.1071	-0.1133
7	7	0.8547	0.1453	-0.1570
8	8	0.9259	0.0741	-0.0770
9	9	0.8130	0.1870	-0.2070
10	10	0.8403	0.1597	-0.1740
11	11	0.8000	0.2000	-0.2231
12	12	0.8403	0.1597	-0.1740
13	13	0.7813	0.2188	-0.2469
14	14	0.8333	0.1667	-0.1823
15	15	0.8475	0.1525	-0.1655
16	16	0.7752	0.2248	-0.2546
17	17	0.7463	0.2537	-0.2927
18	18	0.7353	0.2647	-0.3075
19	19	0.6711	0.3289	-0.3988
20	20	0.7042	0.2958	-0.3507
21	21	0.6452	0.3548	-0.4383
22	22	0.7519	0.2481	-0.2852
23	23	0.6944	0.3056	-0.3646
24	24	0.6494	0.3506	-0.4318
25	25	0.6623	0.3377	-0.4121
26	26	0.6250	0.3750	-0.4700
27	27	0.6579	0.3421	-0.4187
28	28	0.6410	0.3590	-0.4447
29	29	0.6667	0.3333	-0.4055
30	30	0.5682	0.4318	-0.5653
31	33	0.5025	0.4975	-0.6881
32	34	0.5155	0.4845	-0.6627
33	35	0.5208	0.4792	-0.6523
34	36	0.5682	0.4318	-0.5653
35	37	0.5376	0.4624	-0.6206
36	38	0.4831	0.5169	-0.7275
37	39	0.4425	0.5575	-0.8154
38	40	0.5291	0.4709	-0.6366
39	41	0.5650	0.4350	-0.5710
40	42	0.4762	0.5238	-0.7419
41	43	0.4831	0.5169	-0.7275
42	44	0.4167	0.5833	-0.8755
43	45	0.4310	0.5690	-0.8416
44	46	0.4274	0.5726	-0.8502
45	47	0.4115	0.5885	-0.8879
46	48	0.3650	0.6350	-1.0080
47	49	0.4098	0.5902	-0.8920
48	50	0.3817	0.6183	-0.9632
49	51	0.4098	0.5902	-0.8920
50	52	0.3636	0.6364	-1.0116

[a]Time relative to the first NMR measured.

Variation of molar fraction with time for methanolysis of **37a**.

Entry	Time[a]/min	X_{37a}	X_{37}	$Ln(X_{37a})$
1	0	1.0000	0.0000	0.0000
2	1	0.9080	0.0920	-0.0965
3	2	0.9101	0.0899	-0.0942
4	3	0.9250	0.0750	-0.0780
5	4	0.8172	0.1828	-0.2019
6	5	0.8163	0.1837	-0.2029
7	6	0.7547	0.2453	-0.2814
8	7	0.7241	0.2759	-0.3228
9	8	0.7011	0.2989	-0.3550
10	9	0.6250	0.3750	-0.4700
11	10	0.6395	0.3605	-0.4470
12	11	0.6339	0.3661	-0.4558
13	12	0.5897	0.4103	-0.5281
14	13	0.6082	0.3918	-0.4972
15	14	0.6053	0.3947	-0.5021
16	15	0.5313	0.4688	-0.6325
17	16	0.5662	0.4338	-0.5688
18	17	0.4911	0.5089	-0.7112
19	18	0.5082	0.4918	-0.6769
20	19	0.4571	0.5429	-0.7828
21	20	0.4876	0.5124	-0.7183
22	21	0.3902	0.6098	-0.9410
23	22	0.3980	0.6020	-0.9214
24	23	0.4393	0.5607	-0.8227
25	24	0.3968	0.6032	-0.9243
26	25	0.4138	0.5862	-0.8824
27	26	0.3621	0.6379	-1.0159
28	27	0.3793	0.6207	-0.9694
29	28	0.4037	0.5963	-0.9072
30	29	0.3182	0.6818	-1.1451
31	30	0.3113	0.6887	-1.1671
32	33	0.3121	0.6879	-1.1644
33	34	0.2405	0.7595	-1.4250
34	35	0.2739	0.7261	-1.2950
35	36	0.2422	0.7578	-1.4180
36	37	0.2263	0.7737	-1.4860
37	38	0.1942	0.8058	-1.6386
38	40	0.2229	0.7771	-1.5011

[a]Time relative to the first NMR measured.

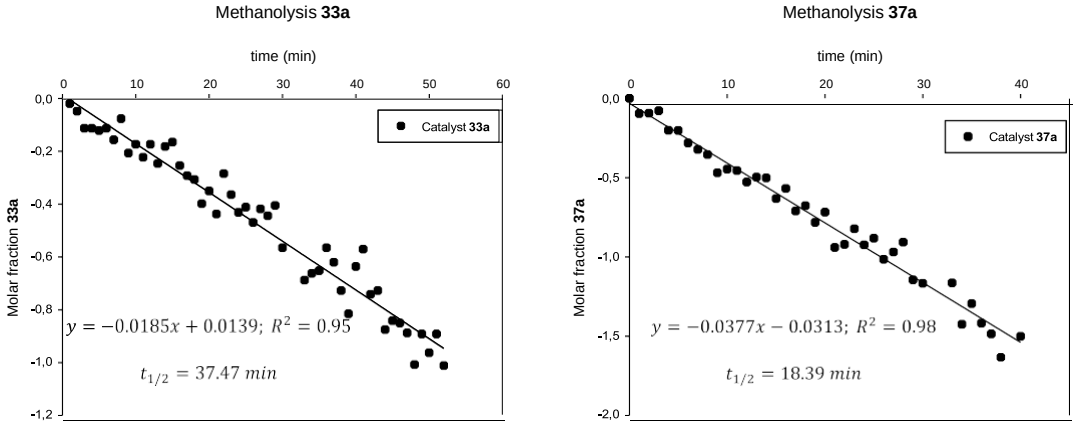

Plotting of Ln[X_{33a}] vs time (left) and Ln[X_{37a}] vs time (right).

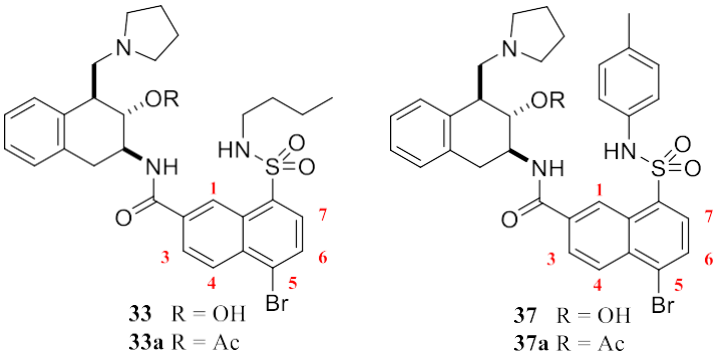

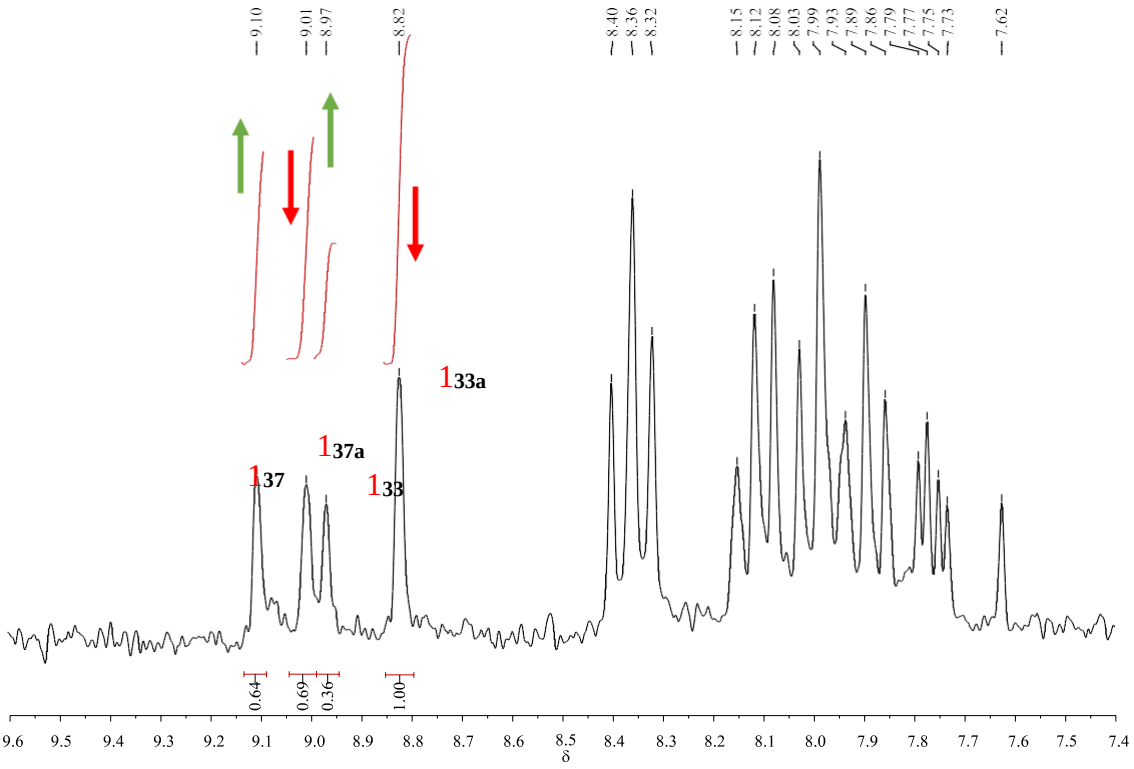

*[1]H NMR spectra (7.4-9.6 ppm) for methanolysis of **33a** and **37a** at 12 min relative to the first NMR measured in CD_3OD 5% in $CDCl_3$.*

Catalyst **39**

1_{39}, 1_{39a}, 1_{33} and 1_{33a} signals from the ^{1}H NMR spectra of 0 were integrated to calculate the molar fraction (X). All data are collected in 0 and 0; plotting Ln[$X_{33a-39a}$] *versus* time gave the equation shown in 0 from which the half-life was calculated:

Variation of molar fraction with time for methanolysis of **33a**.

Entry	Time[a]/min	X_{33a}	X_{33}	Ln(X_{33a})
1	0	1.0000	0.0000	0.0000
2	1	0.9524	0.0476	-0.0488
3	2	0.9524	0.0476	-0.0488
4	3	0.9174	0.0826	-0.0862
5	4	0.9434	0.0566	-0.0583
6	5	0.9091	0.0909	-0.0953
7	6	0.8403	0.1597	-0.1740
8	7	0.8621	0.1379	-0.1484
9	8	0.8621	0.1379	-0.1484
10	9	0.8475	0.1525	-0.1655
11	10	0.8547	0.1453	-0.1570
12	11	0.8264	0.1736	-0.1906
13	12	0.8197	0.1803	-0.1989
14	13	0.7813	0.2188	-0.2469
15	14	0.7634	0.2366	-0.2700
16	15	0.7463	0.2537	-0.2927
17	16	0.7463	0.2537	-0.2927
18	17	0.6711	0.3289	-0.3988
19	18	0.6667	0.3333	-0.4055
20	19	0.7353	0.2647	-0.3075
21	20	0.7042	0.2958	-0.3507
22	21	0.6452	0.3548	-0.4383
23	22	0.6410	0.3590	-0.4447
24	23	0.6623	0.3377	-0.4121
25	24	0.6135	0.3865	-0.4886
26	25	0.5882	0.4118	-0.5306
27	26	0.5814	0.4186	-0.5423
28	27	0.6061	0.3939	-0.5008
29	28	0.6369	0.3631	-0.4511
30	29	0.5780	0.4220	-0.5481
31	30	0.5848	0.4152	-0.5365
32	31	0.5464	0.4536	-0.6043
33	32	0.5236	0.4764	-0.6471
34	33	0.5747	0.4253	-0.5539
35	34	0.5208	0.4792	-0.6523
36	35	0.4926	0.5074	-0.7080
37	36	0.4854	0.5146	-0.7227
38	37	0.4673	0.5327	-0.7608
39	38	0.4310	0.5690	-0.8416
40	39	0.4878	0.5122	-0.7178
41	40	0.4717	0.5283	-0.7514
42	41	0.4115	0.5885	-0.8879
43	42	0.4831	0.5169	-0.7275
44	43	0.4695	0.5305	-0.7561
45	44	0.4484	0.5516	-0.8020
46	45	0.4098	0.5902	-0.8920
47	46	0.4405	0.5595	-0.8198
48	47	0.3831	0.6169	-0.9594
49	48	0.3953	0.6047	-0.9282
50	49	0.3984	0.6016	-0.9203
51	50	0.3968	0.6032	-0.9243
52	51	0.3817	0.6183	-0.9632
53	52	0.3717	0.6283	-0.9895
54	53	0.3690	0.6310	-0.9969
55	54	0.3390	0.6610	-1.0818
56	55	0.3584	0.6416	-1.0260
57	56	0.3497	0.6503	-1.0508
58	57	0.3534	0.6466	-1.0403
59	58	0.3509	0.6491	-1.0473
60	59	0.3472	0.6528	-1.0578
61	60	0.3401	0.6599	-1.0784
62	61	0.3311	0.6689	-1.1053
63	62	0.3521	0.6479	-1.0438
64	63	0.2994	0.7006	-1.2060
65	64	0.3300	0.6700	-1.1086
66	65	0.2865	0.7135	-1.2499
67	66	0.3106	0.6894	-1.1694
68	67	0.2890	0.7110	-1.2413
69	68	0.2770	0.7230	-1.2837
70	69	0.2703	0.7297	-1.3083
71	70	0.2674	0.7326	-1.3191
72	71	0.2667	0.7333	-1.3218
73	72	0.2865	0.7135	-1.2499
74	73	0.2469	0.7531	-1.3987
75	74	0.2618	0.7382	-1.3403
76	75	0.2778	0.7222	-1.2809
77	76	0.2481	0.7519	-1.3938
78	77	0.2347	0.7653	-1.4493
79	78	0.2169	0.7831	-1.5282
80	79	0.2381	0.7619	-1.4351
81	80	0.2198	0.7802	-1.5151
82	81	0.2174	0.7826	-1.5261
83	82	0.2169	0.7831	-1.5282
84	83	0.1931	0.8069	-1.6448
85	84	0.2331	0.7669	-1.4563
86	85	0.2049	0.7951	-1.5851
87	86	0.2188	0.7812	-1.5195
88	87	0.1946	0.8054	-1.6371
89	88	0.2174	0.7826	-1.5261

[a]Time relative to the first NMR measured.

Variation of molar fraction with time for methanolysis of **39a**.

Entry	Time[a]/min	X_{39a}	X_{39}	$Ln(X_{39a})$
1	0	1.0000	0.0000	0.0000
2	1	0.9200	0.0800	-0.0834
3	2	0.8434	0.1566	-0.1703
4	3	0.7683	0.2317	-0.2636
5	4	0.7045	0.2955	-0.3502
6	5	0.6782	0.3218	-0.3884
7	6	0.6392	0.3608	-0.4476
8	7	0.6136	0.3864	-0.4884
9	8	0.5698	0.4302	-0.5625
10	9	0.5444	0.4556	-0.6080
11	10	0.4756	0.5244	-0.7432
12	11	0.4828	0.5172	-0.7282
13	12	0.4400	0.5600	-0.8210
14	13	0.4206	0.5794	-0.8662
15	14	0.3846	0.6154	-0.9555
16	15	0.3558	0.6442	-1.0335
17	16	0.3364	0.6636	-1.0893
18	17	0.3256	0.6744	-1.1221
19	18	0.3307	0.6693	-1.1065
20	19	0.2642	0.7358	-1.3312
21	20	0.2540	0.7460	-1.3705
22	21	0.2847	0.7153	-1.2564
23	22	0.2583	0.7417	-1.3537
24	23	0.1860	0.8140	-1.6818
25	24	0.1776	0.8224	-1.7280
26	25	0.1842	0.8158	-1.6917
27	26	0.1948	0.8052	-1.6358
28	27	0.1654	0.8346	-1.7993
29	28	0.1606	0.8394	-1.8289
30	29	0.1418	0.8582	-1.9530

[a]Time relative to the first NMR measured.

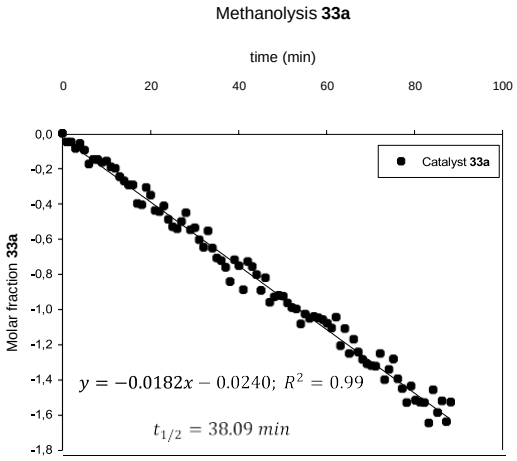

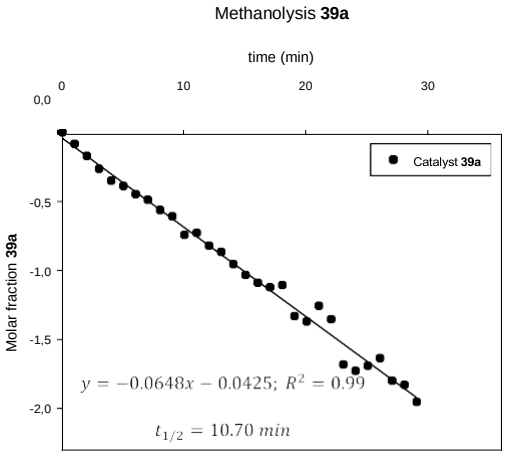

Plotting of Ln[X_{33a}] vs time (left) and Ln[X_{39a}] vs time (right).

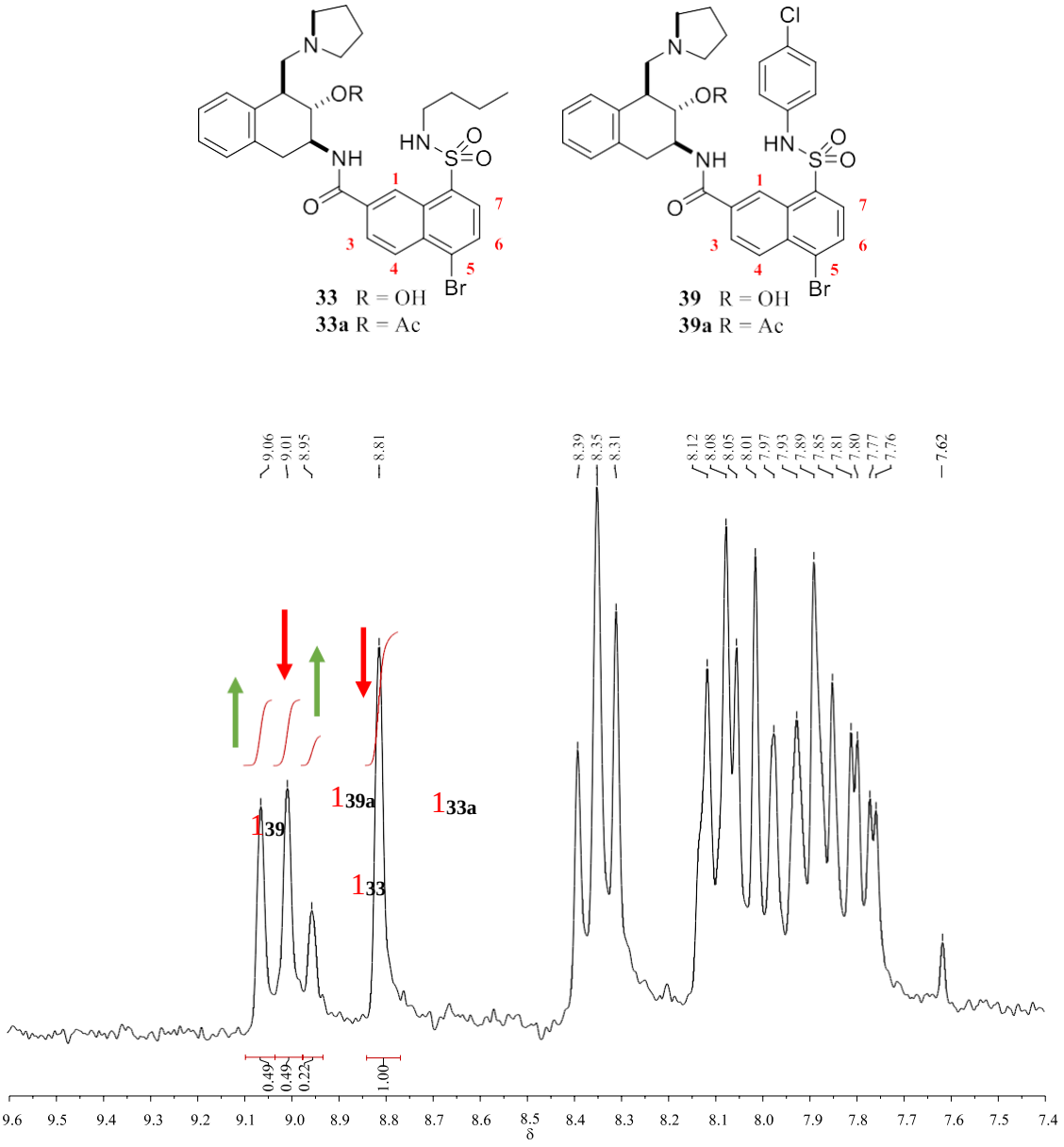

*^{1}H NMR spectra (7.4-9.6 ppm) for methanolysis of **33a** and **39a** at 9 min relative to the first NMR measured in CD_3OD 5% in $CDCl_3$.*

Catalyst **44**

1_{44}, 1_{44a}, 1_{33} and 1_{33a} signals from the ^{1}H NMR spectra of 0 were integrated to calculate the molar fraction (X). All data are collected in 0 and 0; plotting Ln[$X_{33a-44a}$] *versus* time gave the equation shown in 0 from which the half-life was calculated:

Variation of molar fraction with time for methanolysis of **33a**.

Entry	Time[a]/min	X_{33a}	X_{33}	LnX_{33a}	Entry	Time[a]/min	X_{33a}	X_{33}	LnX_{33a}
1	10	0.9747	0.0253	-0.0257	26	35	0.6782	0.3218	-0.3883
2	11	1.0000	0.0000	0.0000	27	36	0.7331	0.2669	-0.3104
3	12	1.0477	-0.0477	0.0466	28	37	0.6966	0.3034	-0.3615
4	13	0.9447	0.0553	-0.0569	29	38	0.6061	0.3939	-0.5008
5	14	0.9005	0.0995	-0.1048	30	39	0.5967	0.4033	-0.5164
6	15	0.9276	0.0724	-0.0751	31	40	0.6061	0.3939	-0.5008
7	16	1.0199	-0.0199	0.0197	32	41	0.5765	0.4235	-0.5507
8	17	0.9005	0.0995	-0.1048	33	42	0.5439	0.4561	-0.6090
9	18	0.9058	0.0942	-0.0989	34	43	0.6361	0.3639	-0.4523
10	19	0.8323	0.1677	-0.1836	35	44	0.6061	0.3939	-0.5008
11	20	0.8699	0.1301	-0.1393	36	45	0.5200	0.4800	-0.6539
12	21	0.9390	0.0610	-0.0630	37	46	0.5831	0.4169	-0.5394
13	22	0.8602	0.1398	-0.1506	38	47	0.5557	0.4443	-0.5875
14	23	0.7737	0.2263	-0.2566	39	48	0.5271	0.4729	-0.6403
15	24	0.8699	0.1301	-0.1393	40	49	0.6523	0.3477	-0.4272
16	25	0.8323	0.1677	-0.1836	41	50	0.4636	0.5364	-0.7687
17	26	0.8278	0.1722	-0.1890	42	51	0.4751	0.5249	-0.7443
18	27	0.8554	0.1446	-0.1561	43	52	0.5537	0.4463	-0.5911
19	28	0.8147	0.1853	-0.2050	44	53	0.4527	0.5473	-0.7925
20	29	0.8104	0.1896	-0.2103	45	54	0.5498	0.4502	-0.5983
21	30	0.6998	0.3002	-0.3570	46	55	0.5382	0.4618	-0.6195
22	31	0.7161	0.2839	-0.3340	47	56	0.4474	0.5526	-0.8042
23	32	0.7161	0.2839	-0.3340	48	57	0.4918	0.5082	-0.7098
24	33	0.6904	0.3096	-0.3705	49	58	0.4461	0.5539	-0.8071
25	34	0.6693	0.3307	-0.4015					

[a]Time relative to the first NMR measured.

Variation of molar fraction with time for methanolysis of **44a**.

Entry	Time[a]/min	X_{44a}	X_{44}	$Ln(X_{44a})$
1	0	1.0000	0.0000	0.0000
2	1	0.8101	0.1899	-0.2106
3	2	0.9787	0.0213	-0.0216
4	3	0.8627	0.1373	-0.1477
5	4	0.7090	0.2910	-0.3438
6	5	0.6565	0.3435	-0.4208
7	6	0.6047	0.3953	-0.5031
8	7	0.6147	0.3853	-0.4867
9	8	0.4844	0.5156	-0.7248
10	9	0.4767	0.5233	-0.7408
11	10	0.4279	0.5721	-0.8488
12	11	0.3953	0.6047	-0.9280
13	12	0.2959	0.7041	-1.2176
14	13	0.3467	0.6533	-1.0593
15	14	0.3473	0.6527	-1.0576
16	15	0.2754	0.7246	-1.2894
17	16	0.2861	0.7139	-1.2516
18	17	0.2451	0.7549	-1.4059
19	18	0.2881	0.7119	-1.2446

[a]Time relative to the first NMR measured

Plotting of Ln[X_{33a}] vs time (left) and Ln[X_{44a}] vs time (right).

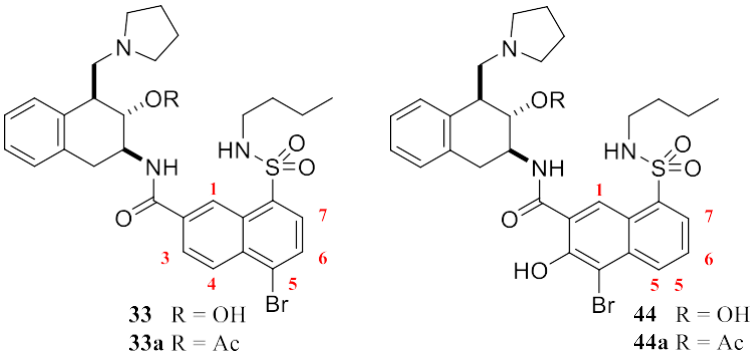

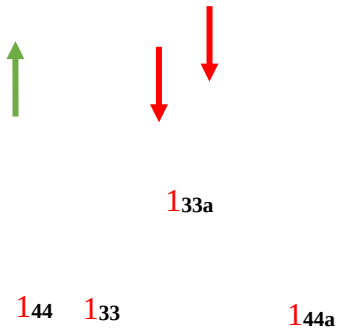

*^{1}H NMR spectra (7.4-9.6 ppm) for methanolysis of **33a** and **44a** at 10 min relative to the first NMR measured in CD_3OD 5% in $CDCl_3$.*

Catalyst **48**

1_{48}, 1_{48a}, 1_{33} and 1_{33a} signals from the ^{1}H NMR spectra of 0 were integrated to calculate the molar fraction (X). All data are collected in 0 and 0; plotting Ln[$X_{33a-48a}$] *versus* time gave the equation shown in 0 from which the half-life was calculated:

Variation of molar fraction with time for methanolysis of **33a**.

Entry	Time[a]/min	X_{33a}	X_{33}	Ln(X_{33a})	Entry	Time[a]/min	X_{33a}	X_{33}	Ln(X_{33a})
1	0.0000	1.0000	0.0000	0.0000	25	21.0400	0.6061	0.3939	-0.5008
2	0.8767	0.9804	0.0196	-0.0198	26	21.9167	0.5848	0.4152	-0.5365
3	1.7533	0.9709	0.0291	-0.0296	27	22.7933	0.5747	0.4253	-0.5539
4	2.6300	0.9259	0.0741	-0.0770	28	23.6700	0.5714	0.4286	-0.5596
5	3.5067	0.9259	0.0741	-0.0770	29	24.5467	0.5405	0.4595	-0.6152
6	4.3833	0.8621	0.1379	-0.1484	30	25.4233	0.5682	0.4318	-0.5653
7	5.2600	0.8621	0.1379	-0.1484	31	26.3000	0.5128	0.4872	-0.6678
8	6.1367	0.8197	0.1803	-0.1989	32	27.1767	0.5587	0.4413	-0.5822
9	7.0133	0.8197	0.1803	-0.1989	33	28.0533	0.5155	0.4845	-0.6627
10	7.8900	0.8065	0.1935	-0.2151	34	28.9300	0.5025	0.4975	-0.6881
11	8.7667	0.8197	0.1803	-0.1989	35	29.8067	0.4808	0.5192	-0.7324
12	9.6433	0.7692	0.2308	-0.2624	36	30.6833	0.4717	0.5283	-0.7514
13	10.5200	0.7692	0.2308	-0.2624	37	31.5600	0.4808	0.5192	-0.7324
14	11.3967	0.7692	0.2308	-0.2624	38	32.4367	0.4695	0.5305	-0.7561
15	12.2733	0.7353	0.2647	-0.3075	39	33.3133	0.4831	0.5169	-0.7275
16	13.1500	0.7246	0.2754	-0.3221	40	34.1900	0.4695	0.5305	-0.7561
17	14.0267	0.6944	0.3056	-0.3646	41	35.0667	0.4545	0.5455	-0.7885
18	14.9033	0.7143	0.2857	-0.3365	42	35.9433	0.4464	0.5536	-0.8065
19	15.7800	0.6803	0.3197	-0.3853	43	36.8200	0.4274	0.5726	-0.8502
20	16.6567	0.6623	0.3377	-0.4121	44	37.6967	0.4016	0.5984	-0.9123
21	17.5333	0.6289	0.3711	-0.4637	45	38.5733	0.3876	0.6124	-0.9478
22	18.4100	0.6410	0.3590	-0.4447	46	39.4500	0.4032	0.5968	-0.9083
23	19.2867	0.6452	0.3548	-0.4383	47	40.3267	0.4132	0.5868	-0.8838
24	20.1633	0.5988	0.4012	-0.5128					

[a]Time relative to the first NMR measured.

Variation of molar fraction with time for methanolysis of **48a**.

Entry	Time[a]/min	X_{48a}	X_{48}	LnX_{48a}	Entry	Time[a]/min	X_{48a}	X_{48}	LnX_{48a}
1	0.8767	1.0000	0.0000	0.0000	15	13.1500	0.4229	0.5771	-0.8607
2	1.7533	1.0742	-0.0742	0.0715	16	14.0267	0.4264	0.5736	-0.8524
3	2.6300	0.9852	0.0148	-0.0149	17	14.9033	0.3478	0.6522	-1.0561
4	3.5067	0.8535	0.1465	-0.1584	18	15.7800	0.2270	0.7730	-1.4830
5	4.3833	0.9117	0.0883	-0.0924	19	17.5333	0.2652	0.7348	-1.3273
6	5.2600	0.7429	0.2571	-0.2972	20	18.4100	0.3152	0.6848	-1.1546
7	6.1367	0.7984	0.2016	-0.2251	21	20.1633	0.2581	0.7419	-1.3544
8	7.0133	0.7728	0.2272	-0.2578	22	21.0400	0.1571	0.8429	-1.8508
9	7.8900	0.6400	0.3600	-0.4463	23	21.9167	0.1652	0.8348	-1.8008
10	8.7667	0.5659	0.4341	-0.5693	24	22.7933	0.1670	0.8330	-1.7901
11	9.6433	0.6014	0.3986	-0.5085	25	23.6700	0.1615	0.8385	-1.8231
12	10.5200	0.4904	0.5096	-0.7126	26	24.5467	0.1458	0.8542	-1.9258
13	11.3967	0.5371	0.4629	-0.6216	27	25.4233	0.1293	0.8707	-2.0455
14	12.2733	0.3568	0.6432	-1.0304					

[a]Time relative to the first NMR measured.

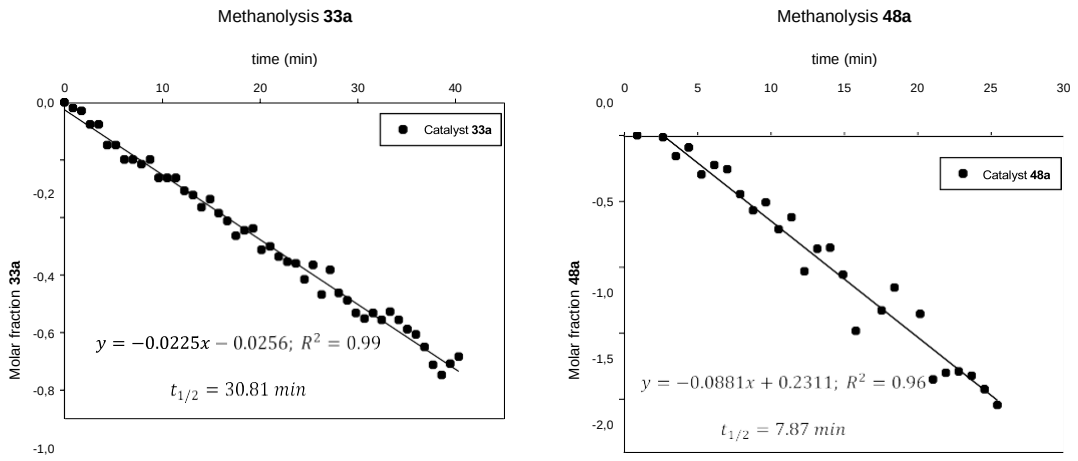

Plotting of Ln[X_{33a}] vs time (left) and Ln[X_{48a}] vs time (right).

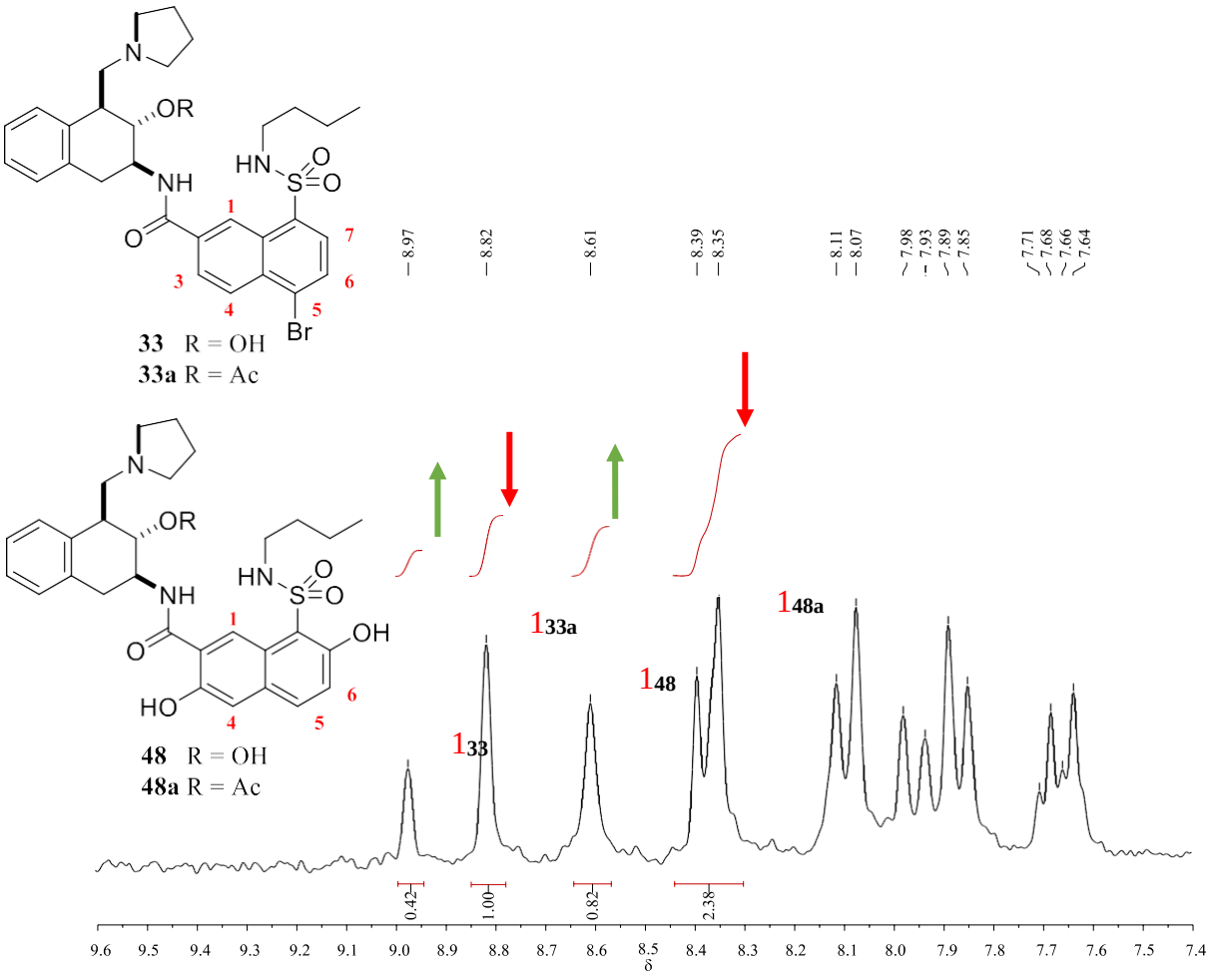

*^{1}H NMR spectra (7.4-9.6 ppm) for methanolysis of **33a** and **48a** at 7.01 min relative to the first NMR measured in CD_3OD 5% in $CDCl_3$.*

Catalyst **52**

1_{52}, 1_{52a}, 1_{33} and 1_{33a} signals from the ^{1}H NMR spectra of 0 were integrated to calculate the molar fraction (X). All data are collected in 0 and 0; plotting Ln[$X_{33a-52a}$] *versus* time gave the equation shown in 0 from which the half-life was calculated:

Variation of molar fraction with time for methanolysis of **33a**.

Entry	Time[a]/min	X_{33a}	X_{33}	LnX_{33a}	Entry	Time[a]/min	X_{33a}	X_{33}	LnX_{33a}
1	0	1.0000	0.0000	0.0000	22	21	0.6849	0.3151	-0.3784
2	1	1.0101	-0.0101	0.0101	23	22	0.6536	0.3464	-0.4253
3	2	0.9524	0.0476	-0.0488	24	23	0.6757	0.3243	-0.3920
4	3	0.9434	0.0566	-0.0583	25	24	0.6494	0.3506	-0.4318
5	4	0.9346	0.0654	-0.0677	26	25	0.6369	0.3631	-0.4511
6	5	0.8850	0.1150	-0.1222	27	26	0.6452	0.3548	-0.4383
7	6	0.8850	0.1150	-0.1222	28	27	0.6173	0.3827	-0.4824
8	7	0.8621	0.1379	-0.1484	29	28	0.5952	0.4048	-0.5188
9	8	0.8696	0.1304	-0.1398	30	29	0.5747	0.4253	-0.5539
10	9	0.8696	0.1304	-0.1398	31	30	0.5747	0.4253	-0.5539
11	10	0.8264	0.1736	-0.1906	32	31	0.5848	0.4152	-0.5365
12	11	0.8130	0.1870	-0.2070	33	32	0.5464	0.4536	-0.6043
13	12	0.7813	0.2188	-0.2469	34	33	0.5747	0.4253	-0.5539
14	13	0.7937	0.2063	-0.2311	35	34	0.5128	0.4872	-0.6678
15	14	0.7519	0.2481	-0.2852	36	35	0.5128	0.4872	-0.6678
16	15	0.7576	0.2424	-0.2776	37	36	0.5102	0.4898	-0.6729
17	16	0.7576	0.2424	-0.2776	38	37	0.4975	0.5025	-0.6981
18	17	0.7246	0.2754	-0.3221	39	38	0.4878	0.5122	-0.7178
19	18	0.7042	0.2958	-0.3507	40	39	0.4878	0.5122	-0.7178
20	19	0.7143	0.2857	-0.3365	41	40	0.4762	0.5238	-0.7419
21	20	0.6849	0.3151	-0.3784					

[a]Time relative to the first NMR measured.

Variation of molar fraction with time for methanolysis of **52a**.

Entry	Time[a]/min	X_{52a}	X_{52}	$Ln(X_{52a})$
1	0	1.0000	0.0000	0.0000
2	1	0.8438	0.1563	-0.1699
3	2	0.7353	0.2647	-0.3075
4	3	0.6563	0.3438	-0.4212
5	4	0.6486	0.3514	-0.4329
6	5	0.5500	0.4500	-0.5978
7	6	0.4412	0.5588	-0.8183
8	7	0.4211	0.5789	-0.8650
9	8	0.3902	0.6098	-0.9410
10	9	0.2927	0.7073	-1.2287
11	10	0.2564	0.7436	-1.3610
12	11	0.2619	0.7381	-1.3398
13	12	0.2000	0.8000	-1.6094

[a]Time relative to the first NMR measured.

Plotting of Ln[X_{33a}] vs time (left) and Ln[X_{52a}] vs time (right).

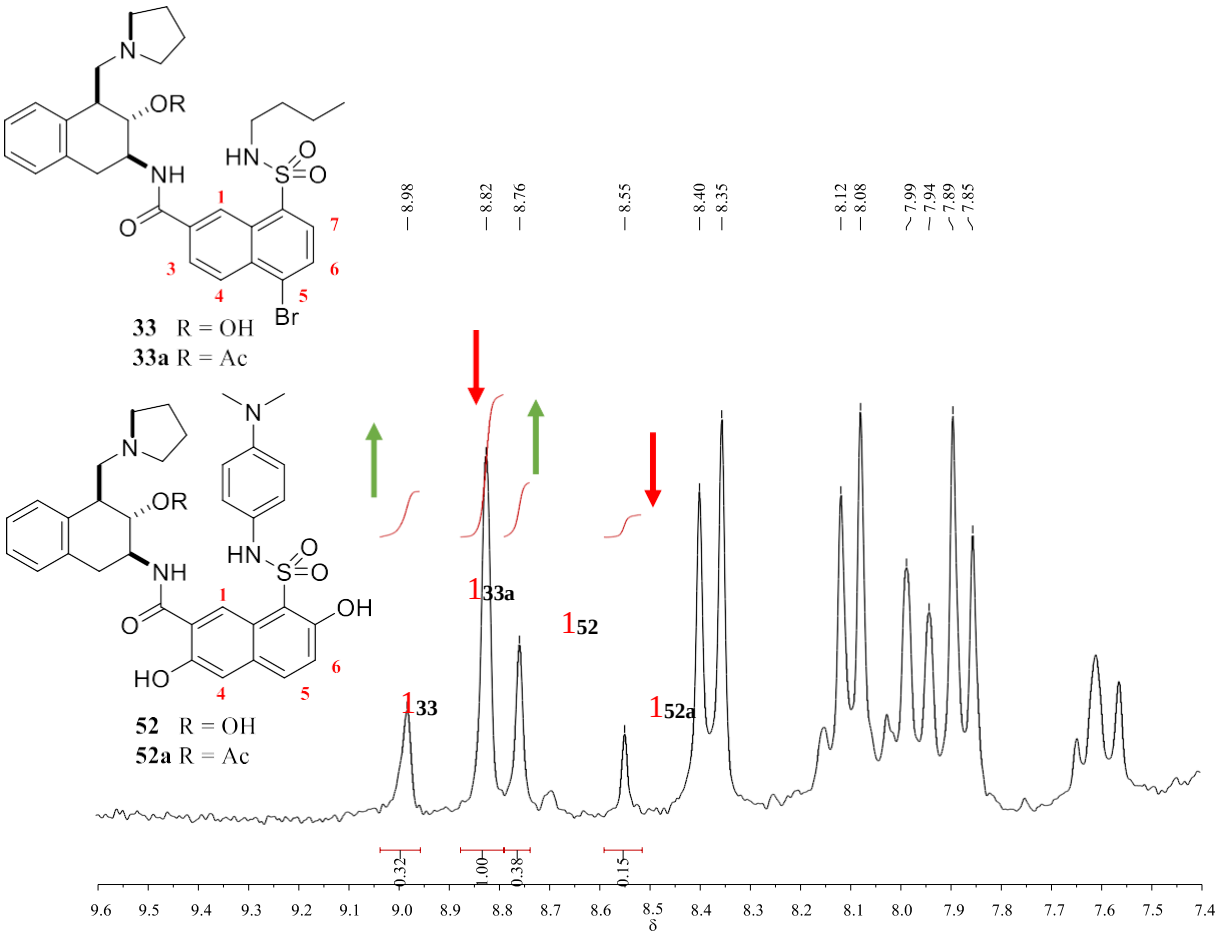

*^{1}H NMR spectra (7.4-9.6 ppm) for methanolysis of **33a** and **52a** at 6 min relative to the first NMR measured in CD_3OD 5% in $CDCl_3$.*

Catalyst **56**

1_{56}, 1_{56a}, 1_{33} and 1_{33a} signals from the ^{1}H NMR spectra of 0 were integrated to calculate the molar fraction (X). All data are collected in 0 and 0; plotting Ln[$X_{33a-56a}$] *versus* time gave the equation shown in 0 from which the half-life was calculated:

Variation of molar fraction with time for methanolysis of **33a**.

Entry	Time[a]/min	X_{33a}	X_{33}	Ln(X_{33a})	Entry	Time[a]/min	X_{33a}	X_{33}	Ln(X_{33a})
1	0.0000	1.0000	0.0000	0.0000	21	20.7140	0.6289	0.3711	-0.4637
2	1.0357	0.9615	0.0385	-0.0392	22	21.7497	0.5714	0.4286	-0.5596
3	2.0714	0.9709	0.0291	-0.0296	23	22.7854	0.5780	0.4220	-0.5481
4	3.1071	0.9434	0.0566	-0.0583	24	23.8211	0.5747	0.4253	-0.5539
5	4.1428	0.9091	0.0909	-0.0953	25	24.8568	0.5155	0.4845	-0.6627
6	5.1785	0.8772	0.1228	-0.1310	26	25.8925	0.5102	0.4898	-0.6729
7	6.2142	0.8475	0.1525	-0.1655	27	26.9282	0.5348	0.4652	-0.6259
8	7.2499	0.7937	0.2063	-0.2311	28	27.9639	0.5155	0.4845	-0.6627
9	8.2856	0.7874	0.2126	-0.2390	29	28.9996	0.4831	0.5169	-0.7275
10	9.3213	0.7937	0.2063	-0.2311	30	30.0353	0.4630	0.5370	-0.7701
11	10.3570	0.7407	0.2593	-0.3001	31	31.0710	0.4464	0.5536	-0.8065
12	11.3927	0.7042	0.2958	-0.3507	32	32.1067	0.4762	0.5238	-0.7419
13	12.4284	0.7042	0.2958	-0.3507	33	33.1424	0.4673	0.5327	-0.7608
14	13.4641	0.6993	0.3007	-0.3577	34	34.1781	0.4464	0.5536	-0.8065
15	14.4998	0.6667	0.3333	-0.4055	35	35.2138	0.4237	0.5763	-0.8587
16	15.5355	0.6579	0.3421	-0.4187	36	36.2495	0.4000	0.6000	-0.9163
17	16.5712	0.6849	0.3151	-0.3784	37	37.2852	0.3861	0.6139	-0.9517
18	17.6069	0.6369	0.3631	-0.4511	38	38.3209	0.4032	0.5968	-0.9083
19	18.6426	0.5714	0.4286	-0.5596	39	39.3566	0.3774	0.6226	-0.9746
20	19.6783	0.6061	0.3939	-0.5008	40	40.3923	0.3390	0.6610	-1.0818

[a]Time relative to the first NMR measured.

Variation of molar fraction with time for methanolysis of **56a**.

Entry	Time[a]/min	X_{56a}	X_{56}	Ln(X_{56a})
1	0.0000	1.0000	0.0000	0.0000
2	1.0357	0.7353	0.2647	-0.3075
3	2.0714	0.6176	0.3824	-0.4818
4	3.1071	0.5000	0.5000	-0.6931
5	4.1428	0.4043	0.5957	-0.9057
6	5.1785	0.3333	0.6667	-1.0986
7	6.2142	0.3000	0.7000	-1.2040

[a]Time relative to the first NMR measured.

Plotting of Ln[X_{33a}] vs time (left) and Ln[X_{56a}] vs time (right).

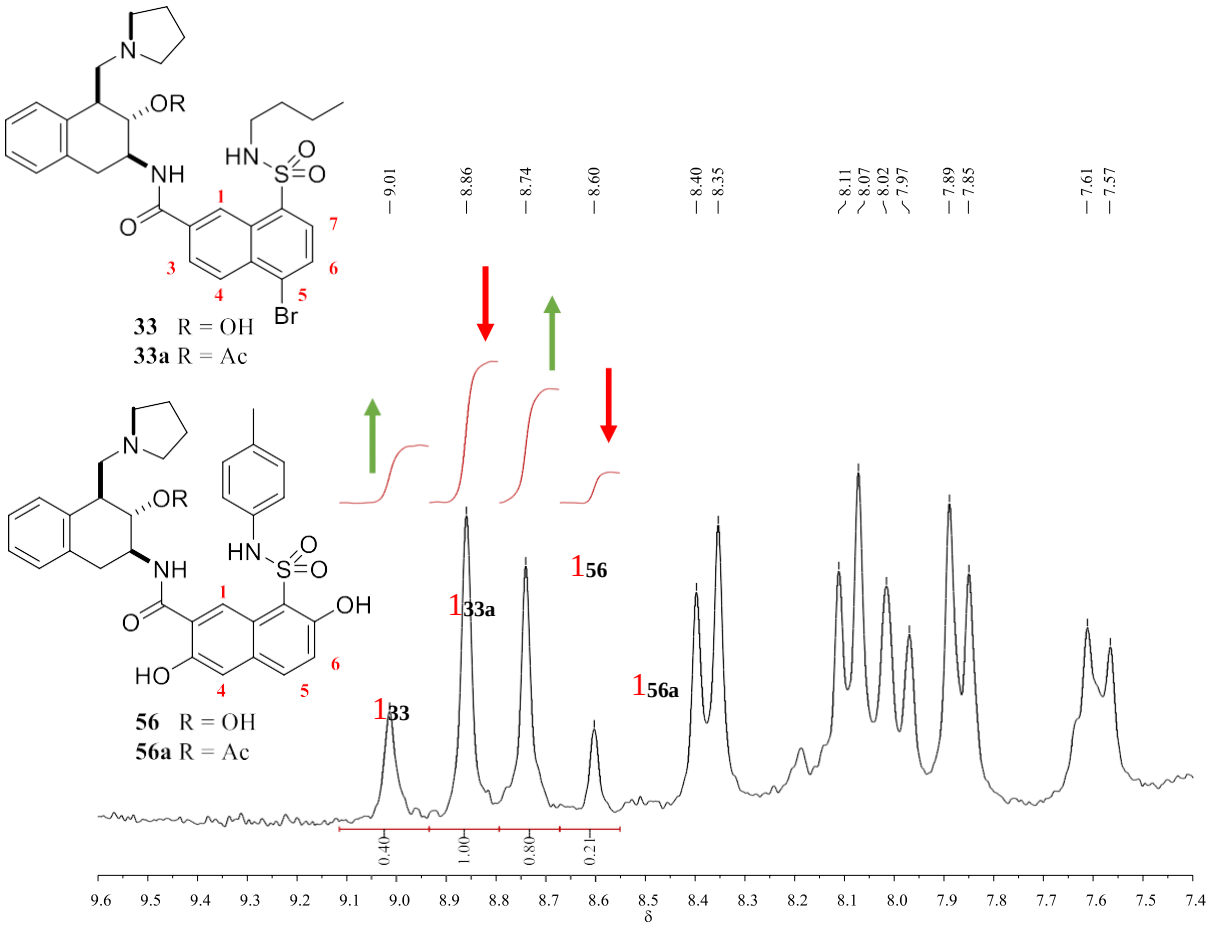

*^{1}H NMR spectra (7.4-9.6 ppm) for methanolysis of **33a** and **56a** at 2.07 min relative to the first NMR measured in CD_3OD 5% in $CDCl_3$.*

Catalyst **61**

1_{61}, 1_{61a}, 1_{33} and 1_{33a} signals from the ^{1}H NMR spectra of 0 were integrated to calculate the molar fraction (X). All data are collected in 0 and 0; plotting Ln[$X_{33a-61a}$] *versus* time gave the equation shown in 0 from which the half-life was calculated:

Variation of molar fraction with time for methanolysis of **33a**.

Entry	Time[a]/min	X_{33a}	X_{33}	LnX_{33a}	Entry	Time[a]/min	X_{33a}	X_{33}	LnX_{33a}
1	0.0000	1.0000	0.0000	0.0000	31	30.3750	0.5181	0.4819	-0.6575
2	1.0125	1.0309	-0.0309	0.0305	32	31.3875	0.5025	0.4975	-0.6881
3	2.0250	0.9901	0.0099	-0.0100	33	32.4000	0.5263	0.4737	-0.6419
4	3.0375	0.9709	0.0291	-0.0296	34	33.4125	0.5495	0.4505	-0.5988
5	4.0500	0.9804	0.0196	-0.0198	35	34.4250	0.5102	0.4898	-0.6729
6	5.0625	0.9259	0.0741	-0.0770	36	35.4375	0.4464	0.5536	-0.8065
7	6.0750	0.8929	0.1071	-0.1133	37	36.4500	0.4525	0.5475	-0.7930
8	7.0875	0.9009	0.0991	-0.1044	38	37.4625	0.4292	0.5708	-0.8459
9	8.1000	0.8929	0.1071	-0.1133	39	38.4750	0.4098	0.5902	-0.8920
10	9.1125	0.9009	0.0991	-0.1044	40	39.4875	0.4292	0.5708	-0.8459
11	10.1250	0.8333	0.1667	-0.1823	41	40.5000	0.4484	0.5516	-0.8020
12	11.1375	0.8850	0.1150	-0.1222	42	41.5125	0.4292	0.5708	-0.8459
13	12.1500	0.8333	0.1667	-0.1823	43	42.5250	0.4348	0.5652	-0.8329
14	13.1625	0.8000	0.2000	-0.2231	44	43.5375	0.4386	0.5614	-0.8242
15	14.1750	0.7246	0.2754	-0.3221	45	44.5500	0.3922	0.6078	-0.9361
16	15.1875	0.7576	0.2424	-0.2776	46	45.5625	0.3704	0.6296	-0.9933
17	16.2000	0.7576	0.2424	-0.2776	47	46.5750	0.4329	0.5671	-0.8372
18	17.2125	0.7692	0.2308	-0.2624	48	47.5875	0.3846	0.6154	-0.9555
19	18.2250	0.6623	0.3377	-0.4121	49	48.6000	0.3623	0.6377	-1.0152
20	19.2375	0.6667	0.3333	-0.4055	50	49.6125	0.3497	0.6503	-1.0508
21	20.2500	0.6452	0.3548	-0.4383	51	50.6250	0.3257	0.6743	-1.1217
22	21.2625	0.6623	0.3377	-0.4121	52	51.6375	0.3597	0.6403	-1.0225
23	22.2750	0.6623	0.3377	-0.4121	53	52.6500	0.3425	0.6575	-1.0716
24	23.2875	0.6329	0.3671	-0.4574	54	53.6625	0.3731	0.6269	-0.9858
25	24.3000	0.5988	0.4012	-0.5128	55	54.6750	0.3289	0.6711	-1.1119
26	25.3125	0.5952	0.4048	-0.5188	56	55.6875	0.3546	0.6454	-1.0367
27	26.3250	0.5952	0.4048	-0.5188	57	56.7000	0.3205	0.6795	-1.1378
28	27.3375	0.5952	0.4048	-0.5188	58	57.7125	0.2597	0.7403	-1.3481
29	28.3500	0.5917	0.4083	-0.5247	59	58.7250	0.2959	0.7041	-1.2179
30	29.3625	0.5714	0.4286	-0.5596	60	59.7375	0.2725	0.7275	-1.3002

[a]Time relative to the first NMR measured.

Variation of molar fraction with time for methanolysis of **61a**.

Entry	Time[a]/min	X_{61a}	X_{61}	$Ln(X_{61a})$
1	0.0000	1.0000	0.0000	0.0000
2	1.0125	0.9683	0.0317	-0.0323
3	2.0250	0.9483	0.0517	-0.0531
4	3.0375	0.8852	0.1148	-0.1219
5	4.0500	0.8833	0.1167	-0.1241
6	5.0625	0.8281	0.1719	-0.1886
7	6.0750	0.7576	0.2424	-0.2776
8	7.0875	0.7869	0.2131	-0.2397
9	8.1000	0.7500	0.2500	-0.2877
10	9.1125	0.6769	0.3231	-0.3902
11	10.1250	0.6667	0.3333	-0.4055
12	11.1375	0.6269	0.3731	-0.4670
13	12.1500	0.5897	0.4103	-0.5281
14	13.1625	0.5556	0.4444	-0.5878
15	14.1750	0.5000	0.5000	-0.6931
16	15.1875	0.5128	0.4872	-0.6678
17	16.2000	0.5062	0.4938	-0.6809
18	17.2125	0.5122	0.4878	-0.6690
19	18.2250	0.4396	0.5604	-0.8220
20	19.2375	0.4304	0.5696	-0.8431
21	20.2500	0.4045	0.5955	-0.9051
22	21.2625	0.3511	0.6489	-1.0468
23	22.2750	0.3297	0.6703	-1.1097
24	23.2875	0.3152	0.6848	-1.1545
25	24.3000	0.3415	0.6585	-1.0745
26	25.3125	0.3197	0.6803	-1.1405
27	26.3250	0.3168	0.6832	-1.1494
28	27.3375	0.2745	0.7255	-1.2928
29	28.3500	0.2600	0.7400	-1.3471
30	29.3625	0.2605	0.7395	-1.3451
31	30.3750	0.2160	0.7840	-1.5325
Entry	Time[a]/min	X_{61a}	X_{61}	$Ln(X_{61a})$

[a]Time relative to the first NMR measured.

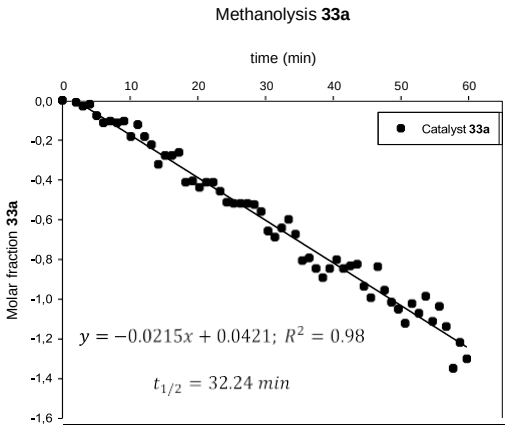

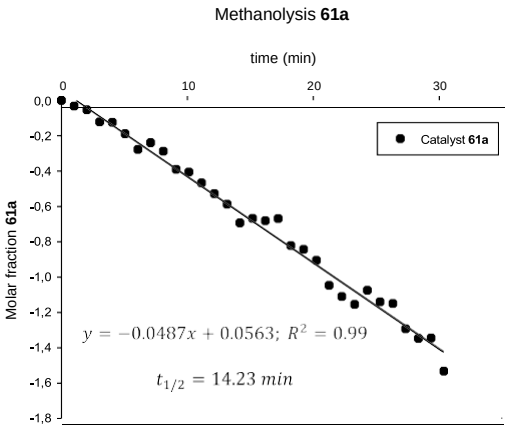

Plotting of Ln[X_{33a}] vs time (left) and Ln[X_{61a}] vs time (right).

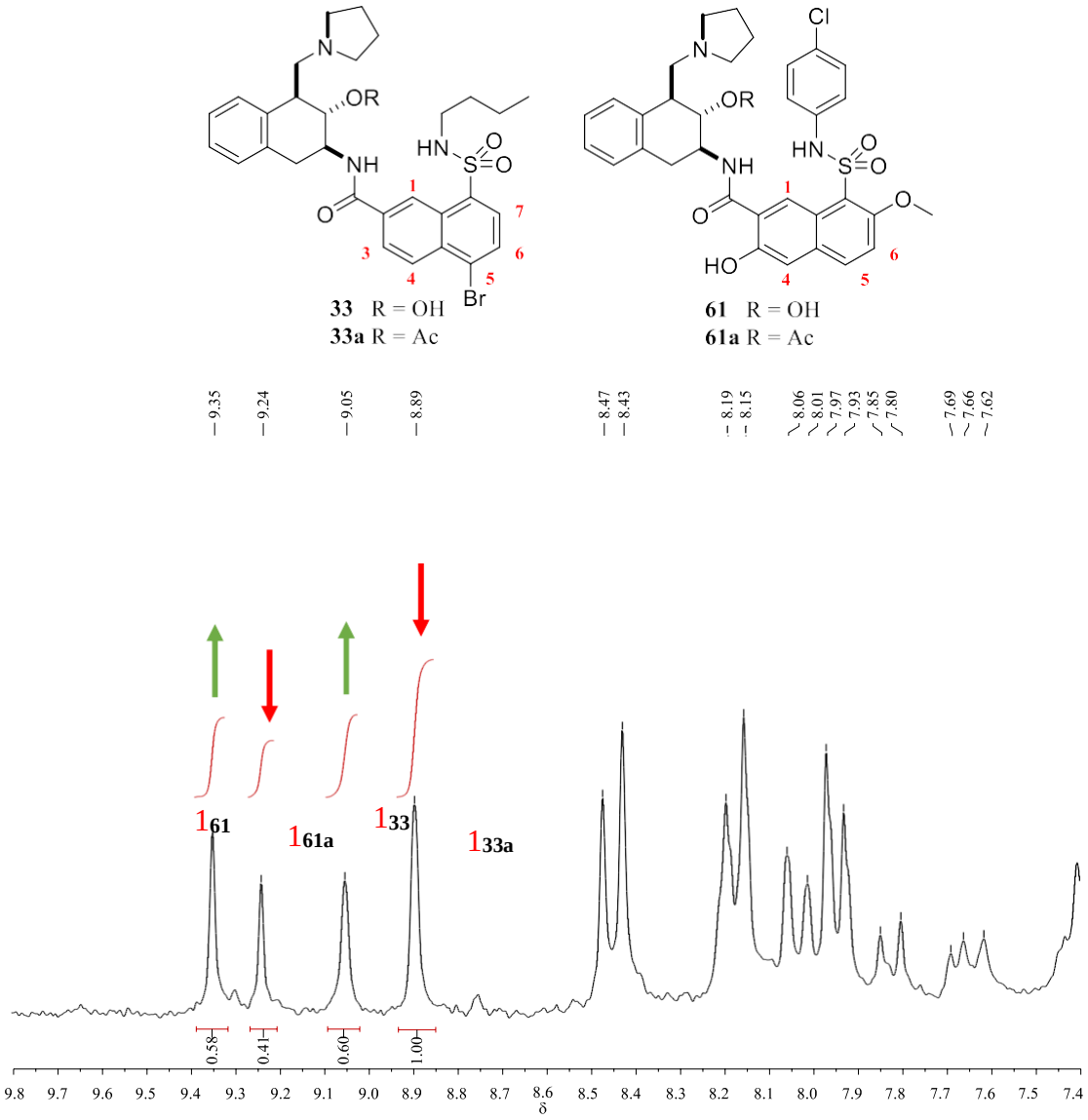

*^{1}H NMR spectra (7.4-9.8 ppm) for methanolysis of **33a** and **61a** at 16.20 min relative to the first NMR measured in CD_3OD 5% in $CDCl_3$.*

Catalyst **60**

1_{60}, 1_{60a}, 1_{33} and 1_{33a} signals from the ^{1}H NMR spectra of **¡Error! No se encuentra el origen de la referencia.** were integrated to calculate the molar fraction (X). All data are collected in **¡Error! No se encuentra el origen de la referencia.** and **¡Error! No se encuentra el origen de la referencia.**; plotting Ln[$X_{33a-60a}$] *versus* time gave the equation shown in **¡Error! No se encuentra el origen de la referencia.** from which the half-life was calculated:

Variation of molar fraction with time for methanolysis of **33a**.

Entry	Time[a]/min	X_{33a}	X_{33}	Ln(X_{33a})	Entry	Time[a]/min	X_{33a}	X_{33}	Ln(X_{33a})
1	0	1.0000	0.0000	0.0000	22	21	0.6135	0.3865	-0.4886
2	1	0.9709	0.0291	-0.0296	23	22	0.5780	0.4220	-0.5481
3	2	0.9524	0.0476	-0.0488	24	23	0.5618	0.4382	-0.5766
4	3	0.9174	0.0826	-0.0862	25	24	0.5556	0.4444	-0.5878
5	4	0.9091	0.0909	-0.0953	26	25	0.5464	0.4536	-0.6043
6	5	0.8696	0.1304	-0.1398	27	26	0.5181	0.4819	-0.6575
7	6	0.8403	0.1597	-0.1740	28	27	0.5208	0.4792	-0.6523
8	7	0.8264	0.1736	-0.1906	29	28	0.5128	0.4872	-0.6678
9	8	0.8000	0.2000	-0.2231	30	29	0.5102	0.4898	-0.6729
10	9	0.8264	0.1736	-0.1906	31	30	0.4902	0.5098	-0.7129
11	10	0.7937	0.2063	-0.2311	32	31	0.4831	0.5169	-0.7275
12	11	0.7463	0.2537	-0.2927	33	32	0.4608	0.5392	-0.7747
13	12	0.7299	0.2701	-0.3148	34	33	0.4717	0.5283	-0.7514
14	13	0.7353	0.2647	-0.3075	35	34	0.4484	0.5516	-0.8020
15	14	0.6897	0.3103	-0.3716	36	35	0.4348	0.5652	-0.8329
16	15	0.6849	0.3151	-0.3784	37	36	0.4425	0.5575	-0.8154
17	16	0.6667	0.3333	-0.4055	38	37	0.4405	0.5595	-0.8198
18	17	0.6289	0.3711	-0.4637	39	38	0.4049	0.5951	-0.9042
19	18	0.6289	0.3711	-0.4637	40	39	0.4016	0.5984	-0.9123
20	19	0.6494	0.3506	-0.4318	41	40	0.4082	0.5918	-0.8961
21	20	0.6135	0.3865	-0.4886					

[a]Time relative to the first NMR measured

. *Variation of molar fraction with time for methanolysis of* **60a**.

Entry	Time[a]/min	X_{60a}	X_{60}	$Ln(X_{60a})$
1	0	1.0000	0.0000	0.0000
2	1	0.5758	0.4242	-0.5521
3	2	0.4333	0.5667	-0.8362
4	3	0.4146	0.5854	-0.8804
5	4	0.2941	0.7059	-1.2238
6	5	0.1765	0.8235	-1.7346
7	6	0.1795	0.8205	-1.7177
8	7	0.1176	0.8824	-2.1401

[a]Time relative to the first NMR measured.

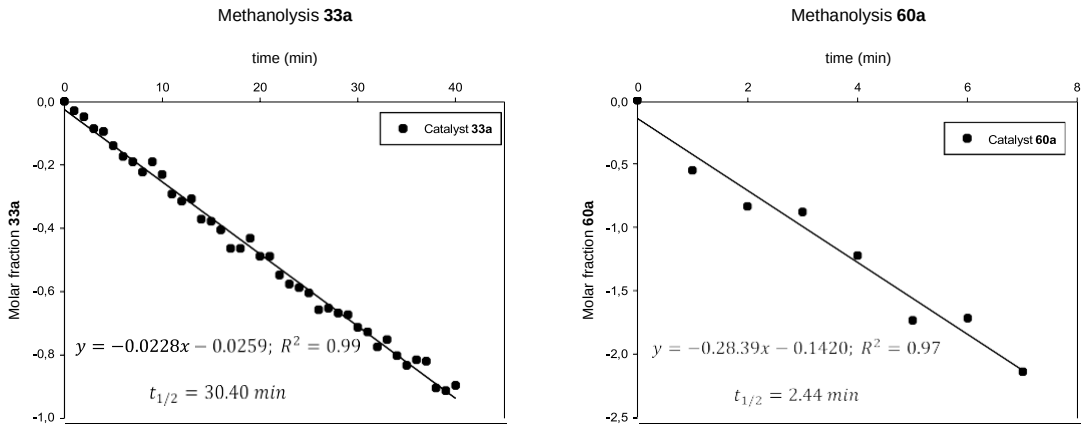

Plotting of Ln[X_{33a}] vs time (left) and Ln[X_{60a}] vs time (right).

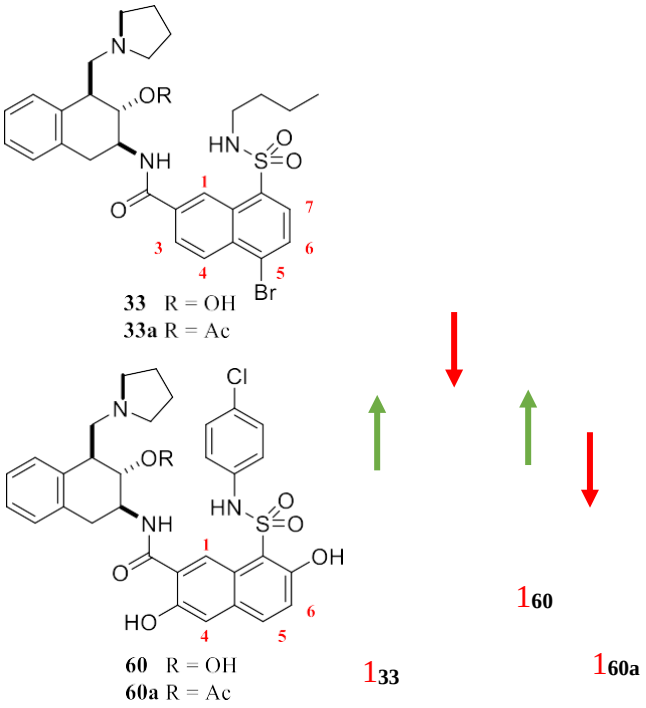

Figure S20. *^{1}H NMR spectra (7.4-9.6 ppm) for methanolysis of* **33a** *and* **60a** *at 1 min relative to the first NMR measured in CD_3OD 5% in $CDCl_3$.*